THE WINDS OF CHANGE: AN ARCHAEOMETALLURGICAL STUDY OF SILVER PRODUCTION IN THE PORCO-POTOSÍ REGION, SOUTHERN BOLIVIA AD 1500-2000

VOLUME I

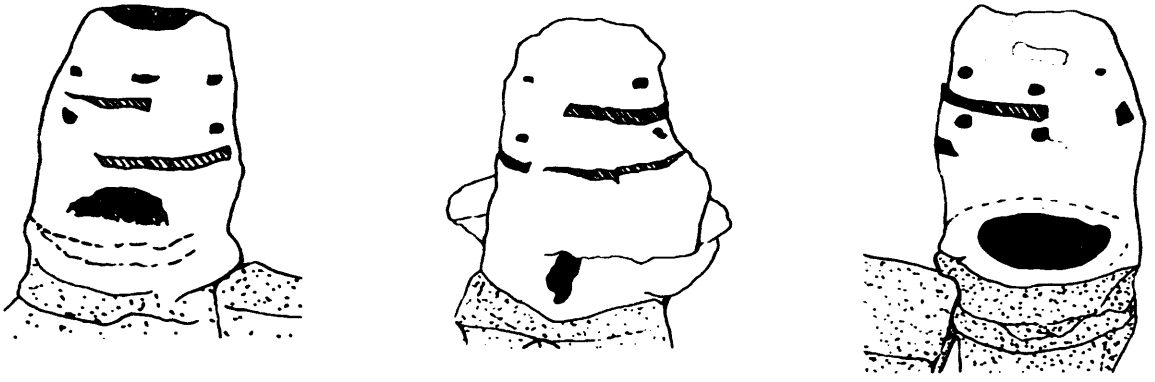

CLAIRE REBEKAH COHEN
UCL, INSTITUTE OF ARCHAEOLOGY

JUNE 2008

ProQuest LLC
789 East Eisenhower Parkway
P.O. Box 1346
Ann Arbor, MI 48106-1346

"I, *Claire Rebekah Cohen* confirm that the work presented in this thesis is my own. Where information has been derived from other sources, I confirm that this has been indicated in the thesis."

ABSTRACT

This thesis considers the technology employed to produce silver within the Porco-Potosí region, southern Bolivia, providing archaeo-metallurgical data on indigenous and European silver production methods in Porco during the period AD 1500 to 2000. The research has been conducted as part of Proyecto Arqueológico Porco-Potosí (PAPP) set up by Dr Mary Van Buren (Colorado State University).

The region of Porco was home to an Inca mine already prior to the Spanish conquest in 1538. Five years later, Spanish rule was established at Potosí. Indigenous technology, such as wind blown furnaces, *huayrachinas*, continued to be used in the region until the introduction of mercury amalgamation from 1570 onwards meant that the indigenous methods of silver production were superseded. *Huayrachina* technology employed at Porco dates back to at least the mid 16th century, with historical indications for earlier usage. PAPP has documented ongoing *huayrachina* smelting near Porco as late as 2003, showing the continuing existence of this technology. In this thesis, different silver production techniques from the archaeological and ethnographic records have been assessed using analytical techniques: Energy Dispersive X-Ray Fluorescence, Optical Microscopy and Scanning Electron Microscopy, and including a historical, archaeological and theoretical review of the relevant data.

In Porco, a diverse range of metallurgical techniques was being used for both small and large scale production. From the early colonial periods onwards both European and indigenous methods were used simultaneously to produce silver. The Spanish influence is evident in the archaeological remains of European furnaces. The analyses of the European furnaces show that these were more efficient in extracting metal than the indigenous *huayrachinas*, at the expense of an increased fuel consumption. A comparison between the archaeological and recent *huayrachina* remains has shown differences in smelting capacity; the latter having a relatively low metal yield and reduced technical efficiency, and indicating a change in ore composition. Recent silver production shows an environmental adaptation taking into account the difficulty and cost in obtaining fuel and ore. The continued use of the *huayrachina* over five centuries shows the persistence of indigenous technology, despite other production methods being available.

The results of this project contribute to a better understanding of the history of the Porco-Potosí region, and to Andean metallurgy.

ACKNOWLEDGEMENTS

This thesis is dedicated to my family: my parents Jeannette and Martin and my brother Avraham. Thank-you for listening and providing me with continued encouragement and much needed distractions.

This research project could not have taken place without the collaboration between Dr Mary Van Buren and all those involved in Proyecto Arqueológico Porco-Potosí (PAPP). It has been a pleasure to work with everyone involved in PAPP. My time in Bolivia has been life changing. I feel so fortunate to have lived and worked in such a beautiful and vibrant country. My thanks are extended to Don Carlos Cuiza for his smelting expertise and Barbara Mills for documenting the 2002 production.

To Professor Thilo Rehren, I will forever be indebted to you. Over the last four years, you have been my mentor and advisor. Despite my protests, I have benefited immeasurably by researching, working and learning from you. It has been a privilege to work with you. You have changed my perception of my own abilities. I have developed into a capable and confident archaeometallurgist. I am quite certain that this is due to your patience and never-ending support. I am extremely grateful to you. I am appreciative for this opportunity to acknowledge you and your contribution to this thesis.

To Dr Bill Sillar, you have challenged my thoughts and always encouraged my research. I have thoroughly enjoyed working with you on and my only regret is that I didn't lure you to Porco! Bill, thank-you for everything.

This PhD could not have been completed without the financial support from: The Institute of Material, Minerals and Mining (IOM3). This research has been sponsored by the awarding of the Stanley Elmore Fellowship 2005-2006, 2006-2007, 2007-2008 and the Heide Stolz Fellowship (awarded through IAMS in 2004).

My thanks are also extended to John Hall formally of Rio Tinto Plc who saw the value of this research project when it was still in its infancy.

Two field seasons in Bolivia were kindly supported by the Institute of Archaeology (IoA) awards and UCL Graduate School funding. As part of my research, I have attended 8 international conferences and these have been funded by IoA and UCL awards. The UCL

Disability Centre has been a great support and source of guidance, thanks go to Ellis, Jenny, Alison and Marion.

I also want to thank the Institute of Archaeo-Metallurgical Studies (IAMS) for their encouragement. The IAMS Trustees and our three-monthly meetings have become part of my routine at UCL.

During my research, the IoA has been my second home. I could not have completed research without the support of colleagues, students and staff at the Institute and UCL. I have to thank the students of room B53 (we suffered flooding and moved offices three times) and room 116. Thanks for the numerous cups of tea and shoulders to lean on. Particular thanks go to those who survived the chaos of my desk: Anna Karatzani, Isabel Villaseñor, Jane Humphris, Geoff Smith, Don Cooper, Paolo Guarino, Claudia Zehrt, Kathryn Piquette, Daniel Jones, Aude Mongiatti, Lorna Anguilano, Anke Cross, Alessandra Salvin, Birger Helgstad, Gabriel Moshenska, Tobias Richter.

I also want to acknowledge the Material Science and Data Research Group whose input and discussion have continued to challenge my research. Special thanks go to Dr Marcos Martinón-Torres who has always been a source of great encouragement and Dr Arlene Rosen whose door was always open for a chat. I am very grateful to Stuart Laidlaw who has supported me in every moment of crisis with *Photoshop* and other design issues. Thanks are extended to all those that work and support the Wolfson Archaeological Laboratories: Kevin Reeves, Phillip Connolly and Simon Groom.

I have to thank my good friends (in no particular order): Jasprit Brar, Isabel Milner, Annette Dick, Anna Razeto, Isabel Rivera Collazo, Paula Worth, Rachel Kelly and Fatma Marii for their open-ears and patience. The constant flow of chocolate and telephone conversations has provided much needed mental support. I also wish to thank Alexandra Mizara who was always there to listen and encourage.

Having reached the point of writing these acknowledgements, I feel overwhelmed by the number of people who have helped me during this research; specifically the support of my supervisors: Thilo and Bill, and my friends and family has meant so much to me. To everyone who I cannot mention personally me thank-you for your: teaching, guidance, intellectual discussion, monetary and emotional support, and friendship.

TABLE OF CONTENTS

TABLE OF FIGURES

TABLE OF TABLES

1. INTRODUCTION

The southern Andes have a rich and diverse metallurgical history spanning some four thousand years from the earliest known metal artefacts from around 2000 BC (Aldenderfer et al. 2008) to the present day. Sustained mineral mining and processing has been a basic means of subsistence for many centuries. The southern Andes have been at the heart of historical and archaeological studies concentrating on mining communities and the influence this region has in wider South America. However, despite the study of mining practise, almost no archaeometallurgical work has been carried out to understand the way in which minerals are processed to produce metal. This PhD research assesses the methods of silver and lead production used over the last 500 years in the Porco-Potosí region of southern Bolivia. It will analyse metal production using historical, ethnographic, archaeological and analytical techniques. These different techniques have been applied to gain a fresh perspective on the way in which political, economic and social factors have influenced and changed technology. This research aims to present an archaeometallurgical discussion that can lead and contribute to Andean as well as wider archaeological debate.

I will argue that the arrival of the Spanish *conquistadors* in the Porco-Potosí region altered the technological methods used to produce silver. These changes can be demonstrated using archaeological and historical evidence, and the results of analytical work carried out in this study will underpin this hypothesis.

In this chapter, the development of this research project is presented along with an introduction to its background, and includes a brief review of the Porco-Potosí region. The main aims and objectives of this research project are outlined and discussed.

1.1. The Porco-Potosí region

The Porco-Potosí region is located in south-western Bolivia (Figure 1.1). One of the main reasons for the high quantity of mineral resources found in this region was the hydrothermal activity during the formation process of the Andes mountain range (Cunningham et al. 1996). It is part of the Bolivian tin belt within the Cordillera Oriental mountain range, and is one of the world's largest silver mining districts. Silver minerals from the Cerro Rico (Rich Mountain), Potosí and surrounding mountain ranges have been mined and smelted for at least 500 years, and possibly longer. The exact quantity of mineral and metal production within the region

during the pre-Hispanic period (prior to 1538) remains unknown. It is estimated that the Cerro Rico has produced some 30,000-60,000 tonnes of silver (Cunningham et al. 1996). During the late 19th century, low prices in silver changed the focus of mining in the region and tin became the main economic ore. The modern Porco mines are today some of the largest producers of zinc in Bolivia (Velasco 2001).

Figure 1.1. A map of Bolivia.

The Porco caldera was formed 12 million years ago, at a similar time to the Cerro Rico, therefore the formation of the rich tin-silver-zinc veins was probably very similar. The mountains are dacitic volcanic domes which experienced internal magmatic activity and hydrothermal heating. "Shortly after the dome (Potosí) was extruded at 13.8 +- 0.2 Ma, it was fractured by renewed movement on the fault system and a large, metal-bearing, hydrothermal system deposited ore and gangue minerals in the veins and caused pervasive alteration of the dacite." (Cunningham et al. 1996, 381). Consequently, the rich mineral deposits found in the Porco-Potosí area were formed by hydrothermal/magmatic fluids. This process involves mineral crystallisation which occurs during hydrothermal precipitation, and is shown by the presence of copper, lead and zinc. When the hydrothermal solution reaches an appropriate physical-chemical environment, the metals (carried as halogens) are deposited as sulphides (Shackleton 1986, 7). Commonly, different hydrothermal fluids mix during the process, resulting in the formation of complex metal veins such as the Cu-Pb-Zn-Au-Ag subtype veins, associated with igneous rock intrusions. Typically, these veins also have Sb, Bi, As, Ga, Ge, and In (Edwards and Atkinson 1986, 147). The Cerro Rico contains zoned areas of metallic veins; in the high temperature zones there is a Sn-W-Bi core surrounded by a core of Ag-Pb-Zn formed in low temperature regions (Cunningham 1996, 385).

Mineralogical analysis of the Porco ore minerals has shown that silver [Ag], Acanthite [Ag_2S], Galena [PbS], Pyragyrite [Ag_3SbS_3], and Stephanite [Ag_5SbS_4] are the predominant minerals containing silver. This thesis considers the types of ores mined and smelted in the archaeological record. In archaeological contexts, raw ore is usually not preserved although identification of those ores which were selected for use can be done using archaeometallurgical debris such as slag.

The domination of mining in the region has led to varied economic and political agendas, especially given Porco-Potosí's location on the edge of the Altiplano region (Highland Plateau) of Bolivia. The Andean Altiplano extends from Chile, Argentina, Peru, Bolivia to Ecuador. The Altiplano is found in between two of the main Andean mountain ranges although it is far from flat because it has hills, volcanoes, salt flats, and valleys.

"Throughout the area (Inca empire), the climate varies more with elevation than with distance from the Equator, so that hot valleys are only a short journey from cold plateau country where little can be grown except potatoes." (Steward 1946, 183).

Vegetation in this area is sparse. During the dry season, night temperatures can drop to -10 °C and the area can be exposed to strong, cold winds. The region receives very little moisture from the Pacific as it is on the edge of the Atacama, although there is precipitation in January and February (Bakewell 1984, 5). The mountains and slopes of the Altiplano can be up to 6000 m high and are inhabited up to 5000 m, the modern village of Porco being 4100 m.a.s.l. Porco's location at such a high altitude means that atmospheric pressure is greatly reduced, to only two thirds of that at sea level. The reduced atmospheric pressure means that more fuel needs to be burnt in order to maintain high temperatures, although the reduced pressure is constant within all metallurgical processes. Compared to low altitudes, reaction rates will be lower, though within the context of this study this does not need to be taken into account as only production at the same altitudes will be considered.

Currently, Porco is worked by two different mining organisations. The official mining company, Corporación Minera del Sur S.A. (COMSUR) are the major Bolivian producers of zinc, silver and lead. A large proportion of the population in modern Porco are employed by COMSUR. An employee of COMSUR will receive medical and insurance benefits. However, other mining organisations exist; small co-operatives that work independently of the main COMSUR owned mines. These co-operatives often involve more dangerous work in previously unexplored mining areas. The cooperative employees do not have the privileges that COMSUR employees receive. The mining organisation of modern Porco is complex and in the context of this research, I wish to highlight the importance of mining and metallurgy in the Porco-Potosí region. Everyone living and working in Porco is affected by mining and the extraction of metal. This will be further considered during the ethnographic documentation of silver production (Chapters 4-7).

1.2. The development of this research project

This PhD has been conducted within the Proyecto Arqueológico Porco-Potosí (PAPP) run by Dr Mary Van Buren of Colorado State University. PAPP was formally established in 1999 and is a multidisciplinary investigation of pre-Hispanic silver mining in the Porco region. PAPP has been conducted with four main *foci*:

i. Archaeological Fieldwork – the fieldwork seasons included conducting an extensive field survey over the Porco area using varied 5 m intervals, and any archaeological remains were noted. As part of my research, the sites (Table 1.1) from survey work carried out in 1999 and 2001 were selected for further study. Material from the sites was cleaned, analysed, and stored in Porco. All artefacts were classified and information recorded. Burnt earth, clay and other construction material associated with smelting was examined and details noted (Van Buren 2005, 1). Dr Jeffrey Eighmy has completed archaeomagnetic analyses to help establish dates for the archaeological sites. I was able to take part in the 2005 and 2006 fieldwork seasons involving surveys and excavations in the Porco area (details to follow in methodology, Chapter 2).

***Huayrachina* sites**	**European style furnaces**	
	Uruquilla domed furnaces	**Dragon furnaces**
Site 24	UR 10	UR EST 10
Huayrachina Alta	UR 11	Don Martin's Dragon
Cruz Pampa Surface	UR 12	
Uruquilla West Saddle Surface		
Uruquilla East Saddle Surface		

Table 1.1. The archaeological sites selected for analytical work in this thesis.

ii. Archival Research - Dr Ana María Presta coordinates the historical archival research undertaken in Bolivia at the *Archivo General de la Nacion* at *Archivo Historico de Potosí* and the *Archivo y Biblioteca Baionales de Bolivia* (Sucre). The work done by Dr Presta and her team will be used by PAPP to contextualise the archaeological work carried out in Porco. The work considers the ethnic origin of the different Indian laborers used in Porco, information on their work ethics, land and mine owners as well as mining in the Porco region during colonial periods (Van Buren 2005; Van Buren and Presta in press).

iii. Ethnographic Silver Production –The ethnographic research documents silver production carried out in 2001, 2002 and 2003 by Carlos Cuiza, a retired miner living near Porco. The process was documented using interviews, photographs and video recordings, and samples

from the process were selected for analytical work (Chapters 4, 5 and 6 discuss the ethnography of silver production).

iv. Ethnographic Research and Education – Dr Pamela Calla, a Bolivian cultural anthropologist, coordinates ethnographic education within Porco. Her work has been focused on conducting interviews with elderly members of the Porco community to understand how different mining and silver production activities were coordinated at a household level (Van Buren 2005, 3). Currently she is concentrating on the educational context of mining and metallurgy.

The long term goal of PAPP is to determine the way in which silver production was organized under different political regimes, with a particular focus on the Inca and early Spanish Colonial periods.

This PhD research project contributes to over ten years of work that Dr Van Buren and her team have carried out in the Porco-Potosí area, and is the first archaeometallurgical project of its scale to be carried out within the Porco region. Only one other archaeometallurgical set of analyses has been carried out: in 2003 an undergraduate student at the Institute of Archaeology, Barbara H Mills, studied current day silver production in Porco for her undergraduate thesis (Mills 2003). Mills carried out preliminary analyses on some of the sampled material from Carlos Cuiza, and her work has been used as a foundation upon which further analyses have been based. The archaeology of lead and silver production, not only in Bolivia, has been severely understudied, and consequently, it is an area which needs further study to understand technological methods and processes within world archaeology.

For continuity, the PAPP survey and excavation procedure was used so that the results of this research can be used by any member of the PAPP. Also, all data connected with PAPP has relevance and is linked to wider research projects.

1.3. The research aim

The aim of this research project is to further our understanding of the historical and technological changes of silver production within the Porco-Potosí region. Different techniques of silver production have been assessed using a contextual review of the historical literature, and a critique and understanding of the archaeological theories related to technological style, change and choice. This has been combined with analysis of current silver production, and consideration of the archaeological excavations in the area done by PAPP. The structure of this

thesis has been determined according to these research areas. Some of the technology employed in the region dates back at least to the early 16th century, but has not yet been dated prior to Spanish conquest despite earlier historical literature providing strong evidence of its use.

Current approaches to the social context of technology and transmission of knowledge have been used to develop methodologies for sampling and analysing materials and interpreting data. This theoretical consideration describes and considers the way in which technology has changed in the region. The theories adopted in this research have provided different viewpoints with which results from analytical work have been interpreted.

The analytical work has been structured into two main archaeometallurgical areas: recent silver production based on ethnographic documentation, and archaeological silver production. The ethnographic documentation carried out by PAPP and Mills (2003) has been summarised in this document. Analytical work has been carried out on selected samples from current day production, and this analysis will be considered in its own right before being compared to archaeological evidence of historical production.

The archaeological production of silver has been divided into two main subsets: archaeological *huayrachinas* (wind blown furnaces) and European furnace technologies. A consideration of these different technologies found in the Porco region in relation to historical information and theoretical concepts has been used to derive a series of research objectives upon which this thesis is built.

The *huayrachina* – wind blown furnaces

A *huayrachina* is a perforated natural draft furnace that uses wind to aid smelting. It is characterised by a cylindrical shaft usually less than a metre tall, which is pierced with a series of holes allowing ventilation from the wind. *Huayrachinas* can be used to produce lead and/or silver metal. They are thought to have stemmed from pre-colonial, native Andean roots; however, at present no conclusive evidence for this is known. The word *huayrachina* comes from Quechua; *huayra* meaning wind and *chi* the causative and *na* transforms the word into a noun. It is often translated as being 'the place where the wind blows through'. The word *huayrachina* also means the winnowing of grain. Colonial literature cites different spellings and names of wind blown furnaces: *guayra, guiara, huayra*. In this thesis the term *huayrachina* is used throughout. The continued use of the *huayrachina* up to the present day within the Porco-Potosí region is one of the main *foci* for this research, therefore this project will consider and review usage of the *huayrachina* during antiquity right through to the present day in modern Porco.

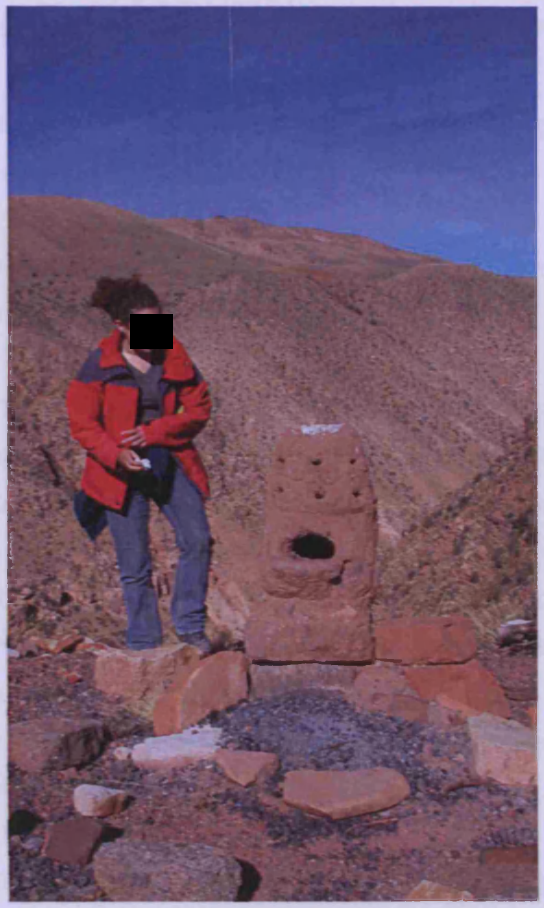

a.

b.

Figure 1.2. The *huayrachina*.
A modern *huayrachina* is relatively small (76 cm high, photographed in image a). Image b shows a 17th century illustration of a *huayrachina* printed in Alonso Barba's Arte de los Metales (Douglass and Mathewson trans., 1923, 199).

1.4. Main objectives

Five main research objectives underpin this PhD thesis.
This research aims to:

1. Describe and analyse recent methods of traditional silver production including the lead smelting technology involved.

2. Document and carry out an archaeometallurgical study focusing on archaeological remains of sites in the Porco region by analysing appropriately selected samples. These examples are analysed with the aim of creating a timeline of production, and the technologies involved in the Porco-Potosí region.

3. Compare and critically contrast archaeological remains of silver production sites to the ethnographic silver production documented in Porco.

4. Consider technological influences from Europe on silver production in Porco over the last 500 years.

5. Consider changes in metallurgical techniques by reference to economic, political and social contexts in the Porco region.

The ethnographic documentation of recent silver smelting by PAPP involved the practise of a retired miner, Carlos Cuiza, who produced silver using a method passed on by his parents. Cuiza's method consists of two main stages, the first being the production of lead via the use of a *huayrachina* followed by the refinement of a high grade silver ore using the lead produced in stage one. These two stages will provide a natural division in my analyses and have structured the methodology for working with these materials. Thus, the ethnographic component of my research will include the lead smelting process using a *huayrachina*. This is the first time in over 100 years that a working *huayrachina* has been recorded. The core of chapter 4 is an analysis of current day silver smelting methodology.

The study of recent silver production is particularly interesting because questions regarding past technologies are similar to those regarding present technologies. Using ethnographic documentation, every stage of the process can be analysed. Information about the yield of the metal produced gives a direct insight into how the furnace functions, as well as the knowledge the smelter has about the process. Questions about the process include how and why the smelter has chosen to produce metal in this way, the efficiency of the process, and how this process can make us aware of economic and social situations in the Porco region. Using this ethnographic documentation, further understanding of the culture involved with the physical smelting process can be gained. In this thesis the *chaîne opératoire* or operational sequence of silver production will be considered, with questions such as how silver was produced and which variables affect its production.

The comprehensive analysis of raw materials (clay, various ores, llareta ash) and products (slags, metals, hearth lining after cupellation) from well documented production processes is only possible with ethnographic or experimental materials. The data from these analyses will enable specific elements to be traced through the entire production process, and this will lead to the detailed study of ethnographic material in turn leading to a successful interpretation of archaeological samples where not all raw materials, products and by-products are available for

analysis. This data will allow for the consideration of differences in slag and hearth lining compositions relating to different raw materials and practices used in the past.

The study of recent silver production methods also has important ramifications for the review of technological choices and how these are affected by different subsistence methods and income strategies. The different subsistence means are also affected by the local environment, e.g. access to water, fuel, and the ability to grow crops. Indigenous cultural practises are shaped by a number of factors, so to understand present day production the cultural aspects of modern Porco-Potosí must be reviewed.

"...the cultural ecology framework has proved beneficial to Andean studies, partly because it helped elucidate aspects of indigenous cultural understanding that are indeed strongly linked to the perception and exploitation of the environment."
(Sillar 2000a, 15).

Archaeological excavations and samples form a critical part of the research, and the project aims to combine present day knowledge of silver production with that of archaeological debris. This will allow for a better understanding and documentation of the technological processes. The archaeological section of the thesis has been guided by the PAPP project director, Dr Van Buren. The methodology of sample selection will be presented later in this document (Chapter 2). The archaeological remains consist of *huayrachina* sites (excavated and surface finds, some of which have been dated from the early to mid 16th century), and late colonial European style furnaces sites (17th and 19th century). Combined with the actual furnaces and direct smelting debris, there are other artefacts that can be linked with metal production such as scorifiers and crucible remains. These will also provide essential information in recreating and understanding the technology employed within the region.

The crucial link between the archaeological remains and the historical literature will be of paramount importance. Complementarities and discrepancies between the two will prove important for gaining overall clarity on the region's history.

Theoretical concepts of technological choice and *chaîne opératoire* are important in interpreting the results of analytical work, for example the factors influencing choice of material, how sequences of production were affected by the availability of natural resources. Using the ethnographic *huayrachina* as a model a suitable *chaîne opératoire* can be easily constructed. For the archaeological *huayrachinas*, reverse engineering has been applied because some aspects of the production process are only theoretically accessible in that they are not directly accessible via analysis of samples. The focus on the technology employed within the Porco-

Potosí region and how it has changed through time is deliberate. Understanding this technology is critical to understanding the history of the region because it has played such a significant role in the history of silver production since prehistory to the current day. Studying the technologies involved will add important knowledge to a previously understudied history. The results of the analytical work will also comment on the emerging patterns concerning the efficiency of technologies used in silver production.

A personal aim of this research is to promote and preserve Bolivian heritage, and consequently I feel very strongly that the documentation and analysis of the work presented in this thesis should be made freely available. The PAPP has worked in collaboration with local schools in Porco to include histories of mining and metallurgy within the curriculum, and the results from this thesis will be used to make a valid contribution to Porco's history. Throughout this period of research, I have presented and published the initial findings from my work at international conferences. With the results of this work, I aim to make an important contribution to the understanding of metal production within the Andean world and hope it will be used as a case study by others interested in technological changes and persistence.

1.5. Structure of the thesis

The research aims and objectives outlined above have structured the methodology around which this work has been carried out. The structure of the thesis has been guided by the nature of the investigation into silver production, and is organised into twelve chapters. This chapter will review the main research aims and objectives as well as the importance of this project within PAPP and the wider Andean community.

Chapter 2 reviews the way in which these research questions have been addressed, and includes the methodologies used in processing the materials. It also considers the different theoretical concepts which have been used for defining these methodologies and interpreting their results.

Chapter 3 gives a broad historical description of the Porco-Potosi region. It mainly focuses on how political and economic factors have shaped the mining and metallurgical communities. Little historical information is available about the history of Porco (Platt et al. 2006). Information regarding Potosí is readily accessible and where no information on Porco was found, data from Potosí has been substituted. This chapter gives a brief review of the changing political climate over the last 500 years, and is used in preparation for the more detailed historical reviews found in chapters 8 and 10.

Chapters 4, 5, 6 and 7 review and present recent methods of traditional silver production. Chapter 4 documents smelting and refining episodes from 2001, 2002, and 2003, chapter 5 presents the results from analytical work undertaken on selected materials from the documented lead productions, chapter 6 presents analytical work done on materials from silver refining, chapter 7 is a discussion regarding the results and the interpretation of the analytical work. These chapters will also include a discussion on the implications of the ethnographic study and its wider social context.

Chapter 8 begins with the presentation of archaeological *huayrachinas*, their samples selected for detailed study, and a historical review of *huayrachinas*. Results from analytical work carried out on specific *huayrachina* sites are presented in this chapter. A discussion and comparison between the modern *huayrachinas* and archaeological *huayrachinas* can be found in chapter 12. This section also discusses persistence and changes seen in their function.

Chapters 10 and 11 presents the European furnaces found in the Porco area. First a review of the historical literature from Europe and South America is presented in chapter 10, and the results of analytical work carried out and a summary of these results are found in chapter 11.

Chapter 12 summarises and discusses all of the analytical work and discusses the ways in which technology has changed in the Porco area, concludes the research and discusses future work.

This thesis aims to provide a comprehensive study of different metallurgical processing techniques within the Porco-Potosí region. Comparison and contrast between these technologies has been conducted to provide a better understanding of the wider technological adaptations in metal production, and the relationship between indigenous and colonial technologies imported from Europe.

2. MATERIAL SELECTION AND METHODOLOGY

This chapter deals with the methodology chosen for this PhD research and the selection of material samples. A combination of historical, theoretical, archaeological and analytical approaches has been used to produce an archaeometallurgical investigation of silver production within the Porco-Potosí region. A brief discussion based on the theoretical methodology considered for this research is presented in the last section (2.3). A review of historical and current literature related to pre-industrial silver production in South America (presented in Chapter 3) was completed in parallel with the analytical study and assessment of samples.

Devising an appropriate method of research should reinforce confidence in the results obtained, requiring a suitable methodological foundation, including the selection of a representative sample set. The chosen method should also have a well developed analytical procedure based on a selection of appropriate techniques which have sound scientific principles. Instrumentation selected must be subject to strict calibration. An appropriate method should include the selection of a suitably qualified person trained to analyse and deal with selected samples (Burgess 2000, 3). Thus, all of these aspects have been considered during the development of my methodology in order to give reliant, fair results.

The methodological approach has been divided into two main categories; the first being an analysis of selected materials, and the second being the review of historical and current literature. This approach has been structured according to the main aims and objectives outlined in Chapter 1. The final methodology has been formed through an adaptive process whereby procedures were initially established but further modifications were made to the process to incorporate new research questions. Thus, new analyses proceeded and informed further re-assessed the data.

2.1. Selection of samples for analysis

Two types of metallurgical debris were available for the analytical sampling:part of this study is based on two sample groups according to the types of metallurgical debris available: the ethnography of silver production (Chapters 4, 5, 6, 7), and archaeological sites (within which two sub-categories were created; the archaeological *huayrachinas* mentioned in Chapter 8 and 9 and the European furnaces discussed in Chapter 10 and 11). Each of these groups has required different ways of considering sampling records and for ease, I shall consider each of

the different metallurgical areas separately, although where possible the methodology has been standardised.

Sampling from the ethnographic silver production debris

The sampling procedure for the current silver production process was limited because samples had already been pre-selected during the original documentation (by Dr Van Buren and the PAPP) and during subsequent analyses undertaken by Barbara Mills for her BSc dissertation (Mills 2003). There were, in total, three sets of present day debris from Carlos Cuiza's lead smelting and silver cupellation; see Chapter 4 for a complete description of the process. These three sample sets correspond to the year of documentation, i.e. silver productions were recorded in 2001, 2002 and 2003. Samples analysed by Mills (2003) were labelled prior to the commencement of this current research project. The numbers already assigned to the samples continued to be used in comparative initial analyses done by Mills (2003). Due to logistical factors (such as limitations in already cut and mounted specimens) re-labelling would have been extremely counter productive. Mills (2003) assigned numbers to each sample that she analysed numbering from 1 to 25 (see Appendices I for full listings).

Those samples were labelled the following way:

Porco 02/SL 1st 2002/ BHM 03

Porco [the number assigned to the sample]/ short coded description (in this case SL=slag) and year of production/ initials of person preparing the sample and year of preparation.

Where further specimens were selected for additional sampling, the short coded description (previously used by Rehren and Mills) would not be used; instead I decided to select simple worded descriptions, i.e. slag rather than SL. When extra samples were prepared they were numbered from 26 onwards, and in total, 51 hand specimens were available for analyses from both the *huayrachina* smelts and the refining episodes. Each hand specimen sent from Bolivia to London was catalogued, bagged and labelled using a note card listing the sample number, a short description of the specimen, and the date and place of collection. Thus, a full list of hand specimens was compiled (Appendices I and II). Analyses conducted by Mills (2003) and Rehren (2001/2002) were used to provide an initial understanding of the materials and the basic metallurgical processes.

Throughout the development of this research project, the samples provided have been analysed to characterise the raw materials and products using my selected parameters. These parameters are in direct response to the research questions and by-products of the current lead smelting process and the silver refining process as previously documented by PAPP. This

analysis has to be done via a review of documented smelting/refining episodes, in turn taking into account the technological processes involved by considering the *chaîne opératoire* as well as technological parameters governing smelting and cupellation techniques. Samples have been selected for analysis only if they can provide further information of the technology and are suitable for the analytical techniques available.

Sampling from the archaeological sites

Sampling from excavated material was approached differently than the ethnographic material. It was subject to other constraints, and therefore it was necessary to follow the protocol that PAPP had established. There were two methods of collecting archaeological material: surface sampling and sampling from stratigraphic layers derived from excavated sites. Excavation of all the archaeological sites was carried out by the PAPP team under the supervision of Dr Van Buren. I was able to attend two field seasons, although some of the samples used in this research were taken prior to my involvement in the project.

I made two trips to Porco to work with Dr Van Buren and her team: the first in June/July 2005 and the second in June 2006, the main field season for this research project being the 2005 trip. The objectives of the fieldwork were to become familiar with the archaeological work carried out by Dr Van Buren and to sample archaeometallurgical debris taken from previously excavated archaeologcial sites. The trip also served as an opportunity to explore the ethnography of silver production by visiting the smelting and refining sites. In 2005, the PAPP team had already identified an area (Uruquilla) of metallurgical interest, and excavations revealed three European furnaces (UR10/11/12) which are described in chapter 10. I supervised with guidance from Dr Van Buren, two of the five excavations on the Uruquilla site. These sites were under my own management, and consequently archaeological illustration, artefact and site documentation were my responsibility.

In 2006 the PAPP team were conducting a more walking extensive survey. Working in teams of five, a walking survey was undertaken using a transect distance of 10 m. The survey discovered some previously unknown *huayrachina* sites and interesting stone working platform, the process involved being extremely useful for gathering information on the landscape surrounding the Porco valley. I also conducted surveys on three different archaeological *huayrachina* sites to review similarities and differences in the hand specimens. The purpose of this review was to complement the analytical results and to assess varability in the size of the furnaces (see Chapter 8 for more information). During the survey, samples of metallurgical interest were photographed and a small selection were taken to London for analysis. Further documentation

of the ethnographic sites was also done, and it was hoped that another ethnographic documentation of the silver production could have followed.

Both the field seasons allowed me to select samples for archaeometallurgical work by checking the whole archaeological record rather than rely soley on Dr Van Buren or other members of the PAPP team. This overview has been important to understand the quantity and breadth of the archaeological record, and where possible archaeologically excavated samples were selected over surface samples for further analysis. This is particularly important when considering the archaeological remains of *huayrachinas*. All excavated sites werehave had their finds recorded using the PAPP recording methods (all documentation was carried out in Spanish). The samples were bagged and a note card was added listing the site name and code, *numero de excavación*/excavation number (NE) or specimen number, stratigraphic layer (nivel 1/2/3 etc...), date, excavator, and a brief one or two word description of the specimen. The NE number corresponds to the year of excavation and is used as a reference point for all samples catalogued. Subsequently, any NE assigned to a sample chosen for further analysis became the number used to identify it because the results of all analytical work will be returned to Dr Van Buren and PAPP.

Samples were thus labelled the following way:

UR10 253/ Slag/ cc 06

Site code NE/ short description/ initials of person preparing sample and year of preparation.

The archaeological huayrachinas

Over the whole Porco-Potosí area there are many undocumented *huayrachina* sites. During extensive survey work carried out by PAPP, ten such sites have been surveyed (Table 2.1), and two of these sites have been excavated. During excavation, it was noted that the *huayrachina* sites had material remains which were confined to the immediate surface, i.e. within one level of stratigraphy, so their excavation did not reveal any further stratigraphic information. It was therefore evident that surface sampling (without defining stratigraphic layering) of *huayrachina* sites would be sufficient, although the lack of any intact *huayrachina* furnaces was interesting. The *huayrachina* sites were located in areas that were exposed to the prevailing winds (a survey was carried out in June and July, known locally as the months with stronger wind). Extreme environmental conditions, exposure to high winds and heavy rain (during the wet season) on ridges where *huayrachinas* stood have contributed to the poor preservation of the *huayrachina* furnaces. In the majority of sites, the furnace fragment remains have been washed down from the original location of the furnace, creating a deposition of archaeological fragments which has no direct meaning to the original site. Consequently, the walls of the

furnace (made from partially baked clay) have been completely eroded in some cases. It should also be noted that there was little evidence of large quantities of slag at the sites, having implications for site re-use and slag re-smelting. Personal communication with Dr Van Buren (2008) indicated that people in Porco have stated that children were occasionally sent out to collect slag when metal prices were high. Erosion of the sites has made any sampling with direct archaeological significance very difficult. Therefore, dating of the sites has been done via surrounding archaeological remains and ceramic debris. Archaeological *huayrachina* fragments were collected to give a simple sample of the types of debris, after which one or two fragments were taken for analysis, together with samples showing any anomalies (interesting slag layering/metallic prills visible, unusual eye or mouth holes). It was decided that the minimum amount of samples should be taken to mainly preserve the sites for future analysis and aid their exportation (samples heavily vitrified with lead based slag became very heavy).

Five sites were selected for sampling (Table 2.1), representing those that have been dated and/or are contextually related to other archaeologically relevant sites. Three such sites (Huayrachina Alta, UR East and West Saddles) were chosen for survey sampling to measure the number of slag layers and size of eye holes on the *huayrachina* fragments. The location of these sites and analytical results will be outlined in chapters 8 and 9.

Site Name	Site Code	Date established for site
Cima Colima veta San Antonio	CCSA	Undated
CP surface	CP	Undated
Huayrachina Alta	HuA1	Early to middle colonial
Juan Equise	JE	Republican
Site 24	Hu24	Early colonial
Site 114	#114	Current day
Site 123	#123	Current day
Site 151	#151	Undated
Site 162	#162	Undated
UR East saddle surface	UR East	Undated
UR West saddle surface	UR West	Undated

Table 2.1. The archaeological *huayrachina* sites found during field survey by PAPP. The five sites shaded in yellow are the sites selected for further analyses.

The European furnaces and other archaeologically excavated sites

Sampling from these archaeological sites has been done according to my own strategy. Fieldwork carried out in summer 2005 and 2006 facilitated a review of all the excavated sites, the most appropriate being selected for sampling. Dr Van Buren's knowledge of local archaeology and history in the region has helped to indicate which sites will provide relevant results to my research questions.

All the sites were excavated using the PAPP protocol and thirteen archaeological sites were available for sampling (Table 2.2). The sites were categorised into those containing European style furnaces, those with refining features such as cupellation hearths, and those with other types of archaeometallurgical features. I primarily selected sites which have provided well stratified and contextually sound material. However, stratigraphy at Porco is shallow and poorly developed, thus, change over time at the site is difficult to establish using stratigraphy.

Samples selected for analysis were taken so that they demonstrated metallurgical practise as fully as possible. From furnaces, a selection of slag, furnace wall and chimney pieces were chosen. From other sites the minimum number of specimens was removed from the collection for analysis, to ensure that material was left within the archaeological record for future analysis.

Site Name	Site Code	Type of site	Date established for site (See Chapter 3 for the specific dating)
Cruz Pampa	CP	R, F	Early colonial with continued used into the Late colonial era.
Don Martin's Dragon	DMD	F	Surface finds without excavation
Hornos	H	F	20th century
Huayrachina and Huayrachina Alta	Hu HuA1	H, R	Early colonial
Site 24	Hu24	R, H	Early colonial
Structure 23	#23	R	Early colonial
Site 35			
Structure 1	~	F	Middle colonial, later than Site 24
Structure 3 associated with feature E, feature G	~	F	Middle colonial, later than Site 24
Structure 7 associated with feature H	~	F	Middle colonial, later than Site 24
Site 80	#80	R	Early colonial or Inca
Site 123	#123	R, H	Undated
Uruquilla 10 Est and Trinchera	UR10 Est	R, F	Early - middle colonial
Uruquilla 10	UR10	F	Early colonial
Uruquilla 11	UR11	F	Late colonial
Uruquilla 12	UR12	F	Late colonial

H = *Huayrachina* site R = Residential site F = Metallurgical sites that do not contain *huayrachinas*

Table 2.2. All the archaeological sites (excluding *huayrachinas*) available for sampling. Site 35 (labelled yellow) was available for sampling but it was not possible to analysis the material during this research. Site 35 may provide evidence for refining and other metallurgical activity in Porco.

2.2. Method for sample analysis

After an initial sample selection *in situ,* permission was received from the Direccion Nacional de Arqueologia Bolivia (DINAR) to bring the samples to London. Once the samples had arrived in London, further sample selection was carried out in preparation for analytical work. All samples taken for analytical work were recorded prior to sending. In this section, the methodology employed for each stage and the relevance of each analytical method is discussed.

Analytical techniques

The selection of a specific analytical technique should always include a review of its suitability and accuracy in relation to the specific research question in mind. My analytical techniques have been shaped by those used by others researching the production of lead and silver in order to facilitate a comparative study, and by economic limitations (Bachmann 1982; Martinón-Torres et al. 2007; Mei and Rehren 2005; and Veldhuijzen and Rehren 2007). Optical Microscopy, Scanning Electron Microscopy and X-Ray Fluorescence have been selected, all of which are available at the IoA Wolfson Archaeological Science Laboratories, UCL. Other analytical techniques could have been selected but the combination of these three techniques provides a complete chemical and mineralogy study of the material. These techniques allow the study of those reactions that occurred during the metallurgical history of the samples.

Energy Dispersive- X-Ray Fluorescence (ED-XRF); (Reed 1996), (Fifield and Kealey 2000), and (Alfassi 2001)

ED-XRF analysis is used to provide bulk compositional data of a sample, for major, minor and trace elements. It works by transmitting a flow of photons (usually in the form of primary X-Rays) onto the (prepared) sample. The sample interacts with the X-Rays and emits secondary or fluorescent X-Rays which can be detected by the Energy Dispersive (ED) detector. Analytical software interprets the detected X-Ray energies and calculates the composition of the sample. During this research a Spectro X-Lab Pro 2000 polarising ED-XRF machine was used. The data has been calibrated using the *turboquant* method, and in the case of elemental samples that are not oxides, the *alloy* method was selected. The ED-XRF can analyse all elements above sodium in the periodic table and in concentrations higher than about 0.005%/50ppm, and is non-destructive although the quality of the data depends on the degree of sample preparation. Hand specimens can be loaded into the sample chamber without the need for cutting and their surface can be analysed for qualitative concentrations of elements. This technique has some limitations, a major limitation being the low penetration of X-Rays into the surface of the sample; only about 1 mm is actually analysed. This can be problematic if the sample is composed of different layers closer to the surface, i.e. corrosion or a thick silicate layer and

then a different composition below. If the surface of the artefact is rough or uneven, this also may alter the quality of the measurements and if more quantitative compositions are required, the specimen needs to be prepared into a pressed pellet. This requires the sample to be fully documented prior to analysis as the pellet preparation process is destructive. The ED-XRF process is a relatively quick analytical tool because each sample can be fully analysed within ten to fifteen minutes, though this is variable according to the method of calibration chosen.

Certified reference materials were analysed together with the specimens prepared from the Porco-Potosí samples to determine the quality of the data produced from the ED-XRF. However, the small number of samples studied does not allow for a proper estimate of the precision of the data produced. All measurements were consistent upon repeated analysis and did not vary by more than a few percent relative to major elements and traces.

For this research, both freshly cut surfaces and polished blocks were used to provide initial 'screening' analyses, and pressed powder pellets for fully quantitative analysis. The former gives less accurate data, but does not require additional sample material or preparation, while the latter normally requires at least 5 to 8 grams of material to be crushed and ground to below 1 µm. Milling of the samples allows for the precise characterisation of the material because it is homogenised. The samples were crushed using a metal piston and then milled using a *Fritsch Pulverisette 7 Mircomill.* The powdered sampls were dried (overnight) in an oven at 100 °C to remove moisture, and a pressed pellet is then made by mixing 8 g[1] of the dried sample with 0.9 g of industrial wax, mixing well and ensuring that the wax and sample are completely homogenised (to improve accuracy of the analysis). The mixture is pressed into an aluminium container using 15 tonnes of pressure for 2.5 minutes, then labelled with sample name and date of preparation.

Many archaeological specimens from the sample set were too small for full pellet preparation, in this case only the surface of a sample was analysed (to reduce destruction of the collection). Due to the rarity of debris from current silver production, only samples which had enough material left over after their initial preparation were selected for pressed pellets.

Optical Microscopy (OM)

OM is an analytical technique used as the primary tool to provide morphological characterisation of a sample's microstructure (Brandon and Kaplan 1999). OM gives both morphological

[1] For samples with high lead contents, less than 8 g was required, the ratio between wax and sample remained the sample (all weights were recorded for future reference).

characterisation and topographic information such as grain size, colour, refractive indices and the degree of crystallinity within the structure of the sample (Brundle et al. 1992). OM can, in the case of slag and other materials formed under high temperatures, reveal the characteristics of the formation process i.e. the history of the material. The most important chemical phases for this research project are opaque such as ore minerals, smelted metals and waste products. Therefore reflected light microscopy (or metallography), rather than thin section petrography was chosen. The preparation of samples for microscopic analysis demands a surface that has been ground flat and is polished free to a mirror-like quality. Thus, epoxy resin blocks were prepared for all samples selected for OM analyses (as discussed below).

Scanning Electron Microscopy with Energy Dispersive Spectrometry (SEM - EDS)

SEM-EDS analyses have been used traditionally in the geological, biological and chemical sciences. In archaeometry, the application of this technique gives specific information on mineral phases within samples and can provide chemical and phase characterisation. It is best preceded by OM to identify specific areas within the sample needing further analysis. SEM works by irradiating the sample with a focused electron beam which is scanned over the sample surface. The electron beam interacts with the sample, emitting different types of signals that can be measured using a variety of detectors. In this research project, the EDS detector has been selected allowing for the chemical analysis of spot samples, i.e. different phases within a sample, and for mass analysis of specific areas. The EDS detector measures characteristic X-Rays, which are expressed as electron Volts (keV). EDS offers chemical analysis with a high spatial resolution down to 3 μm in diameter. It is the most appropriate analytical tool for this research, and is at its most powerful when combined with OM. SEM is primarily used for imaging which can provide topographical (through secondary electrons) and compositional (via mean atomic numbers and backscattered electrons) contrast. The SEM analysis can aid OM by giving increased magnification. It also allows for a high spatial resolution, a large depth of field, simple sample procedure (the analysis is non-destructive after sample preparation), and with EDS gives quantitative elemental analysis within 1% accuracy for major elements, and reasonably good detection limits (≈ 2000 ppm/ 0.2%).

Sample preparation

Before invasive sampling, all the original samples that needed cutting were photographed to provide a visual record. The hand specimen was cut using an abrasive bladed circular saw. The cut surface should reflect the overall nature of the sample and or show areas that may further increase the knowledge of sample formation or the technology involved. Cutting must also take

into account the fragility and rarity of the sample, i.e. whether the sample is unique, or one of many available. When cut, the samples were drawn or photographed with the cut area noted on the record for future reference. The cut surface was then analysed using the ED-XRF to determine an initial qualitative chemical composition of the sample. If the ED-XRF presented interesting analytical results the samples were selected for further analysis (OM, SEM and possibly pressed pellet ED-XRF). They were then mounted in epoxy resin with 30 mm diameter casting cups, ground and polished using standard laboratory procedure to 1 µm particle size.

A PHILLIPS XL30 Environmental SEM with an Inca Oxford spectrometer system was selected to analyse all the samples in this project. Operating conditions for the data collection were as follows: a working distance of 10 mm; accelerating voltage of 20 kV; spot size 5.0-5.3 (INCA conventional units) and a processing time 5 or 6 (dependent on detector deadtime 25-40%) and a livetime of 50 seconds.

The following procedure was used to analyse samples: using the EDS detector, 5 bulk area scans of each sample were taken to give discrete chemical analyses of the area. In the case of slag with large quantities of metallic prills, the prills were avoided. For different crystal phases spot analyses were used. Three to four different crystals were sampled and then the results combined to give the average (allowing for the accuracy of the detector to be checked and investigations of possible variation between different phases). Backscattered electron images (BSE) were taken at the following magnifications: 50x (for bulk area analyses), 100x, and 400x. At my own discretion, subsequent magnifications were taken to highlight anomalies and areas of interest requiring further investigation. Metallic prills were area scanned and individual metallic phases were spot analysed by EDS analysis.

Application of analytical techniques

The natural division between current methods of silver production and the archaeological samples have continued to structure the organisation of the research.

The samples of current silver production

All hand samples within the collection were catalogued, their names noted including assignation to a specific smelting event, briefly described, and date collected. The samples were photographed to document the whole collection and provide a record of the specimens before invasive sampling occurred. As previously stated, the aim of the analytical study into the process of current silver production was to document the technical processes involved, all other variables within the process being known. Thus, the material has been studied via the analysis

of stratified samples from each distinct material group; the two ores used, the *huayrachina* furnaces (slag and ceramic body), the lead metal, the cupellation hearth and lining, the cupellation hearth material (CHM) and the silver produced as a result of the cupellation.

All these materials were combined to give a full metallurgical overview of the technology involved, and each stage of the process was documented via analysis of the materials. This provides a full body of contextualised samples of known metallurgical history, against which the archaeological material can be compared and interpreted.

Mills (2003) had cut and mounted 25 samples in epoxy resin. The mounted samples cut previously were used for further analyses in this research, but where necessary further samples were prepared. The samples were analysed using OM, SEM-EDS and ED-XRF. If prepared for OM or SEM-EDS, the same protocol was followed as for the archaeological material.

The archaeological samples

Archaeological samples were catalogued noting the site, date of excavation, whether sub-sampling has occurred, and included a brief description. If invasive sampling was deemed necessary after initial hand specimen analysis and ED-XRF surface analysis, then the original sample was photographed for documentation. Each sample was assigned a label including the code for the archaeological site, the NE (for comparison to PAPP records), and the date of processing.

The methodology applied to these samples has been designed to address the main research aims discussed in Chapter 1, and is primarily concerned with documenting previously unstudied archaeometallurgical debris. To do this, the Appendices act as a catalogue for all the samples selected for analysis. The main objective of this analytical work has been to understand the function of different metallurgical techniques used in the Porco-Potosí region. Based on this, the development of sampling and analytical work with interpretation of results was done using theoretical models of technological innovation, change and systems. The following section considers these technological models.

2.3. Interpreting the past; a theoretical approach to understanding ancient technologies

The study of technology is not restricted to practical and technical considerations, e.g. the functionality of an object, because it can also discuss changes both in technology and the social

context of material culture. Within this research the concepts of technological choice and style and those concerning the transmission of knowledge are presented and used as a theoretical framework. In the following paragraphs, these theoretical concepts are briefly outlined for further use during this thesis.

What is technology; how and why are things made?

This research aims to consider the production of silver prior to and after the Spanish conquest of the Porco-Potosí region. Technical processes and the influence of social and political regimes on the technology are investigated through analytical reviews of material debris.

Technology can not be separated from the places and peoples that are involved in the process of manufacture. From very early periods metal in the Andes was seen as a luxury material which conveyed the political power of those using and wearing it (Lechtman 1984). Within cultures there must be some systematic organisation materials and techniques. These are manipulated to meet a society's cultural and biological needs, forming a cultural foundation (Hammond 1975). Thus, the study of metal technology and production can contribute to a better understanding of the social, political and religious concerns within society (Lechtman 1984).

Technology is a window through which various social influences regarding the way people make and use things can be observed, and if this is the case, decisions can be hard to assess from just an investigation of hand samples. Great consideration and emphasis on the contextual information must also be written into the methodological approach. Often, commonplace and habitualised social interactions control and underline cultural practise, and in turn cultural change (Dobres 1999, 129). Therefore, choices and variables in the technological process are reliant on environmental, social, economic and political arrangements. Technological processes are always embedded in the material and social environment in which they are used, and are also a medium for defining and expressing personhood (Dobres 1999, 129). Individual people act within their own world view, i.e. within the context of their upbringing. Consequently, their current surroundings are viewed with a particular opinion/stance (Dobres 1999, Epstein 1993, 9).

To further consider how and why an individual makes certain choices regarding the technology they use, their environment must be fully considered:

"Specifically how they {material techniques} differ is causally related to the form, content, and relative complexity of the other component aspects of a people's culture (their economic, social,

and political systems, for example); to the character of their habitat (frozen tundra, tropical rainforest, rocky seacoast); and to their history (centuries of warfare with neighbouring groups or millennia of near total cultural isolation)" (Hammond 1975, 7).

By considering those different variables that can alter the technological processes chosen to produce an artefact, information about that technology's cultural significance can also be gained. With regards to metal production, a consideration of the choices made within the production process can offer a great knowledge of the ancient smelter. Johnson (2003) summarises how information on technology can be gained by considering trade and subsistence patterns and how inferences about hypothetical links between subsistence and trade can be made by using validating evidence:

"...you can't dig up a 'subsistence subsystem', but you can measure and quantify the area of land suitable for arable cultivation round a site, or the meat weight and calorific value represented by the data gleaned from a faunal assemblage" (Johnson 2003, 68).

"Behaviour is to culture as technique is to technology" (Epstein 1993, 21). Epstein assesses the concept that 'technology is knowledge'. He uses the analogy that human creativity is restrained by the physical limitations of the universal processes that govern Earth in that "...if a technology is used to manipulate the environment, the techniques it informs must achieve certain culturally set thresholds of effectiveness." (Epstein 1993, 21). Thus, people will accept technology that functions, even if it provides a very low output. However, a technological process that is ineffective in relation to peoples' need would become extinct (Epstein 1993). Epstein emphasises the concept that technology must be seen as a series of actions, behaviours and techniques. The application of a theoretical framework describing technological choice can be seen as a conceptual bridge linking archaeological remains with the culture behind those remains recovered within the archaeological record (Epstein 1993, 3).

"Treating technology as the knowledge system that informs and constrains attempts to manipulate the environment, rather than treating it as a technique, which is merely the execution of the behaviour necessary to effect the manipulation" (Epstein 1993, 5).

The theory of technology has incorporated two main interrelated themes, the *chaîne opératoire* and the concept of technological choice. These two theoretical approaches have become commonplace within technological studies and have been adapted to this research project to understand the ways in which the people and societies produced silver in the Porco-Potosí region.

The *chaîne opératoire* : linking technological processes

Literally translated, the *chaîne opératoire* is the operational sequence or chain, as in "...a series of operations which brings a primary material from its natural state to a fabricated state" (Cresswell 1976, 6). It refers to any process whereby raw materials are selected and transformed into useable, cultural products (Schlanger 2005, 25). Leroi Gourhan was influenced by the work of Marcel Mauss who believed that every gesture made is done according to the cultural and sociological influences within a society, and he coined the phrase *chaîne opératoire* in the 1950's. Gestures and in turn actions are made on a conscious and unconscious level. Examples of *chaîne opératoire* have been studied in all archaeological periods, most evident in studies from sites of stone tool production where methods of manufacture from core, to waste, to finished artefacts can be traced and analysed (Schlanger 2005). Anthropologists have used the *chaîne opératoire* to observe and document current processes of production where ethnographic observation has lead to variations and similarities seen in the methodological production (Roux 1990). In this thesis, the *chaîne opératoire* of silver production within the Porco-Potosí region is considered although it is not necessarily linear and this must be considered when reviewing technical systems to "overcome the divide between production and consumption, and appreciate the intersecting life histories of objects – in motion as simultaneously social, technical and symbolic accomplishments." (Schlanger 2005, 28).

Technology is about technological choices

Pierre Lemmonier (1986, 2002) addresses the concept of choices within technological systems. Lemmonier was influenced by the work of Mauss and Leroi Gourhan. Technological choices are defined as the selection of technological features that are decided upon through the influences in an agent's life. Lemmonier says that human actions can be described as traditional behaviour which has been learned by individuals through descending generations. "Any technique...is always the physical rendering of mental schemas learned through tradition and concerned with how things work, are to be made, and to be used." (Lemmonier 2002, 3). In this context, mental schemas are always embedded into the wider social consciousness and symbolic system. Lemmonier comments that a consideration of material culture within society is a study of the 'conditions of coexistence and of reciprocal transformations of a technical system and of the socioeconomic organization of the society in which it operates' (Lemmonier 1986). The reviewing of an artefact's style allows access into its production and into the identity of the manufacturer (Lemmonier 1986).

Choices can be considered from a technical perspective regarding raw materials, tools, energy sources and techniques used to produce the product, as well as the sequence that links all the acts together (Sillar and Tite 2000). A production process, therefore, results in a unique product

that has been produced by a certain technical knowledge and bodily practice framed within defined social conditions. Consequently, the factors affecting technological choices can range from constraints imposed by the working properties of the materials to behavioural and sociological factors. A co-dependency on other technologies may also affect the ways in which choices in the production process are made. In effect therefore, culture not nature is controlling the way in which one technological process is selected over another, albeit within the practical possibilities of the social and material environment (Pfaffenberger 1992).

Social Constructionism is the way forward...

Social Constructionists argue that a study of technology must always consider the choices made during observed technological processes. The monitoring of these choices shoud be done regardless of them being open or unconscious, done by individuals or groups. Social Constructionists do not search for an amalgamating theory of technology, they seek to understand and interpret the aims of humanity; explicitly or implicitly (Killick 2004, 572). They are concerned with why one option is selected over another, therefore Social Constructionist mantra is perfectly combined with that of an archaeometrist. It is my aim that Social Constructionist thinking be used in this thesis to interpret the technology employed in the Porco-Potosí region.

A consideration of ethnography and its place in technology studies

Ethnography can provide useful insight into the lives of modern people, observing why and how they do things. The Andes have been particularly fruitful in providing ethnographical observations and studies of traditional technologies (Dransart 1991, Sillar 2000a, b), because pre-Hispanic periods are relatively recent (ending only about 500 years ago) and many traditional technologies have continued to the present day. 'Old' technology may be maintained within a society if it is deemed relevant and utile, these conditions are affected by social and economic contexts. However, the persistence of a particular technique or style does not necessarily indicate stagnation or lack of change. Technology is not permanent and is directly affected by individual conditions these are not the same as they were 500 years ago. The objects produced and the tools used in their production must also be considered. An object's biography and use over time can change, thus its role is integral to human action (Gosden and Marshall 1999).

In the ethnographic component of this research project, one particular interest has been how agents recall and 'do' technologies under observed conditions. When considering this, I have found everyday mundane tasks to be useful as examples:

Thus, if I were to make a cup of tea, I would not have to think about it at all. I would just do it. It would be unconscious. In recalling to another person how I made my cup of tea, I would have to reflect about a number of variables in the process. Did I add the milk first or after? What about my spoonful of sugar? Sometimes I like it black. Do I pour the water before or after adding the tea bag? What type of vessel do I use? Would I make my tea in a teapot? Reflection upon these variables means that I may not always recount the same method of tea making. Do agents always reveal the 'real' process? If I were recounting my tea making, would I tell someone that sometimes I use my fingers to remove the tea bag and not a spoon?

What about the evidence left behind from the making of the tea? An observer may find a vessel contain tea/milk/sugar residues and perhaps a used tea bag. This example illustrates a simplistic technical system and highlights how complex the use of ethnographic records may be when biased or when only partially explained information is given. Bias can also be incurred when the observer asks questions because these questions will ultimately have an agenda behind them.

Using ethnographic observation means that we must be aware that some processes are altered simply because they are being documented. Equally, we must gain a perspective on how we could relate modern studies of people and their technology to the archaeological record. Can the *chaîne opératoire* of this process really be reconstructed? An acknowledgement that agents' act within political, social and environmental constraints is critical to obtaining an understanding of both ethnographical and archaeological technologies. It is also important to note the concept of embedded technology, that artefacts have a specific meaning to each person who has contact with them (Sillar unpublished, Pryce et al. 2007, 555). The agents making the technology, using it, and eventually retrieving it, inevitably find different personal meanings and contexts attached to the artefact (Lucas 2005). Considering the way in which the agent responds to the technology is critical to understanding the embedded nature of technology. Working in a modern environment means that modern social agendas are placed on artefacts. As a result, consideration of those meanings and values from antiquity or within their own cultural group should be an essential part of ethnological and archaeological work.

The application of technological theory: two Andean case studies

Archaeology is a multi-discipline subject encompassing different historical timescales, with theoretical and methodological approaches (Jones 2004). This thesis embraces Jones' approach to multi-disciplinary research. Here research questions address the function of technology in order to consider how silver was produced in the Porco-Potosí region. However, this research

also wishes to address the changes in technology. The measurement of these technological changes will be done via a consideration of the *chaîne opératoire* and technological choices, observed using archaeological, historical and analytical methods. Two Andean cases studies have been selected to illustrate the successful adoption of technological theory in the study of metal production. Firstly, Izumi Shimada's work at Batán Grande shows the use of the *chaîne opératoire* theory within an archaeological context. The project uses a combination of different specialists to achieve an overview of copper metal production processes at all phases and levels.

In parallel with Shimada's work, the second case study is Heather Lechtman's review of 'technology as style'. Her work contributes and adds theoretical consideration to the importance of metals within Andean societies. Her studies on the production of tumbaga (copper-gold or copper-silver alloy) and arsenic indicate that metal technology can also be viewed as stylistic rather than purely technological. Choices made during the production process have been affected by cultural, socio-political environments, and the association and selection of the resulting artefact's aesthetic properties. The interplay between technological constraints and cultural choices within Andean metallurgy emphasises the need to place archaeometallurgical analyses within their cultural context as this thesis aims to do.

Case study 1 – Copper production at Batán Grande

The site of Batán Grande is situated in the La Leche valley, northern Peru. As one of the best preserved metallurgical centres in the Andes, it represents a long term archaeological project that has applied a holistic approach to the study of metal production. Dated from the Middle to Classic Sicán period (AD 900-1100), the site was part of a much wider polity spanning from the Chira to Chicama Valleys (Shimada et al. 2000). Inhabited through the Late Sicán (AD 1110-1375), Chimú (AD 1375-1470), and Inca (AD 1470-1535) periods, the site represents one of the only pre-Inca copper-arsenic production sites, unprecedented in the pre-Hispanic world. Copper and copper-arsenic production is characterised at Batán Grande.

The main archaeological site situated on Cerro de los Cementerios is composed of three different sectors: I, II and III. Each sector is physically linked, indicating a functional relationship between each different area. The ancient road linking these areas would have been used to connect the metallurgical production sites to the mining areas, where copper-rich ore veins were located. Llama caravans would have travelled on the road transporting commodities in and out of the site (Shimada et al. 1982).

Sector I has clusters of adobe and stone debris arranged with an architectural unity not observed in the other sectors. It may have been used to house the main labourers who worked

on the production site (Shimada et al. 1982). Sector II has a series of stone structures that could have been additional housing units, and Sector III contains three parallel platform mounds built up to 3 metres tall. The platforms were used as cemeteries and elaborate tombs containing a variety of funerary objects, the majority of which were gold and copper based metal artefacts (Shimada et al. 1982). Pre-Chimú occupation was established within the funerary areas. The depositional history and radiocarbon dating of excavated stratigraphic layers indicated that the site was occupied for 500 years starting from around AD 1000, and Copper was the first metal to be produced.

A range of metallurgical debris has been excavated from sector III including ore, smelting furnaces, tyueres, slag, *batánes* (large mortar stones up to 1 m in diameter) and *chungas* (rocking stones). Shimada et al. (1982, 955) state that in a 25 m radius over 12 *batánes* were recorded. These are thought to represent only a small quantity of the original numbers at the site. Twenty four furnaces were excavated in sector III, however, it is estimated that over one hundred furnaces would have been used (the remains have been disturbed by looting). A pattern for furnace arrangements was established by Shimada et al. (1982), this showed that they were grouped in clusters of three to four, and aligned north-south, with adjacent furnaces being placed 1 m apart. Furnaces were typically pear shaped (when observed from above). They have a narrow end inset into a low step-like terrace which acted as chimney. The wider end is flared, forming an 'apron' (Epstein 1993, 116). Tuyeres found on site indicate the use of blow pipes to increase air flow. The presence of postholes and other debris indicate that smelting took place under covered structures.

Shimada and his colleagues have developed a craft production strategy which has reconstructed the *chaîne opératoire* of metal production at the site. The reconstruction of metallurgical processes allows for inferences regarding the social context of processes embedded in society to be analysed. To do this they have focussed on a comprehensive study of all phases and levels of metal production including a review of local mines, historical documentation, archaeometallurgical analyses of primary production using archaeological debris, and the production, use and distribution of the resulting metallic artefacts. Shimada (1994) emphases the need to consider metal production and related mining as an integrated project; one should not be considered without the other.

Understanding metal production at Batán Grande

The mining area surrounding Batán Grande has been described as being one of the only few established pre-Hispanic mining areas (Shimada 1994). To assess the ancient mines surrounding the site, Shimada combined a geologist (A. Craig), an archaeometallurgist (J.

Merkel), a local mining engineer (J. Suarez), and a project historian (S. Ramíez). To aid the ground survey, historical, pre-Hispanic, and colonial mining information with modern geological maps was combined with low altitude air photographs to observe ancient roads and workings. Shimada noted that the incorporation of interviews with local animal herders, hunters, and prospectors was particularly useful for the identification of mines (Shimada 1994). In combining these varied techniques and specialists, the project was able to address the ancient mining strategies held by the ancient metal producers. Five mines (four on the northern margin and one on *Cerro Blanco*) were identified as direct suppliers of copper ore for the smelters in Batán Grande (Shimada et al. 1982). It is surmised that pre-Hispanic miners in the region used techniques similar to those found in Chile including the use of hammerstones with wooden wedges to extract ore from the vein. Copper oxides found close to the surface were selected by Sicán smelters. They did not require the pre-roasting treatment of sulphidic ores and hand sorting could be done easily (Shimada 1994). Ores were crushed and sorted using *batánes*. Selected ore would have been mixed with flux ready for smelting (Shimada and Merkel 1991).

Fuel access

Access to fuel may have been gained through the dense sub-tropical forest 70 km north and west of the site (Shimada et al. 1982). The location of the metallurgical site wiith access to suitable fuel source may have been a more important factor than ore sourcing. Algarrobo wood (*prosopis juliflora*) was the primary wood selected for charcoal used at Batán Grande for smelting (Shimada and Merkel 1991).

Smelting at Batán Grande

Raw copper ore was smelted in pear-shaped furnaces (30 cm long, 25 cm high and 25 cm wide). The interior surface of the furnace was lined with refractory mud and showed evidence of relining with 3 or 4 layers. Evidence for blow pipes was seen by the discovery of tuyeres; blowpipes and natural draft were used along side the charcoal to power the furnaces (Figure 2.1). There is archaeological evidence to suggest that an iron compound was added to the charge as a flux. 1.25 to 3.50 litres of charge would have been loaded into the furnace, inferred from slagging on the furnace wall (Shimada and Merkel 1991).

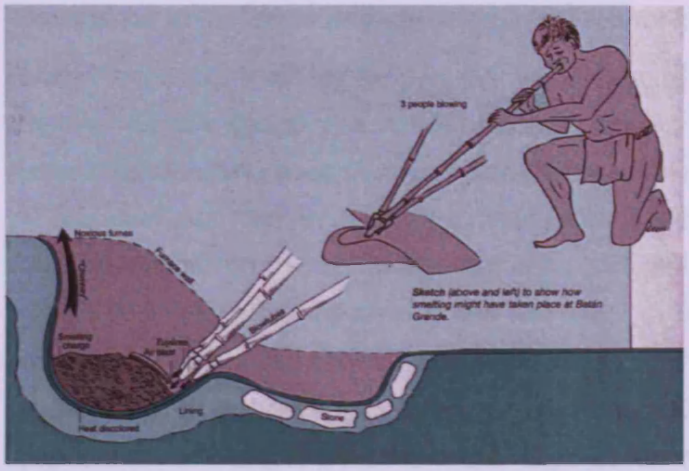

Figure 2.1. A reconstruction of the smelting furnaces at Batán Grande (Renfrew and Bahn 2000, 345).

The furnace capacity was altered according to the different political periods, for example, in the Middle Sicán period, the furnaces were larger (3.3 litres), and by the Chimú and Inca periods their capacity was greatly reduced to 1.4 litres. Regardless of capacity, the smelt created a thick slag. Small copper prills formed in the charge but were unable to move through the dense slag to the base of the furnace. Thus, the slag contained copper-arsenic prills which were extracted using *batán* and *chungas*. The prills recovered would have required re-melting to form an ingot to be ready for transportation. The locations of these refining/melting areas have not been found.

Labour distribution

The distribution of labour at Batán Grande has been established using the archaeological debris and experimental copper production done by members of the Batán Grande project. During the Chimú and Inca periods, groups of six to eight people could have worked the unit areas (three to four furnaces in each unit). This estimate assumes that two people would be responsible for providing air to each furnace (Shimada et al. 1982). Activities at the metallurgical site included:

- Carrying ore/fuel/flux
- The preparation of charge
- The preparation and repair of tuyeres
- Attending the furnaces during the smelt
- Removing products and cleaning the furnace
- The transport of slag to the grinding area
- Crushing the slag to extract copper prills
- The formation of ingots

The crushing of slag and collection of prills could have been done by different labourers, possibly women, elders or children (Shimada et al. 1982, 957). The proximity of batánes and furnaces indicates many of the on-site activities would have been organised by interrelated labour units. Overall administration of the site may have been done on a local level.

Persistence and change in metal production technology

Batán Grande was inhabited for over 600 years. Despite changes in the spatial organisation of the site, furnace design was not substantially altered. However, some minor alterations in furnace function have been observed: furnace capacity was changed to suit different social and political demands. The reduction in furnace capacity allowed for increased smelting efficiency (Shimada and Merkel 1991, 65). Shimada et al. postulate that the dimensions and shape of the furnace were conserved because it was necessary to use lung powered blow pipes, and to create a reducing atmosphere with efficient air flow (Shimada et al. 1982, 955). Changes in furnace lining were also noted; linings during the Chimú period were carefully prepared from specific minerals which were ground and mixed with clay, whereas, the earlier Sicán furnaces showed evidence of simple clay lining. These changes or choices within the *chaîne opératoire* can connect the archaeological remains made through human behaviour to the culture that shaped that behaviour (Epstein 1993, 3).

The combination of different specialists on the Batán Grande site has provided a coherent understanding of all aspects of production. The extraction of a copper-rich ore from local miners would have provided suitable ore for smelting. Smelting was done in the pear-shaped furnaces. While labour organisation and political influence changed over time, the design of the furnaces remained the same. However, furnace their dimensions seemed to have been reduced and their specific construction altered. The presence of Sicán funerary mounds near the industrial smelting site indicated the importance of copper within Sicán cultures. Inside the funerary mounds the excavated burials contained metallic artefacts of copper and gold. A consideration of the labour patterns needed to operate these industrial smelters has been done with a consideration of the archaeological and theoretical information available. A reconstruction of many of the *chaîne opératoire* elements of metal production on the site has been done by Shimada and his team allowing interpretation of the use and function of Batán Grande.

Batán Grande represents a complex Andean metallurgical centre. It produced copper-arsenic alloys on an industrial scale. Metal also played an intricate role in society, and their importance stimulated metal production use and distribution in the wider Andean world.

Case study 2 - Colour and metal in the Andes

In the Andes, the development of metallurgy was restricted to three main metals: copper, gold and silver. Andean metalworkers favoured metal artefacts that were coloured gold or silver. These colours represented a 'visual manifestation of status and power' (Lechtman 1984, 15). However, major metallurgical industries appeared to be based upon copper-alloy production, even though objects coloured gold and silver are prominent in the archaeological record (their

chemical composition shows that they were often copper alloys). The role of different metals within Andean societies allowed for the preferential selection of one colour over another, and the selected colour played a significant part in ritual or political display. Lechtman describes gold and silver during Chavin culture (*circa* 1000 BC) as being carriers of religious iconography. They also held a major role in Andean cosmology and state craft (Lechtman 1977). This role continued until the Late Horizon era (*circa* AD 1470-1532) when all mineral wealth in the Andean empire belonged to the Inca, who controlled the metal production.

"They (gold and silver) were his (the Inca) birthright, for the Inca dynasty began with the offspring of the sun and the moon. The first Inca was the son of the sun" (Lechtman 1984, 14).

During Inca periods, these metals were used in ornaments, woven into cloth, used in buildings and as a means to venerate local elites (Sallnow 1989). Second only to cloth, the colour associated with precious metals was visible in their association with the origin myth of the ruling Inca (Lechtman 1984, 14). The wide symbolic and religious connections of gold and silver have encouraged their manufacture and use.

Gold or silver coloured artefacts could be made directly from precious metals and through the gilding of metal objects. Two prominent copper alloys; copper-silver, and *tumbaga* have been important within Andean metallurgy. Both alloys were worked into sheet metal and required hammering and annealing. The process of annealing softens the metal, allowing it to be worked without cracking. The heating process oxidises the surface of the metal, and during the hammering this oxide layer is removed leaving behind an enriched silver surface (Epstein 1993, 55). *Tumbaga* can be worked in a similar way, but would have been additionally treated with salts or acids to remove the silver concentrations and leave a golden surface. Surface enrichment became standard in Andean metallurgical practice.

The use of *tumbaga* spread throughout the Andes, and local metal workers tailored the concept of depletion and enrichment to their own metallurgical traditions (Lechtman 1984, 29). If copper and pure gold were available, why did ancient Andeans use *tumbaga*? Lechtman states that *tumbaga* was selected because Andeans "liked the colour of *tumbaga* more than gold or copper" (Lechtman 1984, 30). The selection and use of enrichment treatments reflected cultural attitudes towards the nature of technology i.e. the addition of gold to an artefact changed its overall nature and essence:

"The essence of the object, that which appears superficially to be true of it, must also be inside. In fact, the object is not that object unless it contains within it the essential quality, even if the essence is only minimally present." (Lechtman 1984, 30).

If this essence is the addition of gold or silver, then the physical addition of such metals would alter the overall essence of a metallic artefact. The addition of an essence may have had a relationship to *camay,* the Andean concept of giving life or spirit to an object. Lechtman notes that the perception of processes within Andean society greatly influenced the way in which technology functioned, and ultimately changed. As such, she states: 'technological essence must be part structure of the item in order to be realised and made visible on the surface' (Lechtman 1984, 33). Thus, technological knowledge is altered by cultural meaning and definitions. Different belief systems, attitudes towards technology, and materials allowed for development of the technology (Lecthman 1984, 30).

Ultimately, Lechtman observes the influence of culture within Andean metallurgical history by referring to the adoption and use of copper alloys. The style and manufacture of an object is influenced by technology, although the technology is also driven by the style. Technology cannot be removed from the society that makes and uses it.

The application of theory of technology in this thesis

Silver production in the Porco-Potosí region is considered via the investigation of technological choices made within the production process which will help to reconstruct the *chaîne opératoire.* This region has undergone severe political and economic changes over the last 500 years of written history. It has played a critical role in world silver mining and metal production. The area is 4100 m.a.s.l., which has altered and restricted the availability of fuel and affected the thermodynamic and chemical properties of the reactions. The combined influence of all these factors has influenced the technology employed in the region. The theoretical concepts discussed in this chapter will be used in Chapters 7, 9 and 12 to further aid the understanding of the analytical results. This thesis aims to promote a duality between the thoughts and theories of technology discussed in this section and the archaeometric study of material debris.

3. THE TECHNICAL AND HISTORICAL BACKGROUND

Throughout antiquity, different methods of smelting metals have been developed. This chapter will only describe the available methods used to produce lead and silver. It will pay particular attention to Europe in the 15th and 16th centuries AD, in order to gain a comparison of the techniques available to colonizers of the New World, and thus understand the possible influences that could have affected metal production techniques in the New World post Spanish conquest. It will introduce the terminology, technology, and type of equipment involved in the production of lead and silver metal. Also included in this chapter is a brief historical review, focusing on mining and metal production within the Porco-Potosí region. The review considers the historical significance of this region and the different political and economic factors that have influenced metal production processing.

3.1. Lead and silver technology: basic metallurgical practices explained

Silver production past and present predominately used argentiferous lead ore which was smelted to 'bullion', silver-rich lead metal, which was then refined by cupellation to give a pure silver cake. The processes will be dealt with separately, initially considering smelting and then cupellation.

Lead and silver smelting technology and terminology

The term 'smelting' refers to the extraction of metal from a selected ore via heating and chemical reduction. The primary stage in any smelting operation is the beneficiation of mineral ore. Beneficiation is the non-chemical concentration of ore mineral by separating it mechanically from gangue or waste and host rock. The type of beneficiation is technology dependent and the type of smelting conditions and the ore selected will affect the type of beneficiation needed. In general, an increased surface area through crushing or milling means an increased area for the ore to react within the furnace and chemically transform to metal. Beneficiation therefore involves the crushing of mineral ore, often using grinding and hammer stones. This also aids the sorting or separation of different minerals present within the ore body. The archaeological evidence for ore processing is best preserved from the Classical period in the mining district of Lauvion, Greece. There, a series of grinding stones made from volcanic rock were used to produce an ore that had the 'consistency of flour' (Healy 1978, 142). Ore washeries comprising of platforms and a networked series of waterways were used to further concentrate the rich

silver-lead ores. This was done through natural density patterns, the lighter gangue material would be washed away down the flumes while the heavier lead-rich particles would collect within the flumes. This worked perfectly if the ore had been crushed to similar size and shape (Ellis Jones 1986). In the medieval and post medieval world, it was common for ore to be crushed using water or animal powered stamp mills (Hoover and Hoover trans., 1950, 313). This type of processing indicated a much greater intensity of production as ore could be prepared rapidly and without human exertion.

Lead ore can be composed of primarily two differing lead compounds; galena [PbS] and cerussite [PbCO3]. These two minerals cannot easily be separated from each other by traditional beneficiation processes, although the separation of lead ore and gangue minerals (waste mineral unnecessary for the smelt) is possible, due to their different specific gravities. Sometimes galena and cerussite contain naturally occurring silver minerals which, when smelted with the lead mineral create a rich bullion (a silver rich lead metal). The presence of silver does not affect smelting requirements but will determine how the metal is further processed after smelting. Clearly, eyesight and judgment to assess physical properties such as colour, taste, density, and texture have played a definitive role in the selection of ores used during antiquity. Knowledge of the richness of a specific ore means that the smelter can assess the investment of mining and smelting with some knowledge of the economic/financial outcomes (Rehren 1997, 9). Prior to the Renaissance, there is very little documented evidence that more scientific testing of the quality of ores was being practised. However, the technical manuscripts of Agricola, Ercker and Biringuccio explain that a test called fire assay was used by metallurgists to determine the quality of mineral ore and give an exact indication of the amount of achievable nobel metal that could be extracted from the ore (Hoover and Hoover trans., 1950; Sisco and Smith trans., 1951; Smith and Gnundi trans., 1959). Fire assay is a process that is used to test the purity of either mineral ore or metal. It uses the natural affinity of lead to oxygen to form lead oxide, leaving behind the pure noble metal. It is primarily used to test for the presence of silver and gold. This technique has been in continuous use since before the Renaissance period for the testing of minerals, recycled metals, coinage and jewellery. If done correctly fire assay can be an extremely accurate way to determine the silver or gold content in a given ore or metal. It uses the principles of smelting and cupellation (this will be further discussed in 3.1.2) but done on a much smaller scale (Martinon-Torres, Rehren and Van Osten 2003; Martinon-Torres and Rehren 2005). It is still in use in Potosí, Bolivia to test the quality of extracted ores (authors observation).

Roasting is a pre-smelting preparation that is beneficial, but not essential, to lead smelting operations. It helps prepare the ore for smelting by heating it in an oxidising environment (often open fires). Roasting converts sulphides, carbonates and chlorides into oxides, it also

makes the beneficiated ore crumbly and thus can aid further crushing and preparation for smelting (Craddock 1995, 167). Smelting is an operation that demands a high energy input; the roasting of ores can ensure that less heat energy is required during the smelt proper.

Once the ore has been suitably crushed and possibly roasted, it is ready for smelting. This often takes place within a furnace, but can also occur in small quantities within crucibles. Smelting galena demands an environment that has a co-smelting reaction i.e. both oxidation of the sulphur and reduction of the metal occur in the same furnace. Lead is potentially one of the oldest metals produced in antiquity (Pernicka 1990). There is often very little archaeological evidence for the production and working of lead as the process requires very low temperatures. Smelting of lead ore (galena or cerussite) is a simple process. It requires sufficient heat and a suitable furnace atmosphere to separate lead from any gangue components. Lead metal is liquid above 327 °C. If just lead metal is required and optimum yield is not necessary, a smelting furnace is often not required and the metal can be produced using an open hearth or specially dug pits. Agricola describes smelting techniques from Westphalia: they employed piles of wood mixed with as much lead ore as possible, a natural wind would fan the fire enabling smelting to occur and produce lead metal (Hoover and Hoover 1950, 395). This technique is not dissimilar to that of Roman bole smelting found in the Yorkshire dales (Healy, 1978). Large pits known as boles were filled with fuel and ore, then burned to produce lead meta (Cranstone and Willies, 1992).

If a furnace is necessary then the smelter must be able to control the conditions within the furnace, which is primarily achieved via the choice of fuel, the fuel to ore ratio, the air flow, the quality of the ore, and its construction (shape, materials, and location). Charcoal is an excellent fuel because it can burn to give high temperatures while producing carbon monoxide which acts as a strong reducing agent. Throughout antiquity other fuels have played a role in metal production including coke, wood, plant fibres, and dung (Sillar 2000b; Cohen trans., 1968). The choice of fuels within current day silver production in Porco is discussed in Chapter 4. The reactions taking place in the furnace demand that both lead sulphide (PbS) and lead oxide (PbO) be present for the transformation of lead ore into lead metal. Lead metal has a strong affinity for silver and other noble metals. Thus, any silver present in the galena will be extracted preferentially and chemically bound to the main lead metal body.

Of great importance for the interpretation of technological processes within the furnace are the waste products produced during the smelt. A mixture of mineral gangue, possibly fluxes, fuel, and ceramic components from the furnace material combine to form a siliceous compound called slag. The analysis of slag has, in the last forty years, been the predominant method for identifying the technologies of metal production within antiquity (Bachmann, 1982). The

elemental composition and structure of slag contains information about the processes that occur within a furnace. It is possible to see in it the interactions between ore and ceramic furnace material. The chemical constituents within the bulk composition of slag can directly infer the type of reactions happening within the furnace, but also indirectly indicate what source materials were added to the smelt. This information can contribute to compare and identify the *chaîne opératoire* of the production process. The very heterogeneous lead slag from Porco is best described as a rich fruit cake. Each slice may contain a different mixture of dried fruit, nuts, and spongy cake body, providing the consumer with an idea of what initial ingredients were used to make the cake and the conditions needed to bake it. The hidden information about the processing of metal within the slag cannot be so easily known as cutting up a cake, but it can be extracted via the application of scientific techniques and this has now become standard practice within many archaeological institutions.

After the initial lead smelt which may result in the formation of a lead-silver alloy, further refining and cupellation of silver is then necessary.

Cupellation technology

Cupellation is a process used to extract the noble metals (gold and silver) from lead metal by oxidation. It requires temperatures above the melting point of silver (*circa* 960 °C and thus greater than 1000 °C) and demands an oxidising environment. Lead is an ideal agent to use for cupellation in its metallic state it collects at high temperatures gold and silver: it becomes oxidised in conditions where noble metals do not and when molten it is immiscible with the noble metals (Bayley & Eckstein 1995, 108). Thus, during cupellation lead is oxidised and forms lead oxide (PbO/litharge), which then either flows out of the hearth or is absorbed via capillary action into the porous hearth lining (Rehren 2001, 67). The noble metals do not oxidise easily and thus remain behind during the cupellation process. The hearth lining needs to be made from a material that does not contain high levels of silica, as silica will react with lead oxide to form a viscous lead silicate and then clog the necessary porosity in the lining (Bayley & Eckstein 1995, 108). It should be noted that there is a distinction between large scale cupellation on a specially built hearth and smaller refining which takes place in specially made vessels called cupels. Cupels began to be introduced from the late Middle Ages onwards, bone ash was used to prepare the cupels and became common place in cupellation. This document will highlight that it is also possible to cupel silver using plant ash. The silver sitting on top of the litharge was said to be just like 'oil on water' (Pliny the Elder: Rehren and Klappauf 1995). This is technically not true as silver is much denser than liquid litharge and should therefore sink. Bayley (1992) explains that the process of cupellation works efficiently because the liquid litharge is absorbed into the hearth lining while the metal is not and thus it is common to find a slight depression in used cupels or litharge cakes where the pure silver would have collected.

Cupellation should produce a very pure metal, and if done correctly it is a highly effective technique.

A discussion of the types of conditions affecting the furnaces and the cupellation features in this research project will follow in subsequent chapters.

3.2. Metal technology in the southern Andes

For the Andes temporal units are categorised according to changes in pottery and architectural styles. Metallurgy in the southern Andean Highlands did not reach large scale production until later in the 15th century (King 2000). The first use of gold is tentatively dated to the Chavin culture around 1500 BC (King 2000), although newer archaeological evidence by Aldenderfer et al (2008) pushes that date further back to 2000 BC. Thin hammered and annealed sheets of gold were the products of the first metallurgical techniques employed (McEwan 2000). Surface metallurgy such as the gilding and silvering of copper objects became commonly used during the Moche culture (around 0 BC). Moche culture showed a highly developed metallurgical style using complex alloys of gold, silver and copper (Schorsch 1998). The use of different arsenical coppers predominates in Coastal Peru. Bronze formation in the northern Andes started on a large scale from between AD 1000-1476. Lechtman (1976) states that Andean metallurgy was based upon copper metallurgy, and not silver and gold, however, other metals were also employed throughout the Andes, such as *tumbaga* (copper/gold alloy), which had a gold appearance. Nevertheless, the production and use of three main metals; copper, gold and silver has shaped Andean metallurgy. The production of lead has not been located to a particular region and was not a commonly used metal in the Andes.

Archaeological excavations have yielded significant metallurgical finds from northern Peru, such as the metallurgical centre of Batán Grande (Shimada et al. 1982). In the southern Andes, copper producing centres have been found in the north western region of Argentina (D'Altroy et al. 2000, Raffino et al. 1996). In the metallurgical centres of north-western Argentina, Boman attributes the metallurgical activity to the Diaguita communities (Boman 1908). Archaeological and surface survey evidence of smelting showed fragments of thick ceramic with holes; Boman describes the debris as *huayra* remains. Raffino et al (1996) highlight the metallurgically active area of Quillay in the Catamarca Province, Argentina which also has furnaces associated with copper production. In the northern Calchaqui Valley, Argentina, D'Altroy et al. (2000) present the metallurgical evidence for copper and bronze production. The area was a metallurgical centre during the Inca period. Crucibles, slag, moulds and scraps of copper and gold indicate that secondary stages of metallurgy were taking place, such as casting and melting. No evidence for smelting techniques was found (D'Altroy et al. 2000, 22).

Other archaeological evidence for metallurgical activity includes the areas of Aconquija and Jujuy (Scottlin and Williams, 1992; Tarrago and Gonzalez, 1998). The prevalence of copper and gold metallurgy in the northern Andes and north-western Argentina and Chile is contrasted by the tin and silver metallurgy located in the Bolivian highlands and Lake Titicaca basin (West, 1997). However, a lack of primary production sites associated with lead and silver production in the archaeological record have prevented the metallurgical techniques used in pre-Hispanic periods from being identified.

For this research lead metal is also of interest but very little attention has been paid to the production of lead in the ancient Andes. Lead can be used as a material to refine silver via cupellation and is normally associated in the mineralogical formation of silver. Patterson states: "Silver was not cupelled in South America." (Patterson 1971, 316). However, surveys undertaken by Lechtman found metallurgical debris such as litharge cakes associated with cupellation on the southern coast of Peru. This debris has not been dated (Lechtman 1976, 34). The use of silver and lead in pre-Hispanic Peru was occurring, but the exact metallurgical techniques used in production remain unconfirmed.

A rather low quantity of silver artefacts recorded is partially due to the poor preservation of silver artefacts within archaeological contexts but also to the amount of artefacts looted and exported during the Spanish colonisation in the 16th century. King states that the earliest silver objects were small birds used as ornaments for textiles which date to the 1st millennium BC (King 2000, 12). The majority of silver artefacts documented date from the Chimu period (AD 1110-1470) on the northern coast. The silver–rich Porco-Potosí region was a metallurgical centre since pre-Hispanic periods (Platt et al. 2006), but the extent of mining and metal extraction remains uncertain.

The role of metals within the Andean world was very different to that of the Spanish colonialists that followed. Copper, gold and silver were symbols of prestige and held great religious value; objects made from metal were not primary utilitarian items they were symbolic and special. During pre-Inca and Inca times gold and silver was used in exquisite ornaments, woven into cloth, encased entire buildings, gilded and encoded the power of local chiefs, ethnic lords and local elites (Sallnow 1989, 209; D'Altroy 2003). Association between cosmology and metal was part of the Inca mythology and way of life (McEwan ed., 2000; Urton 1999). Silver is often connected with femininity, fertility and the moon. Silverblatt (1987) comments that silver had connotations with gender roles of women within Andean society. The use of noble metals was intimately related to power and hierarchy in Inca society. Within Inca society the use of gold and silver seems to have had political and religious importance. "The warm reflective glow of

gold symbolized the sun, a male deity; the soft, cool sheen of silver symbolized the moon, a female deity and source of life-giving waters. Workers tiling the fields would chant in Quechua, the language of the Inka, *i inti qori paran, killa qolpe paran!* (The sun rains gold, the moon rains silver)." (King 2000, 11). During the Inca period, copper and bronze tools such as crowbars, chisels, axes and knives became more widely available. Prior to the Incas metals had a much more ornamental use (Lanning 1967).

The consideration of metals within Andean cultures has often used the Inca and early Spanish colonialists' writing for understanding pre-Incaic metallurgy. This, however, presupposed that ideas concerning metal and its sociological and economic values had not changed. Even more importantly, many ethnographic accounts have an elitist view of the metals being considered and this can detract from the real value. Thus, despite the identification of some metal workshops and metal production sites, more analyses are needed to interpret the use of metals within pre-Incaic Andes.

During the research presented in this thesis, no pre-Hispanic archaeological sites have been found to provide evidence for metallurgy in Inca and pre-Inca settlements in the Porco-Potosí region. A critical assessment of the origins of *huayrachinas* suggest this technology to be indigenous. Early dictionary sources report the word *huayrachina* as the word used for furnaces used to produce metal (Bertonio 1984 (1612)). To date there are no known archaeological *huayrachina* remains that confirm these were in use prior to the Spanish conquest. The presence of silver and lead artefacts have indicated that those metals were produced in antiquity but it is unclear what types of furnaces were used. Thus, this research has focussed on colonial metallurgical techniques of silver production, where both archaeological and historical evidence are available.

3.3. The history of the Porco-Potosí region

This section gives a brief historical review of the Porco-Potosí region. It will list a few important events that pertain to metallurgical activity. However, more detailed historical work is required before a fuller picture emerges, and this is ongoing with the main PAPP research and other researchers working in the region (Lecoq and Cespedes 1996, Platt et al. 2006).

The Porco-Potosí region has been related to mining and metal production since at least the invasion of the Incas in the mid 15th century AD. It is likely that the region was already exploited during pre-Inca periods for mining and metallurgical activity (Abbott and Woolfe 2003). Historical literature from the early colonial period indicates that this area held religious value and was a pilgrimage area attracting followers from all over the Southern Andes (Platt et

al. 2006, 6). In this section, the history of the region has been separated into seven distinct phases (Table 3.1). These phases have been introduced to clarify the complicated political, economic, and social variables. The seven phases loosely reflect political changes in the region. The history of the pre-Inca period remains very uncertain. The majority of work considered in this thesis lies within the Spanish colonial period. Inca and pre Inca eras are described for reference to the historical context of the silver production, but they are not the focus of this research.

Phase (all A.D.)	Name
1000-c.1470	Pre-Inca
1470-1538	Inca
1538-1570	Pre-Toledan (included in Early colonial phase but forms a separate sub phase)
1538-1650	Early colonial
1650-1780	Middle colonial
1780-1821	Late colonial
1821-onwards	Republican

Table 3.1. Time periods in the Porco-Potosí region.

Pre-Hispanic/Inca Porco

The history and culture of modern Bolivia has been dominated and intimately driven by the mining industry and this has been a major social and economic activity since at least the Inca period. Pre-Hispanic cultures showed a deep affiliation with their own environment. "Andean people literally read their physical surroundings as a resonant text of sacred places and spaces that commemorate a trip across time and changing landscapes from super beings to human beings to present times" (Mosely 2001, 51).

In the Porco-Potosí region the shortage of surveyed or excavated archaeological sites and the absence of any written records prior to the Spanish conquest has made understanding this region's history difficult. The earliest inhabitants of the area were believed to be Aymara speaking tribes (*circa* AD 0-1000). Links between the coastal communities of the Atacama such as Arica and Tarapaca (now in modern Chile) have been suggested (Platt et al. 2006, 25-26). However, the exact historical information remains unclear. Both Porco and Potosí were important *w'akas*, well known by the indigenous communities.

Early Spanish colonial documents state that the Cerro Rico (Rich Mountain), Potosí was never used for mining, although in the wider region prior to the Spanish conquest. It is difficult to establish if the indigenous people knew and used Potosí for mining. It does, however, seem evident that established trade networks during Inca periods were in effect and that minerals

were exchanged for maize and coca, grown in the lowlands (Cochabamba), (Platt et al. 2006, 40).

It is difficult to establish the extent of the metallurgical production during the pre-Inca period and indeed how the infrastructure or organisation of this system can be identified without the discovery of archaeological metal working sites. Recently, Abbott and Wolfe (2003) have analysed lake sediments from Laguna Labato (6 km from the Cerro Rico). The lake has no hydrological connection with the surface water draining from the Cerro. A core was recovered from the deepest portion of the lake and dated using ^{210}Pb, ^{137}Cs and ^{14}C. Five metals (silver, bismuth, lead, antimony and tin) were measured as indicators for metal production. The results indicated that prior to AD 1000, all metal concentrations from the core were stable and relatively low indicating normal geological deposition. Around AD 1130-1150, concentrations of all five metals increased, indicating the onset of metal production. Metal contents in sediments decreased during the mid 13th century. Abbott and Wolfe interpret this to show that metal production was directly linked to the political events occurring to the Tiwanaku state which flourished until the end of the 13th century (Abbott and Wolfe 2003, 1984). Their evidence is one of the only indications of pre-Inca silver and lead production in this region. It suggests that metal production was taking place in Potosí during the early 12th century (the Late Intermediate Period). However, no archaeological evidence has been found to indicate the types of furnaces used to produce this metal. Equally there is no archaeological evidence for settlement patterns or production sites and therefore, no direct confirmation of inhabitation during the Tiwanaku period in this region. Thus, the data from Abbott and Wolfe would ideally require the locating of an archaeologically relevant site to further substantiate their work.

From the archaeological work carried out in the Porco-Potosi region, analysis of ceramic material in the archaeological record has shown no samples from pre-Inca periods. The sites available have been dated to Inca or post colonial periods using structural and ceramic information. Platt et al. (2006) consider that this area was of great religious significance, thus, it would have been regularly visited by different ethnic groups. However, surface surveys carried out on Upu and Huayna Porco (the two summits at Porco) did not reveal evidence for major feasting as would be expected with a pilgrimage site. Abbott and Wolfe's analyses indicate that metal smelting was taking place in the region but no evidence is available to indicate that the processing of silver was taking place in Porco. Metal concentrations in the lake sediments increased substantially after the Spanish conquest of the area in the mid 16th century, which would indicate that prior to the conquest the Incas were producing metal on a relatively small scale, if at all. The lack of pre-Inca ceramics appears to indicate that this area was either uninhabited or inhabited with small scale settlements (personal communication with Dr Van Buren 2008).

The area of Yura 100 km south of Porco was inhabited in pre-Inca and Inca periods. Yura was one of the main sources for food and wood (Rasnake 1988). Porco had very few other resources for permanent inhabitants (Van Buren and Presta inpress). The sparse evidence of pre-Inca settlements leads to a cautious conclusion regarding metallurgical activity in that period. For now little can be concluded regarding either the scale of inhabitations or any metallurgical activity.

The arrival of the Incas

"...metallurgy encapsulates the selective intervention of the Incas in Andean artisanry." (D'Altroy 2003, 303)

The Inca Empire was one of the largest in antiquity "...the largest nation on earth was probably not Ming China or the Ottoman Empire, but Tawantinsuyu, the 'land of the four quarters' as the Incas called their sprawling realm." (Mosely 2001, 7). The Inca state was constructed of four main regions entitled: *Collasuyu, Antisuyu, Cuntisuyu*, and *Chinchaysuyu*, collectively known as *Tawantinsuyu*. The capital of the Inca world was Cuzco which became the centre of the four quarters. The organisation of the Inca Empire was complex; it consisted of some a body of individuals who were linked to the main Inca ruler through bonds of kinship and reciprocity. They dominated over their realm using an intricate governing system, all without a system of writing. "The head of this royal family was the head of state, and at the height of the empire his domain extended over ten million people or more. These individuals were Inca subjects, but they were not Incas because this was a closed ethnic body." (Mosely 2001, 9). The Incas governed with a hierarchical system that saw the main Inca king as the supreme ruler, and specific districts governed by officials appointed from the capital Cuzco (modern day Peru). "By adapting state practices to local circumstances, the Incas forged a policy that relied on a situational mix of alliance, clientage, intensive incorporation, and, on Peru's north coast, dismantling the upper echelon of a potent competitor." (D'Altroy et al 2000, 2). The Inca regional governments allowed the native people to live in relative freedom and practise their own customs and traditions (Moseley 2001).

Early colonial sources have indicated that, prior to the Spanish conquest, the Southern Andes of modern Bolivia consisted of ethnic groups that had their own defined territories. The region was designated under the Charcas Province and under the rule of the Aymara confederation. The Charcas province was under local rules of the Qaraqara Indians (Platt et al. 2006, 126), however, the local indigenous communities kept their own traditions, customs and language, and under the Spaniards the region later became the Audiencia of Charcas.

126 sites within the southern Bolivian Andes, northern Argentina and Chile have been established as Inca mining areas (D'Altroy et al. 2000). Charcas almost certainly became a particular focus of Inca control because of its rich mineral wealth. The region is at a very high altitude which means it has very little agricultural value. The economic history of the region seems to have been driven by the rich mineral wealth, the importance of camelid herding and the unsuitability of much of the soil to agriculture. Juan de Betanzos discusses the Inca ruler, Topa Inca Yupanqui's (AD 1471-1493) visit to the province of Charcas on his return to Cuzco from Chile. "...the Inca was informed by his warriors that these Charcas were lords who had much silver. The Inca asked them where they got the silver, and they told him that they took it from a hill called Porco." (Hamilton & Buchanan trans., 1996 (1576)). According to early colonial sources, the route between Porco and Chuquisaca (Sucre) appears to have been a well used road during Inca periods (Platt et al. 2006, 125).

Archaeological evidence for Inca structures indicates some level of general habitation of the Porco-Potosí area but no archaeological Inca mines or processing areas have been found. Despite a lack of archaeological remains, the historical evidence indicates that the Incas had a strong military system, akin to this they were able to organise and model the workforce and running of state mines via a process of hierarchal systems (Berthelot 1986). There is very limited information on mining and metallurgical practice during the Inca period; therefore archaeological studies remain reliant on the Spanish colonial authors for their documentation of ancient production sites. In general these do not document smelting practice and when they do they present inconsistent methods of smelting from the colonial period rather than pre-Hispanic as they claim in their writing. Other New World colonial sources (Capoche 1585; Barba (Douglass and Mathewson trans., 1951); Parma and Cook trans., (Cieza de Leon 1537)) consider the village of Porco which is 35 km south west of Potosí, to be of Inca origin. Barba says:

"It (Potosí) is completely surrounded by many and very rich Mines, as, for instance, those of Porco, the famous mines of the Incas, and the first from which the Spaniards extracted Silver..." (Douglass and Mathewson trans., 1951 (1640), 68).

It is known that the Incas mined a great variety of minerals and metals. It has, however, been difficult to find archaeological evidence relating to primary production sites. The variety and technical difficulty of many of the Andean metal processing techniques gives an idea of the skill of Inca craftsmen. They were able to smelt, alloy, cast, hammer, *repoussé*, incrust, inlay, solder, and rivet (Steward, 1946). Archaeological evidence from other sites, such as Batán Grande (Shimada et al. 1982), and the Titicaca basin (personal communication with Carol Schulze, 2008)

have provided insight into the different metallurgical practices that were occurring prior to the Inca reign. In the southern Andes, the use of lead and silver has been documented in the Upper Mantaro Valley (Howe and Petersen 1994). It appears that the diversity of peoples and cultures within the Inca territories has lead to a diverse range of metal production techniques.

The arrival of the Incas in the Porco-Potosí region had a dramatic effect on mining and metallurgical technique. We assume sparse inhabitation prior to the Inca invasion in the Porco region, afterwards the region became a metallurgical centre for silver and lead production importing people to work in the mines and smelt the extracted ore. *Yanakuna* were employed by the Inca elites to monitor and control colonies in the Inca Empire. *Yanakuna* were lifelong servants to the Inca (D'Altroy 2003, 267). They were specialists trained in Inca administration, different craft specialities, and taxes. They held no ethnic allegiances and thus, were not members of an *ayllu*. Their only loyalty was to the Inca ruler and state. The *yanakuna* in Porco would have been specialised smelters (Presta in press; personal communication with Dr Van Buren, 2008). The Inca enabled their policies to be flexible according to local environments and politics which was done by improving road networks and by the appointment of provincial governments which monitored the colonised societies (D'Altroy et al. 2000). During colonisation, the Incas intensified craft production which helped distinguish them from colonised society (D'Altroy et al. 2000). In Porco, the mineral wealth encouraged the control of this region. Porco was a beneficial region for the Inca Empire. It is surmised that the *mit'a* system of importing labourers from other communities was employed in Porco; the Inca employed *yanakuna* may have overseen these actions. However, the scale of labour and metal extraction remains unknown.

The arrival of the Spanish

In 1536 Charcas was invaded by the Conquistadores, the Inca Empire crumbled and Spanish rule began. Metallurgical activity within the Inca empire encompassed the central Andean highlands, Pacific coast, *altiplano* Peru/Bolivia, the Atacama dessert of Chile and NW Argentina. These areas have been centres for metallurgical production. The western coast of South America is particularly rich in both native metal and mineral ore bodies. Metallurgy in the New World has, in the past, had a reputation for being behind in terms of technological skill and advancement when compared with the Old World. However, La Niece and Meeks (2000) demonstrate diversity between gold smithing in the Americas and the Old World. Their work further illustrates the complexity of New World techniques and the associated cultural differences. While the New World lacks the technical knowledge of how to smelt iron within the limited historical and archaeological evidence the technological skill can be seen as a direct response to changing environments and evolution via selection of materials. This reflects

a culture that clearly understood some fundamental properties of metallurgy and metal working, over a wider range of environmental conditions.

The arrival of Hernando and Gonzalo Pizarro in the Charcas area (*circa.* 1538) seems to have been a rather rushed affair. Platt et al. (2006, 125) state that they may have used the road connecting Chuquisaca and Porco, that crosses the Pilcomayo river before going up to the site of Porco. Francisco Pizarro endowed his brothers with mines which were guarded and governed by Pedro de Soria. Upon their return to Cuzco, the brothers sent news to Carlos V that Porco was under Spanish control (Platt et al. 2006, 125). The early years of Spanish occupation appear to have been rather casual and very little evidence remains for the way in which the mines and metallurgical processes were being governed. However, the Spanish land owners claimed control and ownership of the mines in Porco and *yanakuna* were employed to organise the mining communities (Presta in press; personal communication Dr Van Buren 2008). The indigenous communities living in the area were drafted using the Inca *mit'a* system from local villages such as Yura. The administration of the Porco-Potosí mines and Charcas areas was directed via La Plata (currently called Sucre), 120 km north-east of Porco (Bakewell 1984, 10).

Figure 3.1. The Virgin Mary and the Rich Mountain of Potosi painted in 1740. It presents the Cerro Rico as the Virgin Mary surrounded by the king of Spain and the Pope. Published in Rishel and Stratton 2006, 447.

The Spanish discovered the ore deposits of Potosí seven years after Porco had already been established as a Spanish freehold, and mining and extraction was already being carried out at Porco. Spanish legend says that in 1545 the mineral veins of Potosí were discovered by an Indian (most probably a *yanakuna*) who told his Spanish master that the Cerro Rico had a wealth of silver ore hidden within. This marked the birth of the Cerro Rico mines which would cause the growth and development of Potosí. As discussed, it is uncertain to what extent the indigenous populations were mining at Potosí prior to the arrival of the Spanish. It would seem logical that mining and metal production were taking place in some capacity at Potosi. Platt et al (2006) suspect Potosi was hidden from the Spanish due to different ownership patterns within Inca social and religious organisations.

The importance of documenting the discovery of the Cerro Rico can be interpreted as a political symbol of power used by the Spanish to determine territorial control (Platt et al. 2006, 31). The hiding of the mineralogical wealth and the important *w'akas* of the Cerro Rico and indeed Porco

(during the early periods of colonisation) marked a period where the rule of the Spanish was not accepted by local populations. Equally, the religious importance of Porco seems to have entitled the Spanish to a different status that previously would have been shown to local deities. The petition by Hernán González de la Casa, a priest assigned to do missionary work in the Porco region describes the discovery of a *w'aka* located near Porco in Caltama (Platt et al. 2006, 182-187; Abercrombie 1998, 267). The *w'aka* consisted of five idols named; *Tata* (Father) Porco (represented by a piece of silver metal and rich silver ores), Cuycoma, Chapoti, Suricaba and Aricaba (Platt et al. 2006, 184). Tata Porco could have resided in the mountain of Porco. The four other idols may have been at other mines in the district, but their location has never been found. In his account, González says that he destroyed the *w'aka*, though upon leaving he was attacked by local Indians. They told him they would kill him unless he returned "Padre' Porco. He was stoned to near death but survived and returned to village to build a church. Pilgrims came from all over the Southern Andes to the Caltama *w'aka* for divination, to inquire about their future, to carry out sacrifices, to remove sins, and to restore their relationship with the gods (Abercrombie 1998, 268). *W'akas* in Andean society were associated with danger; they were the locations which contained deities (Silverblatt 1987, 173). The deities could be destructive but not in the demonic sense that was promoted by 16th century Christian Spanish settlers arriving in Potosí. The area of Porco-Potosí held an important religious position within the Southern Andes. The complicated political situation between the Qaraqara and Charcas confederations encouraged the eventual dominance of the Porco region. Whoever controlled Porco also controlled the local population and the economic climate within the region.

In Porco, indigenous methods of silver production persisted, the beneficiation of ores was done using *quimbaletes;* a mortar constructed from a large stone and a pestle shaped in a half moon which could be moved from side to side to crush the ore placed in between the rocking stone and the mortar (Bakewell 1984, 15). *Huayrachina* furnaces were used during those very early colonial years to produce silver and recorded since the earliest colonial writing (little information is available regarding metal production in Porco, thus colonial sources from Potosí are used).

Luis Capoche (1585) wrote that the *huayrachinas* were positioned around the village of Potosí, where they lit up the mountain from the late afternoon and through the night.

"Llegó los años pasados el número de los asientos de guairas a seis mil cuatrocientos y noventa y siete. En este tiempo permanecen casi todos, aunque están arruinados gran parte de ellos, por no usarse la guaira como solía." (Capoche 1585, 111)

"In past years, the number of *guaira* sites reached 6,497. Most of them have remained throughout this time although a number of them are ruined because the *guaira* is no longer used the way it used to be" (Claire Cohen's translation of Capoche 1585, 111).

The practise of smelting using the *huayrachinas* at night was certainly not for aesthetic reasons, but to make use of maximum wind to power the furnaces, requiring the lowest possible amount of fuel. In the Andes, specifically in the *Altiplano* region, the wind is stronger in the late afternoons and in the winter months. Lighting a furnace at dusk or dim light would also provide the smelter with the advantage of seeing the colour of the flame and molten metal, thus evaluating the temperature of the furnace. It would also seem probable that the furnaces may have been used during the day light hours for several hours in more than one smelt but would have been particularly visible in the evening.

Capoche also states that bellows were not needed for *huayrachina* use but occasionally copper canes were used. Three styles of *huayras* appear to have been in use during the early colonial period:

i. Rough stones, loosely assembled to aerate the charge.

"And for the smelts that necessitate more force, they (Indians) take advantage of the same wind, making the smelts in the countryside, in the areas that are high, some furnaces made from loose stones placed one above another without soil." (Claire Cohen trans. of Capoche 1585, 109).

ii. A furnace built of stones set into clay with holes for air.

iii. A portable clay furnace with pierced holes in the shaft.

Capcoche (1585) assumes that this third type of furnace was invented during the colonial period by Spanish settler, Juan de Marroqui (Capoche 1585, 109). However, this source should be regarded as suspicious and without other direct sources, the origins of *huayrachinas* remain unknown and speculative.

Capoche also describes the ways the *huayrachinas* were used:

"This is the way that they have beneficiated the metal: primarily they grind and wash it, they take the part that has the dead earth, leaving behind the metal parts – and the parts that are most rich it is not necessary to wash. And to two parts of the metal add one part of galena...mix with it...litharge that are the result of old smelts...After this they mix with water, because they don't want the wind to take the metal dust when they put it in the formed clay (that is larger than a vara unusually with 4 angles or corners, extended almost a square, hollow, open above; it has 4 lienoz or made openings or little windows so that it has the most effect from the wind..." (Claire Cohen trans. Capoche 1585, 109)

More descriptions of *huayrachinas,* both historic and modern have been published. Modern authors, such as Bargallo (1967) and Petersen (1970), describe and summarise historic

literature concerning the use of *huayrachinas*, and some introduce the use of native refining furnaces including *tocochimbos* (Van Buren and Mills 2005).

Exploitation of mineral ore for smelting was done on a relatively large scale which is obvious through historical reports, but where is the archaeological evidence? No known source has been found documenting metallurgical practice in Porco during the very early colonial period because the focus of historical sources was on Potosí. How were the indigenous pre-Hispanic population of Porco producing lead and silver metals?

In early colonial Porco, the workers of *huayrachinas* were called *huayradores*. *Huayradores* were often *yanakuna*. The Spanish invasion altered the role of the *yanakuna* and their allegiance shifted to the Spanish landowners. The *yanakuna* would have been responsible for the mining activity (i.e. controlling the exchange and collection of the work force) and directly in charge of smelting and working with the *huayrachinas*. Thus, in the colonial period the workforce remained in ethnic groupings that were controlled by the local Spanish elite. No information is known regarding who was responsible for refining techniques. Archaeological evidence indicates that this may have taken place within households or isolated locations.

The influence of the Spanish within the mining communities was one of the most prevalent as the Spanish were motivated by their desire for precious metals (Steward 1946, 245-246). For the first thirty years of colonisation the use of the wind blown *huayrachina* furnaces continued to produce silver (Bakewell 1984, Platt et al. 2006, 5). By 1540, 85% (by weight) of the precious metals shipped from the New World to Spain were silver based, although the value of silver was far less than that of gold, and it remained that way for the next twenty years (Fisher 1977).

In summary, it appears that the Porco-Potosí region was sparsely inhabited in pre-colonial periods and it is highly probable that the Incas were mining the mountains of Porco for silver. Bakewell (1984) states that during the early colonial period, most workers who were employed in the mines of Potosí came from Porco, and as such this implies that there was a very direct link between Porco and Potosí, as there is today in modern Bolivia.

The early-middle colonial era

The importance of this region during the early colonial era can be seen with the growth and development of Potosí. Since the beginning of the historical records, increased pressure from Spain on silver production encouraged greater invested interest in the mines and workers of Potosí. During the very early years of the conquest, silver and gold were obtained by looking for

artefacts rather than by focussing on the control of mining and smelting. From the 1550s silver production dropped significantly from 379,244 marks (1550) to only 114,878 marks in 1572 (Bakewell 1997, 76). During this period the use of *huayrachinas* to smelt silver continued. All individuals could exploit the mineral wealth but had to pay tax to the King (one fifth of the quantity produced).

When Don Francisco de Toledo, fifth viceroy of Peru (1569-80), came into power it was his recognition that silver quantities were substantially decreasing, prompting the introduction of a new technique for silver extraction called the Patio Process (Bakewell 1997). The new order issued by the Viceroy stated that mercury amalgamation should be the main method for silver production; it modelled itself on the city of Huamanga, Peru started to use this technique in 1565. The Patio Process allowed for the extraction of silver through an amalgamation with mercury using medium to low grade silver ores that would have been previously unsuitable for smelting. During the process silver ore was concentrated at the mine then mixed in refining tanks called cajones with water, salt and mercury. Agents such as iron filings and copper sulphate were also added to speed up the process (Bakewell 1984, 21). The amalgam of mercury and silver then needed to be washed and unreacted ore was washed away. The resulting mixture was compressed to remove any free mercury creating a *pella*. Bakewell says that the *pella* was 80% mercury and 20% silver (1984, 22). The *pella* was pushed into a conical shaped mould and then heated under clay hoods to distil off the mercury, leaving behind refined silver. Compared to methods used in the smelting of silver ores, this process would require relatively low temperatures and hence less fuel. Mercury used in the Patio process was imported from Huancavelica, Peru. The mercury was transported over 1,200 km in leather bags strapped to mules and llamas. When necessary, mercury was imported from Spain (Fisher 1977). The introduction of amalgamation meant the Spanish gained more control over the mining sector; they restarted the system employed by the Incas of using forced workers (Craig 1994). However, the Patio Process did not completely eradicate the use of the *huayrachina* and it is believed that small scale usage continued within indigenous households.

The influence of Europe on silver smelting techniques

In 15th and 16th century Europe, the use of domed furnaces also known as reverberatory furnaces, were used for the processing of rich ore minerals. More commonly, these furnaces have been used to refine via cupellation silver-rich lead to produce pure silver (see Chapters 10 and 11). Various European manuscripts detail the use of domed or reverberatory furnaces. As well as reverberatory furnaces, blast furnaces were used to produce lead, silver and copper. They were constructed with a column shaft made of bricks and luted clay, and often required bellows (Agricola (Hoover and Hoover trans., 1950), Ercker (Sisco and Smith trans., 1951), and

Biringuccio (Smith and Gundi trans., 1959). Comparison of the technology employed within Europe will aid the understanding of knowledge transfer between the Spanish colonisers and native Andean peoples.

Georgius Agricola's *De Re Metallica* (Hoover and Hover trans. 1950) was published in 1556 and was used for its first 180 years of publication as the seminal guide to metallurgy. It remains one of the most important manuscripts for understanding technology in the 16th century. Agricola represents the technological conception and knowledge from 16th century Europe.

Agricola assigned four main furnaces that could be used to smelt silver, gold, lead and copper ores. The different furnaces were selected according to the type of ore that was being smelted. Agricola organised his ores into four categories, each corresponding to the ore being smelted:

1. Rich gold and silver ores;
2. Mediocre ores;
3. Poor gold and silver ores;
4. Ores containing lead or copper but very low in or lacking precious metals such as gold and silver.

All the furnaces Agricola described except those used for ore type 4, were constructed within a building and were basic blast furnaces using a natural draft and bellows to control and maintain temperature. They were constructed with a tall shaft that varies in height and width according to the type of ore to be smelted. The metals produced from all the four furnaces would have required further refinement using a cupellation technique. To date it is uncertain if European blast furnaces were used in the Porco-Potosí region.

The history of mining in the Charcas region and the transition between the production of silver using *huayrachinas*, the newer mercury amalgamation and other European techniques, created an environment where experimentation with different metal production techniques was probably common. Platt et al. say: "Without a doubt...the mining rituals of the 16th century also suggested that there were other ways to understand the mineralisation of the veins and the sacred association of the extraction processes and refinement, and represent some measurement of the older religious practices and convictions of miners today" (Platt et al. 2006, 5).

The introduction of the Patio Process was delayed partly due to the initial wealth and richness of the Potosí mines. The use of mercury amalgam for a rich mineral ore leads to loss of mercury (which would have been valuable as it was imported from Huancavelica, Peru). Indigenous silver production was used until the cost of amalgamation rivalled that of local production techniques. The introduction of amalgamation meant that local indigenous populations had to

be retrained. Spanish land owners were unwilling to invest in new production techniques (Bakewell 1984, 19). The limited availability and high cost of fuel effected and influenced this change in technology. The Patio Process required a much lower fuel quantity than the *huayrachinas*. There were many stimuli that created the shift in technology from indigenous to European production processes. However, as a result Porco was an area where other methods of silver production were experimented with, as Potosí became the main centre for silver production during the colonial period.

A well developed infrastructure related to mining and metal production was quickly adapted within the early colonial period. The necessity for appropriate fuel to be used in conjunction to metal production but also in every day life meant that Potosí required huge quantities of llama dung. Browman (1974, 190) states 800,000 loads of dung however he does not further document quantities. No figures have been located regarding fuel demands in colonial Porco.

The influx of New World riches into Spain completely transformed Spanish society. In Seville, new social and economic values were adopted. The discovery of Potosí and all subsequent trade provided opportunities to acquire great wealth (Pike 1972). *Vale un Potosí* (worth a fortune) became a well known expression of prosperity and is still used today. While the impact and history of Potosí are well documented, rather little is known about Porco. During the early colonial periods the search for new and improved methods to maximise the amount of silver produced was constant. Literature from Potosí reported that fuel sources were very scarce during the 16th century. Hanke (1956, 21) comments that the colonial archives were full of plans and projects to search for new sources of silver. Generally, the early colonial period is viewed as a period which stimulated many technological changes. However, changes were also occurring in the society. The population growth of Potosí was sudden and it expanded from 120,000 inhabitants in 1580 to 160,000 by 1650, making it one of the largest cities in the World in this time (Fisher 1977). The steep influx of different people from all over the Andes, combined with the arrival of Europeans, changed the societies basic principles from estates, ascription, and kinship to one that was driven by class, territory and achievement (Saignes 1995,191). This created a community that was culturally distinct.

The middle to late colonial era (1650-1821)

During the 1700s, exploitation of the Porco mines was only sporadic and by the end of the century the state had halted the assignment of labourers to that zone. By the mid 18th century the political and economic arenas in the Porco-Potosí region were about to undergo significant changes. These changes would condemn the old imperial structure that promoted the precious metals industry. Many of Spain's political and financial advisors found fault with the crown's

desire to gain precious metals at the neglect of the rich agricultural resources. New methods were engaged to increase general economic and commercial activity between Spain and the Americas. At the same time, the reduced supply of mercury from Peru and Spain severely reduced the quantity of metal produced using mercury amalgamation in the Porco-Potosí region (Fisher 1975).

17th century huayrachina *use*

Barba's *Arte de los Metales* provides historical evidence for the technological and the historic past in the Porco-Potosí region. It was written 100 years after the conquest, so the link to pre-Hispanic cultures cannot be heavily relied upon. However, Barba's treatises remain one of the very few manuscripts to document South American metallurgy within the 17th century. He comments on geological rock formation, types of accessible ores, specific furnaces, and equipment for metal formation and working. He states: "The Audience of Silver ores within the jurisdiction of the Royal Audience of Charcas is so great that, if there were no other Silver mines in the World, they alone would suffice to fill it with Wealth." (Douglass and Mathewson trans., 1923, 68)

Barba discusses the *huayrachina* that he calls the *Guayra*, the indigenous furnace: "The natives of this country, who have not yet gotten to the point of using our Bellows, employ, for smelting, furnaces called *Guayras* (Wind Furnaces); the same are still used in this Imperial Village, and in many other parts" (Douglass and Mathewson 1923, 198).

Barba compares three smelting furnaces; A) the European, B) the *Castellano* and C) the Indigenous *Guayra* (Figure 3.2). He discusses the *Guayra*: "...the walls perforated with many holes, through which Air enters when the wind blows, at which time alone they can smelt...They are placed on high locations where wind is usually blowing" (Douglass and Mathewson 1923, 198). These wind blown furnaces could have been used in conjunction with other refining features. Barba mentions the use of *tocochimbos,* indigenous furnaces that are related to muffle furnaces used for assaying. Unfortunately no further information is given about *guayras* and/or *tocochimbos*. The *tocochimbo* may be of Andean origin but further archaeological evidence is needed to support this theory and gain further information about its construction and use. The term *tocochimbo* could have been retained for a new/different style technology that functioned in a similar way to the indigenous *tocochimbo*, however, this remains unsubstantiated.

While the *huayrachinas* described by Barba did not need the use of bellows to smelt their metal, three of the four categories of furnace Agricola mentions demanded the use of bellows. The use

of bellows has remained a technological feature distinct to the Old World. There has yet to be a documented case of pre-Spanish use of bellows in the Americas.

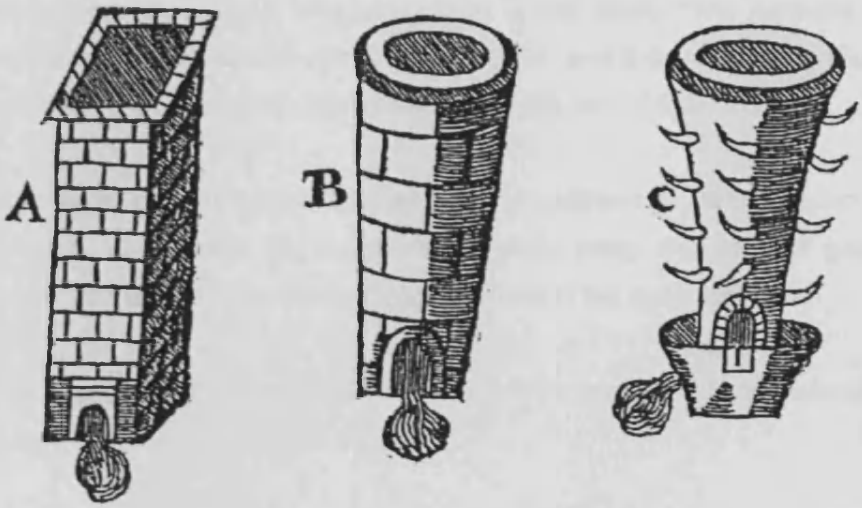

Figure 3.2. Barba illustrates three furnaces that can be used for smelting lead and silver ores. (A) represents the European draft furnace, (B) is the Castellano furnace and (C) the *guiara* indigenous furnace. (Douglass R E and Mathewson E P (trans) 1923, 199).

The Bolivian Republic

The Republic of Bolivia was created in 1825. The late 19th century saw silver prices drop significantly and the mining of tin became more profitable (Bingham 1911); Potosi adapted many of its mines to mine exclusively for tin until 1985 when the tin market crashed (Cunningham et al. 1996). The mining industry was nationalised and developed into small independent mining co-operatives and large nationalised companies, leading to the unionisation of the labour force.

A resurgence of mining occurred at Porco in the late 19th century when the demand for industrial minerals, used in the production of metals such as tin, led to the establishment of a modern concentration plant by Porco Tin Mines, Ltd. Since then tin extraction, and more recently, zinc, has been pursued on a large scale. Modern Porco is still driven by a desire to extract mineral wealth.

The last *huayrachina*

The late 19th century engineer Robert Peele Jr (1893) described the process of silver production. He clearly states that the use of a '*Huairachina*' was common practice among the Indians of Potosí. He says: "...it has an extremely small capacity, and is wholly unsuited to modern

requirements, still, as a survival of the times of the Incas, it possesses some interest as a metallurgical curio" (Peele 1893, 9).

Peele comments on the ore that was being used in the smelt: "The materials treated are galenas, as well as zinc-blend and pyretic combinations, and those containing the high-grade sulphides, such as ruby silver, gray copper, silver sulphide, etc." (Peele 1893, 9).

He also states that in place of galena, litharge could be used and this was collected from 'native refining furnaces'. Thus, were the indigenous smelters using argentiferous galena? Where would they have refined the argentiferous lead produced in the *huayrachina*?

Peele's report was the last documented evidence for this technique, which was subsequently believed to have become extinct (Figure 3.3).

Figure 3.3. *Huayrachinas* in the Porco-Potosí area.
19th century *huayrachinas* photographed and published in 1893 (Peele 1893, 9) image left. An archaeological *huayrachina* site - *Cima Colima Veta San Antonio*. The site is comprised of scattered fragments of furnace wall, slag, and natural rock. CCSA is located high above modern Porco on Huayna Porco.

Current day Porco

The mines at Porco are now operated by COMSUR, although a number of local mining cooperatives also work the deposits. Porco has two small communities which are situated on the remains of old Porco, Agua de Castilla and Porco Village (Figure 3.4). The community of modern Porco comprises predominantly miners and their families. Often families of many generations living in the area have their *estancias* (areas of farm land used to grow potatoes and other vegetables and keep animals, usually llamas). Camelid herding has an important role within the *altiplano*; the animal are a useful source of meat, dung (for fuel), wool, and have also been continuously used as pack animals. The use of camelids has been fundamental to mining and metallurgical processes in the current day and throughout antiquity, especially given

the location of Porco-Potosí within the Cordillera. Modern Porco has a small market and regular buses connect it to Potosí and Uyuni. Miners who work for COMSUR have access to a special medical facility and insurance. Those who work for the cooperatives are not so well cared for. Once people reach retirement age they often move to Potosí or to their *estancias*. Refining of the minerals from the mines is done on an industrial scale. The individual removal of raw ore from the mine is illegal, those caught are subject to losing their jobs. PAPP's work in Porco has indicated that the pocketing of rich ore does occur however, this has been difficult to document. The appropriation of illegal ore has played an important role in metallurgical activity since the early colonial period.

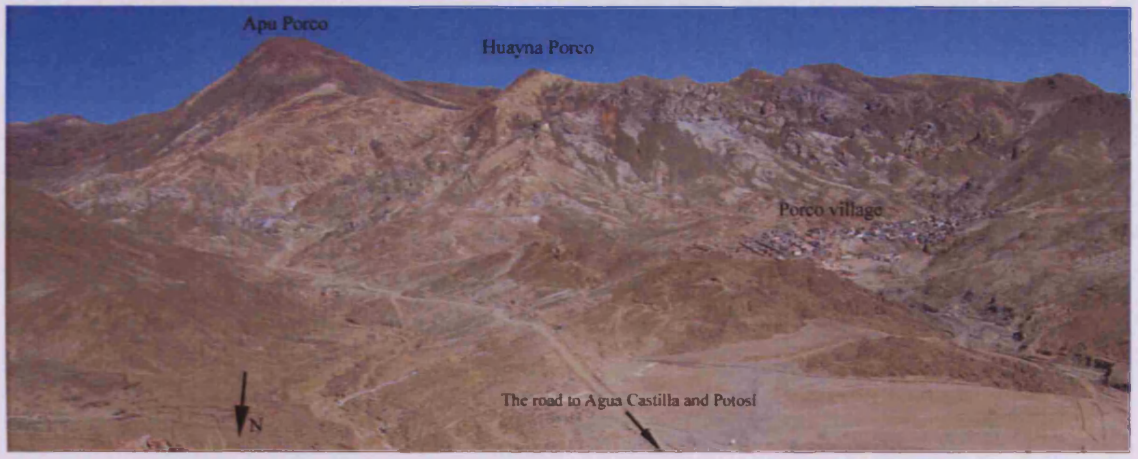

Figure 3.4. The modern Porco mining areas: Apu Porco and Huayna Porco.

In this chapter we reviewed the complex metallurgical and social history of the Porco-Potosí region. Next, the data collected by PAPP on the silver production process of a retired miner who lived outside of modern Porco will be reviewed. Samples taken from the documented productions have been analysed and the results will be presented in the following chapters. This recent metallurgical activity has shown the first documented use of a *huayrachina* in over 100 years.

4. ETHNOGRAPHIC SILVER PRODUCTION USING *HUAYRACHINAS* AND REFINING FURNACES

The ethnographic work carried out by PAPP on Carlos Cuiza's silver production methods provides a basis upon which a technological understanding of metallurgical processes can be gained (Mills 2003, Van Buren 2001, 2003a, 2003b, 2005, Van Buren and Mills 2005). The documented silver production involves the formation of lead metal using a *huayrachina* furnace, and the extraction and refining via cupellation of silver ore; using lead produced previously in the *huayrachinas*. The documented productions can be further understood via an analysis of the materials used and produced (considered in this chapter), and via a review of the chemical and physical processes (discussed in chapter 7). Therefore, this research uses the ethnographic information to document for the first time the lead smelting process and silver cupellation in Bolivia. The use of ethnographic documentation allows for a consideration of all of the stages in the process which has been done by considering the *chaîne opératoire* of Cuiza's silver production and by carrying out analytical work on the products involved in the process. This analysis has focused on smelting as a working *huayrachina* has not been recorded for over 100 years and because the archaeological remains reflect smelting rather than refining activity.

Cuiza's silver production process was documented by PAPP in English although Cuiza spoke Quechua and a member of the PAPP team translated from Quechua to Spanish, and it was recorded by the team using a video camera and photographs. Times, quantities and other information were noted by PAPP (Appendix I). The two stages of the silver production process will be dealt with separately, both for ease and to account for technological disparity between them. The results of these analyses will be documented in Chapter 5 and a discussion will follow in Chapter 6.

4.1. Stage 1– lead production using *huayrachinas*

In 2001 PAPP personnel identified a retired miner, Carlos Cuiza, who used traditional smelting techniques and who agreed to have his production process documented. Carlos Cuiza is the head of his household and is the father of five children (who live on his estate with his second wife, whom he married after his first wife died). He speaks primarily Quechua and does not belong to an *ayullu*. He owns two properties which his wife and children inhabit. His wife tends to their animals (llamas, sheep, cows and chickens) and they grow tubers and beans on their estate (Van Buren 2001). He was a miner but is long since retired. Little else is known about

the other economic activities that the family may be using to generate income; it is assumed that the family have a number of economic methods to bring money into the household (Bolton and Mayer 1977, Deere 1990, Lehmann 1982, and Mayer 1982/2002).

Cuiza said that he learned how to produce silver from his parents who used similar furnaces and sold their silver to the mint in Potosí (Van Buren and Mills 2005). He used to sell his silver privately to Potosíno jewellers. Cuiza was more or less smelting regularly (two/three times a year prior to summer 2004) and produced silver using learnt techniques. His activity was not an artificial reconstruction of an extinct technique but a continuation of traditional knowledge.

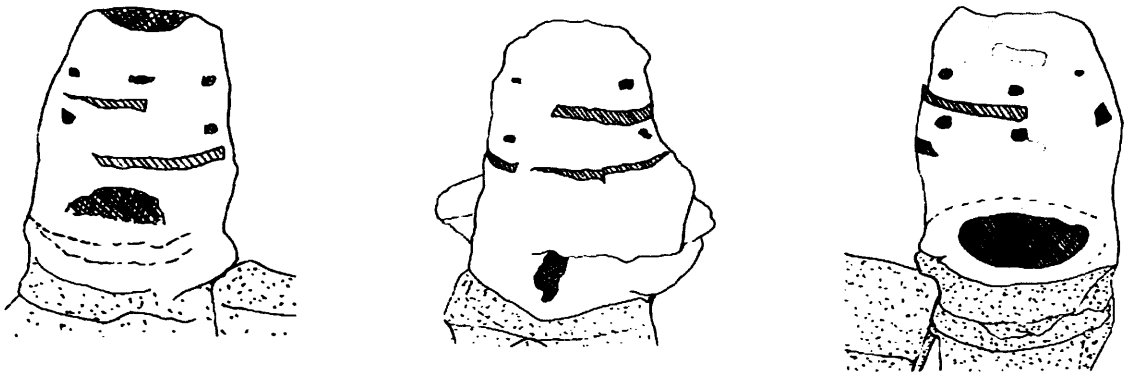

Figure 4.1. Sketches of three different views of one of Cuiza's *huayrachinas*.
This *huayrachina* has two mouths on opposing sides of the column shaft. It is 76 cm high. It is made from natural ravine clay, and has two iron belts incorporated in the shaft for support. The eyes are located on the upper part of the shaft. The *huayrachina* is built onto a large flat base of stones.

His *huayrachinas* sit on a saddle above his house (Figure 4.2), and the metal produced was used to supplement his normal income. Cuiza's *huayrachinas* measured 76 cm high, have an internal height of 45 cm, and sit on top of four or five base stones. The *huayrachinas* had twelve small apertures (referred to as 'air holes' or 'eyes') and two larger openings on opposing sides (referred to as 'mouths') that are facing into the wind (Figure 4.1). The eyes varied in diameter from 2 to 3 cm. They were built from local red clay and had two iron belts that support the column shaft of the furnace. Cuiza called the furnaces variously: *huayrachinas*, *hornos* (Spanish for furnaces) or *abuelitas* (Spanish for little grandmothers).

a.

b.

Figure 4.2. Cuiza's property. His *huayrachinas* sit on the small ridge (right of the centre) above Cuiza's farmstead (mid left).
The small ravine that passes close to Cuiza's homestead houses two refining chambers (a). A closer view of the *huayrachinas* from a side saddle overlooking the site. Cuiza's property and refining furnaces are below on the left hand side outside the image (b).

The PAPP team have recorded and documented three sets of smelts: July 2001, September 2002 and July 2003. In 2001 and 2002 two different smelts were recorded and in 2003 three smelts were documented, thus a total of seven smelts have been recorded.

The 2002 smelt was the most systematically recorded, including documenting input and out put quantities and fully sampling all of the smelting components. There were some variables in the smelting conditions that were necessary to note: smelt times were changed to accommodate observers who had to travel from Potosí to Cuiza's site, and team members rather than Cuiza bought minerals and charcoal (Van Buren and Mills 2005, 10).

The change in starting times may have led to longer smelting periods because wind patterns are variable throughout the day and this directly affects the efficiency of the smelt. Dr Van Buren purchased the minerals (lead and silver ores) in 2002 and 2003, whereas in 2001 Cuiza provided the minerals. Which had not been given to him by acquaintances (Van Buren and Mills 2005, 10). Cuiza owned two *huayrachinas*, but one worked better than the other and during 2002 and 2003 only one was selected for use. The following is a review of Cuiza's smelting

process carried out in 2002 because this is the most complete smelt with some added information regarding sources of ore, fuel and clay. Any differences will also be presented after the review (Appendix I).

Initially Cuiza repaired any cracks or damage on the *huayrachinas*, as they are made from local un-tempered clay and were prone to cracking. It was not necessary to let these fillers dry before the smelt. Cuiza's *compadres* Don Dionisio and Don Juan beneficiated the lead ore by crushing it into fragments of 1 cm in diameter and sorting the pure galena (PbS) from the gangue minerals[2]. Meanwhile Cuiza prepared lumps of used cupellation hearth material (CHM), crushing it to the same size as the ore fragments, which he obtained from his own refining hearth and others in the vicinity of Porco (Van Buren 2003b). The prepared ore and CHM were mixed with urine (provided by Cuiza) ready for the smelt. Cuiza used a mixture of charcoal made from two different woods. He prepared charcoal from *queñua* wood (Van Buren 2003b), and mixed it with *churqui* charcoal which he (or the PAPP team) bought in Potosí. The *huayrachina* was filled with charcoal and donkey dung and lit using *ichu* grass[3] and donkey dung, and the tap hole at the base of the *huayrachina* was plugged with a *queñua* twig. Only when the fire was strong did Cuiza load the charge (beneficiated galena wetted with urine and CHM) in scoop-fulls slowly into the top. Once the furnace was ablaze Cuiza attended to the topping up of the smelt by alternating layers of charcoal, beneficiated ore and CHM.

Occasionally, molten lead was allowed to flow out of the tap hole and Cuiza patiently waited while small quantities of lead metal were tapped from a hole at the base onto an iron dish.

The average smelting process lasted up to eight hours. The total smelt time was highly dependent on the weather conditions as the *huayrachinas* were reliant on strong constant winds to attain high temperatures in their smelting chambers. During the smelt, Cuiza performed *ch'allas*, a symbolic ritual of offerings using coca leaves that were fed into the furnaces, and libations of alcohol. Pieces of slag were removed from the two opposing mouths of the *huayrachina*; Cuiza continuously assessed the slag and decided whether it needed to be re-smelted and thrown back into the furnace or had had the majority of lead removed. When the slag appeared bituminous and less viscous it could be thrown away (Mills 2003, 16). Abram, Cuiza's son said that the discarded slag still contained lead (Van Buren 2001). The result of the *huayrachina* smelt was a quantity (c. 5 kg) of pure lead tapped from the base of the furnace, and larger quantities of irregular lumps of slag (Apppendix I).

---

[2] Gangue is called *charchizo* by Cuiza and his *compadres*.

[3] *Ichu* grass is a spiky grass that grows at high altitude in the Andes.

Figure 4.3. Cuiza using the *huayrachina* to produce lead (Photo by M Van Buren).

Figure 4.4. Lead smelting in the *huayrachinas*. Cuiza in 2001 (Photo by M Van Buren).

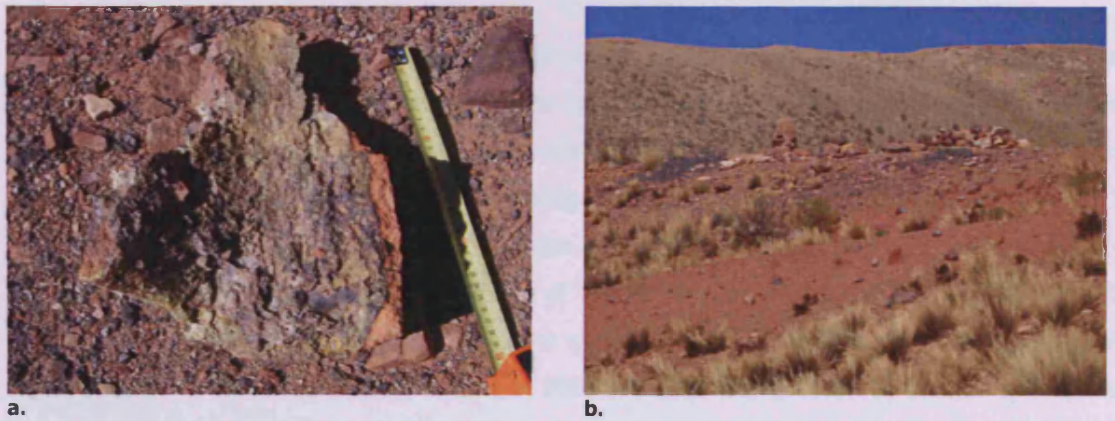

a. b.

Figure 4.5. Older *huayrachina* fragments
Older *huayrachina* fragments around Cuiza's current *huayrachinas* measured in the survey and sampled in 2001 (a).A view of Cuiza's *huayrachina* site (b). The black slag has slid down the ridge. Slag was only collected from the specific documented smelts.

Cuiza is no longer living on his property due to a family dispute and thus is no longer using his *huayrachinas* or producing silver (personal communication July 2006). One *huayrachina* is still

intact but has not been used since 2004 (Figure 4.6). Therefore, understanding this production process is particularly vital as this is currently the last known working *huayrachina* and it provides an opportunity to study traditional Andean silver production in action.

Data and anomalies from the recorded lead smelts

Table 4.1 shows the documented input and output quantities for the seven documented *huayrachina* smelts. The data shows that, in 2001 and 2002, the average amount of lead metal produced was 5 kg per *huayrachina* smelt. The 2001 and 2002 smelts follow the same smelting and time pattern, individual times can be found in the appendix. However, the 2003 smelts are unusual and requires further discussion.

CHM was collected (by Cuiza) for use in the 2003 *huayrachina* smelt from old local cupellation furnaces. Two locations have been documented by the team: Januchupunta (a small *quebrada*/ ravine where CHM was found on the surface: 1.5 kg collected), and Chaco Allana Kullko (an area with three furnaces, possibility more: 4 kg collected). Thus, 5.5 kg of old CHM was collected and mixed with Cuiza's own CHM for the smelt.

The PAPP team purchased the lead ore in Potosí but they experienced difficulty obtaining the ore themselves. The poorer quality of this ore is reflected in the reduced quantity of lead produced in the 2003 smelts. Cuiza noted that his normal ratio of lead mineral to CHM was 2:1, a ratio which he used for the first smelt, although for the second and third smelts he changed this ratio. This change was prompted by 'bad luck' accredited to the presence of a visitor, lack of wind and poor quality of ore.

Thus in 2003 the input ratios differed from those used in the previous years and the amount of lead produced was significantly lower. This is most probably due to the poor quality lead ore that project members bought for Cuiza and may also be due to poor wind conditions. During the smelt, the proportion of litharge in the charge increased considerably for smelt 1 to smelt 3, as did the fuel consumption. For smelt 3, Cuiza initially mixed 16 kg lead ore, 13 kg CHM and 1.5 litres of urine but he only smelted 19 kg of the above mixture (Van Buren 2003b). Despite substantially unchanged total charge weights of around 20 kg and on average considerably higher fuel to charge ratios all the smelts in 2003 were far less successful, producing only half the amount of lead as in previous years. Unfortunately no samples were taken for the 2003 smelts, so I propose that this data only be used to assess the choices made by Cuiza and not as a case study for understanding the *huayrachina's* technological function.

Materials	2001				2002				2003					
	Input Smelt 1	Output Smelt 1	Input Smelt 2	Output Smelt 2	Input Smelt 1	Output Smelt 1	Input Smelt 2	Output Smelt 2	Input Smelt 1	Output Smelt 1	Input Smelt 2	Output Smelt 2	Input Smelt 3	Output Smelt 3
Lead Ore	12 kg		14 kg		12 kg		11 kg		10 kg		14 kg		16 kg	
CHM	7 kg		8 kg		6 kg		6 kg		6 kg		11 kg		13 kg	
Urine	0.5 litres		0.5 litres		0.5 litres		0.5 litres		?		0.75 litres		1.5 litres	
Charcoal	12 kg		?		8 kg		8 kg		15 kg		16 kg		10 kg	
Lead Metal		**4 kg**		**6 kg**		**4 kg**		**5 kg**		**2 kg**		**2.5 kg**		**2 kg**
Slag		**?**		**?**		**9 kg**		**7 kg**		**9 kg**		**16 kg**		**10 kg**

Table 4.1. Input and output data for the all seven documented *huayrachina* smelts. In Smelt 3 2003 only 19 kg of the mixed lead ore and litharge were smelted in the *huayrachina*. CHM=Cupellation hearth material, rich in litharge (PbO) (Data from Van Buren 2001, 2003a,b; Van Buren and Mills 2005).

4.2. Stage 2– refining via the use of cupellation

The lead metal produced in the *huayrachinas* was used to extract silver from rich silver ore. Cuiza had two cupellation furnaces: one built by his parents 30 years ago, and the second built after a family dispute with his brother. The second furnace was built using the measurements of the first, although the older furnace works better, which explains why it was preferentially selected by Cuiza to refine his silver (Van Buren 2001). Both the furnaces were located in small huts, in a ravine next to Cuiza's property. These huts were constructed of stone, bricks, and wood, and had a thatched roof; they were extremely well camouflaged within the surrounding countryside (Figure 4.6). In fact from Cuiza's property was easy to miss the location of the huts. Cuiza said that the furnace and hut need to be repaired regularly (Mills 2003, 20).

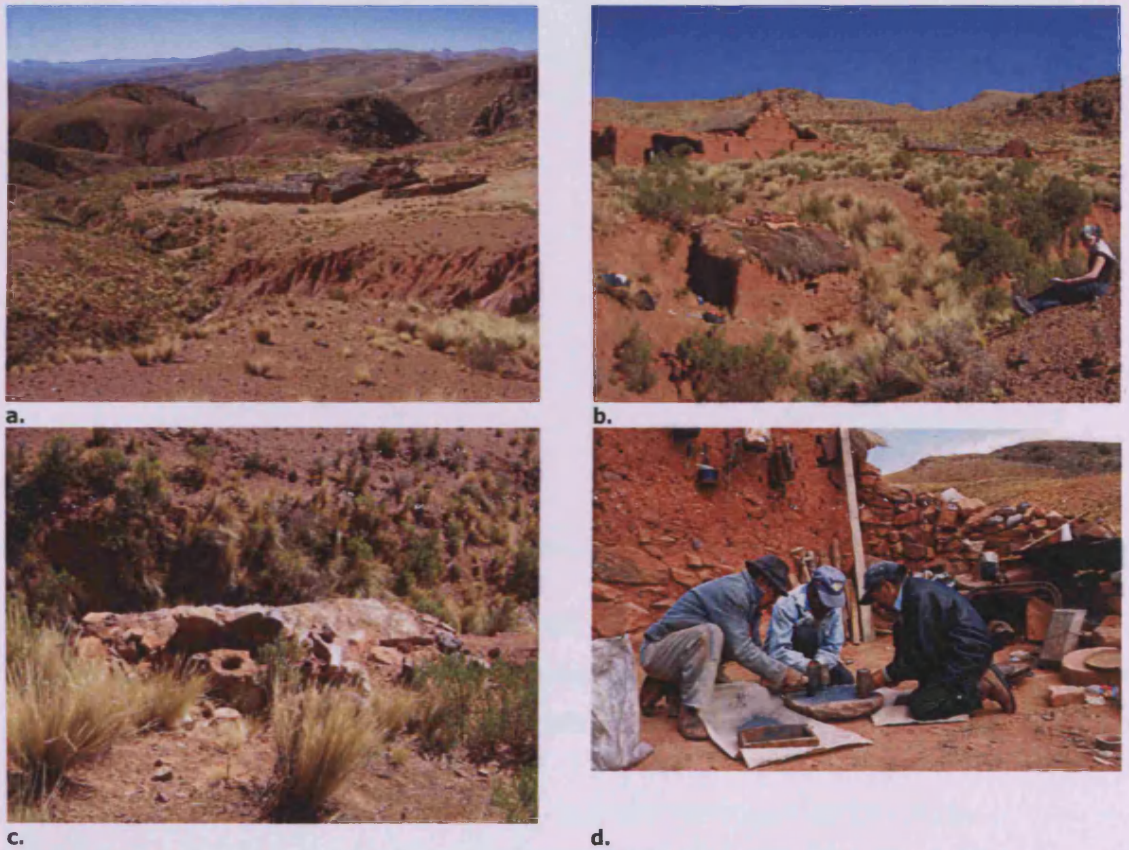

Figure 4.6. Cuiza's refining.
Cuiza refining takes place in a small ravine close to Cuiza's homestead (a). He has two cupellation huts that are well camouflaged in the ravine (b). The hut is hardly visible from above (c). The silver ore is beneficiated using hammers and a large grinding stone (d).

The following is a summary of the cupellation procedure and as with the *huayrachina* smelts any anomalies in the procedure will be explained after the main summary.

The cupellation furnace consists of three chambers: the main chamber which holds a concave hearth, a fire box positioned to one side and slightly below the main chamber, and a chimney on the opposite side of the hearth (Figure 4.7). The furnace uses natural draft to carry the heat and flames from the firebox over the hearth and through the chimney out of the furnace structure. It is made of finely screened clay taken from the local ravine (Mills 2003, 20). The hearth is lined with plant ash made from *llareta (Azorella compacta)* (Van Buren and Mills 2005), a moss-like woody plant native to the *Altiplano (Appendix II, 54)*.

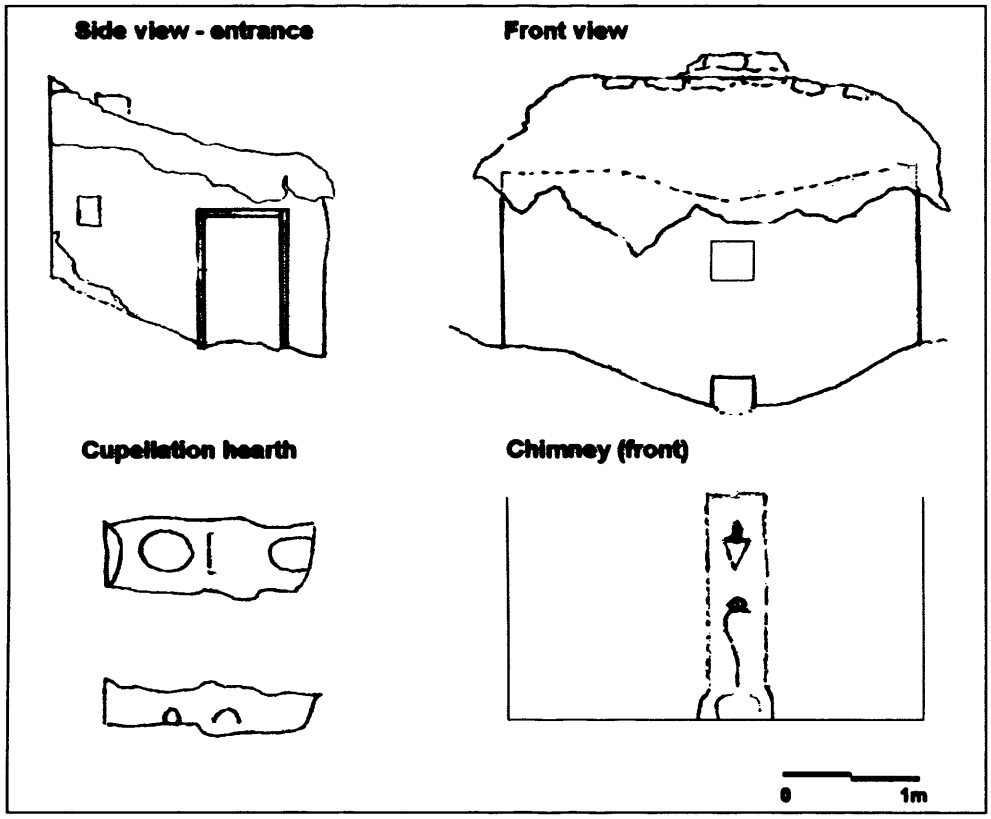

Figure 4.7. A sketch of the cupellation hut and hearth.

It is not known how Cuiza produces the *llareta* ash. Was the *llareta* plant used as a source of fuel as noted in the historical accounts? Or used in a culinary context? What method was used to produce the ash? Was it produced especially for this process? This information remains an anomaly.

The ash acts like a sponge and absorbs the liquid litharge formed during the cupellation process. The plant ash was wetted with urine and packed into the hearth, 1-2 cm thick. Cuiza used a round stone to smooth the hearth into a concave shape, checked the curvature by rolling a marble (Van Buren 2001) and prepared the fire box by loading *uchu*/llama dung and *thola* wood. The lead was placed on the hearth through an opening at the top of the chamber which was then closed. The fire was started using *thola* wood and after approximately one hour the fuel

was changed to llama dung handfuls of which were thrown in continuously at regular short intervals.

Once the lead had melted, Cuiza briefly removed the door from one of the side openings of the central chamber and added finely ground silver ore with an iron spoon (In 2002, the silver ore was beneficiated by Don Dionisio and Don Juan; Figure 4.6 d). Cuiza asked to use his wife's grinding stone and she said that he was not allowed because his work was too dirty (personal communication with Dr Van Buren 2008). The whole process took up to twenty hours during which Cuiza continued adding the *llama* dung and stoking the firebox, and adding as much of the powdered ore as possible.

At the end a button of pure silver remained on top of a litharge cake/CHM. Cuiza described the molten silver as having "...colour and radiance of the sun when it just begins to rise." (Van Buren 2001, 4). Cuiza said the silver was removed from the chamber "..like one removes bread from an oven" (Van Buren 2001, 4). It solidifies immediately after formation and can be removed as a solid piece. The CHM can be removed from the hearth and used as part of the charge in the next *huayrachina* smelt.

A variety of tools were used by Cuiza during the cupellation. Some being specially commissioned by him and made in Potosí. The commissioned tools such as, rabbles and iron dishes, were made out of wrought iron, other tools were constructed by Cuiza using scrap metal and household waste. For example, pieces of sheet metal with holes were used as sieves. Tin cans were commonly used for transporting ore, water and urine.

Cuiza told the team that the silver can become *celosa* (jealous) and in order for the cupellation to work he allowed only people present at the *huayrachina* smelt to attend the cupellation and once the cupellation had begun no one else could look at the furnace. While smelting in the *huayrachina* Cuiza was happy for anyone to participate and ask questions, although during the cupellation he was secretive. He was nervous of people talking too loudly within the chamber as he said the silver would become jealous (Mills 2003). Mills noted that the documentation of the refining process was quite difficult because Cuiza did not answer all her questions. Even with these small problems it is clear that the majority of the process had been documented over the three year period that the team worked with Cuiza.

Data and anomalies from the recorded cupellations

Data from the production process for each consecutive year is available, through the most reliable is the data from 2001 (because it successfully produced a silver cake). The 2003 refining is good although the hearth broke and some of the metal was lost. It is also necessary to note that Cuiza said he modified the silver charge, reducing the quantities to accommodate the PAPP team. He would usually produce greater quantities of silver metal to sell on to jewellers in Potosí. The data from 2001 does show that he used a ratio of about 1:6 (Ag ore : lead metal).

A number of problems occurred with the cupellations during the 2002 and 2003 procedures, in 2002 the PAPP team bought the silver ore. Cuiza commented that the ore was unsuitable for refining as it was of poor quality (this has been confirmed via analysis). Accordingly, the cupellation was very unsuccessful only producing 0.013 kg of silver metal from 1.5 kg of 'silver' ore and 3 kg of freshly smelted lead metal.

Materials	2001		2002		2003	
	Input	Output	Input	Output	Input	Output
Silver ore	0.3 kg		1.5 kg		0.5 kg	
Lead metal	1.8 kg		3.0 kg		6.0 kg	
Llareta ash	~		~		~	
Dung	12 costales		61.5 kg		66 kg *llama* dung, 1 kg *burro* dung	
Other fuel					1 kg firewood, 0.5 kg dry grass	
Silver metal		**0.15 kg**		**0.01 kg**		**0.23 kg**
CHM	**?**	**?**		**5.0 kg**		**6.0 kg**
Slag		**?**		**7.1 kg**		**0.5 kg**

Table 4.2. Input and output quantities for the documented silver refining episodes.

In the 2003 cupellation 6 kg of lead metal was used to cupel the silver ore bought by the PAPP team, that is a ratio of 1:12 (Ag:Pb). However, silver yield per ore quantity for 2001 and 2003 is similar and unfortunately no samples were taken of the silver ore used in 2003. The 2003 production was more successful than the 2002 refining but the hearth lining ruptured during the cupellation and the majority of silver was lost into the hearth. Cuiza said that for this smelt the loss of silver was not detrimental as he would have been able to reclaim the silver via *huayrachina* smelting as well as repeat the cupellation.

4.3. Initial summary of silver production process

The documentation of Cuiza's silver production process provides necessary technical information regarding learned knowledge and the continuation of technological development within the Porco community. The focus of this study has always been to document the production processes with reference to the study of metal production in the past, thus the material samples considered here have been catalogued in the Appendices as reference for other researchers (Appendix I and II). Problems encountered by the PAPP team during the ethnographic documentation concerned the accessibility to raw materials such as fuel, lead ore, silver ore and plant ash. The difficulty obtaining these materials is relevant not only to the current day silver production process but most likely also to silver production in antiquity. Therefore, from each stage of the process more specific research questions arose:

Stage 1 - documented *huayrachina* smelts

Regarding the technological function:

- How does the modern *huayrachina* work? How are the different redox conditions created?
- What is the temperature range in the reaction chamber?
- What sort of slag is produced?
- How efficient is the process i.e. how much lead is produced compared to the amount available in the starting ore?
- What type of fuel is used? How does this affect the reaction and function of the furnace?
- How do variable wind conditions affect the reactions?
- What role do the ventilation holes/eyes play in the smelting reaction?

Regarding the ethnographic study:

- Why is Carlos Cuiza using this method of production?
- Why are the two stages separated?
- How does Cuiza make decisions during the process?
- How often does Cuiza use the *huayrachinas*? What season does he use the furnaces in?
- How does Cuiza access the raw materials needed for continuity of the practise?
- How is the choice of raw materials determined?
- How and why does Cuiza sustain this practise?
- Where does the name *huayrachina* come from? *Huayra* means wind in *Quechua*, does this have implications for the origins of this style of furnace?

Stage 2-cupellation (silver refining)

The process of cupellation is highly specialised, it requires sustainable temperatures greater than 1000°C and oxidising conditions for the process to occur. The separation of smelting and refining also means that unrefined silver ore is added directly to the cupellation hearth. Therefore, reactions in the hearth need to firstly oxidise/roast the ore to remove the sulphur components to ensure sufficient lead is present within the system to allow for cupellation to take place. While this process is unusual from a European point of view, it does not hinder the refining from taking place. It does, however, make the process much longer and harder because more fuel is needed to remove sulphur and heat the hearth sufficiently. We cannot easily assume a working model for the cupellation – the ethnographic data documented is not adequate to describe an 'ideal cupellation', but chemical analyses may provide a more detailed understanding of the refining process.

More specific research objectives have been asked of the cupellation samples selected for analytical work, these have helped to structure the analyses.

Regarding the technological function:

- How suitable was the silver ore? What quantity of silver was present and how much was extracted?
- What is the nature of the hearth lining? How suitable are the components such as llareta ash, fuel etc? What characteristics define the hearth lining? What is its chemical composition?
- How efficient was the cupellation process? How absorbent was the hearth lining, and what happened to the hearth lining during cupellation?
- What heavy metals were present/trapped in the hearth lining? What metals collect in the lead/silver prills?
- How pure was the silver produced?

Regarding the ethnographic study:

- Why was this refining stage more secretive and protected than the smelting stage?
- Why was Carlos Cuiza using this method of production?
- Why are the two stages separated?
- How did Cuiza make decisions during the process?
- Why did Cuiza chose to continue this process rather than any other silver extraction method?
- How many times a year does Cuiza did this?

- How many people knew about Cuiza's silver production? Who did he share his ideas with?

The more specific research questions derived from the detailed study of the ethnographic silver production were used along with the main research aims and objectives to approach the analytical work to be done on selected samples from both stages of the process. From stage 1, the lead smelting in the *huayrachina*, the analytical work carried out on the ceramic furnace wall, CHM, ore, slag and lead metal is presented in Chapter 5. From stage 2, samples were selected from each stage of the process: lead, silver ore, llareta ash, CHM and silver metal. These have been prepared and analysed using the methodology outlined in chapter 2. The results are presented in Chapter 6.

5. RESULTS FROM THE ETHNOGRAPHIC LEAD SMELTING

This chapter deals with the results from the technical analysis and review of the ethnographic lead smelting described in chapter 4. The data is presented using five key material categories from the silver production process: the ore, the cupellation hearth material (CHM, added to the *huayrachinas*), the furnace wall/ceramic, the slag and the resultant lead metal. A partial review of the relevant results obtained from chemical and physical analyses is presented here. A discussion of these results and full interpretation will follow in chapter 6.

5.1. The ore

The ore samples taken from Cuiza's smelt are divided into two categories: selected ore (used in the subsequent *huayrachina* smelts) and rejected ore/tailings. From the 2001 smelts, three samples of ore were available, two selected and one rejected. From 2002 two bags of samples were available; two hand specimens were mounted from the selected ore and four from rejected (Table 5.1). In total, four selected and five rejected ore samples have been analysed.

Mounted blocks	Year of smelt	Description
2	2001	Lead ore 1st smelt
3	2001	Lead ore 2nd smelt
15	2002	Lead ore 2nd smelt
16	2002	Lead ore 2nd smelt
4	2001	Rejected ore 2nd smelt
17	2002	Rejected ore 1st smelt
18	2002	Rejected ore 1st smelt
19	2002	Rejected ore 2nd smelt
20	2002	Rejected ore 2nd smelt

Table 5.1. Samples used in ore analyses.

The selected ore samples range in size from being powders to lumps of 1-2 cm wide (Figure 5.1.a) as they were beneficiated by Carlos Cuiza and his *compadres* prior to use in the *huayrachinas*. The selected ore samples are primarily galena (lead sulphide). They have a distinctive shiny, almost metallic appearance and many of the larger pieces have a light brown/yellow patina.

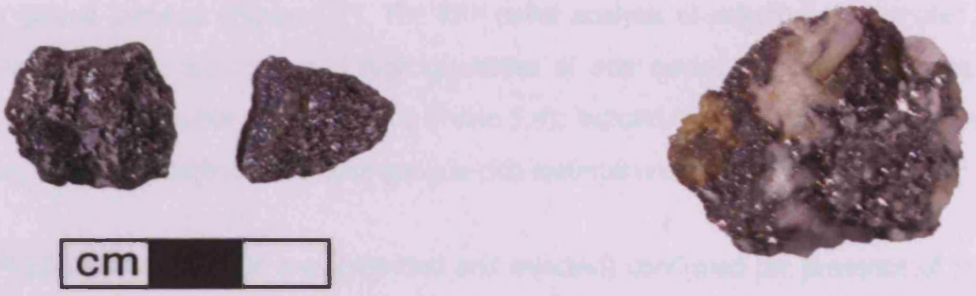

a. b.

Figure 5.1. Beneficiated galena from the 2002 smelt (a). Gangue minerals rejected for smelting in 2002 (b).

The pieces are angular, most probably due to the natural cleavage of the galena crystals. In contrast, rejected ore samples contain large quantities of gangue minerals such as quartz and siderite, but also often galena and chalcopyrite (Figure 5.1. b), unseparable from the gangue, therefore being unsuitable for smelting. It is important to note that during beneficiation, samples are rejected or selected by eye, then crushed and sorted. Thus, samples higher in the dark shiny galena are chosen over whiter pieces richer in these gangue minerals.

OM of the selected ore confirms that the majority of it is galena. With OM, galena is recognised by its distinctive triangular patternation and white reflection. The selected ore also contains pyrite (FeS_2) seen under the OM as cubic, slightly yellow euhedral crystals. Interspersed are crystals of sphalerite (ZnS), lightly textured mid grey crystals. The rejected ore seems to have a much higher gangue content but also crystals of chalcopyrite are seen as bright, shiny crystals with a light greenish yellow colour via OM. Quartz crystals are richly dispersed within the rejected ore (Figure 5.2).

ED-XRF analyses using pressed pellets of the selected lead ore samples confirmed the presence of copper (0.1%), lead (45-76%), sulphur (7-11%), zinc (12%) and highly variable iron (up to 30%); see Table 5.3. The high quantity of iron (30%) and concentrations of manganese (4%) and silica (1%) in sample 3 (2001) indicate the presence of excessive and unwanted gangue mineral in selected ore. This could indicate that the mineral was less than satisfactorily sorted. XRF pellet analyses also confirmed that only minimal quantities of silver (0.2% - 0.07%) were present in the selected ore (Table 5.3). Antimony and arsenic were present at even lower concentrations.

Compared to the selected ore, the rejected ore samples contain less galena and consist of larger pieces of gangue material interspersed with residual areas of galena. Rejected ore samples have a quartz and carbonate matrix and were easily distinguishable by eye from the

rich galena samples (Figure 5.1). The XRF pellet analysis of rejected ore samples 19 and 20 showed that the ore contained high quantities of iron oxides (60%), manganese (3%) and lower lead and sulphur concentrations (Table 5.4); indicating that hand sorting by eye is, in this case, a suitable method to remove gangue-rich material unsuitable for smelting.

SEM-EDS analyses of the ores (rejected and selected) confirmed the presence of chalcopyrite, galena, and sphalerite (Appendix II). The gangue mineral analysed in the majority of the rejected ore appears to be siderite (Fe, Mn, Mg) CO_3.

The analyses have shown that the selected ore used for smelting is predominantly galena (PbS), sphalerite (ZnS), pyrite (FeS_2) and minimal chalcopyrite ($CuFeS_2$). It is a suitable ore for lead smelting, but its silver content is very low.

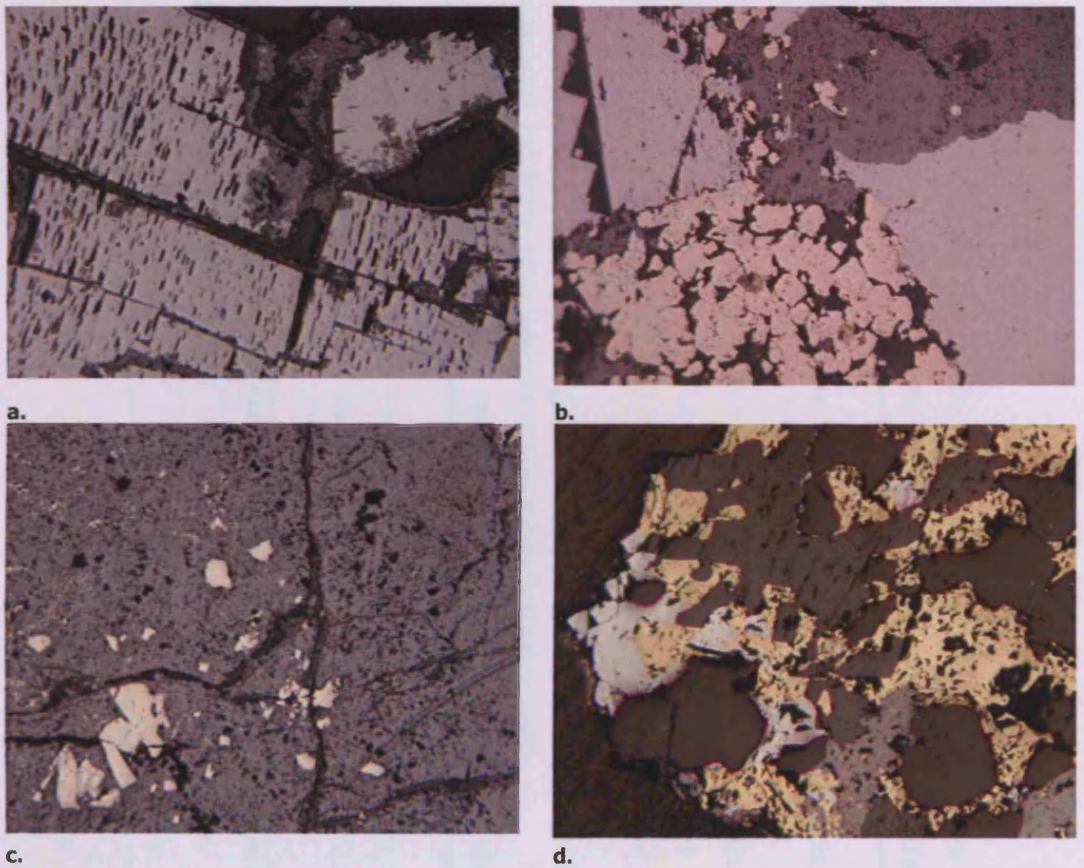

Figure 5.2. Ore from the 2001 smelts.
Selected ore 2 from the 2001 smelt; Image a shows typical galena areas with the distinctive triangular patternation. OM Image b is selected ore sample 3 (2001). Typically the selected ore has a base of galena (PbS), the brightest phase in the images above. Sphalerite (light grey textured phase) and pyrite (light yellow phase) are also present. Large areas of the selected ore consist of sphalerite with small pyritic inclusions (cream/ white); Image c (Selected ore 2 from the 2001 smelt). Rejected ore has a mixture of different phases and chalcopyrite predominates in this image (bright yellow phase); Image d (Rejected ore 18 2002). Quartz, sphalerite and galena are also presented here.

Element	Na	Mg	Al	Si	S	Cl	K	Ca	Mn	Fe	Pb	As	Zn	Cu	Co	Ni	Ga	Cd	Sb	Hf	Ta	Bi
	%	%	%	%	%	%	%	%	%	%	%	%	%	%	µg/g	µg/g	µg/g	µg/g	µg/g	µg/g	µg/g	µg/g
Selected lead ore 16 2002	1.7	0.3	0.1	0.1	23.9	5.3	0.1	~	~	0.1	68.2	0.1	~	~	159	226	159	17	321	405	174	318
Rej ore 17 2002	1.8	2.1	~	4.7	8.5	2.7	~	0.2	2.3	48.9	28.5	~	0.2	~	420	66	100	39	38	312	128	172
Rej ore 18 2002	0.3	0.9	0.3	57.5	9.2	1.5	~	0.1	0.7	16.7	2.2	~	9.6	0.9	161	129	23	153	5	117	134	29
Rej ore 19 2002	0.9	5.8	0.1	~	1.2	~	~	0.4	4.3	75.2	12.0	~	~	~	352	31	72	4	9	84	30	108

Table 5.2. XRF analyses of mounted block ore samples.
Analysed using Turbo quant and displayed as elements in wt% and normalised to 100%.

Element	Mg	Al	Si	S	Ti	V	Cr	Mn	Fe	Pb	Ni	Cu	Zn	As	Ag	Cd	Sb
Selected lead ore 3 2001	0.04	0.20	1.42	6.73	0.02	trace	0.04	4.19	29.69	45.94	0.01	trace	11.41	0.03	0.21	0.02	0.09
Selected lead ore 5 (MB 15, 16) 2002	0.04	0.02	0.02	10.68	0.01	0.02	0.01	0.02	0.78	75.76	0.01	0.10	12.50	trace	0.07	0.02	0.03

Table 5.3. XRF data analyses of lead ore pressed pellets used in *huayrachina* smelts. Analysed via Alloys setting. The data has been normalised to 100 wt%.

Element	MgO	Al2O3	SiO2	SO3	CaO	TiO2	V2O5	Cr2O3	MnO	Fe2O3	PbO	ZnO	As2O3	SrO	Ag	Sb	Tl
	%	%	%	%	%	%	%	%	%	%	%	µg/g	µg/g	µg/g	µg/g	µg/g	µg/g
Rej ore 4 (MB 19, 20) 2002	5.28	0.86	1.23	8.80	0.24	trace	trace	0.01	2.68	58.16	22.58	239	115	143	38	36	533

Table 5.4. XRF data analyses of rejected lead ore pressed pellet analysed using Turbo quant
Data has been normalised to 100 %.

5.2. The Cupellation Hearth Material (CHM) added to *huayrachinas*

The *huayrachina* charge materials also consist of cupellation hearth material (CHM) which was mixed with the beneficiated lead ore. This material was taken from Cuiza's previous refining episodes and collected from other refining furnaces near his property. Samples have been taken from the 2001 and 2002 smelts and four are available for analysis (Table 5.5).

Mounted blocks	Description	Notes
2001		
Not mounted	CHM added to 1st smelt	labelled #5
6	CHM added to 2nd smelt	
2002		
21 (re-labelled 19)	CHM added to 1st smelt	
22	CHM added to 2nd smelt	

Table 5.5. CHM samples added to the *huayrachina* smelts selected for analysis.

Two samples of CHM were prepared for XRF pressed pellet analyses (Samples 5 and 21). The results (Table 5.6; Table 5.7) indicate that sample 21 has a heavy metal content containing lead (70%), zinc (3%), antimony (0.9%), arsenic (1.3%) and silver (0.05%). Sulphur is still present (10%) indicating that the cupellation of an ore took place rather than a metal. Sample 5 is predominately lead oxide (90%), lime (3%) and silica (3%).

Element	Na2O	MgO	Al2O3	SiO2	SO3	K2O	CaO	TiO2	Fe2O3	PbO
Dimension	%	%	%	%	%	%	%	%	%	%
CHM 21 2002	0.00	1.04	0.77	7.01	10.02	0.55	3.40	0.06	0.94	70.00
CHM 5 2001	2.08	0.20	0.51	2.68	0.00	0.24	3.14	0.04	0.19	90.00

Table 5.6. XRF data (major elements) of pressed pellet CHM analyses added to *huayrachinas*. The data has been normalised to 100 wt%.

Element Dimension	ZnO µg/g	As2O3 µg/g	Sb2O3 µg/g	Co3O4 µg/g	NiO µg/g	CuO µg/g	Ga µg/g
CHM 21 2002	29169	13163	9498	31	264	1203	317
CHM 5 2001	304	602	129	58	189	48	169

Element Dimension	SrO µg/g	Ag µg/g	SnO2 µg/g	Ba µg/g	Hf µg/g	Bi µg/g
CHM 21 2002	942	525	221	197	247	1047
CHM 5 2001	958	72	0	137	74	23

Table 5.7. XRF data (minor/trace elements) of pressed pellet analyses of CHM added to *huayrachinas*. The data has been normalised to 100 wt%.

CHM sample 6 2001

Sample 6 was taken from a collection of CHM prepared ready for smelting in the *huayrachinas* in 2001. The origin of this material is unknown, it could have been collected from other refining hearths or from Cuiza's own.

a. b.

Figure 5.3. A selection of CHM samples (a). These samples would have been added to the *huayrachina* in 2001. The mounted CHM sample 6 is shown in image b.

The analysis was done partly to establish if the CHM has the same characteristics as Cuiza's own litharge. Sample 6 was selected for analysis and mounted in resin in 2001. The polished mounted sample has three distinct layers with a yellow strip crossing the bottom of the sample. No metallic inclusions are visible by eye in this sample (Figure 5.3 b). The SEM-EDS images and chemical analyses have shown that this sample contains circa 70% lead oxide and less than 2% of other heavy metal oxides (Table 5.8). The structure is extremely porous and still contains some open pores. The majority of the sample is filled with a pure lead oxide matrix. This matrix is visible in the images as the light grey inter-fill/matrix. In more localised areas, the liquid lead

oxide has absorbed heavy metals including antimony oxide (9%) and copper oxide (2%) (Appendix II). The formation of lead-calcium silicates is very common, and it is likely that this calcium comes from the llareta ash rather than the ore minerals used for the cupellation. Sample 6 has various other crystal phases in smaller quantities; while the focus of this work is not to identify all phase information the following should be documented. The SEM-EDS analyses has shown the presence of black lead silicates with differing complex oxides combinations (Figure 5.4; Table 5.9).

Sampled area	Na2O	MgO	Al2O3	SiO2	K2O	CaO	FeO	ZnO	PbO
Average (n=5)	0.2	0.8	3.0	14.9	2.2	6.3	1.0	1.9	69.7

Table 5.8. CHM sample 6 2001 – average bulk scanned areas of the CHM avoiding metallic prills from the upper lead oxide layer, data normalised to 100 wt%.

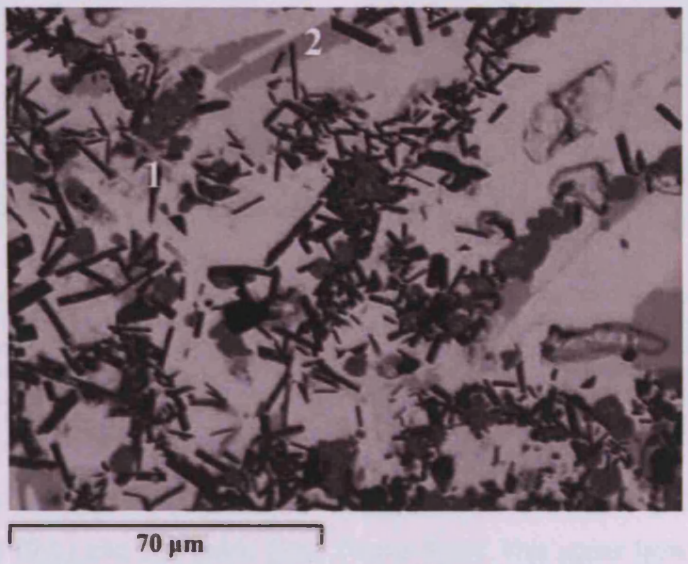

Figure 5.4. SEM image of CHM sample 6 showing different minerals formed in the CHM. Dark angular inclusions (1) and grey semi angular phases (2).

Scanned area	MgO	Al2O3	SiO2	CaO	FeO	ZnO	SbO	PbO
Dark black angular inclusions - low lead high antimony & calcium (1)	1.2	8.4	7.0	22.3	5.9	8.1	37.5	9.6
	0.9	7.9	1.0	20.7	6.2	20.4	36.5	6.4
Mid grey semi angular phases – lead antimony calcium oxide (2)	0.6	4.7	1.5	16.3	3.7	4.8	29.8	38.6

Table 5.9. Different mineral phases within CHM sample 6 (See Figure 5A. 4) . Data has been normalised to 100 wt%.

CHM 21 2002

Sample 21 has two discrete areas: a matrix of free lead oxide with inclusions of well developed crystals particularly in the upper part of the sample. The lower half of the sample is composed of hearth lining partially soaked with lead oxide (Figure 5.5).

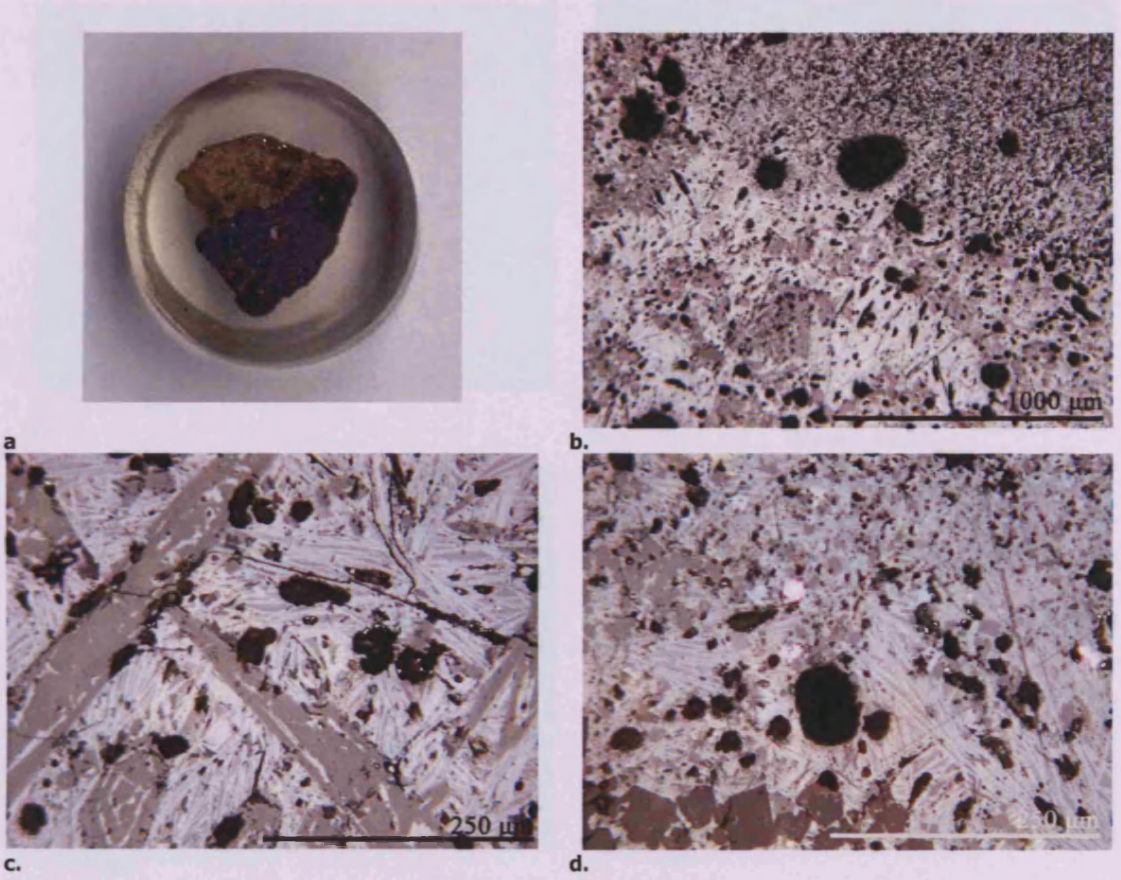

Figure 5.5. CHM sample 21
The mounted block of CHM sample 21 added to the *huayrachina* smelt in 2002 (a). Note the upper half of the sample (yellow/brown) is free lead oxide and the lower half is the hearth lining (purple/brown area). CHM sample 21 shows evidence of interaction between the lead free oxide and the lower hearth lining, seen in image b. The free silicate layer contains different crystal phases embedded in a lead oxide matrix (c and d). Small lead metal prills and lead silicate crystals (bottom grey crystals, d) are found within the lead oxide matrix (d).

The SEM-EDS scanned area analysis of the lower layer confirmed that it was composed of lead oxide (75%), silica (9%) and iron oxide (3%) (Table 5.10). This upper layer also contains zinc and arsenic. The upper section of the sample is composed of lead oxide (51%), ion oxide (29%) and zinc oxide (13%), Table 5.11. Increased concentrations of heavy metals in the system allowed the formation of iron and zinc rich phases and the llareta ash promoted the formation of feldspars. Within the lead oxide matrix, various phases re-crystallise. Darker grey crystals, with lead oxide (47%), lime (23%) and high arsenic oxide content (20%) are associated with light grey angular crystals lower in arsenic oxide (2%) but higher in silica (17%) and lead oxide (67%). Hexagonal crystals of antimony oxide and lime are also present in the lead oxide matrix.

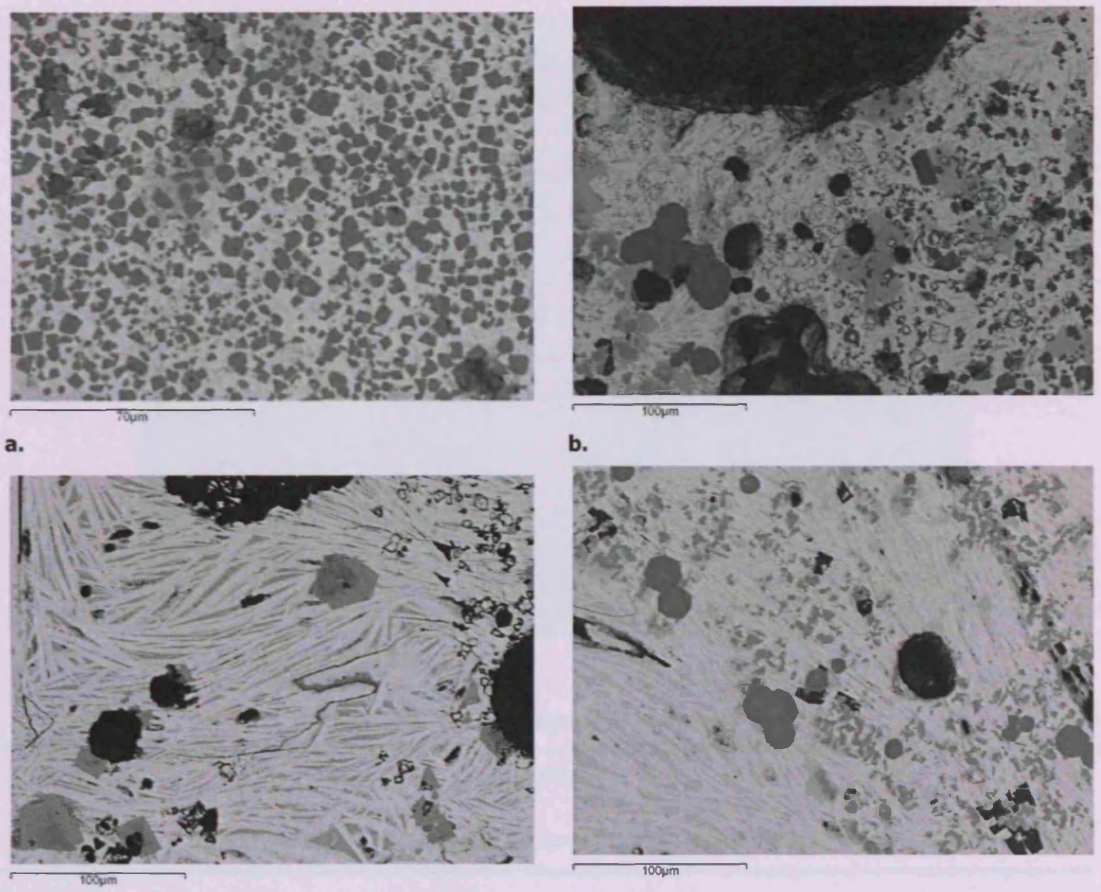

Figure 5.6. This backscattered electron image of sample 21 shows the complex nature of CHM. The lead oxide matrix (light grey) is scattered with mid grey euhedral crystals (c) which are iron and zinc oxides with up to 8% nickel. Also in this micrograph are feldspars (dark black angular crystals upper left of image). CHM sample 21 has calcium antimony silicates (light grey crystals) and a matrix of free lead oxide (long thin needle like crystals), image d.

Spectrum	Na2O	MgO	Al2O3	SiO2	CaO	FeO	ZnO	As2O3	PbO
1	~	~	1.6	9.5	6.1	2.9	1.4	2.0	76.5
2	0.5	0.8	1.8	9.5	7.6	3.5	2.2	1.1	73.2
3	~	0.9	1.4	9.2	6.2	3.1	1.8	1.0	76.5
Average CHM 21 lower layer	**0.2**	**0.6**	**1.6**	**9.4**	**6.6**	**3.1**	**1.8**	**1.4**	**75.4**

Table 5.10. SEM-EDS bulk area analyses of the lower lead oxide layer of sample CHM 21. The data has been normalised to 100 wt%.

Spectrum	Al2O3	SiO2	CaO	FeO	NiO	ZnO	As2O3	PbO
1	0.8	3.5	0.7	28.8	1.4	13.9	1.3	49.7
2	~	3.8	0.6	29.6	1.8	12.5	~	51.7
3	0.8	3.1	0.6	28.1	2.0	11.4	1.6	52.5
Average CHM 21 upper layer	**0.5**	**3.5**	**0.6**	**28.9**	**1.7**	**12.6**	**0.9**	**51.3**

Table 5.11. SEM-EDS bulk area analyses of the upper layer of sample CHM 21. The data has been normalised to 100 wt%.

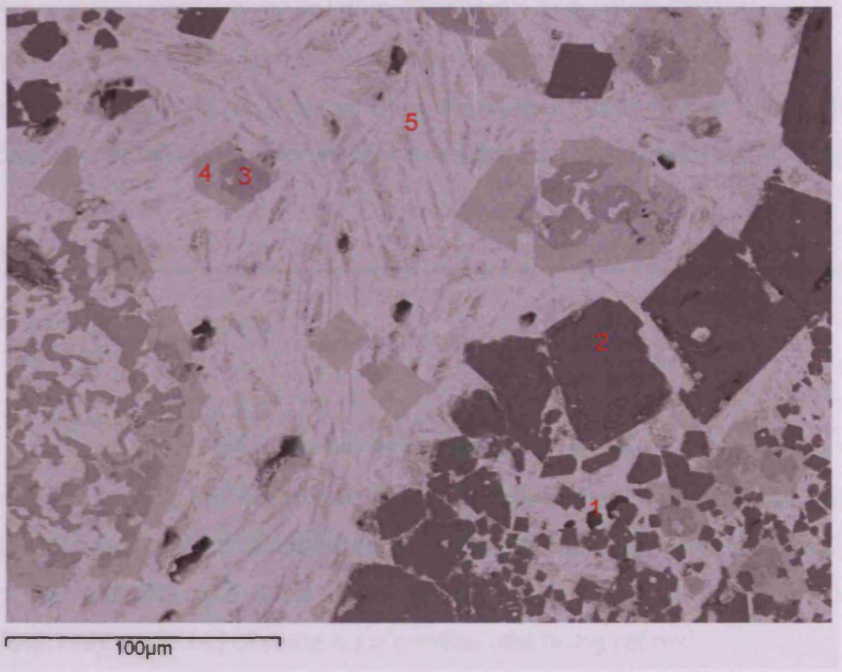

Figure 5.7. SEM image of CHM sample 21.
Five different labelled areas indicate the variability in the structure of the sample. N.B. Area 5 is free lead oxide.

Scanned areas	MgO	Al2O3	SiO2	K2O	CaO	FeO	CoO	NiO	ZnO	As2O3	PbO
Area 1 (n=3) Leucite	4.1	21.9	36.8	28.7	~	3.0	~	~	5.7	~	4.8
Area 2 (n=6) Spinel	~	1.8	~	~	~	64.5	1.1	8.1	21.2	~	1.9
Area 3 (n=2)	~	~	6.7	4.1	22.8	~	~	~	~	19.6	46.9
Area 4 (n=6)	~	0.5	18.6	~	11.2	0.4	~	~	~	2.1	67.3

Table 5.12. SEM-EDS scanned area analyses of CHM sample 21.
The data has been normalised to 100 wt%.

Sample 21 appears to be CHM material made from the interaction between a hearth lined with llareta ash and free lead oxide. ED-XRF analysis of llareta ash presented in chapter 6 shows that it is composed of silica (36%), lime (31%), potash and alumina, magnesium oxide, iron oxide and soda. The silica content in the llareta ash reacts with the free lead oxide to form lead silicate lime crystals. The presence of heavy metals such as zinc and iron within the CHM indicates that an ore mineral may have been refined during this process. If metal were being refined these metals would not be present.

CHM 22 2002

CHM sample 22 would have been added to the *huayrachina* smelts in 2002. The SEM-EDS analyses of this sample is different to CHM 21 in that less crystal phases are present. It has a chemical composition of lead oxide (76%) with silica (13%), lime (7%), and alumina (3%),

Table 5.13. No metallic phases were found in the sample and unlike CHM 21, no iron oxide was present. The crystal phases found in this sample are simpler and easily identifiable as lead-calcium silicates (Appendix II). Analysis of the main matrix indicates that it was almost always pure lead oxide, and possible remains of plant ash were also analysed in this sample.

Scanned area	MgO	Al2O3	SiO2	K2O	CaO	FeO	ZnO	PbO
Average bulk area of CHM sample 22 (n=5)	1.0	2.9	12.7	0.3	7.1	~	~	76.1

Table 5.13. SEM-EDS data of bulk area scans of CHM sample 22 2002. Data has been normalised to 100 wt%.

The CHM samples added to the *huayrachina* are composed of primarily free lead oxide, and the documentation of lead calcium silicates show interaction between the lead oxide and plant hearth lining. No metallic prills were found in this sample, indicating the efficiency of the refining process. Here we could assume a pure metal was being refined.

Why did Cuiza add CHM to the *huayrachina* smelt?

The CHM added to the *huayrachinas* contribute lead oxide to the smelting process. The addition of CHM to the lead smelting process allows for co-smelting reactions to take place between lead oxide and lead sulphide. Heavy metals such as Zn, As and Sb have been found in the CHM samples, but Cuiza would not be interested in extracting these metals. Thus, he was not adding this material to reclaim the metals, but to initiate the smelting process.

5.3. The *huayrachina* furnace wall

One sample of furnace wall (sample 9) was collected during ethnographic documentation from the 2002 smelt. In addition to sample 9, a bag of *huayrachina* fragments was sampled during the 2001 smelt from Cuiza's smelting site representing older furnaces used prior to PAPP studying Cuiza, i.e. before 2001. One fragment from the older *huayrachina* fragments was analysed and labelled sample 17 (Table 5.14).

Mounted blocks	Associated Year	Description
17	2001	Old *huayrachina* fragment found at Cuiza's smelting site
09	2002	Furnace fragment
24	2002	Clay from a *quebrada*/ravine close to Cuiza's smelting site used to repair the *huayrachina* from 1st smelt

Table 5.14. *Huayrachina* fragments and clay samples available for analysis.

Carlos Cuiza's *huayrachinas* were constructed with natural ravine clay. A sample of the clay used to repair the *huayrachinas* in 2001 was also collected for analysis (sample 24). The analytical work has considered the nature of the clay used by Cuiza: was it tempered with filler? How does the charge react with the furnace wall? Does the clay used to fill the *huayrachinas* differ from the ceramic of the furnace wall? This section will present the results of analytical work carried out on furnace fragments and the clay samples.

The *huayrachina* fragment – sample 9

The *huayrachina* fragment (sample 9) is a red ceramic piece (Figure 5.8), ranging in thickness from 2 to 3 cm. The ceramic appears to be very fine and un-tempered. In the centre of the fragment is an opening which would have been one of the 'eye' holes of the *huayrachinas*, with a diameter of 3 cm. Externally, the red clay has been finished to a smooth texture and transformed to a fully baked ceramic. Internally, the surface is covered by a thin layer of vitrification up to 1-2 mm thick. This vitrification appears to have been a liquid slag, and the resulting vitreous layer has a glossy and flowing texture (Figure 5.8).

Sample 9 was prepared for XRF analysis, ensuring that any vitrification from the internal wall was removed before pellet production. Clay used to repair the *huayrachinas* prior to smelting in 2002 (sample 24) was also sampled for XRF analysis to be compared with the clay used in production of the *huayrachinas* (Table 5.15). XRF analysis shows that sample 9 is composed mostly of silica (68%), alumina (18%), and iron oxide (3%). This, together with several wt% of potash and lime, indicates that the ceramic is not particularly refractory. The clay used to repair the *huayrachina* is composed of silica (60%), alumina (20%), and iron oxide (6%). The composition of the repair clay is comparable to the *huayrachina* fragment analyses and differences could be attributed to different mineral inclusions or temper contents.

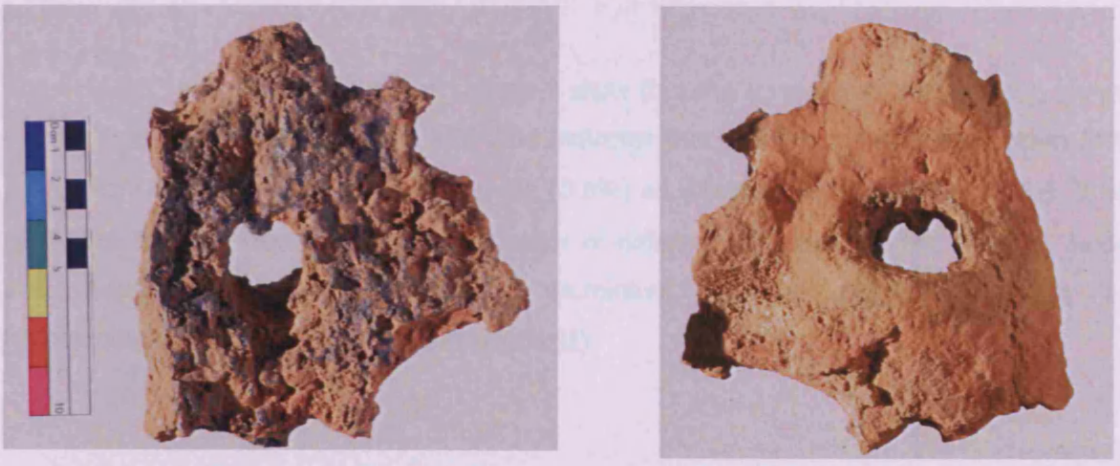

Figure 5.8. Sample 9, 2002 furnace fragment.

Samples	Na2O	MgO	Al2O3	SiO2	P2O5	SO3	K2O	CaO	TiO2	Fe2O3	BaO	PbO
24 (2002)	0.4	1.8	20.0	59.3	0.2	1.8	3.5	5.3	0.6	6.4	0.2	0.5
9	2.7	0.7	17.9	67.7	0.2	trace	4.1	2.0	0.5	3.3	0.1	0.7

Table 5.15. XRF analysis of pressed sample 24 clay pellets used to patch *huayrachinas* before use in 2002, and sample 9 a *huayrachina* fragment.
The pellets were analysed using Turbo-quant and the data had been normalised to 100 wt%.

The OM shows that the majority of the furnace wall is composed of semi rounded quartz grains, present as natural inclusions. There is no information from ethnographic documentation regarding the construction the furnace and or acquisition and treatment of clay. However, the ceramic has a highly porous structure. The voids in the structure are most probably relict space from organic materials which could have been burnt away during the smelt, or indicate incomplete working of the clay prior to use. The source of the clay must have had some organic temper.

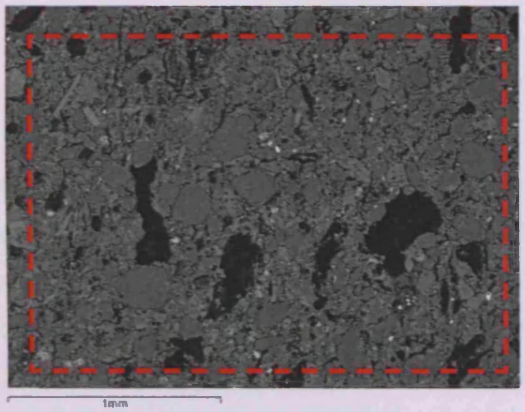

Figure 5.9. SEM backscattered image of the ceramic body.
Bulk scans were taken using large sample areas marked within the dashed red square. The matrix has a number of different crystals with a large proportion of the matrix consisting of quartz grains (smooth grey crystals).

The SEM-EDS bulk scanned areas of sample 9 show that the ceramic has silica (75%), alumina (12%), lime and iron oxide (4%). XRF data indicates that the minor oxides are potash (4%), magnesium oxide (0.7%) and titanium oxide (0.6%) as shown in Table 5.16, Figure 5.9. It also confirmed that the ceramic contains a number of different minerals including titanium oxides, iron oxide rich particles, potassium aluminium silicates, possibly feldspars and hornblende/amphibole (Figure 5.10, Appendix II).

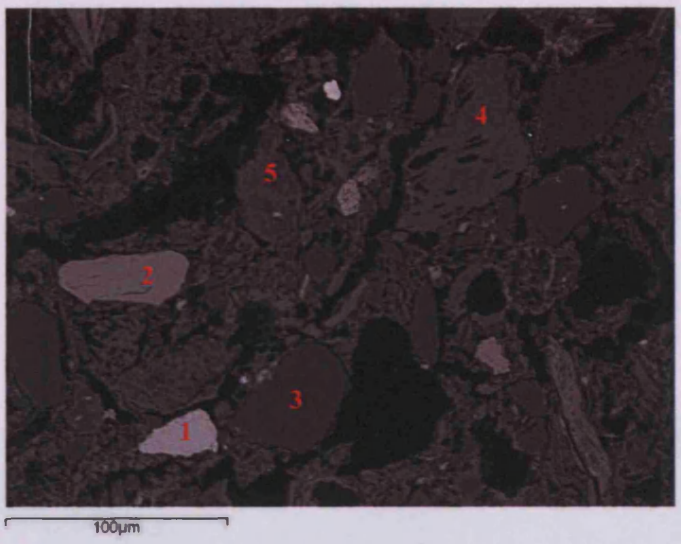

Figure 5.10. SEM backscattered image of the different minerals found in the *huayrachina* sample 9. 1 = iron oxide, 2 = titanium aluminium, 3 = quartz, 4 and 5 = feldspars

The *huayrachina* sample has a layer of vitrified material coating the inner surface; this is less than 2 mm thick and has not penetrated the sample very deeply. The penetration of lead oxide was recognised and defined in depth using SEM images (Figure 5.11). The lead oxide formed during the smelt reacted chemically with the silica rich *huayrachina* ceramic, forming a vitreous layer of lead silicate. Analysis of this layer showed that it contained lead oxide (53%), silica (31%), alumina (6%), iron and zinc oxide and lime (3%). The zinc and lead oxide content comes from the interaction between lead oxide and the furnace wall. The slag lining contains about 50 wt% lead oxide, and the amounts of silica and alumina are accordingly only about half of that found in the un-reacted ceramic. However, both lime and iron oxide are less diluted while zinc oxide occurs as a further component. This indicates that the slag contributed not only lead oxide, but also zinc and iron oxide and lime, in accordance with minor minerals found in the ore. The thin layer of vitrification and shallow penetration of the lead silicate indicates that conditions within the furnace were not suitable to produce large quantities of reactive lead oxide. The partially molten lead oxide was unable to flow into the ceramic wall, indicating that the *huayrachinas* operate at a relatively low firing temperature.

Scanned area	NaO	MgO	Al2O3	SiO2	K2O	CaO	TiO2	FeO
Average (n=11)	**0.4**	**1.1**	**12.2**	**74.6**	**2.9**	**4.2**	**0.6**	**4.0**
Min	0.4	0.7	8.1	70.7	1.8	3.1	0.5	2.4
Max	0.9	1.3	14.1	82.7	3.8	5.4	0.9	5.0

Table 5.16. Bulk scans of ceramic body sample 9. Data has been normalised to 100 wt%.

Scanned areas	MgO	Al2O3	SiO2	K2O	CaO	FeO	ZnO	PbO
1	~	5.4	27.7	1.3	1.8	2.0	3.8	58.0
2	0.9	6.0	32.4	0.7	3.0	3.6	3.6	49.8
3	0.7	6.1	31.8	1.6	2.7	2.9	3.4	51.0
Average	**0.5**	**5.9**	**30.6**	**1.2**	**2.5**	**2.8**	**3.6**	**52.9**

Table 5.17. The vitrified lead silicate layer (illustrated in Figure 5.11) found on the internal side of the *huayrachina* fragment.
Data has been normalised to 100 wt%.

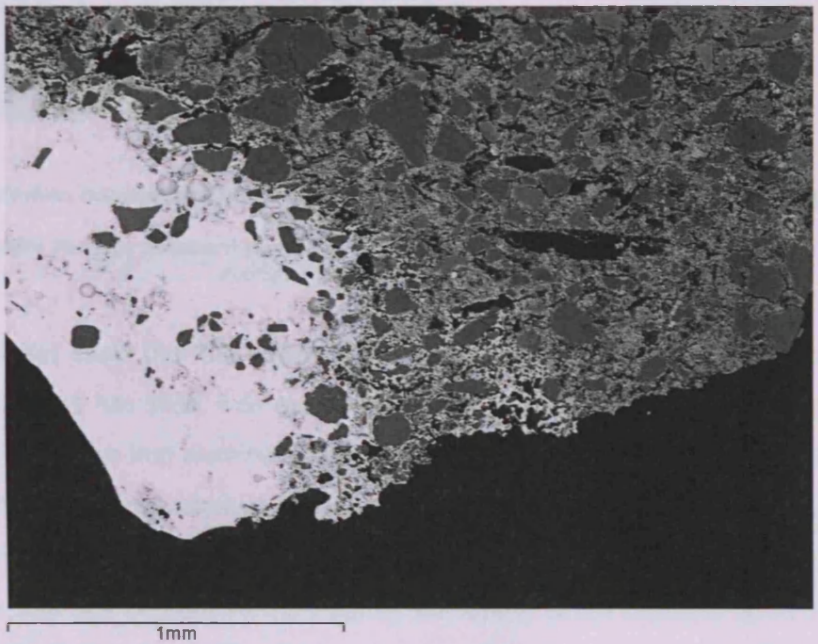

Figure 5.11. The vitrified layer on the *huayrachina* fragment, sample 9.
The lead rich silicate (bright) is attacking the ceramic matrix (gray). Quartz grains (dark grey angular crystals) remain the last mineral to be absorbed/dissolved into the lead silicate.

Older *huayrachina* fragments sampled in 2001; period of use *unknown* – sample 17

In 2001, a sample of scattered furnace fragments from Cuiza's smelting sites was collected (Figure 5.12. a). One of these fragments has been mounted in resin and analysed using SEM-EDS. While the exact time of use of this *huayrachina* is unknown, it is likely that it was built and used by Cuiza or his parents and therefore is suitable for the ethnographic material analysis.

Furnace fragment sample 17 was selected for analysis. It had a 2 cm thick red ceramic body with a dense, vitreous black slag attached. The slag measured up to 1.5 cm thick and contained

large pieces of charcoal, metallic prills and large gas bubbles. The cut surface revealed a grey/yellow slag. The ceramic is fine, with inclusions of quartz crystals (Figure 5.12.b).

a. b.

Figure 5.12. Broken *huayrachina* fragments found scattered around Cuiza's smelting site (a) during my site visit in 2005 and 2006.
In 2001, an older furnace fragment was sampled by PAPP. It was mounted in epoxy resin and polished ready for OM and SEM analyses (b).

SEM-EDS analyses show that the ceramic body (Table 5.18) is predominately silica (65%), and alumina (20%), and has soda, iron oxide and lime (3%). The minerals composing the ceramic body were shown to be iron alumina silicates and quartz. The lead slag (Table 5.19) attached to the ceramic body contains relatively high lead oxide levels (33-57%) with zinc oxide (5-12%), iron oxide (4%), and lime (6%), and is shown in Figure 5.13. The slag has concentrations of lead sulphide that has partially reacted during the smelt, which contains up to 10 wt% silver (area analysis). Prills of metallic silver and lead were analysed and while these metallic inclusions are limited and small, they indicate that silver was present in the system.

Scanned area	Na2O	MgO	Al2O3	SiO2	K2O	CaO	TiO2	FeO	PbO
1	2.5	1.0	22.1	64.3	2.5	3.5	0.4	3.8	~
2	1.2	1.6	18.1	66.1	2.5	2.9	0.9	5.1	1.7

Table 5.18. Bulk area scans of *huayrachina* fragment sample 17.
Data has been normalised to 100 wt%.

Spectrum	MgO	Al2O3	SiO2	P2O5	K2O	CaO	TiO2	FeO	ZnO	PbO
Average (n=5)	1.2	6.4	33.1	0.8	2.0	5.3	0.1	3.9	7.1	40.0

Table 5.19. SEM-EDS bulk area scans of the sample 17 slag.
The data is normalised to 100 wt%.

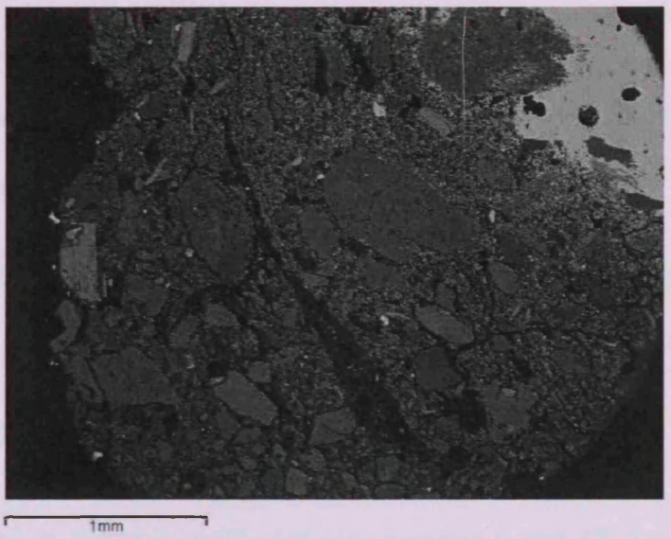

Figure 5.13. An SEM image of *huayrachina* fragment sample 17.
The bright white area (top right) is the slag layer attached to the ceramic furnace wall (grey area).

Scanned areas	S	Ag	Sb	Pb
Lead sulphide areas	9.1	4.0	1.1	85.8
	4.7	7.1	2.8	85.4
	6.1	7.4	2.1	84.3
	7.5	6.1	2.2	84.3
	7.4	6.0	1.9	84.7
	~	9.7	3.4	86.8
	~	8.7	3.1	88.3
Silver rich prills	~	82.4	11.8	5.8
	~	24.7	~	75.3

Table 5.20. Lead sulphide and silver prills recorded during SEM-EDS analyses of the slag on furnace fragment 17.
The data has been normalised to 100 wt%.

A comparison between Cuiza's older furnaces and samples from 2002

A review of the hand samples showed that the two ceramic furnace fragments have different quantities of slag attached. Sample 9 has a very thin coating of lead silicate slag, whereas, sample 17 has a slag layer of up to 1.5 cm thick. The slag layer on sample 17 contains metallic prills, lead sulphide and a piece of charcoal. It consists primarily of lead oxide and silica, with lower concentrations of lime and alumina, zinc and iron oxides. The presence of zinc and iron in the slag indicate that the interaction was taking place between the ceramic wall and the charge material rather than an interaction between lead oxide gases and ceramic. The location of sample 17 within the overall structure of the furnace is not possible to determine. It may be possible that, given the thickness of the slag, it came from the lower half of the furnace where charge material would have had time to interact and form a dense slag. However this is a working hypothesis. The presence of metallic prills indicates that silver was present in the

system; either from the selected ore or from CHM added to the smelt. No metallic prills were recorded in sample 9. The ceramic bulk area analysis shows that alumina and silica contents were variable between the two samples (Table 5.21). However, all other elements seem to be similar.

Average bulk area scan	Na2O	MgO	Al2O3	SiO2	K2O	CaO	TiO2	FeO	PbO
9 (n=11)	0.4	1.1	12.2	74.6	2.9	4.2	0.6	4.0	~
17 (n=2)	1.9	1.3	20.1	65.2	2.5	3.2	0.7	4.5	0.9

Table 5.21. SEM-EDS bulk area scans of *huayrachina* fragment samples 9 and 17. The data has been normalised to 100 wt%.

There is a difference in the slag quality between samples 9 and 17. The presence of silver within sample 17 is very significant, it indicates that some silver was present in the reaction system. This silver may have come from the ore source and thus may also show that Cuiza was smelting argentiferous galena, although without more samples this is difficult to substantiate. For the seven documented smelts, Cuiza did not select argentiferous galena for smelting. Personal communication with Dr Van Buren (2008) clarified that Cuiza's older smelting operations may have used ore with some silver content. Local miners brought ore to Cuiza and he would smelt their ore for a share of the resulting metal. This will be further discussed in Chapter 6.

Survey of the eye holes and dimensions of Cuiza's furnaces

A small survey of the *huayrachina* remains found at Cuiza's smelting site was done to observe the dimensions of the furnace in order to compare and contrast furnace changes between archaeological furnaces (see Chapter 9) and those used today. Six fragments containing eye holes were measured for the diameter and thickness fragment of the eye openings (Table 5.22) The average diameter of the eye holes is 2.9 cm and the average thickness of the fragment is 2.7 cm. On Cuiza's intact *huayrachina* the eye holes were smaller (2 cm diameter). The thickness of the furnace wall was measured from the opening of the eye hole to the internal surface of the shaft, and the thickness of the furnace was much deeper, ranging from 7 cm on the upper layer of eyes (towards the top of the column) to 10 cm on the lower row (Table 5.22).

The *huayrachina* remains from Cuiza's site showed a slightly larger eye diameter, almost 1 cm more as compared to the intact *huayrachina*. The difference could be attributed to changing methods of furnace production.

Sample measured	Eye diameter (cm)	Eye width thickness (cm)	Notes
1	2.5	3.0	Samples showed evidence for erosion
2	3.0	300	
3	3.0	2.5	
4	3.0	2.5	
5	3.0	3.0	
6	3.0	2.0	
Average surveyed *huayrachinas*	**2.9**	**2.7**	
Cuiza's intact *huayrachina*	**2.0**	**7.0**	Upper row of eyes
	2.0	**10.0**	Lower row of eyes

Table 5.22. Dimensions of survey ethnographic *huayrachina* eyes (samples 1-6) and the measurements of Cuiza's intact *huayrachina*.

Observation of the eye holes showed that the ceramic of the furnace had been partially fused around the holes during the previous smelts, causing the diameter of the holes to decrease. There is a clear difference in eye width and diameter between the surveyed fragments and the intact *huayrachina*. Some of the surveyed ethnographic samples had an eroded outer ceramic wall, which could explain the reduced wall thickness. However, it is also possible that Cuiza changed the dimensions of his furnaces. In Chapter 9, measurements from archaeological *huayrachina* will be presented and a discussion will compare the ethnographic and archaeological *huayrachina* dimensions.

5.4. The slag

Six samples have been selected from the 2001 and 2002 smelts (Table 5.23), while there are no slag samples available from the 2003 smelt. Only one sample from the 2001 smelt was available and was cut in half, creating two samples; samples 9 and 9A (Sample 9 was labelled by Mills (2003), unfortunately there is furnace fragment 9 and slag sample 9). Having two samples from one piece of slag provided a better overall perspective on its compositional and textural qualities.

Mounted Block	Associated year	Description
9	2001	Slag 1st smelt
9a	2001	Slag 1st smelt
1	2002	Slag 1st smelt
2	2002	Slag 1st smelt
10	2002	Slag 1st smelt
3	2002	Slag 2nd smelt
4	2002	Slag 2nd smelt
~	2002	Slag 1st smelt
~	2002	Slag 2nd smelt

Table 5.23. Slag samples selected for analysis.

All the slag samples were discrete pieces of slag and were not attached to the furnace wall. The majority range in diameter from 2 cm to 10 cm (Figure 5.14). The following is a generic description of all slags, and anomalies will be highlighted separately. The slag is dark grey-black in colour. It has a number of different inclusions ranging from stones (gangue from the ore), through to large pieces of charcoal, to prills of lead sulphide and lead metal. The slag is not very vitreous; it clearly was never fully molten within the furnace. The slag has a high specific gravity most probably due to its high lead content.

Microscopy of the slags has shown that there is a great deal of variation between samples. Even from a single smelt, the slag produced is not uniform. As a collection of samples, it is difficult to generalise them so therefore it will be necessary to consider the slags as individual specimens. In order to consider slags as a group, a discussion will follow regarding the overall slag.

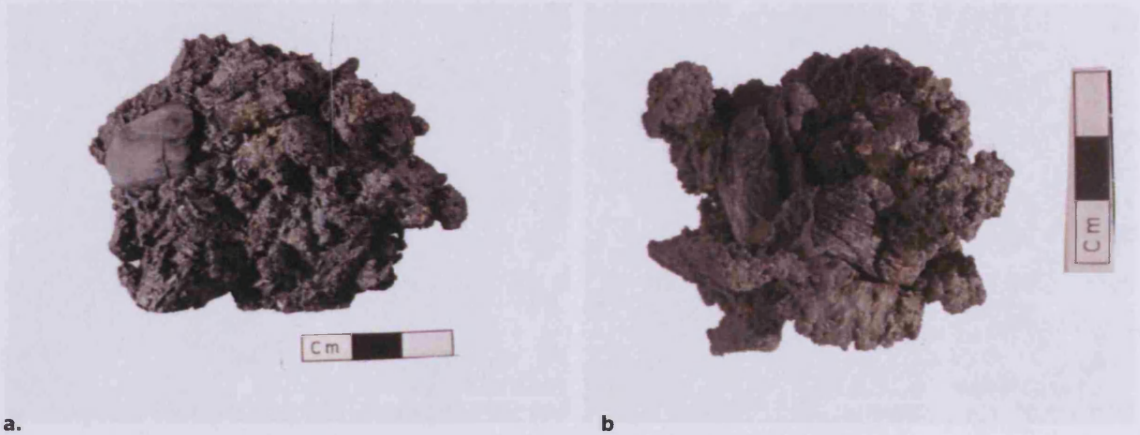

a. b

Figure 5.14. Slag sample 10 from the 1st smelt in 2002 (a) and Slag sample 9 from the 2001 smelt (b).

Slag samples 9 and 9A 2001

Samples 9 and 9A come from the same piece of lead slag taken from the 2001 lead smelts, and OM images indicate that it is a multi-crystalline system. It contains a matrix interspersed with different crystalline phases, metallic prills of lead metal and partially reacted lead sulphide (Figure 5.14). The crystalline matrix has different phases which appear to have grown out of the siliceous matrix. A few traces of residual charcoal were also noted.

Sample analysed	Na2O	MgO	Al2O3	SiO2	P2O5	SO3	K2O	CaO	MnO	FeO	ZnO	PbO
Average 9	1.1	0.5	4.4	30.9	1.6	0.6	1.1	7.0	0.9	12.2	8.9	30.8
Average 9A	~	1.4	3.8	29.2	1.1	0.6	1.6	7.8	0.4	12.8	11.1	30.3
Average 9 + 9A	0.6	1.0	4.1	30.1	1.3	0.6	1.4	7.4	0.6	12.5	10.0	30.5

Table 5.24. SEM-EDS bulk area analyses of the 2001 glassy slag matrix. The data has been normalised to 100 wt%.

SEM-EDS analysis of the glassy slag matrix shows that it is mostly composed of lead oxide (31%), silica (30%), iron and zinc oxide (13, 10 %), lime (7%), and alumina (4%). Potash, magnesium oxide, and phosphate sulphur were also recorded (Table 5.24). Mineral phases such as olivine, leucite and spinels were noted. Zinc and lead sulphide was also found in the sample.

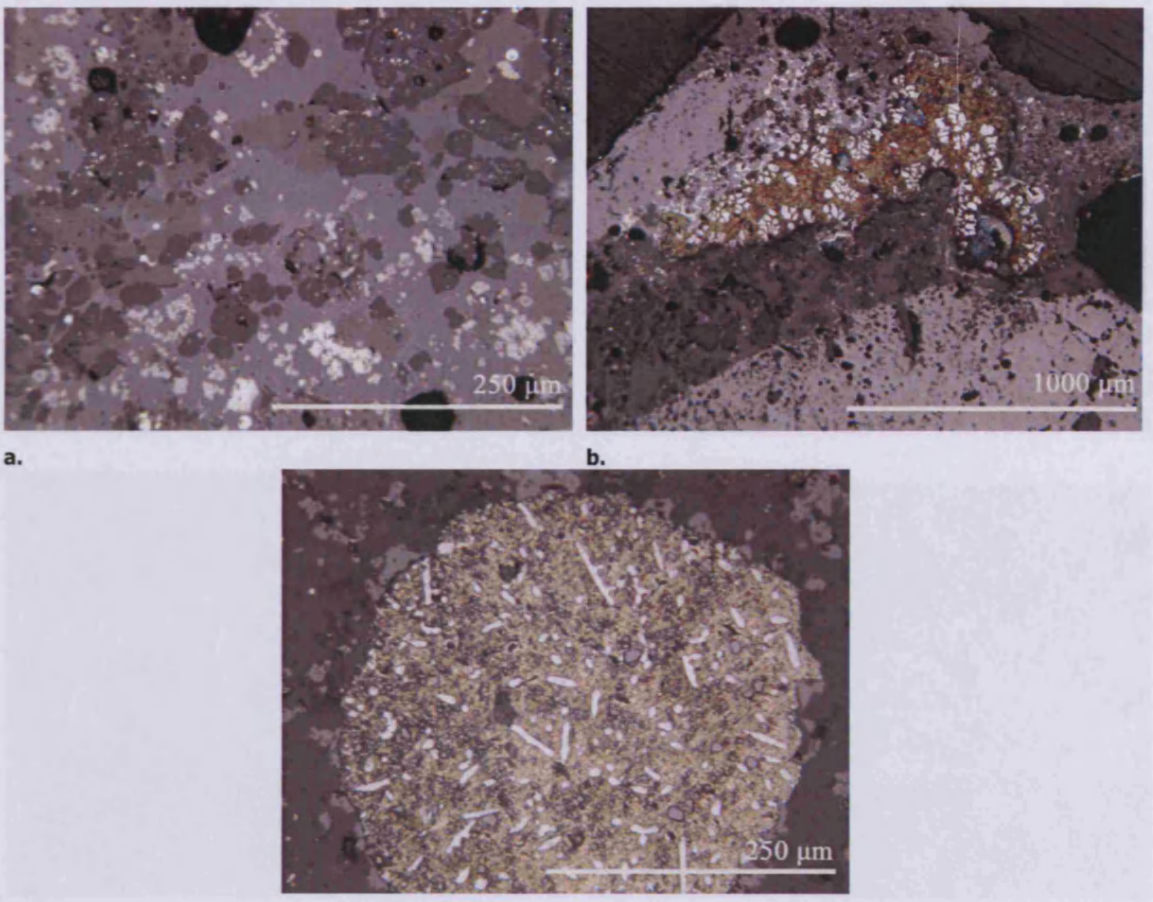

a. b. c.

Figure 5.15. A typical section of the slag from 2001.
Sample 9 (a) contains various silicate based phases. The whitest crystals/phases are re-crystallised lead sulphides that have not reacted to form lead metal and are instead trapped in a lead-silicate matrix. OM of sample 9A shows that the lead slag is highly heterogeneous, some areas are filled with large islands of lead metal. The brown phase is lead metal, the white phases are partially reacted lead sulphide while being transformed into lead metal. Large metallic lead prill were commonly found to be trapped within the slag matrix (c). The white thin phases are areas of lead sulphide that have not been fully converted to lead metal (brown).

Slag - sample 1 2002

Slag sample 1 is taken from the 1st smelt documented from the 2002 *huayrachina* lead smelts. The hand sample is a black/grey slag that has visible inclusions of gangue, charcoal and metallic prills. The outer surface is not glassy and appears to have never been fully molten.

This slag sample is similar to the 2001 samples because it is a silicate matrix with embedded crystalline phases, residual areas of gangue and many metallic inclusions warranting further analyses. The slag matrix contains two different crystalline phases in addition to the lightest areas which are lead sulphide intermixed with pure lead metal. Charcoal was also found in the polished cross section (Figure 5.16).

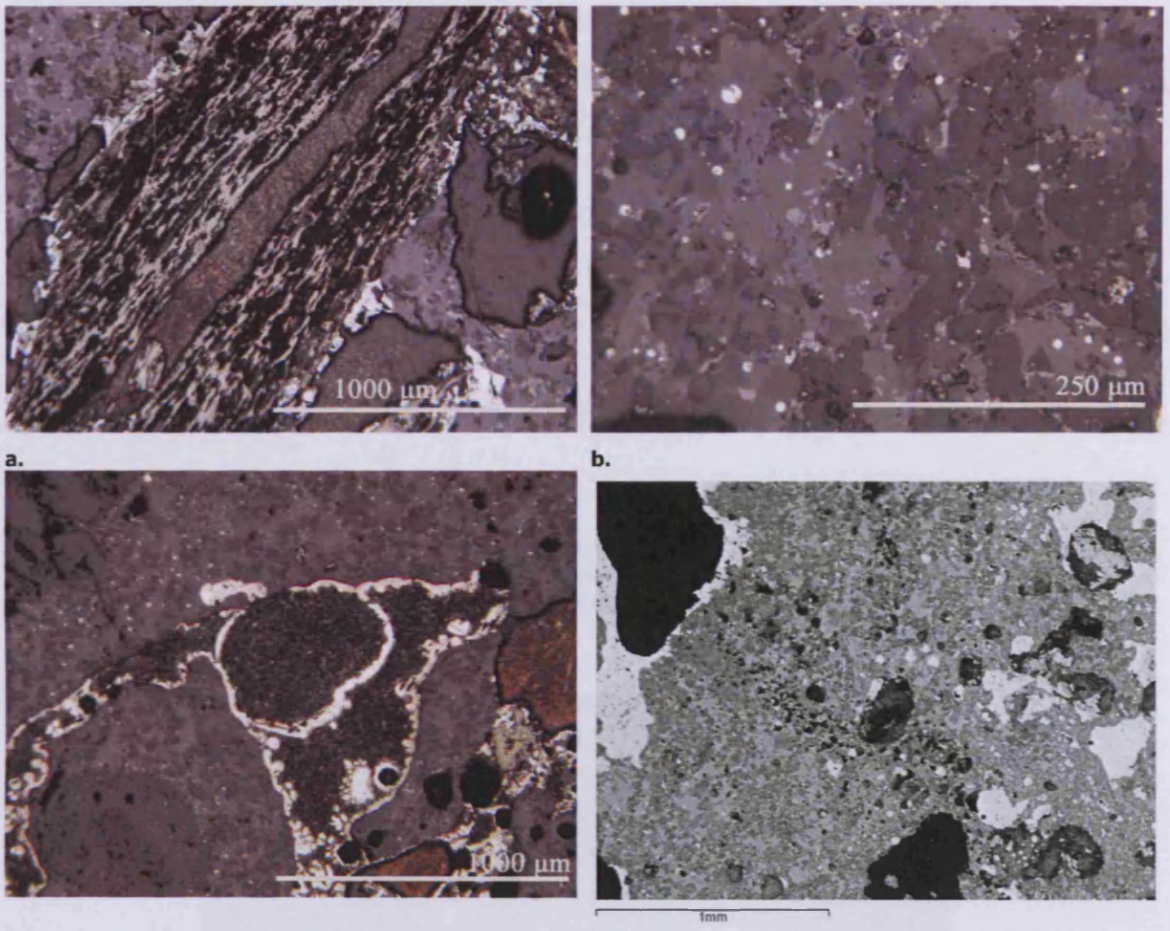

Figure 5.16. Charcoal inclusions are common slag sample 1 2002 within the current day *huayrachina* slag. OM image (a) was taken of the charcoal embedded in slag sample 1 (2002). The matrix of slag sample 1 is glassy and contains intergrowths of different crystalline phases (mid-grey in colour), image (b). Bright prills of lead sulphide were also common. Large metallic lead islands are a common feature in the slag (c). SEM imaging shows the multiphase texture of the sample (d). The brightest areas are partially reacted lead sulphide.

ED-XRF pellet analyses showed that the slag contained predominately lead oxide (38 wt%), silica (38 wt%), sulphur tri-oxide (13%), which is most probably lead sulphide. Heavy metals such as iron and zinc oxide were also recorded. Copper (700 ppm) and silver (200 ppm) were also found to be present.

SEM-EDS area analyses of the bulk slag composition were different to the overall XRF bulk analyses. The sample is characterised by a lead and iron silicate, but with greatly reduced lead only (11 wt% lead oxide), increased iron oxide (10 wt%) while the silica content remained the same (40 wt%, Table 5.25). These differences are most likely related to the number of metallic prills and partially reacted ore areas in the sample. The SEM-EDS cannot fully represent the bulk composition, however SEM bulk analyses are beneficial because they indicate the chemical differences found within the slag structure. The glassy slag matrix has low quantities (3%) of lead oxide and very high quantities of iron oxide (35%);Table 5.33, Figure 5.17. The matrix also contains zinc oxide (7%). The high quantity of iron oxide in the glassy matrix may come from

the ore and it reflects the non-homogenous nature of *huayrachina* slag that it would not be seen in XRF bulk chemical analyses. Slag sample 1 has a large number of metallic and partially reacted gangue inclusions (already previously noted in the OM). The majority of these inclusions are lead metal and lead sulphide, with up to 6% zinc sulphide. Isolated areas of zinc sulphide are also common. Large quantities of sulphidic gangue components remain only partially reacted in the slag matrix. Crystalline phases include pyroxenes, leucite, and spinels with high iron oxide (Appendix II).

Area scanned	MgO	Al2O3	SiO2	P2O5	SO3	K2O	CaO	MnO	FeO	ZnO	PbO
Average sample 1 (n=5)	2.1	8.4	39.1	0.2	2.2	5.3	14.3	0.9	10.0	6.5	11.0

Table 5.25. SEM-EDS bulk area analyses of slag sample 1 (2002). The data has been normalised to 100 wt%.

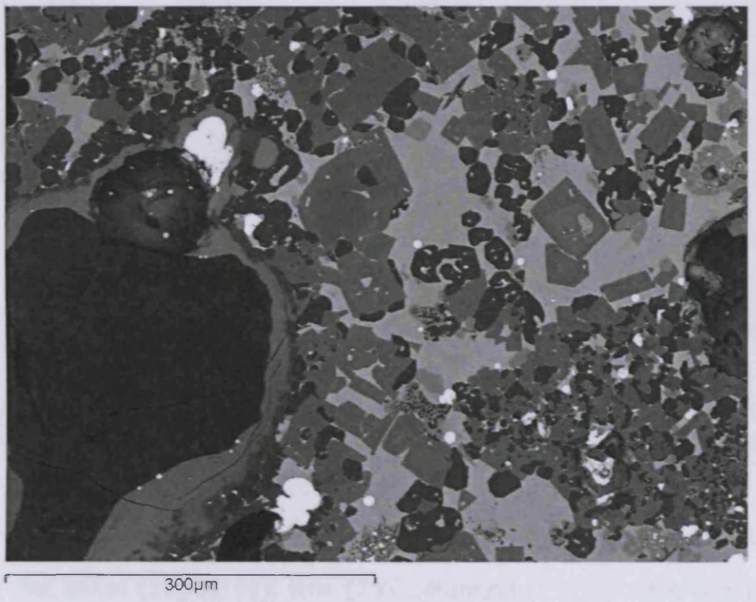

Figure 5.17. Slag sample 1 (2002) contains many crystalline minerals surrounded by a glassy silicate matrix (light grey). A large quartz grain is embedded in the slag (left dark grey). The brightest areas are partially reacted lead sulphide.

SEM-EDS analyses have shown that slag sample 1 is relatively high in iron. However, ED-XRF analyses indicated that iron oxide concentrations are only 3%, due to a large quantity of lead sulphide included in the XRF analysis. The slag is a lead silicate containing large quantities of residual sulphidic ore.

Slag – sample 2 2002

Slag sample 2 was created in the 1st documented smelt of the 2002 lead productions. The hand sample contains very few visible metallic prills and has a stone-like texture with many pores and inclusions of charcoal and ore. The cut surface revealed an extremely porous central area and a more vitreous outer section. OM showed that the mounted sample contained very little glassy slag the majority of which was located on the outer edge of the sample (Figure 5.18). The bulk of the sample is primarily quartz.

No bulk area analyses were done on this sample because it contained very few vitreous slag areas. In the areas of siliceous slag, the silicate matrix, individual phases and metallic prills were analysed (Appendix II).

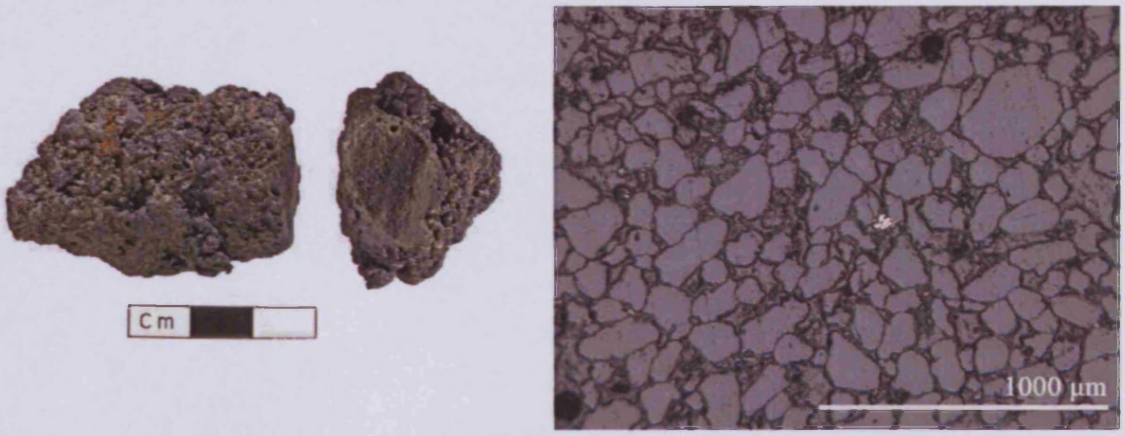

a. b.

Figure 5.18. The hand specimen of slag sample 2 from the 1st smelt (2002, a). The microscopic texture of slag sample 2 showed that it contained large quantities of gangue minerals (b).

SEM-EDS analyses shows the glassy slag matrix of sample 2 contains lead oxide (24%), silica (34%), iron and zinc oxide (14; 11 %), lime (7%), alumina (5%), potash (2%), and phosphate (1%); Table 5.33. Olivines and leucite were also recorded.

Slag - sample 3 2002

Slag sample 3 was taken during the second day of smelts in 2002. The SEM showed a glassy slag matrix with a number of different crystalline phases (Figure 5.19). Lead metal and lead sulphide were also noted. Like sample 1, the slag matrix has some areas containing sulphur although the majority of this sample is low in sulphur. Silica, iron oxide, zinc oxide, and lead oxide are variable but constitute the major components of the slag (Table 5.26). Lime and alumina were also recorded in the bulk area scans. Zinc and lead sulphides are interspersed

within the slag matrix and the zinc sulphide contains up to 6% iron. Silicate phases such as olivine and leucite are embedded in the slag matrix.

Sampled area	MgO	Al2O3	SiO2	P2O5	SO3	K2O	CaO	TiO2	MnO	FeO	ZnO	PbO
Average sample 3	1.9	8.9	45.2	0.4	0.4	4.7	10.2	0.1	0.4	8.5	7.1	12.2

Table 5.26. SEM-EDS bulk area analyses of slag sample 3 (2002). The data has been normalised to 100 wt%.

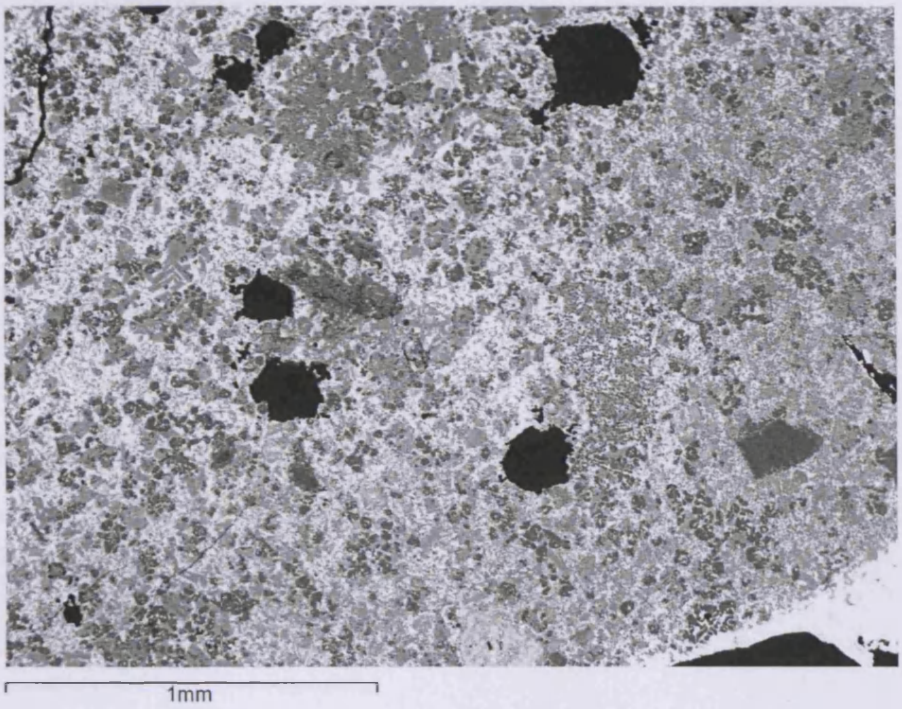

Figure 5.19. SEM image of slag sample 3 (2002), showing the general bulk appearance of the slag.

Slag - sample 4 2002

Slag sample 4 was taken during the second day of smelts in 2002. OM showed that a large majority of the matrix is composed of lead sulphide. It has inclusions of gangue minerals that are trapped in large areas of lead sulphide (Figure 5.20). Lead sulphide was confirmed as being the major component of this slag (Table 5.27), containing only very little silica, lime and iron and zinc oxides. Some areas show the formation of lead metal trapped as discrete islands in the slag.

Overall this is a very rich slag, containing large amounts of lead as metal and as lead sulphide and should not have been discarded as waste material.

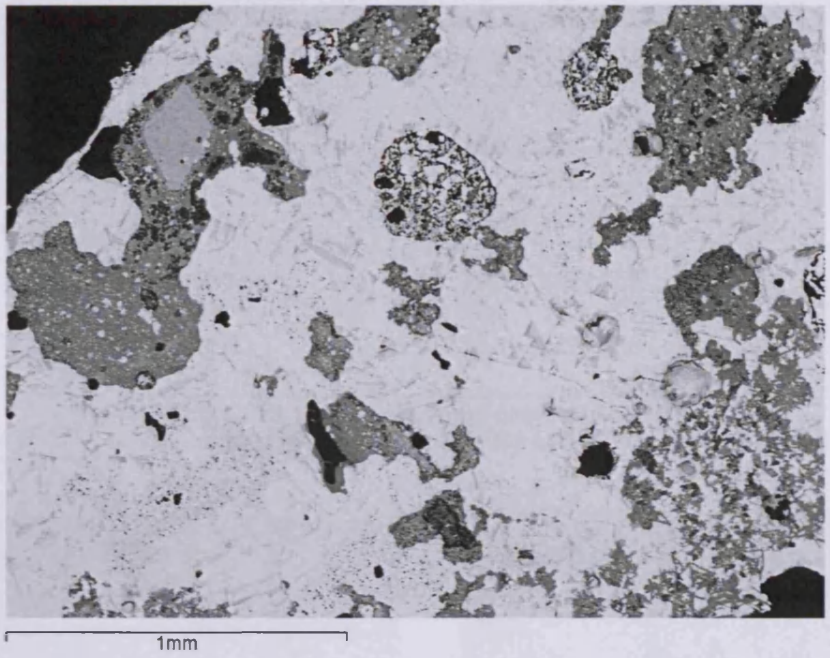

Figure 5.20. Bulk area used for SEM-EDS analysis on slag sample 4 (2002).

Spectrum	MgO	Al2O3	SiO2	SO3	K2O	CaO	FeO	CuO	ZnO	PbO
Average sample 4	0.2	1.0	7.1	22.5	0.6	3.9	2.4	0.3	2.7	59.3

Table 5.27. SEM-EDS bulk area analyses of slag sample 4 (2002). The data has been normalised to 100 wt%.

Slag – sample 10 2002

Slag sample 10 was taken from the 1st smelt in 2002. The sample is almost pure lead sulphide (Figure 5.21). Lead metal began to form, accounting for the presence of silica (3 wt%) and oxygen in bulk SEM data (after polishing, the lead metal converts to lead oxide in the presence of oxygen, and the silica most probably comes from the polishing crystals trapped in the soft lead metal); Table 5.28. Higher magnification on the SEM shows that the sample has undergone sufficient heating to produce lead metal but also to produce re-crystallised zinc sulphide along grain boundaries (Figure 5.21).

Scanned area	O	Si	S	Fe	Zn	Pb
1	5.2	~	13.1	1.4	2.8	77.4
2	3.2	~	13.8	2.4	2.3	78.4
3	~	~	15.3	2.5	2.2	80.0
4	6.4	3.6	9.8	1.3	2.6	76.3
5	~	3.7	14.3	1.6	2.4	78.0
Average	**3.0**	**1.5**	**13.3**	**1.8**	**2.5**	**78.0**
Min	3.2	3.6	9.8	1.3	2.2	76.3
Max	6.4	3.7	15.3	2.5	2.8	80.0

Table 5.28. Bulk area scans of sample 10 (2002). Data has been normalised to 100 wt%.

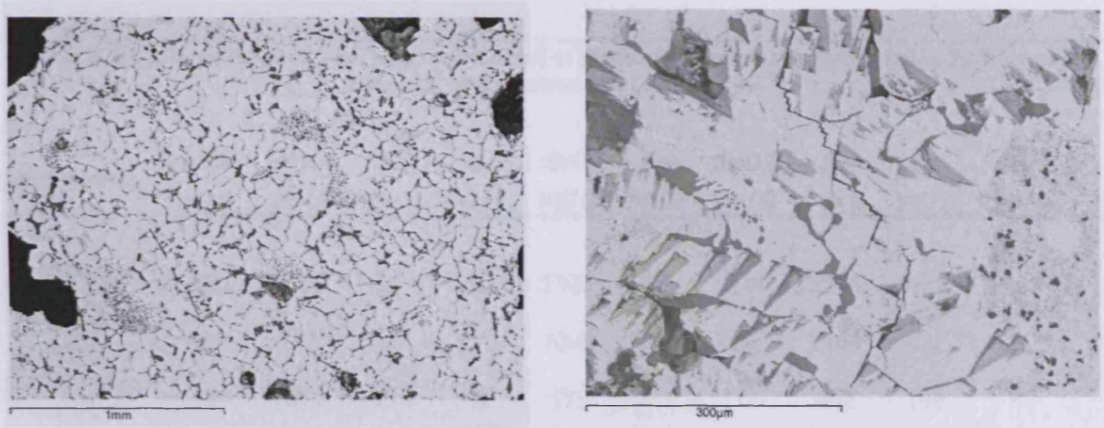

a b

Figure 5.21. An SEM image of slag sample 10 (2002)
Image a; sample 10 is almost pure lead sulphide with zinc sulphide on grain boundaries (dark grey). The lead sulphide shows evidence for re-crystallisation (b). It also shows how the lead sulphide changes to lead metal; right corner.

Summary and basic discussion of all the *huayrachina* slag analyses

Only one out of the six mounted slag samples have been analysed using ED-XRF pellets (Sample 1 2002). Additionally, two other samples were prepared for XRF bulk analyses; one of these samples coming from the 1st smelt in 2002 and the other from the 2nd 2002. The results of these analyses are in Table 5.29 and Table 5.30. Sample 10 is pure PbS. The disparity between the slag samples can be clearly recognised in the XRF results; PbO, FeO, CaO, SiO_2, ZnO, and SO_3 make up the major composition with trace concentrations of Ni, Cu, As, Ag, Sn, and Ba. The variability of lead oxide ranges from 25% to 43%, and analyses from individual areas (see below) indicate that this range can be even larger. A relatively high quantity of sulphur was measured in all samples (ranging from c.7 to 18 wt% when expressed as SO_3), indicating that conditions were not heavily oxidising. Most of the slag sampled is siliceous with silica concentrations ranging from 19 to 34%. Zinc oxide is also highly variable (1.6-15%), most likely reflecting the composition of the lead ore. From the ethnographic documentation we know

that the lead ore is not roasted prior to smelting and thus enters the system raw as PbS, ZnS, or FeS_2. The bulk chemical analyses showed that the slag has a number of different heavy metals present; particularly Ni (0.02%), Cu (0.06%), As (0.11%), and Ag (0.04%). Concentrations of these heavy metals have come directly from the lead ore used for smelting.

Compounds	MgO %	Al2O3 %	SiO2 %	SO3 %	K2O %	CaO %	TiO2 %	MnO %	Fe2O3 %	PbO %	ZnO %	As2O3 %
1st smelt slag 2002	1.8	5.5	28.4	6.5	2.5	9.1	0.2	0.6	10.5	28.3	5.4	0.6
2nd smelt slag 2002	0.9	2.9	20.3	12.4	1.5	5.7	0.2	0.2	5.4	44.4	5.1	0.3
Slag sample 1 2002	0.3	3.3	37.8	12.6	0.8	2.2	0.1	0.1	2.6	38.1	1.5	0.2

Table 5.29. XRF pellet analyses (major elements) of three slag samples analysed using Turbo-quant. Data has been normalised to 100 wt%.

Compounds	Co3O4 µg/g	NiO µg/g	CuO µg/g	Ga µg/g	SrO µg/g	Ag µg/g	SnO2 µg/g	Sb µg/g	Ba µg/g	Hf µg/g	Bi µg/g
1st smelt slag 2002	431	358	1264	20	1328	249	234	1556	522	208	0
2nd smelt slag 2002	255	487	2195	273	1096	487	95	1466	411	242	160
Slag sample 1 2002	76	252	734	0	655	213	72	692	146	68	0

Table 5.30. XRF pellet analyses (minor elements) of three slag samples analysed using Turbo-quant. Data has been normalised to 100 wt%.

A comparison between XRF bulk composition and SEM analysis shows that there are some obvious discrepancies. Lead concentrations are greatly reduced in the SEM-EDS data, in one case by 30%. The main difference, and probable cause, for this discrepancy is the very heterogeneous nature of the material, and the full inclusion of lead sulphide lumps in the XRF but not in the SEM-EDS, which tends to focus more on the siliceous part of the slag.

Bulk area scans of the slag samples 9a (2001), 1, and 3 (2002) show that they are all chemically similar to each other (Table 5.31). Lime levels within the slag are high (10-19%). Iron, zinc and lead oxides predominate with a silicate base (40%).

Analysis of slag from the 2001 and 2002 smelts was done to gain a complete characterization of the phases present, and to interpret the type of reactions occurring in the furnace. Nine main phases have been identified (Table 5.32).

Bulk area scans of sample	MgO	Al2O3	SiO2	P2O5	SO3	K2O	CaO	TiO2	MnO	FeO	ZnO	PbO
9a (2001)	1.9	8.0	37.8	0.7	0.4	4.1	19.7	~	0.3	11.8	9.7	5.6
1 (2002)	2.1	8.4	39.1	0.2	2.2	5.3	14.3	~	0.9	10.0	6.5	11.0
3 (2002)	1.9	8.9	45.2	0.4	0.4	4.7	10.2	0.1	0.4	8.5	7.1	12.2
Average	**2.0**	**8.4**	**40.7**	**0.4**	**1.0**	**4.7**	**14.7**	**0.0**	**0.5**	**10.1**	**7.8**	**9.6**

Table 5.31. Comparison of the average bulk area scans of ethnographic slag samples. Data has been normalised to 100 wt%.

The main glassy slag matrix consists of a lead silicate that also contains on average 10% zinc oxide and c. 15% iron oxide (Table 5.33). The average lead oxide and silica content is c. 30% each. Crystal phases identified include leucite, olivine and high iron spinels, zinc sulphide, lead sulphide, and lead metal. These reflect the interaction between gangue minerals, ceramic wall and lead ore, and indicate relatively reducing conditions (olivines, sulphides).

Areas of residual ore minerals were found within all slag samples, ranging from zinc sulphide to quartz and feldspar (seen in Figure 5.21 and Table 5.33).

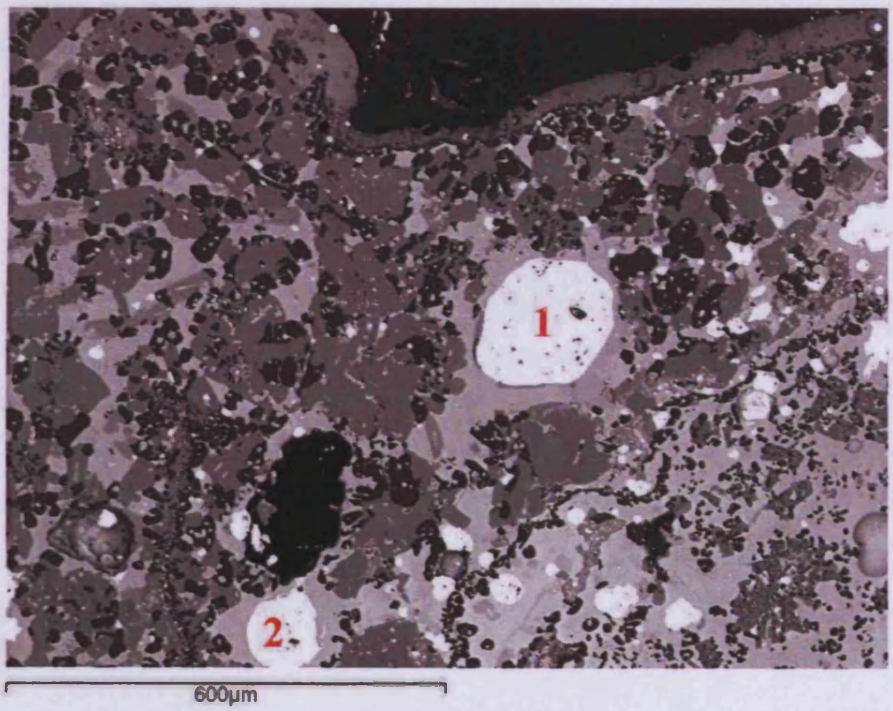

Figure 5.22. SEM-EDS image of slag sample 9 (2001). The metallic prills analysed were pure lead metal (labelled 1) and lead tin metal (labelled 2).

Phases identified	Chemical formulae	Brief description
Slag matrix	~	Slag matrix refers to the interstitial matrix containing high quantities of silica. It can be considered as the sponge within the system that soaks up remaining elements not used in other crystal formations.
Leucite	$KAlSi_2O_6$, Potassium Aluminium Silicate	Leucite has a distinctive euhedral crystalline structure and appears very dark in back-scattered images.
Olivine	(Mg, Fe, Ca, Zn) $2SiO_4$, Magnesium Iron Silicate	Seen on SEM images as flattened, tabular boxes, olivines are easily recognizable. Chemically they contain high levels of CaO (up to 35%) and about 40% SiO2.
Spinels	$Me^{2+}\ Me^{3+}{}_2\ O_4$	Spinel crystals with a cubic crystal structure. They can incorporate bi- and tri-valent metal oxides.
Lead metal	Pb	Found in areas of PbS where transformation of PbS into Pb is occurring. Distinctively noted because of the embedded SiC crystals from the preparation of samples.
Lead Sulphide	PbS	Many inclusions of PbS have re-crystallised and show a much more spherical growth structure. The presence of PbS indicates a low oxidizing area within the furnace. These areas often contain ZnS and other gangue minerals.
Zinc Sulphide	ZnS	Found both as re-crystallised ZnS, but also as partially molten remaining gangue mineral. Much of the Zn should have been lost via evaporation but the presence of ZnS indicates low oxidising conditions.
Chalcopyrite	$CuFeS_2$	Areas of residual ore.
Quartz inclusions	SiO_2	Remaining gangue minerals frozen in the slag matrix. The outer edges of these crystals show erosion from the surrounding glassy slag matrix. With more time and greater temperatures the system would absorb and react with the quartz grains, creating more slag matrix.

Table 5.32. Phases identified within the slag from current lead smelting.

Slag sample 9 perfectly illustrates the nature of *huayrachina* slag. Figure 5.22 shows the different crystal phases present in the slag (in the darkest phase, the leucite, mid grey rectangular crystals are olivines, the whitest phase indicates lead sulphide, and light grey areas are the slag matrix). Prills of lead metal are occasionally found embedded into the matrix of all of the slags analysed, labelled on Figure 5.22 as 1 and 2. Analysis of the metallic prills indicates that they are nearly pure lead metal though containing some antimony, zinc and iron (all found as components of the starting lead ore).

Samples	Na2O	MgO	Al2O3	SiO2	P2O5	SO3	K2O	CaO	TiO2	MnO	FeO	ZnO	As2O3	PbO
4 2002 extreme area analysed	~	0.1	2.9	17.1		~	0.7	2.1	~	~	5.2	7.6	~	64.4
1 2002	~	6.2	2.4	33.0	1.5	0.2	0.7	6.7	0.1	3.1	36.5	7.3	~	2.7
9 2001	1.1	0.5	4.4	30.9	1.6	0.6	1.1	7.0	~	0.9	12.2	8.9	~	30.8
9A 2001		1.4	3.8	29.2	1.1	0.6	1.6	7.8	~	0.4	12.8	11.1	~	30.3
2 2002	~	1.1	5.3	33.9	1.0	~	1.8	6.8	0.3	1.0	13.5	11.4	~	24.0
3 2002	~	0.3	6.4	36.5	0.7	~	1.4	5.5	0.1	0.7	9.3	11.0	0.6	27.7
4 2002	~	0.9	4.6	32.9	1.3	~	1.4	6.5	~	0.6	12.5	9.6		29.7
Average (9 2001-4 2002)	**0.2**	**0.8**	**4.9**	**32.7**	**1.1**	**0.2**	**1.5**	**6.7**	**0.1**	**0.7**	**12.1**	**10.4**	**0.1**	**28.5**
Min	1.1	0.3	3.8	29.2	0.7	0.6	1.1	5.5	0.1	0.4	9.3	8.9	0.6	24.0
Max	1.1	1.4	6.4	36.5	1.6	0.6	1.8	7.8	0.3	1.0	13.5	11.4	0.6	30.8

Table 5.33. SEM-EDS glassy silicate matrix. The data has been normalised to 100 wt%. Samples 4 (extreme area) and 1 have not been included in the average slag matrix because they contain high quantities of lead oxide (sample 4) and high iron oxide (sample 1).

5.5. The lead metal

During smelting, the metals produced from the *huayrachinas* dribble onto an iron dish. The samples taken for analyses reflect the production of the smelting process. Most show flow pattern indicating the formation of the metal as it dripped from the bottom of the furnace onto the iron dish. It has a shiny metallic grey colour and no visible inclusions (Figure 5.23).

a b C

Figure 5.23. Lead metal produced in the 2nd smelt (2001, a), 1st smelt (2001, b and c) .

XRF analysis of the lead metal produced in the *huayrachina* indicates that the metal was very pure, containing around 98% lead metal (Table 5.34). Only 1 wt% of silver is present and there are trace concentrations of other heavy metals and sulphur.

Sample analysed	S	Co	Ni	Cu	Zn	As	Ag	Sb	Pb
Lead metal block 7 (2001)	0.02	0.01	0.02	0.03	0.06	0.09	1.07	0.41	98.28

Table 5.34. XRF data of the lead metal produced in the *huayrachina* smelts. The Alloys method was used in the XRF analyses.

5.6. Discussion

The *huayrachina* slag has shown that conditions inside the furnace were highly variable, creating a co-smelting environment. Analysis of the starting ore confirmed that it is predominately lead sulphide with minor zinc sulphide and iron sulphide. This ore is easily separated from the gangue minerals and should produce a pure lead metal in a reducing atmosphere. CHM added to the *huayrachina* smelts have introduced lead, zinc, nickel, iron oxides, and slag-forming light oxides into the system; the lead oxide is useful to promote the transformation of lead sulphide to lead metal.

Interactions between the furnace wall and the charge material produced a very thin layer of vitrification on the inner surface of the *huayrachina*. If higher temperatures would have occurred inside the *huayrachina,* we should have expected a more fluid slag which would have reacted with the silicate rich ceramic wall, creating a thick vitrification layer. In the sampled *huayrachina* fragments, the slag layer is less than 1 mm thick, indicating that the temperatures inside the furnace were relatively low. SEM images indicate that only minimal interaction between the slag and ceramic matrix has occurred. The lead silicate produced shows that lead oxide formed during the smelting process, dissolving the ceramic matrix.

The slag analyses have also shown the presence of large amounts of lead sulphide in a lead-silicate rich slag matrix, indicating that the system was not strongly oxidising. Therefore, while we must pay attention to the location within the furnace where the slag has formed, we cannot deny that the system displays a highly sulphuric environment. If the conditions had been more oxidising, then more sulphur would have been burned away; whether or not this would result in higher lead metal production or simply increased formation of lead silicate in the slag would depend on the exact circumstances within the *huayrachina*. The compositional analysis of the slag shows that, while the furnace clearly yields some lead metal, the slag still contains considerable quantities of lead, both chemically bonded as lead silicate and mechanically trapped as lead sulphide and lead metal aggregates. Also apparent from the analysis is the heterogeneity of most slag lumps with regards to the redox conditions preserved in them, and the insufficient separation of the sulphides from the silicate smelt, indicating insufficient operating temperatures.

So in summary, the current day *huayrachinas* are suitable but not very efficient for producing lead metal. The high sulphur content and presence of partially reacted mineral ore within the slag indicate that the furnace conditions were not heavily oxidising and it is clear that a lot of potential lead was lost into the slag matrix.

6. RESULTS FROM THE ETHNOGRAPHIC SILVER REFINING

The ethnographic silver production documentation consists of two stages, Chapter 5 considered the production of lead metal via smelting in *huayrachina* furnaces and this Chapter presents the results from the second stage: silver refining via cupellation. Samples taken from the silver refining process are listed in Table 6.1. They have been sampled from two different refining episodes done in 2001 and 2002. Samples were collated into the following groups; llareta ash, silver ore, Cupellation Hearth Material (CHM), and the silver metal produced in the cupellation. The Chapter will be structured around these four groups. The chemical analyses of the sampled groups are presented and briefly discussed.

Description	Year	Mounted block
llareta ash	2002	25
Silver mineral	2001	13
Beneficiated silver mineral used in cupellation	2002	24
CHM	2001	15 MVB
CHM	2001	15 cc
CHM	2001	16 MVB
CHM	2001	16 cc
CHM	2001	16a
CHM/2	2002	6
CHM/3	2002	7
CHM/4	2002	8
silver metal	2001	14
AgM {13}	2002	13
silver retrieved from CHM	2002	?

Table 6.1. Samples taken for analyses from the silver refining process.

6.1. The *llareta* ash

The *llareta* plant (*Azorella compacta* [Apiaceae]) is a member of the Cushion plant family. These are low growing, woody, herbaceous plants (Kleier and Rundel 2004). They come in a variety of shapes, from semi spherical to hummock and possibly flat mat (Ramsay and Oxley 1997). They have been found in various parts of the world and are extremely hardy and able to

survive in extreme climates; low temperatures, strong wind, and seasonal drought. They are predominant in the southern Andes. The plants have lateral branches that form a canopy structure which is made of small leaf rosettes. Below the open canopy, the branches are physically closer to wood than shrub (Kleier and Rundel 2004, 462) and there is a peaty interior that is built up by the decay of leaves and branches. The *llareta* plant is also very slow growing; Kleier et al. (2004, 462) estimate that the radial growth rate is 1.7 cm per fourteen months, thus a plant that is greater than 10 m would be at least 700 years old. It has been used in the Andes as a source of fuel and as a medicine. It is still used in rural areas as a fuel source because it burns with very little smoke, and is in constant supply in the *Altiplano* where other vegetation is sparse.

Earl Hanson (1926) describes his visit to three small villages located in the north of Chile. Hanson says that the primary source of income is agriculture; the men tend to the fields in the spring and summer, but during the winter they collect *llareta* from the Loa basin. He says that it is used locally as a fuel but also taken further afield to be used on a much larger scale in chemical processing plants. Llamas were used in the transportation of the *llareta* (Hanson 1926, 367-368). It is apparent that *llareta* is a well known commodity in the Andes although its uses for cupellation had never been documented prior to this ethnographic study.

Only one sample of *llareta* ash from the 2002 refining episode was collected. The sampled ash is a fine-grained grey powder. The reason this ash was analysed was to establish its chemical composition, to understand why it had been selected for use as the hearth lining, and to compare it to the hearth material of used cupellation installations. Unfortunately, only one sample of ash was available for analysis, therefore a comprehensive understanding of this ash may be difficult to achieve.

According to XRF pressed pellet analyses the *llareta* ash is composed of silica (36%), lime (31%), potash (11%), alumina (9%), magnesium oxide (5%), iron oxide (3%), and trace quantities of soda, sulphur, and phosphate (Table 6.2). The silica content is higher than expected for cupellation hearth lining materials, where a low quantity of silica is preferable.

SEM-EDS analyses were carried out to allow a more detailed study of the ash. Bulk scans of areas taken at x50 magnification were analysed and the data is consistent with the XRF data (Table 6.3). A more detailed review of the ash's microstructure showed that there are two major grain types characterising it; an angular grain, and a rounded grain (Figure 6.1). The angular grains (labelled 1 in Figure 6.1) have a typical composition of silica (40%), iron oxide (20%), alumina (15%), magnesia/ potash (10%), and only trace quantities of lime (Table 6.4).

The rounded grains contain a much higher silica content of 60 to 80 wt%. Potash and alumina contents are similar to the angular grain but magnesia and iron oxide are reduced to only 1% (Table 6.4).

Sample	Na2O	MgO	Al2O3	SiO2	P2O5	SO3	K2O	CaO	Fe2O3
llareta ash pressed pellet	2.2	4.7	8.7	**36.2**	1.2	2.5	10.6	31.0	3.0

Table 6.2. XRF analysis of pressed pellet llareta ash .
The data has been normalised to 100% and oxygen calculated via stoichiometry.

Sampled area	Na2O	MgO	Al2O3	SiO2	K2O	CaO	FeO
Average (n=5)	1.7	4.2	7.5	44.3	8.0	31.9	2.5

Table 6.3. SEM-EDS bulk scanned area analyses of the llareta ash.
Data has been normalized to 100 wt%.

Sample area	Na2O	MgO	Al2O3	SiO2	P2O5	K2O	CaO	TiO2	FeO
Average angular grains	~	11.2	15.1	38.8	0.5	10.2	0.6	4.8	18.8
Average round grains	1.8	0.1	14.3	72.3	~	8.7	2.1	~	0.7

Table 6.4. The different grains within the llareta ash (sample 25).
Data has been normalised to 100 wt%.

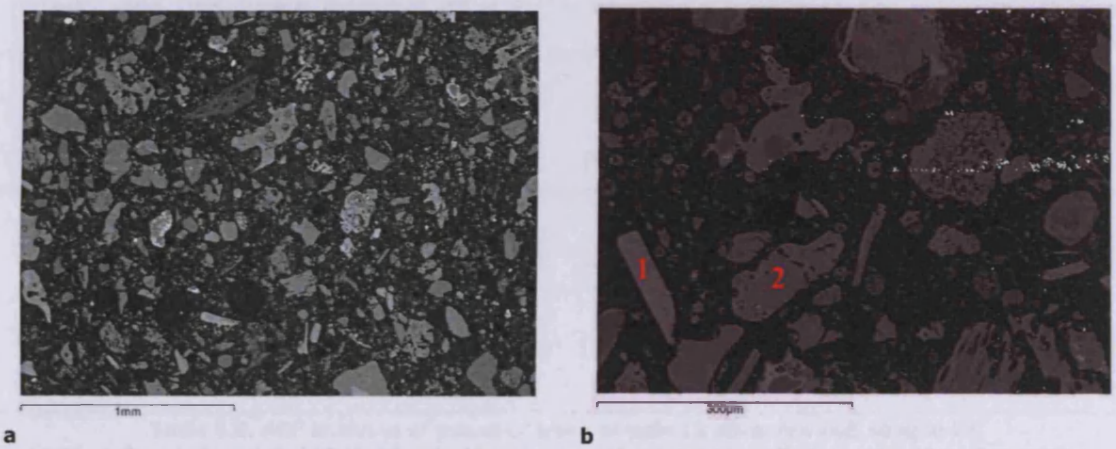

a b

Figure 6.1. SEM-EDS Backscattered 50x micrograph of llareta ash mounted in resin.
An example of the bulk crystals making up the llareta ash. The dark grey coloured matrix is the resin, lighter shaded crystals are the llareta ash (a). Micrograph b shows the two major crystals that compose the llareta ash and (1) are the long angular grains which have lower silica contents than the rounded (2) grains.

The *llareta* ash has relatively high quantities of silica and is therefore not ideal for cupellation. However, it provides a fine-grained porous material which is mechanically suitable for cupellation, and the integration of this plant within Andean society may have other interesting aspects. In Chapter 6, the selection of *llareta* ash and its properties will be considered.

6.2. The silver ore

Two samples of silver ore were available for analyses. One comes from the successful 2001 cupellation but is infact silver gangue (sample 13). The other sample is a selected silver ore from the unsuccessful 2002 refining. However, the possibility of studying a failed cupellation is also very useful, thus the ore was prepared for XRF analysis using the pressed pellet method.

Figure 6.2. Rejected silver ore from the 2001 cupellation (sample 13).

Rejected ore sample 13 (Figure 6.2) could not be prepared for the pressed pellet method as there was an insufficient amount, therefore the resin mounted sample was analysed by XRF. The XRF results shown in Table 6.5 indicate that the ore was composed primarily of zinc sulphide, very little lead (1.5%), and even less silver (0.1%). These results seem to indicate that sorting this ore by hand was sufficient to remove minerals low in silver.

The silver ore sample taken from the failed 2002 refining contains lead (59%), sulphur (12%), antimony (16%), and zinc (9%). The silver content is only 1.6 % (Table 6.5), rather low for a 'rich silver ore'. It is not the most adequate silver ore to be selected for this type of silver refining, and this choice probably reflects the limited experience of the team members in obtaining silver ore rather than Carlos Cuiza's methods.

Sample analysed	Na	Mg	Al	Si	S	Fe	Pb	Sn	Sb	As	Zn	Cu	Ag
Silver ore sample 13 MVB 2001	0.8	0.7	0.5	10.9	27.8	4.6	1.5	0.2	0.3	2.1	50.1	0.1	0.1
Silver ore sample 24 2002	~	~	~	1.0	12.3	1.1	59.0	~	15.8	0.1	9.0	trace	**1.6**

Table 6.5. XRF analyses of mounted block sample 13 silver ore and sample 24.
XRF analyses of mounted block sample 13 silver ore (The data was collected using the alloy setting, presented in elements and normalised to 100%) and sample 24 (pellet) silver ore taken from the 2002 refining episode (The data was collected using the alloy setting, presented in elements and normalised to 100%).

6.3. The Cupellation Hearth Material (CHM)

The cupellation hearth is prepared from finely powdered *llareta* ash, wetted in place with urine. During the cupellation process (described in more detail in Chapter 4), the *llareta* ash acts as a

sponge absorbing liquid lead oxide and other waste produced during cupellation which, when cooled, forms the CHM.

The ethnographic CHM samples have been organised into four categories: CHM from Cuiza's documented refining episodes, CHM added to the *huayrachinas*, CHM from Cuiza's own refining hearths, and other material collected from other hearths in locations surrounding Porco. In this section, the results from analyses of Cuiza's own material are presented and then compared to the CHM added to the *huayrachinas* (previously discussed in Chapter 5). Do the CHM samples taken from other refining areas use plant ash for the hearth lining? Do the processes correlate? What was the type of refining? These questions are central to the analytical work carried out and displayed with regards to the current day CHM.

CHM made during the documented silver refining production

There are 11 samples of CHM available for analysis coming from two separate cupellation episodes. The 2001 cupellation was a successful refining episode, but the 2002 cupellation produced very little silver due to bad quality ore. Unfortunately, during the 2003 cupellation the hearth lining ruptured and thus this cupellation may not reflect a typical refining episode and is hence not considered for analytical study. The data and analysis from the 2001 cupellation is therefore of key importance because it is an example of a working cupellation. The CHM samples are presented in the following section and are grouped according to the year of documentation, and therefore production. Anomalies in the data are also presented.

Cupellation 2001

Two samples of CHM from the 2001 refining episodes are available for analysis (Table 6.6). From these two samples, five pieces of CHM have been selected for analytical study. The numbers assigned have no significance because they were initially assigned when the sample arrived at the UCL Institute of Archaeology for preliminary analysis. I have continued to use the numerical label assigned for ease of documentation.

Mounted blocks	Description
15 MVB	CHM
15 cc	CHM
16 MVB	CHM
16 cc	CHM
16a	CHM

Table 6.6. Samples taken for analyses from the 2001 cupellation.

The CHM samples reflect the inconsistent nature of this material; they consist of three dense pieces of CHM (sample bag 15) and loosely packed pieces of ash, metal and CHM (sample bag 16). Sample bag 15 contains yellow/brown dense CHM that has a luminescent/shiny appearance. The body of the samples is textured and porous. The cut surface of samples 15 MVB and 15 cc reveal regions of different coloured areas, ranging from green and orange to brown. No visible metallic prills were observed. In contrast, the CHM from sample bag 16 is made up of pieces ranging in size from being powders to pieces 2 cm wide. Many have large prills of metal embedded in the surface. Some of the pieces resemble samples from sample bag 15, yellow in colour with a porous structure, whilst others are metallic and grey in colour with a smooth outer layer. These pieces could have been remnants of the skimmed material that Carlos Cuiza removed from the molten metal during the cupellation process. Regardless of origin, all of these samples are classed as being CHM and have been analysed using the same methodology.

Figure 6.3. Selected samples of CHM from sample bag 16.

The OM images correlated with the differences seen in the hand samples. Those from bag 15 showed an open porous structure composed mainly of free lead oxide. The texture of these samples is very fine with few metallic inclusions (Figure 6.3). Samples from bag 16 (16 MVB, 16 cc, and 16a) have a large metallic component; they appear as areas of lead oxide with embedded metallic lead and silver (Figure 6.4). The microstructure is composed of a complex mixture of lead oxides, lead silicates and metallic prills of differing metallic components (Figure 6.4). The metallic prills seen in the OM images have different phases (Figure 6.5). Gangue materials were found such as lead sulphide which had only partially reacted in the lead oxide matrix.

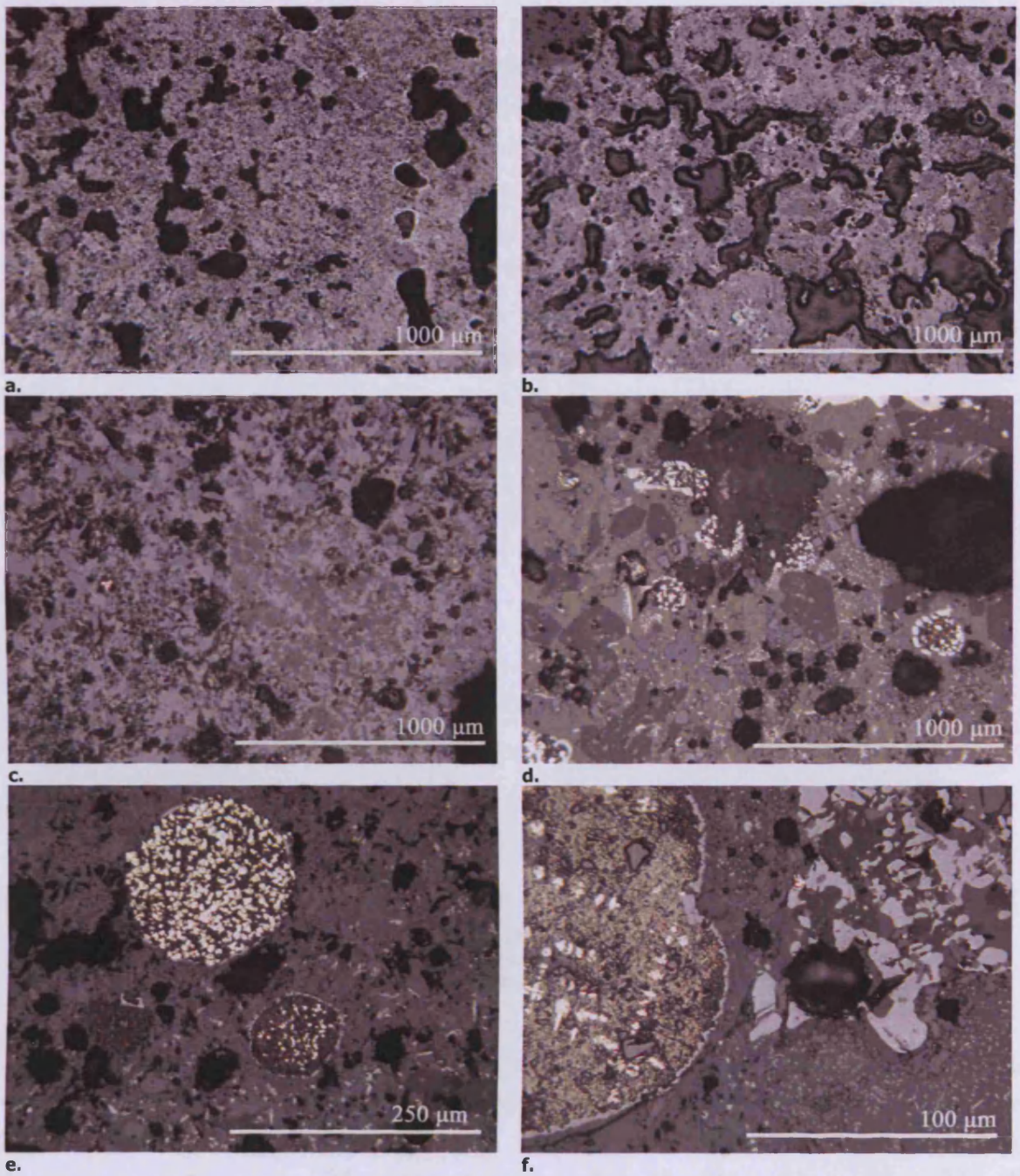

Figure 6.4. OM images of CHM 2001.
The OM showed that the CHM has a porous structure (a - sample 15 cc 2001 and b sample 15 MVB 2001). OM image a and b have a matrix with consistent of dense lead oxides and silicates with very few metallic prills. However, not all the CHM samples were alike; CHM from sample 16a and CHM sample 16 MVB have a complex structure which has open pores, lead oxide, and metallic prills. CHM is composed of different mineral phases (lead oxide and lead silicate), open pores, metallic prills of lead and silver CHM (images c and d - sample 16 MVB 2001). Metallic prills observed using the OM (e -sample 16 MVB 2001). The prills are found within the lead oxide matrix. The yellow lustre of the prills indicates the presence of silver metal. The smaller of the two prills is composed predominately of lead metal. Close up magnification (f) on the CHM indicates the presence of lead sulphide (white areas) and silver metal (yellow dendritic areas within the brown lead metal), left).

The SEM-EDS analyses of bulk scanned areas of CHM have shown that samples from the 2001 refining contain a variety of chemical constituents. The quantity of lead oxide is circa 63% (Table 6.7). The heavy metals such as zinc, silver, antimony and tin (and possibly iron),

identified in the CHM have come from the silver ore being refined. Concentrations of these are variable, but for this refining episode up to 20% zinc oxide and 6% iron oxide are trapped within the CHM. It is necessary to note the presence of silver (0.5 %) because while this cupellation was successful, some silver was left behind in the CHM. The recycling of this material would allow the lost silver to be salvaged. Noticeable in both the bulk area analysis and on the micrographs is the presence of significant quantities of re-crystallised ore, reflected in the analyses with the measurement of sulphur. This is an indication that not all of the starting ore had an opportunity to react and oxidise from sulphides to metal and oxides. The impregnated hearth lining (CHM) is porous, typically with large inclusions. It has a broad range of different phase/mineral inclusions.

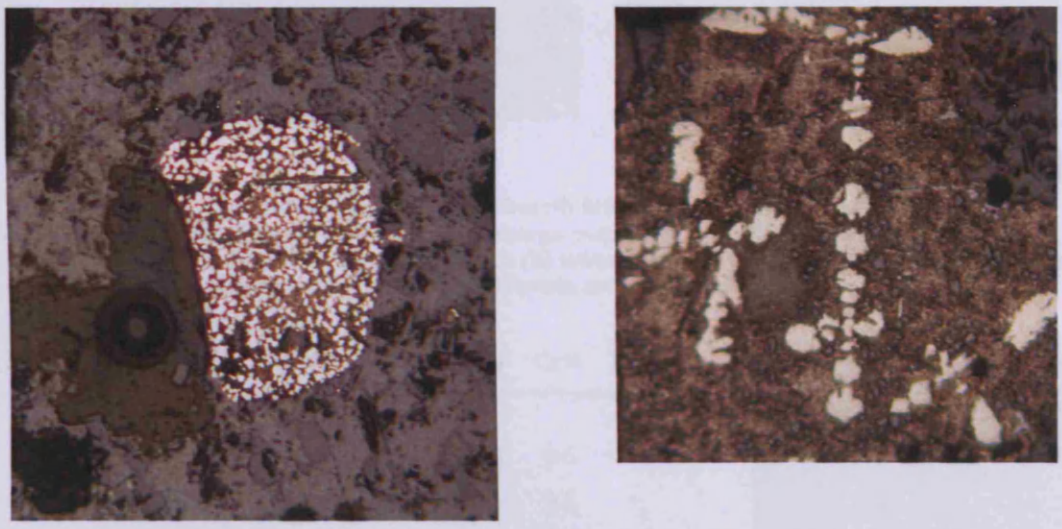

Figure 6.5. A large metallic prill trapped in the CHM sample 16cc 2001 (mag x200), image a. A close up OM image b of a lead prill within sample 16cc 2001 (mag x500). The cream coloured dendrites are silver.

Average composition CHM	Na2O	MgO	Al2O3	SiO2	K2O	CaO	SO3	TiO2	FeO	ZnO	As2O3	Sb2O3	AgO	PbO
15 MVB	0.9	2.3	5.4	17.9	4.0	8.4	~	0.3	1.7	0.9	~	~	~	58.3
16 MVB	~	~	1.1	6.4	~	~	1.7	~	5.6	23.9	0.5	0.6	0.3	59.9
16 A	~	0.2	0.7	4.9	~	0.3	~	~	2.5	21.7	0.2	~	0.6	68.8

Table 6.7. SEM-EDS bulk scanned areas of CHM. Data has been normalised to 100 wt%.

Anomalies and differences in the 2001 CHM

Sample 15 indicates the complex nature of CHM. In this sample, the *llareta* ash is reacting with the litharge/lead oxide produced during cupellation. Figure 6.6 shows a backscattered SEM image of sample 15 MVB. The *llareta* ash used to line the hearth has reacted, being partially dissolved within the main litharge matrix. Derivatives of the *llareta* ash particles are common

within the matrix and have been categorised as feldspars. Table 6.8 shows that these feldspars have silica (65%), alumina (20%), potash (9%), lime (4%), and soda (3%) contributing to their overall composition. Also present within the CHM are crystals of calcium-lead silicates.

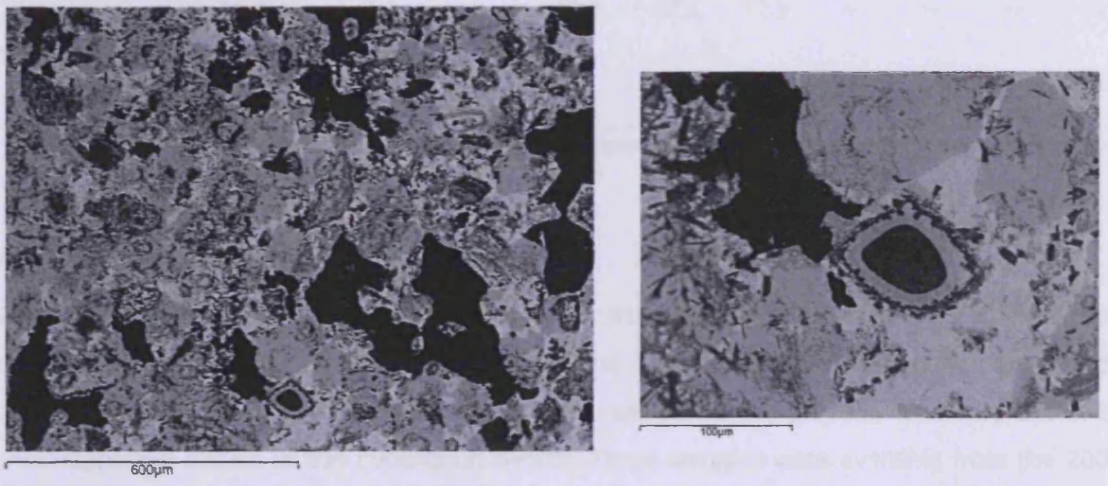

a b

Figure 6.6. CHM sample 15 2002 is the hearth lining soaked with litharge/lead oxide. The SEM backscattered image shows the main litharge matrix (a). In the bottom centre of the image a, a residual ash grain is visible. The magnified grain (b) when analysed was found to be residual feldspar thought to be from the original llareta ash within a lead oxide matrix.

Scanned area	Na2O	Al2O3	SiO2	K2O	CaO	FeO
1	1.1	12.3	71.8	12.9	0.6	1.3
2	5.7	25.1	59.6	1.0	8.5	~
3	2.3	17.7	67.1	12.9	~	~
4	2.3	18.0	66.8	12.5	0.4	~
5	4.8	24.5	58.7	3.7	8.3	~

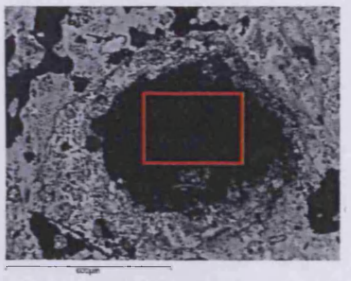

Table 6.8. SEM-EDS data from CHM sample 15 MVB 2001- Feldspar interacting with lead oxide matrix. Data has been normalised to 100 wt%.

In Figure 6.6, there is a residual feldspar grain which can be seen in greater detail in the magnified image. The grain itself is being attacked by liquid lead oxide, which has reacted with the silica in the grain to form the various crystal layers. The centre of the grain has been analysed (Table 6.9 row 2) and the chemical analysis reveals its resemblance to original *Llareta* ash particles (Table 6.9 row 1).

Areas analysed	Na2O	MgO	Al2O3	SiO2	K2O	CaO	FeO	ZnO	PbO
Feldspars analysed in the Llareta ash	1.8	0.1	14.3	72.3	8.7	2.1	0.7	~	~
Bulk analysis of residual grain in Figure 6.6	2.3	~	17.7	67.1	12.9	~	~	~	~
Mid grey layer between inner grain and black crystal layer (Figure 6.6)	2.9	~	3.5	25.7	2.1	2.7	1.7	~	61.4

Table 6.9. SEM analyses normalised to 100% , with oxygen content being calculated via stoichiometry.

Cupellation 2002

The 2002 cupellation only produced 13 g of silver from 1500 g of silver ore. As a result, this cupellation represents an unsuccessful silver refining episode. Given that ethnographic records documented precise quantities of the inputs and outputs of the process, it will be useful to understand the nature of this cupellation hearth. Three samples were available from the 2002 cupellation (Figure 6.7). The results from analyses of these samples will be discussed generally and then any anomalies outlined.

6 (CHM/2) **7 (CHM/3)** **8 (CHM/4)**

Figure 6.7. Images of available CHM samples from the 2002 cupellation.

The CHM sampled from the 2002 refining episodes are much larger pieces of hearth material than the samples taken in 2001. The samples are multilayer fragments which contain remnants of hearth lining (*llareta* ash), metallic prills, and layers of yellow lead oxide. These different layers are very distinct and easy to recognise (Figure 6.8). The layers match the ethnographic documentation of the 2002 cupellation, and during the cupellation Cuiza requested for more silver ore, reporting that the hearth contained too much lead. Samples 6, 7 and 8 have an upper layer of pure lead oxide (up to 1 cm thick) which had not been soaked up by the CHM, in turn reflecting the excessive presence of lead in the system (Figure 6.8). Sample 7 has three distinct layers; a base layer of hearth lining (this layer has a dominant silicate base and could be the hearth wall/clay), a middle layer rich in metallic prills, and an upper layer of lead oxide.

OM revealed a complex microstructure. Lead silicates, a matrix of lead oxide, partially reacted crystal phases, and metallic compounds were observed (Figure 6.9). The different layers seen in the hand specimens were also recognised in the OM.

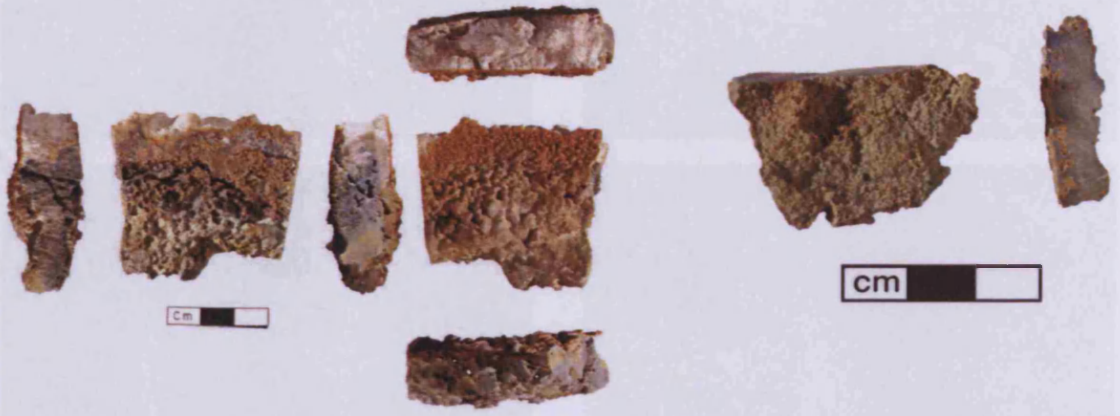

a b

Figure 6.8. CHM 6 2002
Image a - one piece shown from all angles. This sample has been analysed using XRF bulk analysis and full SEM-EDS study. The grey layer is the packed llareta ash, which was wetted into place with urine prior to cupellation. The orange coating is a layer of almost pure lead oxide that has been slowly interacting and sinking into the packed ash. Image b is the hand specimen of the CHM sample 8.

The samples have a matrix of free lead oxide, seen in the OM as a grey opaque phase (Figure 6.9 d). Figure 6.9 b and c show the upper layer of the hearth, which is mostly composed of free lead oxide. The thin needle-like crystals interspersed between the grey matrix are characteristic of lead oxide/litharge (Figure 6.9 c). The opaque lead based matrix contains numerous different crystal phases, but not all were identifiable using the OM. Embedded in the matrix of lead oxide are metallic prills of lead and silver metal, and partially reacted lead sulphides (Figure 6.9 e, f, g). Lead sulphide was only found to be present in the upper layers of the samples. Sample 7 contains a large quantity of the outer hearth in the lower part of the sample, which appears to be clay based (Figure 6.9 h).

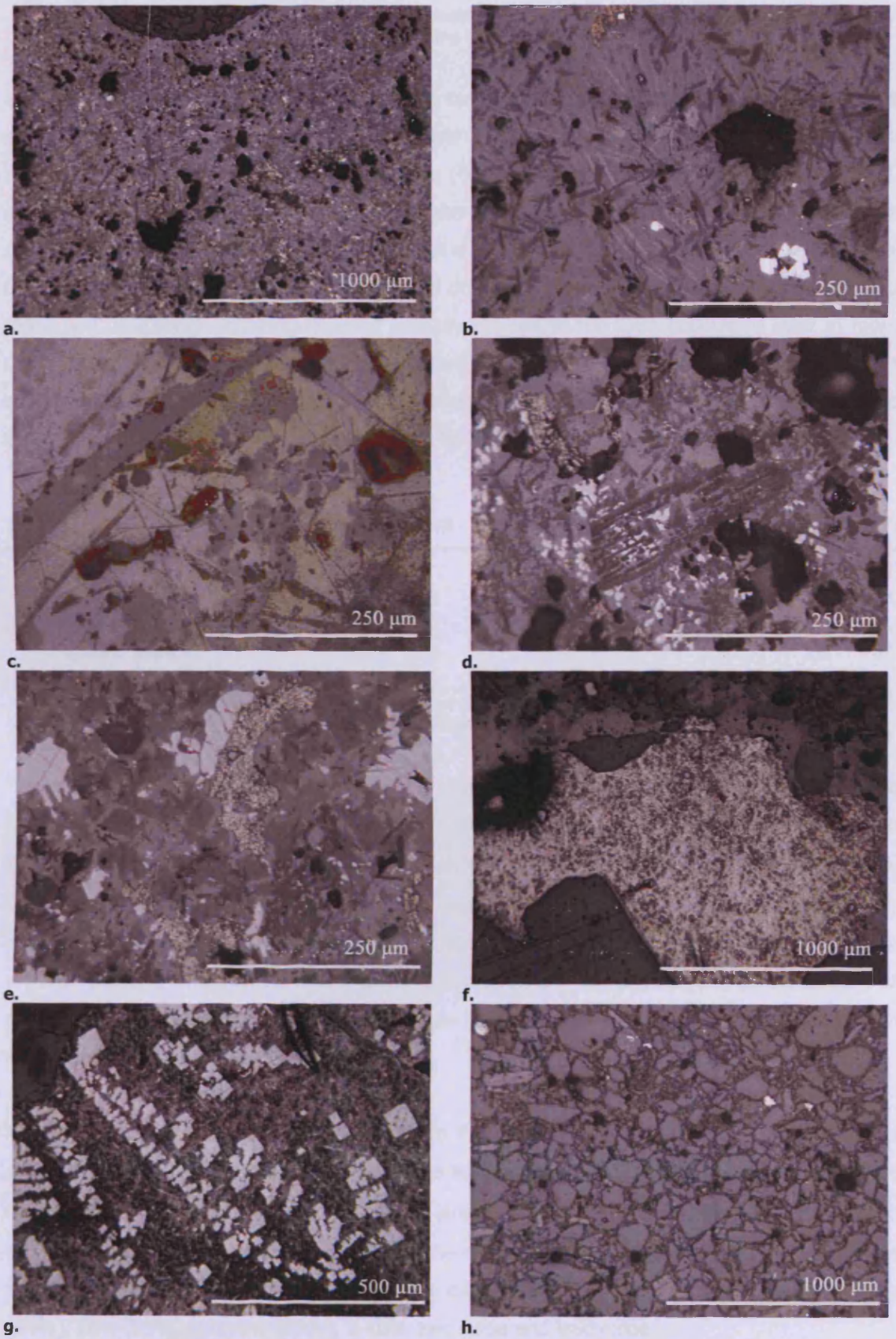

Figure 6.9. OM image showed the porous nature of the CHM 7 and 8
Image a sample 7 and Image b sample 8 2002. CHM sample 8 has a free lead oxide layer with different silicate phases and large pores (Image c). CHM sample 7 has different chemical phases (Image d). Metallic prills of lead and lead sulphide in the lead oxide matrix are common (Image e and f). The CHM

has partially reacted with lead sulphide re-crystallised in the lead oxide matrix (g). Sample 7 has remnants of a clay layer (Image h).

SEM-EDS bulk area analyses of the three CHM samples indicate that samples 6 and 7 have very similar chemical compositions whereas sample 8 has a slightly different bulk composition. Samples 6 and 7 are composed of lead oxide (64%), silica (12%), lime (6%), alumina (3%), and magnesium oxide (1%). These samples also contain heavy metals such as antimony oxide (10%) and zinc oxide (1.5%). The heavy metal concentrations measured in the samples are from the processing of the silver ore, both as dissolved chemical components in the free lead oxide and as distinct ore/gangue areas partially reacted in the CHM (discussed later in more detail). Sample 8 has a higher lead oxide content (80%) and lower levels of heavy metals. This difference may be due to the sampling of different areas within the CHM, and highlights the variability of this type of material. It is difficult to classify a standard CHM composition.

Average bulk area analyses	Na2O	MgO	Al2O3	SiO2	K2O	CaO	FeO	ZnO	Sb2O3	PbO
CHM 6 2002	~	1.0	2.3	11.4	0.4	5.4	0.9	1.9	11.9	64.8
CHM 7 2002	0.1	0.9	2.9	12.9	1.1	5.7	0.6	1.3	10.1	64.4
CHM 8 2002	~	0.7	1.4	7.4	~	5.7	~	1.7	2.3	80.9

Table 6.10. Bulk area scans of CHM from the 2002 refining. Data has been normalised to 100 %.

To analyse how the chemical reactions are happening during cupellation, separate area analyses of the CHM matrix (lead oxide) were done. The quantity of free lead oxide is variable (Table 6.11- sample 6 illustrates this particularly well), ranging from 62 to 86%, as is silica (0-21%). In the majority of sampled areas, the lead oxide matrix has absorbed/dissolved heavy metals such as antimony, arsenic and zinc. In some cases alumina, lime, potash and iron oxide are also present. When these light element compounds are not present, the concentrations of silica are also greatly reduced and the areas measured are almost pure lead oxide with significant antimony oxide (14%).

The CHM from 2002 exhibit similar porosity to that observed in the CHM from 2001. It has a structure that is complicated to interpret, due to the continued interaction between free lead oxide and the hearth lining (Figure 6.11). As already observed, feldspar interaction is common and mineral grains are readily dissolved by the matrix (Appendix II). The system exhibits the formation of other crystals such as complex calcium/antimony crystals with antimony oxide (40%), lime (23%), alumina (10%), 5-10% zinc oxide and lead oxide.

Sampled area	MgO	Al2O3	SiO2	K2O	CaO	FeO	ZnO	As2O3	Sb2O3	PbO
1	~	1.5	10.0	~	~	~	2.4	2.9	14.2	69.0
2	~	3.3	20.6	0.9	2.6	0.7	2.3	5.6	~	64.1
3	~	3.2	21.7	1.1	1.3	1.4	2.8	4.0	~	64.4
4	0.6	1.9	14.4	~	~	~	0.9	~	9.8	72.5
5	~	~	3.1	~	~	~	~	1.4	15.0	80.5
6	~	~	~	~	~	~	~	~	14.0	86.0
7	~	~	1.8	~	~	~	~	~	12.8	85.5
8	~	3.8	20.4	~	~	~	13.7	~	~	62.2

Table 6.11. SEM-EDS area analyses of the lead oxide matrix of CHM from sample 6 2002. Data has been normalised to 100 wt%.

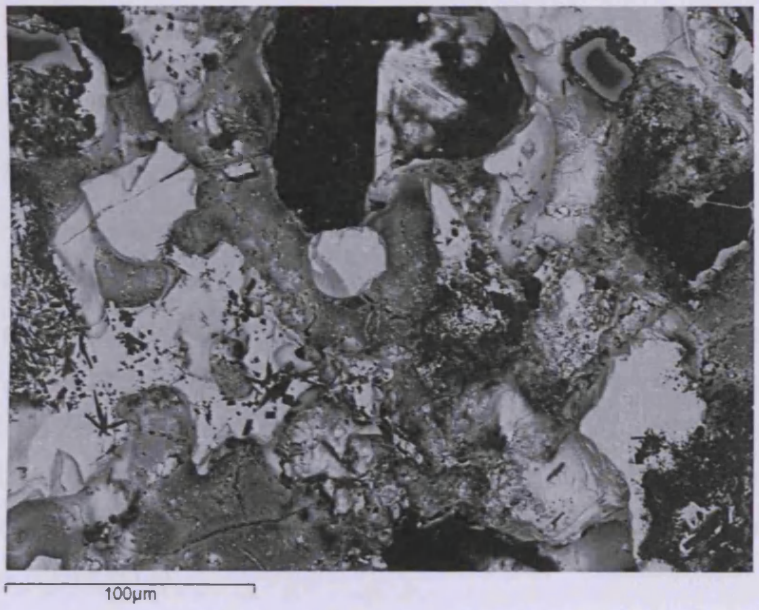

Figure 6.10. SEM-EDS backscattered image of CHM sample 6. The sample shows a mixture of different phases. Dissolving feldspars are common in this sample (e.g. top right hand corner).

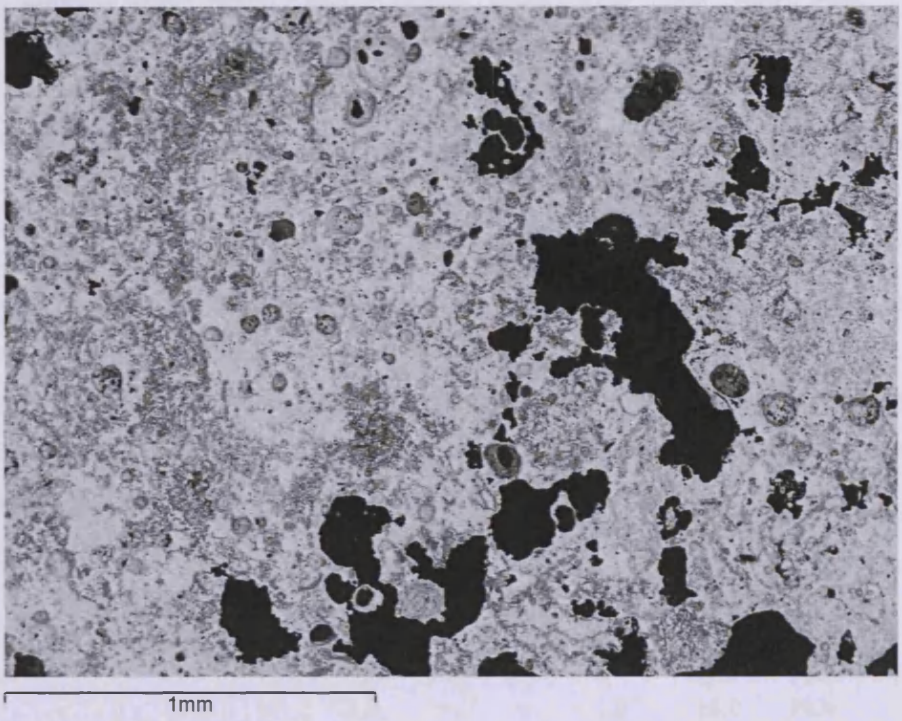

Figure 6.11. SEM-EDS image of bulk area scanned from sample 6. Porosity is a characteristic feature of the CHM (dark regions).

Anomalies and differences in the 2002 CHM

SEM-EDS results have shown that metallic areas found in the CHM are often lead prills containing discrete areas of silver metal with variable concentrations (Table 6.12). Sample 7 is a good example of CHM containing a large quantity of metallic areas. The presence of these metallic areas indicates the cupellation process; some are partially reacted ore samples because they still exhibit concentrations of sulphur. The prills can contain up to 60 at% copper and 8 at% sulphur. The metallic areas consisting of mostly lead always contain silver (16 at%) and lead (83 at%). Finally, SEM-EDS analysis confirms that the lower half of the sample is made of a quartz-rich clay (Table 6.13).

Sampled areas	S	Cu	Ag	Pb
1 (sample of silver rich area)	4.3	~	89.3	6.5
1 (bulk scan)	~	~	16.9	83.1
2	8.7	62.1	~	29.2
3	4.8	~	90.8	4.4
4	2.8	27.5	65.4	4.2

Table 6.12. SEM-EDS area analysis of silver rich areas within lead metal prills (CHM sample 7). Data has been normalised to 100 wt%.

Sampled area	Na2O	MgO	Al2O3	SiO2	K2O	CaO	FeO	PbO
1	1.2	0.7	12.2	76.9	3.2	1.6	2.5	1.8

Table 6.13. CHM sample 7, SEM-EDS area analysis of the clay hearth bottom. Data has been normalised to 100 wt%.

Area analyses were taken to look at the matrix of the upper layer of CHM sample 7 to consider the content of the lead oxide/silicate layers seen in the optical microscopy. The areas are predominately lead oxide (75%), with antimony oxide (11%), and occasionally arsenic oxide (1%). The extremely reactive lead oxide was chemically dissolving, the silica, resulting in lead silicate areas containing around 1 to -20 wt% silica (10%). Here we observe the lead oxide reacting with the gangue minerals from the ore and the hearth lining.

Sampled area	Al2O3	SiO2	CaO	FeO	As2O5	Sb2O3	PbO
1	4.1	12.4	1.2	0.8	~	9.3	72.3
2	~	3.8	~	~	1.0	16.9	78.4
3	1.1	17.3	2.7	~	~	~	78.9
4	2.3	11.2	1.7	~	~	13.9	71.0
5	1.7	17.0	5.2	~	~	3.1	73.0
6	4.1	12.1	~	1.0	~	10.1	72.7
7	~	4.5	~	1.3	~	18.8	75.4
8	~	2.6	~	~	~	17.3	80.0

Table 6.14. SEM-EDS analyses of lead oxide areas that had absorbed gangue from silver ore (CHM 7). Data has been normalised to 100 wt%.

SEM-EDS analyses also indicated the presence of some crystal formations, predominantly those of feldspars possibly formed from the *llareta* ash lining and/or the clay lined base, confirming interaction between the ash and lead oxide.

Summary of cupellation episodes 2001 and 2002

The analyses of the CHM have shown that it is composed of a mixture of pure antimonial lead oxides, residual and partially reacted *llareta* ash minerals, newly formed silicates and many other crystalline phases. The hearth lining appears to have been reacting with the liquid lead oxide to form lead silicates. This interaction between hearth lining and lead oxide has, in 2002, been the cause of a failed cupellation when lead oxide build-up occurred (clearly visible on all of the samples). The lining of the hearth became saturated and excess lead oxide could not be absorbed and so remained above the lining. During cupellation, liquid metal and lead sulphide seeped through the ash layer into the centre of the sample. These areas were then coated by a layer of lead oxide, which reacted and flowed into the upper ash layer. The lead oxide/silicate layer sat above the metallic prills creating the layer seen in this sample; therefore the lead

oxide could not flow easily into the lining because the porosity was blocked by the silicate. Here we see the cupellation process frozen at a crucial point, metallic prills are trapped within the lining, this being extremely detrimental to the overall collection of the silver.

The cupellation in 2001 represents a successful cupellation, and the results of the analyses indicate that the CHM produced contained up to 70% lead oxide and some lime, silica and soda. In contrast, the 2002 CHM has higher lead oxide quantities (65-80%) and increased antimony within the system due to different ore being refined (Table 6.15).

CHM	Na2O	MgO	Al2O3	SiO2	K2O	CaO	SO3	TiO2	FeO	ZnO	As2O3	Sb2O3	AgO	Pb
15 MVB	0.9	2.3	5.4	17.9	4.0	8.4	~	0.3	1.7	0.9	~	~	~	58.
16 MVB	~	~	1.1	6.4	~	~	1.7	~	5.6	23.9	0.5	0.6	0.3	59.
16 A	~	0.2	0.7	4.9	~	0.3	~	~	2.5	21.7	0.2	~	0.6	68.
6 2002	~	1.0	2.3	11.4	0.4	5.4	~	~	0.9	1.9	~	11.9	~	64.
7 2002	0.1	0.9	2.9	12.9	1.1	5.7	~	~	0.6	1.3	~	10.1	~	64.
8 2002	~	0.7	1.4	7.4	~	5.7	~	~	~	1.7	~	2.3	~	80.
Average	**0.2**	**0.9**	**2.3**	**10.2**	**0.9**	**4.3**	**0.3**	**0.1**	**1.9**	**8.6**	**0.1**	**4.2**	**0.2**	**66.**
Min	0.1	0.2	0.7	4.9	0.4	0.3	1.7	0.3	0.6	0.9	0.2	0.6	0.3	58.
Max	0.9	2.3	5.4	17.9	4.0	8.4	1.7	0.3	5.6	23.9	0.5	11.9	0.6	80.

Table 6.15. SEM-EDS bulk area analyses of CHM samples. Data has been normalised to 100 % wt%.

CHM from Cuiza's documented refining episodes versus CHM added to the *huayrachinas*

SEM-EDS data of bulk scanned areas of all CHM are displayed in Table 6.16. The heavy metal elements (those coming from the ore) are removed to allow a comparison between the used CHM and the original *llareta* ash. Quantities of iron oxide are variable, ranging from 2 to 38%. CHM containing high iron oxide indicates that the ore being refined had a high iron content and that the CHM absorbs these gangue components. Silica concentrations between the CHM and *llareta* ash fluctuate from 43-57%. Potash also appears to have been depleted from the CHM material in samples 21, 16 MVB, 16A, 7 and 8. Soda and lime levels are also variable. This variability may be accounted for by the *llareta*'s chemical composition. Only one sample of ash was available from the 2001 production, and logically this bears some similarity to the 2001 CHM samples. No sample of ash was taken from 2002. The variability between *llareta* plants and their different chemical constituents has not been addressed within this thesis. However, it is apparent that all samples of CHM material have been made from *llareta* ash. CHM sample 6 was added to the *huayrachina* in 2001 and its origin is unknown. The chemical composition of

this sample is similar to other samples made from the ash, and it would therefore be a suitable suggestion that sample 6 also be made with a hearth lined with *llareta* ash.

Sample	Na2O	MgO	Al2O3	SiO2	K2O	CaO	SO3	TiO2	FeO
CHM 6 to be added to the *huayrachina* in 2001	0.6	2.8	10.7	52.5	7.7	22.2	~	trace	3.6
CHM 21 to be added to the *huayrachina* in 2002	0.9	2.8	7.4	43.7	~	30.7	~	~	14.4
CHM 15 2001	3.2	3.5	11.8	44.8	8.8	23.4	~	1.1	3.4
CHM 16 MVB 2001	~	~	7.4	43.2	~	~	11.5	~	37.8
CHM 16A 2001	~	2.3	8.1	57.0	~	3.5	~	~	29.1
CHM 6 2002	0.6	2.8	10.7	52.5	7.7	22.2	~	~	3.6
CHM 7 2002	0.5	3.6	11.9	53.4	4.5	23.7	~	~	2.4
CHM 8 2002	~	4.8	7.4	48.9	~	38.9	~	~	~
llareta ash	1.7	4.2	7.5	44.3	8.0	31.9	~	~	2.5

Table 6.16. Llareta ash vs CHM. A comparison between SEM-EDS analyses of CHM minus the heavy metals and the llareta ash. The data has been normalised to 100%. Sample 21 has 14% FeO, and this high quantity is most probably due to a different ore source used for the cupellation.

Element	Na2O %	MgO %	Al2O3 %	SiO2 %	SO3 %	K2O %	CaO %	TiO2 %	V2O5 %	Cr2O3 %	MnO %	Fe2O3 %	PbO %
CHM 5 2001	2.08	0.20	0.51	2.68	0.00	0.24	3.14	0.04	0.00	0.01	0.02	0.19	90.42
CHM 6 2002	0.00	1.98	0.60	6.21	10.74	0.67	2.80	0.05	0.01	0.00	0.00	2.37	67.18

	Co3O4 µg/g	NiO µg/g	CuO µg/g	ZnO µg/g	Ga µg/g	As2O3 µg/g	SrO µg/g	Ag µg/g	SnO2 µg/g	Sb µg/g	Ba µg/g	Hf µg/g	Bi µg/g
CHM 5 2001	58	189	48	304	169	602	958	72	0	129	137	74	23
CHM 6 2002	724	1599	999	14199	496	46291	852	404	137	5046	153	160	1578

Table 6.17. XRF analyses of pressed pellets CHM samples 5 2001 and 6 2002. Data has been normalised to 100 wt% and measured using Turbo-quant.

6.4. The silver metal

The metal produced during the cupellation appeared as a shiny white bullion/cake. In 2001 a large cake of silver bullion was produced weighing 145 g, and measuring almost 10 cm in length. The silver produced was very pure and SEM-EDS analyses showed that 97% of the sample was silver with only 3% lead. SEM images show that the metal had a typical cast alloy structure with lead and bismuth gathering on the grain boundaries. The bismuth must have entered the system through the silver ore and joined the silver during the cupellation process (bismuth was recorded in the XRF data in the CHM). The silver metal produced has very few pores and no other inclusions.

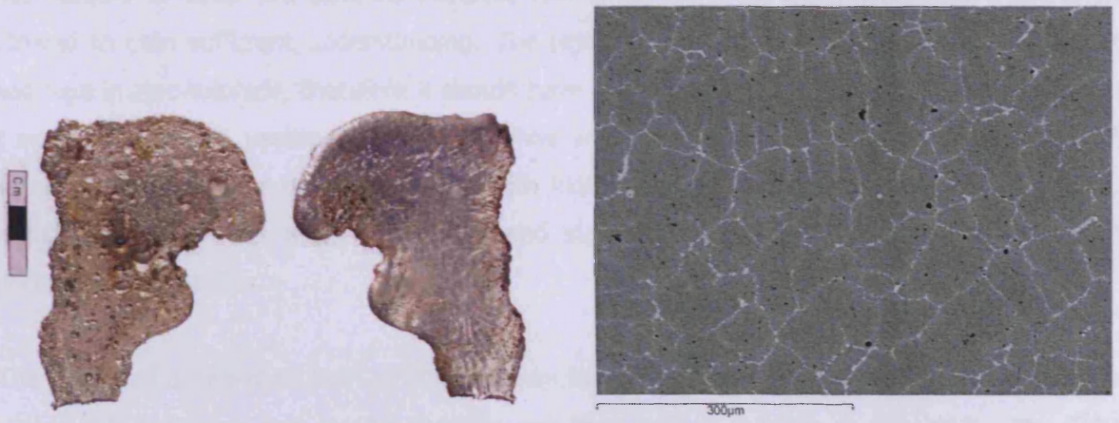

a. b.

Figure 6.12. Silver metal produced from the cupellation 2001 (a).
The image to the left is a view of the base of the cake, note the textured surface from the llareta ash base. SEM backscattered micrograph of silver metal (b). This image shows the grain boundaries of the metal. The inter-fill of the boundaries is a high in bismuth and lead.

Elements	Ag	Pb	Bi
Average bulk scan areas	97.2	2.8	~
Grain boundaries			
SI4	24.4	14.4	61.3
SI9	17.0	18.0	65.0
SI9	6.6		93.4

Table 6.18. SEM-EDS analysis of the silver metal produced in the 2001 cupellation.
The data has been normalised to 100 wt%.

6.5. Summary of the ethnographic silver refining

The ethnographic silver refining has been considered using four main categories of materials; *llareta* ash, silver ore, CHM, and silver metal.

The analyses of the *llareta* ash have shown that it is predominantly composed of lime, silica and alumina, and that it consists predominately of two different minerals that have variable quantities of silica. The high quantity of silica in the *llareta* ash appears to have negatively affected the refining process, as lead oxide is highly reactive with silica. This interaction was clearly observed in the CHM.

The number of silver ore samples available was small and thus the analyses have not been allowed to gain sufficient understanding. The rejected ore analysed from 2001 shows that it was high in zinc sulphide, therefore it should have been considered a gangue mineral, for when it was analysed, no usable quantities of silver were recorded. Ore analysed from the 2002 refining was composed of lead sulphide with high antimony. Only 2 % silver was recorded, which is rather low for a good silver ore and explains the small amount of silver recovered during the cupellation.

The results of analyses on the CHM have shown that the samples contain up to 80% lead oxide (Table 6.15), though this can be variable and the average quantity is only 66%. The CHM absorbs the heavy metals from the ore, such as antimony, zinc, iron and arsenic. The quantities of these also fluctuate according to the selected ore used for refining, the lead ore used to produce the lead metal and the area sampled in the cupellation hearth may also vary the quantity of heavy metals in CHM. The CHM has an average silica content of 10%. The chemical and optical data has indicated that the liquid lead oxide reacted with the *llareta* ash hearth lining, creating lead silicates and other silica-rich phases. This interaction is unfavourable because it blocks the absorptive properties of the cupellation hearth as demonstrated in 2002, where residual lead oxide created a layer above the reacted hearth material.

The analysis of several CHM samples, calculated without the heavy metal oxides, indicates that in all samples, llareta ash or a very similar material was used as the cupellation hearth lining. The occurrence of antimony and/or zinc in the CHM shows that it was most likely that an ore was being refined in all cases, rather than a silver rich lead bullion. Despite the difficulties with the refining process, relatively pure silver bullion is produced and this can then be taken by Carlos Cuiza for sale in Potosí.

7. DISCUSSION AND CONCLUSIONS FROM THE ETHNOGRAPHIC SILVER PRODUCTION

The documentation of the ethnographic silver production has allowed an in-depth review of the chemical and operational processes within the furnaces. In this Chapter, the function and efficiency of this production process is considered. The *chaîne opératoire* of the process will be examined with a reflection on the social and economic factors involved in current day silver production. The production process will initially be reviewed in relation to the two stages; lead production, and silver refining as presented in chapters 5 and 6; followed by a general overview.

7.1. Stage 1 – Smelting to produce lead

The results from analytical work carried out on the lead production samples indicate that only low quantities of lead metal were produced, with a low yield compared to the amount of lead present in the charge. Low reaction temperatures, minimal ceramic wall interaction, and a review of the slag formation process showed that high quantities of lead were lost during the process, either chemically as lead silicate or mechanically as lead metal and sulphide prills. The following section considers the technological function of the *huayrachina* both outside (by reviewing the operational sequence and an assessment of the inputs and outputs within the process) and inside (via the consideration of the chemical processes).

Outside the *huayrachina*: technological function discussed

The efficiencies of the documented *huayrachina* smelts have been assessed using the percentage yield of metal produced and information on mass balances (Table 7.1 and Table 7.2). The *huayrachina* furnace is successful in producing lead metal, but the amount of metal produced compared to the amount of input ore is rather low. The variability in the ratio between fuel and ore may alter the efficiency of the *huayrachina*, but it does not massively increase yield.

A more detailed review of the data indicates that the lead smelting process is not very efficient for metal yield, but may have other inherent benefits. All the smelts were operated with a ratio (by weight) of galena to CHM in the charge of around 2:1, and a fuel to charge ratio of around 1:2, with the exception of smelt 1 (2003) where the fuel to ore ratio was almost 1:1. The fuel to charge ratios are significantly less than the ratios usually encountered in traditional metal

smelting, which range often from 1:1 to 3:1, or even higher (Anguilano et al. in press). This low ratio clearly does not facilitate high temperatures or strong reducing conditions. Nevertheless, in four out of seven of the documented smelts, Cuiza produced around 5 kg of lead metal from a typical charge of *c.*20 kg (Table 7.1). If a lead metal content of 80% in the ore and 50% in the CHM is assumed, then it is possible to estimate that each charge contains between 11 and 17 kg of total lead metal.

	2001		2002		2003		
	Smelt 1	**Smelt 2**	**Smelt 1**	**Smelt 2**	**Smelt 1**	**Smelt 2**	**Smelt 3**
Total input of charge (kg)	19	22	18	17	16	25	19
Estimated Pb in PbS (kg)	10	11	10	9	8	11	8
Estimated Pb in PbO (kg)	4	4	3	3	3	6	4
Estimated Pb in charge (kg)	13	15	12	12	11	17	13
Pb produced (kg)	4	6	4	5	2	3	2
Pb yield	**31 %**	**39 %**	**32 %**	**42 %**	**18 %**	**15 %**	**16 %**

Table 7.1. Lead metal production - the efficiency of the *huayrachinas* reviewed. This table lists both the lead available from the ore and litharge, as well as the quantity of lead finally produced by the *huayrachina*. The average quantity of metal produced is 5 kg. The total lead yield is only about one third of the possible available lead.

Cuiza uses a mixture of galena and CHM as his charge, thus he not only extracting the lead present in the galena but also recycling the lead within the CHM from previous smelts. Ideally, the lead oxide from the CHM reacts with the lead sulphide from the ore to form lead metal and sulphur dioxide, thus the addition of CHM is inherently beneficial. However, almost two thirds of the charge's lead content are still lost in the process, either as fumes and dust, by being absorbed onto the furnace wall, or discarded as solid slag lumps. Thus, the 2001 and 2002 smelts yielded on average only about 30–40% of the combined lead metal contained in the ore and CHM. The 2003 smelts produced even less lead metal than the other years documented, with only 2 kg of metal. The average lead yield in 2003 was only 17% of the potential metal available, and there are a number of factors that influenced the reduced quantities of lead metal during these smelts. Cuiza commented on the poor quality of the lead ore acquired by the PAPP team and as a result, he added increased amounts of ore and CHM to the smelt. He also commented on lower than usual wind conditions. It seems probable that the lack of wind and reduced quality of galena adversely affected the smelt. Unfortunately, no slag samples from the 2003 smelts were available for further analytical work. One may assume that Cuiza would re-smelt some of the slag to reclaim the lost lead (since he had recycled slag back into the *huayrachina* during the smelts) although this is unknown. It is apparent that the 2003 smelts were not consistent with earlier recorded smelts. Although the fuel to ore ratio was not substantially different, the quantity of the charge smelted was increased in smelt 2 (2003).

Wind strength and quality of the smelted ore seem to have affected the smelt negatively by reducing metal yield despite increased fuel consumption.

	2001	2002		2003		
	Smelt 1	Smelt 1	Smelt 2	Smelt 1	Smelt 2	Smelt 3
Total input of charge	19 kg	18 kg	17 kg	16 kg	25 kg	19 kg
Charcoal	12 kg	8 kg	8 kg	15 kg	16 kg	10 kg
Fuel : ore (charge)	**0.6**	**0.4**	**0.5**	**0.9**	**0.6**	**0.5**
Fuel : metal	3	2	1.6	7.5	7.2	5

Table 7.2. Fuel consumption versus quantity of metal produced and ore used. There is no data on fuel from Smelt 2 2001.

Crucially, other factors such as the timing of the documented smelts may have influenced metal yield. To measure these factors, the times of the smelts will be reviewed in the following section.

Timing of the smelts and the resulted variability

The PAPP team noted that Cuiza produced silver on a regular basis (3-4 times) a year prior to 2005. However they did not document when, during the year or what time of the day, these smelts occurred. It could be assumed that they would not have occurred during the wet seasons (January-March) although the exact time of the year is unknown. The time of year in which a smelt was conducted raises important concerns regarding the effect of wind on the smelt. It also allows for further understanding of the role of metal production within Cuiza's daily life. Is it a seasonal activity related to the weather/wind conditions or the rotation of different tasks according to agricultural responsibilities? Is it related to the accessibility of resources (when fuel, ore and other materials in the area are readily available)? Personal communication with Dr Van Buren 2008, confirmed that Cuiza smelted when local miners or acquaintances brought him ore. Thus, the seasonality of the task may also be related to the times of the year that ore was obtained. The role of Cuiza's smelting as a result of the potential illicit acquisition of ore is still undefined; it is apparent that he was smelting ore that may have been obtained illegally when required, but the details of this activity remain shrouded and undisclosed. Nevertheless, during the PAPP smelts Cuiza continued to use his normal smelting methods, and some of the basic functions of the furnace can still be analysed. Historical sources state that smelting occurred in the afternoons and late evenings (Capoche 1585). Did Cuiza continue this practise during his normal smelting episodes?

The documented smelts occurred in July (2001 and 2003) and September (2002). The dry season is from May to September, during these months winds are strong in the afternoon and

evening. From the documented smelts, the duration of a smelt varied from 5 to 8.5 hours (Table 7.3). In 2001, the second smelt was terminated because the furnace did not become hot enough to melt the lead ore. The successful smelt in 2001 started at 11.30 am and in 2002 at 11.30 am and 1.00 pm. The different start times of the smelts may have influenced the smelting conditions within the furnace. The dates and times of the documented smelts were partially determined to suit the PAPP team, therefore it is unclear when Cuiza would normally use the *huayrachinas*.

The *huayrachina* is partially powered by wind, thus it requires constant strong wind to function efficiently. Without constant wind, the system will suffer from reduced temperatures and inconsistent oxygen levels within the reaction chamber, causing poor smelting conditions. Thus, successful smelting needs a regular flow of air to keep temperatures constant, which is even more important when fuel is of poor quality or is in short supply. In Cuiza's *huayrachina* the fuel to charge ratio is typically 1:2, indicating a choice to use a low quantity of fuel which is expensive and in short supply. However, using lower than ideal quantities of fuel requires suitable wind power. In 2003, Cuiza commented on the lack of wind and the quantity of lead metal produced was greatly reduced (2-3 kg). If the wind levels are increased, one might assume that the duration of the smelt would be reduced because temperatures would remain constant and the reactions occur more quickly. An investment of 5-8 hours is quite a substantial amount of time to produce 5 kg of lead. However, Cuiza only requires sufficient lead to cupel enough silver, therefore the time investment must be outweighed by the amount of income the silver will bring into his household. However, there are still questions relating to Cuiza's silver production that remain unanswered: How much time per year would Cuiza have devoted to metal production? Does seasonal variability in wind influence the time that Cuiza smelts?

Smelt	Time taken in total
1st day smelt 1 2001	**8.5 hours**
1st day smelt 2 2001	**4 hours but smelt was terminated as furnace never became hot enough to melt the lead**
2nd day smelt 1 2001	**7.5 hours**
1st day smelt 1 2002	**5 hours**
2nd day smelt 2 2002	**Final time not noted**

Table 7.3. The time taken to produce lead in the documented smelts. Note that no data is available from the 2003 smelts.

Thus far, conditions and variables outside of the *huayrachina* have been considered. Here the focus changes to review the chemical and physical reactions taking place inside the *huayrachina*. How does a *huayrachina* work?

Reactions inside the *huayrachina*

Closer inspection of the situation within the modern *huayrachina* reveals that the temperature and redox conditions are highly dependent on the location; if closer to the eye holes, the ore will be under highly oxidising conditions and will also experience higher temperatures. In the main body of the *huayrachina*, conditions will be reducing i.e. there will be a lack of oxygen. These variable conditions mean that different reactions will occur concurrently.

Within the furnace, several reactions are occurring including the transformation of lead sulphide mineral into lead oxide, lead sulphide conversion to pure lead metal. If lead oxide is present without siliceous material to react with, and inside the furnace with sufficient carbon monoxide to drive the reduction, that too can be reduced to form lead metal (Figure 7.1). Evidence of all stages is represented in the slag matrix.

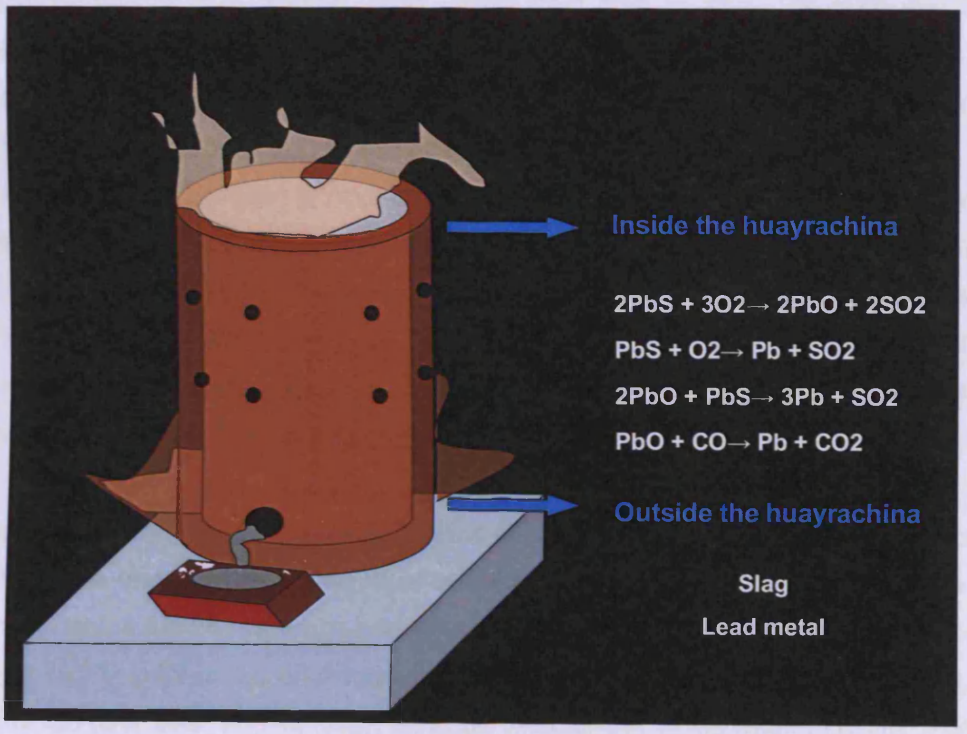

Figure 7.1. Reactions inside the *huayrachina* and products.

The balance between these four stages is crucial as it represents the skill of the smelter and affects the efficiency of the furnace. Litharge (PbO) is a necessary component to facilitate the transformation of lead sulphide to lead metal, although it is highly reactive and will combine with any silicate material to form a lead silicate. This has been noticed on the furnace walls, with 2-3% of lead oxide being absorbed into the ceramic matrix. This type of chemical reaction is common in any lead smelting furnace but the amount of penetration and thickness of the vitrified material is very low, which is further evidence for the lack of temperature within Cuiza's *huayrachinas*. If the smelting materials were fully molten they would have had an opportunity

to react more strongly with the furnace wall, if they remained semi-molten, the surface area for interaction is greatly reduced and hence there is only limited vitrified material left behind on furnace fragments.

The analytical results

Chemical analysis has revealed the heterogeneous nature of the *huayrachina* slag. It is highly variable, and some pieces contain 80% lead sulphide. Their structure indicates that not all of the partially molten lead sulphide matrix reached sufficient temperatures and/or correct redox conditions to transform to lead metal. These samples often have re-crystallised zinc sulphide on the grain boundaries. Other pieces of slag have been formed in different regions within the furnace, and as a result they can show up to 40% iron oxide within the glassy matrix and as little as 2% lead oxide. The slag is so varied that numerous mineral phases are present and the relative proportion of each mineral varies widely from area to area. The main slag sample consists of a lead silicate glass that also contains up to 8% zinc oxide and c. 10% iron oxide. The average lead oxide content is only 9% and silica content is 40%. Crystal phases identified include; leucite, olivine, high iron spinels, zinc sulphide, lead sulphide, and lead metal. These reflect the interaction between gangue minerals, the ceramic wall and lead ore, and are also indicative of the initial ore source since recrystallised galena (PbS), chalcopyrite ($CuFeS_2$), and sphalerite (ZnS) are still visible as distinct phases within a complex slag base. Consideration of the different phases within the slag has been of key importance to understanding the type of reactions occurring. This slag does not follow an average compositional pattern, indicating that the conditions inside the *huayrachina* were highly variable.

The presence of large amounts of lead sulphide in a lead-silicate rich slag matrix indicates that the system was, on the whole not strongly oxidising, and so while we must pay attention to the location within the furnace where the slag has formed we cannot deny that the system overall displays a highly sulphurised environment. If the conditions had been more oxidising, more sulphur would have been burned away, although whether this would result in higher lead metal production or simply increased formation of lead silicate in the slag would depend on the exact circumstances in the *huayrachina*. The compositional analysis of the slag from the 2001 smelts shows that, while the furnace clearly yields some lead metal, the slag still contains considerable quantities of lead which chemically bonded as a lead silicate and mechanically trapped as lead sulphide aggregates.

Analysis of slag adhered to an older *huayrachina* fragment found on Cuiza's smelting site has shown that the slag contains rich silver prills, and areas of partially reacted argentiferous lead sulphide (sample 17, see Appendix II). The slag on this sample is glassy and less

heterogeneous than the slag pieces analysed in the documented smelts. Conditions within this area of the furnace would have been hotter and possibly more oxidising than those recorded in the acknowledged smelts. The presence of silver indicates the use of a different ore source from that of the current day situation. Importantly, the smelting practise was different to past smelting episodes, but the exact time of this smelt remains uncertain.

The environmental adaptation

In the ethnographic lead production, we can observe environmental adaptation. Cuiza needed to use charcoal for the smelt, but charcoal is expensive to buy, since the *Altiplano* region of Bolivia has scarce plant material and fuel is generally costly. Cuiza did make his own charcoal, but this required considerable a time investment of around one week to produce enough charcoal for a week of smelting. Cuiza used a mixture of different fuels in the *huayrachina*. He prepared his own charcoal using *queñua* wood, which was mixed with *churqui* charcoal (bought from Potosí). During the initial lighting of the furnace, *ichu* grass and donkey dung were used and only later, once the furnace was hot, the charcoal was added. The preferential selection of these fuels did have an effect on the way in which the smelt functioned. Green wood was available to Cuiza (*queñua* wood), but he selected charcoal for his smelting. The use of charcoal rather than green wood allowed for higher temperatures to be obtained in the reaction chamber and required lower quantities of fuel for ignition. The high altitude of Porco (4100 m.a.s.l.) reduces atmospheric pressure which would have affected the temperatures at which evaporation, thermal decomposition and chemical reactions would have occurred. Thus, even with suitable charcoal that burns and reaches high temperatures, more fuel would probably be required in high altitudes compared to smelting at lower altitudes.

By reducing the amount of fuel used in the smelt, Cuiza could economise on the cost of fuel and invest more time into the refining of his silver ore. The main consequence of economising on the quantity of fuel was a reduction in the quantity of lead produced from the *huayrachina* smelts. This decreased yield would have been acceptable as Cuiza only needed sufficient lead metal to refine his rich silver ore in the cupellation chamber. These adaptations were driven by a necessity to create access to cash (other methods of income may have been based on a barter/exchange trade system). Cuiza only produced silver three to four times a year, so the investment of time needed to be proportional to the profit resulting from selling silver in Potosí.

Cuiza's *huayrachinas* did not produce large quantities of lead metal. They appear to have been optimised for fuel efficiency as well as using the power of the wind to provide adequate temperatures and furnace conditions. The *Altiplano* region of Bolivia has a severe fuel shortage, and most wood has to be imported from lower altitudes while silver poor lead ore is easily

available. Under these conditions, creating a furnace using relatively little fuel is very sensible (Winterhalden et al. 1974) even if it is wasteful in its ore consumption. The technology requires a relatively low capital investment for Cuiza since he already had his *huayrachinas* which required very little extra care because they only needed replacing every 2 to 3 years. Although he had to buy some of the charcoal for the *huayrachina*, he could prepare small quantities of charcoal and other necessary fuel from his farm.

Ore acquisition

One of Cuiza's substantial investments would have been the acquisition of the ore used to produce silver. He would need to have had access to good quality silver ore but also good lead ore. His knowledge of ores and their properties will have almost certainly governed his choice and selection of ores in this process. However, PAPP noted that Cuiza would also smelt ores brought to him by local miners. Thus, it is difficult to ascertain the time invested by Cuiza in ore acquisition. One could assume that he may never have needed to acquire his own ore because smelting would have taken place when miners approached him to smelt their ore.

Cuiza used both lead ore (galena) and recycled litharge as a source of lead metal, which enabled him to control the batch composition within the smelting charge. Furthermore, Cuiza continuously checked the appearance of the slag produced, which would have informed his decisions about whether to discard or re-feed it for further smelting, and possibly also regarding the amount of fuel needed. This provides an interesting opportunity to analyse the variable input factors within the smelting process; including the degree of desulphurization during the smelt, and the degree of liquefaction and homogenisation of the charge. At present, it appears that the *huayrachina* operated not at a stable equilibrium, but provided a wide range of oxidising and reducing conditions and very variable temperatures. The limited metal yield has to be seen in conjunction with the cost of lead ore and charcoal bought for cash, and the effort once necessary for Carlos Cuiza to procure litharge and other fuel (Cohen et al. in press).

The main variables affecting the smelting conditions in the *huayrachinas* are the wind and quality and quantity of ore and charcoal. Thus, the location of Cuiza's *huayrachinas* played an important role in the smelting operation. High windy locations were favoured in antiquity, and it seems that the ridge where the *huayrachinas* were built (close to Cuiza's *estancia*) was also selected for this purpose. The location chosen for *huayrachinas* also needs to provide access to strong constant winds, but presumably it also needed to be close to a good fuel source (if a large quantity of fuel is necessary, the fuel needed to be transported to the site). The locality of the *huayrachinas* may have also been influenced by the materials required to build them i.e. the location of suitable clay and access to water. All of these variables would have affected Cuiza

and his family's decisions when choosing a location for the *huayrachinas*. The ridge chosen catches the wind as it is surrounded by two smaller peaks which direct the wind towards and over the ridge.

So in summary, the current day *huayrachinas* are suitable for producing lead metal. The high sulphur content and presence of partially reacted ore within the slag indicate that the furnace conditions were not heavily oxidising, and it is clear that a lot of potential lead was lost into the slag matrix. For Cuiza, this loss is acceptable because he only needed sufficient lead metal to refine his silver ores. He did not have to invest heavily into producing a more effective smelting furnace with a higher lead yield. The separation of silver and lead production also requires a smaller investment in the smelting process. If the result of smelting is lead metal which is not the final desired metal, then only the minimum amount of charcoal needs to be used to smelt a sufficient quantity of lead metal. Thus, Cuiza economised on fuels and instead invested time and energy into the cupellation process. Slag containing a large quantity of lead sulphide can also be recycled back into the *huayrachina* to reclaim some of the lost lead.

7.2. Stage 2 – silver refining via cupellation

The lead produced in the *huayrachinas* is used in stage 2 to refine rich silver ore using cupellation. In this section the function and properties of Cuiza's cupellation hearth are considered. It starts with a review of the fuel selection and the process efficiency, and then a consideration of the input and outputs generated during the refining process.

Fuel used by Cuiza during the cupellation

Cuiza selected a number of different fuels (llama dung, *thola* wood, and donkey dung) to power the reactions in the cupellation hearth. The selection and use of these fuels differed from those used in the smelting, and indicates a preferential selection.

Dung as a resource is readily available to Cuiza. On his properties he cared for sheep, llamas and cows. Llamas regularly defecate in the same area, and thus collection of dung is straightforward. Llamas and other herbivores produce up to four times their body weight in dried dung per annum (Winterhalder et al. 1974, 89). Dung burns similarly to grass/straw/other plant material because a herbivore's diet is plant based. Herbivore dung has a compact, porous structure that burns steadily (Sillar 2000b, 46). Cupellation requires high temperatures to melt the silver ore and conditions need to be sufficiently oxidising to stimulate the production of lead oxide. Wood would have been another suitable choice for fuel, however, wood was an expensive and time consuming commodity for Cuiza. The use of dung was therefore a sensible

choice because it is easily collected, will burn smoothly, and give sufficient heat to cupel the silver ore. The selection of dung over wood may have been one of economic rather than technical preference (i.e. a decision based on costs rather fuel efficiency). Materials that were easily available to Cuiza such as dung may have also influenced the technological choices involved in the refining process. (Rice 1987). The use of varied fuel sources is a sensible use of resources in the *Altiplano* environment and within a *campesino* mixed income economy. Typically Andean peasants use llama dung and the *llareta* plant as sources of fuel (Sillar 2000a, 106), so the selection of llama dung for cupellation is not surprising.

Construction of hearth and its efficiency

Cuiza owned two cupellation hearths built within different small adobe brick huts. For the documented cupellations, Cuiza chose to use the first hearth built by his parents 30 years before. The adobe huts were located within a small ravine close to Cuiza's house. They were constructed using traditional methods, and the walls were made from adobe bricks and lined with local clay, with a thatched roof made from local *ichu* grass covering the hut. This sheltered the cupellation hearth from the extreme Andean weather. Cuiza said that the cupellation hearths needed protection from the wind and from rain to prevent damage (Van Buren and Mills 2005, 13). This is in complete opposition to the *huayrachina,* which needed exposure to the wind to function. What can this separation tell us about the origins of this technology within Andean metallurgy?

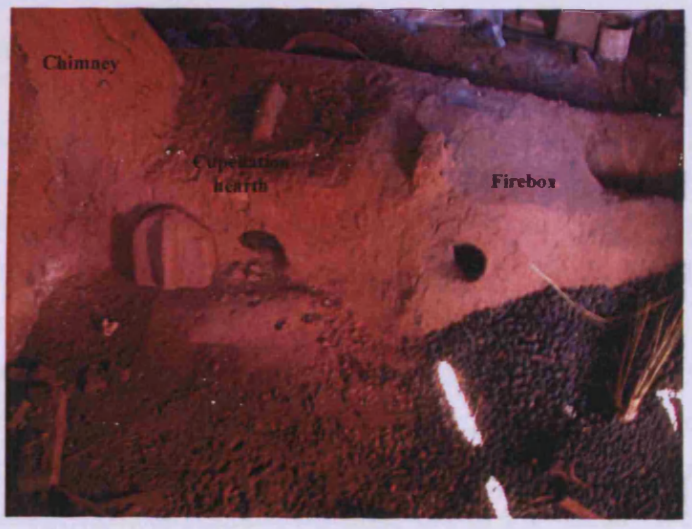

Figure 7.2. Cuiza's cupellation hearth.

The cupellation chamber is constructed of local ravine clay and segmented into three compartments; the fire box, the cupellation hearth, and the chimney (Figure 7.2). The cupellation hearth has some similarities to the traditional Andean cooking hearths (Sillar 2000a, 106). The size of the reaction hearth restricts the quantity of silver produced. The *llareta* ash

layer can only absorb a defined quantity of lead oxide and if the quantity of lead exceeds this limit, the hearth will become blocked and cupellation will stop. Cuiza used the same size of hearth for each of the documented refining episodes.

The documented cupellations took up to 19 hours with the 2001 refining starting at 9.30 am and finishing at 6 am the next day. The overall process required constant attention and Cuiza did not leave the furnace unattended for long periods of time. Inside the cupellation hut there was little space and Cuiza performed the cupellation process by lying on his side, tending and monitoring the firebox and hearth.

Materials	2001		2002		2003	
	Input	Output	Input	Output	Input	Output
Silver ore	0.3kg	~	1.5 kg	~	0.5 kg	~
Lead metal	1.8 kg	~	3.0 kg	~	6.0 kg	~
Fuel	12 costales	~	62 kg llama dung	~	66 kg llama dung, 1 kg donkey dung, 1 kg firewood, 0.5 kg dry grass	~
Silver metal	~	**0.15 kg**	~	**0.01 kg**	~	**0.23 kg**
CHM	**Not recorded**	**Not recorded**	~	**5 kg**	~	**6 kg**
Silver ore:lead metal	**6**		**2**		**12**	
Silver ore:silver metal	**0.5**		**0.0006**		**0.5**	

Table 7.4. Input and output quantities for the documented silver refining episodes.

The efficiency of the refining episodes has been considered via a review of the ore to silver metal ratio and the silver ore to lead metal ratio (Table 7.4). The 2001 and 2003 cupellations have similar ratios of 2:1 for silver ore to silver metal. Despite the 2003 cupellation being unsuccessful due to the hearth rupturing, the ratio remains the same as in the successful 2001 refining. The ratio of silver ore to lead metal does not seem to have been constant in the documented refinings. The successful refining in 2001 had an ore to lead metal ratio of 1:6. The 2003 episode used more charge and the silver ore to lead metal ratio was 1:12 though cupellation still took place with 0.2 kg of silver metal being produced. The 2002 cupellation was unsuccessful, which can be attributed to a poor ore source with very low quantities of silver. As a result of Cuiza's attempt to mitigate this problem by adding more silver ore, the ratio between lead metal and ore does seem rather unusual at 1:2. This may have contributed to the poor silver yield.

Analysis of the cupellation process

The analytical work carried out on Cuiza's refining process has considered the input and output materials. The starting materials were *llareta* ash and silver ore (the *llareta* ash and hearth lining have been assessed for their suitability to the process), and the products were CHM and silver metal.

The starting materials

Silver ore

The small number of samples available for analytical work limited the chemical information that could be gained from analysis. However, silver ore analysed from the 2002 refining was composed of lead sulphide with high antimony. Only 2 % silver was recorded which is very low for a good silver ore and explains the small amount of silver recovered during the cupellation. The analytical work carried out on rejected ore from the 2001 refining showed that it was composed of sulphidic compounds, expected for gangue minerals. Unfortunately no silver ore selected for refining in 2001 was sampled for analytical work (all the ore went into the cupellation). The use of a poor ore in 2002 resulted in a very low silver yield; out of a total of 1500 g of ore, only 10 g was refined. In this process the quality of the silver ore is important and poor ore results in low metal yield. The quantity of silver yield is limited by the size and depth of the llareta hearth lining and the ratio of lead to silver ore.

During the ethnographic documentation, Cuiza was reluctant to discuss where he sourced his silver ore. Sourcing of the silver ore raises important questions regarding the illicit trading of minerals. Cuiza was a retired miner and he would still have had acquaintances working in the mining trade. It would have been easy for him to gain access to good quality ore through the communal trading of goods; however, for miners working in the Porco mines the removal of ore is illegal. Cuiza had hinted that local miners would bring him ore to smelt and then refine. He would receive half of the resulting metal (personal communication with Dr Van Buren 2008). No further information is available regarding ore acquisition. However, despite circumstances of ore acquisition, Cuiza's cupellation works successfully to form an economically valuable silver cake. If the silver-rich ore was sourced from a miner, then the expertise of this miner would have meant a suitably rich silver ore would have been selected. When members of the PAPP team selected the ore, their inexperience in mineral quality created an unexpected vaiation from the normal cupellation process.

Llareta ash

Cuiza's cupellation hearth is lined with *llareta* ash. It is a common source of fuel for rural communities located in the *Altiplano* region where other wood is scarce and expensive. Traditionally, wood and plant ash was used for cupellation in Europe (Craddock 1995). Since the medieval period, bone ash was preferred because it contained no silica. This is favourable because litharge is highly reactive with silicate material; during cupellation a lining low in silica is preferred.

Why did Cuiza select *llareta* rather than bone ash? In the Porco region trees are scarce, thus *llareta* ash is the most obvious plant ash available for cupellation. If the *llareta* plant had been used for other means in Cuiza's property, such as a fuel, it may have been easier for Cuiza to prepare *llareta* ash rather than make or buy bone ash (which can be both a time and fuel consuming operation). The use of bone ash in an Andean environment seems rather unlikely due to the lack of a large centralised butchery in the *Altiplano*. Camelids have less bone than cattle. However, this part of the *chaîne opératoire* is unknown. Why did Cuiza select this ash rather than another for cupellation? It is necessary to establish the role of *llareta* within metal refining? Is it technically or sociologically preferred?

No information is known regarding the preparation of the *llareta* ash prior to use in the cupellation hearth. Since llareta is used locally as a fuel, it is likely that Cuiza collected ash from his domestic hearths, although this is currently unsubstantiated. The hearth was prepared using a mixture of *llareta* ash and urine. The resulting mixture was pressed into the concave shaped hearth, ensuring a smooth surface.

Analytical work conducted on the *llareta* ash showed that it contained *circa* 40% silica, 30% lime, and 10% potash. The high lime and relatively low silica content make *llareta* ash an advantageous choice. It is preferable to grass, straw ash or even llama dung ash due to their assumed higher silica levels. However, it still contains relatively high levels of silica for cupellation and thus is not the ideal hearth lining (Cohen et al. forthcoming b). A comparison to European tree ash (beech and oak) shows that silica levels are increased in the *llareta* ash (Table 7.5). However, despite the higher than desired silica quantities, the *llareta* ash allowed cupellation to occur successfully in Cuiza's cupellation hearths.

Sample	Na2O	MgO	Al2O3	SiO2	P2O5	SO3	K2O	CaO	Fe2O3	TiO2	MnO
Cuiza Ilareta ash	2.2	4.7	8.7	**36.2**	1.2	2.5	10.6	31.0	3.0	~	~
Beech ash*	0.6	7.0	0.9	**18.0**	15.3	~	20.0	31.0	0.9	0.1	6.2
Oak ash*	0.5	4.3	1.9	**7.1**	3.1	0.7	14.9	64.5	2.5	0.1	0.4

Table 7.5. ED-XRF analysis comparing tree ash to the Ilareta ash used by Cuiza. The data has been normalised to 100 wt% and oxygen calculated via stoichiometry. *Beech and oak ash data taken from Jackson & Smedley 2004, 39.

As a result of cupellation, Cuiza produced silver metal and CHM. A review of the products formed via cupellation now follows.

The products

CHM analysis

SEM imaging of hearth lining soaked in litharge (known as Cupellation Hearth Material – CHM) shows that the *Ilareta* ash reacted with the litharge as well as absorbing it mechanically. Area SEM-EDS scans of CHM have shown that the samples contained up to 80% lead oxide, although the average quantity is only 66%. The impregnated hearth lining is commonly porous with large inclusions of different minerals from the initial ash and metallic oxide inclusions such as antimony, zinc, iron and arsenic oxides (derived from the silver ore). The quantities of these fluctuate according to the ore used for refining, the lead ore used to produce the lead metal, and the area sampled in the cupellation hearth.

It is apparent that the *Ilareta* ash used to line the hearth had been reacted with and been partly dissolved into the main litharge matrix. This interaction is unfavourable because the lead silicate phases block the absorptive properties of the cupellation hearth, as demonstrated in 2002, where residual lead oxide was not absorbed but instead created a layer above the reacted hearth material. The remaining high level of porosity in the used CHM also indicates that the *Ilareta* did not act fully as a sponge to soak up the liquid litharge.

Silver metal

The silver cake produced from Cuiza's cupellation hearth in 2001 is almost pure silver (97 at%) with small concentrations of lead (3 at%) and trace quantities of bismuth. The 2001 cupellation was successful in producing pure silver that could be sold in Potosí without the need for further refining.

In 2002 the process did not work, and this is partially due to the project team members obtaining a poor/low grade silver ore, as well as the fracturing of the *llareta* ash hearth, with molten metal being partly lost in between the cracks. The analysis has therefore indicated that the *llareta* ash is not an ideal material to be used for cupellation, yet it is an interesting technical choice because it can adapt to given environmental conditions.

The cupellation process

Cuiza's cupellation furnace functioned under oxidising conditions (Figure 7.3). Cupellation requires a strong and steady heat to oxidise the lead metal and refine the silver ore. For cupellation to occur successfully, the reaction must happen in a vessel that is made from material that will not react with litharge. Thus, the reaction vessel must have a low silica content. Cuiza used *llareta* ash to line the cupellation hearth (made from local clay). The *llareta* hearth lining partially reacted with the liquid litharge to form a lead silicate. The reaction between the litharge and *llareta* created CHM (cupellation hearth material). While interaction between the hearth lining and litharge is not desired, some reaction is acceptable as long as sufficient quantities of litharge can drain through (via capillary action) into the lining. If large quantities of lead silicate are formed, this will block the porosity and will prevent litharge from draining away from the hearth lining. A careful balance needs to be maintained between the quantity of silicate and litharge. Analytical work on CHM from Porco shows that silicate build up is common, which may contribute to the reduced silver yield. Cuiza's cupellation process produced relatively pure silver which did not require further refining. Overall, it seems that Cuiza was confident that this process would win him enough silver to sell for profit in Potosí. Any silver lost in the process could have been potentially regained by recycling the CHM back into the *huayrachinas* (see *chaîne opératoire*).

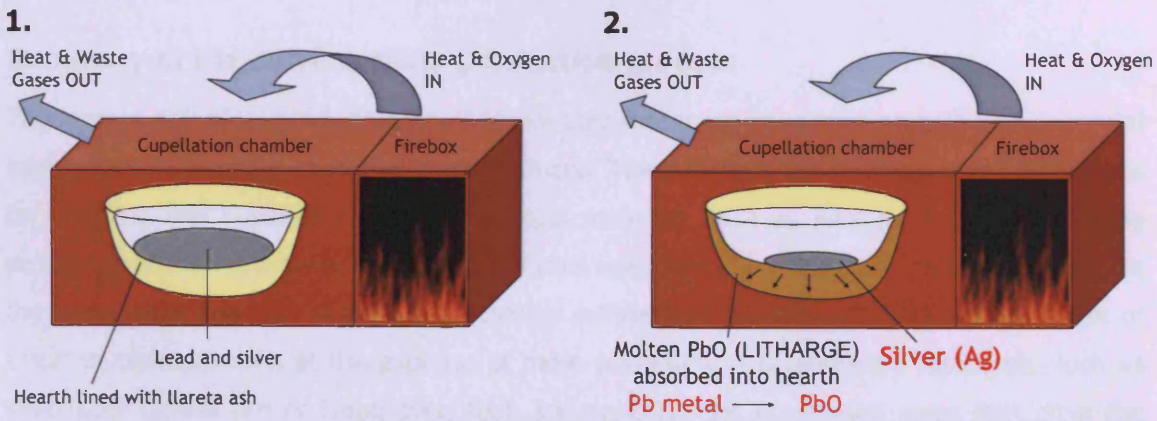

Figure 7.3. Stages of Cuiza's cupellation.

Environmental adaptation seen in the cupellation process

The use of *llareta* as a fuel is well known in the Andes, and it is highly probable that this ash was much more readily available than any other lower silica based ash. The selection of llama dung rather than any other fuel also showed environmental adaptation, since as an abundantly available fuel source it would be preferential to wood. Of greater interest was the clear separation between the lead smelting and silver ore refining. The use of two separate fuels could have allowed a much lower investment of time into the overall process, i.e. by mixing wood and llama dung Cuiza could have maintained higher temperatures with less fuel (wood burns with a fiercer flame and higher temperatures than dung). The choice of fuel also showed a strong adaptation to the environmental condition, in particular the shortage of fire wood. Using dung as the main fuel instead of brush wood preserved this scarce resource. Clearly Cuiza was using a process that was well adapted to the high altitude Andean environment.

Hidden nature of the process

The silver refining process also has a secretive nature to it. Cuiza allowed only people present at the *huayrachina* smelt to attend the cupellation; once the cupellation had begun no one else could look at the hearth. While smelting in the *huayrachina* Cuiza was happy for anyone to participate and ask questions, but during the cupellation he was secretive. He was nervous of people talking too loudly within the chamber as he said the silver would become jealous (Mills 2003). Why did Cuiza hide some parts of the process, while others were open? What did this signify? If the refining was secretive, is that the reason that very few archaeological refining sites have been found? Could the need for secrecy be linked to illicit sourcing of minerals or the value of the product? No gender differences have been documented; Cuiza said that both men and women could take part in silver production, unlike mining communities where woman are not permitted in the mines (Nash 1979).

Summary of the current silver production process

The current day silver production process indicates that there have been several environmental adaptations to the way silver has been produced. These include the selection of different fuels for smelting and cupellation, the use of local materials such as *llareta* ash for the refining process, and the remarkably low fuel to ore ratio used in the *huayrachina* smelting. All indicate the preferential selection of available materials sufficient for the process, minimising the use of wood or charcoal even at the expense of more wasteful use of abundant resources, such as silver-poor galena ore or llama dung fuel. and ensuring the economical gains that drive the continuation of this technology to this day.

7.3. Cuiza's silver production

Analysis of the smelting process in the current day *huayrachinas* has shown that these furnaces had very low yield, and in relation to the metal extraction from the ore they were relatively inefficient. However, very low quantities of fuel were necessary for a smelt, an obvious adaptation the limited accessibility of fuel within the Andes. With access to good quality silver and lead ore, Cuiza was able to produce highly refined silver.

The lead made in the *huayrachinas* was used to refine silver in cupellation chambers. The cupellation process uses a hearth that has been lined with plant ash; lead metal produced in the *huayrachinas* is melted and used to cupel a high grade silver ore. This cupellation process is not in itself very efficient, and some metal is left behind with other waste material. But ethnographic observation has shown that the recycling of these waste materials in subsequent smelts could lead to an overall balanced process. The CHM produced by Cuiza as well as other local refining sites was recycled back into the system via *huayrachina* smelting. Thus, lost silver or even lead (in the form of lead oxide) could be regained during the smelt. This process (which appears to be rather inefficient for lead production) is in effect efficient for silver production. There is almost no silver loss because even in unsuccessful cupellations the silver can be re-smelted and then re-refined. The observation of *ch'allas* or ritual blessings was seen during both stages of the process. Libations of alcohol and coca leaves were fed to both furnaces. These would not be possible to observe in the archaeological record.

Prior to 2005, Cuiza was producing silver three to four times a year. The sale of the refined silver provided his family with another source of income in addition to subsistence farming. The use of multi-subsistence strategies is common within the Andes. Peasant economy is often driven by the need to bring in extra cash to methods of primary subsistence, usually via agricultural activity, or trade and exchange (Harris 1995; Mayer 2002). The necessity for cash means that Andean peasant households are reliant on a number of different economic strategies to survive. "Seasonal trading trips, migrant labour, artisan production, and animal husbandry may all be engaged in by a single household, but none is relied upon as the sole source of income" (Sillar 2000a, 46). Carlos Cuiza and his family demonstrated very obvious examples of different methods upon which extra income could be brought into the household. Cuiza had a number of different animal herds and other farming activities which he was reliant on for his primary income. The investment made into the production of silver was primarily in time, but clearly this was supported by his ability to obtain the fuel and lead minerals at a lower cost than silver sold in Potosí (llama dung, *llareta* ash and galena/lead ore, all obtained with low capital investment).

Figure 7.4. A *chaine operatoire* of Carlos Cuiza's silver production (page 169)

PLEASE SEE INSERTS AT THE BACK OF THIS THESIS FOR AN A3 VERSION OF THIS DIAGRAM

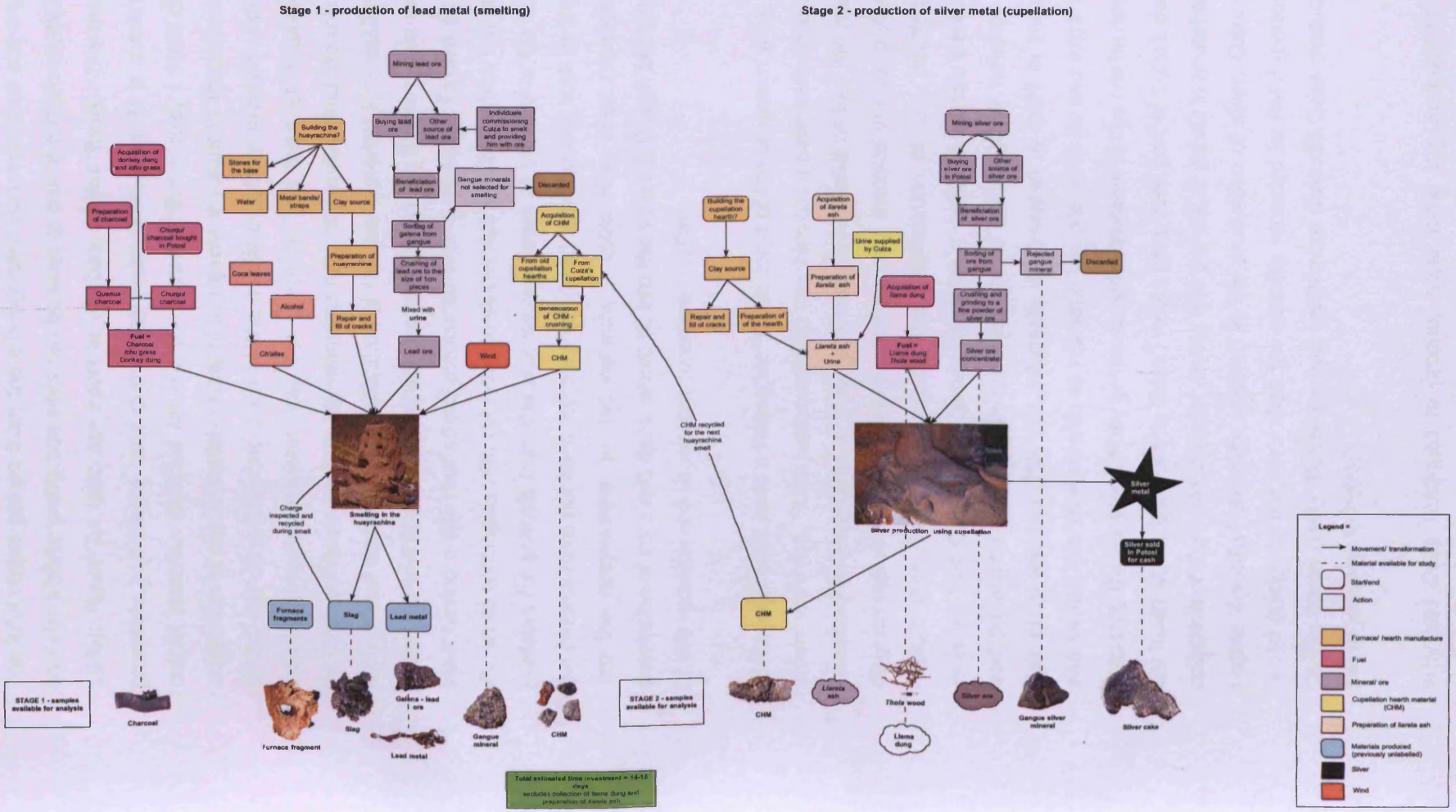

The information gained from the ethnographic documentation and analytical work carried out on Cuiza's silver production sites can be used to create a *chaîne opératoire* model (Lemmonier 1986); Figure 7.4 (also see insert at the back of this thesis). This model aims to present the processes and stages used during the metal production. It is concerned with the input and output materials selected for use by Cuiza. In this model, I have chosen to start with the acquisition of raw materials rather than represent stages of the process that remained outside of the ethnographic work (such as the formation of ore minerals and/or mental schemas that indicate thoughts invested into the process). The focus of acquisition regarding materials includes processes such as the manufacturing of furnaces and the collection of input materials such as fuel and ore. The preparation of the raw materials for metallurgical activities has been addressed in the sequential processes labelled on the diagram, and each different material or input having a different colour associated with it. Materials formed as part of the process are shown as rectangles with curved corners (except for silver which is a star). Pictures of samples available for analysis from the process are shown at the end of the schema. Some aspects of the process have not been represented in very much detail, such as the introduction of *ch'allas* into the *huayrachina*. In this instance, it could have been expanded to consider how the acquisition of coca and liquor would fit into the schema, though but this has not been the focus of this research and so was not considered further.

This model does have a time scale. While some of the processes were documented and timed, others were not. These undocumented variables could have been done over a much longer time scale and an estimation of these processes would take us into the realm of fiction. Thus, this diagram represents the possible variables once involved in Cuiza's silver production without a notable time scale. However, for the beneficiation of ore, smelting, and refining we can ascertain that Cuiza's silver production took a minimum of two weeks; two to three days for lead production (in the *huayrachinas*) and a day for silver refining, but also one week for charcoal production (this was informally documented by PAPP in 2002). This estimate should also include the time needed to resource the ore minerals and extra fuel, as well as that for preparing the furnaces. Many of the activities involved in the *chaîne opératoire* (Figure 7.4, also see insert at the back of this thesis) would have been part of Cuiza's daily routine; for example, collection of the llama dung for drying and the use of *llareta* in household fires. That should not negate the effort and time involved in the production of silver. Cuiza stated that normally he would produce more silver than the quantity recorded by PAPP (personal communication with Dr Van Buren 2008). Therefore, how much more silver did Cuiza produce? What quantity did he sell to jewellers in Potosí?

Why had Cuiza continued to produce silver using this method? Other techniques such as mercury or borax refining are available in Potosí but Cuiza continued to use the silver processing technique he had learnt from his parents. Why? Why had the use of a *huayrachina*

persisted even though in current economic terms the one Cuiza used was relatively inefficient? Technological innovation and change require the individual to be open to change. Resistance to change can occur when the newer technology is perceived as being risky, when it requires capital investment or skills that are not yet available. Cuiza learnt his metal production from earlier generations in his family, thus the technology was predictable and known. Other techniques may have been regarded with a conservative mind because they would require personal investment and possibly have financial risk associated with them. One of the key priorities Cuiza had was to generate money as a source of income, so any activity that had too much risk associated with it would surely be ruled out. Risking change in a technological method would require a suitable back-up system to be in place (Costin et al. 1989, 108). Foster (1973) states that many traditional societies can create cultural, social and psychological barriers which prevent them from changing technologies. Within Andean peasant communities or the local subordinate systems, the use of traditional technology can be described as being "...dialectically opposed to the homogenous cultural forms which the dominant institutions try to impose on them" (Rabey 1989, 168). Cuiza and his family may have experienced heavy sociocultural pressure to conform his traditional technologies to those of the state organised metal production. However, in comparison to that of the large smelting operations, Cuiza's scale of production was small and his activity may not have been monitored by external society. The secret nature of the silver refining may have been promoted by underlying social pressure and therefore there was a necessity for Cuiza to have hidden his technique and method of refining. It is difficult to measure the extent of sociocultural influences on Cuiza and his technological choices made regarding his silver production. However, the reliance on familiar, learned technology is evident.

Cuiza's technological experience and subsistence needs may have influenced his choices when producing silver. Technology can be considered as being an adaptation to ones' local social and environmental situation (Rabey 1989, 168). It is embedded in the agents' surroundings (Sillar, unpublished). The embedded nature of Cuiza's production process was seen within his technological choices. However, the modification within Cuiza's technique were problematic to measure. It would be interesting to consider, or have asked Cuiza, if he had modified the methods of silver production he had learned from his parents. What, if anything, has he altered to improve or simply change the technology?

The adoption of new technology by Cuiza for the production of silver would have meant an investment of capital. The most commonly used methods for modern, small scale silver production involve the use of boric acid or mercury. The use of mercury to refine silver ores has been employed within the region since colonial periods. Thus, an infra-structure exists within Porco to buy materials necessary for mercury amalgamation. However, Cuiza would have needed to have a suitable amount of capital to fund the change in technology. As a *campesino*

using a multi-subsistence strategy to generate income, it is unlikely that he had reserves of money to spend on the set up of new production processes. Therefore, the persistence of more traditional methods such as the *huayrachina* may not have only been due to risk assessment, but also to do with initial set-up costs. Continuing with well established processes that do not demand large investment is always preferential to introducing those techniques that demand high costs initially, despite increased yield or long term profit.

Cuiza appeared to be the only known individual using this method to produce silver in the Porco valley, despite other apparently recent *huayrachina* sites being identified during survey. Recent surveys in the Porco area completed in 2006 (site 123) found an *estancia* owned by a Porceno woman. The area contained various buildings, one of which had a refining furnace of similar design to Cuiza's (Figure 7.5). On the hill above the *estancia,* fragments of *huayrachina* furnaces were found. No samples were taken from the site as the owner was unwilling to talk to PAPP. However, photographs were permitted. This site shows that in the last ten years someone else was producing silver using similar production techniques to Cuiza. Unfortunately, during this thesis there has been no further opportunity to talk with Cuiza.

If Cuiza is the last to produce silver using these techniques, who does he have to discuss his processes with? The lack of other skilled people to discuss his methods of silver production with would isolate him. Has this affected the way in which Cuiza produces silver? It is extremely likely that others know/use this method, although they are unwilling to discuss it with PAPP. Cuiza asked his *compadres* Don Dionisio and Don Juan to help with the recorded productions; although how much do they know about the process? Do they also produce silver?

Cuiza's choices regarding the technology must have been made with strong economic factors in mind and the environmental adaptation that we can see from the process can bring another dimension into the understanding and variability of Andean metallurgy both past and present (Cohen et al. forthcoming b).

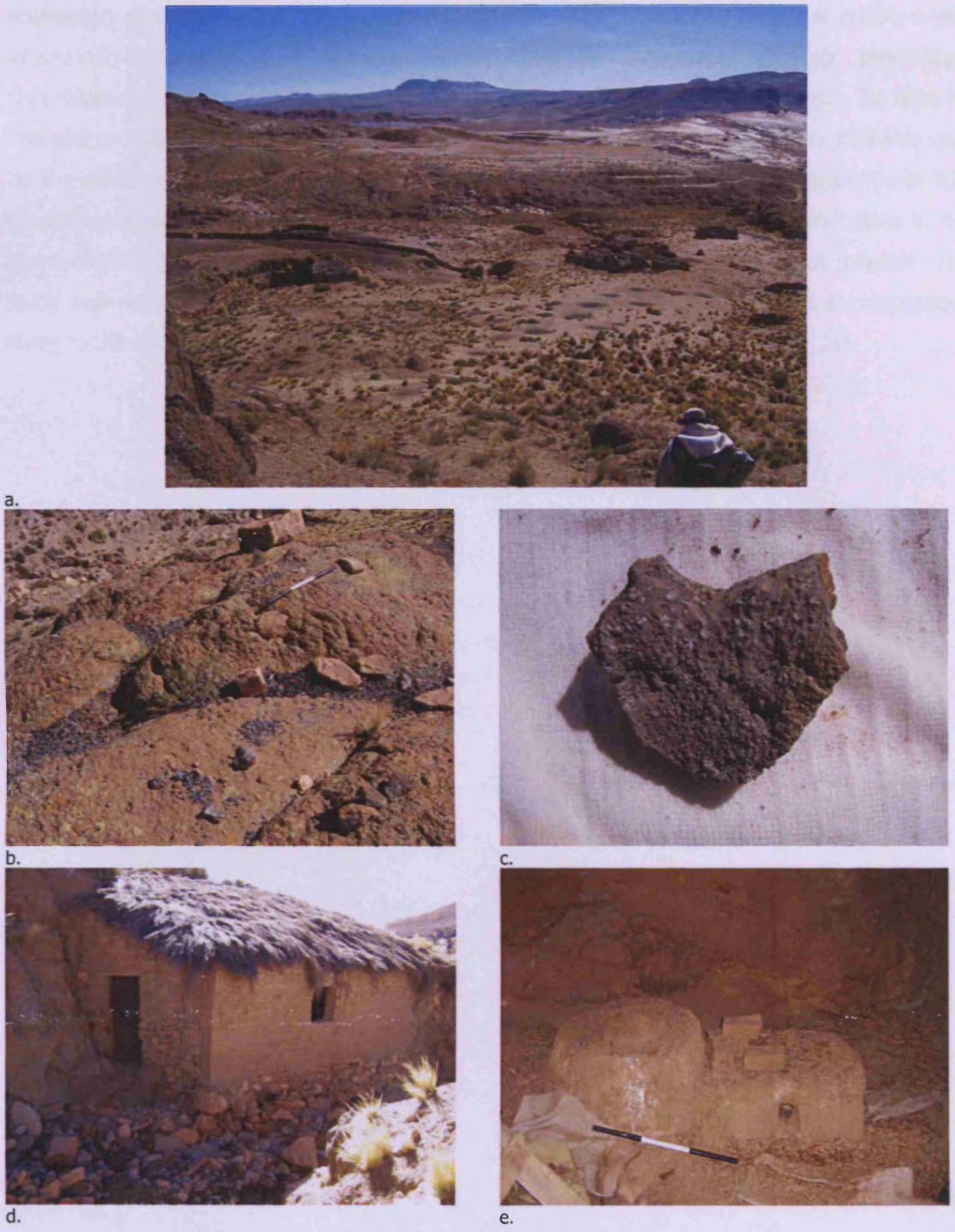

Figure 7.5. Site 123 is an estancia found during field season 2006.
The estancia (a) is owned by a Porceno villager who knows Carlos Cuiza. The owner did not want to talk to Dr Van Buren or PAPP. The site seems to be abandoned. The estancia is located near Porco village. On the hills to the west, *huayrachina* fragments where found (b and c). Within the complex of buildings, a small refining hut was discovered (d and e).

7.4. Summary of the ethnographic work

It was hoped that during this thesis other

production processes could have been recorded for their archaeometallurgical merit. I was interested to observe (and question) Cuiza about his processes of silver production. Unfortunately, this has not been possible because Cuiza no longer lives in Porco. To date no one else in Cuiza's family has admitted currently producing silver, and it is likely that this may be the last known working *huayrachina*. The field survey carried out in 2006 identified site 123 (described above) which has provided evidence for other current-day silver production in the Porco region. Thus, the archaeometallurgical study of this process is of great interest. The study and documentation of this unique production process has been used as a comparative study to the archaeological remains found in the Porco-Potosí area (Chapters 8 - 11).

8. ARCHAEOLOGICAL HUAYRACHINAS

Thus far this thesis has considered the ways in which silver is currently manufactured which involves the use of *huayrachinas* and refining furnaces. Archaeological evidence exists in the Porco-Potosí region which suggests that *huayrachinas* have been used since the Spanish conquest. Although there is no datable evidence it is widely believed that *huayrachinas* were in use prior to the arrival of the Spanish (Ohem 1984, Lechtman 1976). This chapter focuses on the archaeological *huayrachina* sites that surround the modern village of Porco. Five sites have been selected for analysis, although there were more than ten available for sampling (Table 8.1). In this chapter, the archaeological and historical information for each site will be discussed individually and in the conclusion and discussion, all the sites will be summarised and compared. The results of analytical work carried out on selected archaeological samples are presented in this chapter. A discussion and a comparison between the archaeological and current day use of *huayrachinas* will be presented in Chapter 9. This discussion will use the results from this chapter and chapter 5, survey results carried out on two different archaeological *huayrachina* sites, and a consideration of colonial literature.

8.1. *Guayras, huayras* or *huayrachinas*? A summary of the significance of wind blown furnaces in Andean metallurgy

Within the Andes, the use of the wind (natural or mouth blown) to produce metal is a uniting factor between the various metallurgical furnaces recovered archaeologically (Boman 1908; Bray 1978, 28; Epstein 1993; Lechtman 1976; Lleras Pérez 2005; Raffino et al. 1996; Shimada and Merkel 1991; Scottlin and Williams 1992; Shimada et al. 1982; and Tarrago and Gonzalez 1998). In Ecuador and Columbia, blowpipes were the standard manufacturing method for gold production (Bray 1978; McEwan 2000). To aerate the furnaces, smelters in the Andes used natural draft furnaces and blowpipes rather than bellows (often selected in European and Asian metallurgy). Within the body of literature smelting furnaces are generally referred to as *huayras* or *huayrachinas* (Oehm 1984, Bargallo 1969, Petersen 1970). '*Huayra*' means wind in both Aymara and Quechua. A *huayraatha* is described as "*Fundir metal con ayre*", to smelt metal using wind (Bertonio 1612, 157).

The site of Batán Grande has some of the best preserved examples of pre-Hispanic smelting furnaces. The furnaces were inset into the hillside and used both natural wind and blowpipes to smelt copper ores (Shimada et al. 1982). The slag was crushed using the large *batánes* to extract the metallic prills. This method of production continued until the mid 15th century. As

discussed in Chapter 2, throughout the 600 years the site has been occupied, furnaces showed some diachronic changes, although their overall design remained unchanged.

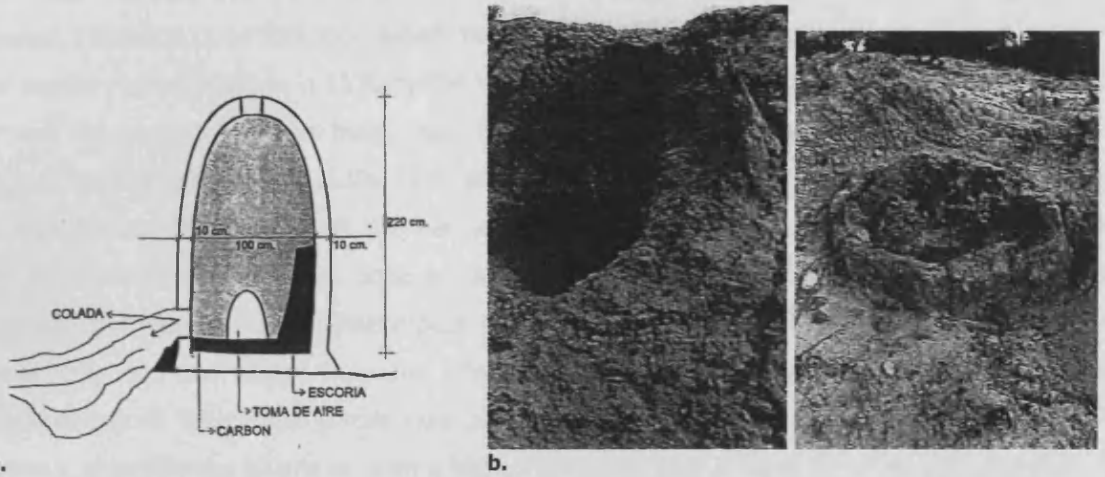

Figure 8.1. A reconstructed of a *huayra* (a) and photographs of the furnace remains at Quillay Argentina image b (Raffino et al. 1996, ?)

Copper producing areas have also been observed in the north-western region of Argentina and northern Chile. Raffino et al (1996) highlight the metallurgically active area of Quillay in the Catamarca Province, Argentina, which has furnaces associated with copper production. Fourteen furnaces, introduced there as *huayras,* were located there. These *huayras* were constructed from adobe (Figure 8.1). The site has been dated to the Inca period using radiocarbon dating. The reconstruction of this furnace did not appear to have a pierced shaft and thus, this furnace may have functioned with natural draft. Raffino et al hypothesise that small holes at the base of the furnace shaft may have been used as openings for blow pipes (similar to furnaces at Batán Grande). These may have aided smelting when wind/natural draft conditions were poor. Other examples of archaeological furnaces have been shown to be situated high on terraces (Lechtman 1976).

The use of wind aided furnaces is not unique to the Porco-Potosí region. Nor are furnaces that have pierced shafts. The region represents some of the only known silver and lead production sites in the southern Andes. Generally, copper production rather than lead or silver has been documented in the Andes. The role of Porco's *huayrachinas* within Andean metallurgy is difficult to clarify and lies outside the remit of this thesis. However, the use of wind in Andean metallurgy is a uniting factor between other Andean metallurgical techniques.

The lack of written sources from pre-Hispanic periods in the Andes has made identifying techniques of metal production difficult. In pre-Hispanic Andes, it is unclear how silver and lead were produced. No known example of a pre-Hispanic smelting furnace has been located. The scarceness of pre-Hispanic archaeological remains has meant that an understanding of the metallurgical history of the Porco-Potosi region has been limited to colonial sources often written up to 100 years after the first conquest of the area (Barba 1640 – Douglass and

Mathewson trans. 1923). This project documents and analyses furnace remains dating from the colonial period to the current day. It is hoped that the documentation of these early colonial furnaces will help to further understand the technology employed during the early Spanish period. Historical documentation details the use of indigenous methods prior to the introduction of mercury amalgamation in 1570 by the Viceroy Toledo de Peru (Bakewell 1997, 77). In Porco-Potosí the *huayrachina* was being used as a means of silver production from soon after the point of colonisation in the 1530s. Most of the written sources after this point claim that it is of native Andean origin, although this has yet to be archaeologically proven. Clearly, exploitation of minerals for smelting was done on a relatively large scale, as is obvious from historical reports, but where is the archaeological evidence? How were the indigenous people of Porco producing lead and silver? How and why did the practice continue after the introduction of amalgamation? What type of ore was being smelted in the *huayrachinas*, for example pure galena, argentiferous galena or even a high grade silver ore? If these furnaces were not directly producing pure silver, then where were the refining furnaces? How has the technology changed over the last 500 years? The historical literature provides an excellent basis upon which to study material debris, and has provided questions of technological choice and function, which this thesis will address.

The next section presents the archaeological *huayrachina* sites used in this study. In preparation for the presentation of the analytical work done archaeological *huayrachina* debris

8.2. Archaeological *huayrachina* sites in Porco

In the next section of this chapter, each of the archaeological *huayrachina* sites will be discussed. The historical, archaeological and material information will be outlined in preparation for the results of analytical work presented in this chapter. The five sites chosen for analytical work are shown in Table 8.1. A map of the *huayrachina* sites has also been included here to give an overview of their locality (Figure 8.2).

***Huayrachina* sites**	**Uruquilla domed furnaces**	**Dragon furnaces**
Site 24	UR 10	UR EST 10
Huayrachina Alta	UR 11	Don Martin's Dragon
Cruz Pampa Surface	UR 12	
Uruquilla West Saddle Surface	UR 14	
Uruquilla East Saddle Surface		

Table 8.1. List of archaeological sites selected for analysis. The column left shows the available *huayrachina* sites.

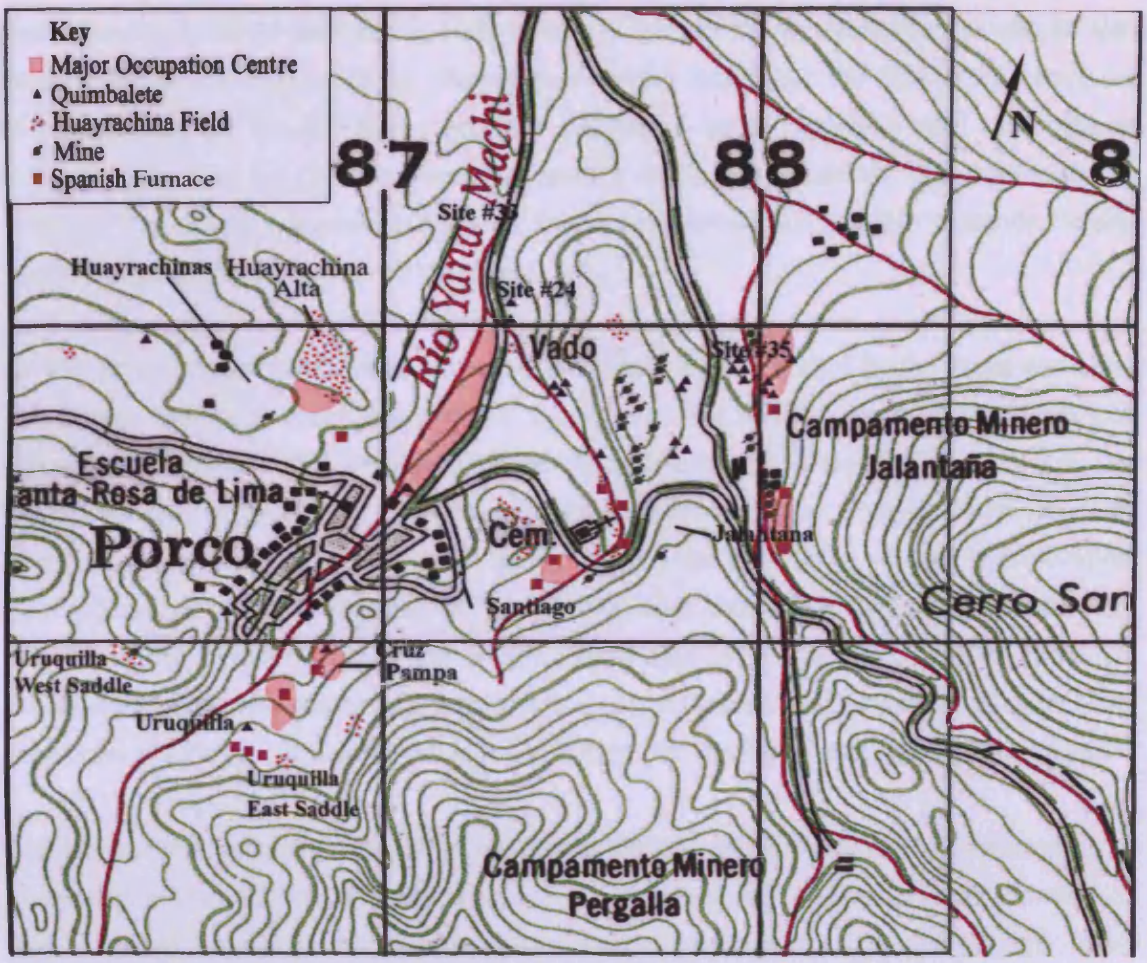

Figure 8.2. Map of the Porco region.

Cruz Pampa Surface

The main Cruz Pampa site is located on the flanks of Huayra Porco, south-east, and directly above the modern village of Porco (Figure 8.2). It has various structures that seem to have been used for domestic purposes, but the overall plan is obscured by animal corals that now cover the site. The high density of Inca ceramic material and the structure of the buildings indicate that the use of Cruz Pampa occurred during the Inca period and continued into the early colonial period. A small colonial European style furnace was excavated and one burial pit was also found. Samples from the site include excavated and surface samples, and archaeological *huayrachina* fragments from nearby saddles. Those samples selected for analysis were two fragments of this archaeological *huayrachina*; the fragments are multi-layer including a slag layer.

Site *Huayrachinas* and Huayrachina Alta

The sites shown on the map as *Huayrachinas* (Figure 8.2) consist of numerous circular and rectangular structures indicating Inca architectural storage buildings known as *qollqas*. The designation of this site is confusing. The lower part of the sites consists of Inca storage

structures that were re-used during early colonial times (personal communication with Dr Van Buren). The site is referred to as '*Huayrachina*' by the locals, but the *huayrachina* furnaces themselves are on the hill above and are designated as 'Huayrachina Alta'. The site of '*Huayrachinas*' does not have *huayrachina* furnaces on it; it is residential with some refining features. The site of 'Huayrachina Alta' has only *huayrachinas*, with no clear evidence for any residential structure, and hence no clear date.

Dr Van Buren suggests that these remains may have been constructed by the Incas and used for storage and provisions necessary for the miners and smelters working near this site (http://lamar.colostate.edu/~mvanbure/sitedescriphyrachinas.htm, May 2008). Although the site shows clear architectural evidence for Inca settlements, there is evidence of its reuse during the early colonial period, and some of the structures have yielded archaeological evidence indicating that at least two of the buildings were built during the colonial period. This site shows the complexity of dating archaeological sites within the Porco region since the continuing mining presence has allowed sites to be reworked on a regular basis. *Huayrachinas* have been included in the sample set as an important site first constructed during Inca times.

The *huayrachina* remains on the ridge top above the site of '*Huayrachinas*' are referred to as 'Huayrachina Alta'. Huayrachina Alta is situated to the north east of *huayrachinas* and west of Site 24. It has a series of *huayrachina* remains and archaeological debris, and may also have had a more permanent housing structure, though this has been destroyed by a modern electricity pylon. PAPP excavated one of the *huayrachinas*. The site of '*Huayrachinas*' was constructed during Inca times, but Huayrachina Alta probably consisted of a palimpsest of remains - Inca and later. *Huayrachina* fragments from the excavation have been selected for analysis.

For survey of the site in 2006, two sample areas were selected from the overall Huayrachina Alta site. These have been labelled areas A and B (more details to follow in this chapter).

Site 24

Site 24 is located on a ridge next to a series of mines due west of site 35 (Figure 8.2). The site is on top of the north-south Zodillos ridge, whose spine is formed by a mineral-bearing vein radiating from Cerro Huayna Porco to the north. The area has been mined and nineteen pits and vertical mine shafts have been documented during surface survey. It has an irregular line of small boulders that could have been used as platforms for *huayrachina* furnaces, with nineteen discrete clusters consisting of *huayrachina* debris, ceramic material and other remains from the smelting process (Figure 8.3). 'The presence of Spanish olive jar shards as well as decorated Late Horizon wares among the *huayrachina* remains at Site 24 suggests a sixteenth century date, an interpretation that is supported by local oral tradition which indicates that

these mines were worked by the early Spaniards' (http://lamar.colostate.edu/~mvanbure/sitedescriphyrachinas.htm, May 2008).

The results of the archaeological survey show that site 24 and the excavated *huayrachina* debris are similar to the current *huayrachina* debris found and documented by the Projects' team at Carlos Cuiza's property. Thus the site is important for a comparison and understanding of current local and historical *huayrachina* smelting.

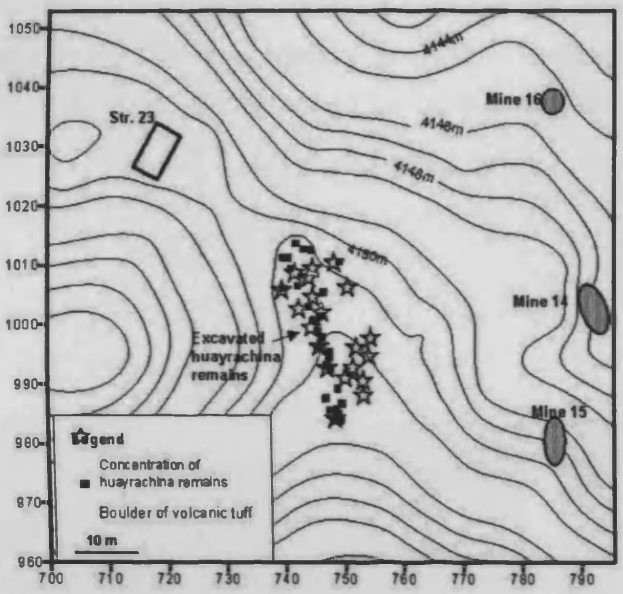

Figure 8.3. A map of site 24 and structure 23. The stars represent *huayrachina* remains. Squares are volcanic tuffs used as wind breakers.

Structure 23 is located northwest of the *huayrachina* debris within site 24. It is a rectangular building that could have been used for the supervision of smelting and mineral processing (Van Buren & Mills 2005).The smelting features found within the building may have been refining furnaces and could have been used in association with the *huayrachinas* in site 24 and in combination with site 35.

The true date and purpose of site 23 is harder to interpret and the various 'unusual'/different smelting features that are not related to current smelting practice (or at least practices that have been documented) found within the structure indicate that it may be concurrent to the '*Huayrachinas*' site and the local mines, thus early to mid colonial. These sites form an integral part of metal processing history within the region, and further clarity on the dating of these sites can only come with time and further excavation. Samples have been taken from the unusual hearths found in structure 23 and *huayrachina* fragments from well stratified levels of site 24.

Uruquilla East & West Saddle Surface

The *huayrachina* sites labelled Uruquilla West Saddle and Urquilla East Saddle are located in hills above the main complex (Figure 8.4; Figure 8.2). These two sites have been selected for surface sampling because they represent two large *huayrachina* sites close to modern Porco. Uruquilla West Saddle is on a small ridge (15 m wide) to the West of the main complex. It has three to four *huayrachina* bases, i.e. areas with discrete scattered *huayrachina* and slag fragments. The majority of the *huayrachina* remains have fallen down the eastern side of the ridge. Most of the UR West samples have come from the top of the ridge, although a wider

survey of *huayrachina* fragment measurements was done following the methodology described in Chapter 9. Large pieces were measured for wall thickness, and if eye holes were present the diameter of these was noted.

Uruquilla East Saddle is similar to Uruquilla West Saddle, located on the eastern side of the main complex on a large ridge. It has seven *huayrachina* bases which have scattered furnace fragments of variable size, and the site appeared to be relatively undisturbed. The ceramics found at the site were plain red ware but they were not suitable for dating the site. The *huayrachina* bases are so well defined that they may be relatively modern furnace sites. This ridge is very windy (excellent for wind blown furnaces), but many of the *huayrachina* fragments are badly eroded and difficult to survey, thus they have not been included in the surface survey.

a. b.

Figure 8.4. A view of Uruquilla East Saddle (a).

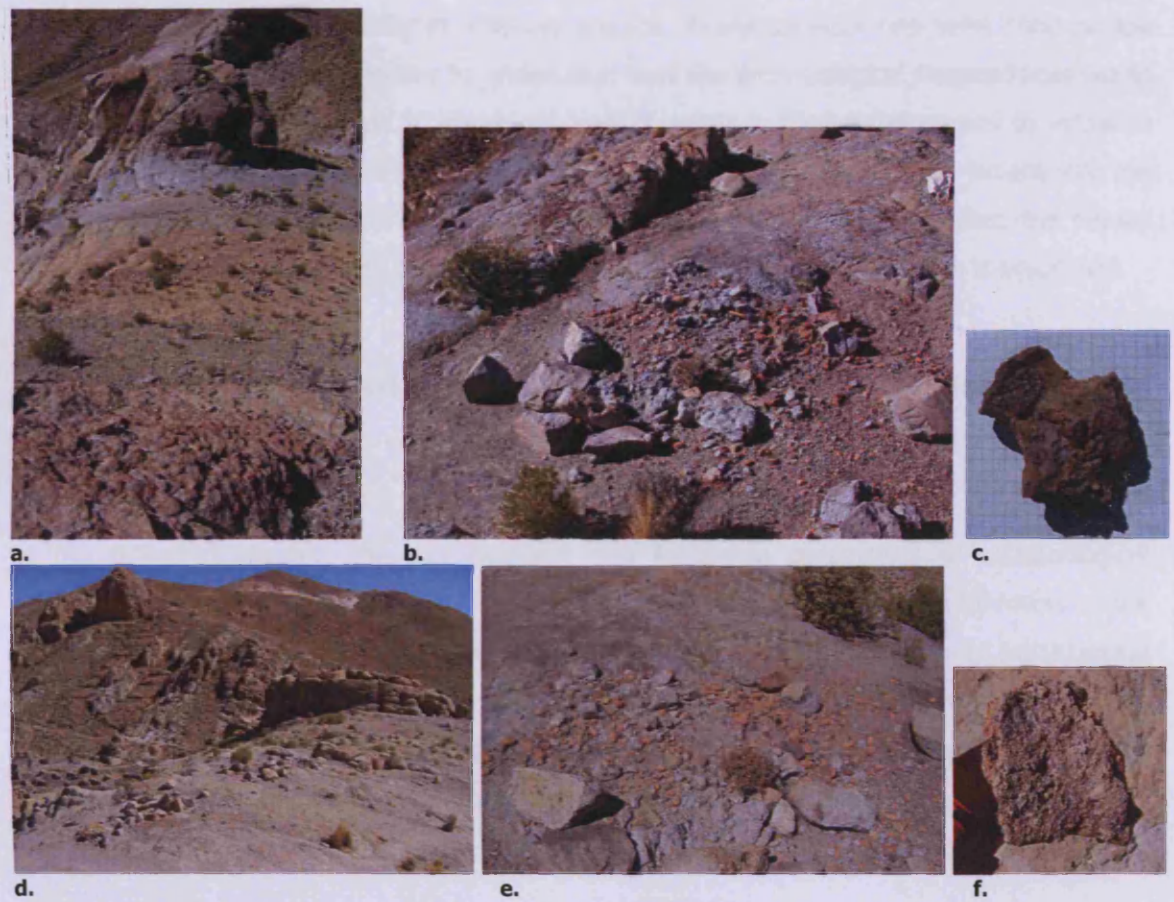

Figure 8.5. The UR West Saddle
The UR West Saddle (a). UR West Saddle *huayrachina* remains (b). A large *huayrachina* fragment which appears to have the remainder of two eye holes from UR West Saddle (c). The UR East Saddle (d). UR East Saddle *huayrachina* base (e). A large *huayrachina* fragment taken from UR East Saddle (f).

While un-stratified and un-excavated, these sites can still provide valid information regarding the history and smelting practice within the Porco-Potosí region. These samples have undergone detailed metallurgical analysis to determine the type of ore being smelted and to understand the technological functions of the furnaces.

Summary

The five archaeological *huayrachina* sites reviewed above have been selected for further analytical work. The two excavated sites 24 and HuA1 have been tentatively dated to the early colonial period. However, both display ceramic ware and other artefacts that would indicate that the sites were in use prior to the arrival of the Spanish. Stratigraphic dating on *huayrachina* sites is not possible because the sites consist of surface remains with very little deposition. Nevertheless, sampling from undated sites such as CP and UR WS/ES is still beneficial and will allow the documentation of metallurgical practise within the Porco region.

The material debris from the archaeological *huayrachina* sites has been chosen for sampling because one of the objectives of this thesis is to compare and contrast the archaeological use of

huayrachinas throughout the colonial period to the present. The comparison between sites will allow for a measure of variability in smelting practice. Analytical work has been done on the selected samples with the objective to understand how the archaeological *huayrachinas* would have functioned, the conditions which would have occurred in their furnaces and to establish which ores would have been selected for smelting. This information will allow insight into the methods of silver production in the Porco-Potosí region. In the following chapter, the results from the analytical work carried out on selected archaeological *huayrachina* sites is presented.

8.3. Survey and analytical results from the archaeological *huayrachinas*

In the following chapter, the morphological and functional parameters of archaeological *huayrachinas* are considered via the measurement of air holes (eyes) and the thickness of the furnace wall. Two sites were selected for a surface survey to analyse the types of metallurgical debris found at a *huayrachina* site. The analytical work done on the five archaeological *huayrachina* sites is presented in conjunction with the survey results. Data from each site will be presented separately, and the results from a comparative review will be shown in chapter 9.

Archaeological *huayrachina* site surveys

After the initial sample selection in 2005 of the archaeological *huayrachina* debris, various similarities between samples found at different sites were observed. Thus, a preliminary survey of the archaeological remains found at different sites was conducted in 2006. The main objective of the survey was to understand the types of metallurgical debris found at *huayrachina* sites. It also aimed to further investigate the construction of older *huayrachinas* by considering the thickness of the furnace wall and dimension of air holes.

In June 2006, two sites were selected: Huayrachina Alta (HuA1) and Uruquilla West Saddle (UR WS). HuA1 was selected for the main survey site because it had undergone prior excavation and sampling work, and it had a large area within which relatively well preserved *huayrachina* remains had been previously documented and dated to early colonial periods. Two different areas in the site were selected for survey and labelled block A and B (Figure 8.6).

Block A is located on the crest of the site (on one of the uppermost parts of the hill). Block B is further down the hill on a steep slope below block A. Both areas were selected because they are rich in archaeological debris. The material remains had fallen from the upper slopes and down through the ravine, most probably carried by rain water from the upper slope. The exact position of samples within the survey area thus became irrelevant because the original orientation of the *huayrachina* was impossible to determine. Despite this, on the HuA1 site, the

selected blocks were marked out with flags and string to orientate the spatial distribution of the finds within a closed system. Transects of 2.5 m were walked and any finds were documented. A find can be linked to a transect line. In contrast, the UR WS site contained less surface debris than the HuA1 site and was contained within a small area. The survey was conducted by walking around the site and noting finds, although specific locations were not recorded and no area was marked out (Appendix IV-for more detailed information on survey).

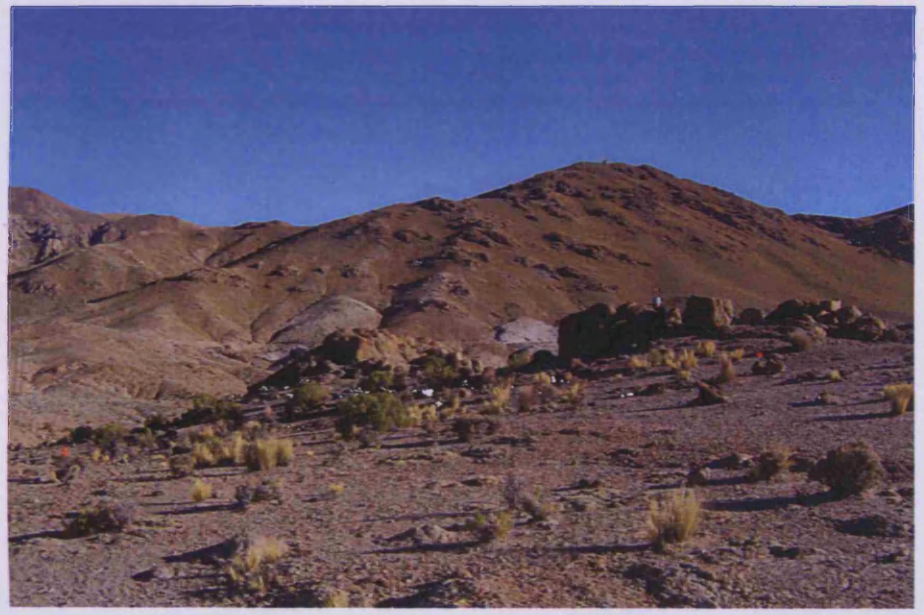

a.

b.

Figure 8.6. Photographs of HuA1 Block A (a) and Block B (b) survey areas. Note the steep ravine that survey block B was located in.

The same procedure for the observation of finds was used at both sites. Any *huayrachina* fragments found were considered by: a brief description of the fragment, thickness of the fragment, number of slag layers, and if an air hole was identified the thickness and diameter were also noted (Figure 8.7).

Slag layers were defined as an individual layer of vitrified material. In the archaeological record, some furnace fragments show evidence of relining and multiple layers of slag (Figure 8.8 b). If multiple layers were recorded, the overall thickness of the fragment would be increased, and the number of layers noted although the original thickness of the wall would be difficult to assess.

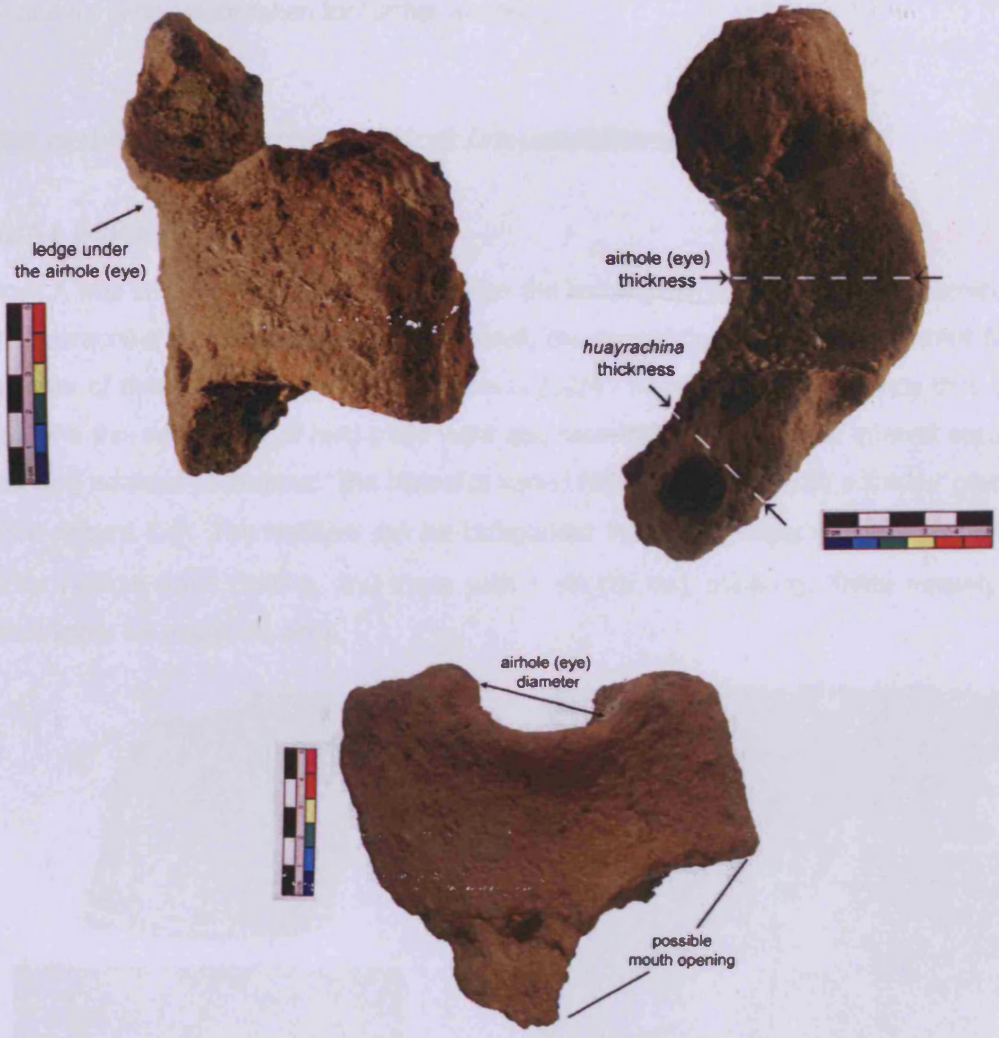

Figure 8.7. Measurements taken on *huayrachina* fragments.
This fragment from un-sampled site 114 was selected rather than one from surveyed sites because it best illustrated ledges located underneath air holes.

If a fragment contained an air hole then evidence of a clay ledge was checked. Ledges are described by Peele (1893) as a platform made of ceramic, located on the outer surface below the hole. Peele states they were used to hold burning charcoal pieces. Ledges have been noticed in the historical literature, but not recorded in current day practice. It is unclear when this stylistic feature began and indeed when it was discontinued. The presence of a ledge was anticipated as a possible variant within this survey. If present, the ledge can complicate the measurement of the eye thickness; to effectively evaluate the eye thickness, ledge thickness

needs to be clearly defined and measured separately. Prior to the survey it was unknown how many samples would have a ledge. At other archaeological *huayrachina* sites, ledges had been observed such as site 114, not selected for analytical work in this research but one fragment has been photographed to present ledges (Figure 8.7).

During the survey a selection of the fragments were photographed. None were taken for further analysis. Any other archaeological finds were also documented and photographed where necessary (some were taken for further analysis).

The results of the archaeological *huayrachina* surveys

HuA1 Block A

Block A was an area of 27.5 by 10 m. Within the rectangular survey area, five discrete clusters of *huayrachina* fragments were found. Overall, the survey documented 43 different finds. The majority of these were *huayrachina* fragments (32/43 finds). Ten ceramic finds that contained slag or a thin white layer of lead oxide were also recorded. These were of interest because they had slag adhered to ceramic. The ceramics varied from fine red ware to a thicker coarser plain ware (Figure 8.8). The residues can be categorised into two groups; those which have a thin white /yellow oxide coating, and those with a silicate slag adhering. Three ceramic samples were taken for analytical work.

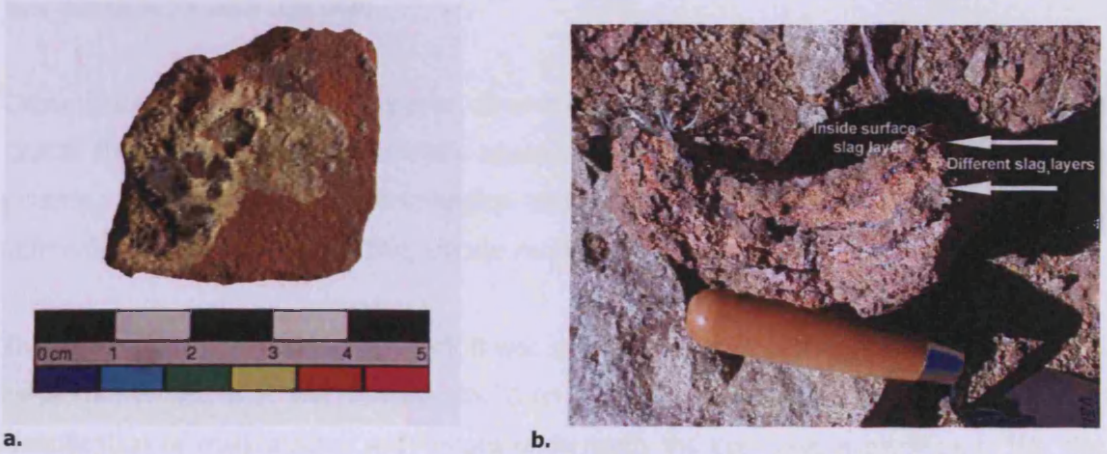

a. b.

Figure 8.8. Ceramic with slag adhering (a) observed in HuA1 block A (sample N7) and multilayer *huayrachina* fragments found at UR WS (b).

The average *huayrachina* wall thickness recorded was 2.9 cm (measured including slag layers). Those fragments with eyes had an average thickness of 3.3 cm and an average diameter of 4.1 cm. No ledges were recorded. Out of the 28 samples containing slag, 26 had only one slag layer and 2 had multiple layers. The type of slag found on the samples was variable, ranging from a thin yellow/grey to heavy black. Informal measurements of the slag layer indicated that it was from 0.5 to 1 cm thick. No correlation was recognisable between the thickness of the slag layer and the size of the eye hole. Thickness of the eye hole does not appear to be very

different to the overall thickness (the average thickness is 0.4 cm thicker, perhaps due to slag build up inside the furnace). The measurement of the thickness will not vary greatly because no fragment in the HuA1 sample area was shown to have ledges, and so the overall thickness of the samples would be unlikely to change (see Appendix IV for the detailed survey data).

HuA1 Block B

The HuA1 block B covers a rectangular area of 20 by 4 m. The survey area was located in a steep ravine; finds would have been washed/blown down from the upper and flatter platform (Block A). The number of samples recorded in Block B were greatly reduced in comparison to the total number in Block A, so to was the total survey area. However, despite the small number of finds recorded (11 finds and only 3 fragments with air holes) and reduced survey area, the data is still valuable for comparison.

Five *huayrachina* samples were recorded. The average thickness of the fragments was 3.5 cm. Eye diameter was 4 cm and thickness of the fragments varied between 2.3 and 4 cm (For detailed information see Appendix IV). Two of the fragments recorded have small ledges underneath the eye hole, on the outer surface of the fragment[4]. The presence of these ledges would result in an increased wall thickness, although since only two fragments were measured, this increase is difficult to identify. The ledges show that almost no wall erosion had taken place and the thickness of the hole indicates the original thickness, however, given the small sample size this data remains tenuous.

Other finds included fine and coarse ceramic ware that had metallurgical residues adhering. One of the ceramics taken for analysis appears to be a crucible and has beads of metallic lead adhering to the surface. The metallurgical residues (like those of HuA1 Block A) take various different forms; thin white coating, silicate residues, and metallic prills.

The number of finds recorded in Block B was small. This survey has its limitations and it should be acknowledged that the sample size cannot reflect a normal sample set. However, the identification of *huayrachinas* with ledges underneath the eye holes is significant. The size of the eye diameters is similar to those previously observed in Block A.

UR WS survey

Survey work from site UR WS was a smaller and less monitored process, mainly because finds were confined to the individual *huayrachina* bases (Figure 8.9). I decided that surveying in

[4] Peele (1893, 9) photographed *huayrachinas* with small ledges. This has not been observed in the ethnographic process.

transects would be unnecessary. Seven *huayrachina* fragments were recorded from the site. The average thickness was between 2.5-2.8 cm (Appendix IV).

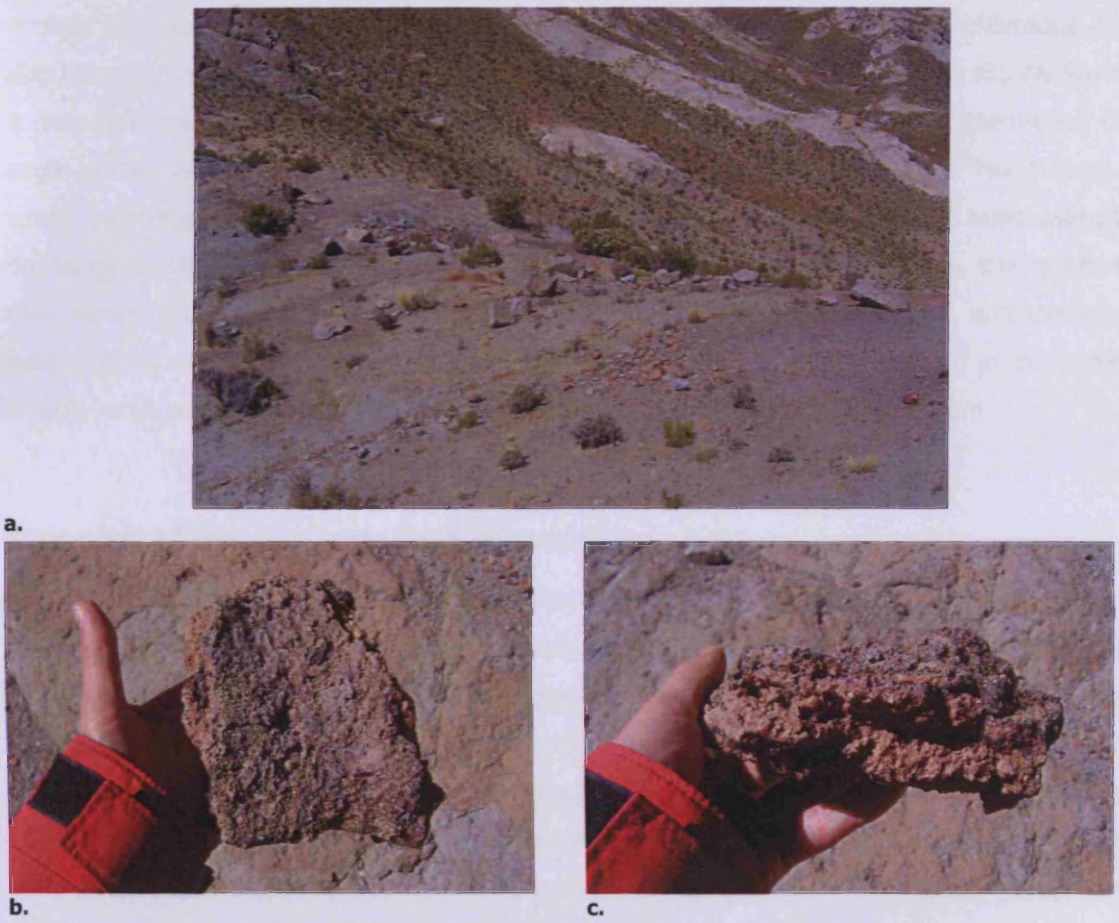

Figure 8.9. The archaeological *huayrachina* site of UR WS.
The area contains three or four *huayrachina* bases (a). These bases consist of ceramic with slag adhered. *Huayrachina* fragments are typically large, up to 10 cm or more long, and with a heavy grey slag adhered to a partially fired ceramic (c and d).

Only three of the samples had parts of an eye, but two out of three had two eyes per fragment. The eye holes were 5 cm in diameter. Most of the samples contained only one layer of slag, although one contained three distinct layers. Generally, the slag was dark grey and relatively thick (less than 0.8 cm, Figure 8.9). Some of the fragments had visible erosion visible on their outer ceramic surface.

A site comparison

Despite sites HuA1 Block B and UR WS having only small number of finds, an informal comparison was done to understand any similarities/differences in the thickness of *huayrachina* fragments. The average thickness was between 2.5 and 3.3 cm. However, samples from the UR WS site were smaller, between 2.3 and 2.7 cm. Samples from UR WS showed some external erosion of the ceramic wall, which may account for the differences. *Huayrachina* sites are located in windy, exposed areas. Furnaces located on these areas would have experienced strong winds (during dry months) and heavy rain (during the wet season). On the outer surface of the furnace, the ceramic would have remained less fired, i.e. it would have experienced some

thermal alteration due to internal heat from the reaction chamber although it would not have been fully baked. As a result, the ceramic would be easily eroded by water and wind. Thus, the ceramic fragments seen in the archaeological finds at UR WS may not necessarily represent the original thickness of the *huayrachina*. The location of each fragment within the furnace may also have had an effect on the thickness. If the column shaft of the furnace was slightly flared, it may well have been made thicker at the bottom and thinner at the top. Determining the angle of the ceramic shaft was not possible from the fragments. In the case of HuA1 Block B where two fragments had visible ledges this would indicate that erosion had not taken place as the ledge would not have been preserved had the fragment been eroded. Thus, the results of this survey have provided only general evidence for the thickness of archaeological *huayrachinas* walls. However, an estimate of the diameter of air holes measured in this survey is more reliable and the survey showed eyes varied in size between 3.6 and 5.0 cm.

Summary of the archaeological *huayrachina* survey

The survey carried out on the two archaeological *huayrachina* sites has shown that a hand specimen can provide some information regarding the construction and design of *huayrachinas*. Two fragments in HuA1 Block B were recorded with ledges underneath the eye holes. These samples give an indication as to the appearance of the shaft's outer surface and are significant finds illustrating the design of furnaces in antiquity (further discussion continues in Chapter 9). The air holes measured with ledges did not show significant difference in thickness which would indicate that little erosion had taken place. However, the small size of the survey makes data generated on wall thickness rather tenuous.

Ceramic debris found at the site include two different wares: a fine grained red ceramic with a silicate slag adhering to it, and a coarse ceramic with a layer of lead oxide on the internal surface. Further investigation is needed to understand the nature of these ceramics and how they have been used in the process.

The survey has been small and a much larger selection of different sites would be recommended for future work to fully identify the style of older *huayrachinas*. A comparison between these results and that of Cuiza's furnace will be presented in Chapter 9.

This chapter continues with the results of analytical work carried out on the archaeological *huayrachina* samples from the archaeological sites of Cruz Pampa, Huayrachina Alta, Site 24, the Uruquilla West Saddle and East Saddle.

Archaeological analyses: samples from Cruz Pampa Surface (CP)

From the Cruz Pampa saddle, two specimens of *huayrachina* wall and slag were analysed. Both fragments have a dense, glassy black slag adhering to a red baked ceramic. The fragments were cut and a sample of slag was mounted: sample 344A being only slag, and sample 344B a sample of slag with some ceramic material attached (Figure 8.10 a and b).

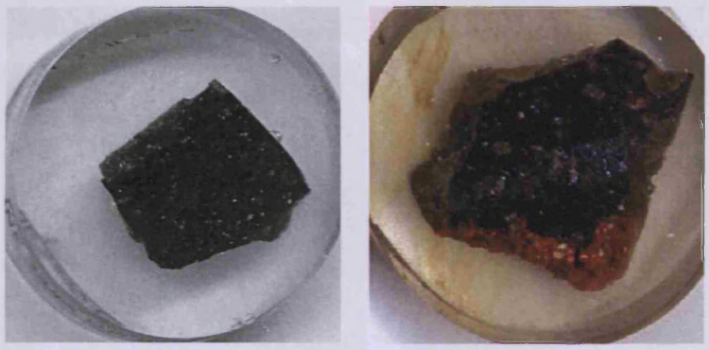

a. b.

Figure 8.10. Two samples mounted from CP *huayrachinas* were selected for analytical work: samples 344A (a) and 344B (b).

OM has shown that sample 344A has a multi-component slag consisting of a glassy slag matrix with different mineral inclusions, residual lead sulphide, and metallic prills. Sample 344B has a glassy slag attached to un-tempered ceramic. The slag contains lead sulphide and a number of metallic prills (Figure 8.11).

Initial ED-XRF screening of sample 344A showed that the slag is composed of silica, lead oxide, lime, iron, zinc oxide, potash, and phosphate. The trace element analysis showed the presence of silver, tin, and antimony. SEM-EDS bulk area analyses show that the sample is composed of lead oxide, silica, lime (13 %), iron and zinc oxides (Table 8.2).

The SEM-EDS analysis confirmed that the slag was composed of a lead silicate containing leucite, pyroxenes, and spinels with high tin content. Metallic prills and lead sulphide were commonly observed in the sample. There were two types of metallic prills analysed, those with lead as the major component and those rich in silver prills.

The presence of lead sulphide, metallic lead, and silver in the slag show that the ore selected for smelting would have been argentiferous galena. The glassy nature of the slag and low abundance of lead sulphide indicate that operating temperatures were high. The low number of samples analysed limits further interpretation of these archaeological remains.

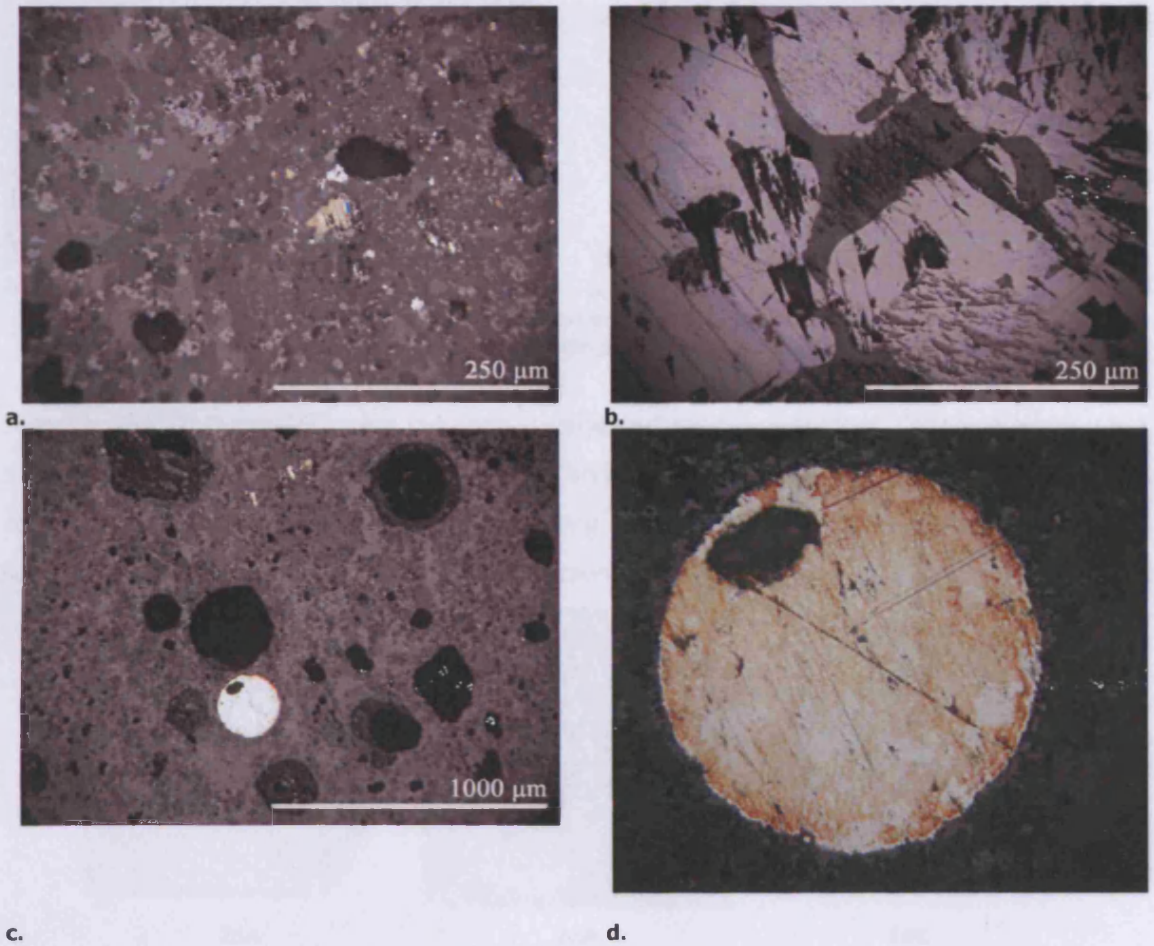

Figure 8.11. CP *huayrachina* slag
The CP *huayrachina* slag has a multi phase slag matrix (sample 344A, image a). Islands of partially reacted mineral ore (Sample 344B lead sulphide, image b) and silicate based minerals compose the slag. Metallic prills are common as seen in image c and a close up in image d.

Sample	MgO	Al2O3	SiO2	P2O5	K2O	CaO	TiO2	FeO	ZnO	PbO
CP 344A (n=1)	1.9	5.4	32.3	2.0	3.3	12.4	0.9	10.8	9.3	21.7
CP 344B (n=2)	2.5	1.6	29.6	2.3	2.9	12.9	1.1	10.0	11.4	26.1

Table 8.2. SEM-EDS bulk area analyses of CP samples 344A and 344.
The data has been normalised to 100 wt%.

Site 'Huayrachinas' and Huayrachina Alta (HuA1).

Seven archaeological *huayrachina* samples from HuA1 were analysed (26A, 26B, 26C, 27, 27A, 29, and 31). The slag sample is adhered to a partially baked, red furnace wall. The slags are grey/black in colour with different crystalline and metallic inclusions (visible without microscopy). The slag adhered to the furnace wall is generally 2-3 cm thick. The cut surface has revealed large gangue inclusions within the slag layer. The *huayrachina* fragments from this site are multi-layered; they have intermediate layers of slag and ceramic indicating possible reuse and relining of the reaction chamber (Figure 8.12). Relining was not seen in the ethnographic *huayrachinas*.

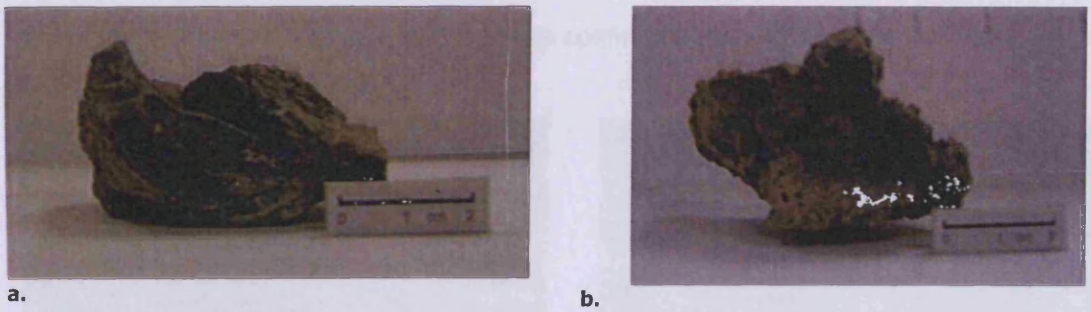

a. b.

Figure 8.12. Samples 26A (a) and 26C (b) hand samples.
Note the multi-layer structure of 26A. Both specimens have a 2 cm thick layer of grey slag.

Samples 26A, 26B and 26C were cut from a large *huayrachina* fragment. Different areas were sampled to give an overview of the reactions and processes happening. Samples 27 and 27A come from two slag samples taken from a bag of slag. Samples 29 and 31 were selected because they come from layered *huayrachina* fragments (Figure 8.13).

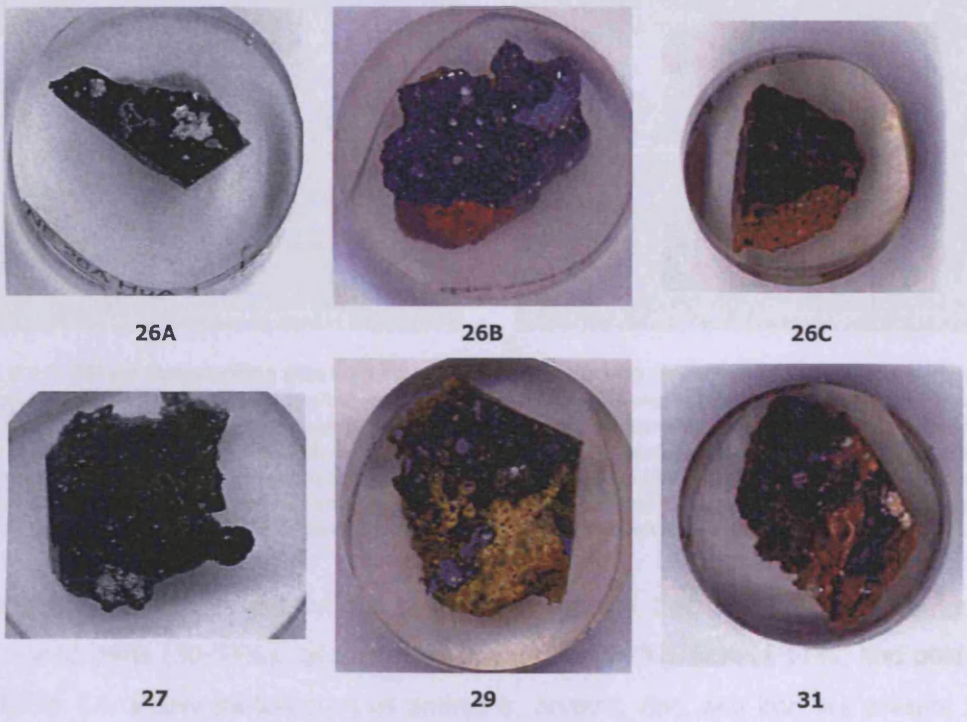

Figure 8.13. Cut and mounted resin blocks of the HuA1 samples.

OM of the seven HuA1 samples has shown that the slag has a consistently glass-rich matrix (Figure 8.14). Partially reacted gangue minerals predominate the slag matrix. The most common gangue minerals recorded were quartz and sulphidic ores. In the OM, lead sulphide and large metallic prills were commonly observed. The metallic prills were composed of different metallic phases. Inclusions of charcoal were recorded in sample 26C. Sample 29 is a multi-layered *huayrachina* fragment. OM showed that the mounted sample has three different mineralogical areas. The upper layer is a massive slag layer attached to the furnace wall, and the middle layer represents the interaction between ceramic and siliceous slag which created a lead silicate. Finally, the third and bottom layer is the furnace wall. Within the slag layer proper (upper layer), a large number of metallic prills remained trapped in the silicate matrix. Metallic prills seen in the OM commonly had a lead metallic centre which was surrounded by a halo of

lead sulphide (Figure 8.14). SEM-EDS analysis confirmed that metallic lead prills also contained other metallic phases (see below).

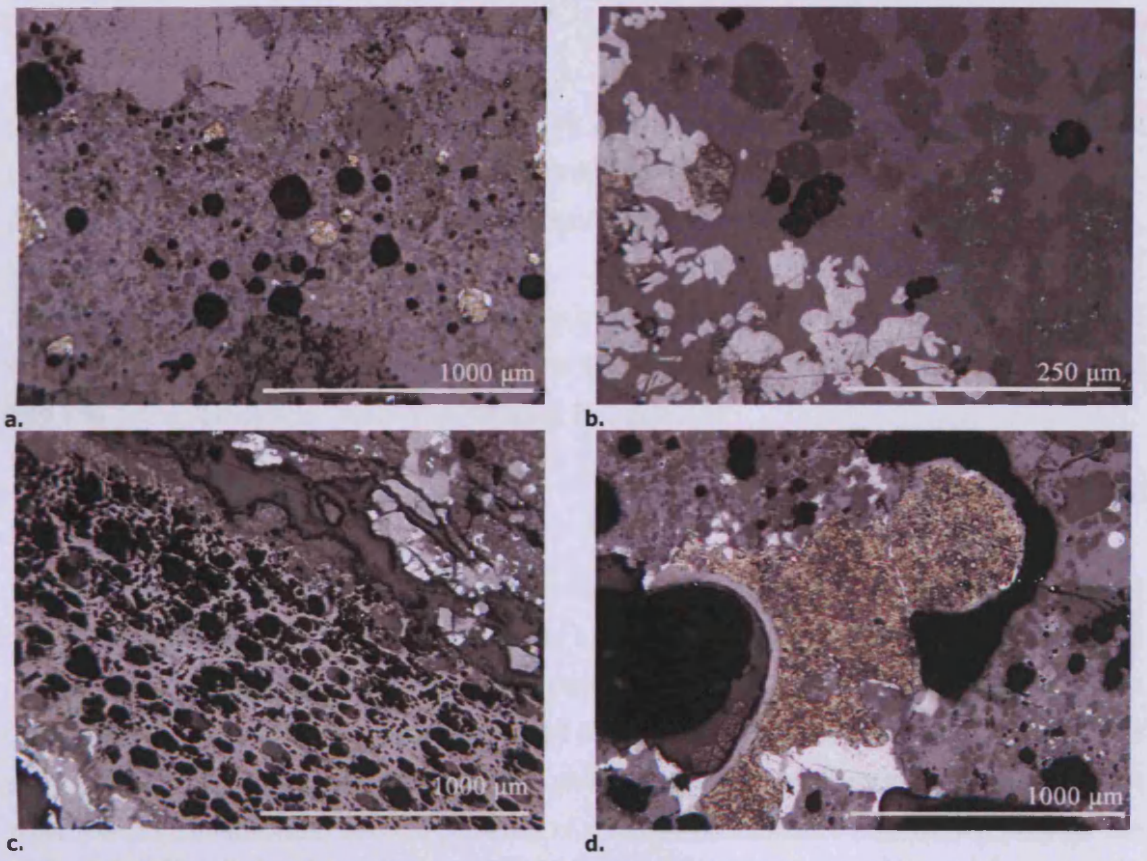

Figure 8.14. OM on Huayrachina Alta slag samples showed a glassy matrix with different silicate phases. Image A (sample 26A) shows a typical slag sample with small metallic lead prills scattered throughout the body of the slag. Image b (sample 26B) shows the crystals formed in HuA1 slag: the glassy slag matrix (lightest grey), the lead sulphide (white), Leucite (dark hexagonal crystals), and olivines (mid grey crystals). A Large charcoal inclusion was observed in slag sample 26C (c). Metallic lead was common in all slag samples, particularly in sample 29 (d). The metallic lead is brown in colour and has areas of lead sulphide (bright white) around the outer rim.

SEM-EDS analysis carried out on the samples has shown that the bulk area composition contains lead oxide (30-53%), silica (22-34%), alumina (5-7%), lime (1-11%) and potash (2-3%); Table 8.4. Heavy metals such as antimony, arsenic, zinc, and iron are present in the bulk composition of the slag from HuA1. Sample 26C has significantly higher sulphide concentration; OM indicated that there was a large quantity of sulphur present as lead sulphide.

Analysis of the glassy slag matrix has shown that the matrix is composed of large quantities of lead oxide (50-71%). Heavy metals such as iron, zinc, arsenic, and antimony are present in the glassy matrix, but in relatively low quantities (Appendix V). Mineral inclusions in the slag matrix include olivine and leucite (Appendix V).

The ceramic furnace lining was analysed using bulk area analyses on the SEM-EDS. Three samples (26B, 29, and 31) were analysed. The ceramic appeared to be non-tempered and of a typical ceramic composition with silica (68%), alumina (15%), potash (5%), iron oxide (2.5%)

and lime (2%). Small quantities of lead oxide were recorded in two of the samples, and it is assumed that these were caused by lead oxide reacting with the ceramic body during the smelt (Table 8.3).

Sample 31 demonstrates how the lead silicate was formed from the ceramic body and the reactive lead oxide. Leucite crystals were recorded forming from the surrounding lead silicate. Zinc calcium silicates were a common phase found within the slag matrix of sample 31.

Metallic prills analysed in the slag were mainly composed of lead metal but contained up to 5 wt% of silver. Small metallic prills of pure silver were recorded in sample 26A. Partially reacted lead and zinc sulphide was recorded in samples 26C and 27A.

Summary of site HuA1

The HuA1 slag is glassy and heavily leaded (up to 52% lead oxide from bulk area scans). Areas of lead and zinc sulphide were recorded in the majority of samples although the slag was well oxidised, and areas of sulphidic inclusions were small. Metallic prills within the slag were composed of pure lead metal and alloys of lead and silver. PAPP have dated this site within the early colonial era. The analytical results have shown that the *huayrachinas* were used to smelt argentiferous lead sulphide, and the presence of sulphidic components indicate that no prior ore roasting occurred. The metal from these *huayrachinas* would have required further refining to extract the silver.

Samples	Na2O	MgO	Al2O3	SiO2	P2O5	K2O	CaO	TiO2	FeO	PbO
26B	2.0	0.6	14.9	72.3	~	6.5	1.3	~	2.4	~
29	3.0	0.7	16.6	61.7	1.4	4.5	3.4	~	2.5	6.2
31	2.6	~	13.3	69.7	~	4.3	1.6	0.6	2.5	5.4
Average ceramic	**2.5**	**0.4**	**14.9**	**67.9**	**0.5**	**5.1**	**2.1**	**0.2**	**2.4**	**3.9**

Table 8.3. Bulk area analysis of the ceramic body of archaeological *huayrachina* samples HuA1. Data has been normalised to 100 %.

Sample	Na2O	MgO	Al2O3	SiO2	SO3	K2O	CaO	TiO2	MnO	FeO	ZnO	As2Ox	Sb2O3	PbO
26B	~	1.0	4.8	23.6	~	1.6	8.2	0.3	~	4.9	13.4	~	~	42.2
26C	~	0.7	6.2	23.5	1.1	2.8	8.3	~	~	4.9	15.5	2.8	~	34.2
27A	~	1.6	5.3	22.2	~	3.1	11.4	~	0.4	13.4	11.1	~	~	31.5
29	0.8	~	8.2	30.5	~	2.4	1.0	~	~	1.6	~	1.0	1.8	52.7
31	0.4	0.8	7.0	34.1	~	2.7	5.8	1.1	~	7.3	11.1	~	~	29.7
Average	**0.2**	**2.5**	**4.7**	**26.8**	**0.2**	**2.5**	**6.9**	**0.3**	**0.1**	**6.4**	**10.2**	**0.8**	**0.4**	**38.1**
Min	0.4	0.7	4.8	22.2	1.1	1.6	1.0	0.3	0.4	1.6	11.1	1.0	1.8	29.7
Max	0.8	8.2	7.0	34.1	1.1	3.1	11.4	1.1	0.4	13.4	15.5	2.8	1.8	52.7

Table 8.4. SEM-EDS bulk area analyses of slag samples from HuA1. Data has been normalised to 100 wt%.

Site 24

Five samples of *huayrachina* slag were selected for analysis from the *huayrachina* debris from site 24. The labelling of these samples derived from the numbers assigned to the samples when originally collected. Some of the samples have the same number although all are separate pieces of slag that are from the same historical period but may or may not have originated from the same smelting episode. All the samples selected have been analysed using OM and SEM, and some were specifically selected for XRF. The results of these analyses are presented in this section.

Figure 8.15. A selection of hand specimens sample bag 77 from site 24.

Samples 76A and 76B come from a group of slag samples that are relatively small (less than 3 cm wide) grey/brown vitrified pieces. Samples 77A, 77B and 77C are also from a large collection of slag samples (Figure 8.15). All the slag pieces are porous and heterogeneous containing pieces of charcoal, metallic inclusions, and pieces of gangue material. The five samples selected for analysis are shown in Figure 8.16.

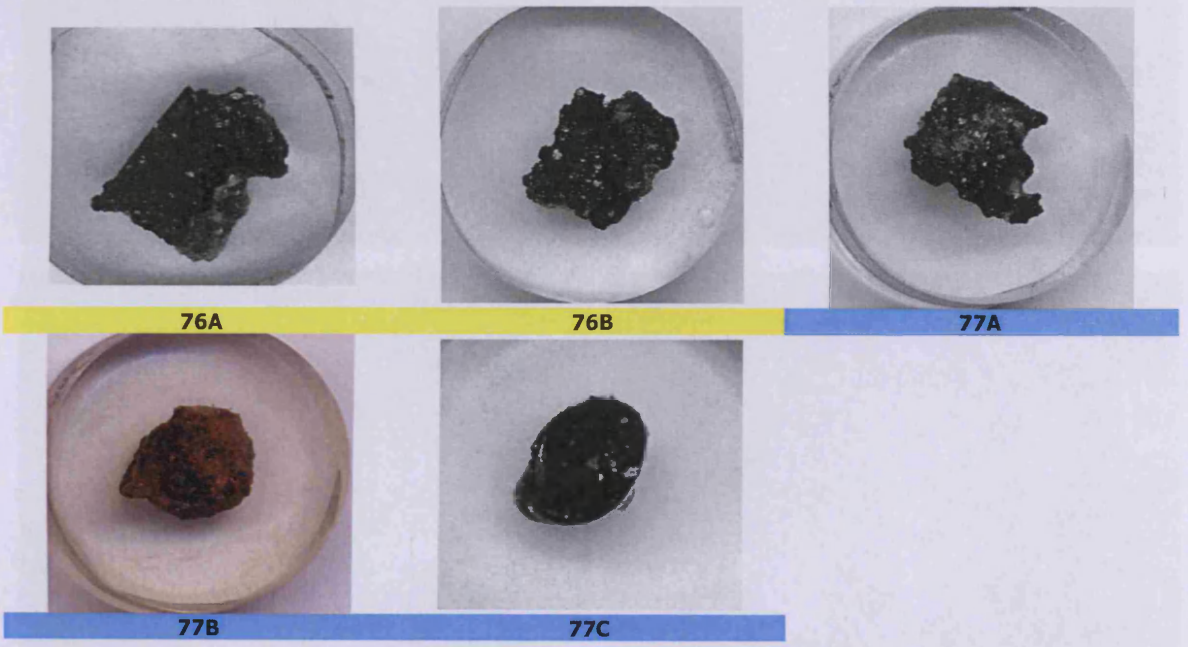

Figure 8.16. Cut and mounted samples from Site 24.
Yellow samples come from the sample numbered bags, but are different samples.

From the OM, all five samples exhibit a high degree of variability. Slag sample 76A is very vitreous and glassy containing metallic prills dispersed throughout the sample. Other crystal phases are present, but in very small quantities. However, in sample 77B the slag has a textural composition including many crystal phases, and is not very vitreous. These differences indicate the variable conditions occurring in the *huayrachina*. Typically, the slags had a glassy matrix

(seen as light grey in the OM) with different crystalline inclusions and gangue minerals such as zinc sulphide. Quartz was a commonly occurring mineral present within the slag matrix (Figure 8.17).

SEM-EDS bulk area scans (Table 8.5) indicate that the variability in the samples, seen optically and by eye, is also chemically visible. The silica content ranges from 19 to 35%, and the quantity of lead oxide from 8 to 50%. The inconsistent quantity of lead oxide mirrors the results of slag analysis from the current day *huayrachinas*. The quantities of gangue minerals absorbed into the slag body can be assessed by considering the zinc and iron oxides, lime, alumina and potash contents. Sulphur was detected in only one of the slag samples and this was less then 1 %. The variability detected between the five slag samples only continues to highlight the inconsistent nature of this type of smelting operation, i.e. the changing temperatures and oxidising zones in the furnace. Low sulphide contents indicate that conditions were highly oxidising.

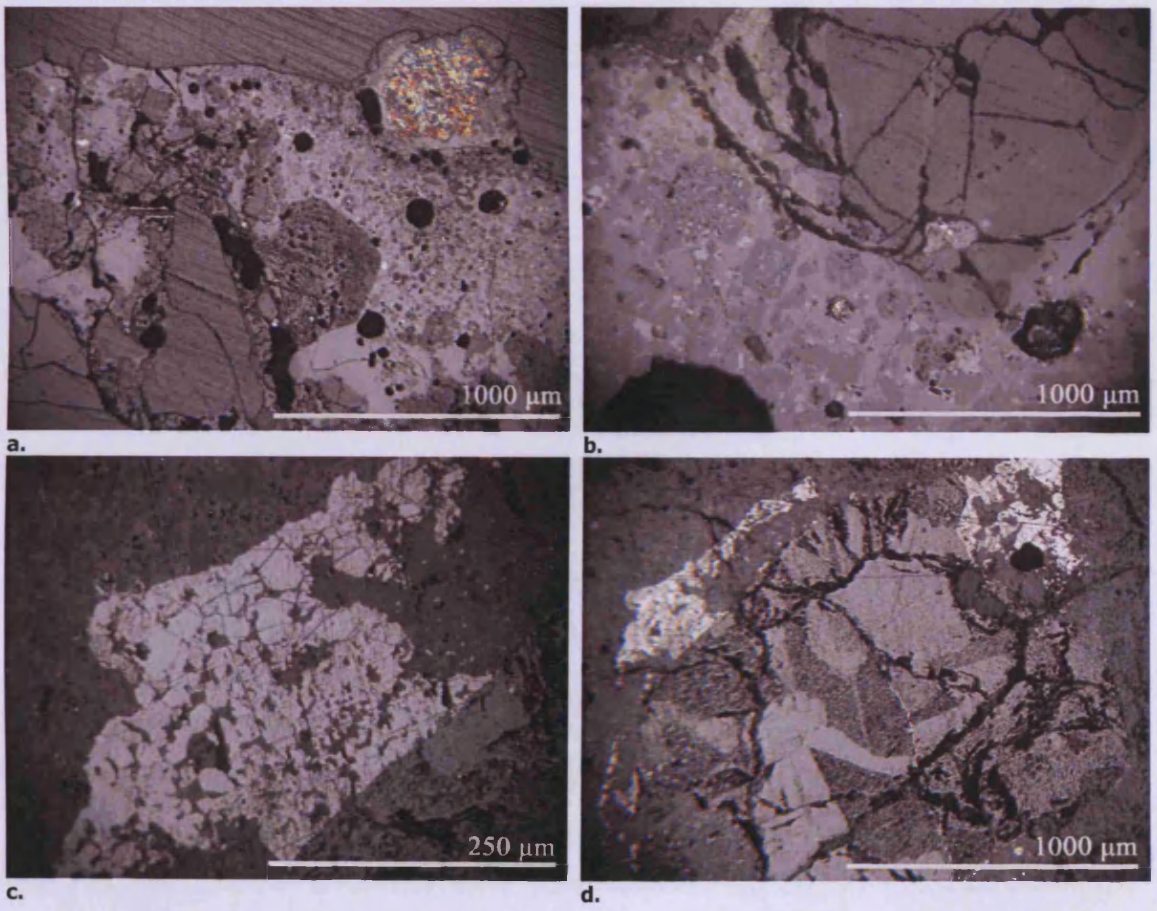

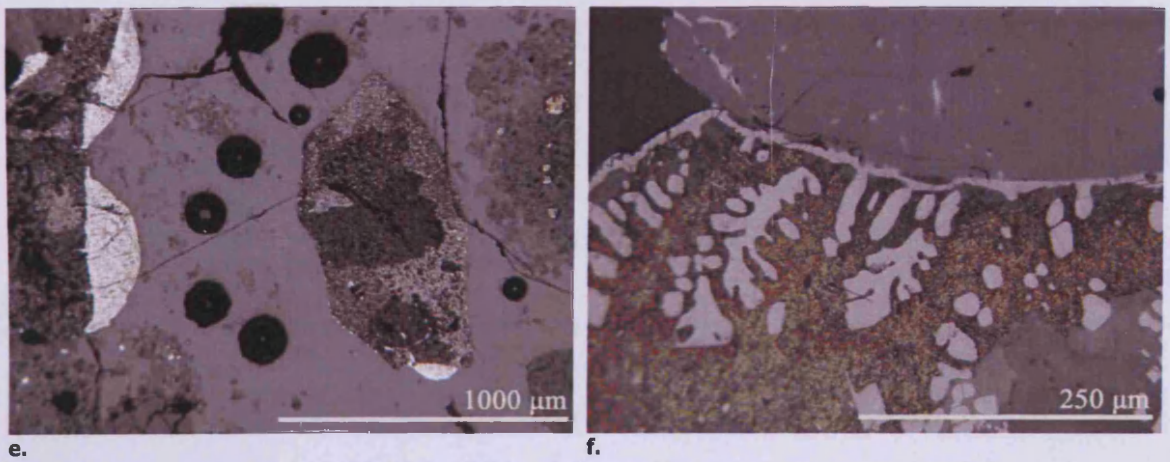

e. f.

Figure 8.17. OM of Hu24 slags

OM of Hu24 slags show a multi-textural slag with different crystal and metallic components (slag sample 77A, image a). Quartz crystals (grey) are also present (slag sample 77A, image b). Areas of partially reacted ore minerals were also recorded such as lead sulphide (bright white, image c) and zinc sulphide (light grey, image d). Some of the slag samples were more glassy (mid grey) such as 77C (image e). Image e also shows inclusions of lead sulphide (bright white), sphalerite (mid grey) and other smaller crystal phases. Areas of lead metal (brown) found in the Hu24 slag have shown partially reacted lead sulphide (white) – image f (slag sample 76B).

Sample	MgO	Al2O3	SiO2	P2O5	SO3	K2O	CaO	TiO2	FeO	ZnO	PbO
76A	2.2	8.0	33.5	~	~	3.7	14.1	~	14.4	4.9	19.2
76B	2.1	7.3	34.5	~	~	3.7	12.7	0.2	7.2	17.2	15.1
77A	1.6	4.2	24.3	~	~	0.8	11.1	0.4	8.0	18.5	31.2
77B	1.7	3.3	19.1	~	~	0.7	11.7	0.7	5.2	5.4	52.3
77C	3.5	5.9	32.8	1.2	0.9	2.4	23.5	0.2	10.3	11.6	7.7
Average slag matrix	**2.2**	**5.7**	**28.8**	**0.2**	**0.2**	**2.3**	**14.6**	**0.3**	**9.0**	**11.5**	**25.1**
Min	1.6	3.3	19.1	1.2	0.9	0.7	11.1	0.2	5.2	4.9	7.7
Max	3.5	8.0	34.5	1.2	0.9	3.7	23.5	0.7	14.4	18.5	52.3

Table 8.5. SEM-EDS bulk area scans of slag samples taken from site 24. The data has been normalised to 100 wt%.

Analysis of the glass slag matrix has shown that it is primarily composed of lead oxide (13-74%) and silica (15-33%). Elevated lead oxide levels in the glassy matrix indicate that the slag contains high quantities of lead, which at the time flooded the system creating a lead based silicate matrix. The matrix absorbed gangue material such as iron, zinc, arsenic, and titanium oxides (Table 8.6). Lime, alumina, potash, magnesium oxide and phosphate also contribute to the overall composition. Sample 77C has an unusual composition with low lead oxide (13%), high iron, zinc oxide and phosphate levels. These differences probably reflect inconsistent ore composition. It is important to note that no silver was recorded in the glassy matrix.

Sample	Na2O	MgO	Al2O3	SiO2	P2O5	SO3	K2O	CaO	TiO2	MnO	FeO	ZnO	As2O3	SnO2	PbO
76A	0.2	2.0	7.9	32.9	0.7	~	3.2	13.3	0.2	~	14.2	4.5	~	~	20.6
76B	~	2.0	5.5	31.2	0.6	~	2.5	8.0	~	~	9.2	14.8	0.5	~	25.7
77A	~	1.0	3.6	23.6	0.4	~	2.7	3.2	~	~	5.0	15.7	~	~	44.8
77B	~	~	1.7	14.9	~	~	~	2.9	~	~	4.6	1.0	0.5	0.5	73.9
77C	~	2.5	5.6	31.9	3.1	1.1	5.8	10.3	0.5	0.2	14.3	12.3	~	~	12.5
Average glassy slag	**~**	**1.5**	**4.8**	**26.9**	**1.0**	**0.2**	**2.8**	**7.6**	**0.1**	**~**	**9.4**	**9.7**	**0.2**	**0.1**	**35.5**
Min	0.2	1.0	1.7	14.9	0.4	1.1	2.5	2.9	0.2	0.2	4.6	1.0	0.5	0.5	12.5
Max	0.2	2.5	7.9	32.9	3.1	1.1	5.8	13.3	0.5	0.2	14.3	15.7	0.5	0.5	73.9

Table 8.6. SEM-EDS analysis of the glassy slag matrix in slag sample from site 24. Data has been normalised to 100 wt%.

SEM-EDS analyses of the crystalline phases present in the slag showed that olivines and leucitic compounds predominate (Appendix V). The olivines consist of lime, silica, and zinc oxide with the latter comprising of up to 20 % of the overall composition indicated an environment rich in zinc. This is confirmed by the bulk area analysis. The leucite crystals were easily identified via their small hexagaonal/angular shape. Other minerals such as spinels, have also been recorded in slag sample 77A (Appendix V). High alumina, iron, and zinc characterise these spinels, with some containing tin oxide. Pockets of gangue tin oxide were also analysed (Appendices V). Other gangue compounds remain in the slag, such as zinc sulphide and lead sulphide.

The slag body included metallic prills. The majority of the prills analysed were lead metal based. Some were pure lead metal, others contained quantities of silver (samples 76A, 76B and 77C). Residual lead sulphide recorded in the slag shows evidence of partial heating and semi transformation into lead metal.

Summary from site 24

Slag samples from site 24 have shown that they are composed of a lead silicate. The slag has been produced under oxidising conditions, indicated by the near absence of sulphur, a presence of high lead oxide levels and zinc oxides in the matrix and other crystalline phases. Partially reacted sulphidic ores have indicated that, while the overall conditions in the furnace were oxidising, there were pockets which were not. Their presence also indicates the absence of roasting. Tin oxide found in the furnaces showed evidence of poor sorting prior to smelting. Importantly, the presence of silver within trapped metallic prills indicated the use of argentiferous lead ore to produce an argentiferous lead metal. This metal would have then required further treatment to extract the silver.

Uruquilla East & West Saddle Surface

The two saddles of Uruquilla East (UR ES) and West (UR WS) were used as locations for *huayrachina* sites in antiquity. Samples taken from these sites were selected because they are typical examples of metallurgical debris found on *huayrachina* sites. In this section the results of analyses done on samples collected from UR ES and UR WS are presented.

Uruquilla East Saddle Surface

Four samples from the UR ES site were selected for analysis: 343A, 343B, 343C and 343D. These samples represent a selection of the overall surface remains. Only four samples were collected because the UR ES site is small and difficult to date. These samples were selected to provide preliminary data about the way in which these furnaces functioned and the types of ore once selected for smelting.

Samples 343A and 343B are pieces of slag (less than 2 cm in width) without ceramic adhered. The hand specimens are black/mid grey in colour with a granulated surface texture, and their cut surfaces show a porous structure with the occasional fragment of charcoal. Samples 343C and 343D are *huayrachina* furnace fragments. Both have a red ceramic wall upon which slag has adhered. Sample 343C has a 1 cm thick layer of dark grey slag. The external texture of the slag is dimpled with a pock marked surface, internally the cut surface has different inclusions but is mainly composed of a grey coloured matrix. Sample 343D was selected because of its form, which appears to connect two eye holes (Figure 8.18, lower left fragment). The slag layer is very thin and a much lighter grey than sample 343C. Cutting of both samples was done to ensure that both the slag and ceramic layer were available for analysis.

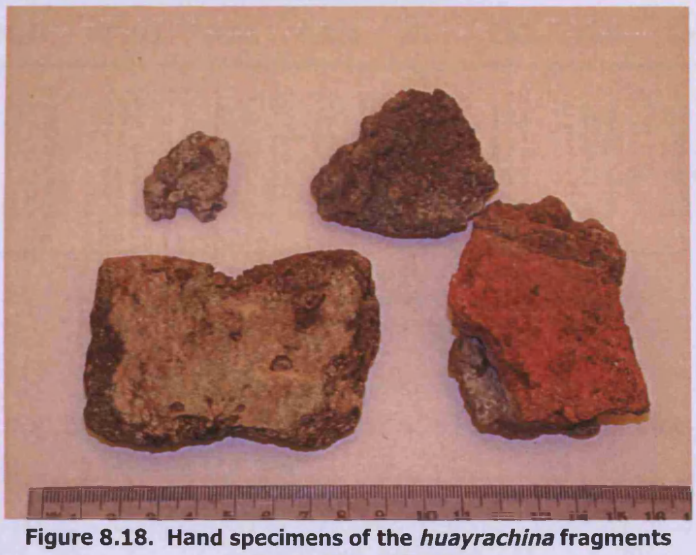

Figure 8.18. Hand specimens of the *huayrachina* fragments collected from UR ES.

OM work done on sample 343A has shown that it is composed of a silicate base matrix with a number of different mineral and metallic inclusions. A number of multi-phase metallic prills were

observed. Slag sample 343B has a large number of lead metal inclusions. The basic silicate matrix appears similar to sample 343A. OM of the two *huayrachina* wall fragments (343C and 343D) showed that the ceramic layer is relatively porous and composed predominantly of quartz grains. Both samples contained prills with areas of lead metal and lead sulphide in the slag (Figure 8.19).

SEM-EDS bulk area analysis of slag from the four ES samples has shown that samples 343C and 343D have similar quantities of lead oxide but their other components vary, samples 343A and 343B chemically different (Table 8.7). Each of the samples will be discussed separately, followed by an overall review.

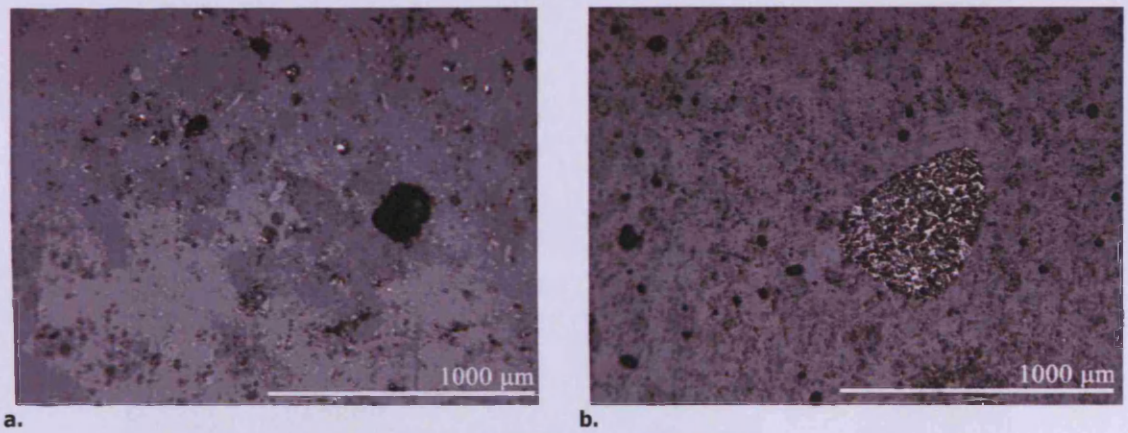

a. b.

Figure 8.19. OM images of ES 343A.
OM images taken of UR ES 343A show that the slag contains different silicate minerals (a) and ore minerals (b). OM imaging of sample 343B showed the presence of lead metal with partially reacted lead sulphide (white phase).

Average bulk composition	MgO	Al2O3	SiO2	P2O5	K2O	CaO	FeO	ZnO	SnO2	PbO
ES 343A (n=5)	2.4	5.4	29.0	~	3.0	14.4	6.0	24.4	~	15.4
ES 343B (n=5)	1.7	6.6	29.3	1.2	3.9	15.3	6.8	5.2	12.6	17.5
ES 343C (n=3)	1.2	4.8	19.4	~	1.9	7.8	3.1	4.0	~	57.7
ES 343D (n=2)	0.6	5.2	10.8	~	~	1.4	1.0	13.9	~	66.4

Table 8.7. Bulk area compositions of ES slag samples.
The data has been normalised to 100 wt%.

Sample 343A is a slag containing higher than expected quantities of zinc oxide (24%). This sample is best described as being a zinc silicate, rather than a lead silicate. Silica, lime, and lead oxide make up the primary composition of the slag. The high quantity of zinc observed in the bulk analyses is present as areas of zinc sulphide (Figure 8.20) but also recorded in the glassy matrix; 25 wt% zinc oxide was measured. The glassy matrix is composed of zinc oxide, lead oxide and silica (Table 8.8). Other mineral phases included complex olivines which are zinc-rich

(20%) with lime (32%), and silica (37%) seen in Figure 8.20 as the darkest coloured angular minerals (Appendix V).

Glassy silicate matrix	Na2O	MgO	Al2O3	SiO2	P2O5	K2O	CaO	FeO	ZnO	As2O3	PbO
Average 343A (n=3)	~	2.3	4.2	27.6	0.9	5.4	5.2	5.5	22.8	0.3	25.6
343B (n=1)	0.9	~	1.7	18.2	~	~	2.4	3.2	~	0.9	72.8
Average 343C (n=3)	~	1.2	3.2	17.9	~	0.8	4.7	2.8	3.8	~	65.7

Table 8.8. SEM-EDS area analysis of the glassy matrix of sample UR ES. The data has been normalised to 100 wt%.

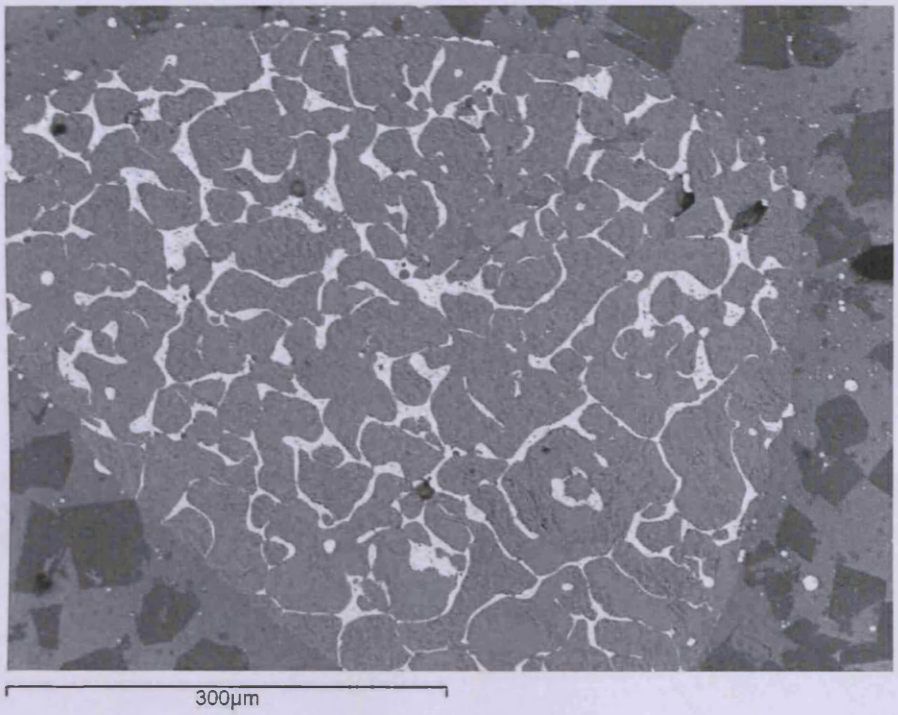

**Figure 8.20. A backscattered electron image of a large zinc sulphide mineral found in sample UR ES 343A (OM image seen in Figure 8.15 b).
The mid grey areas are zinc sulphide, and bright white veins are lead sulphide. The dark angular minerals are zinc silicates.**

Sample 343B is an unusual slag sample. Bulk area analysis indicated the presence of tin oxide (13%), which is unique to this sample. It also contains silica (29%), lead oxide (18%), lime, alumina, zinc, iron oxide, and phosphate. Quantities of lime within this sample were also higher than expected. Metallic prills analysed in the SEM-EDS are composed of lead metal but also contain variable quantities of silver, tin, and antimony (Table 8.9).

Spectrum	Ag	Sn	Sb	Pb
Prill C	~	11.1	~	88.9
Prill B	6.6	6.7	3.8	82.9
Prill A	4.7	10.5	2.4	82.4
Area c	3.3	9.7	4.2	82.8
Area d	4.0	11.8	3.8	80.5
Area E	~	16.9	9.4	73.7

Table 8.9. SEM-EDS area analysis of metallic prills in sample 343B. The data has been normalised to 100 at%.

Samples 343C and 343D have a slag composition containing high quantities of lead oxide (c. 60%) and variable quantities of silica, zinc and iron oxide, lime, potash, and alumina. No metallic prills were analysed in 343D. The ceramic matrix seems to be normal clay with higher silica (Table 8.10).

Area analyses	Na2O	MgO	Al2O3	SiO2	K2O	CaO	TiO2	FeO	PbO
343C (n=3)	1.2	0.7	16.1	71.0	5.7	0.7	0.6	3.0	1.0
343D (n=1)	0.9	~	13.2	79.0	6.0	~	~	0.9	~

Table 8.10. Ceramic bulk SEM-EDS area analyses of furnace wall sample 343C/D. The data has been normalised to 100 wt%.

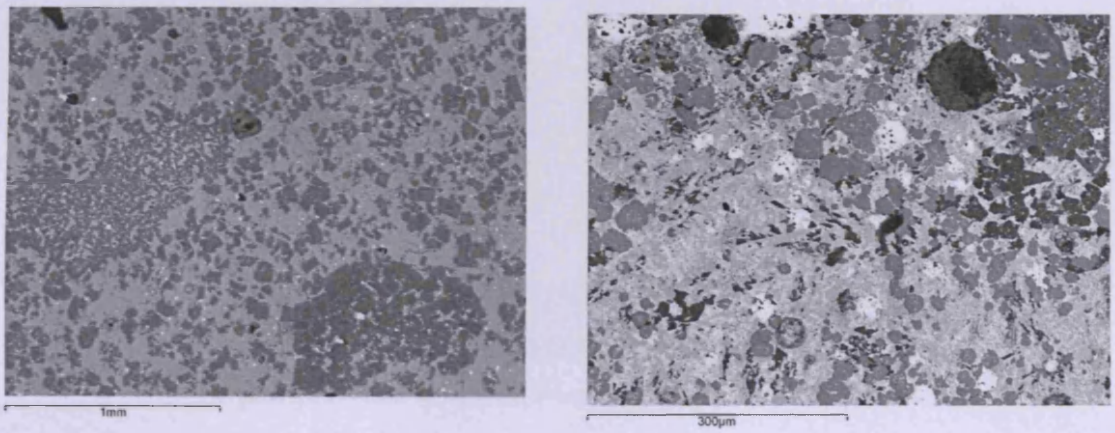

a. b.

Figure 8.21. SEM images of UR ES 343A.
A SEM image of 343A, the slag body with zinc silicates (dark grey crystals, a). Sample 343B in comparison is a slag containing many metallic phases (bright white prills) and different silicates (b).

Summary from UR ES

The samples recorded from UR ES have a silicate slag containing widely variable quantities of lead oxide (16-66 wt%). The predominant phases identified in the UR ES samples are olivines and leucite. Lead and zinc sulphides were also identified. The high quantity of tin in sample 343B is rare, but would perhaps indicate the poor separation of lead/silver rich ores from a tin-

rich gangue. The Porco region is rich in tin and thus, the presence of tin is not abnormal, however one assumes that the ore would be sorted to ensure that lead and silver ores were selected rather than tin. The ceramic from the furnace wall appears to be made from un-tempered sandy clay. This site was not dated, but from analytical results, the *huayrachinas* were used for smelting argentiferous lead sulphide which may have been poorly sorted (to account for the areas of high tin). The slag is highly oxidised with areas of sulphides being relatively low. However, sample 341A shows that the original ore would have contained significant amounts of zinc sulphide. This site was used for the processing of sulphidic ore which would not have required pre-roasting.

Uruquilla West Saddle Surface

From the WS site, six samples were selected for analytical work: 342A, 342B, 342C, 342E, 342F, and 342G. Each of these were taken from separate *huayrachina* fragments sampled from the surface of the site. The fragments are of variable size and shape, and all had slag attached to the inner surface of the ceramic.

Figure 8.22. Hand specimens taken for analysis from site UR WS.

Samples 342 B, F and G are heavily slagged ceramic; the slag is light grey and has a light yellow coating on the exposed surface. The cut surface of the slag is matt and has a porous texture. Samples 342A, 342C and 342E are wall fragments composed of dense red clay. The slag is dark grey in colour and heavy to the touch, indicating a high lead content. The cut surfaces of these fragments have shown metallic prills and some zoning of a shiny metallic mineral (most probably galena). The surface texture of the slag is granular and covered in a brown patina.

OM analysis has shown that the samples are very heterogeneous (Figure 8.23). All the samples except for 342C have some ceramic adhered to the slag layer. The slag has a glassy matrix with many different crystalline phases present. Metallic prills are common within all the samples, and all samples contain partially reacted lead sulphide minerals. Sample 342A has inclusions of lead and zinc sulphides that are extremely angular indicating that they have not reacted with the surrounding melt. Sample 342E has a striated texture composed of three main layers: the ceramic wall, a layer of lead sulphide, and an upper slag layer.

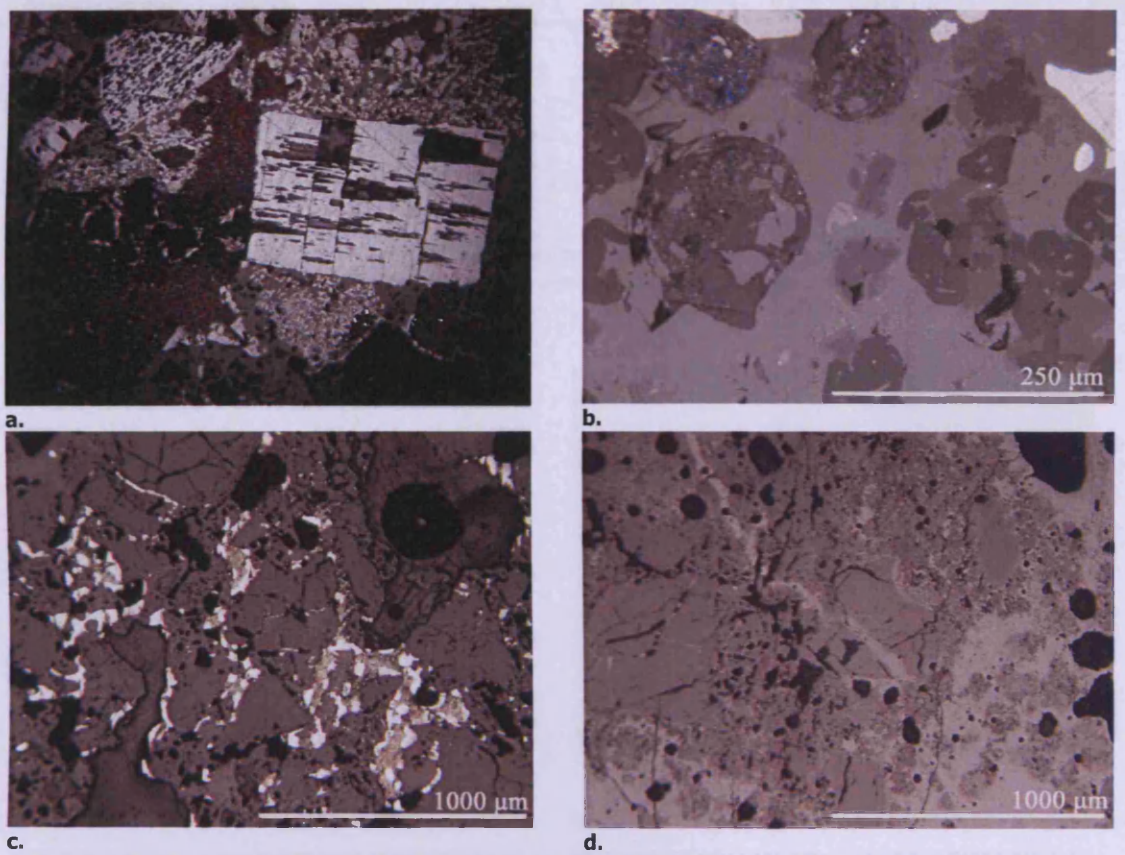

a. b. c. d.

Figure 8.23. OM images taken from the WS assemblage.
Sample 342A has angular lead sulphide inclusions (a) (need scale). OM images 342B and 342C have silicate matrices with silicate mineral inclusions (b and c). Sample 342C has inclusions of lead sulphide shown in white (c). Some samples from the assemblage are pure lead silicates like sample 342F (d).

Sample 342F is extremely glassy, and initial OM analysis has shown that the majority of the sample appears to be silicate based. The ceramic analysed from all the samples with ceramic adhered to the slag appears to be un-tempered

SEM-EDS analysis of the bulk composition has confirmed the variability already noted in the OM and hand samples. The primary slag component is lead oxide (28-66%), however the large presence of sulphur in 342A, B, and C make these totals unreliable (Table 8.11). In sample 342A, the high incidence of sulphur would make it more than likely that the lead is present as lead sulphide rather than lead oxide. The bulk composition also consists of silica (9-30%), alumina (1-17%), lime, iron, and zinc oxide. Sample 342F has a higher than average alumina (17 %). This is reflected by a high number of leucitic crystals found in the slag matrix.

The analysis of the ceramic adhering to the slag fragments has indicated a normal ceramic body with silica (c. 70%), alumina (19%) and potash (5%) and low quantities of lime, soda, iron, magnesium, and titanium oxide.

Area scanned	Na2O	MgO	Al2O3	SiO2	SO3	P2O5	K2O	CaO	FeO	ZnO	PbO
WS 342A (n=5)	0.2	~	0.8	8.8	12.4	~	0.2	1.8	7.5	2.6	65.7
WS 342B (n=5)	0.5	0.4	7.9	29.8	2.9	~	4.1	3.8	2.4	4.4	43.7
WS 342C (n=3)	~	1.3	7.5	26.9	3.1	~	3.6	6.7	4.8	12.7	33.4
WS 342F (n=3)	1.0	3.3	17.1	26.6	~	0.4	4.9	8.4	3.7	6.9	27.6
WS 342G (n=5)	~	1.3	5.1	21.2	~	~	2.1	9.2	3.1	6.2	51.9

Table 8.11. SEM-EDS bulk area analyses of UR WS slag samples. The data has been normalised to 100 wt%.

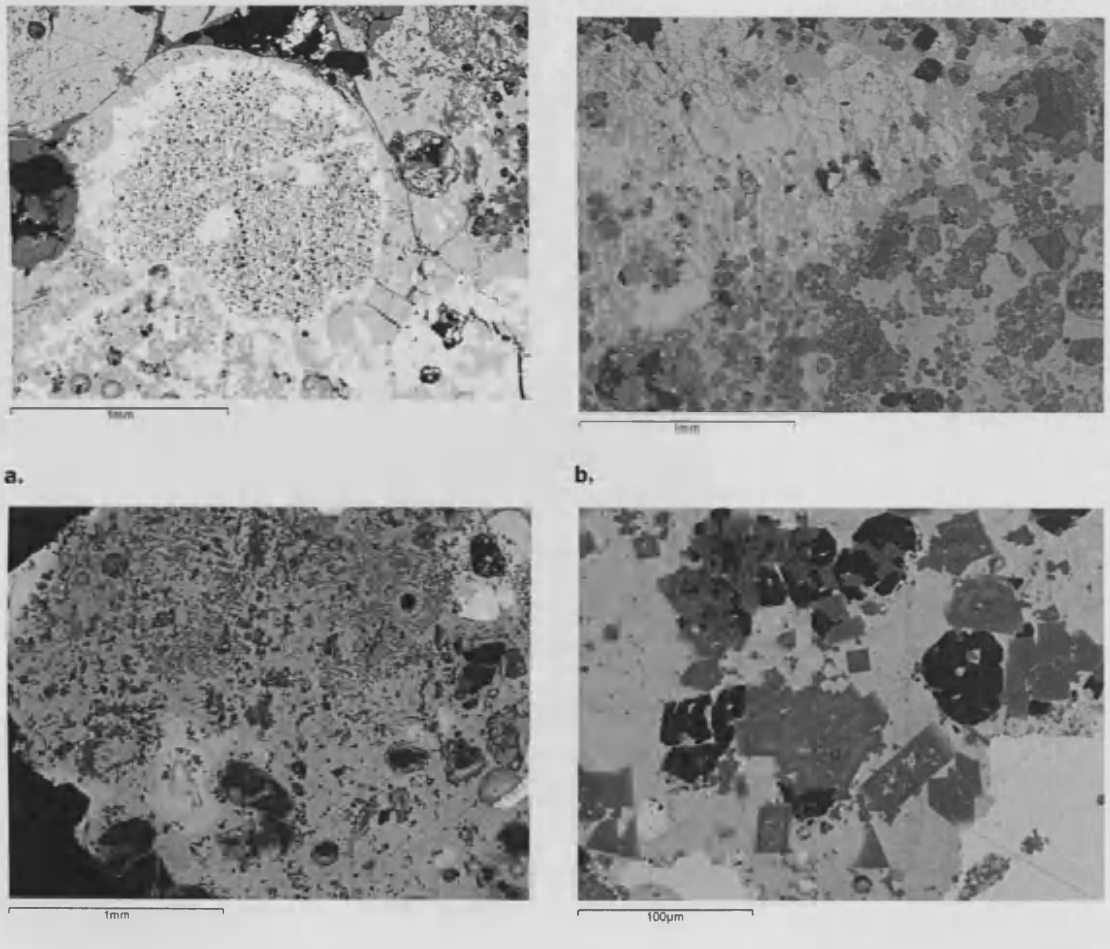

Figure 8.24. SEM-EDS images of the bulk area analyses from UR WS samples show that all the slag samples contained different silicate phases such as leucite, olivines and metallic lead prills. Image a shows a lead prill surrounded by lead sulphide (342B). Images b and c show typical bulk area analyses from sample 342B and 342C. The different phases within sample 342C are illustrated in image d.

The different silicate mineral phases seen in the OM were analysed using SEM-EDS and found to be leucite, zinc calcium silicates, zinc silicates, iron oxides, and iron silicates. The formation

of the zinc based phases occurs in samples with high zinc sulphide present (samples 342A, 342B, 342C and 342E). Metallic prills analysed have shown that the majority are lead metal based. Many have halos of lead sulphide on their outer edge, with some containing up to 8 at% silver.

Summary from UR WS

The UR WS slag has high levels of partially reacted lead sulphide. Sample 342A has residual lead sulphide minerals that have an angular appearance. This indicates the beneficiation of the ore minerals by crushing prior to smelting. Only two of the slag samples do not contain quantities of lead sulphide in the bulk matrix. Zinc silicates and oxides were recorded in the slag. The UR WS slag is composed of a glassy lead silicate. The presence of sulphidic minerals (without any silver recorded) in the glassy matrix indicates that these furnaces were used to produce lead metal. However, metallic prills analysed contain up to 8 at% silver. This site, like UR ES is un-dated and thus very little contextual information is available.

Average bulk composition	Na2O	MgO	Al2O3	SiO2	P2O5	SO3	K2O	CaO	TiO2	MnO	FeO	ZnO	As2Ox	Sb2O3	SnO2	PbO
Hu24 77C	~	3.5	5.9	32.8	1.2	0.9	2.4	23.5	0.2	~	10.3	11.6	~	~	~	7.7
Hu24 76B	~	2.1	7.3	34.5	~	~	3.7	12.7	0.2	~	7.2	17.2	~	~	~	15.1
ES 343A	~	2.4	5.4	29.0	~	~	3.0	14.4	~	~	6.0	24.4	~	~	~	15.4
ES 343B	~	1.7	6.6	29.3	1.2	~	3.9	15.3	~	~	6.8	5.2	~	~	12.6	17.5
Hu24 76A	~	2.2	8.0	33.5	~	~	3.7	14.1	~	~	14.4	4.9	~	~	~	19.2
WS 342F	1.0	3.3	17.1	26.6	0.4	~	4.9	8.4	~	~	3.7	6.9	~	~	~	27.6
HuA1 31	0.4	0.8	7.0	34.1	~	~	2.7	5.8	1.1	~	7.3	11.1	~	~	~	29.7
CP 344A	~	1.9	5.4	32.3	2.0	~	3.3	12.4	0.9	~	10.8	9.3	~	~	~	21.7
CP 344B	~	2.5	1.6	29.6	2.3	~	2.9	12.9	1.1	~	10.0	11.4	~	~	~	26.1
Hu24 77A	~	1.6	4.2	24.3	~	~	0.8	11.1	0.4	~	8.0	18.5	~	~	~	31.2
HuA1 27A	~	1.6	5.3	22.2	~	~	3.1	11.4	~	0.4	13.4	11.1	~	~	~	31.5
WS 342C	~	1.3	7.5	26.9	~	3.1	3.6	6.7	~	~	4.8	12.7	~	~	~	33.4
HuA1 26C	~	0.7	6.2	23.5	~	1.1	2.8	8.3	~	~	4.9	15.5	2.8	~	~	34.2
HuA1 26B	~	1.0	4.8	23.6	~	~	1.6	8.2	0.3	~	4.9	13.4	~	~	~	42.2
WS 342B	0.5	0.4	7.9	29.8	~	2.9	4.1	3.8	~	~	2.4	4.4	~	~	~	43.7
WS 342G	~	1.3	5.1	21.2	~	~	2.1	9.2	~	~	3.1	6.2	~	~	~	51.9
Hu24 77B	~	1.7	3.3	19.1	~	~	0.7	11.7	0.7	~	5.2	5.4	~	~	~	52.3
HuA1 29	0.8	~	8.2	30.5	~	~	2.4	1.0	~	~	1.6	~	1.0	1.8	~	52.7
ES 343C	~	1.2	4.8	19.4	~	~	1.9	7.8	~	~	3.1	4.0	~	~	~	57.7
WS 342A	0.2	~	0.8	8.8	~	12.4	0.2	1.8	~	~	7.5	2.6	~	~	~	65.7
ES 343D	~	0.6	5.2	10.8	~	~	~	1.4	~	~	1.0	13.9	~	~	~	66.4

Table 8.12. The average bulk SEM-EDS area scans of all the archaeological *huayrachina* slag samples. The data has been arranged according to increasing lead content. Colour coded according to site.

Overall summary

A comparison between all of the SEM-EDS bulk area scans (Table 8.12) indicated that there is a large chemical variability between the *huayrachina* samples analysed. Lead oxide content varies between 8% and 67%. Other heavy metals such as iron and zinc oxides are almost always present and range from a few percent to 17%. Silica content in the slag is variable according to the lead oxide content. Some samples lie outside of the norm such as UR ES 343B which contains up to 13% tin oxide, indicating a different ore source. Sample UR WS 343A contains a large proportion of lead sulphide and therefore contains very little silica (only 9%). Sample HuA1 29 is an anomaly because it contains higher than expected magnesium oxide (8%), with relatively low lime and some antimony. Here, there has been a very different ore vein used for smelting. Evidence for ore crushing and beneficiation was recorded in the UR WS site, and sample 342A has angular, almost un-reacted pieces of lead sulphide. All the sites produced argentiferous lead metal which would have required further refining.

The analysis of these archaeological *huayrachina* sites has shown that in all of the sites, argentiferous galena was used as the smelted ore. The furnaces appear to have been made from local, un-tempered clay. The presence of sulphidic minerals such as galena and sphalerite was observed in all of the sites. Metallic prills of lead metal and lead silver alloys were common in all of the slags. All the slag is glassy and in the majority of samples is heavily leaded. Silicate phases are common components found in the slags. Conditions within the furnaces appear to be relatively oxidising, although the majority of samples still contain some quantities of sulphidic components. The presence of sulphidic phases shows that perhaps those areas not near eyeholes were not as oxidising as those located close to eye openings. Roasting prior to smelting does not appear to have been part of the production process. In the dated sites, evidence for poor sorting has been recorded via the higher than expected quantities of tin oxide and sphalerite or zinc oxides recorded (samples from site 24 particularly Hu24 76A).

The results of this chapter will be discussed further and compared to ethnographic slag samples in chapter 9.

9. RECENT AND ARCHAEOLOGICAL *HUAYRACHINAS* DISCUSSED

This chapter summarises the differences and similarities observed between the ethnographically documented *huayrachinas* (Chapters 4, 5, 6 and 7) and the archaeological *huayrachinas* sampled and analysed (Chapter 8). It will consider continuity and changes in the technical function and design of the furnaces. To review these changes, a brief summary of the analytical results done on the archaeological *huayrachinas* will be presented. In parallel with the analytical work, a small surface survey was conducted on two archaeological *huayrachina* sites, as previously presented in Chapter 8. The results of the survey allow consideration of the structural characteristics of the furnaces, such as, the diameter of air holes (eyes). Measurements were taken of the ethnographic *huayrachinas* and a comparison between the current day and archaeological surface surveys is reviewed in this chapter. What, if any, changes have occurred in the function and use of *huayrachinas* in the Porco-Potosí region?

9.1. Conclusions from the analysis of archaeological *huayrachinas*

The majority of slag samples analysed and presented in Chapter 9 contain silver-rich lead prills as well as residual sulphidic components such as galena and sphalerite, indicating that an argentiferous galena was smelted in the *huayrachinas*. Mineral compounds found in the slag are leucite, spinels, and olivines. The variation seen in the samples was likely caused by different ore concentrations and differences in temperature and redox conditions inside the furnace. Conditions within the huayrachina seem to be co-smelting, that is reducing and oxidising. The presence of silver within lead rich areas indicates that the archaeological huayrachinas were producing a lead/silver bullion. Only occasionally did the slag contain increased levels of arsenic, antimony, or tin which indicates that complex silver rich ores played no major role in this metallurgy.

The huayrachina samples analysed have a thick lead slag adhering to the ceramic wall. The slag has a high lead content, confirmed by the chemical analysis. These furnaces operated via the burning of charcoal and the constant flow of air (from the holes pierced into the shaft of the furnace). Air flow into the reaction chamber maintained temperatures and allowed for the oxidation of sulphidic compounds. The quality of the ore and charcoal, and quantity of airflow would have affected temperatures and redox conditions within the system. No information was available, the possible presence of CHM as part of the charge. Similarly, no archaeological refining features were identified so far. However, it is clear from the nature of the lead/silver

bullion (trapped as prills in the slag) that such refining, equivalent to European cupellation, must have taken place after the huayrachina smelting to obtain pure silver.

The analysed current day *huayrachina* fragments exhibited a thin vitreous coating (furnace fragment sample 9 only had 1-2 mm of slag). This thin layer of vitrification and shallow penetration of the lead silicate indicates that conditions within the furnace were not suitable to produce large quantities of reactive lead oxide. The partially molten lead oxide was unable to flow into the ceramic wall, indicating that the huayrachinas operate at a relatively low firing temperature. Slag analysed from the current day smelting was taken from material that was discarded during the smelt as waste. The slag analyses have shown the presence of large amounts of lead sulphide in a lead-silicate rich slag matrix, indicating that the system was not strongly oxidising. During the PAPP documentation of the smelting, CHM material was recorded as part of the input charge. The current day production separates the production of lead and silver. Lead is produced in the *huayrachina* and silver ore refined in a different process but using the lead produced previously.

A comparison between the archaeological and current day *huayrachina* shows that the basic furnace design has remained similar, however, the technical function has altered. The archaeological material analysed shows that the furnaces operated under higher temperatures and more oxidising conditions than the current day. These differences and similarities will be further discussed in section 9.3.

A reconstruction of the processes involved in archaeological silver production has drawn upon the ethnographic chaîne opératoire described in Chapter 7 (see inserts at the back of this thesis). The schematic *chaîne opératoire* of archaeological silver production uses reverse engineering to model production methods, this will be discussed later in this chapter. Many of the stages of the process are variable and rather uncertain. These uncertain variables have been labelled in grey to further emphasise the overall aspects of the system that have been confirmed. In parallel to the chaîne opératoire of archaeological silver production a web of archaeometallurgical research has been constructed. The next section of this chapter discusses the surveyed *huayrachinas*, as well as the results of ethnographic and archaeological surveys. The final section uses the *chaîne opératoires* and the web constructed during this research to consider the differences and similarities observed between the current day and archaeological *huayrachinas*.

9.2. Ethnographic *vs.* archaeological survey data

The purpose of the surface survey was to understand more about the dimensions and design of the *huayrachina* furnaces, both in the current day and within the archaeological record. The

survey was conducted on two archaeological sites (HuA1 and UR WS) and on a small review of the ethnographic furnace debris. Measurements were taken of the *huayrachina* wall thickness, and the air hole diameter and thickness. The number of slag layers was also recorded, as this was previously noted to be different in the archaeological record. Results from the archaeological sites showed that the original thickness of furnace wall could not easily be identified from this survey.

In the ethnographic survey, samples from Cuiza's smelting site were measured to document the eye hole diameter and width (presented in Chapter 5). The results showed that the older furnace debris had a slightly larger eye diameter almost 1 cm more, as compared to the intact *huayrachina* (2 cm diameter). These differences could be attributed to a change in furnace design.

Sample measured	Eye diameter (cm)	Eye thickness (cm)	Notes
Surveyed ethnographic *huayrachinas* average	2.9	2.7	~
Cuiza's intact *huayrachina*	2.0 2.0	7.0 10.0	Upper row of eyes Lower row of eyes
HuA1 Block A average	4.2	3.6	~
HuA1 Block B average	3.6	2.7	~
UR WS average	5.0	2.8	~

Table 9.1. A comparison of the diameter and thickness of *huayrachina* eyes from an archaeological and ethnographic context.
The eyes measured on the intact (ethnographic) *huayrachina* appear to have been partially sealed during the smelt.

The results presented in Chapter 8 from the archaeological surface survey have shown that the diameter of eye holes can vary between 3.6 and 5.0 cm (Table 9.1). HuA1 Block A has the highest number of furnace fragments measured. The average eye diameter from this site was 4.2 cm. UR WS had an average of 5.0 cm for the diameter, whereas HuA1 Block B has an average eye diameter of 3.6 cm. These changes in size may reflect a number of different variables, such as the methods of manufacture and the location of the eye holes within the furnace.

Also recorded during the archaeological survey was the thickness of the *huayrachina* fragments. It was noted that there was a discrepancy between the wall thickness of the intact furnaces (7-10 cm measured as eye hole thickness) and the thickness of ethnographic debris (2.7 cm) and archaeological fragments (2.7 to 3.6 cm). It is proposed that these differences were possibily partly due to the erosion of the partially-baked ceramic on the outer surface of the shaft. The heat from the reaction chamber transferred through the thickness of the furnace shaft. In Cuiza's furnaces, low temperatures were observed by the low interaction between the furnace wall and slag, the slag being recorded with partially reacted galena. If Cuiza's *huayrachinas*

worked at low temperatures, the penetration of heat into the previously unfired ceramic furnace shaft would be rather limited. Unfired clay is more susceptible to erosion from wind and rain, and as a result would dissolve more readily. It appears likely that this scenario happened both at Cuiza's site and at the archaeological sites where erosion was noted on the outer surface of furnace fragments.

In the archaeological *huayrachina* sites, the presence of fragments with eye holes was common. This is to be expected because weaknesses in the *huayrachina* structure would force cracks to propagate from air hole to air hole, thus preferentially creating pieces which have sections of air holes.

Cuiza's *huayrachinas* have two iron belts that help support the shaft. In the archaeological record, these have not been documented. The addition of the iron belts could account for the smaller air holes noted on Cuiza's furnaces (Table 9.1). It is plausible that the design of larger holes combined with a stronger slag build-up created a strong column shaft. Thus, within the archaeological record air hole furnace fragments are more common than other pieces which weathered at a faster rate. It was also noted that on Cuiza's intact *huayrachina,* some of the eye openings appeared to have been reduced in diameter due to slag formation.

Evidence of relining of the furnace shafts has been observed in a number of multilayer furnace fragments, although in the overall sample the quantity of layered fragments was very small. When multilayered samples were measured, the overall thickness of the furnace wall was increased; as a result the multilayered fragments were left out of the average thickness and diameter data. No relining has been observed in the ethnographic record.

Slag thickness was not specifically measured during the survey, although abnormal changes in slag thickness were recorded. It was noted that the archaeological material typically contained a heavy, vitrified layer of slag. The analytical work carried out on the archaeological material has confirmed that the majority of slag is lead silicate based, which would explain the weight of the furnace fragments. Ethnographically analysed samples have rather thin silicate layers and are typically light. The differences observed in slag thickness possibly indicate different temperature and redox conditions within the furnace.

The HuA1 block B survey recorded small ledges underneath the eye holes. This is particularly interesting because in 1893 Peele photographed *huayrachinas* with ledges (Peele 1893). No obvious ledges were recorded in the ethnographic *huayrachina.*

On the archaeological sites, some larger loose stones were found. On the UR WS site some had a black vitrified coating. These may have been used as base stones for a *huayrachina.* However, the sites do not provide evidence of how these bases would have been constructed. Nothing is

known about the height of *huayrachina* bases. Measurements taken by Peele (1893) seem to only consider the furnace shaft and not the base. In Cuiza's furnaces, the bases were constructed of three or four large flat stones. They also had an uppermost stone which had a groove cut out to aid the flow of the metal, indicating that the *huayrachina* would have been built directly on top of the base stones. Cuiza did not discuss what technique he used to build the furnace. It would be interesting to consider the height of archaeological base stones and how this may have altered the overall height of the furnace as a unit. Due to the limited information, nothing further can be concluded.

The survey results show that the archaeological *huayrachinas* have a larger eye hole diameter than the ethnographic. In particular, the intact ethnographic furnace used for the majority of the current day documentation has much smaller eye diameters than those recorded in the archaeological survey.

9.3. Discussion comparing the archaeological and ethnographic *huayrachinas*

In Porco, the use of *huayrachinas* persisted for several hundred years until recently. How had the technology evolved, and if so how did it experience technological adaptation? The *huayrachina* was initially the primary form of technology deployed under elite control to smelt relatively abundant rich ores during Inca and very early colonial times. As new techniques for metal production were introduced by the Spanish, such as mercury amalgamation, peasant/proletarian households used *huayrachinas* to supplement marginal incomes. Thus, not only has the physical and technical function of the *huayrachina* changed over the last 500 years, its social context has also changed. The continued use of the *huayrachina* until recently reflects its importance in the metallurgical history of the region. Accompanying the chemical analysis, a review of the historical literature has been considered and discussed above, along with the surface survey.

The survey and review of the physical/morphological qualities of archaeological and ethnographic *huayrachina* samples has shown that there are differences in the size of the furnace walls and eye holes. The air holes in the shaft appear to have been larger in antiquity. A 19th century source reports that air holes were up to 6 cm in diameter (Peele 1893). An evaluation of illustrations from historical literature indicated a slight adaptation in the shape and height of the *huayrachinas* (Figure 9.1). The earlier furnaces appear to have been taller, with a shaft that flared at the top. Small ledges were built underneath each of the eye holes. During the archaeological surface survey two fragments were found with ledges. Figure 9.1 a is an illustration from the 16th century. The furnaces have a shaft which appears to have ledges underneath the air holes. Peele (1893) says these ledges were used to place charcoal on. Could

charcoal have been added into the eye holes as well as through the top of the shaft, and how would that have affected metallurgical reactions and fuel consumption?

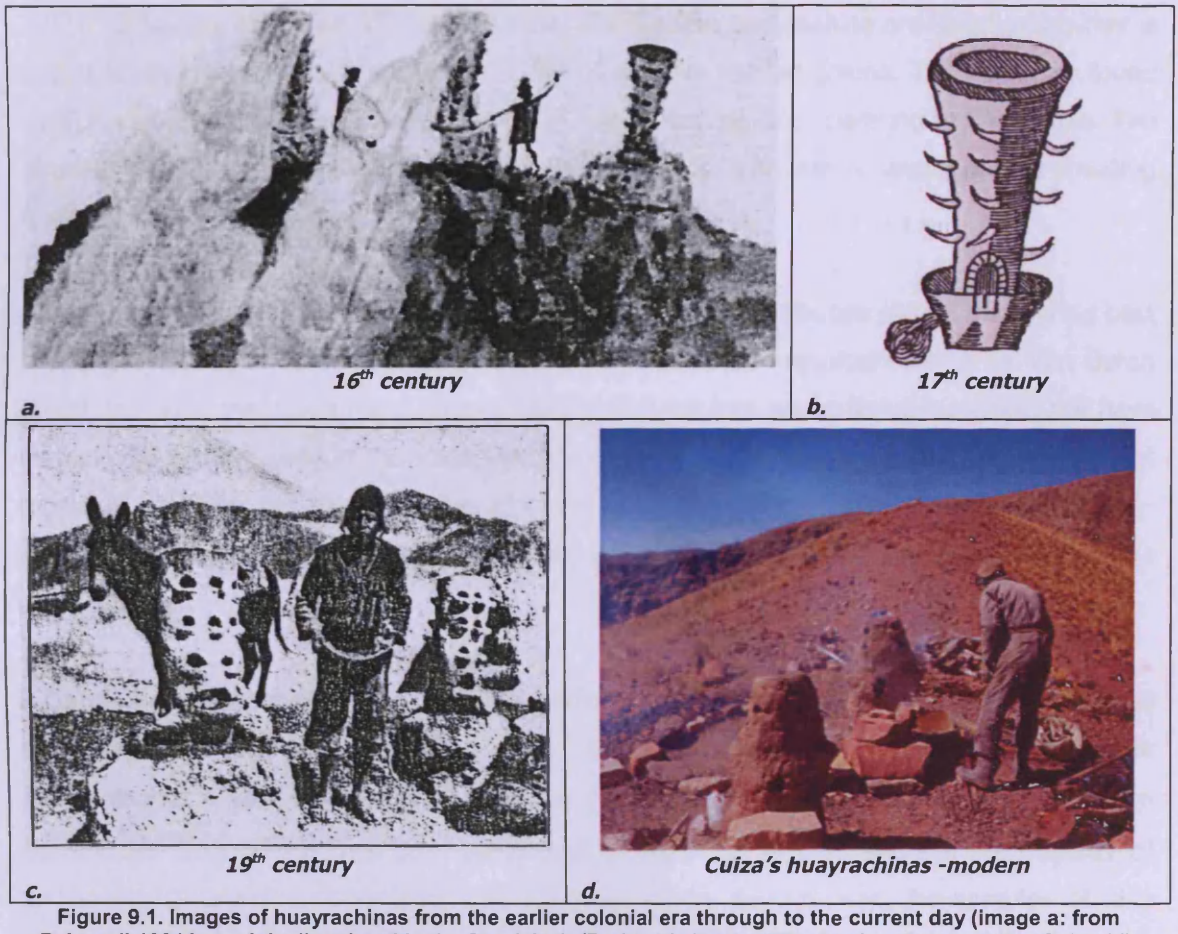

Figure 9.1. Images of huayrachinas from the earlier colonial era through to the current day (image a: from Bakewell 1984 but originally printed in the Sea Atlas), (Barba, b), (Peele 1893, 9 , c) and current day Cuiza (d).

Cuiza's modern *huayrachinas* have a vertical shaft and no ledges. Historical huayrachinas may well have been 86 cm tall, whereas the modern day huayrachina is only 76 cm (Peele 1893 and Table 9.3). A larger furnace would have allowed a greater metal yield but would have also demanded increased fuel quantities.

The analytical results of the archaeological huayrachinas have shown that they functioned under relatively higher temperatures compared to the ethnographic ores. This created an environment suitable to smelt the rich silver ores and force the majority of silver into the lead metal areas to form a lead/silver alloy. The archaeological slag appears to have less lead metal and lead sulphide trapped than the modern slag, indicating a significantly higher yield and overall lead recovery from the ore. The resulting bullion would have required further refining (see the next section for a discussion on refining in antiquity).

The use of rich silver ores for smelting differs from the current day study of huayrachina use, where for the documented smelts, Cuiza is separating lead production from silver refining. He only smelts galena in his furnaces to produce lead metal. The choice of the ore added to the

smelt was made by the PAPP team. Thus, the use of galena rather than a rich-silver ore may differ from the normal/standard practice. CHM was added during the procedure. Analysis of the ore has shown that up to 1 wt% of silver was recorded, but overall the ore was lead sulphide with small quantities of zinc and iron sulphide. The modern huayrachina produced a slag that is not particularly glassy and has large inclusions of partially reacted galena. The slag layer found on Cuiza's furnaces was very thin, less than 1 mm indicating low operating temperatures. The abundance of lead metal and lead sulphide in the slag is indicative of unsatisfactory smelting conditions.

Analysis of an older furnace fragment found on Cuiza's smelting site has shown that during past smelting episodes, he used argentiferous galena. Personal communication with Dr Van Buren (2008) indicated that Cuiza relied on local miners to bring him ore to smelt. He would not have normally bought ore used in the smelt. Thus, the choice of galena by the PAPP team does not represent the usual ore that Cuiza would smelt. It is assumed that miners would pocket rich-silver-rich ore and bring it to Cuiza to extract the silver. Cuiza would then share half of the resulting silver.

A comparison between SEM-EDS bulk area analyses has shown that archaeological *huayrachina* slag has much higher quantities of lead oxide, indicating that conditions within the archaeological furnaces were highly oxidising (Table 9.2). Some of the slag analysed from current day *huayrachinas* has been constituted of individual pieces, whereas the majority of archaeological samples came from slag adhering to the furnace wall. No samples of slag adhering to the furnace wall were available from the ethnographic collection for two reasons; a) the slag layer was very thin and this meant that sampling was difficult and b) only two fragments of furnace lining were available for sampling. Cuiza's modern *huayrachinas* have a vertical shaft and no ledges. Historical *huayrachinas* may well have been 86 cm tall, whereas the modern day *huayrachina* is only 76 cm (Peele 1893 and Table 9.3). A larger furnace would have allowed a greater metal yield but would have also demanded increased fuel quantities.

Average bulk composition	Na2O	MgO	Al2O3	SiO2	P2O5	SO3	K2O	CaO	TiO2	MnO	FeO	ZnO	As2O5	Sb2O3	SnO2	PbO
Cuiza's slag sample9a (2001)	~	1.9	8.0	37.8	0.7	0.4	4.1	19.7	~	0.3	11.8	9.7	~	~	~	5.6
Hu24 77C	~	3.5	5.9	32.8	1.2	0.9	2.4	23.5	0.2	~	10.3	11.6	~	~	~	7.7
Cuiza's slag sample 1 (2002)	~	2.1	8.4	39.1	0.2	2.2	5.3	14.3	~	0.9	10.0	6.5	~	~	~	11.0
Cuiza's slag sample 3 (2002)	~	1.9	8.9	45.2	0.4	0.4	4.7	10.2	0.1	0.4	8.5	7.1	~	~	~	12.2
Hu24 76A	~	2.2	8.0	33.5	~	~	3.7	14.1	~	~	14.4	4.9	~	~	~	19.2
WS 342F	1.0	3.3	17.1	26.6	0.4	~	4.9	8.4	~	~	3.7	6.9	~	~	~	27.6
HuA1 31	0.4	0.8	7.0	34.1	~	~	2.7	5.8	1.1	~	7.3	11.1	~	~	~	29.7
CP 344A	~	1.9	5.4	32.3	2.0	~	3.3	12.4	0.9	~	10.8	9.3	~	~	~	21.7
CP 344B	~	2.5	1.6	29.6	2.3	~	2.9	12.9	1.1	~	10.0	11.4	~	~	~	26.1
Hu24 77A	~	1.6	4.2	24.3	~	~	0.8	11.1	0.4	~	8.0	18.5	~	~	~	31.2
HuA1 27A	~	1.6	5.3	22.2	~	~	3.1	11.4	~	0.4	13.4	11.1	~	~	~	31.5
WS 342C	~	1.3	7.5	26.9	~	3.1	3.6	6.7	~	~	4.8	12.7	~	~	~	33.4
HuA1 26C	~	0.7	6.2	23.5	~	1.1	2.8	8.3	~	~	4.9	15.5	2.8	~	~	34.2
HuA1 26B	~	1.0	4.8	23.6	~	~	1.6	8.2	0.3	~	4.9	13.4	~	~	~	42.2
WS 342B	0.5	0.4	7.9	29.8	~	2.9	4.1	3.8	~	~	2.4	4.4	~	~	~	43.7
WS 342G	~	1.3	5.1	21.2	~	~	2.1	9.2	~	~	3.1	6.2	~	~	~	51.9
Hu24 77B	~	1.7	3.3	19.1	~	~	0.7	11.7	0.7	~	5.2	5.4	~	~	~	52.3
HuA1 29	0.8	~	8.2	30.5	~	~	2.4	1.0	~	~	1.6	~	1.0	1.8	~	52.7
ES 343C	~	1.2	4.8	19.4	~	~	1.9	7.8	~	~	3.1	4.0	~	~	~	57.7
WS 342A	0.2	~	0.8	8.8	~	12.4	0.2	1.8	~	~	7.5	2.6	~	~	~	65.7
ES 343D	~	0.6	5.2	10.8	~	~	~	1.4	~	~	1.0	13.9	~	~	~	66.4

Table 9.2. SEM-EDS bulk area scans of archaeological huayrachina slag and Cuiza's slag. Samples from archaeological sites have been highlighted a different colour. Cuiza's slag is pink.

The data has been sorted by increasing lead content, and normalised to 100 wt%.
Carlo Cuiza's = pink CP = salmon pink Hu24=Site 24 (blue) HuA1= Huayrachina Alta (purple) ES = Uruquilla East Saddle (yellow)
WS=Uruquilla West Saddle (not highlighted). ~ = below SEM-EDS detection limit.

The only older slag (from non documented episodes) available for sampling was the slag adhered to furnace wall and collected as waste from Cuiza's property. The lower lead content in the ethnographic/recent slag is a noted difference between the recent and archaeological slag. The overall low quantity of slag seen in the ethnographic records reflect the lower temperatures and oxidising conditions of Carlos Cuiza's *huayrachinas*.

The *chaîne opératoire* of silver production within Porco-Potosí

The *chaîne opératoire* is an appropriate method to understand the processual schema used to produce silver. The *chaîne opératoire* (previously discussed in Chapter 7) of Cuiza's silver production has highlighted that the current day process required him to invest considerable time and possibly some money into the process. It takes approximately two weeks for Cuiza to produce silver. This is an estimated time frame based on the recorded smelting, refining, and preparation times documented by PAPP over three consecutive years. However, many of these variables were difficult to calculate precisely; for example, the preparation for the silver production may have been spread over a longer period rather than being a solid block of time. Unfortunately this data was not recorded.

From the *chaîne opératoire* it is clear that a significant quantity of time needed to be invested into the collection and acquisition of ore, CHM and fuels. Overall, an extended period of time is required to prepare and produce metal, although it is difficult to establish how many of the tasks involved in the production would have required Cuiza to expel extra energy and time, i.e. was the collection of dung done as part of Cuiza's usual subsistence or exclusively for the purpose of silver production?

The review of ethnographic silver production can provide a model which could have similarities to the archaeological production, where information on the production process is limited. In this research only the archaeological smelting has been reviewed using reverse engineering. In this model, rather than show the starting processes in the operational sequence, I present the archaeological material that has formed the basis for analytical study. The use of a reversed process showing the final archaeological products has been applied here to illustrate the reconstruction process. Entitled 'a web of archaeometallurgical research' (Figure 9.2 – also see inserts at the back of this thesis) this model is presented to aid in understanding the methodology used in this thesis and to confirm the known processes in the *chaîne opératoire* of archaeological silver production (Figure 9.3 – also see inserts at the back of this thesis).

The archaeological remains found at *huayrachina* sites include large stones used in the construction of the base, furnace fragments with slag adhering, the occasional piece of rejected ore, and ceramics coated in lead silicate or lead oxide. Analytical work done on samples from the archaeological furnace wall fragments and their adhering slag has shown evidence of the

selection and processing of ore, the reactions within the furnace, the metal produced, and the formation of the *huayrachina* furnace.

The adhering slag samples contain charcoal fragments, demonstrating the use of charcoal rather than dung as a fuel source. The slag produced is heavily leaded and contains silver alloyed with lead metal and as pure metallic prills. This shows that a silver/lead bullion would have been produced from the *huayrachinas*, which would have required further refining.

Also included in the archaeological *huayrachina chaîne opératoire* is the presence of possible tools on the archaeological sites (Figure 9.3 - see inserts at the back of this thesis). During the archaeological survey, a number of ceramic sherds coated in lead silicate material were observed. The analysis of these (Kulhanek 2007) has shown that they have very similar chemical nature to that of the *huayrachina* lead silicate. Little is known about the use of these sherds during the archaeological process. It is surmised that they may have been used as tools, perhaps to close eye holes when necessary, or even as dishes to collect the metal. However, further work is necessary to establish the nature or these ceramics and their role within the use of *huayrachinas*.

A review of the archaeological sites has shown that they are located in windy high locations, and close to mining areas. Thus, the need to have wind to power *huayrachina* has influenced the location of the smelting sites (Figure 9.2 and Figure 9.3 - see inserts at the back of this thesis).

The analytical work has shown that ore was beneficiated (UR WS 342A; and identified as residual and partially reacted galena; Appendix V). Peele (1983) states that argentiferous galena or in fact a rich silver ore may have been selected for smelting. Thus, in the schema all of these ore types have been listed as being used in the *huayrachina*. It is not known how in antiquity the minerals would have been acquired. They could have been acquired via trade, exchange, direct mining and/or acquisition of ore via smelting. It is apparent that the ore would have been beneficiated i.e. sorted and crushed prior to smelting. In Cuiza's *huayrachina* smelt, CHM is used in the furnace. Here, no direct archaeological evidence has been found for the addition of CHM in the past. However, the nature of the material and the smelting process make it unlikely that CHM remains would have survived sufficiently in the *huayrachina* to make analysis viable. It has been placed on the chaîne because it was available during the colonial period and may have been used in the process (Figure 9.3). Analysis of the ceramic wall showed that the clay was un-tempered. Areas closer to eye or mouth openings appear prominently within the archaeological record. It seems that the slag adhering to these areas has strengthened the area, making it more resistant to erosion.

Key ingredients of the smelt	Ethnographic data from Carlos Cuiza. Data taken between 2001-present	19th C. Peele - adapted from Van Buren and Mills (2005, 10)	Colonial sources of silver production	Archaeological survey and analytical work (Colonial to 19th century)
Fuel types	Primarily charcoal: mixture of two types (one made by Cuiza and the other bought in Potosí)	Good quality charcoal	Charcoal	Charcoal found in analytical work otherwise unknown
Fuel preparation	One week to prepare charcoal	Unknown	Unknown	Unknown
Quantity of fuel used	Fuel:ore 1:2	Fuel: ore 1:1 – alternating layers	Unknown	Unknown
***Huayrachina* manufacture**	Local ravine clay- untempered	Unknown	Unknown	From analytical review untempered local clay
Height of *huayrachina*	76 cm	76-86 cm	1 vara =84 cm	Unknown
Diameter of eye holes	2 or 3 cm	5 x 6.4 cm		Between 4 and 5 cm
Ledges underneath eye holes	Not done	Yes small ledges present	Barba describes ledges used to hold charcoal	Found during site survey HuA1 block B
Ore selection	Bought by PAPP team and not selected by Cuiza - Galena with some sphalerite and pyritic inclusions	Argentiferous galena mixed with high grade silver ores; ruby silver, gray copper, and silver sulphide.	High grade silver ore mixed with lead sulphide (Capoche 1959?)	Argentiferous galena which always contains sphalerite and iron compounds
Ore preparation	Crushing using hammers and a basalt mortar. Size?	Beneficiated to pea sized pieces	Ground beneficiated (Capoche)	Angular fragments found in UR WS which indicate crushing. Other sites unknown
Ore roasting	Not done	Not done	Not done	Sulphidic components found in the slag assumed not done
CHM selected?	Added to smelt and taken from old cupellations	Litharge added when no galena found	Flux such as litharge added (Capoche)	Unknown
Time of smelt	Between 5 to 8 hours	12 hours	Unknown – over night	Unknown
Conditions inside the *huayrachina*	Co-smelting but only very weakly oxidising	Unknown	Unknown	Co-smelting with areas of strong oxidation
Metal produced	Lead	Lead/silver alloy	Lead/silver alloy	Lead/silver alloy
Slag produced	Lead silicate with large quantities of partially reacted lead sulphide	Unknown	Unknown	Lead silicate (often extremely glassy) with mineral inclusions. Some residual sulphidic components observed.
Refining?	Yes via cupellation	Yes, place unknown	Yes, in tocochimbos (Barba)	Yes, some sites identified

Table 9.3. A comparison between the ethnographic, archaeological, and historical *huayrachinas*.

The use of a reverse engineering schema on the archaeological *huayrachina* production process has provided information on the technical function of these furnaces; the ore selected, the conditions within the furnaces, and the metals that may have been produced (Figure 9.2 - see inserts at the back of this thesis). It has allowed a possible *chaîne opératoire* to be produced (Figure 9.3 – also see inserts at the back of this thesis). However, there is more work to be done on the role of these furnaces within colonial Porco. What sort of scale were these furnaces operated on? The historical literature states that over 6000 furnaces lined the hills of the Cerro Rico, Potosí (Capoche 1585). In colonial Porco, the workers of *huayrachinas (huayradores)* were *yanakuna* employed by Spanish mine owners to oversee metallurgical production and the employment of labour. Was mining and smelting done by different (groups of) people, and if so, how was their interaction and co-operation organised?

Labour patterns in Porco

The labour patterns in Porco during the early colonial period would have been driven by the Spanish mine owners (Bakewell 1984). The Spanish would have ownership of mines but also the mineral extracted from those mines. As a consequence, the land owners would have control over the *yanakuna* and mit'a labourers who worked for them. The *yanakuna* would take a share of the silver metal produced but the metal belonged to the land owner, and in fact a fifth belonged to the Spanish crown (Presta in press). It is not known how much of the royal tax was collected. The use of *yanakuna* would have allowed for concentrated specialist labour to be employed. Very little is known regarding the origins of these *yanakuna*, and equally their technical expertise. Colonial sources state that mit'a labourers came from Lupaca and Carangas (West of Lake Poopó). In the 1567 census, interviewees stated that under Inca rule, they had been required to work in Porco to extract silver (Van Buren and Presta in press, 12).

Two tables have been constructed to show agency and time invested within metal production in Porco (Table 9.4 and Table 9.5). These tables are meant to highlight the uncertainty regarding historical production and to consider the differences between both archaeological methods and Cuiza's operation.

It remains unclear how the workforces behind metal production would have been organised in the early colonial period, although, in Cuiza's production process he was a largely autonomous agent. He controlled all aspects of the smelting but had no involvement in the mining and if someone brought him ore to smelt, he may not even have chosen which ore to smelt. Despite the obvious gaps in our knowledge of colonial labour organisation, historical sources have shown that *huayrachinas* were used on a much larger scale. Many agents would have been involved in the production process compared to Cuiza's clandestine smelting.

Figure 9.2. A web of archaeometallurgical research
(page 221)

PLEASE SEE INSERTS AT THE BACK OF THIS THESIS FOR AN A3 VERSION OF THIS DIAGRAM

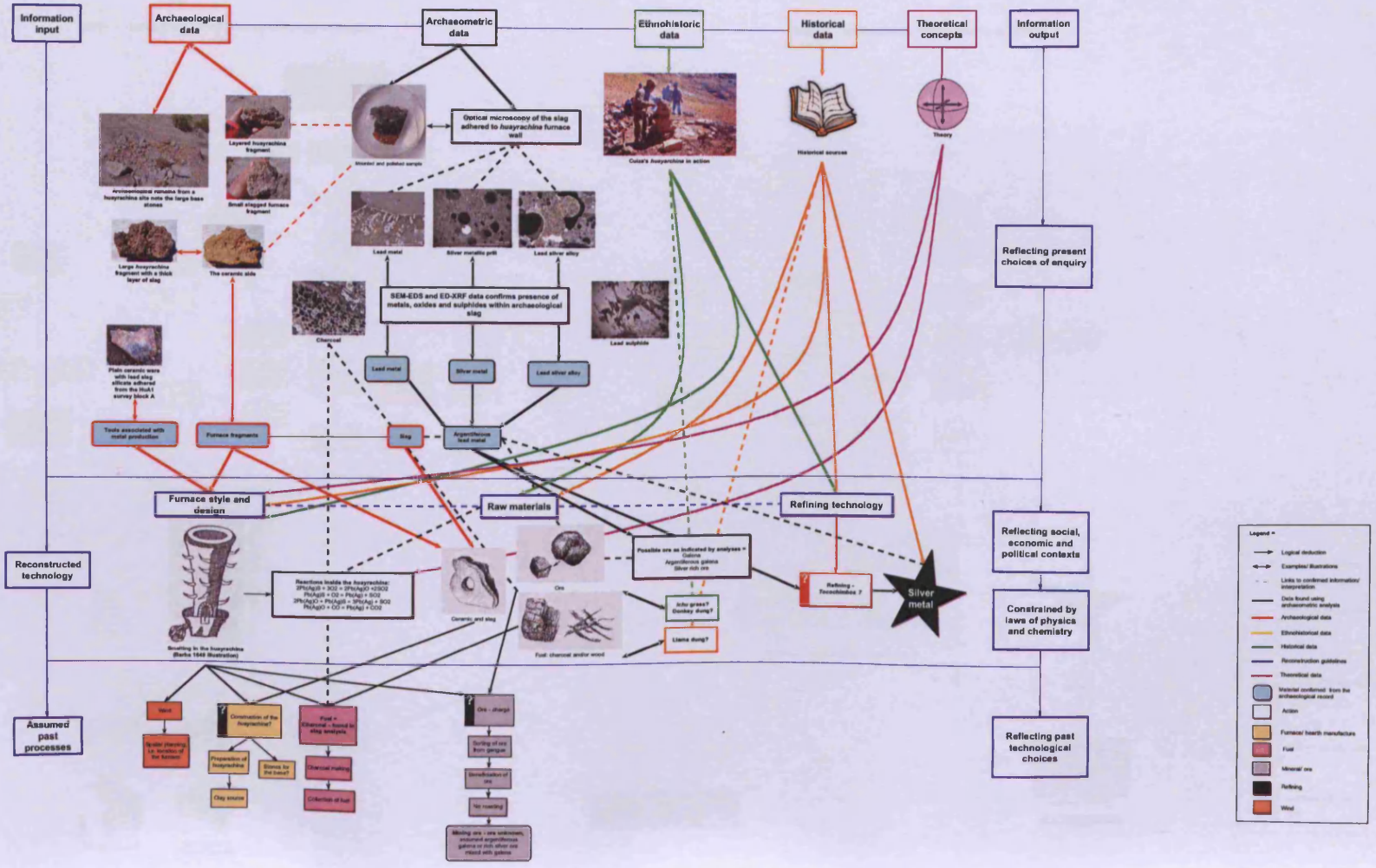

Figure 9.3. A *chaine operatoire* of archaeological *huayrachina* use - production of silver rich lead metal (smelting) and pure silver (refining)

(page 222)

PLEASE SEE INSERTS AT THE BACK OF THIS THESIS FOR AN A3 VERSION OF THIS DIAGRAM

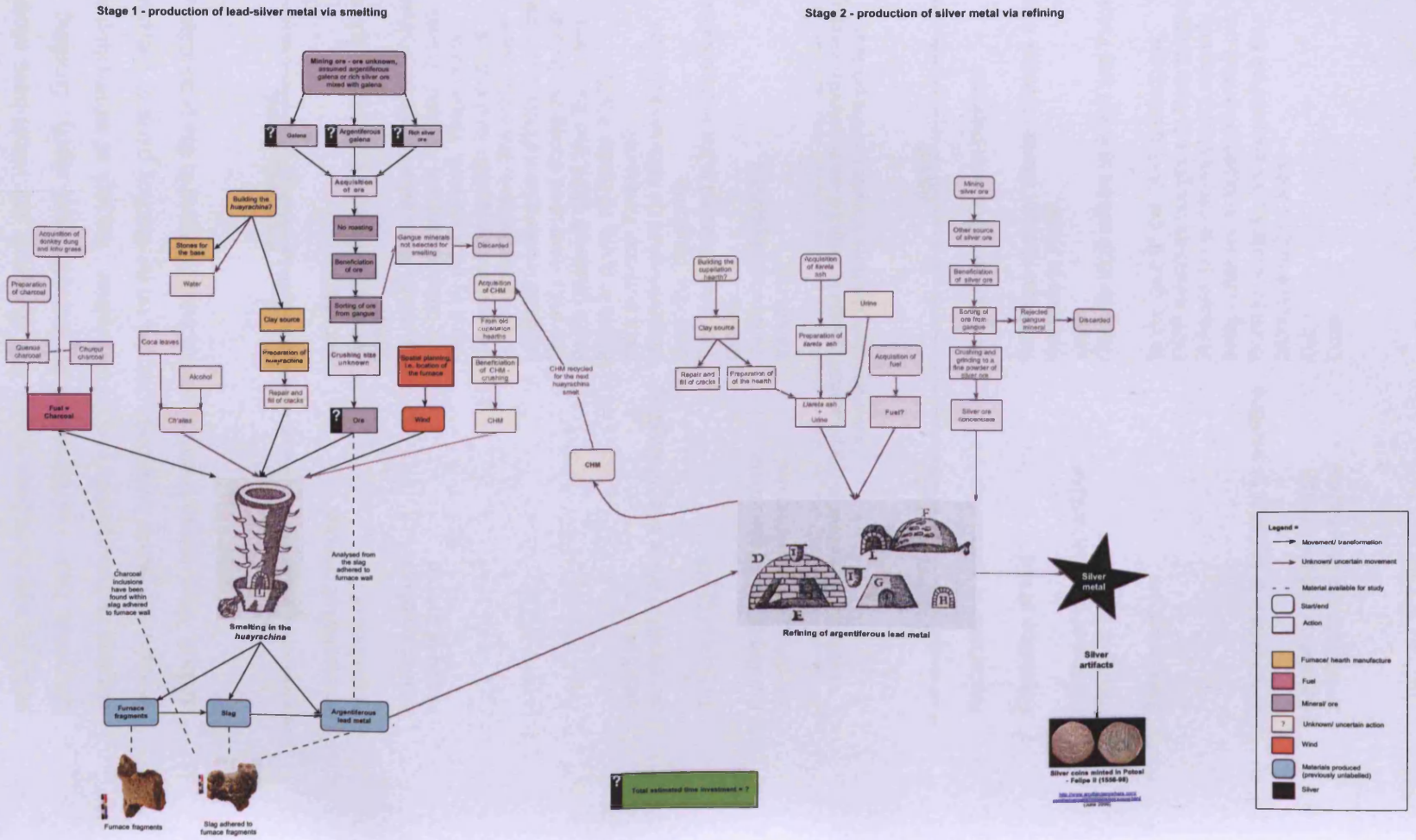

The changes in technical function can be observed using the *chaîne opératoire* and through a consideration of metal production stimuli. The combined data has indicated that furnaces in antiquity may have been larger. This change in size would have allowed a greater metal yield, but would have also demanded an increased fuel supply. Smelting practice may have been dictated by huayradores/*yanakuna*, however, the lack of information regarding the structure of workers and labour in antiquity makes understanding parts of the *chaîne opératoire* extremely difficult. Thus, labour practice has not been included in the production schema (Figure 9.2).

Process/activity	Proposed agent	Time invested
Preparation of charcoal	Uncertain	Uncertain
Acquisition of fuel	Assumed to be from Yura (pc Van Buren 2008)	Uncertain
Acquisition of ore	*Yanakuna* responsible for ore acquisition	Uncertain
Mining of the ore	The ore was mined in Apu and Huayna Porco by mit'a workers. These miners were owned by Spanish land owners (such as the Pizarro). The mit'a were imported workers from different regions. The mit'a were used during the Inca in Porco (Bakewell 1984, Van Buren and Presta in press, pc Presta 2008)	Mit'a workers employed for a year or more. Quantities of ore unknown, thus time invested unknown.
Selection of ore	Mit'a workers? *Yanakuna*?	Uncertain
Beneficiation of ore prior to smelting	Uncertain-could be Mit'a workers who assist the *Yanakuna*	Uncertain
The use of CHM?	This is unconfirmed in the archaeological record	Uncertain
Building of the *huayarachina*	*Yanakuna*?? Uncertain	Uncertain
Smelting in the *huayrachina*	*Yanakuna*	Uncertain

Table 9.4. A review of the proposed agents involved in early colonial *huayrachina* production with a consideration the time invested in the process.

Process/activity	Agent	Time invested
Preparation of charcoal	Cuiza prepared *Quenua* charcoal	1 week for one batch of charcoal
Acquisition of fuel	PAPP team bought churqui charcoal from the Gato in Potosi.	1 day
Building of the *huayrachina*	Cuiza	Uncertain
Mining of the ore	Done by local miners in Porco and Potosi.	No time investment for Cuiza
Selection of ore	In the case of the PAPP productions, PAPP members bought ore from miners in Potosi. Local miners would normally bring Cuiza pre-selected silver-rich ore.	Uncertain (No time investment for Cuiza)
Beneficiation of ore prior to smelting	Done for Cuiza by his *compadres*: Don Dionisio and Don Juan.	Half a day
Acquisition and use of CHM	Cuiza	Uncertain
Smelting in the *huayrachina*	Cuiza	5 - 8 hours (variable according to wind conditions

Table 9.5. A review of Cuiza's *huayrachina* smelt and the time invested.

Change and innovation

The differences in the production process allows changes within the technology to be identified. It is appropriate to consider both the choices selected and those rejected during the process. Innovation and change do not normally take place statically. The exact points at which innovations become more permanent changes are difficult to establish. "Every such dynamic system is always fluctuating: it is repeating anterior behaviour ('behaving traditionally') and introducing new behaviour ('innovating'). The difference in the two is not in what is happening (or what happened after), but in what has happened before" (Torrence and Leeuw 1989, 8). A production process is viewed as a constantly evolving method, where innovation is always occurring, though whether new changes are accepted is related to the effectiveness of the process and traditions associated with it. "Change is not always due to external sources, and innovation is not always inevitable in the face of change" (Loney 2000, 648).

Technological choices can be considered from a technical perspective regarding raw materials, tools, energy sources, and techniques used to produce the product, as well as the sequences linking all the acts together (Sillar and Tite 2000). Therefore, a production process results in a unique product that has been produced within a certain technical knowledge and bodily practice framed within defined social conditions. Epstein considers copper production in the northern coats of Peru, stating that 'technology is knowledge'. He refers to the analogy that human creativity is restricted by the physical limitations of the universal processes that govern Earth, as well as their culturally specific socio-economic conditions. "If a technology is used to manipulate the environment, the techniques it informs must achieve certain culturally set thresholds of effectiveness" (Epstein 1993, 21). Thus, people will accept technology that functions, even if it provides a very low output. A technological process that is ineffective in relation to people's need would become extinct (Epstein 1993). Using this framework, the *huayrachina* fulfilled the needs of its users. This is certainly the case in the ethnographically documented furnaces. Cuiza had adapted his technology to suit the limitations of his surroundings and his economical and cultural influences. The economic factors limiting the quantity of good quality fuel and ore have influenced the metallurgical practice. However, while the technology employed may seem inefficient for lead yield, the overall process produced well refined silver which could have then been sold to generate monetary income for Cuiza, which was the main aim of the process. Clearly, the modern use of the *huayrachina* fulfilled Cuiza's need to bring an extra income to his household. It is more difficult to identify specific motivations of ancient smelters, but one may assume that the variety of metallurgy used in the Porco-Potosí region reflects the differing and changing needs of a complex society.

Task Constraints

- Level of acceptance of *huayrachina* technology within the society – who uses it? To what scale?
- Efficiency of the metal production process and thus, indirectly, the efficiency of the furnace
- Quantity of metal needed to be produced
- Quantity of raw resources available: fuel and ore. Possibly clay?
- Time available for smelt and associated preparation and acquisition of ore
- Consequences of the *huayrachinas* not performing (risks)

Locational Constraints

- Altitude and its affects on metallurgical process
- Location with suitable wind conditions
- Access to ore/clay/fuel
- Relationship to alternative subsistence activities

Material Constraints

- Availability of materials and associated costs
- Ease of working with the *huayrachina*

Technical Constraints

- Available technology i.e. other types of metal production techniques
- Production costs
- Repair of furnace and tools associated with production
- Skill required for smelting in a *huayrachina*

Socioeconomic Constraints

- Transport capacity
- Available labour
- Storage capabilities
- Social networks – access to materials, sale and trade of product
- Economic system e.g. degree of reciprocity, cash economy, value of silver ore

Ideological Constraints

- Meaning and value of silver
- Knowledge transfer e.g. learning networks

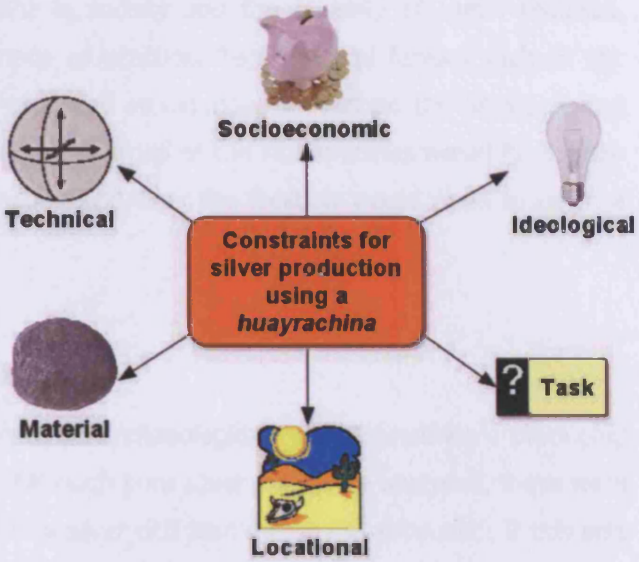

Table 9.6. A schematic representation of the constraints on silver production using *huayrachinas* in the Porco-Potosí region, adapted and influenced by Hayden 1998, 5.

The changes observed in *huayrachina* usage indicate that over time, the size of the furnace has been reduced, different ore has been selected for smelting, and thus the function of the *huayrachina* has changed and conditions within the furnace altered.

Importantly, technological changes do not always create an improved or more efficient function. The influence of change has greater social and cultural values that are embedded in local beliefs and external forces can often be secondary to these more defined cultural roots (Loney 2000, 646). There is a direct link between the practical outcomes of a technology and the survival of that technology (Horsfall 1987). The continued persistence of the *huayrachina* within the Porco region provides evidence for the continuity of this technology within indigenous communities all be it at a much reduced level to earlier periods. To observe changes in the technology, we can consider possible constraints that may have limited and/or defined the use of *huayrachinas* in Porco (Table 9.6). These limitations show that the initial task constraints, such as the acceptance of the *huayrachina* in society and the quantity of metal required, affected the technological function and mode of practice. Technological factors such as the quantity of ore, fuel needed, and metal produced would have influenced the selection and choice of this production method. The choice of location of the *huayrachinas* would have been limited because they required wind to function and thus the location would need to be in a suitably windy place.

Where were lead/silver alloys refined?

The analytical work has shown that the sampled archaeological *huayrachinas* were producing lead metal and/or a lead-silver metal alloy. Although pure silver prills were analysed, these were in low quantity and it seems more likely that a silver rich lead metal was produced. If this was the case then this alloy would require refining in an oxidising environment to obtain pure silver. Where were the archaeological refining chambers located? Who did the refining? Did the same group of artisans smelt the mineral? What type of furnace/technology was employed to refine the silver? Once the refined silver was produced where was it taken? Was it sold in Potosí or was this a centralised operation where metal workers produced metal and all trade was dealt with in Porco? If *huayrachinas* were in use during the early colonial period, how was the production of metal taxed?

The studied ethnographic silver production has shown that a closed cupellation furnace was used to refine silver ore. The use of this type of furnace is often associated with European technology, and there has been little evidence for cupellation in the Andes. Lechtman (1976) makes for an interesting comparison to the archaeological refining furnaces described in the colonial historical literature. Refining features are described as tocochimbos. Van Buren and Mills (2005) discuss the relevance of these historical sources and that of Carlos Cuiza's furnaces.

As discussed in Chapters 4-7 of this document, Cuiza produced silver using two stages and during the second stage, silver ore was refined using lead produced in the *huayrachinas*. Trace quantities of silver were found in the slag from recent *huayrachinas* (Appendix II - sample 17 furnace fragment with slag adhered) but in such minimal quantities that the silver almost

certainly came from additional CHM or occurred naturally in the galena being smelted. Regardless of this trace silver's origin within the slag, there is a noticeable difference in the separation of lead and silver production between the archaeological and Cuiza's *huayrachinas*. The current day silver refining is done in a small hut, hidden from the outside world. Is it possible that in antiquity this second refining stage was also done in secluded locations?

The two stages from Cuiza's production required different resources: *huayrachinas* required charcoal and a source of wind, whereas cupellation/refining require flame-producing fuel as well as a good flow of air (oxygen). This flow needs to be controlled in order for the oxidation of lead to occur. It would thus seem logical that the refining occurred in a location not exposed to strong wind. However, the distance between refining and smelting furnaces is difficult to establish. In the current day documentation, refining furnaces were located close to Cuiza's estancia and his choice of fuel (llama dung). The hut was in a small ravine. It was constructed of mud sourced locally and had a thatched roof made using ichu grass, which grows in the surrounding area.

This secretive nature of the refining could have implications for the identification of archaeological refining sites. Where were they located? Some possible clues to older refining sites have come from the ethnographic documentation. Cuiza collected CHM from two different refining sites: Januschupunta (located in a small quebrada), and Chaco Allana Kullko (an area with three furnaces, possibility more). These are thought to have been used within the last 100 years, but no other information is known about the sites. PAPP have also found another refining site at Hornos. The Hornos site is a series of cupellation hearths; one cupellation hearth was excavated in this series of three. The site is located away from the modern village of Porco, accessible via a dirt track road. The furnace sites are totally obscured from the road, hidden within a distinctive rock formation (Figure 9.4 a and b). On inspection, further refining sites were observed in sheltered locations in between the rocks. These were identified due to the presence of thick lead oxide layers which had fused with the rock surface (Figure 9.4 c.). The site is roughly dated to the 20th century, as an iron truck spring was found there.

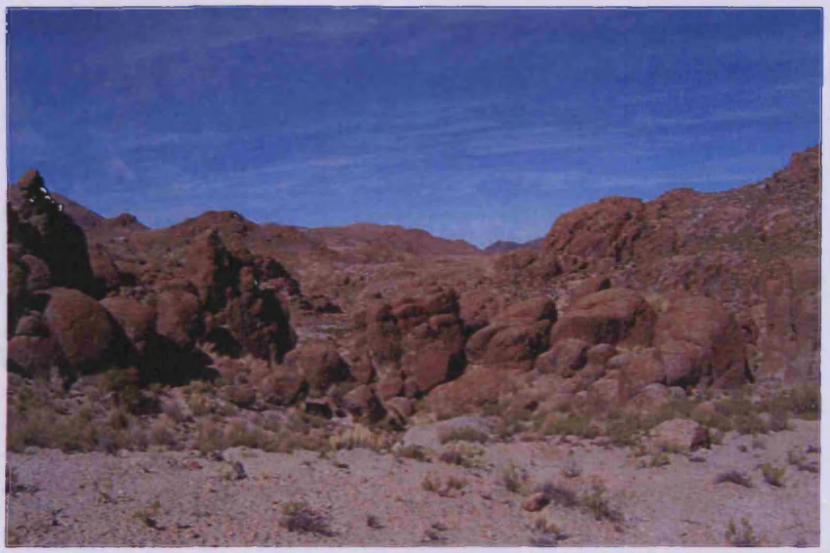

a.

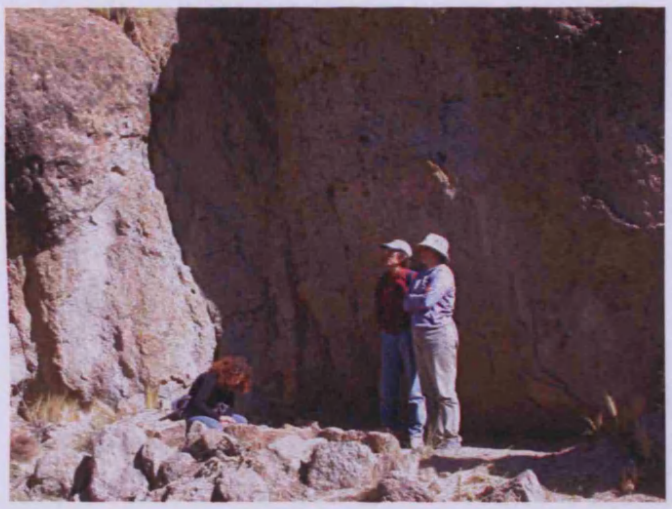

b.

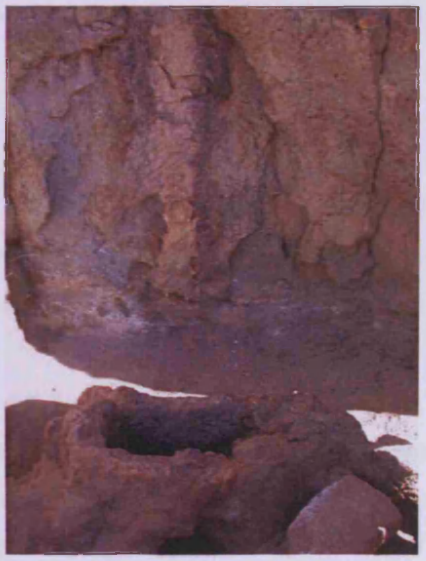

c.

d.

Figure 9.4. The Hornos refining site.
The Hornos refining site is located in a rock outcrop (a). Cupellation furnaces are hidden within the rock formation (b). The furnaces are badly preserved, but the location of the chimney flume is visible due to a heavy lead oxide/silicate coating (c.) Samples excavated from one of the furnaces consist of possible furnace walls (d).

Samples taken from the excavation of one of the Hornos cupellation furnaces include slagged ceramic, lead metal, possible furnace fragments and CHM. No analytical work has been undertaken on these samples. At the Hornos site, it does not seem easy to understand how and where fuel would have come from. The location is relatively remote and located in an arid zone.

However, the position and identification of these different refining sites indicates that smelting and refining have occurred at different locations. Within earlier periods, the identification of refining sites has proven more difficult and so far none have been discovered during survey work.

9.4. Overall conclusions for archaeological *huayrachina* production

In conclusion, the basic function of the *huayrachina* has not changed for 500 years although the social and economic settings within which these furnaces have been used has changed dramatically. The use of the *huayrachina* may reflect an underlying cultural practice that has its roots in Andean technology. The continued use of the *huayrachina* until the present day reflects its importance in the metallurgical history of the region.

Archaeological *huayrachinas* are located on high windy ridges all over the Porco region. Due to lack of stratigraphic and other architectural structural information, dating an archaeological *huayrachina* site is difficult. However, in two of the five sites studied here, dates have been established using ceramic finds and by the presence of other archaeological sites in close proximity.

The *huayrachina* in the Porco region was a smelting furnace used to produce lead and/or silver-rich lead bullion. The resulting lead/silver alloy would have then required refining in a different furnace (the technical function of this furnace is unconfirmed but assumed to be based on cupellation). The analytical work done on the archaeological *huayrachina* slag has shown that local silver-rich ore was selected for smelting. No roasting of this ore would have occurred. The archaeological slag shows evidence for high temperature operations, whereas the current day slag still contains large quantities of partially reacted sulphides indicating lower operating temperatures.

Higher temperature operating conditions would require more fuel; the availability of this would primarily indicate the high priority to produce silver, particularly in the early to middle colonial periods. Fuel was in short supply and would probably have been imported to Porco and Potosí. As silver production by *huayrachina* moved from a general method of production to a rare and possibly clandestine one, the changing needs of the agents making silver may have altered the functionality of the furnace.

The change in the role of the *huayrachina* within society was brought on by the arrival of the Spanish in the region. Their arrival had a delayed effect on metallurgical technology. For the first thirty years of colonisation, indigenous communities still controlled silver production using

the *huayrachina*. It was only after 1570, when the Spanish introduced large scale silver production using mercury amalgamation, that control and influence of specific metal production was altered (Bakewell 1997). This change in control seems to have stimulated a top-down change within metallurgical practice (Costin et al. 1989). However, despite the large stimuli (from the Spanish authorities) to reduce the use of *huayrachina,* the practice continued during periods when high quality ore was available.

The archaeological survey and a review of the historical literature indicate that in the past furnaces may have been constructed with larger eye holes and ledges, and possibly slightly larger and more flared shafts (the latter is harder to substantiate). The changes in design, i.e. the reduction in eye hole size, may have been caused by innovation or influenced by constraints within the economic, political and social environments. For example, if we consider Cuiza's furnace, he introduced iron belts to the structure of his *huayrachina*. He told PAPP that he did this to increase the lifespan of his furnaces. This new feature may have lead to thicker walls and smaller holes. This was an innovation that he created to enable him to do less maintenance work on the furnace throughout the year.

Many of the archaeological *huayrachina* fragments analysed in the survey showed erosion to the outer unbaked ceramic wall. However, the presence of ledges in a small number of samples is a good indication against significant erosion. As a result the degree of variability in furnace size, noted in this chapter, between historical sources and Cuiza's furnace is difficult to establish.

Some evidence for relining was seen in the archaeological survey although nothing concrete could be established about whether this was standard practice. Certainly no relining was recorded within current day smelting.

The co-existence of *huayrachina* use, mercury amalgamation and European style smelting furnaces in the Porco-Potosí region showed that specific socio-economic situations enabled the continued use of the *huayrachina*. The PAPP archaeological excavations have provided evidence for the use of European style furnaces in the region during the early and middle colonial periods, in addition to the archaeological *huayrachina* remains discussed here (the use of European style furnaces is discussed in the next chapter). The continuation and persistence of the *huayrachina* despite the existence of other suitable methods of silver production is important to note. In the early to middle colonial period the technology continued because the Spanish did not have to invest any capital since it was a low risk activity. As the use of the *huayrachina* began to reduce in scale (middle to late colonial), it continued at a household level. The activity became rather illicit and was done in parallel to other European methods until recently when only one known individual was smelting. His activity seemed clandestine and technically inefficient. However, it continued to be used as it was relatively low cost to Cuiza.

The organisation of smelting during early to late colonial times is difficult to discuss due to a lack of information. After the introduction of amalgamation, it is unclear exactly who continued to smelt using *huayrachinas*. Were they family groups? The *yanakuna*? Individuals who were mining, smelting and then refining? Was the activity seasonal? Was it done by specialists or part-time smelters (like Cuiza)? These issues are mentioned in this thesis, but further analysis would go beyond the scope of this research.

The results from this chapter have contributed to a better overall understanding of *huayrachina* use and technological function within the Porco region. A *chaîne opératoire* of archaeological *huayrachina* use has been prepared using a web of archaeometallurgical research (please see the inserts at the back of this thesis). It is hoped that this will act as a case study for other archaeologists, anthropologists and historians working on technological change.

In the next chapter, the use of European style furnaces during the early to middle colonial periods will be discussed, and Chapter 12 will compare and contrast the use of different technologies to produce silver in the Porco region.

10. HISTORICAL AND ARCHAEOLOGICAL INFORMATION ON THE EUROPEAN FURNACES

Prior to the 1570's, the use of indigenous methods to smelt rich silver ores dominated in the Porco-Potosí region (the *huayrachina* furnaces further discussed in Chapters 4, 5, 6 and 7). After 1570, the extraction of silver through amalgamation with mercury was introduced, which became the most common of all the silver production processes (Bakewell 1997). However, archaeological remains in Porco have shown that other types of silver producing furnaces remained in use during the colonial era. The archaeological remains documented by PAPP show similarities with furnaces used in 16th century Europe. Two stylistically different metallurgical furnaces have been identified: the Dragon furnace (with a domed roof and a flared-side chimney) and the reverberatory or domed furnace (with a domed roof but no flared-side chimney). In this chapter, the historical and archaeological evidence for these two types of furnaces is described. Chapter 11 presents the results from analytical work done on archaeological samples and discusses the significance of the results. What did these furnaces produce? How did they work, and how did they relate to the other forms of metallurgical activity in the Porco region?

10.1. Historical information on European furnaces

In 15th and 16th century Europe the use of domed furnaces, also known as reverberatory furnaces, was partly associated with the processing of rich ore minerals. More commonly, however, these furnaces have been used to refine (via cupellation) silver-rich lead metal to produce pure silver. Various European manuscripts detail the use of domed or reverberatory furnaces. In particular, the works of Georgius Agricola (published in 1556) and Vannoccio Biringuccio (published early 16th century) are used as examples of the type of furnace technology employed in Europe. In this chapter, Bolivian metallurgy is compared to the European furnace technology using the manuscript of Alvaro Alonso Barba (originally published 1640) and via archaeologically excavated sites.

European furnaces

According to Vannoccio Biringuccio a reverberatory furnace commonly has a circular base, but can also be rectangular (Smith and Gnudi 1990, 151/152). A reverberatory furnace is a round domed furnace that has an opening on one side for the flames to enter from an attached fire box. The hearth is slightly inclined and a small channel is made through which the metal can be

tapped/removed (Smith and Gnudi 1990, 151). Holes on the side of the dome act as viewing windows and openings for bellows (Figure 10.1). On the domed roof, four holes allow the flames and waste gases to be expelled. Reverberatory furnaces require wood rather than charcoal as a fuel source (Smith and Gnudi 1990, 151). Biringuccio acknowledges that reverberatory furnaces have beneficial effects for smelting ores. Lead based ores require a more gentle heat because they evaporate readily. The domed roof contains these reaction gases and allows the temperatures to be stabilised.

Figure 10.1. A reverberatory furnace used for smelting (Biringuccio (Smith and Gnundi 1990, 151)).

Biringuccio states that this type of furnace is not very efficient, although he also said that he had never seen this furnace in use (Smith and Gnudi 1990, 151). He preferred to use a blast/shaft furnace for smelting rather than a reverberatory furnace (Figure 10.2). In his manuscript, he gives a description of what others have described rather than his own observation (Smith and Gnudi 1990, 150).

Ore used for smelting in reverberatory furnaces must be prepared via the following method: the selected ore should be broken into small pieces, the size of a small bean (Smith and Gnudi 1990, 153). The ore should be washed and sorted well. A half to one third of galena minerals should also be added to the prepared ore. This mixture should then be charged to the preheated furnace. Biringuccio describes in detail smelting in blast furnaces, but only briefly mentions that in a reverberatory furnace, slag and metal should be separated via the use of separate tapholes (Smith and Gnudi 1990, 154).

Figure 10.2. Blast furnaces, the preferred method of smelting ores. (Biringuccio Smith and Gnudi 1990, 150).

In contrast, Georgius Agricola (*De Re Metallica,* 1556) associates the use of domed furnaces with cupellation and the refining of metal alloys to produce silver metal. "Lead is separated from gold or silver in a cupellation furnace, of which the structure consists of rectangular stones, of the two interior walls of which the one intersects the other transversely, of a round sole, and a dome'" (Hoover and Hoover 1950, 467).

Agricola's domed cupellation furnaces have a circular base wall composed of stone. The wall has five air holes spaced out around the circumference of the wall one foot above the ground. An extra hole is made at the top of the wall to allow the litharge (liquid lead oxide) to flow out of the hearth. The holes in the base are ventilation holes which allow moisture to escape from the hearth lining which is fragile and could easily fracture with excess gases and pressures from below (Hoover and Hoover 1950, 467). The internal walls that transect the circular outer wall are made from brick and form the shape of a cross. In between the spaces of the internal walls one wheelbarrow of slag is placed and on top of the slag layer charcoal dust is added. Mounted on top of the transecting inner walls is a stone sole touching the outer wall. The stone sole slopes at the front so that the litharge can flow out of the hearth. The dome described by Agricola used in these furnaces is constructed of different sized iron bands and a lid. The dome has various apertures used as openings for bellows and to allow access to the hearth platform (Figure 10.3).

A—An artificer tamping the crucible with a rammer. B—Large rammer. C—Broom. D—Two smaller rammers. E—Curved iron plates. F—Part of a wooden strip. G—Sieve. H—Ashes. I—Iron shovel. K—Iron plate. L—Block of wood. M—Rock. N—Basket made of woven twigs. O—Hooked bar. P—Second hooked bar. Q—Old linen rag. R—Bucket. S—Doeskin. T—Bundles of straw. V—Wood. X—Cakes of lead alloy. Y—Fork. Z—Another workman covers the outside of the furnace with lute where the dome fits on it. AA—Basket full of ashes. BB—Lid of the dome. CC—The assistant standing on the steps pours charcoal into the crucible through the hole at the top of the dome. DD—Iron implement with which the lute is beaten. EE—Lute. FF—Ladle with which the workman or master takes a sample. GG—Rabble with which the scum of impure lead is drawn off. HH—Iron wedge with which the silver mass is raised.

A—Chamber of the furnace. B—Its bed. C—Passages. D—Rammer. E—Mallet. F—Artificer making tubes from litharge according to the Roman method. G—Channel. H—Litharge. I—Lower crucible or hearth. K—Stick. L—Tubes.

a. **b.**

Figure 10.3. Preparation of iron vaulted cupellation furnaces from Agricola (Hoover and Hoover 1950, 470).
The wetted ashes are backed onto the sole stone to form a crucible in the centre and a shallow moat round the outside (a). Cupellation hearths from Freiberg, Germany (b).

The sole stone is then lined with lute (a mixture of fine clay and charcoal dust) and straw which is compressed using a wooden rammer. Balls of wetted ash are placed on top of the hearth (Hoover and Hoover 1950, 468) and smoothed into place. A crucible or shallow dish is created in the centre of the sole stone. A series of channels is created: one for the litharge to run out of the hearth and two or three others for the placement of fuel and to allow access to the crucible when the dome is placed on top. The person preparing the ashes can, and should, use his feet to smooth the hearth making the shape of the outer edge of the crucible and the crucible itself (Hoover and Hoover 1950, 471). Dry ashes are sieved over the smoothed hearth and wetted ash is packed densely around the edge of the crucible/hearth to prevent any liquid reagents escaping.

Once ready, the iron domed roof is lowered onto the prepared hearth and charcoal and burning coals are then added. Different iron tools are used during the production process. A triangular

hook is used to stir the charcoal. The hearth is heated for three hours and left to cool for two hours. After heating, the hearth is swept and washed with a cloth, rubbed with doeskin, and any cracks are filled. Agricola states that the central crucible could also be lined with powdered incense mixed with egg white, or a liquid made of egg white and bullock's blood, marrow, or powdered lime. Once lined a weighed quantity of lead alloy cakes is added to the crucible (straw prevents the alloy from touching the carefully prepared heath), and the alloy cakes are arranged in the hearth through the opening at the top of the dome. Once the furnace has been loaded the opening at the top of the dome is sealed and the edge of the iron dome is luted tight.

These cupellation furnaces require the use of large bellows, and Agricola notes that a water source is necessary to power the bellows. In order for cupellation to take place a complex series of heating episodes must be carried out, and wood and charcoal are added through the channels and openings in the dome. Long and large wood sticks are then placed into the channels. After the lead is molten for two hours the flame and fire may be decreased (Hoover and Hoover 1950, 474). Agricola states that alloys of lead and silver are difficult to separate and that the refiner may add copper and/or charcoal powder to help the cupellation. Other mixtures including Venetian glass, *sal-ammoniac*, Venetian soap and saltpetre can also be added to improve the smelt (Hoover and Hoover 1950, 474). Once the reaction starts the lead oxide will begin to be absorbed into the crucible or hearth lining. At that point the refiner can take out a ladle full of the molten mixture and assay it to check the quantity of silver in the metal. Agricola states that the reaction is finishing when "...the colour begins to show in the silver, bright spots appear, some of them being almost white, and the moment afterward it becomes absolutely white" (Hoover and Hoover 1950, 475). After cooling, this metallic cake is removed by wetting the furnace with water and chipping off any adhering litharge and hearth lining.

Agricola also considers fixed domed cupellation hearths found in Freiberg (in Saxony), Germany, which are composed of cement (the circular base), bricks (the domed roof), and lute. This furnace has a simpler construction to the iron domed furnaces. The main dome is four feet high and has two or three openings large enough for the person preparing the internal crucible to crawl through.

Polish and Hungarian cupellation furnaces are similar, but they have no ventilation holes; instead they have a hole connecting the main crucible to a separate fire box (Figure 10.4). Unfortunately no further details about their construction or operation were found in the literature. (Hoover and Hoover trans. 1950, 483).

Figure 10.4. Polish and Hungarian furnaces as illustrated and described by Agricola in *De Re Metallica* (Hoover and Hoover 1950, 482).
These furnaces have a separate firebox preventing the internal reactions being touched by the flames and fire.

Bolivian furnaces

In Bolivia, Alonso Barba describes the production of lead and silver in his seminal work *el Arte de los Metales* (Douglass and Mathewson 1923). Barba's manuscript also notes that in 17th century Bolivia various techniques for silver extraction were coexisting. This is consistent with the archaeological excavations carried out in the Porco- Potosí region:

"And, although, as has been said in previous treaties, all the ores of Gold and Silver may be amalgamated, for many of them smelting is necessary, and for the very rich it is more suitable; and it is thus that its use in this Village (Potosí), and in other mining Districts of the Kingdom, has never been interrupted" (Douglass and Mathewson 1923, 185).

Barba states that ore-smelting furnaces are made from stones, mud or adobe (Douglass and Mathewson 1923, 187). He states that the choice of mud for the adobe should not be sandy nor salty and the earth must be free from salts. The furnace bottoms (*mazacotes*) may require the use of the same clay used for the adobes or in some instances a mixture of earth and round charcoal called *carbonilla* (Douglass and Mathewson 1923, 187). Barba also describes reverberatory furnaces used to roast silver and lead ores. He states that the floor should be around 1 vara wide (1 vara = 0.8359 m, subdivided into 3 *pies*) and the rest of the dimensions

can be adjusted according to necessity. Muffle and reverberatory furnaces were constructed in the same way.

'Leave a fire-door at the most convenient point, and opposite to it a chimney to carry off the smoke' (Douglass and Mathewson 1923, 189). Flames enter via a bridge located between two doors and a fire box with grating is used for the fuel (wood) and allows the ash to be separated from the new fuel. Muffle furnaces can have circular or square sides. Iron sheeting can be used as a hearth base rather than adobe flooring to aid and save on fuel and time (Douglass and Mathewson 1923, 189).

Roasting of ores occurs in the reverberatory furnaces described above. The ore can be burned using firewood, *llareta* or llama/cow dung. Barba also notes that ores can be roasted in furnaces similar to those used for the heating stages of the amalgamation process (Douglass and Mathewson 1923, 193).
Barba writes about four different furnace types used to smelt ores:

- Reverberatory furnaces using wood as fuel.
- Pit furnaces using wood and charcoal as the fuel source.
- Muffle furnaces or *tocochimbos* using only charcoal.
- *Castellaňo* (shaft) furnaces, in which ore is reduced using charcoal.

To make the reverberatory furnace, a square wall of bricks should be constructed of two to three vara width (*circa* two metres) and one and a quarter vara high (*circa* one metre). Within the square outer wall an inner circular wall should be constructed. The circular area inside the circular wall should be filled three quarters full with 'good earth' (Douglass and Mathewson 1923, 194) after which snowballs of *carbonilla* be thrown one at a time into the hearth. The *carbonilla* should be spread over the furnace so that the form of a cup is produced. The lining can be rammed with wooden tampers or large stones to ensure all the slopes have a common point (Douglass and Mathewson 1923, 194). This lining should be at least four or five fingers thick. These furnaces have a domed roof described by Barba as a 'chapel' or 'arch' and he states that it is smaller than a bread oven's dome. The roof had a hole big enough for a person to enter to prepare the hearth (Figure 10.5).

The firebox and its gratings are linked to the dome via a bridge where flames can enter (Douglass and Mathewson 1923, 195). Barba states that in front of the firebox and to the opposite side holes should be left for smoke to escape, and he notes that these can be closed and opened using adobe when necessary. On the two other remaining sides of the furnace, triangular doors should be made to allow access for bellows and to watch the charge.

"..in one of these doors a Bellows may be fixed when it is desired to scorify or cool off the furnaces; the same equipment may be used in smaller furnaces thus arranged to refine Gold and Silver. The other door is used for watching the charge, rabbling when necessary, skimming the slag when the charge is finished, or feeding when smelting on a lead bath; lastly, it is used to tap off the Litharge in cupelling, and through this door the bottoms or sheets of Gold and Silver are removed" (Douglass and Mathewson 1923, 195).

To improve the quality of smelting in these reverberatory furnaces, a flared chimney can be added and Barba discusses this addition:

"To the Reverberatories there is added, on the end opposite the fire bridge, a tail-like extension, which, on account of its shape and the amount of ore it swallows, some call the "Dragon." It is not vertical like the aforesaid chimney, or a Castellano furnace, but inclined" (Douglass and Mathewson 1923, 201).

Lead ore is smelted in the Dragon and the hearth can be used to refine the metal if necessary.

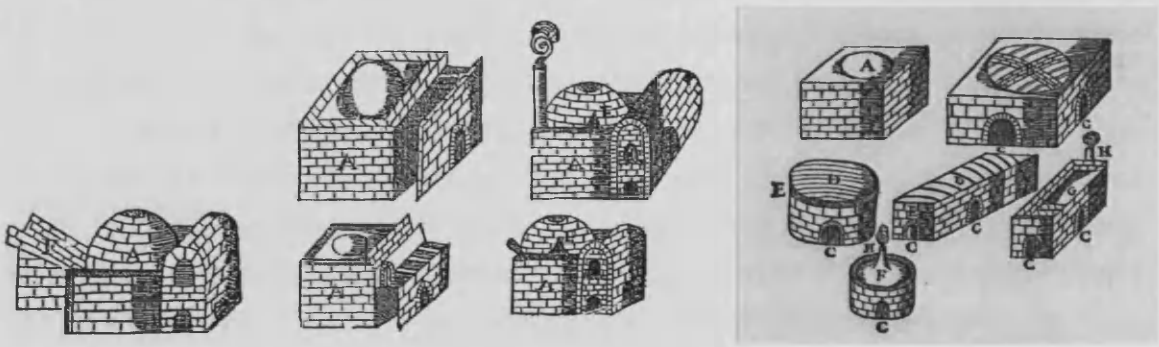

a. b. c.

Figure 10.5. Alonso Barba wrote *'el Arte de los Metales'* in 1640 , in it he describes various metallurgical practises used in colonial Bolivia.
Illustration a is a diagram of a 'Dragon' furnace used to smelt lead ore. The Dragon refers to the sloping chimney (left of the dome, Douglass and Mathewson 1923, 201). Barba also describes reverberatory furnaces (b) used for smelting rich silver ores (Douglass and Mathewson 1923, 196). The fireboxes are always represented on the right hand side of the domed hearth. The chimney (if present) is on the opposite side to the firebox. Reverberatory and muffle furnaces were also commonly used during this time period (Barba 1923, 190, c).

Historical records from 15th and 16th century Europe consider the use of domed or reverberatory furnaces as refining chambers that can be associated with the production of silver, whereas Alonso Barba's treatise on metallurgy in Southern Bolivia considers reverberatory furnaces in the context of smelting chambers used to change raw ore into metal. In the Porco-Potosí region, archaeological evidence for Alonso Barba's furnaces is widespread. Dragon, domed, and cupellation chambers have all been found.

19th Century Peruvian furnaces

Pfordte (1893) describes smelting/refining technology from the nineteenth century in the Cerro de Pasco, Central Peru. The style of production is similar to the one documented from Bolivia, and is a useful comparison to current day silver production in Porco. Quite fittingly, he comments on this technology as follows:

"Although the subject has no practical bearing on the metallurgy of the present day, it may not be entirely uninteresting to note how the art of silver-lead smelting has been, and in a few remote districts of Peru, is still practised by an old method, and under conditions widely different from our own" (Pfordte 1893).

Pfordte is quick to emphasise the lack of fuel available to the residents of Cerro de Pasco; he claims that this lack of fuel prevented large scale production necessary for the exportation of metals. This suggests that this reduced availability also affected the type of smelting technique. Pfordte describes a small reverberatory furnace with a shallow hearth for cupellation. It was an enclosed structure built out of fire-resistant rock lined with clay and sealed externally with lime and sand. The furnace consists of a fire box, concave hearth and a chimney made out of adobe, 10-18 ft high. Pfordte says that these furnaces are generally contained within an adobe thatched house, and require the following tools: a rabble, scraper, poker, and a paddle-shaped spatula for extracting litharge. The furnace needed to be air dried before use after which a fire was started. The heat slowly increases over a four-day period via the use of *taquia* (dried llama dung). "It [the furnace] is generally fed in such a manner that a small quantity is constantly being thrust rapidly through the fire-door with a thin board or sheet of tin; this operation having also the advantage of producing at the same time a slight draft'" (Pfordte 1893, 27).

Pfordte is very specific regarding the way in which the furnace was charged: 100-125 pounds of lead metal and/or litharge was first put in, which was allowed to melt and reduce. Then 400 pounds of an easily fused material such as a lead carbonate or lead oxide was added, and finally the ore (galena and grey copper (fahlore)) containing c. 50 ounces silver per ton or ruby silver (argentite) which had been crushed (3-8 inches screen) was added to the bath. The temperature of the furnace is slowly increased and any slag formed is removed; this process took up to 4 hours. Once the lead had begun to be oxidised, the process took a further 7-8 hours. If the charge was poor it may need further refining. The litharge produced was saved and used in further smelts. This detailed account is one of the most important for understanding traditional 19th century silver refining. The key features of this process are similar to the cupellation observed in Porco-Potosí; the use of a closed hearth, llama dung as fuel, and the charging of sulphidic ore directly onto the cupellation hearth. Only the scale differs by an order of magnitude.

European literature has shown that domed furnaces were used during the 16th century mostly exclusively for the refining of metal alloys. This is in contrast to the evidence from 17th century Bolivia, where Barba discussed the use of domed reverberatory and muffle furnaces for both the smelting and refining of silver and lead metal and ore. The use of different furnaces indicates that the technological choices made within the Porco-Potosí region were varied and complex, responding not only to differences in the ore but also to the scarcity of fuel. The archaeological debris reflects this variety. The next section of this chapter will describe the archaeological sites available for study.

10.2. Archaeological sites with Dragon furnaces

PAPP have discovered two archaeological sites containing Dragon furnaces, namely Don Martin's Dragon (DMD) and Uruquilla Est 10 (UR Est 10). Both examples are well preserved and appear to have been used during colonial periods and more recently (DMD).

Don Martin's Dragon (DMD)

The DMD site consists of one well preserved furnace apparently identical to the one excavated at UR Est 10 (see below) which is circumstantially dated to the Spanish colonial period. Historical documents place this type of furnace as originating from the 17th century (Douglass and Mathewson 1923). The site is over an hour's walk from Porco village, on the property of Don Martin (Figure 10.6). The DMD site is located at a height of 4086 m.a.s.l, with GPS coordinates of 19K0811750 7812262. The site was found during interviews with locals in Porco village carried out by PAPP anthropologists Sara Hoerlein and Christy Eyler. Don Martin told Sara that he owned a furnace similar to the one at Uruquilla (see below). Information on the history of this site is limited and Don Martin told us that he remembered his family owning this homestead and farming on the land to grow tuber crops. He does not remember his family using the furnace.

An initial investigatory surface survey of the site indicated there was no useful pottery to indicate the date of this furnace. The furnace was well preserved with part of the domed roof still intact. It has not been fully excavated, but surface samples have been taken and the furnace was well photographed. Don Martin's Dragon cannot be well dated but helps in understanding the technology and therefore stands out as an example of a well preserved furnace from other sites within the sample set.

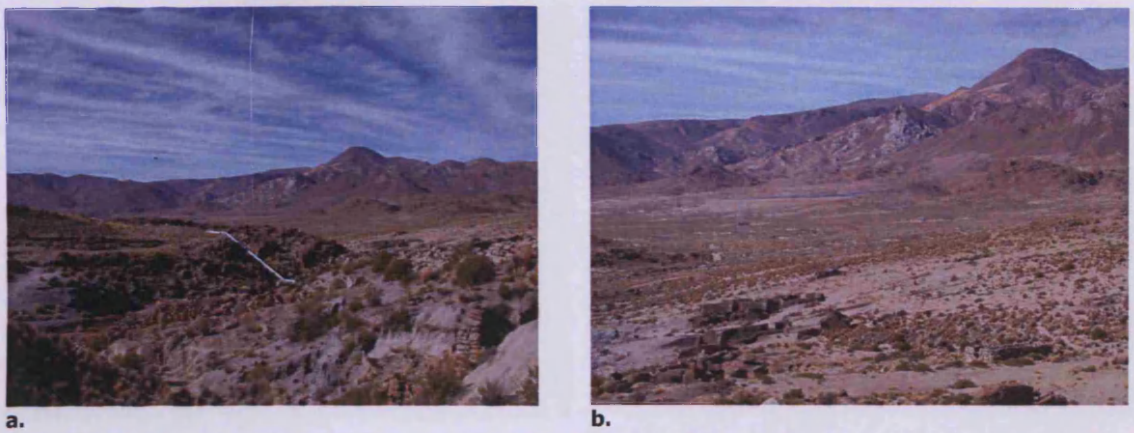

a. b.

Figure 10.6. The view from DMD to Porco (a). The Uyuni road runs in between the site and Porco (b).

The DMD furnace consisted of a firebox, a central domed reaction area, and a flared chimney. The firebox is a rectangular box (50:80:80 cm; l:w:h) made of clay and local stone. It has a clay layer 1 cm thick and has 3-5 mm of charring (Figure 10.7, Figure 10.8). The firebox is linked to the hearth via a trapezium shaped opening. No gratings or other internal structure remained from the firebox. It seemed apparent that the fire box had a level below which heating occurred which could indicate the level at which gratings could have been placed, but none of it is preserved. The whole structure is above ground level, and no excavation was necessary to see the shape and construction of the DMD furnace.

The main reaction hearth has a domed roof and a circular furnace wall. The greatest diameter of the furnace hearth is 120 cm. The dome is built from stone, lined with clay and has a wall thickness of 15-20 cm. The dome has a layer of black vitrified material (created by the partial reaction between the metallurgical gases, heat from the furnace and the domed roof) which starts 30-40 cm from the floor level on the right hand side of the furnace and only 0.1 cm from the left hand side (viewed from the front). The change in vitrification layers indicates that the hearth would have been strongly tilted. The domed roof has two air holes or openings on the right hand side (12x10 and 14x9 cm); (Figure 10.7).

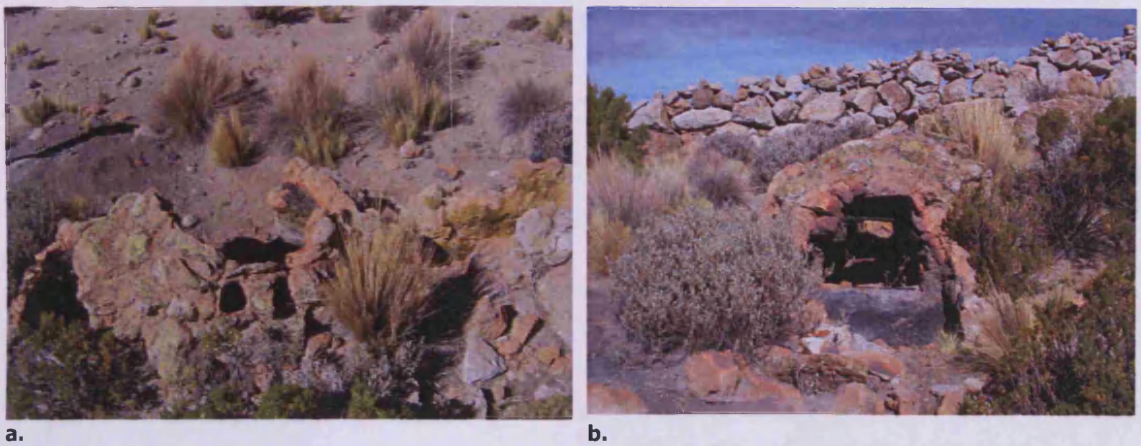

a. b.

Figure 10.7. The DMD furnace from the side looking at the hearth and intact domed roof that has two openings (a) and a view through the firebox (b).

a.

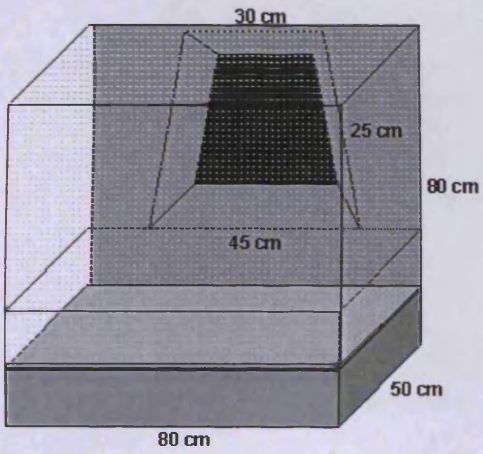

b.

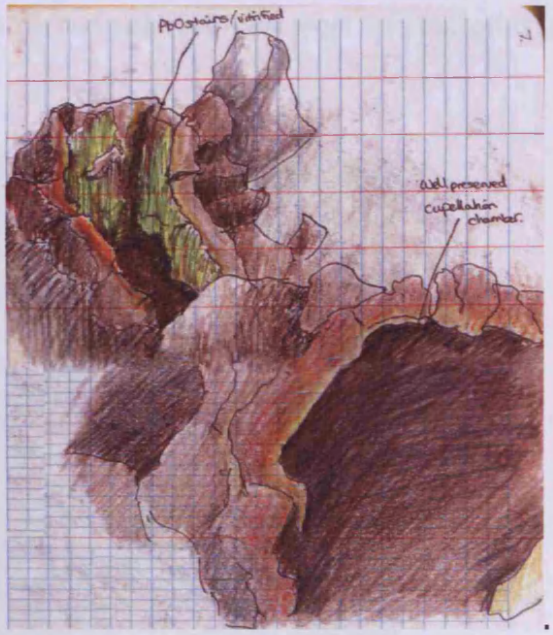

c.

Figure 10.8. The DMD firebox.
It has an oval shape on the left hand side and a square on the right. Image a is a sketch of the firebox. Image b shows the dimensions of the box and threshhold to the reaction hearth. Image c is a sketch of the domed reaction hearth which leads on to the chimney.

From the hearth, a small trapezium door leads through to a large chimney area which measures 95 cm from the end of the opening to the internal end of the chimney. The chimney is 38 cm wide and the trapezoid opening 34 cm. The chimney is internally covered with a layer of vitreous green material which is 20 cm in height (measured from the remaining top of the

chimney). The floor of the chimney is slightly sloping. The furnace is surrounded by scattered dense black slag.

Samples were taken of the slag, chimney wall, furnace wall and ash/residue from the firebox. The results of their analyses are presented in section 8B of this chapter.

Uruquilla Est 10 (UR Est 10)

The archaeological area of Uruquilla sits to the southwest of Cruz Pampa and south of modern Porco (Figure 10.9) and is also known as Porco Viejo (Old Porco). Uruquilla has three distinct areas classified here via the type of metallurgical activity (Table 10.1), the first, considered to be the main area, being a complex settlement enclosed by stone walls containing a large Dragon furnace; Uruquilla Est 10. The second area located to the south of the main complex has three smelting furnaces (UR10, 11 and 12), and some outlying storage buildings. In 2005, excavations were conducted to investigate the second area and gain more information on the three smelting features.

Figure 10.9. The Uruquilla complex.

The third area is located in the hills surrounding the main complex. Discrete clusters of *huayrachina* fragments were found both to the east and the west of the main site. These sites are called UR East saddle and UR West saddle. They are documented further in Chapter 7.

The high density of Inca ceramics found at the main Uruquilla site indicates that this area was inhabited and built during Inca times, although continued occupation by subsequent generations meant that it was used well into the colonial period. Therefore the archaeological

area of Uruquilla has evidence of European (Domed and Dragon furnaces) and indigenous Bolivian metallurgical practice (*huayrachina* debris found in UR ES and UR WS).

***Huayrachina* sites**	**European furnace sites**	
	Dragon furnaces	**Domed furnaces**
Uruquilla West Saddle Surface (UR WS)	UR Est 10	UR 10
Uruquilla East Saddle Surface (UR ES)		UR 11
		UR 12
		UR 14

Table 10.1. Metallurgical sites found in the Uruquilla archaeological area.

Within the main Uruquilla site is a European type furnace labelled UR Est 10. It has a very well defined fire box, circular hearth and flared chimney made from large local stones and clay. The fire box measures 110x45x100 cm. It is an oval shape with straight sides and rounded edges. The hearth has an internal diameter of 160 cm, and the openings for the firebox and chimney intersect the circular hearth. The hearth and chimney connect via a trapezoidal opening. It is highly likely that the firebox was connected via a similar shaped opening, but the archaeological remains now only have the curved threshold (Figure 10.11).

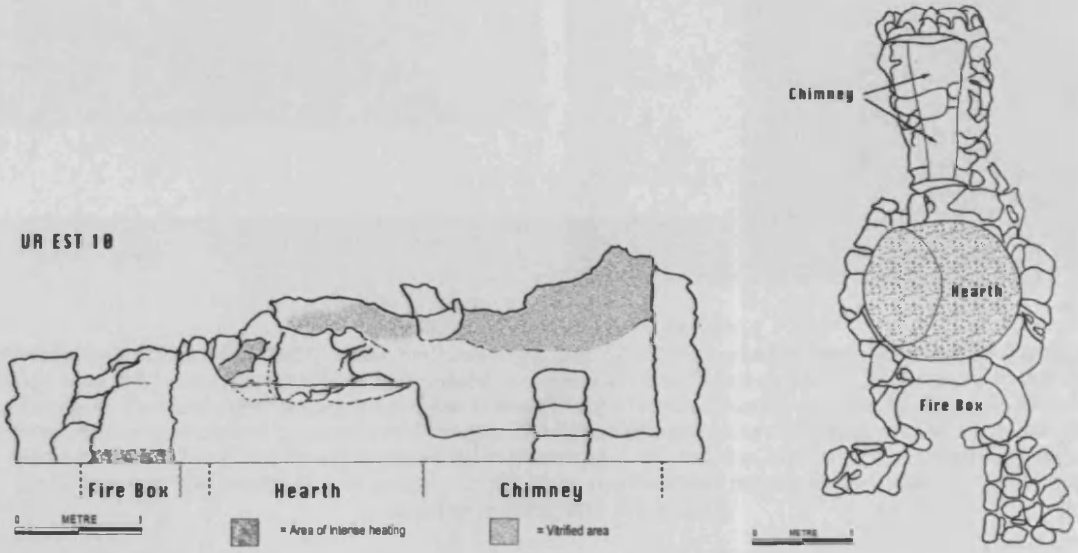

Figure 10.10. Archaeological site plans of furnace UR10 Est 10.

a.

b.

c.

d.

Figure 10.11. The UR10 Est Dragon.
Photograph of the UR10 Est Dragon from a-far (a). It is possible to see the large firebox (centre right of image b on left) and the remains of the domed furnace roof. The flared chimney can be seen in the far left of image b. Currently the Dragon sits in llama corrals used to store llamas overnight. It would have been located inside the original Uruquilla settlement. The flared chimney has a vitrified green layer adhering to the chimney wall (c). The fire box shows no evidence of grills, but the bridge or threshold between the box and into the hearth is well preserved (d). Note the carefully moulded threshold of the firebox opening leading into the hearth.

The chimney is large, measuring over one third (140 cm) of the overall length of the furnace. It is lined with a 1 cm layer of green/yellow vitrification. The original floor of the chimney was not intact. The base of the chimney was eroded but there was evidence for a support structure on the floor in the centre of the flared chimney (Figure 10.10 and Figure 10.11). There may have been an upper raised floor directing the flames and smoke up and out of the hearth. The solid chimney used in this type of furnace appears to have substantial archaeological remains which would survive in the archaeological record even if the upper parts were to erode further.

During excavation, the PAPP team also recorded a drainage system that consisted of a series of interconnected shallow trenches originating from the chimney end and leading away to the outer surroundings of the furnace.

"DMD verus UR Est 10"...

The two Dragon furnaces found during archaeological survey work by PAPP contribute different information to the sparse historical documentation of these European furnaces. The DMD furnace is smaller (120 cm Ø) than the UR Est 10 (160 cm Ø) furnace and has little archaeological context. The location some distance away from Porco village, the lack of ceramics and other indicating factors, do not provide information on the relationship of this site to Porco. However, it does show evidence of silver production, the remote location could indicate that the furnace was used to smelt illicitly obtained ores as seen in the current day silver production process (Chapter 4 and Van Buren 2005). In contrast, UR Est 10 is located within a distinct archaeological zone. Detailed excavation of the furnace and surrounding area has been undertaken by PAPP. Dr Van Buren's assessment of the site indicates that it was probably in use prior to Spanish contact, and used continuously after that point. The remains found during excavation would indicate the furnace was in use from the early to middle colonial periods (personal communication Dr Van Buren 2007). On a positive note, the remote location of the DMD furnace has meant that the external structure has been well preserved. The domed roof remains almost fully intact, whereas the UR Est 10 furnace has no roof remains. Both furnaces have large flared chimneys that share similar green vitrification due to the presence of lead silicate. The designs of the linking bridges between the firebox and hearth area, and between the hearth area and the chimney are also similar. Neither firebox was fully enclosed nor did they have any gratings (which have been observed in the illustrations of Barba and Agricola).

Excavation of the UR Est 10 furnace showed that it had an extensive drainage system and a large workshop associated with it. Ideally, the most suitable furnace for analytical work would have been UR Est 10, however the samples available for metallurgical study were poor and little contextual slag was found. No recognisable roof fragments were available. In contrast, the DMD furnace area provided many surface samples suitable for study from the firebox, chimney, hearth wall as well as large slag samples. Thus it was decided that archaeological information from UR Est 10 would be included in this thesis, although analytical work was only carried out on samples from the DMD furnace.

10.3. Archaeological sites with reverberatory furnaces

Three furnaces from the archaeological site of Uruquilla have been excavated and all these were included in the analytical study in this research project; UR10/11/12 (Figure 10.12). The stratigraphy of the site appears to indicate that these furnaces were used during similar time intervals. Ceramic chronology showed early colonial influences. In the following section, information about the excavation of, and details of, these furnaces will be included.

Figure 10.12. The Uruquilla archaeological area.
In the foreground the three furnaces UR10/11/12 (left to right) and in the background in the stone walled settlement (top left) UR Est 10 – The Dragon.

UR10

Excavation of this site was carried out by PAPP in 2005 and in total an area of 20m^2 was opened using 2x2 m units. Archaeological finds were catalogued and bagged following the excavation protocol. Any changes in stratigraphic layers were recorded and any important features were also detailed in the excavation reports.

The first area revealed the burnt hearth of the UR10 furnace. The total width of the furnace is just under 3 m and the total length 3.5 m (including the firebox), Figure 10.13 and Figure 10.14. UR10 is composed of an oval shaped furnace with an internal hearth at the centre. The internal wall is composed of adobe bricks and the outer wall, local stone. To the west of the hearth is a firebox joined via a small bridge of clay lined stone. The firebox is angled due North with four

large gratings made from clay that cross over the width of the firebox. There appeared to be a lower level to the firebox where ash could be collected and scraped away.

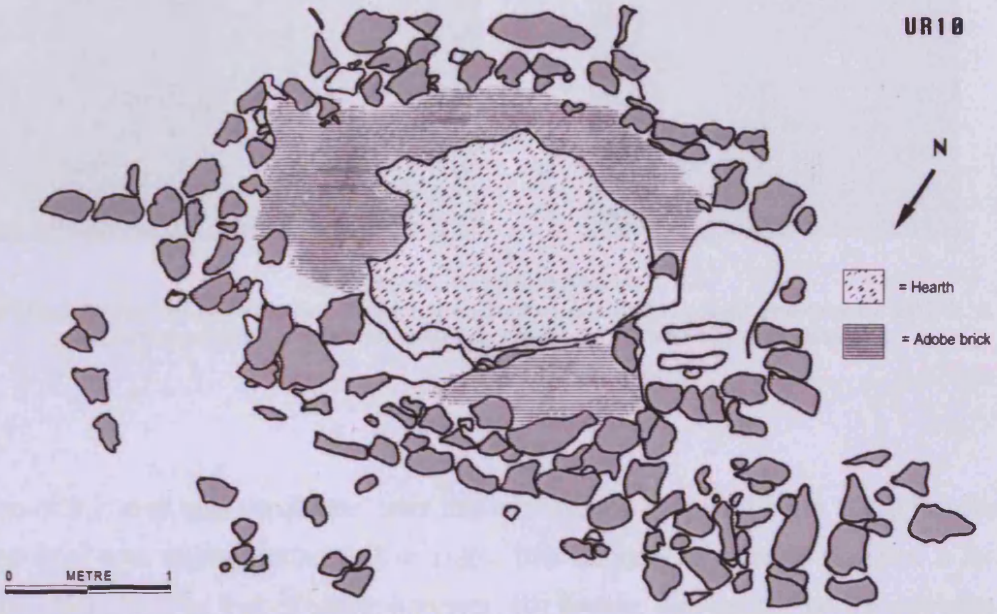

Figure 10.13. Archaeological plan of furnace UR10.

A small 1x1 m^2 trench was dug into the hearth area to further understand the construction. The stratigraphy was such that four texturally different clay layers were identified; alternating in colours from white to red and with some areas even containing a fine green powdered layer. In between each layer was evidence of heating and ground clay, orange in colour, and ash. Surrounding the oval shaped hearth was one layer of adobe bricks that had been used as an internal lining. The external wall of the furnace was constructed with large stones.

Aarchaeological evidence has indicated that the hearth would have been a little larger than the present residual fragments and may even have been slightly angled downwards towards the front.

a.

b.

c. d.

Figure 10.14. The UR10 furnace.
A view of UR10 furnace from above (a). The front of the furnace (hearth right and firebox left); b. A side view looking across the firebox into the hearth (c). A view of the firebox (d).

UR11

Excavation of this area was conducted after the excavations of the adjacent UR10 furnace. An equivalent 20m^2 was opened using 2x2 m units. The archaeological work revealed a furnace with similar dimensions to that of UR10, however, the firebox was located on the opposite side (Figure 10.15).

The furnace consists of a hearth, a firebox located north-east of the hearth and two surrounding walls (internal and external). The construction and style of this furnace is similar to UR10, but it has a different firebox grating. Holes rather than grates compose the upper firebox base (Figure 10.16).

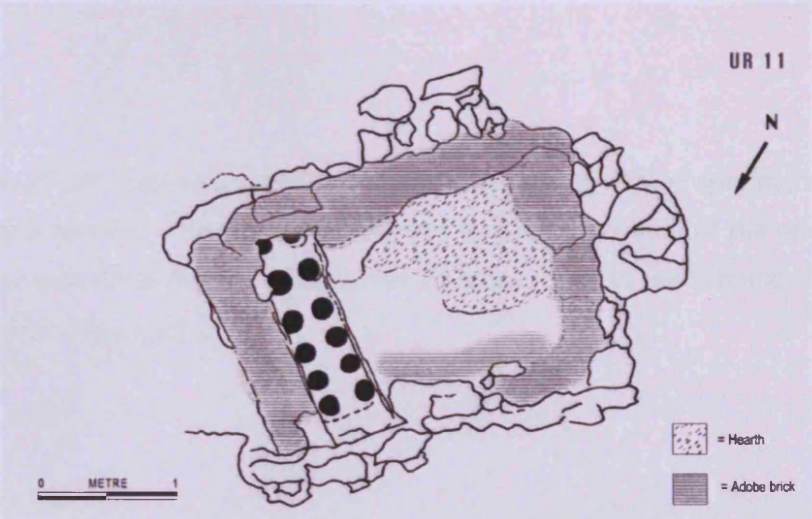

Figure 10.15. Archaeological plan of UR11.

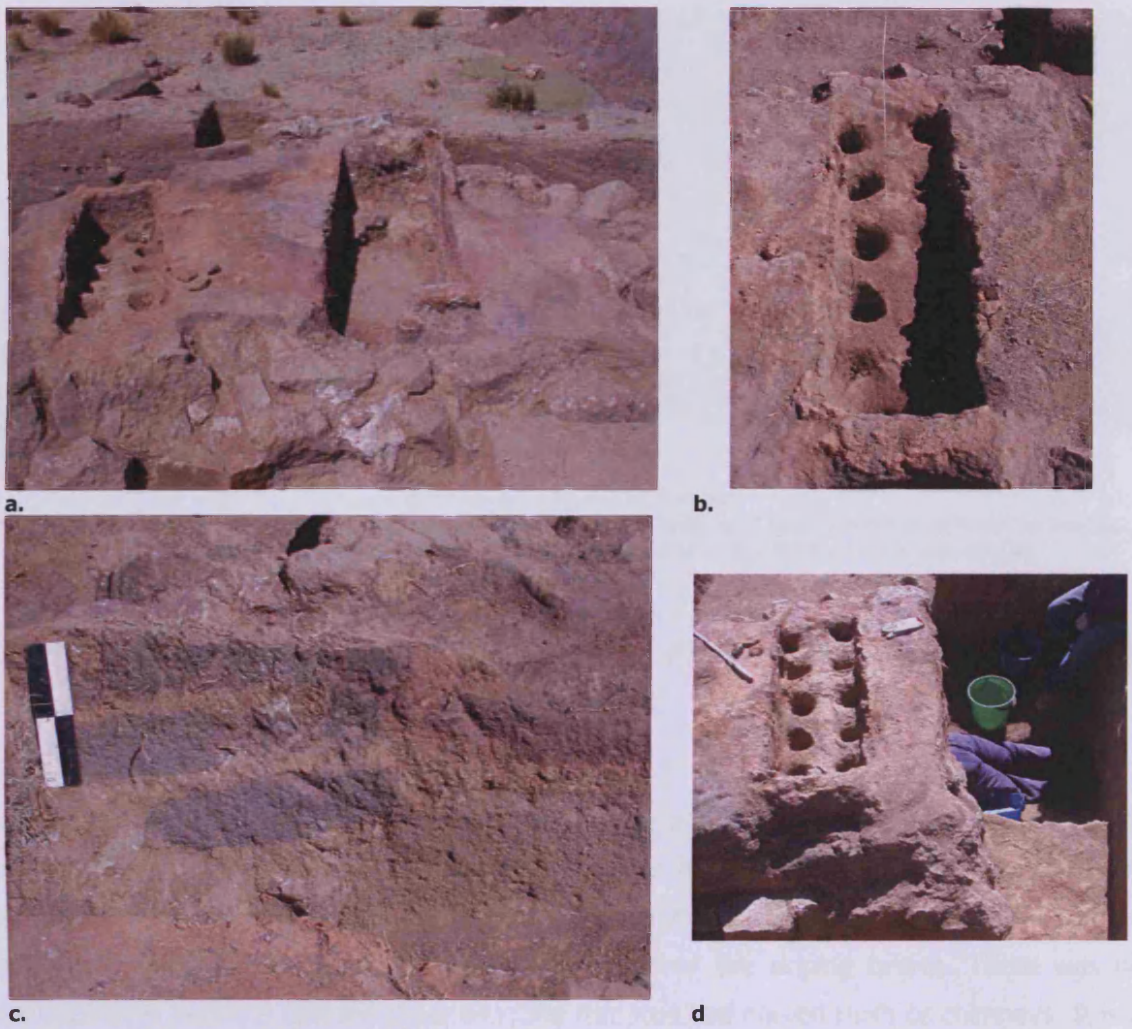

Figure 10.16. The UR11 furnace.
A view from the front of furnace UR11 looking south (a). Detailed view of UR11's firebox. A cross section of the furnace wall in UR11 (c). The adobe bricks that were used to make the inner furnace wall are clearly visible as blue grey rectangles. The firebox has a large lower section that was filled with loose sand and ash (d).

UR12

Surface analysis of UR12 showed burnt stones and a scattering of slag specimens. 2x2 m units were opened and revealed a very poorly preserved furnace. Very little of the original structure remained. Some superficial firebox holes similar to those of UR11 were found. No real hearth structure remained (Figure 10.17).

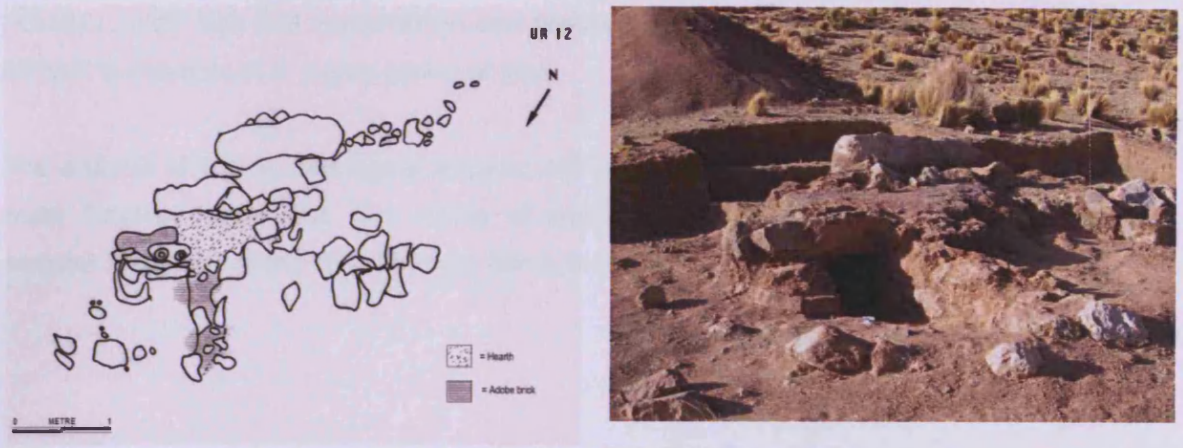

a. b.

Figure 10.17. The UR 12 furnace.
Archaeological plan of the UR12 furnace (a). The original structure of this furnace is difficult to assess. The front view of furnace UR12 where only the remains of the firebox is on the left (b).

10.4. Comparison of the Dragon and other reverberatory furnaces

Differences and similarities between the two Dragon and the three Uruquilla reverberatory furnaces are immediately apparent. The most obvious is the lack of archaeological chimney remains for the latter. Both Dragon furnaces have a large side flared chimney, as well as evidence for the domed roof which would have covered the sloping hearth. There was no archaeological evidence that the three Uruquilla furnaces had domed roofs or chimneys. It is a tentative hypothesis that the Uruquilla furnaces would have had a domed hearth area like the illustrations seen in Alonso Barba and Agricola. During the excavation, no chimney remains were discovered in areas opened due south, nor was there evidence for external chimneys. Thus the chimneys, if present at all, may have been upright and attached to the dome. The historical literature represents these types of furnaces but as yet no direct archaeological evidence can confirm this.

All the European style furnaces had fireboxes with gratings (round or rectangular grates). The presence of gratings indicates the use of pure wood/brushwood rather than dung as a fuel source. Dung would have fallen through the grates and would have been a poor choice of fuel for these large furnaces. All the furnaces would have required large quantities of fuel to function efficiently. Given the size of the furnace hearths and the dimensions of the fireboxes, one can assume that these furnaces would have had a long firing period. However, given the scarcity of appropriate fuel in the Porco-Potosí region, these furnaces would have been expensive to run. European furnaces, in particular the three domed ones at Uruquilla, would probably have been used in conjunction with *huayrachinas* to produce silver-lead bullion. These furnaces must have made large quantities of metal in comparison to the smaller *huayrachinas*.

However, their high fuel consumption and probable high labour investment would have been difficult to maintain over a long period of time.

The analysis of the archaeological remains will be used to further address the way in which these furnaces functioned. The results of analytical work done on selected archaeological samples on the European style furnaces follow in chapter 11.

11. RESULTS FROM ANALYSES OF EUROPEAN FURNACES

This chapter covers the presumed European furnace technology in the Porco-Potosí region. The chapter is divided into two sections according to furnace type/morphology: the results relating to the so-called dragon furnaces, and the results from the reverberatory furnaces without surviving evidence for chimneys.

11.1. Results of the Dragon furnaces

Two dragon furnaces have been found in the region surrounding modern Porco, Don Martin's Dragon (DMD), and Uruquilla Est 10. No excavation has taken place at DMD, but samples were collected from the surface. DMD is very well preserved but has little archaeological context. The collection of samples represents a well preserved and previously unstudied furnace type. The small number of samples (only four were taken for analysis) and their lack of dating is not ideal, but analysis of this sample set is valuable because it will provide information on the technological function of these furnaces.

A number of samples were taken from the excavation of the UR Est 10 dragon furnace, but turned out to be unsatisfactory as indicators of metallurgical analysis. Thus they are not further discussed here.

Samples analysed from DMD

Four samples were taken from the DMD site: one sample of slag (341A), one sample of furnace wall (341C), one sample of chimney wall/lining (341B), and one piece of ash from the firebox (341D).

Slag: sample 341A

Sample 341A is a black glassy slag (Figure 11.1). It is heavy and has a series of ripples on the upper surface. The surfaces are easily distinguishable with a defined top and bottom. The bottom has a porous texture and the upper surface has flow lines indicating the viscosity of the molten slag (Figure 11.1). By eye the slag has no metallic inclusions and appears fully vitreous.

Initial XRF analysis of the hand sample indicated that the sample is predominately silica and lead oxide.

The OM showed that the slag has very few crystalline phases present; it has a light grey glassy matrix with occasional crystallised angular dark grey phases. Extremely small prills of lead sulphide/metal are scattered throughout the entire slag matrix (Figure 11.2.).

a. b.

Figure 11.1. DMD slag sample 341A from the side (a) and bottom (b), note the texture of the base.

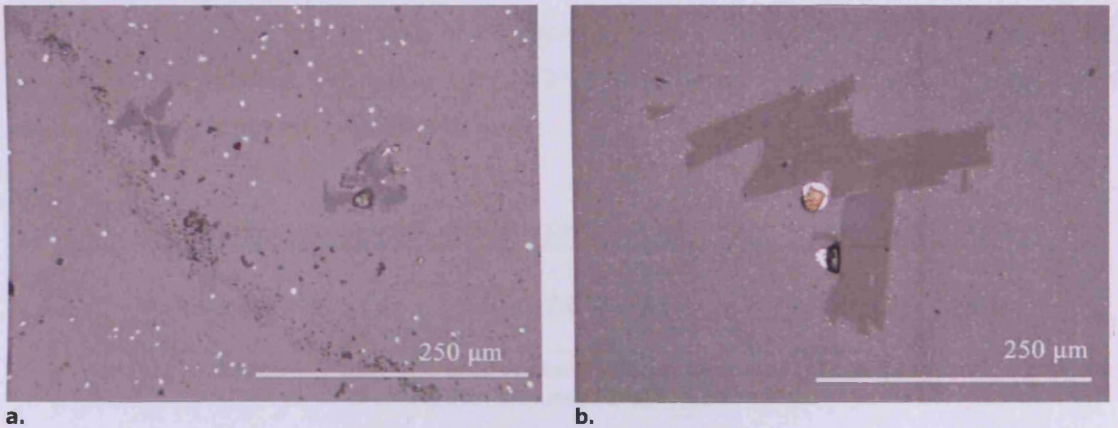

a. b.

Figure 11.2. OM images of DMD 341A slag.
OM image of the 341A slag body scattered with white prills (PbS); image left. OM image (b) shows the darker silicate phases present in the slag. Note in the centre the small metallic prill of lead metal surrounded by a halo of lead sulphide.

Pressed pellet XRF analysis done using turbo quant showed that the slag contains minor quantities of heavy metals such as tin (0.05%) and copper (0.01%), see Table 11.1. The presence of these metals is indicative of the ore selected for smelting. No silver was recorded.

Sample	Na2O	MgO	Al2O3	SiO2	P2O5	SO3	K2O	CaO
341A DMD	0.24	0.29	1.92	16.10	0.01	4.48	0.47	3.14

TiO2	Cr2O3	MnO	Fe2O3	PbO	ZnO	As2O3	SnO2	CuO
0.13	0.01	0.01	2.21	67.47	3.23	0.20	0.05	0.01

Table 11.1. ED-XRF analysis of the DMD slag sample 341A. Pressed pellet analysis done using turbo-quant.

SEM-EDS bulk area scans (Table 11.2) show that the slag has a relatively high lead oxide content (60%) and also contains silica (22%), lime (4%), zinc oxide (6%), iron oxide (3%), and alumina (3%). The darker angular crystals have a silicate base (35%) with lime (26%), zinc and lead oxide (16 and 18%) and low concentrations of alumina, magnesium and iron oxide (1-2%) (Appendix VII); these may be melilithe.

Analysis of the largest prill present in the sample, with a diameter of 30 μm, showed that it consists of lead sulphide with zinc sulphide (2%) surrounding a metallic prill. The metallic part was analysed as lead metal with 8 at% silver.

Scanned area	MgO	Al2O3	SiO2	K2O	CaO	FeO	ZnO	PbO
Average (n=5)	**0.4**	**2.8**	**22.2**	**1.2**	**4.2**	**3.2**	**5.9**	**60.1**

Table 11.2. SEM-EDS bulk scanned areas of DMD slag sample 341A. The data has been normalised to 100 wt%.

The slag from the DMD furnace is extremely glassy, indicating that it was created in a furnace that could generate high temperatures sufficient to fully melt the charge. The chemical analyses have shown that the slag contains little lead sulphide, providing evidence that conditions must have been highly oxidising. The single metallic prill analysed shows the presence of a considerable amount of silver in a lead matrix, surrounded by lead sulphide. The presence of iron and zinc indicates that an ore was smelted in this furnace, as opposed to the cupellation of metal done in European domed furnaces.

Chimney wall: sample 341B

The most distinctive feature of the dragon furnaces is the flared chimney. The DMD chimney wall is constructed of brick and lined with a red ceramic. It has a thin vitrified layer (less than 1

cm), and a shiny green/yellow layer of glassy slag (Figure 11.3). A sample from the DMD chimney wall was taken for analysis to compare with the slag proper and labelled 341B.

a. b.

Figure 11.3. A close up view of the DMD vitrified chimney wall (a), samples taken from the chimney wall (b).

Initial ED-XRF analysis indicated that the yellow/green vitrified layer was a lead silicate. The sample was cut and the polished cross section studied using OM, which showed that the lead silicate layer contained few crystal phases, and no metallic inclusions. The chimney wall appeared to be made from an extremely coarse material (Figure 11.4). The mineral phases were angular and the ceramic was heavily quartz tempered.

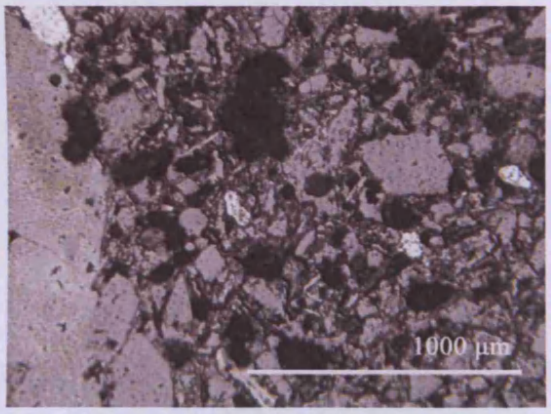

Figure 11.4. OM of the chimney wall (multi-phase area, right) and the vitrified layer (left).

The chimney's ceramic material was analysed by SEM-EDS; bulk scanned areas were used separately to determine both the composition of the chimney wall and the vitrified layer. These analyses showed that the chimney wall had a typical ceramic composition, with only limited contamination by the lead oxide (Table 11.3). The sample contained a large quantity of pure quartz grains, and mineral phases with high titanium (35%) and iron oxide (62%).

The SEM-EDS results of the green vitrified area confirmed the initial ED-XRF analysis which showed that the green vitrification was lead silicate containing lead oxide (51%), silica (34%), alumina (7%), iron oxide and potash (2%), with traces of soda, lime and zinc oxide (Table 11.4). Within the lead silicate there are various crystal phases present. There are many crystal

phases that have been partially dissolved by the surrounding lead silicate. SEM-EDS area analysis of these minerals show that they have a high silica content (60%), generally containing alumina (20%), with variable potash concentrations (8-14%). In some cases, lime was substituted for potash (see area scans 2 and 3). These minerals were most probably feldspar. Surrounding these mineral phases there is often a secondary or interactive layer between the mineral and the lead silicate. This layer has a chemical composition intermediate between the mineral phases already discussed, and the surrounding lead-oxide rich melt.

Scanned area	Na2O	MgO	Al2O3	SiO2	SO3	K2O	CaO	TiO2	FeO	PbO
1	1.5	0.8	16.2	67.9	~	4.0	1.8	1.4	4.7	1.6
2	1.8	0.7	17.3	64.6	~	4.5	2.7	1.7	4.7	2.0
3	1.6	0.7	14.1	70.6	~	5.7	1.4	1.1	3.4	1.5
4	1.9	0.7	16.0	67.8	1.0	4.4	2.5	1.5	4.3	~
5	2.0	0.6	15.9	68.9	~	5.1	1.7	1.0	3.4	1.4
Average	**1.8**	**0.7**	**15.9**	**67.9**	**0.2**	**4.7**	**2.0**	**1.4**	**4.1**	**1.3**

Table 11.3. SEM-EDS bulk area analysis of the chimney wall (sample 341B). Area scans at a magnified image of 50X. Data has been normalised to 100 wt%.

Scanned area	Na2O	MgO	Al2O3	SiO2	K2O	CaO	TiO2	FeO	ZnO	PbO
1	1.2	0.6	6.5	34.4	1.9	1.5	~	2.1	1.2	50.6
2	0.7	~	6.6	34.3	2.1	1.6	~	1.8	1.1	51.8
3	1.2	~	6.6	33.5	2.0	1.5	~	1.7	~	53.5
4	1.3	~	6.7	33.9	2.2	1.5	~	1.9	~	52.5
5	1.3	~	8.9	36.8	3.6	1.5	~	1.8	~	46.1
6	0.6	0.5	6.4	29.9	1.5	1.2	~	1.6	1.0	57.3
7	1.2	0.7	7.3	35.6	1.7	1.8	1.3	3.1	~	47.3
Average	**1.1**	**0.3**	**7.0**	**34.1**	**2.1**	**1.5**	**0.2**	**2.0**	**0.5**	**51.3**

Table 11.4. SEM-EDS bulk area analysis of the lead silicate layer/green vitrification from sample 341B. The data has been normalised to 100 wt%.

The chimney wall appears to have been made from clay that was very sandy/quartz rich. The layer of green vitrification on the chimney wall has been identified as a lead silicate. This lead silicate was dissolving the ceramic wall, evident from the partly dissolved mineral phases trapped in the siliceous layer.

Table 11.5 shows the chemical differences between the bulk chimney wall and the vitrified silicate layer. The silicate glass shows on average half the amount of oxides as the main chimney wall, and contains 50 wt% lead oxide with 0.5 wt% zinc oxide. The chimney wall itself contained about 1 wt% lead oxide and no zinc oxide. Therefore, the vitrification seen on the chimney wall comes to about equal parts from lead oxide fumes and the ceramic lining of the

chimney wall. The proportionally higher lime content in the vitrified layer was probably due to a fuel ash component in the flue gas. The apparently low concentration of titanium may be due to the refractory nature of the ilmenite mineral grains in the ceramic, due to the detection limits of the SEM-EDS analyses, or both.

Scanned area	Na2O	MgO	Al2O3	SiO2	SO3	K2O	CaO	TiO2	FeO	ZnO	PbO
Chimney wall bulk	1.8	0.7	15.9	67.9	0.2	4.7	2.0	1.4	4.1	~	1.3
Silicate glass	1.1	0.3	7.0	34.1	~	2.1	1.5	0.2	2.0	0.5	51.3
Glass/wall (%)	61.8	38.0	44.1	50.1	~	45.1	73.3	13.2	48.9	~	~

Table 11.5. SEM-EDS area analyses showing the bulk chimney wall versus the vitrified silicate glass.

Comparison of the ceramic and its vitrified glassy layer to the slag proper was done to test whether the slag proper is lead oxide fluxed with furnace wall or was made with other components (ore/gangue). The SEM-EDS analyses of the slag proper show elevated zinc oxide levels; this would suggest that ore smelting rather than cupellation of lead metal bullion was occurring. We can assume two thirds of the slag proper (66%) is 'clear' ore (lead and zinc oxide). This then leaves one third of the slag to be either interaction with the furnace wall or gangue components such as quartz from the slag. Consideration of the furnace wall ceramic shows that average alumina content is 16% (Table 11.5). In the slag proper, alumina contents are low (3%). If the lead and zinc oxides (clear slag) were only interacting with the furnace wall, we would expect around 5% alumina (one third of the 16% found in the ceramic wall). The slag proper also has slightly elevated lime levels (4%), compared to the ceramic wall. The lime most probably comes from the gangue minerals or fuel ash contributions.

Thus, if we consider the overall composition of the slag proper, two thirds oxidised ore minerals, one sixth ceramic, and one sixth gangue or fuel ash contributions. This composition shows that the furnace was being used to smelt good ore concentrate. However the possible addition of CHM, as suggested in historical sources, may further complicate the situation.

Furnace fragment: sample 341C

Sample 341C was collected from inside the chimney. It is most probably from the bottom of the chimney. This sample has been selected to juxtapose sample 341B and to further study how the furnace fumes interacted with the furnace wall. This sample is a dense grey brick coated in

a very thin layer of brown vitrified material (Figure 11.5). Basic XRF analyses of the hand sample indicated that the vitrified layer was lead silicate with some alumina and potash.

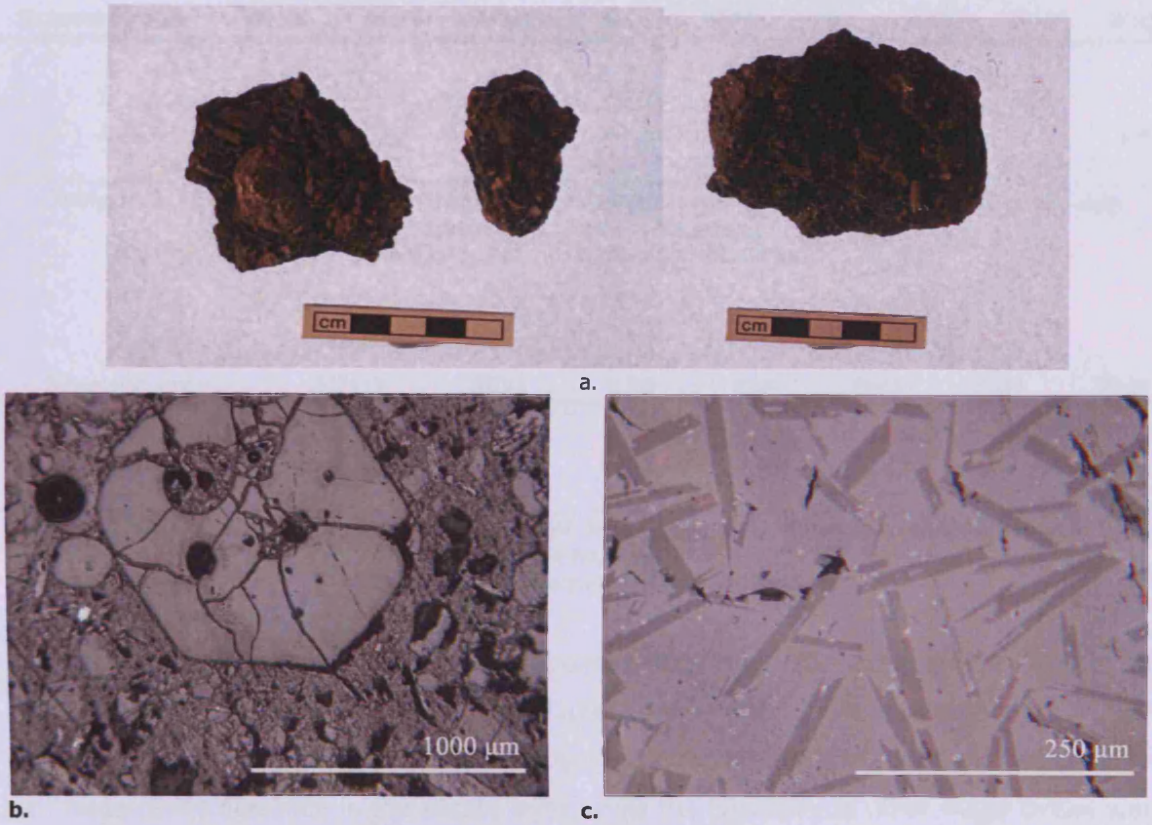

Figure 11.5. Furnace fragment DMD 341C.
Image a is furnace fragment sample 341C from the bottom (left) and from the top (right). OM of furnace fragment sample 341C, the ceramic/brick layer with a large quartz grain in the centre (b). The sample has a lead silicate layer with newly formed crystals (c).

OM showed that there were two distinct areas within the sample: the ceramic/brick that would have lined the furnace prior to use and a thin layer of slag/vitrified material. The brick has a multiphase texture matrix (seen in Figure 11.5 b as the mid grey areas) and dispersed throughout the matrix are different mineral phases. Figure 11.5 b shows a very large quartz grain and is a typical image from the brick layer. The lead silicate layer adhering to the brick was thin. Enclosed within the silicate layer are fragments that are residual brick/ceramic, having been chemically attacked by the lead oxide. The chemical reaction between the lead oxide and brick layer caused different siliceous phases to crystallize in the silicate matrix (Figure 11.5 c). Analysis of this vitrified layer confirmed that its composition is dominated by lead oxide (50%) and silica (33%), as well as minor quantities of alumina (9%), iron oxide (4%), potash (2%) and zinc oxide (2%), similar to the layers seen in sample 341B (Table 11.7). Analysis of the matrix without the phase inclusions showed that there is little chemical difference between the overall bulk analysis and individual phases other than a slight increase in lead oxide (50-55%). The angular crystallised silicate phases seen in the SEM were analysed; compared to the silicate

matrix they have much higher silica (47%), increased potash (7%) and alumina (18%) but reduced iron (1.5%) and lead oxide (24%).

Scanned area	Na2O	MgO	Al2O3	SiO2	K2O	CaO	TiO2	FeO	PbO
1	~	0.7	21.3	66.9	5.6	~	1.0	4.5	~
2	0.4	0.9	17.0	67.7	3.9	0.7	0.8	7.3	1.4

Table 11.6. SEM-EDS bulk area analyses of large brick/ceramic inclusions surrounded by the slag (sample 341C-furnace fragment). Data has been normalised to 100 wt%.

Scanned area	Al2O3	SiO2	K2O	CaO	FeO	ZnO	PbO
1	8.8	32.5	2.1	1.4	3.7	2.0	49.6

Table 11.7. SEM-EDS analysis of a bulk area scan of the vitrified coating on the brick layer (sample 341C-furnace fragment). Data has been normalised to 100 wt%.

Sample 341C is composed of a brick/ceramic base with a layer of lead silicate adhering to one side. The glassy lead silicate layer of 341C is much thinner than the lead silicate layer in 341B. Comparison of the silicate layer to the underlying ceramic indicates that lead oxide (50%) and zinc oxide (2 %) dominate in the silicate layer, while the quantities of other major oxides were reduced by half (Table 11.8). The presence of the lead silicate indicates that this furnace produced strong lead oxide fumes.

Scanned area	Na2O	MgO	Al2O3	SiO2	K2O	CaO	TiO2	FeO	ZnO	PbO
Furnace fragment	0.2	0.8	19.2	67.3	4.8	0.4	0.9	5.9	~	0.7
Silicate layer	~	~	8.8	32.5	2.1	1.4	~	3.7	2.0	49.6
Silicate layer/FF (%)	~	~	45.8	48.3	43.2	394.3.	~	62.0	~	~

Table 11.8. SEM-EDS bulk area analyses of the silicate layer versus main furnace fragment composition.

Ash: sample 341D

Sample 341D was taken from the remains of the firebox and was thought to be a sample of ash. The hand sample is dark grey, extremely porous with a grainy texture and is light (Figure 11.6).

Figure 11.6. The hand sample of 341D prior to sample analyses.

OM showed that this sample appears to be composed of difference minerals, the majority being quartz and is therefore not organic ash. Most of the phases are angular and randomly dispersed in a fine clay matrix (Figure 11.7). Little more information can be gained from the OM.

The SEM-EDS bulk area scans of the sample indicate the presence of silica (66%), alumina (20%), potash (4%), lime (3%), iron oxide (3%), traces of soda, magnesium oxide, and titanium oxide (Table 11.9). Thus, this sample is almost chemically identical to the ceramics found in samples 341B and 341C. Individual phases in the sample were characterised and found to be iron-rich silicates, feldspars, iron titanium oxides, and quartz (Appendix VII).

This sample is clearly not ash from the fire box. From the analytical data, many of the phases present are quartz, feldspars, and iron rich silicates which correlate with furnace fragment sample 341C. This sample is most likely a sample of fine soil similar to un-reacted furnace wall or lining, indicating that the furnace was built (as expected) from local clay.

Scanned area	Na2O	MgO	Al2O3	SiO2	P2O5	K2O	CaO	TiO2	FeO
1	1.3	1.6	20.5	63.3	~	4.9	1.4	1.2	5.7
2	1.9	0.8	17.8	68.6	~	4.9	1.6	0.9	3.5
3	2.0	0.8	19.2	66.5	~	5.0	1.9	1.0	3.6
4	2.1	0.7	19.5	67.2	~	4.1	2.9	0.6	3.1
5	1.6	0.9	18.0	66.3	1.0	3.6	2.3	1.1	4.8
Average	**1.8**	**1.0**	**19.0**	**66.4**	**0.2**	**4.5**	**2.0**	**1.0**	**4.1**

Table 11.9. Bulk area scans of sample 341D using SEM-EDS. Data has been normalised to 100 wt%.

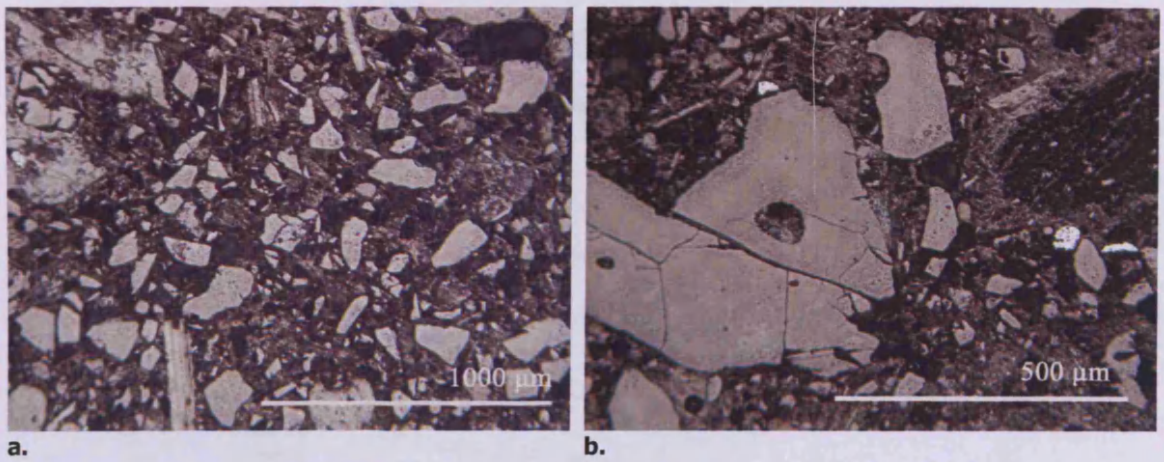

a. b.

Figure 11.7. OM image of the sample DMD 341D ash (a). Multiphase inclusions with large quantities of silica (large smooth light grey inclusions). Closer magnification (b).

Overall summary

The analyses carried out on the DMD samples have shown that this furnace was used for smelting ore in highly oxidising conditions to produce lead-silver metal and a lead rich siliceous slag. The DMD slag (sample 341A) has evidence of flow lines and ripples indicating that high temperature conditions were achieved when producing this slag.

The analytical results have shown that the slag is composed of lead oxide (67%) and silica (16%). The presence of iron, zinc and sulphur was also noted. The small number of metallic prills left in the slag matrix may indicate that this furnace was very efficient in producing a siliceous slag containing very little metallic residues. The metallic prill analysed contained silver and lead metal, with a halo of lead sulphide surrounding it. This indicates that primary ore was used to smelt rather than pre-roasted ore, which should have had the sulphidic component removed during the roast. The presence of sulphur in the bulk analyses is a useful indicator of the original mineral ore chosen for smelting and it would seem highly probable that argentiferous galena was selected for smelting. Zinc oxide levels present in the slag indicate the presence of sphalerite in the ore. Therefore, the DMD furnace would have produced lead metal (enriched with silver) and a lead oxide rich slag from the local argentiferous lead/zinc ore.

The composition of the slag can be used to evaluate the temperatures in the furnace. The PbO-ZnO-SiO2 composition of the DMD slag has been plotted onto the phase diagram. An approximation of the temperatures within the DMD furnace can be gained by using this diagram. The slag falls on the 900 °C line. Temperatures may even have been slightly lower due to lime and iron contents in the slag. Thus, the overall functioning temperature of this furnace was relatively low.

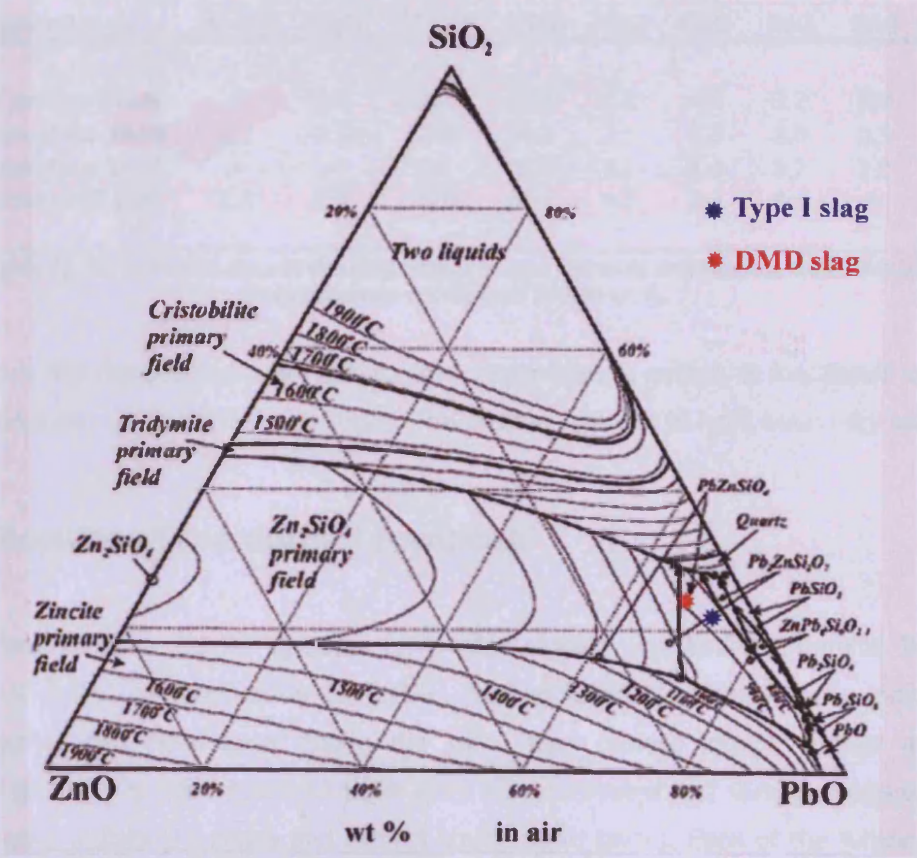

Figure 11.8. The PbO-ZnO-SiO2 phase diagram.
DMD slag shown by a red star (personal communication with Thilo Rehren, 2008).
Blue star = average Type I UR series slags. Red star = DMD slag

Analyses of the furnace wall and chimney also support the processing of lead in this furnace. A comparison of the slag proper (341A), chimney, and chimney base fragments (341B and 341C) indicate that there is a difference between the slag proper and the vitrified silicates found on the furnace fragments. The slag proper contains a much higher zinc oxide content (6%), and has a lower Al2O3:SiO2 (1:7) ratio whereas in the ceramic material analysed the Al2O3:SiO2 ratio was higher (1:4), akin to the ratio in ceramic. Differences in the silica ratio indicate that the slag had absorbed additional silica (most probably from the quartz in the gangue from the ore), whereas the vitrified ceramic material from the chimney has maintained its original alumina to silica ratio (Table 11.10). The addition of quartz as a flux seems less likely at present because there is no need for such a flux in lead smelting. It is also noted that the slag proper contains metallic prills of lead sulphide whereas the chimney wall and furnace fragments do not. There is an increased lime content in the slag compared to the ceramic material indicating the introduction of calcium into the system (Table 11.10). There are two possible options for the increased lime content; it may have come from the gangue materials, or from a fuel ash. Historical evidence indicated that these furnaces could have had ash lined furnace hearths, which could also have added lime to the slag.

Scanned area	Na2O	MgO	Al2O3	SiO2	K2O	CaO	FeO	ZnO	PbO
Slag proper 341A	~	0.4	**2.8**	22.2	1.2	4.2	3.2	**5.9**	60.1
Silicate glass 341B	1.1	0.3	7.0	34.1	2.1	1.5	2.0	0.5	51.3
Silicate glass 341C	~	~	8.8	32.5	2.1	1.4	3.7	2.0	49.6
Chimney wall bulk	1.8	0.7	15.9	67.9	4.7	2.0	4.1	~	1.3

Table 11.10. SEM-EDS data of the slag proper versus chimney and furnace wall silicates. Data has been normalised to 100 wt%.

In summary, this furnace has been used to smelt argentiferous galena. It functioned under high temperatures and very oxidising conditions. The process appears to have been very efficient.

11.2. Results of the domed furnaces

Samples from all three domed furnaces have been studied analytically: Uruquilla 10 (UR10), Uruquilla 11 (UR11), and Uruquilla 12 (UR12). The archaeological stratigraphy indicates that these furnaces had been used during the same time period, though further analysis is necessary to clarify specific dates. All three were fully excavated and samples collected can be traced to their individual furnace and distinct stratigraphic layers. Each of the furnaces will be presented individually and the results then discussed as a group. Samples were selected to represent the archaeological debris found at the sites, and primarily analysed using XRF.

UR 10

UR 10 is the first of the three furnaces in the Uruquilla series. It has a well preserved grated firebox and a multilayer hearth platform. The inside layer of the furnace was lined with adobe bricks and the outer layer constructed from natural rock. There is no evidence for a chimney and no samples remain of the furnace roof's internal structure. More detailed descriptions and images are in Chapter 10. Samples taken for analysis were predominately slags, as well as a few ceramics with slag/metal adhered to them. No suitable furnace fragment remains were found for analysis. The samples will be discussed per category; the results of the slag samples and the results of the ceramic samples.

Results of the UR10 slag analysis

Eleven slag samples were selected for analysis. The samples analysed can be grouped into two main sub-categorises according to their chemical composition: lead-rich and zinc sulphide-rich (Table 11.11). For clarity, each group shall be discussed individually and then a more general

summary of the results will be considered (two of the samples lie outside of the groups and are presented individually).

Type I –lead rich	Type II –zinc sulphides rich	Others
209	250B	89
250A	255	268B
253A	268A	
253B	268C	
254		

Table 11.11. Slag samples from UR10 organised into selected categories.

Type I - lead rich slags

Analysis of slag samples from site UR10 indicated that five of the samples (209, 250A, 253A, 253B and 254) can be collated in the Type I - lead rich slags category.

All the slag specimens in this group are extremely vitreous. They have a glassy, black appearance with few or no visible inclusions. The cut surface revealed numerous pores and the occasional metallic prill. Sample 250A exhibited a multi-layered structure possibly indicating a tapping process. The uppermost surface of sample 250A has conchoidal fracture marks and ripples. These ripples also occur on one other sample. Type I slags are generally smooth and without large inclusions on the outer surface (Figure 11.9).

209 **250A** **253B**

Figure 11.9. Type I lead-rich slags.

Characteristically for the Type I slags, OM showed a glassy slag matrix with metallic prills of lead and partially reacted lead sulphide crystals. Sample 254 is so glassy that it has no metallic prills or crystalline phases (Figure 11.10). In the extremely glassy slags, increased porosity was frequent (samples 254 and 250A). Type I slags contain pieces of ore minerals within the slag matrix; residual quartz was recorded in sample 253A, (Figure 11.11). Sulphidic prills were universal, typically small crystals of lead sulphide peppering the matrix (Figure 11.10). Other sulphidic components were also recorded such as the sulphide prills with a blue sheen

(indicating the presence of copper) that were found in sample 253B. Metallic prills of lead metal were found in samples 209, 253B, and 253A.

ED-XRF pellet analysis of four slag samples (samples 209, 250A, 253A and 254) indicated a low silica content (10-22%) and the overall lead oxide content measured 69%. Considerable sulphur was present in the bulk chemical analyses (6%). No silver was measured in the bulk analyses, however nickel, strontium, and barium were all recorded.

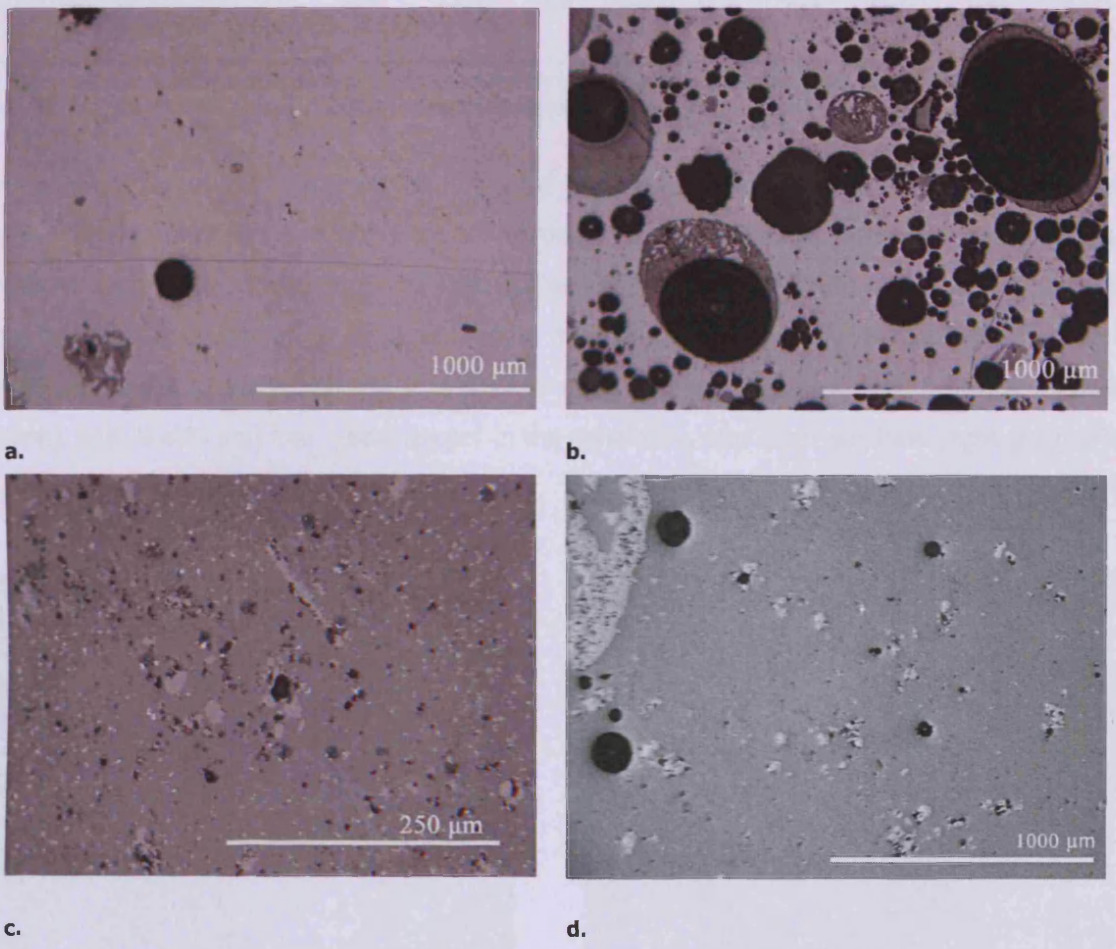

Figure 11.10. Type I slags.
Type I slags typically have a vitreous texture. OM analysis on sample 254 shows the glassy slag matrix (a). Heavy porosity was also commonly noted within Type I slags (sample 254 b). While type I slags are glassy, they also contain a variety of crystal phases. The OM of sample 250A (c) illustrates this. OM image of slag sample 209 glassy matrix with lead sulphide inclusions (d).

SEM-EDS analysis of the bulk area scans further characterised this group. The slag is comprised of lead oxide (c. 60%), and silica (c. 20%) (Table 11.12). Heavy metals such as zinc, iron and antimony are also present in the slag. Low quantities of lime, potash and alumina are characteristic of this slag sample set. No arsenic was recorded.

Groups	Sample	MgO	Al2O3	SiO2	K2O	CaO	MnO	FeO	ZnO	Sb2O3	PbO
Lead rich slags	209	~	1.9	17.3	~	0.2	1.0	12.4	1.7	~	65.5
	253A	0.1	3.3	24.8	0.8	0.4	~	5.4	6.6	0.8	57.8
	253B	~	3.5	25.3	0.9	0.8	~	4.7	5.6	0.3	58.8
	254	~	2.9	18.9	1.5	1.8	~	6.0	2.8	~	66.1
Average Type I (n=4)		**~**	**2.9**	**21.6**	**0.8**	**0.8**	**0.3**	**7.1**	**4.2**	**0.3**	**62.1**

Table 11.12. Average SEM-EDS bulk area analyses of slag samples from UR10 Type I "lead rich slags. Data has been normalised to 100 %.

Ore minerals found in the slag during OM were already identified as being sulphidic, and SEM-EDS analysis confirmed the presence of partially reacted sulphidic ores and other gangue minerals such as quartz. Sample 253A illustrates the presence of these ore minerals, such as the residual quartz seen in Table 11.12. Higher magnification revealed a multiphase ore mineral area with lead sulphide containing 2 at% silver (brightest white phase), zinc sulphide (darkest phase), with 9 at% iron and 1 at% copper in the sphalerite, and silver sulphide (light grey) with 2 at% copper (Figure 11.11)

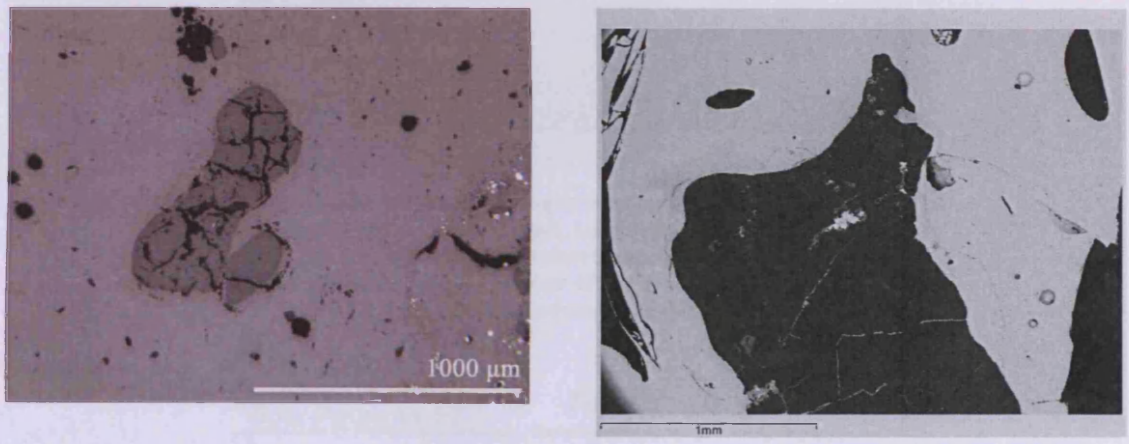

a. b.

Figure 11.11. OM images of slag sample 253A.
The slag is very clean and contains gangue components (mid grey island); (a). SEM image of slag sample 253A (b). Quartz gangue components stuck in the slag matrix.

Other crystalline components analysed in the Type I slag were found to have an iron silicate base containing silica (37%), iron oxide (24%), alumina (16%), potash (10%), manganese (8%), and titanium oxide (5%). The slag also contains zinc olivines (Appendix VII).

Metallic prills analysed were found to be both lead and silver based. Sample 209 has up to 6 at% silver within the analysed lead prills. Sample 253B has high silver prills, two were analysed.

Prill 1 consists of 80% silver, 5% copper, sulphur, and lead. Antimony was also found. Inside prill 1 an area of lead sulphide was analysed with 3% copper present. Prill 2 showed the presence of copper (22-57 at%), lead (32 at%), and sulphur (40 at%), with up to 9 at% silver (Table 11.13).

Scanned area	S	Cu	Ag	Sb	Pb
Prill 1 area 1	3.8	3.8	88.6	1.8	2.0
Prill 1 area 2	7.9	7.9	79.2	1.8	3.1
Prill 2 area 1	33.4	57.0	9.6	~	~
Prill 2 area 2	43.2	22.6	2.3	~	32.0

Table 11.13. Metallic prills 1 and 2 analysed using SEM-EDS. The data has been normalised to 100 at%.

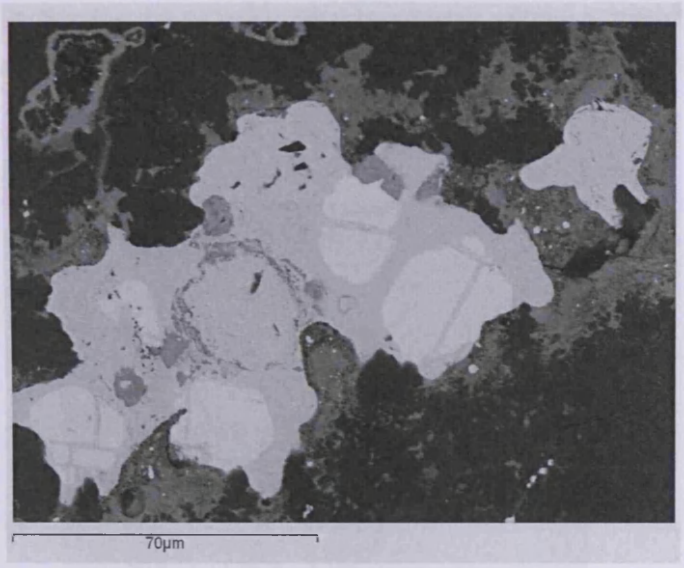

Figure 11.12. SEM images from slag sample 253A. UR10 of residual ore minerals. Lead sulphide, silver sulphide, and zinc sulphide were recorded trapped in a silica the quartz grain (This is magnified image of the quartz grain where this ore mineral is trapped Figure 11.11).

Scanned area from Figure 11.12	S	Fe	Cu	Zn	Ag	Pb
Silver sulphide (mid grey phase)	39.0	~	1.8	~	59.2	~
Zinc sulphide (darkest grey phase)	50.0	8.7	1.3	39.2	0.8	~
Lead sulphide (brightest phase)	50.0	~	~	~	2.3	47.6

Table 11.14. SEM-EDS analysis from Figure 11.12 residual ore minerals in slag sample 253A. Data has been normalised to 100 at%.

Type II - Zinc sulphide rich slag

Four out of the eleven slags analysed fit together in a category classed 'zinc sulphide rich slags' or Type II (250B, 255, 268A, 268C). Here a summary of the characteristic components of these slags is presented.

Typically, the hand specimens are glassy and black (similar to Type I), but often have a brown patina coating on the outer surface. OM analysis has shown that the matrix is mostly vitreous. Unlike the Type I slags, Type II slags have a greater density of areas with partially reacted ore particles. These were identified as sphalerite and galena. Quartz crystals were also noted. Other crystals scatter the slag micro morphology. Areas rich in galena often contain pure lead metal, as seen in Figure 11.13. Metallic prills are more common within Type II slags and are generally multi-metallic with a number of different phases present within a metallic lead base. Prills usually contain areas of lead sulphide, found in discrete halos surrounding the outer edge of the prills (Figure 11.13 b).

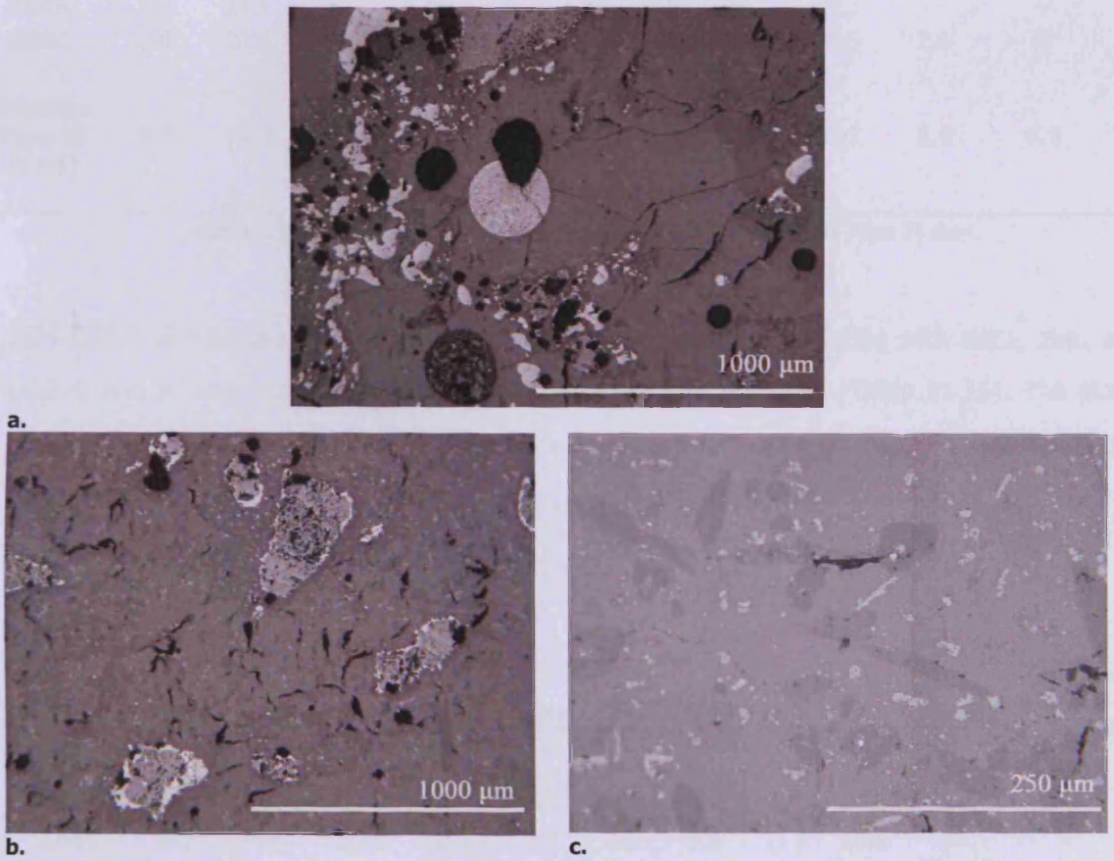

Figure 11.13. Type II slag.
Type II slag has a glassy matrix with metallic and sulphidic inclusions. Other crystalline phases were recorded. Slag sample 250B (a) illustrates the typical round metallic prills and scattered white lead sulphide islands that are common within these samples. Slag sample 255 (b) has a matrix with many small islands of sphalerite (light grey)/galena (bright white). Type II slag typically has a silicate matrix with recrystallised lead sulphide (white inclusions) and lead silicates/zinc olivines (mid grey angular crystals, c).

The high quantity of zinc registered in the bulk area scans (c. 20% ZnO) and the presence of sulphur (c. 5% SO3) were characteristic for this slag type. The OM imaging showed that large areas of residual sulphidic gangue were present in the slag matrix. Most of the sulphur is found associated with lead and zinc sulphide rather than in its oxidic state. The SEM-EDS images and data from residual ore confirmed the presence of zinc sulphide and lead sulphide (Figure 11.15). Areas of lead sulphide analysed within the slag were found to contain considerable quantities of zinc (9%), iron (3%), and some arsenic. Only sample 255 contained silver (Appendix VII). The zinc sulphide measured within the four Type II slags is very homogenous and contains less than 2% iron (Appendix VII). Metallic prills within the sample are primarily composed of lead metal with up to 5% antimony, 10 at% silver, and 11 at% arsenic (Table 11.17 and Figure 11.16).

Sample	Al2O3	SiO2	P2O5	SO3	K2O	CaO	MnO	FeO	ZnO	As2O3	Sb2O3	PbO
250B	1.9	18.4	~	6.0	0.7	~	~	6.5	22.3	1.3	0.7	42.2
255	3.5	25.9	0.3	8.9	0.9	1.3	0.5	9.5	20.6	~	~	28.6
268A	3.3	24.6	~	4.6	1.0	1.5	0.5	11.7	25.2	~	~	27.6
268C	2.4	20.4	~	0.5	0.7	0.7	0.4	23.7	16.6	2.6	~	32.0
Average Type II (n=4)	**2.8**	**22.3**	**0.1**	**5.0**	**0.8**	**0.9**	**0.4**	**12.9**	**21.2**	**1.0**	**0.2**	**32.6**

Table 11.15. Average SEM-EDS bulk area analyses from UR10 Type II slag. Data has been normalised to 100 wt%.

SEM-EDS bulk area analyses of the slag show a lead oxide base (33%) with silica, zinc, iron oxides, and sulphur making up the majority of the slag composition (Table 11.15). The glassy slag matrix is primarily composed of lead oxide (c. 50%), and silica (c. 25%); Table 11.16. The high quantity of zinc in the slag system has produced crystalline phases rich in zinc, such as zinc/iron silicates, possibly zinc olivines (Figure 11.17), and zinc oxides (spinels).

Spectrum	MgO	Al2O3	SiO2	P2O5	K2O	CaO	MnO	FeO	ZnO	As2O3	Sb2O3	PbO
250B	~	2.8	20.8	0.4	1.0	~	~	8.4	10.1	2.2	2.2	52.2
255	0.2	4.8	32.5	0.8	1.6	2.5	0.8	11.8	10.5	~	~	34.6
268A	~	2.9	29.1	~	1.4	2.4	~	12.1	13.7	~	~	38.3
268C	~	2.2	25.1	~	1.1	1.1	0.6	8.5	12.3	3.1	~	46.1

Table 11.16. SEM-EDS glassy slag matrix analysis of zinc rich slags. The data has been normalised to 100 wt%.

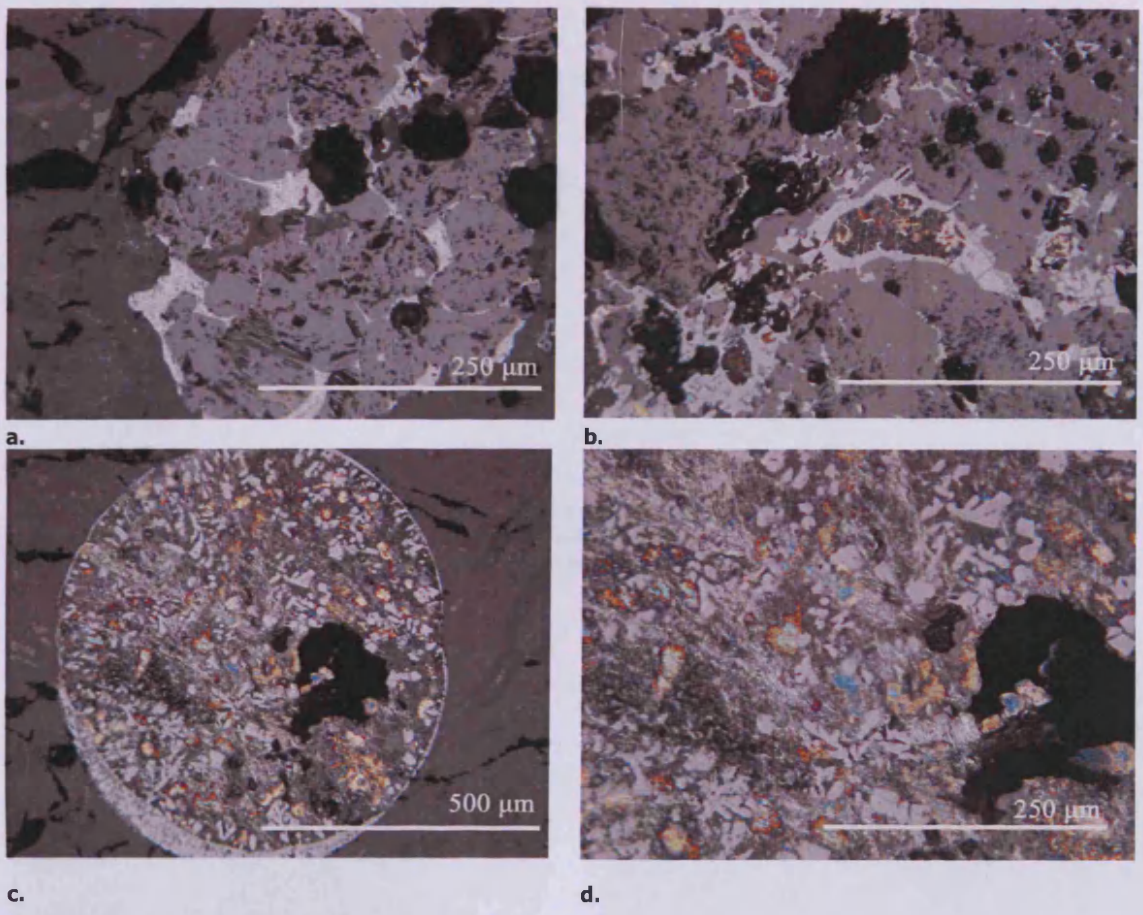

a. b.

c. d.

Figure 11.14. The OM analysis showed that trapped ore was a common feature of Type II slag. Slag sample 268A (a) illustrates this with a large ore mineral, predominantly sphalerite (light grey) and lead sulphide (brightest phase) that has partially reacted with the surrounding matrix. Slag sample 250B (b) shows the glassy slag matrix which often has metallic lead inclusions surrounded by lead sulphide. Other metallic prills within the slag generally have a matrix of lead metal (brown) with *dendritic* intergrowths of lead sulphide and prills of silver (creamy yellow). This is best shown in sample 268A (c and d) where different metallic intergrowths are shown. Mid grey inclusions are silver rich dendrites, dispersed in a lead metal matrix.

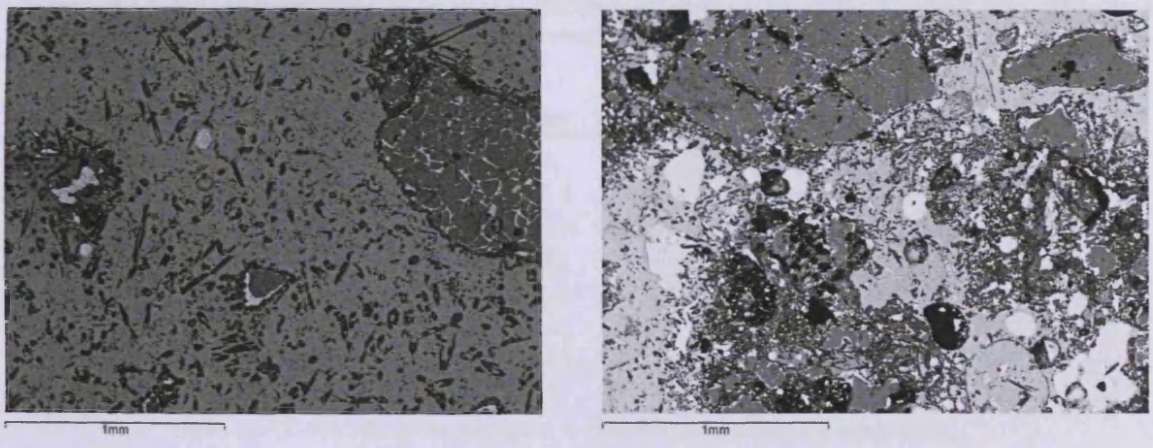

a. b.

Figure 11.15. SEM image (a) shows sample 268A's slag matrix (light grey) with ore minerals (predominately zinc sulphide; mid grey islands) scattered randomly. Zinc/iron silicates are re-crystallised throughout the slag matrix (dark grey crystals). A similar microstructure was seen in samples 250B and 255. SEM-EDS image (b) shows different crystalline phases present in slag sample 250B. Large sphalerite inclusions (mid grey), zinc silicates (dark grey), sulphidic and metallic prills (bright white) are dispersed throughout the slag matrix.

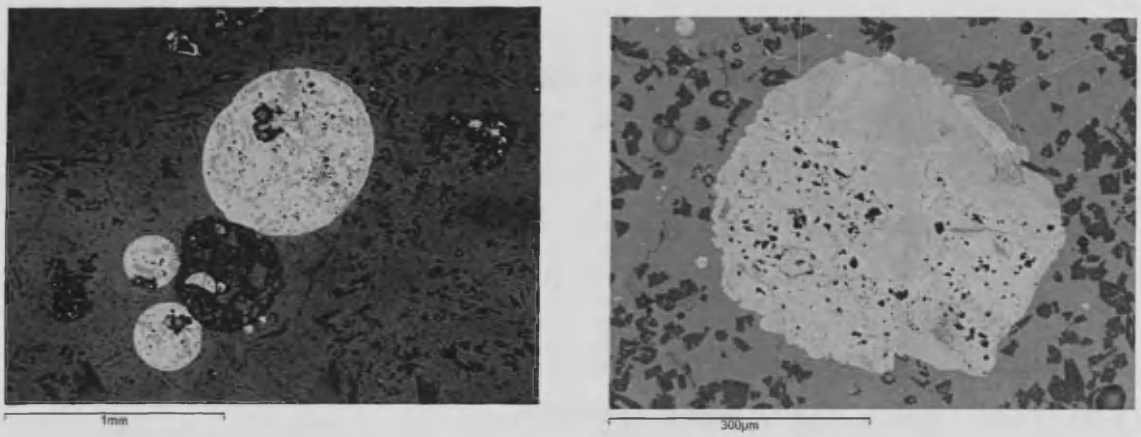

a. b.

Figure 11.16. The Type II slags contained many metallic and sulphidic prills. SEM images and EDS analysis showed metallic prills within the lead silicate matrix such as sample 268A (a) or sample 268C (b). These prills are multi-metallic containing silver, lead, and often traces of copper, and antimony.

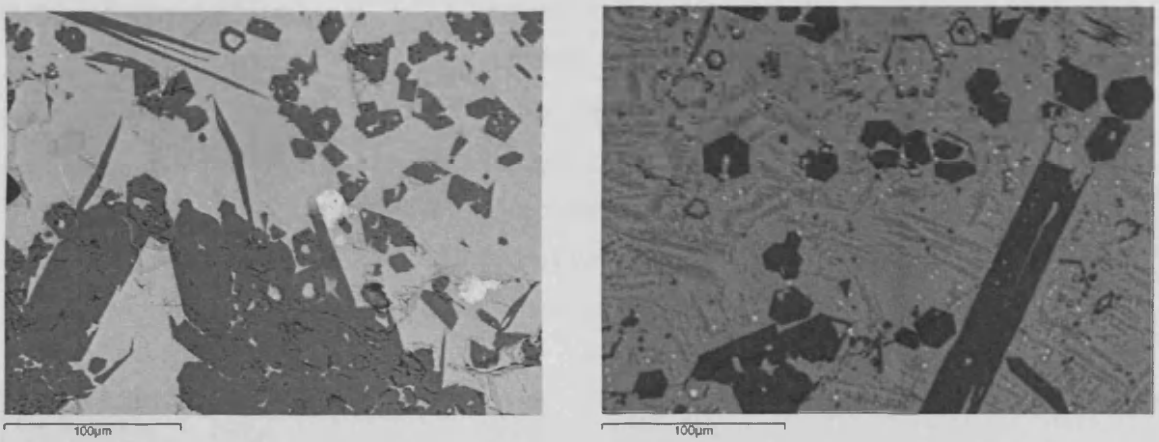

a. b.

Figure 11.17. Type II slags have numerous zinc silicates within the slag matrix. Samples 268A (a) and 225 (b) show the typical morphology of these crystals (dark grey).

Spectrum	Zn	As	Ag	Sb	Pb
SI6 3	~	6.4	~	5.0	88.6
SI8 1	~	11.8	8.7	4.0	75.5
SI8 2	~	7.1	~	3.3	89.6
SI9 4	4.8	6.1	~	4.1	85.0
SI10 3	16.6	~	10.9	4.0	68.5
SI12 1	14.2	7.3	5.6	3.2	69.8

Table 11.17. Metallic prills analysed in the silicate matrix of sample 268C. Data has been normalised to 100 at%.

'The Others' - slag samples from UR10 that cannot be categorised

Two samples remain outside of the Type I and II categories; slag sample 89 and 268B. Each will be discussed individually in the following section.

Slag sample 89

Slag sample 89 is black and glassy. Macroscopically, the majority of it has no obvious mineral inclusions, however, one area has an extremely dense collection of quartz crystals. Externally, one of the surfaces has a thin light brown coating or patina (Figure 11.18). XRF analysis of the cut, hand specimen indicated that the slag was composed of a lead silicate with smaller concentrations of alumina, iron and zinc oxides, lime and potash.

Figure 11.18. The hand sample UR 10 89.

OM of sample 89 shows the slag has two different mineralogical areas: a porous area with partially reacted ore and gangue and a dense glassy/vitreous area (Figure 11.19). The two areas are adjoined by an intermediate area that becomes more fluid and glassy but remains very porous. The dense area of the slag contains crystalline phases embedded in the glassy matrix (Figure 11.20, b, c) and scattered white prills of residual lead sulphide. Metallic lead prills are uncommon in the glassy area but are found in the porous gangue-rich region. These prills usually contain halos of lead sulphide as seen in Figure 11.20 (a).

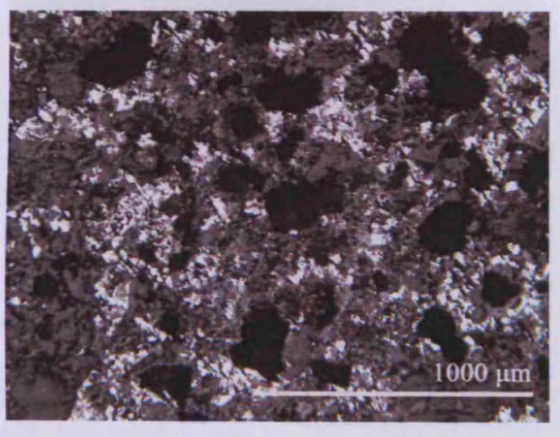

a.

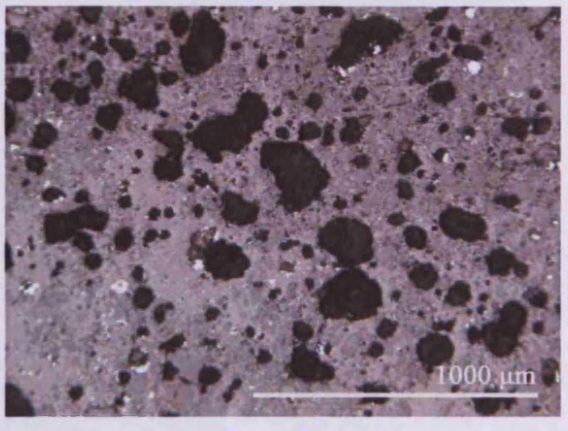

b.

Figure 11.19. OM image of partially reacted gangue area in slag sample 89.
This OM image (a) shows the heavy porosity (dark black holes) and the clusters of partially reacted lead sulphide (galena), the brightest white areas. Other areas in sample 89 (b) show the partially reacted gangue and its interaction with the glassy area.

SEM-EDS bulk area analyses show that the glassy area of the slag contains silica (42%), lead oxide (24%), alumina (10%), iron and zinc oxides (6% each), lime and potash (5% each) and minimal amounts of magnesium oxide (Table 11.18). In contrast the porous gangue area is

extremely variable; it contains up to 13% sulphur and 50% lead expressed as lead oxide. Silica levels range between 16-44%.

No silver was found in this sample. In gangue-rich regions metallic prills of lead metal and lead sulphide were analysed. Analysis of one prill indicated that antimony (4%) is present in the metallic area. The silicate/glassy areas of the slag prove to be the most metallurgically interesting because the glassy matrix has a variety of phases. The basic glassy slag matrix is composed of lead oxide (30%) and silica (35%). It also contains zinc oxide, iron oxide, lime, alumina, and potash (Appendix VII). Included in this are crystals of leucite, and zinc/lead silicates that appear to have crystallised during cooling of the slag. Feldspars were also analysed in the matrix. The white crystal phases seen in the OM were analysed and confirmed to be lead sulphide.

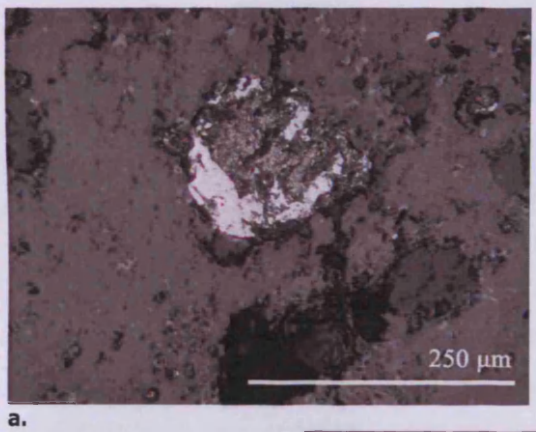

a.

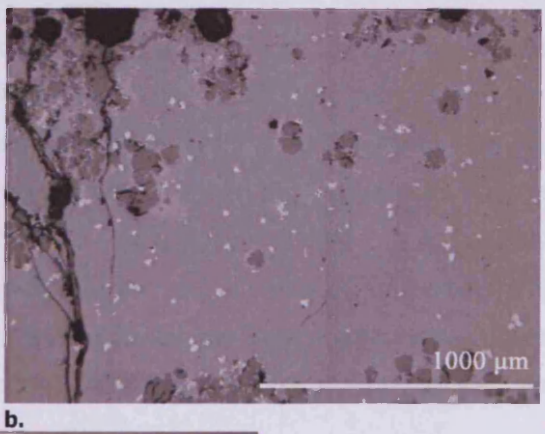

b.

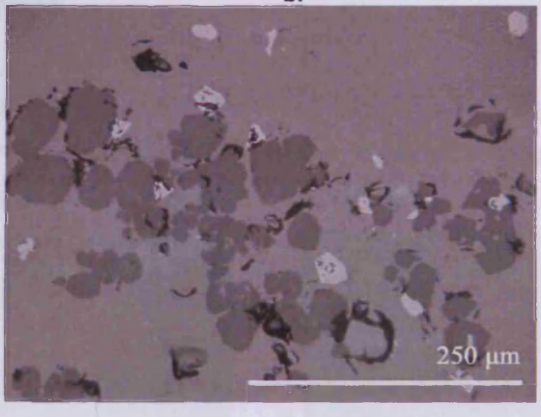

c.

Figure 11.20. Image a shows a partially reacted lead/lead sulphide prill embedded in the slag. This prill contains metallic lead in the centre (brown shiny area) and a halo of partially reacted lead sulphide (white). Image B illustrates the glassy which has very little porosity, embedded in glassy matrix are grey crystals and the white minerals which are lead sulphide inclusions. Crystalline phases are common in the sample; image c.

Sample 89 is a complex crystalline slag and has trapped gangue material. It is a lead silicate and contains remnant ore fragments rich in lead sulphide.

Scanned area	MgO	Al2O3	SiO2	K2O	CaO	FeO	ZnO	PbO
1	0.9	11.1	41.7	5.8	5.3	5.6	5.6	24.0
2	0.9	10.6	41.1	4.7	4.6	5.5	5.2	27.4
3	0.8	10.3	49.0	6.1	3.7	5.3	6.2	18.5
4	1.1	9.0	38.5	4.1	5.5	7.0	8.0	27.0
5	1.1	10.5	40.9	5.7	5.1	6.1	5.8	24.9
Average	**1.0**	**10.3**	**42.2**	**5.3**	**4.8**	**5.9**	**6.1**	**24.3**

Table 11.18. Bulk area analyses of slag sample 89. SEM-EDS data has been normalised to 100 wt%.

Slag sample 268B

Figure 11.21. UR 10 268B hand sample.

Slag sample 268B is a black, glassy slag (Figure 11.21). On the upper surface it has a brown/green sheen and the lower base is black with a texture indicating that the liquid slag may have been poured or tapped onto a soft surface. The cut internal surface is black and appears to have no macroscopic inclusions. Initial XRF analysis indicated that the slag consists of lead oxide, silica and iron oxide as its base components. Silver, antimony, alumina, sulphur, zinc oxide and phosphate were also recorded.

OM revealed that the slag has a vitreous glassy matrix which contains a lighter grey crystal phase, white (lead sulphide) prills and recrystallised minerals. The slag also has very small prills of lead metal scattered throughout the matrix.

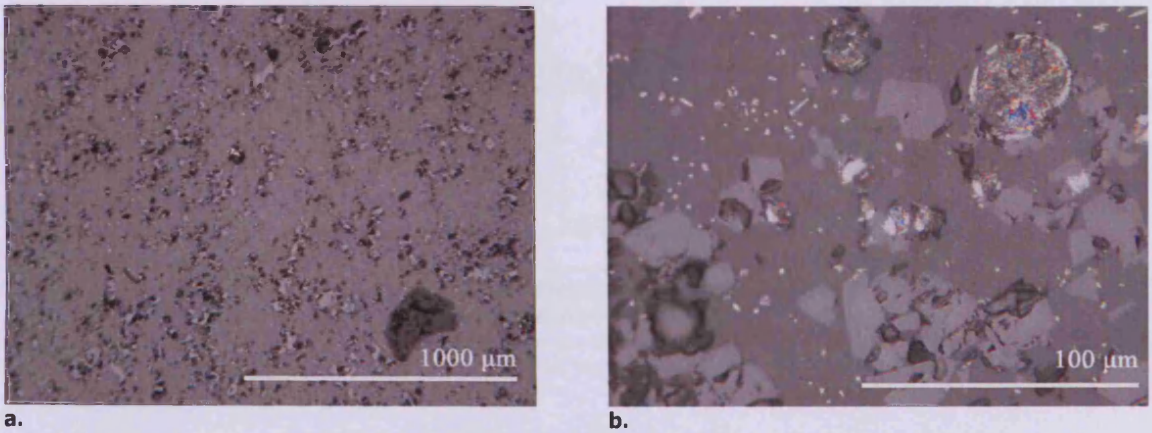

a. b.

Figure 11.22. UR10 sample 268B.
Sample 268B has a glassy slag body (a). The slag body reveals different crystalline phases in the slag. Lead prills and grey spinel crystals predominate in the slag matrix. Lead sulphide inclusions are dispersed throughout the slag (b).

SEM-EDS bulk area analyses indicate that it is comprised of lead oxide (49%), iron oxide (17%), silica (13%), antimony oxide (12%), zinc oxide (8%), and alumina (2%); (Table 11.19). The glassy slag matrix has a much higher lead oxide content (57%) and slightly increased silica and antimony oxide values (16%). Antimony is rare within the other slag samples, and to see 12 % within a general matrix is highly unusual. Iron and zinc oxide concentrations are the same (5%) (Appendix VII).

The lighter grey crystals observed in the OM were analysed on the SEM and they are composed of iron oxide (77%), zinc oxide (18%), alumina (4%), and trace quantities of antimony, tin, silica and titanium (Appendix VII). They are most likely a spinel phase. The brightest phases seen on the OM were confirmed as lead sulphide in the SEM-EDS. In the majority of spot analyses, the lead sulphide was pure but it was also found to contain up to 2 or 3 at% of copper, antimony, zinc and iron (Appendix VII).

Metallic prills analysed in the slag matrix ranged in their lead compositions from 93 at% - 40 at%. Silver was present and in one spot analysis 49 at% was measured. Antimony was also measured in the silver/lead alloys (9%), Table 11.20.

Scanned area	Al2O3	SiO2	K2O	FeO	ZnO	Sb2O3	PbO
1	1.6	12.7	0.6	17.8	7.9	11.6	47.9
2	1.7	12.7	~	17.5	7.3	12.0	48.8
3	1.6	12.7	0.4	15.7	7.3	12.1	50.1
4	1.7	12.5	~	18.0	8.1	11.8	48.0
5	1.7	13.3	~	16.0	7.5	12.1	49.4
Average	**1.6**	**12.8**	**0.2**	**17.0**	**7.6**	**11.9**	**48.8**

Table 11.19. Bulk area analyses (SEM-EDS) of slag sample 268B. The data has been normalised to 100 wt%.

Spectrum	Cu	Fe	Ag	Sb	Pb
1	~	~	4.8	2.0	93.2
2	~	~	39.2	9.1	51.7
3	1.4	~	48.8	9.4	40.4
4	~	2.8	39.1	10.6	47.6

Table 11.20. Metallic prills found within slag sample 268B. The data has been normalised to 100 at%.

Summary of UR10 slag samples

The UR10 slag samples have been categorised into two main groups according to their physical and chemical properties: Type I and Type II. Two samples remain outside of these groups: samples 89 and 268B (Table 11.21). Regardless of groupings, all the slags analysed are lead silicates containing lead and zinc sulphides, metallic lead prills, and different crystalline minerals. The primary differences between Type I and II are the quantities of lead and zinc. Type I slags contain higher lead oxide contents and less crystalline phases than Type II slags, which contain high levels of zinc sulphide and as a result have numerous zinc silicates in their silicate matrix.

Groups	MgO	Al2O3	SiO2	P2O5	SO3	K2O	CaO	MnO	FeO	ZnO	As2O3	Sb2O3	PbO
Type I (n=4)	0.0	2.9	21.6	~	~	0.8	0.8	0.3	7.1	4.2	~	0.3	62.1
Type II (n=4)	~	2.8	22.3	0.1	5.0	0.8	0.9	0.4	12.9	21.2	1.0	0.2	32.6
89	1.0	10.3	42.2	~	~	5.3	4.8	~	5.9	6.1	~	~	24.3
268B	~	1.6	12.8	~	~	0.2	~	~	17.0	7.6	~	11.9	48.8

Table 11.21. SEM-EDS bulk area analyses of all UR10 slag samples. Data has been normalised to 100 wt%.

The overall slag matrix contains heavy metals such as iron, zinc, arsenic and antimony, the quantities are variable but zinc and iron oxides are common between all of the samples. The heavy metals come from the ore selected for smelting and the variability between samples is attributed to the different ore minerals used in the smelt. The presence of sulphur in the majority of the metallic prills found in the slag also indicates the lead ore processed was sulphidic, and most probably lead sulphide.

In the majority of slags the conditions in the furnace appear to have promoted the formation of a glassy, fluid and oxidised slag containing very few metallic prills. This would indicate a clean separation of slag and metal, unlike the slag seen in Cuiza's *huayrachinas* used to produce lead, and archaeological *huayrachinas* used for silver production. The high level of lead in the system of the UR10 slag and the presence of silver in metallic prills suggests that these furnaces produced a silver/lead alloy.

Uruquilla 11 (UR11)

Uruquilla 11 (UR11) is the second of the three furnaces in the Uruquilla series. It is similar to UR10 in that it has a large hearth and a well preserved firebox. The firebox is constructed of 12 holes rather than slats as in UR10, and it is located on the east side of the furnace. The inside

layer of the furnace was constructed with adobe bricks and the outer layer constructed from natural rock. There is no evidence for a chimney.

Samples were taken from stratified layers during the 2005 excavations of this furnace. Five samples of slag were selected for analysis. The results of analyses from each of the five samples are presented below and a discussion of the characteristics and results of the UR11 slag group will then follow.

Slag sample 222A

Slag sample 222A is a vitreous black slag which appears to have very few inclusions (Figure 11.23). OM confirmed that this slag sample has a very glassy slag matrix which is studded with white recrystallised crystals (later identified in the SEM as iron/zinc oxides). Also embedded in the slag are small metallic prills (Figure 11.24)

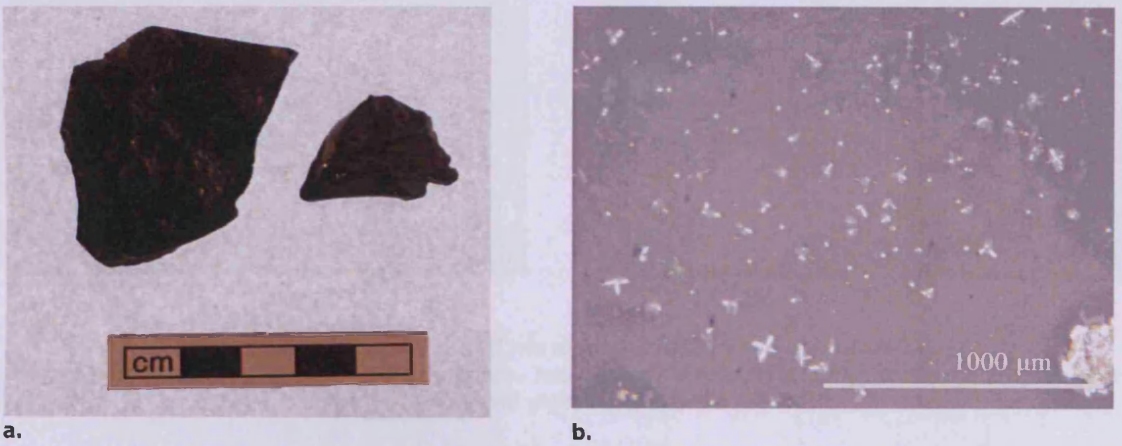

a. b.

Figure 11.23. UR 222A.
Hand specimen of slag sample UR11 222A (a). OM analyis of 222A shows a glassy slag matrix withe slag with lead sulphide prills (b).

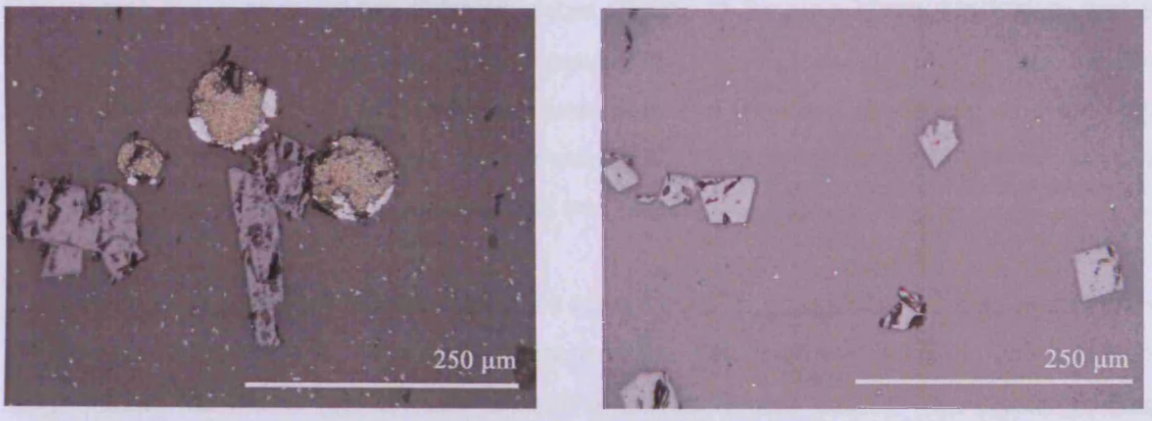

Figure 11.24. OM images of UR 222A.
OM image of 222A slag containing lead prills (yellow) and oxide crystals (light grey). (a). The 222A slag matrix with oxides (b).

SEM-EDS analysis shows that the slag is lead oxide with around 10 wt% each iron and zinc oxide (Table 11.22). The glassy slag matrix is compositionally similar to the overall bulk scans because the sample is very homogenous with very small crystalline and metallic inclusions (Figure 11.25). Metallic prills within the slag are lead based and some contain up to 7 at% silver. Four out of the seven prills analysed contain silver. One of the prills contained residual sulphur indicating that the ore used for smelting was a sulphidic lead ore.

Scanned areas	MgO	Al2O3	SiO2	P2O5	K2O	CaO	TiO2	FeO	ZnO	PbO
Average (n=)	0.5	3.2	22.6	1.2	1.2	3.0	0.3	10.7	8.9	48.5

Table 11.22. SEM-EDS bulk area scans of slag sample 222A. Data has been normalised to 100 wt%.

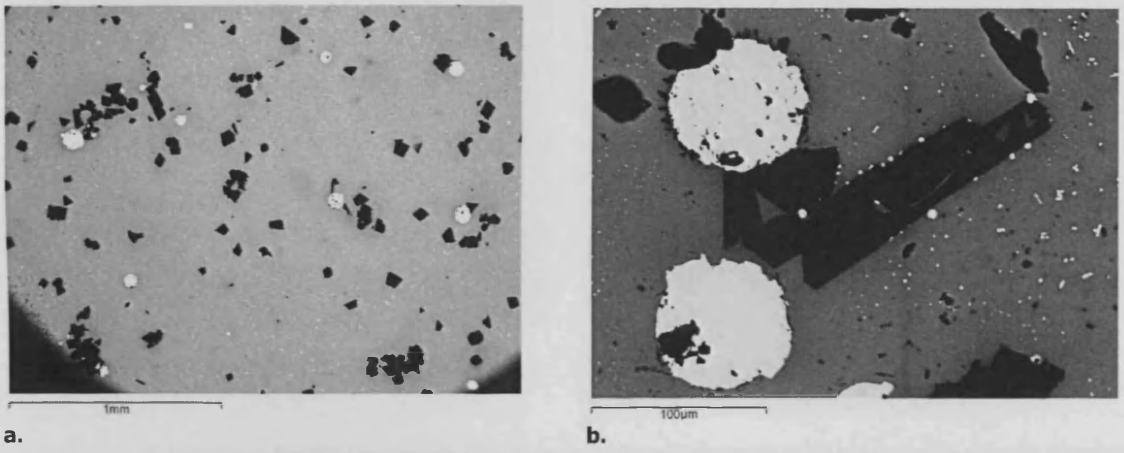

a. b.

Figure 11.25. SEM backscattered low magnification image of sample 222A (a). High magnification (b) showed that this sample has a glassy slag matrix (grey) scattered with iron-zinc oxides (black) and metallic lead prills (white).

Slag sample 251

Slag sample 251 consists of two different pieces (Figure 11.26 a): a glassy black slag, and a denser brown tinged slag with a light brown patina. The dense brown slag was chosen for OM and ED-XRF analysis. No metallic inclusions were visible in the hand specimens, and the slag had very few distinguishing features. Hand specimen ED-XRF analysis indicated that this sample is a lead silicate that also contains sulphur and iron oxide.

The OM revealed a multiphase microstructure consisting of a glassy/vitreous slag matrix with interspersed crystal phases. At low magnification, the slag appeared homogenous but high magnification the matrix had obvious crystalline phases (Figure 11.26). The crystal phases present in the matrix include: grey semi-euhedral crystals (crystallised within the main slag

body), white snow-flaked shaped lead sulphide dendrites, and metallic prills (Figure 11.26). These prills were lead metal with lead sulphide Figure 11.27 and Table 11.24.

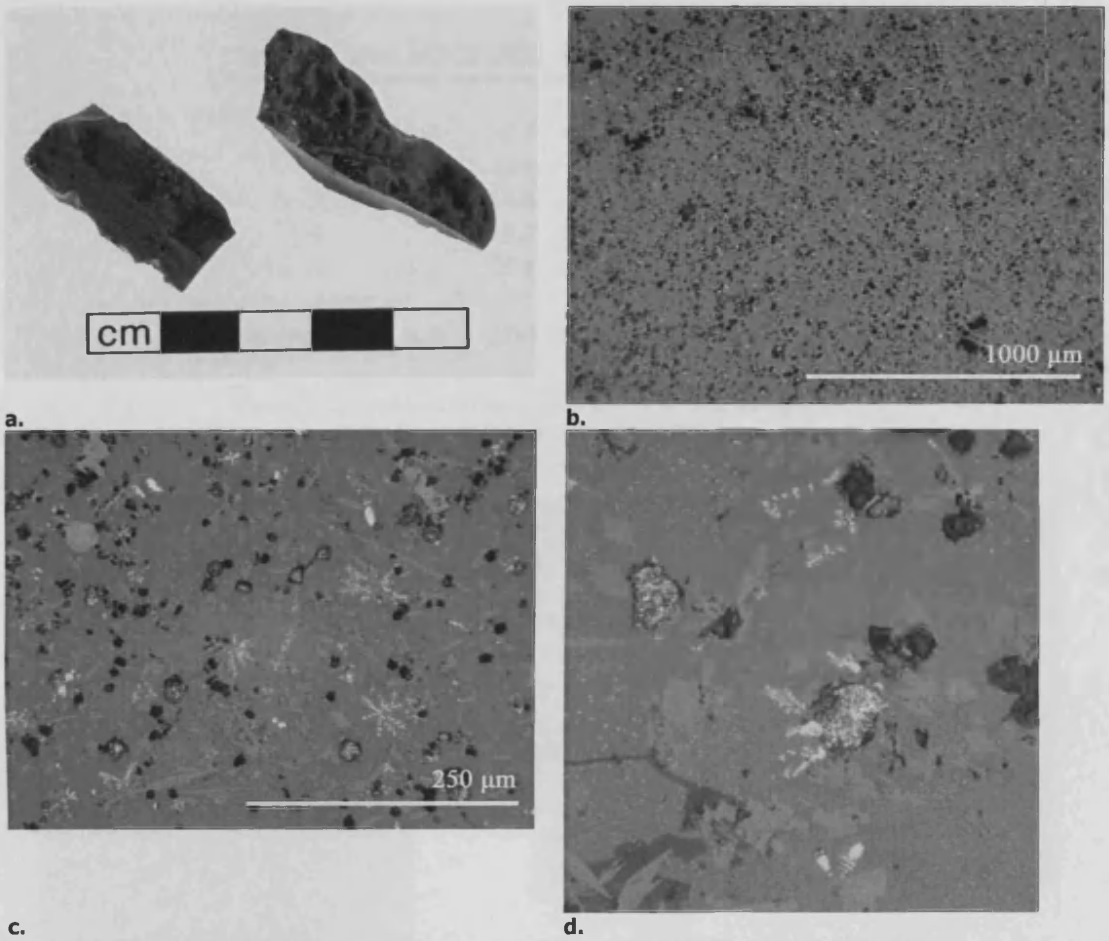

a. b. c. d.

Figure 11.26. Slag sample 251 comprises two samples (a)one of which is a layered slag sample (lower left) and a glassy slag (upper right).
OM of sample 251 indicated a glassy matrix studded with different crystal and metallic phases (b). Close up microscopy shows the slag matrix (mid grey) which contains different crystal inclusions: the lighter grey crystals forming from the slag matrix, white snow flake-like crystals of lead sulphide, and metallic prills (c and d, mag x500).

Bulk area analyses done using SEM-EDS showed that this sample was extremely high in lead oxide (71%). Silica (15%) and iron oxide (10%) made up the rest of the sample's composition. Smaller quantities of zinc oxide (2%), alumina (1%), and traces of lime and antimony were also measured (Table 11.23). Analysis of the slag matrix indicated that it contained less iron oxide only 4% then the bulk, and slightly increased lead oxide levels (76%), most probably due to iron being concentrated in spinels.

The grey silicates seen in the OM were analysed in the SEM and shown to be lead/iron silicates containing lead oxide (57%), iron oxide (19%), silica (15%), tin oxide (7%), and alumina (1%) (Table 11.23). General metallic prills analysed showed lead metal containing silver (7 at%) (Table 11.25). The metallic prill shown above (Table 11.24) was analysed using SEM-EDS; the prill consists of a lead metal matrix (SEM image white , OM image brown), lead sulphide (SEM

image dark grey, OM image brightest cream/white), and silver metal (99 at%) with small quantities of lead (1%) (SEM image mid grey, OM image purple grey).

Scanned area	Al2O3	SiO2	CaO	FeO	ZnO	Sb2O3	PbO
1	1.4	15.5	~	9.4	1.7	~	72.0
2	1.4	14.4	~	12.7	1.9	~	69.6
3	1.5	14.8	~	9.8	2.1	~	71.8
4	1.3	15.3	0.6	8.8	1.3	1.7	71.1
5	1.5	15.4	~	10.4	1.5	~	71.3
Average	**1.4**	**15.1**	**0.1**	**10.2**	**1.7**	**0.3**	**71.2**

Table 11.23. SEM-EDS bulk area scans of slag sample 251. Data has been normalised to 100 wt%.

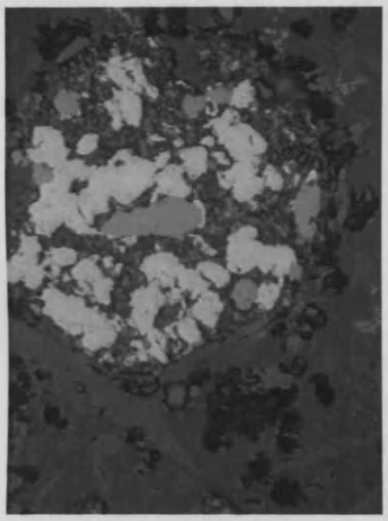

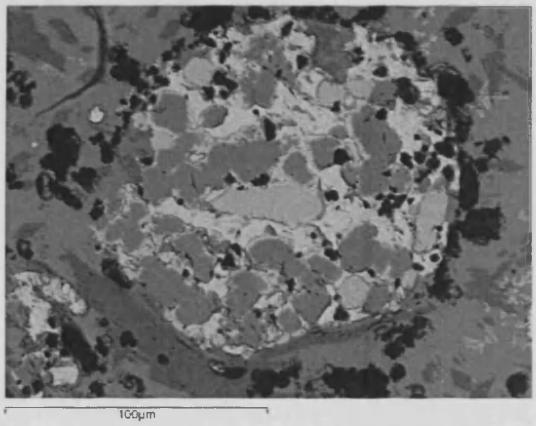

Spectrum	S	Ag	Pb
Light grey area	~	98.6	1.4
Whitest area	~	~	100.0
Mid grey	51.8	~	48.2

Table 11.24. SEM-EDS spot analyses of different metallic phases in Figure 8B. 6 (SEM image above).

a. **b.**

Figure 11.27. This prill found during OM in slag sample 251 has different metallic and sulphidic phases present (a OM image mag x500).
SEM-EDS analyses have shown that this prill has a matrix of lead metal (brown), a light grey phase (PbS), and white silver (a). The SEM backscattered image is shown on the right (b).

Spot analysed	S	Ag	Pb
1	~	8.4	91.6
2	51.0	~	49.0
3	~	7.1	92.9
4	51.0	~	49.0

Table 11.25. Lead metal and lead sulphide spot analysis in sample 251. Data has been normalised to 100 at%.

This slag sample is a lead rich silicate slag with very little zinc oxide. Most of the iron is present as iron and lead silicates. It has metallic inclusions that indicate the smelting of a lead sulphide containing silver.

Slag sample 259

Sample 259 is a black, extremely glassy slag. It has heavy ripples or flow lines that are visible on the upper surface (Figure 11.28) and a defined bottom which has small stones and debris impacted. This slag may have been tapped onto a textured surface as the base shows indentations from when the slag solidified. Internally, the slag appears to be very glassy and could be mistaken for obsidian. Macroscopically, small gas bubbles are present in the slag matrix but no other inclusions can be seen. XRF analysis of the hand specimen indicated the predominance of lead oxide with silica, sulphur, iron oxide and alumina making up the rest of the composition. OM correlated with the macroscopic observation, the slag has very few crystalline inclusions. It is composed of a dense glassy slag matrix (light grey) and very occasionally it has small white crystal inclusions, probably lead sulphide (Figure 11.28).

a.

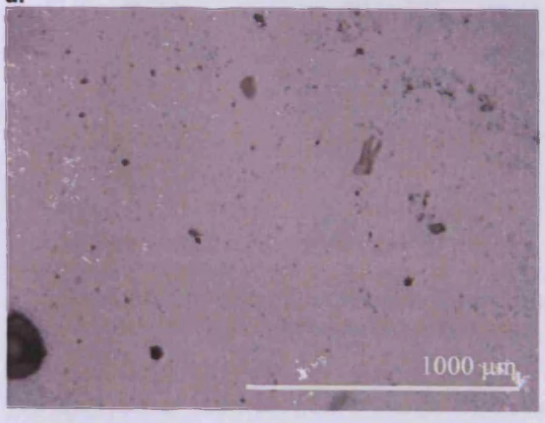

b.

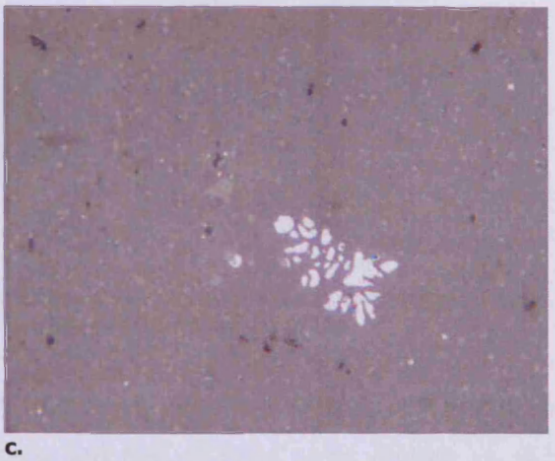

c.

Figure 11.28. OM images of UR11 29.
The hand specimen of slag sample 259 has a rippled outer surface (a). The OM showed that the sample is extremely glassy and contains very few crystalline inclusions (b). However, some white crystals of lead sulphide were found in the matrix of the slag (c - mag x500).

Bulk area analyses using SEM-EDS showed that the slag has a very high concentration of lead oxide. The rest of the sample consists of silica, iron oxide, zinc oxide, alumina and lime, and potash (Table 11.26).

Scanned area	Al2O3	SiO2	K2O	CaO	FeO	ZnO	PbO
Average (n=5)	2.3	17.9	0.9	1.8	5.8	3.0	68.3

Table 11.26. SEM-EDS bulk area scans of slag sample 259. Data has been normalised to 100 wt%.

The white crystals noted in the OM were confirmed during the SEM-EDS analyses as lead sulphide. One of the small lead sulphide particles also had some silver present in the spot analysis.

Slag sample 263

Slag sample 263 was selected from a bag of slag collected from the same excavation layer. The slags are black and appear to be less glassy than the other slags analysed from the UR11 site. On the surface they are encrusted, have a pitted texture, and some have small ripples (Table 11.26). One piece was selected to represent all the slags in this sample set and labelled sample 263. Once cut and mounted, macroscopically, the sample's internal surface revealed a number of different gangue inclusions. It has a very thin brown patina (Table 11.26). Initial XRF analysis indicated that the sample contained silica with lead oxide, alumina, iron and zinc oxide, lime and potash.

a. b.

Figure 11.29. Samples from the same stratigraphic layer and labelled as a group 263 (a). Mounted slag sample 263 taken from the collection of 263 slags (b).

OM analysis of sample 263 showed that the slag matrix has very few metallic inclusions. In some areas it is porous but the majority is vitreous and free of large pores (Figure 11.30). Several prills are present in the slag and contain multiple phases (Figure 11.31). They appear to be quite blue in the OM, which may indicate the presence of copper in the prills.

SEM-EDS analysis of the bulk area confirmed the initial XRF analysis, this slag is composed of lead silicate with relatively low levels of iron and zinc oxide (5%), alumina (4%), lime and potash (1%); (Table 11.27). Analysis of a metallic prill within sample 263 (Figure 11.31) show that lead/copper/silver sulphide (area 3) was used to produce silver metal (area 1). A small area of lead sulphide is also present, and within this a silver metallic prill. The majority of the prill is composed of silver-copper sulphide (Table 11.28).

Only one sample was prepared for pellet analyses (sample 263) {see appendices for data} the bulk composition showed that it is composed of lead oxide, silica and sulphur.

Scanned area	Al2O3	SiO2	K2O	CaO	FeO	ZnO	Sb2O3	PbO
1	3.5	24.5	0.5	0.9	4.3	4.8	2.1	59.4
2	3.3	24.2	0.6	0.5	4.5	6.0	~	60.9
3	3.5	24.7	0.7		4.6	5.6	~	61.0
4	3.4	24.9		0.6	4.9	5.1	~	61.1
5	3.9	25.5	0.7	0.5	4.4	5.7	~	59.4
Average	**3.5**	**24.7**	**0.5**	**0.5**	**4.5**	**5.4**	**0.4**	**60.4**

Table 11.27. Bulk area analyses of sample 263. SEM-EDS data has been normalised to 100 wt%.

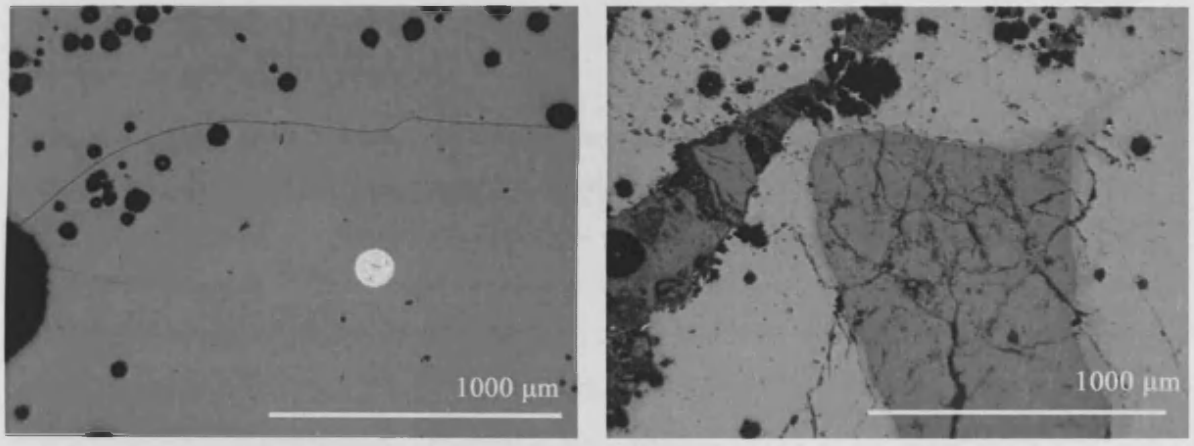

a. b.

Figure 11.30. OM analysis of slag sample 263 shows that the slag matrix is very glassy, only one large metallic prill was found (a). Slag sample 263 also contains residual gangue crystal inclusions (mid grey/brown phase) (b).

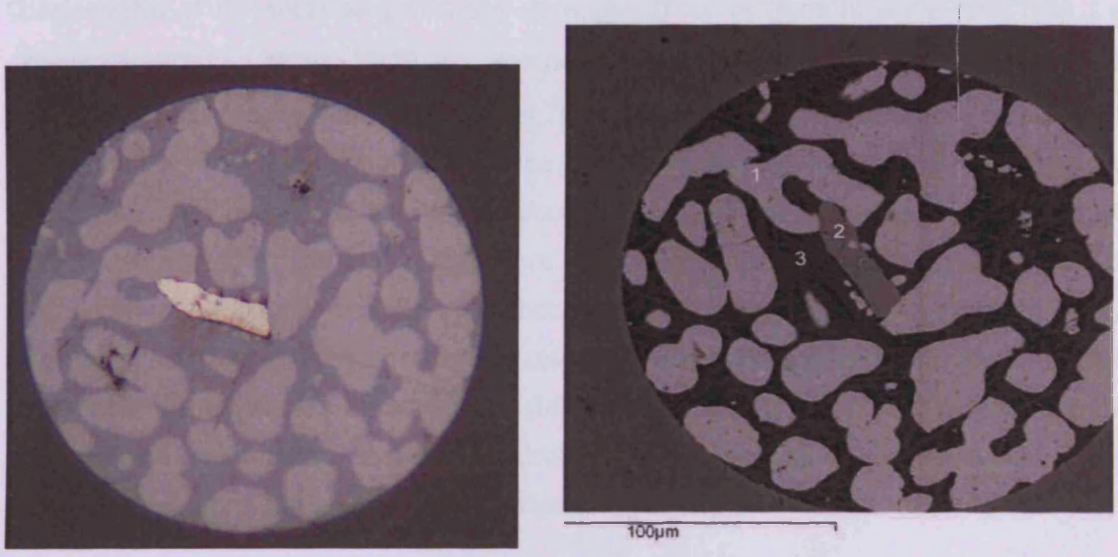

Figure 11.31. A complex metallic prill found in sample 263 (left -mag x500). SEM backscattered image of a prill containing lead sulphide (1), silver (2), and silver/copper sulphide (3).

Spot analyses	S	Cu	Ag	Pb
1 – lead sulphide	50.9	2.7	~	46.4
2 – silver	~	2.5	97.5	~
3 – silver copper sulphide	34.5	33.2	32.4	~

Table 11.28. Different metallic phases present in Figure 11.31 slag sample 263.

Summary of UR11 slag analysis

Four slag samples from the UR11 site have been analysed using OM, SEM-EDS and ED-XRF analyses. The slag from this assemblage is very vitreous and relatively pure with few inclusions. SEM-EDS analyses of the UR11 samples show that the slags are composed of lead oxide (49-71 %), silica (15-25 %), iron and zinc oxides (5-11%; 2-9%). Small amounts of antimony and titanium oxides were also recorded (Table 11.29). The high level of lead oxide in the slag system would indicate that the metal being produced was lead, while the repeated occurrence of silver-rich prills demonstrate the richness of this metal.

The lime, alumina and phosphate content showed that these quantities are relatively variable. The relatively high concentration of iron, zinc, tin and antimony in the slag would indicate the starting ore. Lime, alumina and phosphate may also have originated from the ore. It is highly likely that the starting ore was sulphidic as sulphur was regularly recorded in the bulk composition and in prills found within the slag samples. Lead sulphide was found in all four samples and copper-silver sulphide was recorded in sample 263 (Table 11.28).

Consideration of the UR11 slag analyses show that three of them fit within the Type I slag category established by the UR10 slag analyses (Table 11.29 and Table 11.30). The OM and SEM analyses confirmed that these samples had a lead rich silicate matrix with few crystalline inclusions. The high level of lead seen in the slag would indicate a lead rich mineral vein that would have been mined and used for smelting. Metallic prills analysed within the UR11 slags have shown that silver and lead metals were the predominant metals produced. Sample 222A falls in between Type I and Type II and therefore remains separate. The correlation between slags from UR10 and UR11 is significant because it indicates that, despite the design difference observed in the archaeological excavations (i.e. different firebox designs and placement), these changes have not affected the technological efficiency/workings of the furnaces. The slag analysed does not reflect these stylistic changes.

Sample	MgO	Al2O3	SiO2	P2O5	K2O	CaO	TiO2	FeO	ZnO	Sb2O3	PbO
222A	0.5	3.2	22.6	1.2	1.2	3.0	0.3	10.7	8.9	~	48.5
251	~	1.4	15.1	~	~	0.1	~	10.2	1.7	0.3	71.2
259	~	2.3	17.9	~	0.9	1.8	~	5.8	3.0	~	68.3
263	~	3.5	24.7	~	0.5	0.5	~	4.5	5.4	0.4	60.4
Average	**0.1**	**2.6**	**20.1**	**0.3**	**0.7**	**1.4**	**0.1**	**7.8**	**4.7**	**0.2**	**62.1**

Table 11.29. SEM-EDS bulk area analyses from UR11 slags taken from SEM-EDS data. The data has been normalised to 100 wt%.

Sample	MgO	Al2O3	SiO2	K2O	CaO	MnO	FeO	ZnO	Sb2O3	PbO
253A	0.1	3.3	24.8	0.8	0.4	~	5.4	6.6	0.8	57.8
253B	~	3.5	25.3	0.9	0.8	~	4.7	5.6	0.3	58.8
263	~	3.5	24.7	0.5	0.5	~	4.5	5.4	0.4	60.4
209	~	1.9	17.3	~	0.2	1.0	12.4	1.7	~	65.5
254	~	2.9	18.9	1.5	1.8	~	6.0	2.8	~	66.1
259	~	2.3	17.9	0.9	1.8	~	5.8	3.0	~	68.3
251	~	1.4	15.1	~	0.1	~	10.2	1.7	0.3	71.2

Table 11.30. SEM-EDS bulk area analyses from UR10 (black) and UR11 (red). These samples have been classified as Type I – lead rich slags. The data has been sorted according to lead oxide content.

UR12

Uruquilla 12 (UR12) is the third and final furnace in the Uruquilla series. It is the worst preserved furnace of the series. Very little evidence remains to indicate its original shape. However, two or three holes indicate the firebox may have been similar to UR 11. There is no evidence of a chimney.

Samples were taken from stratified layers during the 2005 excavations of this furnace. Three slag samples were selected for analysis. The results of analyses from each of the three samples are presented below, and a discussion of the characteristics and results of the UR12 slag group will then follow.

Slag sample 293

Sample 293 is a black vitreous slag. OM shows that the slag is composed of a glassy matrix which has metallic and crystalline inclusions (Figure 11.32). Analysis of the metallic prills within the glassy matrix indicated the prills are multi-phase containing lead, silver and in the majority of prills a halo of sulphides (Figure 11.32). Within the slag matrix large residual/partially reacted ore minerals are present (Figure 11.33).

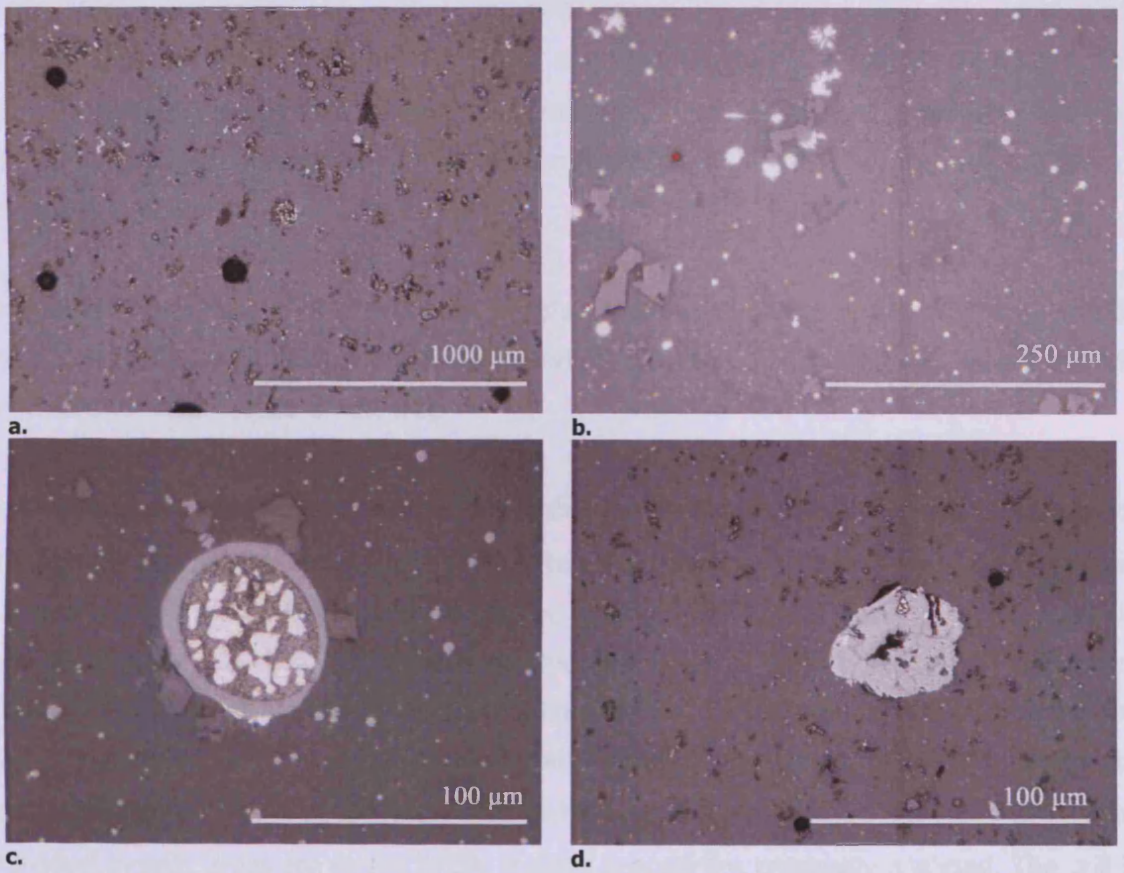

Figure 11.32. Slag sample 293 has a very glassy silicate matrix (a). Metallic prills are loosely scattered in the matrix (b). Close up OM taken at mag x500 showed droplets of lead sulphide prills (c and d).

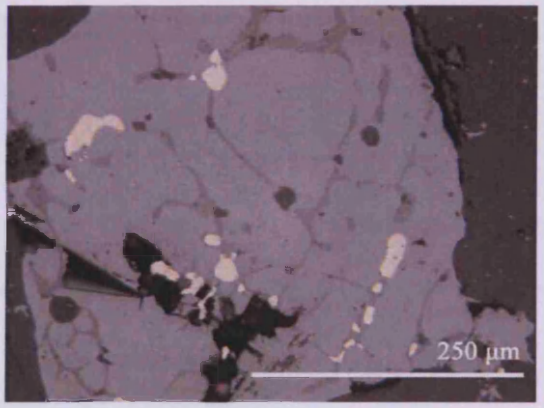

Figure 11.33. OM image of ore minerals in the slag sample 293 – zinc sulphide with lead sulphide inclusions.

SEM images (Figure 11.34 and Figure 11.35) confirmed that the sample has a glassy silicate matrix with inclusions of iron/zinc oxides and metallic prills. The sample is composed of predominately lead oxide (72%) with a remaining composition of silica (16%), iron oxide (5%), zinc and antimony oxide (2%), alumina (2%), and trace quantities of lime (Table 11.31). The silicate matrix shows very little variation from the overall bulk analyses. The similarity between the matrix and bulk analyses is due to the homogeneity of the slag, i.e. the low quantity of mineral inclusions.

Embedded in the lead silicate matrix are angular crystals composed of complex iron/zinc rich oxides (Appendix VII). Also interspersed in the lead silicate matrix are lead silicate crystals which are common in lead silicate slag.

Several residual ore minerals are embedded in the slag matrix. Figure 11.34 is an SEM image of one partially reacted ore area, showing five different phases (A-E). Four of these areas contain substantial amounts of sulphur, and they can be classified as lead sulphide (A), copper sulphide with some silver (15 at%, C), partially reacted lead sulphide (D), lead, copper, and silver sulphide (E). Silver (B) was also found indicating that the ore had partially reacted during the smelt. This slag sample also contains metallic prills dispersed throughout the matrix. Analysis of one of these prills (Figure 11.35) has shown that they contain lead, silver, copper, and sulphur. Individual metallic areas are similar to the residual gangue ore previously analysed. The prill is composed of five main areas ranging from partially reacted lead sulphide (A), metallic silver (B), copper silver sulphide (C), reacted lead sulphide and gangue minerals (D/E), Table 11.34.

Scanned area	Al2O3	SiO2	CaO	FeO	ZnO	Sb2O3	PbO
1	2.1	16.2	0.8	5.1	2.1	2.8	71.1
2	~	16.2	0.7	5.1	2.0	2.0	73.9
3	2.0	16.2	0.7	5.2	2.3	2.4	71.2
4	1.9	15.9	~	5.5	2.3	1.7	72.7
5	2.2	16.2	~	6.1	2.7	1.9	70.9
Average	**1.6**	**16.2**	**0.4**	**5.4**	**2.3**	**2.2**	**71.9**

Table 11.31. Bulk area scans of slag sample 293.
Data has been normalised to 100 wt%.

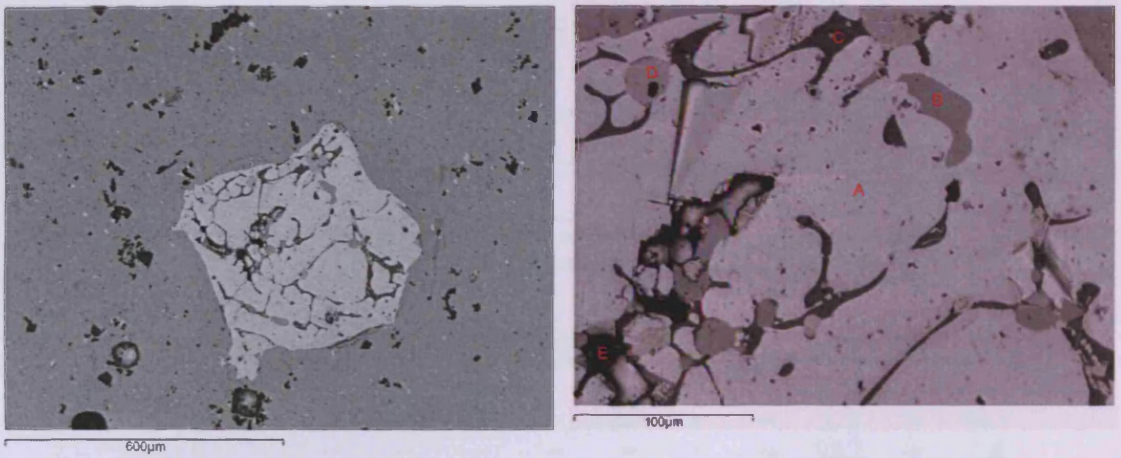

a b

Figure 11.34. SEM backscattered image of lead sulphide inside slag sample 293.
Note the black iron/zinc oxides crystals formed in the surrounding lead silicate matrix (a). Close up of the inclusion (b); silver, copper, and lead sulphide were all recorded

Spot analysis	Si	S	Cu	As	Ag	Sb	Pb
A - Lead sulphide	~	51.1	0.7	~	~	~	48.3
B - Silver	~	1.2	1.1	~	95.8	~	1.9
C - Copper sulphide with silver	~	40.7	44.1	~	15.2	~	
D - Partially reacted lead sulphide	4.2	17.4		2.7	~	4.8	70.9
E - Lead, copper and silver sulphide	~	34.7	15.2	~	18.5	~	31.6

Table 11.32. Analytical date from residual ore minerals in Figure 11.34.
Data has been normalised to 100 at%.

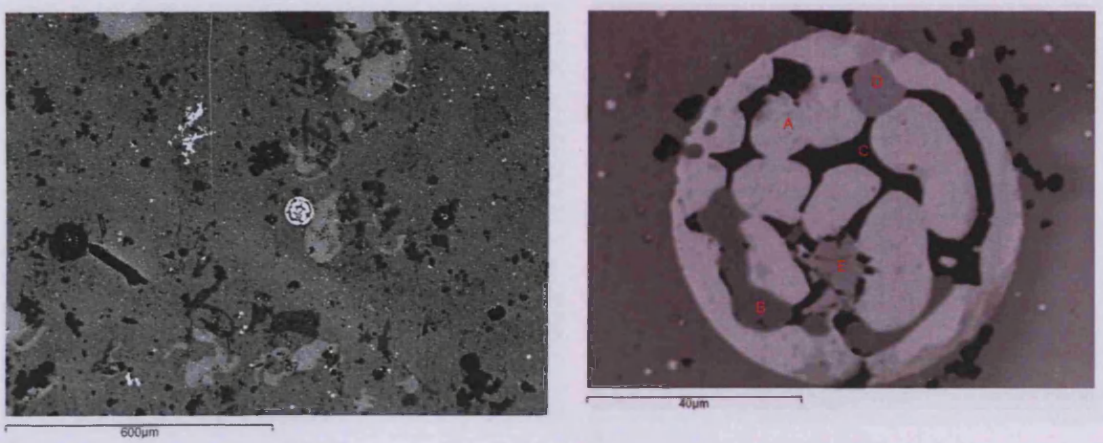

a. b.

Figure 11.35. SEM image of slag sample 293, a large sulphide prill is embedded in the matrix (a) and a close up view where analyses was undertaken (b).

Scanned area	S	Cu	Ag	Pb
Total area	40.7	12.4	16.9	30.0

Table 11.33. Total area scan of the metallic prill seen in Figure 11.35. Data has been normalised to 100 at%.

Spot analyses	Al	Si	S	Fe	Cu	Zn	As	Ag	Sb	Pb
A	~	~	49.4	~	2.7	~	~	1.2	~	46.7
B	~	~	~	~	~	~	~	98.2	~	1.8
C	~	~	38.6	~	42.6	~	~	18.8	~	~
D	2.3	14.2	9.0	2.9	~	4.2	1.8	~	5.5	60.1
E	~	4.6	26.6	~	12.0	~	1.5	4.1	1.3	49.9

Table 11.34. Spot analysis on a metallic prill found in slag sample 293 (Figure 11.35.). Data has been normalised to 100 at%.

Slag sample 297

Slag sample 297 is very similar to 293, a black vitreous slag with no visible metallic inclusions. Hand specimen XRF analyses showed that the slag was lead based with high quantities of zinc oxide, silica, alumina and iron oxide. The OM showed a glassy slag matrix with very scarce metallic prills and other mineral inclusions dispersed throughout the matrix (Figure 11.36). Like slag sample 293, gangue minerals are also present.

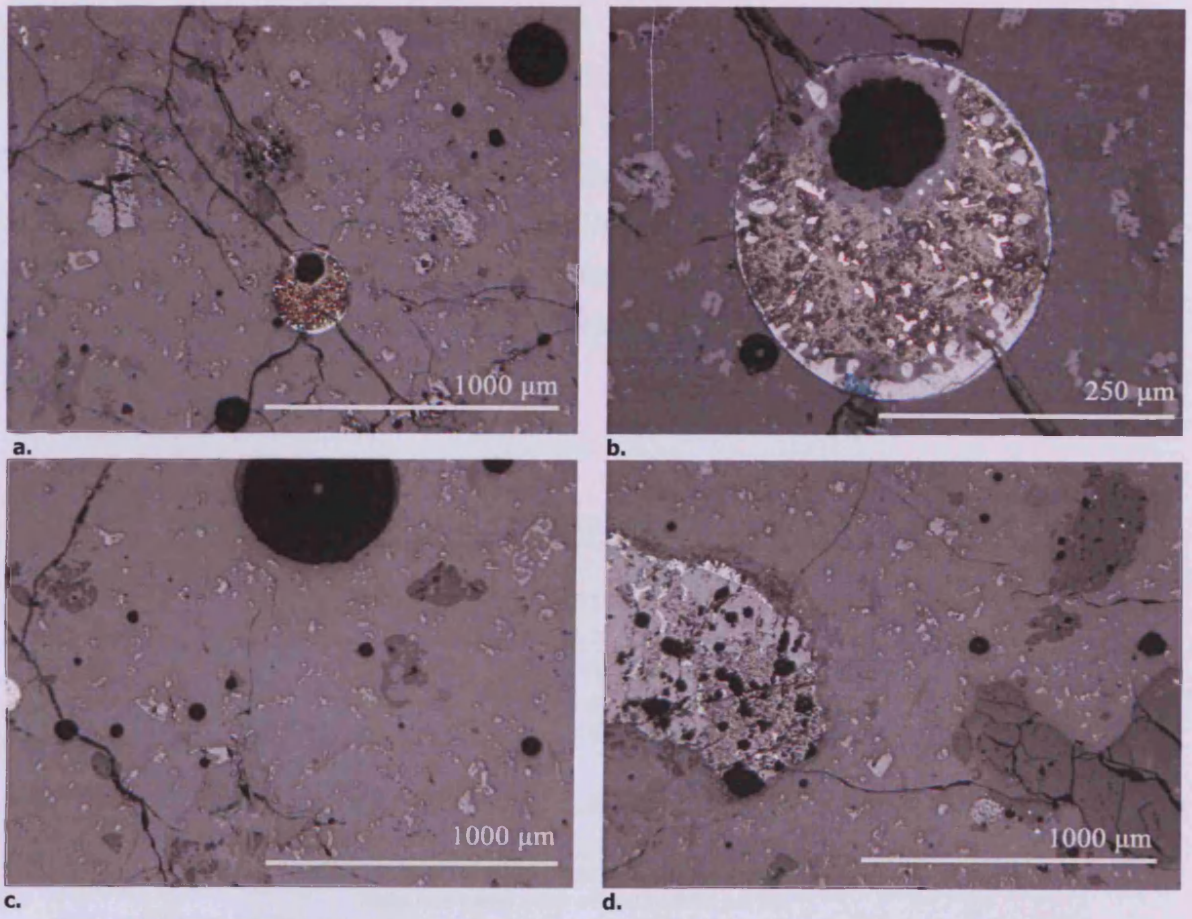

Figure 11.36. The bulk area scans showed that sample 297 has a glassy matrix (a and c) with the occasional metallic prill (b). Gangue inclusions of zinc sulphide (light grey) and quartz (dark grey) were also common (d).

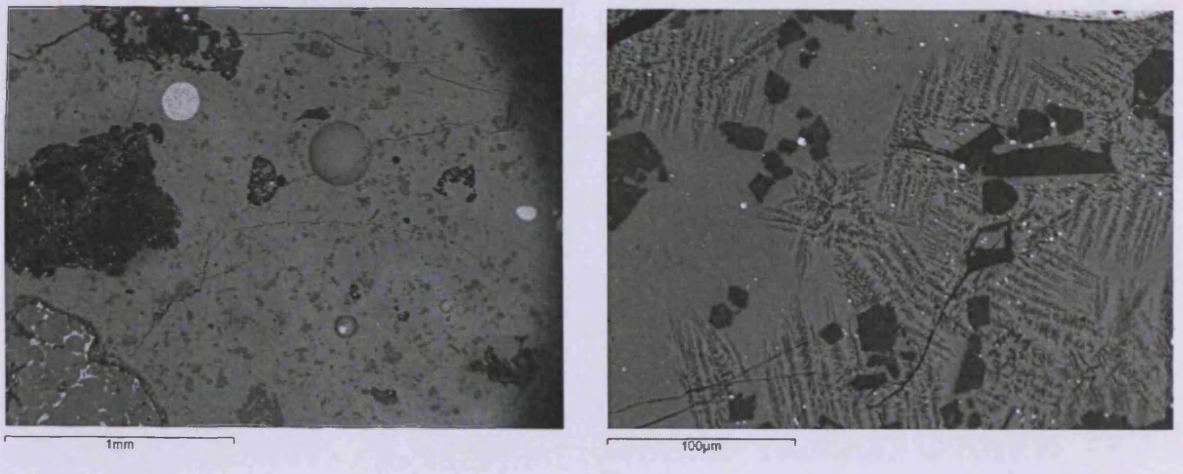

Figure 11.37. Image a shows a typical area used for bulk SEM-EDS area analyses. Image b: Zinc silicates in the slag matrix of sample 297. The darker black crystals are zinc silicates, mid grey crystals to the left of the image (smaller and more cubic) are zinc/iron oxides.

SEM-EDS bulk analyses confirm that the slag is a lead silicate with relatively low lead oxide, silica (33%), iron oxide (14%), zinc oxide (11%), lime, potash, and phosphate (2%). Sulphur was also recorded in the sample (Table 11.35). The slag is composed of five main components: the glassy slag matrix, metallic prills, zinc silicates found in the slag matrix, iron/zinc oxides, and gangue minerals embedded and partially reacted in the slag (Figure 11.37).

Scanned area	MgO	Al2O3	SiO2	P2O5	SO3	K2O	CaO	FeO	ZnO	PbO
1	~	5.4	32.7	2.1	~	2.3	3.0	14.1	10.0	30.4
2	~	4.8	32.5	2.1	~	1.9	3.1	13.8	10.2	31.8
3	~	6.2	34.5	1.4	3.3	2.5	2.4	12.2	9.8	27.6
4	0.8	4.5	31.5	1.6	1.7	1.9	2.9	15.1	11.3	28.9
5	~	5.8	33.0	1.6	~	2.4	2.8	13.4	11.3	29.8
Average	**0.2**	**5.3**	**32.8**	**1.8**	**1.0**	**2.2**	**2.8**	**13.7**	**10.5**	**29.7**

Table 11.35. Bulk scan analyses of slag sample 297. Data has been normalised to 100 wt%.

The slag silicate matrix and the overall bulk composition show very little variability between the major components. Zinc silicates (Figure 11.37), iron/zinc oxides, and leucite form the silicate matrix. Gangue particles were recorded in the silicate matrix and a close up of the gangue. Zinc silicates, zinc sulphide, lead sulphide, and lead metal were also all present in this partially reacted ore mineral (Figure 11.38). The prills found in the slag reflect the minerals found in the gangue particles.

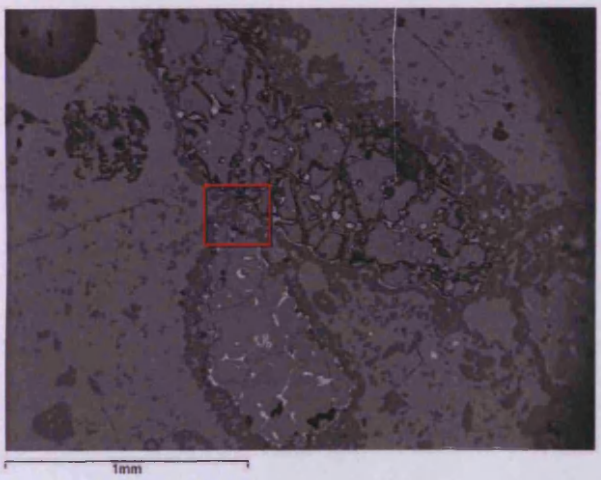

A = Zinc silicates
B = Zinc sulphide
C = Leucite
D = Lead metal
E = Lead sulphide
F = Slag matrix

a.

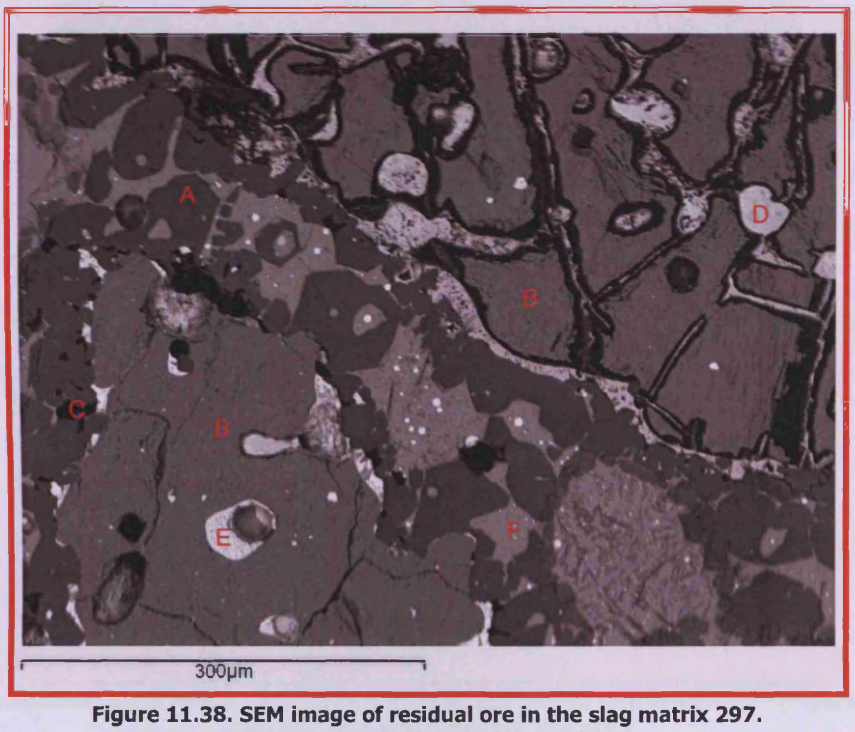

Figure 11.38. SEM image of residual ore in the slag matrix 297. Image b is a magnified area of the residual ore.

Two prills were recorded in detail. The first has less than 100 µm in diamter a base of lead and zinc sulphide (Figure 11.39). The zinc sulphide areas contain copper, iron (3%) and silver (6%); Table 11.36 (area B). Furthermore, they also contain various alloy mixtures of lead and silver metal (labelled in Figure 11.39 as areas C and D). Lead metal appears to form around the outside of the prill and contains 8% silver (area E).

The second prill analysed is almost 300 µm in diameter (Figure 11.40). It also has multiple metallic phases. Lead sulphide areas were found on the outer halo of the prill. Inside the prill shown in Figure 11.40 (b), lead metal with 9% silver was analysed (area A), small islands of

metallic silver (areas Band D) had formed within the lead metal. Silicon carbide crystals are embedded in the soft lead metal from the polishing process (Table 11.37).

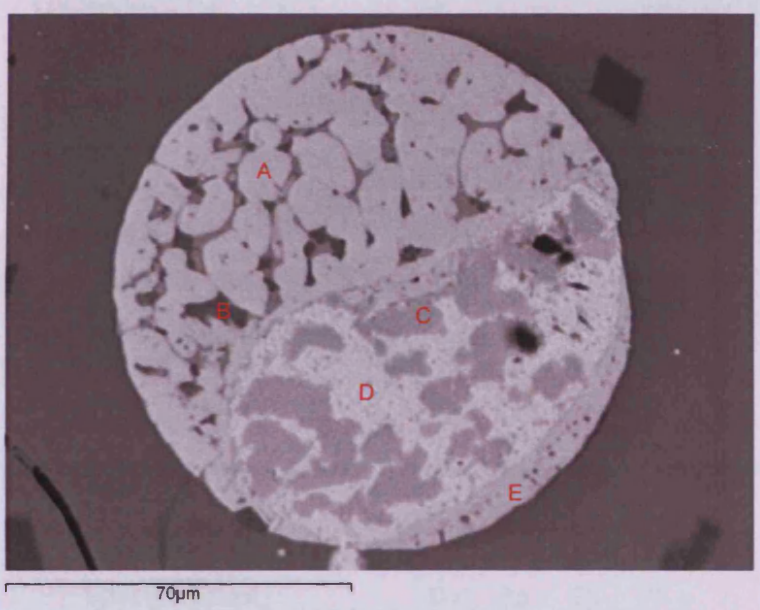

Figure 11.39. A metallic prill found in the slag 297.

Spot analyses	S	Fe	Cu	Zn	Ag	Sb	Pb
A - lead sulphide	53.6	~	~	~	~	~	46.4
B – zinc sulphide	55.6	3.8	2.9	30.5	5.9	~	1.3
C – lead/silver metal	~	~	~	~	49.8	4.5	45.7
D - lead/silver metal	~	~	~	~	58.3	8.2	33.6
E – lead metal	~	~	~	~	7.6	~	92.4

Table 11.36. Analysis of metallic phases in a metallic prill within slag sample 297 (Figure 8B. 14). Data has been normalised to 100 at%.

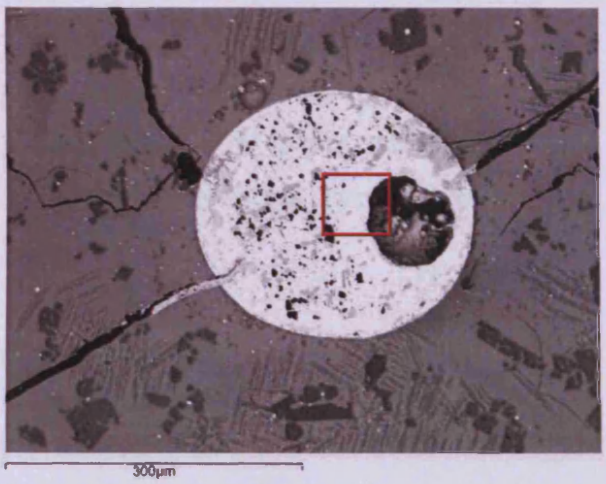

a.

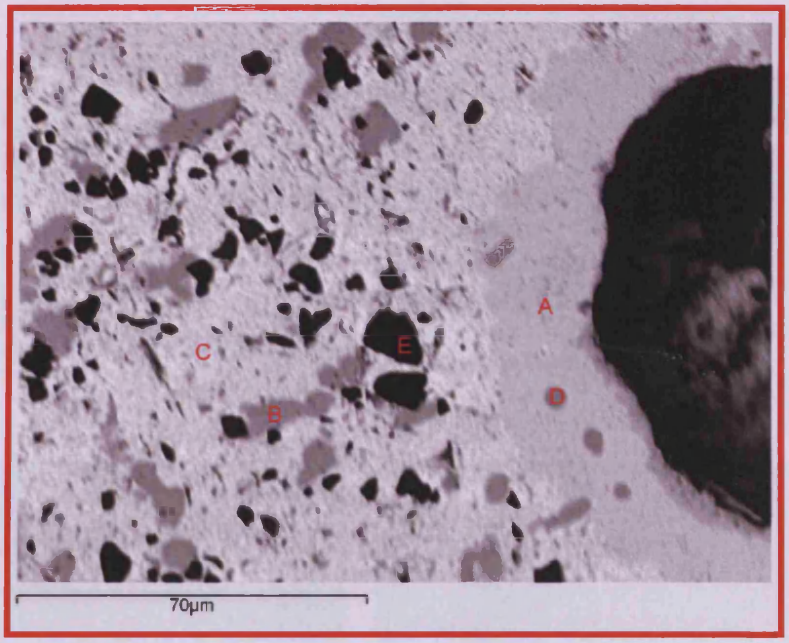

b.

Figure 11.40. Prill 2 embedded in slag sample 297 (image a). Image b is a magnified image of prill 2.

Spot analyses	Cu	Ag	Sb	Pb
A – Lead metal with silver	~	8.8	~	91.2
B – Silver metal	0.8	94.7	3.3	1.3
C – Lead metal	~	5.3	~	94.7
D – Silver metal	~	94.6	3.5	1.9
E – Silicon carbide crystal	~	~	~	~

Table 11.37. Spot analyses of prill 2 found in slag sample 297 (Figure 11.40). Data has been normalised to 100 at%.

Slag sample UR12 298

Sample 298 is a black vitreous slag. It is light to the touch and has flow lines on the outer structure (Figure 11.41a). No metallic prills were visible on the surface. OM revealed a slag matrix that is extremely glassy with a few metallic prills and almost no other crystalline phases (Figure 11.41b). The largest metallic prill has a complex microstructure and a blue colour indicating the presence of copper (Figure 11.41c).

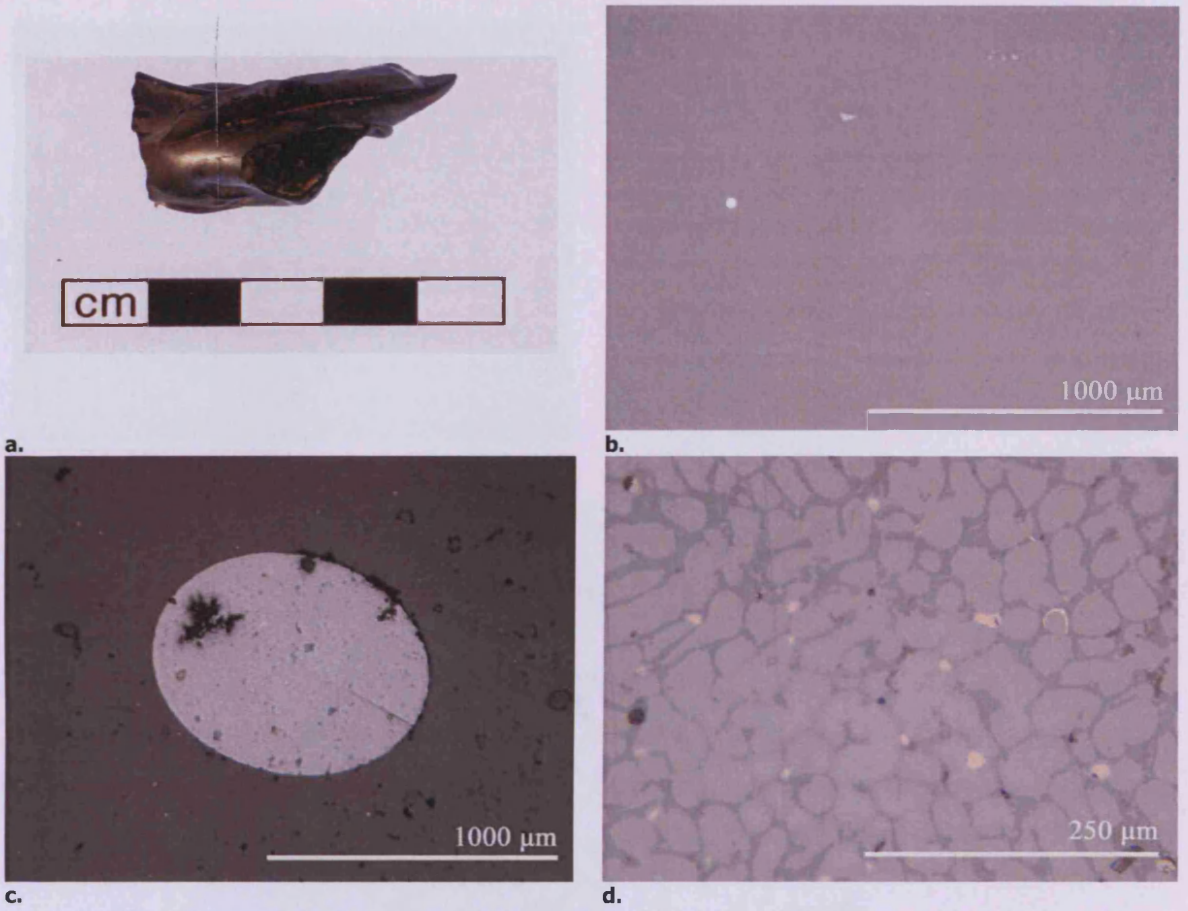

Figure 11.41. Hand specimen of slag sample 298 (a). OM showed that the slag was extremely glassy (b) and contained one large metallic prill (c). Close magnification of the prill indicated multi-metallic phases (d).

The SEM-EDS analysis shows that the slag is predominantly lead oxide (45%) with silica (31%), and iron oxide (11%) making up the rest of the composition (Table 11.38). Smaller quantities of alumina, zinc oxide, potash, phosphate, lime and manganese were also recorded. Analysis of the prills found in the slag showed that they still contain a large quantity of sulphidic components. The largest prill was analysed (Figure 11.42) and was found to be lead-copper sulphide (area 2 Table 11.39) with little silver present. An overall area scan indicated that only 2 at% silver was present. Copper sulphide appeared within the grain inter-fills (area 3); Figure 11.42. Nickel and antimony were also recorded in other metallic prills.

Scanned area	Al2O3	SiO2	P2O5	K2O	CaO	MnO	FeO	ZnO	PbO
1	3.3	31.0	1.7	1.1	1.9	0.9	11.9	3.2	45.1
2	3.3	32.0	1.6	0.9	1.9	0.8	10.7	3.1	45.8
3	3.5	32.2	1.3	1.0	1.9	0.8	10.1	3.4	45.8
4	3.0	30.6	1.5	1.0	2.1	0.8	12.1	4.1	44.9
Average	**3.2**	**31.4**	**1.5**	**1.0**	**2.0**	**0.8**	**11.2**	**3.4**	**45.4**

Table 11.38. Bulk area analyses of slag sample 298. The data has been normalised to 100 wt%.

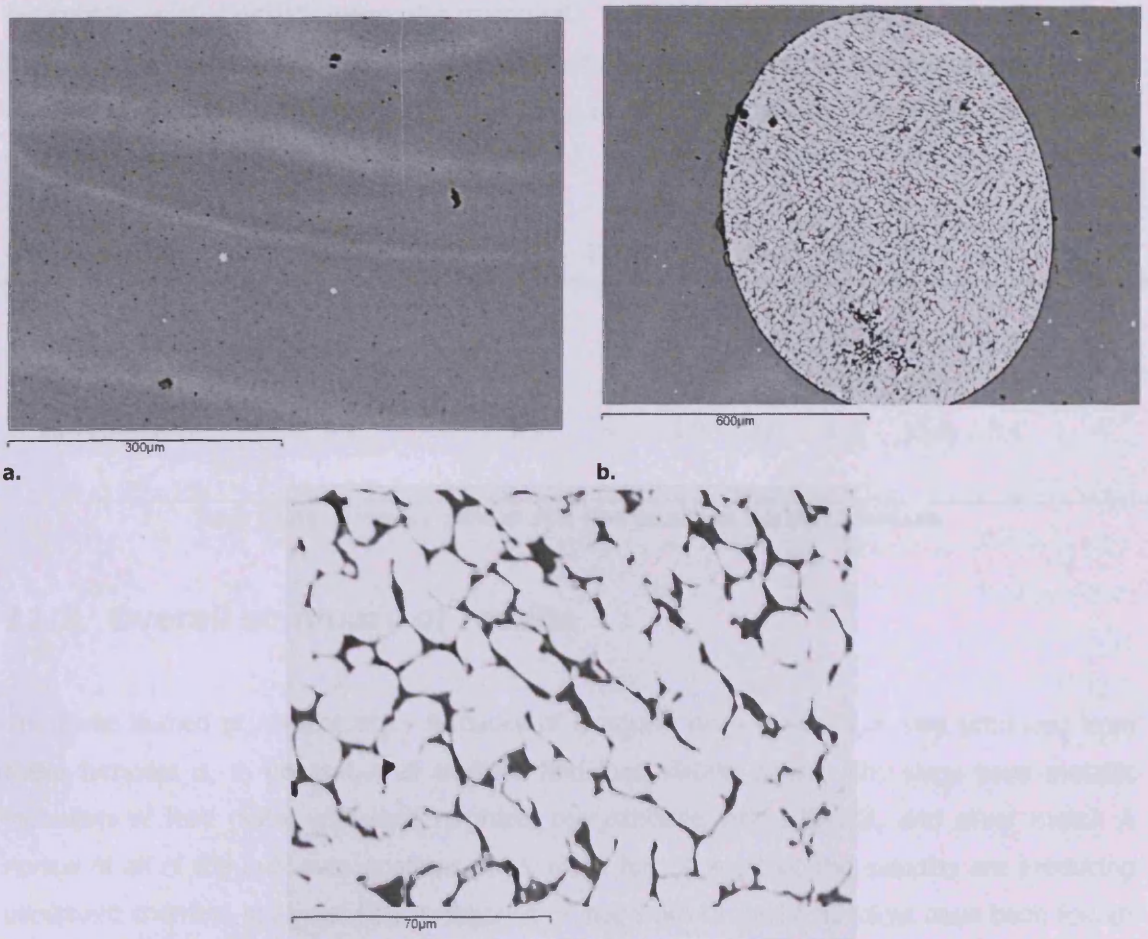

Figure 11.42. Slag sample 298 has a very glassy matrix with very few inclusions as seen in image a. One large prill was recorded in the matrix (b). Magnification of this prill revealed a very distinct grain structure (c).

Analysed area	S	Fe	Cu	Ag	Pb
Area scan of the whole prill	**44.9**	**1.2**	**22.0**	**2.3**	**29.6**
Spot analyses					
1 – mid grey interphase	45.0	~	38.8	0.8	15.5
2 - dark areas	46.1	2.3	47.0	1.7	3.0
3 - white interfill.	49.5	~	1.6	~	48.9

Table 11.39. SEM-EDS data of the largest prill found in slag sample 298. Data has been normalised to 100 at%.

Summary UR12

The analytical work carried out on three slag samples from furnace UR12 has shown that the slag is lead silicate based. It contains lead oxide (30-72%), silica (16-33%), and smaller quantities of iron, zinc, and antimony oxide (Table 11.40). Trace components of sulphur, lime,

phosphate, and alumina were also recorded. There is variation between samples which indicates the variability of ore and smelting patterns throughout the lifetime of the furnace. Lead metal analysed within the UR12 slags has a relatively high silver content indicating the use of a silver lead rich ore.

Sample number	MgO	Al2O3	SiO2	P2O5	SO3	K2O	CaO	MnO	FeO	ZnO	Sb2O3	PbO
293 (n=5)	~	1.6	16.2	~	~	~	0.4	~	5.4	2.3	2.2	71.9
297 (n=5)	0.2	5.3	32.8	1.8	1.0	2.2	2.8	~	13.7	10.5	~	29.7
298 (n=4)	~	3.2	31.4	1.5	~	1.0	2.0	0.8	11.2	3.4	~	45.4

Table 11.40. Summary table of SEM-EDS data from the UR 12 furnace.

11.3. Overall summary of results

The three domed or reverberatory furnaces of Uruquilla have shown that slag produced from these furnaces is, in general, well oxidised and lead silicate based. The slags have metallic inclusions of lead metal with lead sulphide, recrystallised zinc sulphide, and silver metal. A review of all of the bulk area analyses on all slags has shown that the samples are producing consistent chemical analyses. Four categories of slag from Uruquilla furnaces have been found: Type I, II and III and 'The others'. A brief review of the general properties of each group, and then a more general discussion regarding the relationship between the slags and the type of furnace will follow. The slag proper from the DMD furnace has been included in the Type I lead rich slags for comparison to the slags of the Uruquilla sites.

Type I - lead rich slags

The hand specimens of the lead rich slags were notably similar. They are extremely black and glassy. Many had a ripple texture on the outer surface. Optical microscopy confirmed that the glassy texture seen on the hand specimen was true of the microstructure. Metallic lead prills and prills of lead sulphide were scattered throughout the glassy slag matrix. Other crystalline phases were recorded. SEM-EDS revealed that these are iron and zinc silicates and iron and zinc oxides. The bulk composition of lead rich slags contains relatively high lead oxide (58-72 %). No sulphur or phosphate was recorded in the overall bulk composition (Table 11.41).

The slag also contains silica, iron and zinc oxide, and alumina, the next most important oxides. Very low quantities of lime and potash characterise this slag type. Metallic prills found in the matrix contained silver and lead alloys.

Consideration of the DMD slag already showed that it had been formed from a lead sulphide rich ore. The analyses from the Uruquilla furnaces also support the same hypothesis. Comparison of the slag data shows that heavy metal concentrations differ between the individual slag samples, presumably due to the use of slightly different ores. Lime and potash are elevated in the DMD slag, although silica and alumina contents are similar.

Type II - zinc sulphide rich slags

The second group consists of zinc sulphide rich slags. The SEM-EDS bulk area analyses showed that this group of slags has much lower lead oxide (32 %) compared to Type I slags (65%), but elevated silica, zinc and iron oxides (the majority of the zinc is zinc sulphide); (Table 11.42). Low quantities of phosphate and lime were present in the slag composition. SEM-EDS analyses confirmed that all zinc rich slags contained ore components such as quartz grains, tin oxide, zinc, and lead sulphides. The presence of iron, zinc, arsenic and antimony in the lead silicate matrix can all be attributed to the starting ore. These slags contain crystalline phases that are rich in zinc such as zinc olivines, iron and zinc oxides (spinels). Many of the zinc silicates recorded have different structures and when analysed have variable chemical compositions.

Sample	MgO	Al2O3	SiO2	K2O	CaO	MnO	FeO	ZnO	Sb2O3	PbO
UR 10 253A	0.1	3.3	24.8	0.8	0.4	~	5.4	6.6	0.8	57.8
UR 10 253B	~	3.5	25.3	0.9	0.8	~	4.7	5.6	0.3	58.8
UR 11 263	~	3.5	24.7	0.5	0.5	~	4.5	5.4	0.4	60.4
UR 10 209	~	1.9	17.3	~	0.2	1.0	12.4	1.7	~	65.5
UR 10 254	~	2.9	18.9	1.5	1.8	~	6.0	2.8	~	66.1
UR 11 259	~	2.3	17.9	0.9	1.8	~	5.8	3.0	~	68.3
UR 11 251	~	1.4	15.1	~	0.1	~	10.2	1.7	0.3	71.2
UR 12 293	~	1.6	16.2	~	0.4	~	5.4	2.3	2.2	71.9
Average lead rich slag	**~**	**2.6**	**20.0**	**0.6**	**0.8**	**0.1**	**6.8**	**3.6**	**0.5**	**65.0**
DMD slag 341A	**0.4**	**2.8**	**22.2**	**1.2**	**4.2**	**~**	**3.2**	**5.9**	**~**	**60.1**

Table 11.41. SEM-EDS bulk area scan analyses from UR10, 11 and 12 of Type I – lead rich slags. The data has been normalised 100 wt%.

Sample	MgO	Al2O3	SiO2	P2O5	SO3	K2O	CaO	MnO	FeO	ZnO	As2O3	Sb2O3	PbO
UR 10 268A	~	3.3	24.6	~	4.6	1.0	1.5	0.5	11.7	25.2	~	~	27.6
UR 10 255	~	3.5	25.9	0.3	8.9	0.9	1.3	0.5	9.5	20.6	~	~	28.6
UR 12 297	0.2	5.3	32.8	1.8	1.0	2.2	2.8	~	13.7	10.5	~	~	29.7
UR 10 268C	~	2.4	20.4	~	0.5	0.7	0.7	0.4	23.7	16.6	2.6	~	32.0
UR 10 250B	~	1.9	18.4	~	6.0	0.7	~	~	6.5	22.3	1.3	0.7	42.2
Average zinc sulphide	**~**	**3.3**	**24.4**	**0.4**	**4.2**	**1.1**	**1.3**	**0.3**	**13.0**	**19.0**	**0.8**	**0.1**	**32.0**

Table 11.42. SEM-EDS bulk area scans of UR10/11/12 slags - Type II zinc rich slags. The data has been normalised to 100 wt%.

These slag samples are characterised by the presence of metallic prills containing mostly lead metal and smaller quantities of silver, copper and antimony. In some samples such as 268A, 268C and 250B, complex metallic prills contain areas of silver with as much as 76 at%. Only two of the samples contain no silver traces.

Type III - slags with increased lime and phosphate

The third group of slags are the lead silicates with elevated lime and phosphate contents: only two samples can be grouped in this category; (Table 11.43). These two slags have lead oxide levels of 45-50% and also contain silica, iron & zinc oxides, lime (3%), alumina & phosphate (1%), and potash (1%). Raised quantities of phosphate and lime could have come from the hearth lining or increased fuel ash. Evidence for this still requires further analytical investigation. It may also be possible that these slags form a low-lead variant of Type I slags.

Sample	MgO	Al2O3	SiO2	P2O5	SO3	K2O	CaO	MnO	TiO2	FeO	ZnO	PbO
UR 12 298	~	3.2	31.4	1.5	~	1.0	2.0	0.8	~	11.2	3.4	45.4
UR 11 222A	0.5	3.2	22.6	1.2	~	1.2	3.0	~	0.3	10.7	8.9	48.5

Table 11.43. SEM-EDS data of bulk area scans of Type III - slags with increased lime and phosphate from UR10/11/12.
The data has been normalised to 100 wt%.

The others - slags that cannot be categorised

Two residual slag samples do not fit into the grouped categories already discussed. Samples 89 and 268B are both from furnace UR10. Sample 89 is a very high silicate slag (42% SiO_2). Quantities of alumina, lime, potash are elevated when compared to the zinc rich slags while iron, lead, and zinc are reduced. Sample 268B has a very glassy microstructure with residual lead sulphide scattered throughout the matrix and contains 12 wt% antimony, which is highly unusual. It also has high quantities of iron and zinc oxides. Silver content in the metallic prills is high, with discrete areas of pure silver droplets within metallic lead prills.

Further debate and discussion- UR furnaces?

The analysis of the slags from the UR furnaces has identified two main types of slag and two other minor/individual types. The analytical groupings of these slag types show that the ore used in these furnaces came from two main mineral veins, one which was lead rich and a second which was richer in zinc. Within the Type II zinc-rich slags, high iron content (13%) reflects pyrite from the smelted ore. The presence of tin oxide, observed in spinel phases within the slag, shows that the ore was locally sourced. Tin is a characteristic element of mineral

deposits in the Porco-Potosí region. The relatively low alumina content in the all the slags analysed (c. 3%) indicates low furnace wall contribution in the slag formation. The gangue minerals in the slag remain the same for all types.

There appears to be no correlation between the selection of ore and the types of furnaces used. Therefore the slags have been grouped according to the results of the analytical work rather than by individual furnace classifications. In either case, the smelting of argentiferous galena was the primary function of these furnaces. Thus, a smelt would have produced a silver/lead bullion. This bullion would have then required further refining to extract the silver. The location of these refining sites is still unknown.

The confirmation that these furnaces were used for smelting rather than refining would indicate that there was little connection between *huayrachinas* and the reverberatory furnaces. The European style furnaces may have been operated by different ethnic groups although nothing is known regarding the labourers once employed to work at this site, nor of how fuel would have been acquired.

Dating of the site remains tenuous because stratigraphy from the site is poor and there appears to be very little difference in stratigraphic layers.

Differences in technological style observed in the fireboxes of the UR furnaces did seem to have affected the technological function of the furnace. No difference except for different ore selection was observed in the analysed slags.

11.4. Conclusions and future work

The two different types of colonial furnaces seen in the Porco region are the Dragon furnaces and the domed or reverberatory furnaces. According to the historical literature, these furnaces were certainly in use during the mid 17th century if not before. The 16th century European literature describes domed reverberatory furnaces that were used to refine metal rich in silver. However, the analytical work carried out on slags from the UR and DMD furnaces shows that smelting was occurring in these European style furnaces, as opposed to refining. There is an interesting parallel to Carlos Cuiza's cupellation/refining hearth (Chapters 4 and 6). Cuiza's refining hearth has a similar design but a different technological function.

The differences in design of the UR furnaces are not linked to the technological function or the selection of different ores for smelting. Despite the differences in style of the Dragon and

domed furnaces, metallurgical function does not appear to be affected and the slag produced correlates chemically.

The analytical results have shown that two main types of slag could be identified (Type I and II), along with some minor types (Type III and others). All the slag types reflect the selection of raw (un-roasted) local ore.

The UR European furnaces area surrounded by *huayrachina* sites. However, little is known regarding the work force employed to make and use European style furnaces. Indigenous style *huayrachinas* would have probably been operated by indigenous members of the Porco community. Who commissioned and used the European furnaces? Were European furnaces used diachronically with the indigenous *huayrachinas*? The analytical work has shown differences in the metallurgical function between the two types of furnace. The European UR furnaces were producing silver on a much larger scale than the *huayrachinas*. The relatively large fire boxes indicate the need for access to high quantities of good quality wood. The use of more fuel in the process would have facilitated a better separation between metal and slag. Thus it is tentatively argued that this process may have been a tapping process. The metal, being heavier, would have sunk to the bottom of the furnace hearth, tapped until no further metal flowed. The hole would have been plugged and then the slag tapped before the furnace cooled. However, relatively little slag was found during the excavation. If this process produced slag, where is it now?

From the archaeological domed furnaces, no evidence remains for the roof and chimney. Thus, it is not known where, if at all, the chimneys would have been placed. Where is the debris from the domed roofs?

Both types of furnaces played a role in the early-middle colonial metallurgical history, however, in order to place the UR furnaces in a clear chronological order, there is a need for clearer dating. Analysis of the slag has shown that the furnaces functioned between around 900 and 1000 °C (Figure 11.8). Large quantities of brush wood would have been required for the furnace to function effectively. There must have been a high economic investment into these furnaces. Their sustained use must have been difficult given the high labour and economic costs.

12. OVERALL DISCUSSION AND CONCLUSIONS

The Porco-Potosí region has played a major role in the extraction of minerals and production of metal for at least the last 500 years. Historical and archaeological evidence indicates that the mining area of Porco has been inhabited by the Incas prior to the arrival of the Spanish in the early 16th century. Spanish chroniclers documented their arrival in Porco and noted the large mineral wealth that the mountain contained. For centuries, the region has influenced world silver economies and continues to be Bolivia's largest mining area. However, despite the importance of this region, almost no archaeometallurgical study has been carried out on historical silver production techniques. The only known lead and silver production sites in the southern Andes are found in this region. Thus, this project represents the first archaeometallurgical study of lead and silver production. This thesis has addressed the different techniques of metal production observed in the archaeological, historical, and ethnohistorical record. In this chapter, conclusions from each of these areas will be summarised, starting with current day ethnographically documented silver production methods, followed by the archaeological evidence for the smelting of lead and silver ores in *huayrachinas*, and the use of European furnaces. Finally, silver rich ores and lead/silver alloys refined via cupellation methods to produce silver are discussed.

The archaeological evidence for silver production has shown that several different methods were employed in Porco. The Spanish conquistadors stimulated and ultimately forced changes in technology. This was prompted by their desire to win as much silver as possible. Indigenous methods of production such as the *huayrachina* were only employed until newer technologies became financially viable. Since the early colonial period the region has been a 'hot spot' (Presta in press) for technical innovation and change. Different methods of silver production were being used simultaneously. To address changes in technology, the smelting techniques in the region will be compared using the analytical work presented in this thesis. What ore was being selected? How did the different furnaces function? What type of fuel was consumed? A reverse *chaîne opératoire* has been used to understand archaeological *huayrachinas* and this has been used in comparison to the current day *chaîne opératoire.*

Refining technology was almost certainly occurring in antiquity in association with smelting furnaces. While archaeological evidence is sparse, historical and ethnohistorical studies of refining techniques have provided a source of knowledge regarding metallurgical refining practice. This chapter will assess the existence and continuation of these techniques.

Finally, conclusions from this thesis and ideas for future work will also be presented at the end of this chapter.

12.1. Recent silver production

Prior to this PhD thesis the current day silver production process had been sequentially documented and small scale analysis of some samples from the process had been undertaken (Mills 2003). The study of current silver production in modern Porco by Carlos Cuiza has shown that he employed a technically adaptive method to produce silver. Two processes were used to produce silver: the smelting of galena (PbS) in the *huayrachina* and the refining of silver ore (probably pyrargyrite, Ag_3SbS_3) in a cupellation hearth using the lead from the first stage of production (Chapters 4-7). The separation of these techniques is rather unusual and shows technical disparity between the archaeological, current day silver production (analysed here), and silver production techniques observed in other parts of the world.

This research has produced a schematic of Cuiza's smelting *chaîne opératoire* (see insert at the back of this thesis and chapter 7) which involves a series of different steps used to produce lead metal. Collection and acquisition of raw materials such as wood for charcoal, water, ore, and clay is required for a smelt. Of equal importance to the raw materials are the conditions required for a smelt, primarily the presence of strong wind. This variable is harder to control than the others. A successful smelt is reliant on Cuiza's learnt knowledge regarding appropriate smelt times and seasons, selection of ore, fuel and the ability to control the *huayrachina*. The presence of the PAPP team at the documentation of the smelt appears to have altered Cuiza's normal smelting practice. It is acknowledged within this thesis that the ethnographic data taken has its limitations. Conclusions regarding the selection of ore chosen for smelting are limited due to the influence of PAPP. Despite this and other changes such as different seasonal and timing conditions, the function of the furnace can still be monitored through the analytical work presented in this thesis.

The analytical results have confirmed that Cuiza smelts galena (which contains little or no silver) to produce lead metal. The process is technically inefficient, functioning at low temperatures, and involving rather high losses in lead. Lead is trapped within the slag as partially reacted lead sulphide, lead oxide, and lead metal. It is also lost into the environment as lead oxide fumes. The technical inefficiency of the process has its own inherent benefits. Cuiza has reduced the quantity of fuel (charcoal) added to the *huayrachina*; the fuel to ore ratio being 1:2 (Chapter 7). By reducing the quantity of expensive fuel needed in the process, Cuiza can economise on capital invested into the process. Cuiza can then invest time into the cupellation/silver refining stage which requires a greater time investment (up to 24 hours to compete one cupellation).

The cupellation process used by Cuiza requires a hearth that has been lined with plant ash (*llareta*). Lead metal produced in the *huayrachinas* is melted and used to cupel a high grade silver ore. The practice of adding silver ore directly into the cupellation hearth without roasting or prior smelting is rather peculiar because it requires the sulphide components to be removed before strict cupellation can occur. This process is not in itself very efficient and metal is left behind in the waste material (CHM). However, ethnographic observation has shown that the recycling of these waste materials in subsequent smelts can lead to an overall balanced process. (Cohen et al. forthcoming b). Analysis of the CHM showed that the *llareta* ash reacts with the lead oxide to form a lead silicate. In some instances this reaction blocked the system and prevented further refining from occurring. However, given the other plant material available to Cuiza for hearth lining the selection of *llareta* seems more appropriate than the ash from straw or *ichu* grass, as it contains less silica.

Cuiza's technological choices were monitored in this research by reviewing the *chaîne opératoire*, analysis of the material debris from the process, documentation of the inputs and outputs of the system as well as his comments regarding the production documented by the PAPP team. The results of this work confirm that technological choices were modified according to environmental, social, and economic factors. Cuiza produced silver as a means of income for his household along with agricultural and other undefined activities. So the process was also affected by the needs of Cuiza and his family to gain extra income.

Cuiza may have been the only known individual using this technology, but others were aware of his production. He produced silver for other agents who brought him ore to process and he also used (for the PAPP documented productions) his *compadres* Dons' Dionisio and Juan to process ore and assist him during the *huayrachina* smelting. Although technical, Cuiza appears to have been isolated, he was part of an social group that were connected via the need to produce silver. This group would have had some input into the nature of the silver production, the provision of ore, frequency of production, and to some extent the organisation of the production (through provision of labour). The limited information gained regarding the individuals involved in current day silver production has been hard to assess. Within the archaeological record, this information would not be visible at all.

Prior to the documentation of Cuiza's silver production, a working *huayrachina* had not been seen for 100 years. The last being reported by Peele (1893). The review of current day practice has been beneficial in understanding indigenous metallurgical activity in Porco. Cuiza's practice was taught to him by his parents, representing a learnt technique that had been used for a series of generations. Thus, the study of this technology, and the materials/objects associated

with it, reveals knowledge regarding the cultural and environmental factors affecting Cuiza. Rowlands' summarises: "Objects are culturally constructed to connote and consolidate the possession of past events associated with memories and striking events associated with them." (Rowlands 1993,144). Cuiza's separation of smelting and cupellation in the silver production process allowed for a distinction between the two different metallurgical techniques. Variations have also been discussed between location and technical differences in the processes. These variations can help to understand the situation in early colonial Porco. Historical documentation (Oehm 1984; Capoche 1585; Barba 1640 (Douglass and Mathewson trans 1923) discusses the need for separation between smelting and refining technologies. However, little is known regarding refining technologies in the Porco region.

12.2. Archaeological silver production

Archaeological silver production is split into two sections. Production within early colonial Porco was done using several methods; including smelting using *huayrachinas* and European reverberatory furnaces, refining of silver-rich lead bullion, and mercury amalgamation. To date no archaeological evidence has been found for mercury amalgamation in Porco, although the introduction of this method in 1570 had severe consequences for metal production in Potosí. It is highly probable that mercury amalgamation would also have been used within Porco. This thesis has not considered the technicalities of mercury amalgamation. In this conclusion, it is referred to only as a comparative technology and is brought into the discussion as a method of assessing other production techniques.

Smelting in the past – *huayrachinas*

Archaeological and historical evidence for smelting in the Porco-Potosí region has indicated that initially the *huayrachina* had a predominant role in the production of silver. *Huayrachinas* are present in the archaeological record from the beginning of the Spanish colonisation (1538), and the presence of *huayrachina*-like furnaces in Porco prior to the arrival of the Spanish is highly likely.

The *huayrachina* design found in Porco-Potosí is different to that of other Andean furnaces such as those found at the archaeological site of Batán Grande (northern Peru) and north western Argentina (Shimada et al. 1982; Raffino et al. 1996). Both these examples provide evidence for pre-Hispanic furnaces but are associated with copper technology. These copper producing furnaces would have employed natural draft and blow pipes whereas *huayrachinas* found in Porco-Potosí did not require blow pipes; they used wind power. Other styles of furnaces such as the 17th century European furnaces required the use of bellows rather than wind.

To-date there is little documented evidence regarding silver and lead producing furnaces in the Andes; this thesis is the first known research to explore the furnaces, their design and function.

The origins of the *huayrachina* are difficult to establish. One may argue that it was an Andean technology employed prior to the arrival of the Spanish. However, the lack of archaeologically dated pre-colonial archaeometallurgical sites makes this difficult to demonstrate. The name *huayrachina* originates from Quechua (the language used by the Incas) but was also used in Aymara and means the place where the wind blows through. The use of *huayrachina* to indicate smelting and/or metal furnaces has become commonplace within Andean literature. Questions related to the origins of the *huayrachina* are beyond the scope of this thesis, however, it seems logical to assume that some variant of the furnace described as the *huayra/huayrachina* in colonial sources may have been indigenous to the Andes.

In this research project no archaeological *huayrachina* site has been found that can be dated with clarity to pre-Hispanic periods. Dating of archaeological *huayrachina* sites is difficult due to the lack of stratigraphic evidence (all sites are typically surface debris), and their location on high windy ridges exposing debris to water and wind erosion, affecting the quality of the remains. Other structures which could be used for dating the sites are rarely located close to the *huayrachina* sites. Re-use of furnace sites has also made their earliest occupation difficult to establish. In this research the dating has been done by Dr Van Buren using historical evidence, ceramic sherds and where possible the use of architectural remains where stratigraphic context may be observed and translated to the *huayrachina* sites. Archaeological *huayrachina* samples from Porco were selected from two datable and three un-dated sites. The two dated sites (HuA1 and Hu24) are considered to have been in use during the early to middle colonial period. However, both sites yielded Inca style ceramics which were commonly used post-conquest. The results of analytical work showed continuity in ore selection and slag compositions between samples from different sites (Chapters 8 and 9).

Survey of archaeological *huayrachina* remains indicated that debris from the un-baked furnace wall may have experienced erosion leaving samples that do not necessarily reflect the original furnace. The review of *huayrachina* remains must be treated with caution. Areas of vitrification allow for fragments to be better preserved within the archaeological record. The design of the furnace allows cracks to appear connecting the air holes. Thus, comparatively more furnace fragments with partially preserved air holes were found during survey. The results from the brief survey of two archaeological *huayrachina* sites indicate that air holes in antiquity were larger than those of the recent day *huayrachinas*. Possible erosion of the outer surface of fragments and ledges located underneath air holes makes measurement of the thickness of the

archaeological furnaces difficult to estimate. Colonial literature provided evidence that furnaces may have been larger in the early colonial period. The shape of the shaft may have also altered, from being slightly flared to vertically straight. The surveys carried out cannot confirm this change in size, however, a change in construction was noted between current and ancient *huayrachinas*. Cuiza introduced the use of iron belts into the shaft. This innovation was carried out to strengthen and prolong the life of the furnace. I hypothesise that furnaces in antiquity would have internal strength due to the slightly larger eye holes. The slag generated around the eye holes would have provided support to the shaft. Cuiza's modern furnaces did not have this internal support. It is probable that the earlier furnaces were slightly larger but to what extent it is difficult to confirm from the archaeological remains analysed in this small survey (Chapters 8 and 9).

The analysis of the *huayrachina* ceramic body indicated that the furnaces were built from local clay which was possibly tempered with an organic filler. It is unclear whether this filler was added intentionally. This thesis has shown that the selection and smelting of argentiferous galena was common practice. Analysis of slag adhering to archaeological *huayrachina* wall fragments has shown that ore was beneficiated and placed raw/un-roasted into the furnace. Compositional studies of archaeological slag have shown that the composition is highly variable (Table 12.1). Quantities of lead oxide range from 66 to 8 wt%. The presence of heavy metals in the slag such as zinc, iron, tin and lead are directly correlated to the composition of the raw ore. Some slag samples contain significant sulphur contributions as high as 12% (Table 12.1 UR WS 342A). Lime and alumina compositions were contributed to by the interaction of the lead oxide with the ceramic body of the furnace. Metallic prills are commonly found within the slag, which are typically lead metal or silver-rich lead metal. The slag analysis shows that furnaces operated under high temperatures and relatively oxidising conditions. These redox conditions created a lead silicate slag with different silicate phases and inclusions of silver-lead metallic prills. A silver-rich lead bullion would have been produced that would have needed further refining.

The *huayrachina* has persisted for five centuries in the Porco-Potosí region. Prior to 1570 the *huayrachina* in association with the *tocochimbo* (a refining hearth, very little is known regarding this style of furnace) was the primary method of silver production. As the use of the *huayrachina* began to decline (middle to late colonial era), its use continued at a smaller scale within Andean households. The users of these furnaces changed from elite to peasant/proletarian agents and it became a rather illicit activity, done in homes away from centralised Spanish areas. Historical evidence has shown that the *huayradores* were *yanakuna* employed by the Spanish elites to smelt rich silver ore (Van Buren and Presta in press). As different methods of silver production were introduced, labourers from different ethnic groups

encouraged the continuation of Andean trading systems and the combination of a multi-economic strategy:

"Mining is the most striking case: it generated a waged labour force in the colonial period; however, such people did not live solely for their wages but supplemented them with independent extraction of ore and sometimes with agriculture. They were, and still are, complemented by a large temporary labour force that combines waged work with agriculture, or at least retains long-term rights to land." (Harris 1995, 375).

This multi-subsistence strategy is still implemented today by many Andean communities but during the colonial period may have encouraged the use of the *huayrachina*.

This research documented the activities of one individual (Carlos Cuiza) who was using a *huayrachina*. His activity seemed clandestine and technically inefficient. However, the *huayrachina* (and his cupellation hearth) continued to be used as it was relatively low cost to Cuiza. The last known *huayrachinas* provide us with valuable and unparalleled information for the way in which these furnaces functioned. If we assume that prior to 2006 there were a few other individuals as well as Cuiza using *huayrachinas* then perhaps we are observing the death of this technology rather than continuation of a practice. Nevertheless the comparison between large scale industrial *huayrachina* use in the early colonial era to the current day situation is noteworthy. The death or decline of one technology over another is of great importance to technological studies.

To visually represent the methods used to understand *huayrachina* use in Porco a web of archaeometallurgical research has been presented. Furthermore, the evidence gained from the analyses in this thesis have allowed for the construction of a possible *chaîne opératoire* of archaeological *huayrachinas* (see the insert attached located at the back of this thesis). This figure can be used to compare the limited level of information available from archaeological debris to the detailed information about recent day *huayrachina* use, and provides a different way of representing results from the analytical, historical, and archaeological data gathered during this research. It is hoped the use of both the web and archaeological *huayrachina chaîne opératoire* can aid archaeologists and theoretical discussion.

The use of the *huayrachina* has been complemented by other methods of silver production. In the next section a summary of conclusions from the European furnaces analysed will be presented.

European furnaces

Three different types of reverberatory furnaces have been found in the Porco-Potosí region; in the archaeological record domed and dragon furnaces, and in current day practice the use of a cupellation hearth which is similar in design to European dragon furnaces. This section will discuss the conclusions from this thesis regarding these furnaces and their interaction with other metallurgical practices.

Archaeological smelting furnaces; domed and dragon furnaces

European historical literature states that reverberatory furnaces were traditionally used for refining. A domed roof intensifies the heat and allows reactions to take place under strongly oxidising conditions. These properties can also be valuable during smelting, creating a high temperature reaction chamber. Barba's 17th century manuscript establishes that domed or reverberatory furnaces were used for smelting and that some contained a large flared chimney used only for lead smelting (the dragon furnace). Barba states that, although the technique of mercury amalgamation was accepted practise for production of gold and silver metal, it was not necessarily the most suitable and within Potosi and other mining districts, older methods of smelting still remained the current and more popular mode of production (Douglass and Mathewson trans., 1923, 185). There was no evidence of a chimney or domed roof in the archaeological remains documented here. However, the intact fireboxes and hearths link very well to the historically drawn domed furnaces depicted by Barba who was, in fact, familiar with the metallurgical activities that were carried out in Porco (Cohen et al. forthcoming c).

During initial excavations (summer 2005), the location of the domed furnaces close to the UR *huayrachina* sites (UR ES and UR WS) led to some speculation regarding the role of these furnaces in the overall technological repertoire of the colonial period. It was hypothesised that these European reverberatory furnaces could have been used to refine the argentiferous metal smelted in the *huayrachina* furnaces located on mountainous saddles surrounding the site. However, the relationship between the European furnaces and the indigenous *huayrachina* furnaces is difficult to understand. The results from the analyses conducted in this research have shown that the European furnaces were not used in the refining process and that they were in fact smelting furnaces. Therefore, no direct functional link between the metal produced in the *huayrachinas* and the furnaces can be established. At present the relative dating of domed and dragon furnace types is unclear (the domed furnaces are tentatively dated to the late colonial period but they may be slightly earlier), and further work is necessary to establish the relationship between the furnaces and to understand the sequential technological influences and changes in furnace technology. The remote location of the smaller DMD furnace seems to

indicate that small scale ore smelting was being undertaken away from central Porco; this practice is not dissimilar to Cuiza's *huayrachina* and cupellation (to be discussed below).

Analytical work has shown that sulphidic argentiferous galena was the ore selected for smelting in the European furnaces. Results from the UR domed furnaces indicated two ore sources which varied by quantities of zinc. No roasting process was occurring prior to smelting in either the domed or dragon style furnaces (Chapter 11). Compositional data of analysed European slag has shown that it fits within the archaeological *huayrachina* slag (Table 12.1). This indicates that similar ore was being selected for both indigenous and European furnaces. The ore was smelted directly producing a vitreous black lead slag and a lead-silver rich bullion. This bullion would require further refinement via the use of a cupellation hearth. The location of these refining sites is presently unknown. Small cupellation furnaces have been encountered during archaeological surveys, but date later in time and are associated with isolated indigenous households.

Judging from the quality of the slag, the reverberatory furnaces would have required large quantities of fuel (wood) to operate. This was a scarce resource and so the use of these furnaces was not sustainable in the long term. The selection of European furnaces to produce silver represents the short-term priorities of the Spanish conquistadors (who had direct control into the manufacture and use of these furnaces). The necessity to extract high quantities of silver was far greater than the need to invest in long-term strategies of subsistence and local development. These furnaces would have required high quantities of fuel but they were able to produce larger quantities of silver than the smaller and more fuel economical *huayrachina*.

The lack of archaeological remains indicating the style of the dome at the UR furnace site is problematic. A review of Barba's (Douglass and Mathewson 1923 trans., 196) illustrations of reverberatory furnaces showed that the dome was made from bricks and could have a chimney at one edge of the base or in some cases no chimney was necessary, with instead there being an opening at the top of the dome acting as a vent. For the UR furnaces, the lack of debris from possible roof areas and evidence of chimneys mean that the exact construction remains a mystery. Equally puzzling is the lack of slag. Considering the size if the furnaces and scale of metal formation, slag would have been an abundant waste product. During excavation only very small quantities of slag were recovered. It is hypothesised that slag could have been scavenged and re-melted to extract any trapped metal.

production moved to Potosí. There is no historical evidence to identify who would have worked the European furnaces.

A comparison between the two different styles of furnaces used in the Porco region shows that there were different scales of production occurring. The UR furnaces would have produced much more metal per furnace in comparison to the smaller reaction chamber of the *huayrachina*. The larger capacity of the European furnaces would have required larger quantities of fuel, and the good quality slag indicates a high fuel to ore ratio. The high fuel consumption of these furnaces would have allowed them to be used in the short term, but long term use was impractical. The use of these furnaces was more than likely due to the political power that the Spanish/Europeans had over indigenous populations. The demise of the European furnaces, contrasted by ongoing *huayrachina* use, may well be due to a combination of environmental and socio-economic factors. Their increased fuel consumption would not have been sustainable long-term, and they would have fitted less in a typical subsistence strategy of the population of European decent, in contrast to the mixed strategy followed by the indigenous peasant populations which enabled the survival of *huayrachina* smelting. Despite these socio-economic differences and the different furnace design, it seems that in all cases the same type of ore was being smelted.

SEM-EDS bulk area analyses on slag samples from Cuiza's and the archaeological *huayrachinas*, and European furnaces (Table 12.1) show that all the samples have high chemical variability, for example lead oxide ranges from 6 to 66 wt%. The chemical composition of the slags shows that they come from a similar lead rich ore type. The lead rich ore selected for smelting varies according to heavy metal content recognised in the slag by the concentrations of SnO2, Sb2O3, ZnO (ranging from 3 to 24 wt%) and FeO (ranging from 1 to 14 wt%). The seemingly low lead oxide content of Cuiza's slag is due to the exclusion from the SEM-EDS analysis of the large and numerous inclusions of galena, lead sulphide and lead metal. Thus, it represents the lower smelting temperature in his *huayrachina* rather than a higher efficiency of his technology. A detailed assessment of his operation (Chapter 4 and 7) has shown that he only recovers about one third of the total lead in the furnace charge.

12.3. Registering changes in technology within the Porco-Potosí region

As already noted in this thesis, very little was known regarding silver and lead production techniques in southern Bolivia. The lack of archaeological silver and lead production sites within the Andes has meant that knowledge of mineral processing and extraction has remained undocumented. The review of silver production techniques used throughout the colonial era has provided insight into the infrastructure of colonial metallurgy. Changes and similarities in production techniques have been identified through historical and archaeological evidence. However, what motivated change or continuity within metallurgical production?

The arrival of the Spanish in the Porco-Potosí region stimulated changes within the technological systems already in place in the region. Those technological systems are currently poorly defined, early colonial accounts document the use of *huayrachinas* to smelt ore minerals, however to date, there is no datable archaeological evidence for this. Despite limited evidence within the first fifteen years of colonisation, new methods were introduced by the Spanish governors. Costin et al (1989) argue that technological change can be monitored via a consideration of control within society. Those agents that have control of production and technology can influence and command society. Two models govern changes in technology:

i. Top-down: where local elites control production methods.

ii. Bottom-up: models that allow change to take place on a commoner level that then affects the larger community.

Adoption of a new technology would be stimulated by changes in subsistence needs due to changes in population, new access to resources perhaps via social and economic changes, and changes in settlement patterns (Costin et al. 1989, 107).

Top-down changes were imposed by the Spanish conquistadors as they implemented strategies to gain control over local indigenous groups. A similar strategy has been widely adopted by the Incas who were able to conquer and control different geographical and sociological zones. They did this through a carefully balanced approach between state leadership, regional development, application of social, political, and cultural styles, and allocation of resources.

"By adapting state practises to local circumstances, the Inkas forged a policy that relied on a situational mix of alliance, clientage, intensive incorporation..." (D'Altroy et al. 2000, 2).

The centralisation of metal production (mercury amalgamation) introduced by Viceroy Toledo in 1570 allowed the Spanish governors to manage technological production and then in turn direct

the economic profits that increased metal production would encourage. The implementation of a top-down strategy was initially costly for the Spanish because it required significant capital and labour investment to maintain control over mining and metal production technologies. However, it was beneficial beyond the increased silver output. Given the status of metal within Andean communities and the significance of the Porco-Potosí region, whoever controlled this region and its metallurgy would appear powerful and legitimise their rule over the local population.

Prior to the introduction of mercury amalgamation, the indigenous population were controlling the production of silver via the use of *huayrachinas* and other refining techniques (possibly *tocochimbos*). It is difficult to identify the influence of the Spanish on metal production technology during these early colonial periods. Archaeological *huayrachina* sites located in this project have shown re-use patterns indicating that sites may have been in use both prior to and after the Spanish invasion. Analytical work on the archaeological *huayrachina* samples has shown that furnaces were generally used to smelt an argentiferous galena. The mining and selection of this ore would have been done close to the furnace sites. The *huayrachinas* would have produced a silver-rich lead bullion which would have required further processing. The site of these refining sites and the technology used remains unknown and rather speculative.

The introduction of amalgamation should have made the use of the *huayrachina* unnecessary. Amalgamation can refine lower grade ores and needs less fuel. Thus, it is more cost effective. However, the use of *huayrachinas* to produce metal seems to have continued on a smaller or local scale. Were family or *allyu* units smelting mineral that they could access? This demonstrates a resistance by the indigenous community to fully accept the Spanish technological changes. This resistance may have been due to a number of different factors such as uncertainty in the predictability of new technology resistance to social change, and a loss of autonomy (Costin et al. 1989 108). A perceived risk in the new technologies enforced by the Spanish may have allowed for the continuation of the use of more traditional techniques of silver production. 'When results of a new process are unknown, people must either risk inadequate production or maintain back-up systems.' (Costin et al. 1989,108). Rabey comments that different sociocultural systems adapted according to their own social and natural environment needs and concerns (Rabey 1989, 168).

Table 12.2 compares different archaeological production techniques used to produce silver. The use of the *huayrachina* requires very little initial set-up. Ore preparation techniques were small scale and easy with basic sorting and no roasting required. Access to quality charcoal as fuel would have been the major investment.

The introduction of mercury amalgamation represented a large capital investment by the Spanish. Processing plants for ore preparation and areas for *cajones* needed to be built. Mercury was imported from Peru and in later periods it was brought from Spain. The low grade ore selected for amalgamation required processing much more intensively than the high grade ore. However, the overall process could be done with lower quality fuel. Mercury amalgamation produced pure silver, whereas the European furnaces and *huayrachinas* would have required further refining. Scales of production varied with amalgamation processing large quantities of ore and *huayrachinas* having the smallest quantity per furnace. The results of the analyses of European and *huayrachina* furnaces have shown that for both, silver-rich argentiferous galena was selected for processing. Mercury amalgamation allowed lower grade silver ores to be accessed. The concurrent use of all of these techniques shows the diversity of the metal production in a region stimulated by the desire to extract as much silver as possible. The use of multiple strategy metal production techniques restricted the control and quantity of metal produced. Porco has a diverse archaeometallurgical tradition and more work is required to understand the arrangement of labour forces during the Spanish colonial era. The persistence of some methods over others shows selection based on economically, socio-political and environmentally practical technology.

12.4. Final conclusion

This PhD project is the first of its kind to document silver and lead production in the southern Andes. It uses unique ethnographic data to analyse the only known working *huayrachina* for 100 years and archaeological evidence of colonial silver production. In this work the application of archaeometric, theoretical, historical, and ethnographic data has given an overview of the technology used in the Porco-Potosí region.

Technological changes observed in the archaeological record were initially stimulated by the Spanish conquistadors' desire to extract as much silver as possible. However, the location of Porco away from the governmentally regulated Potosí allowed a symbiotic relationship between different technologies to occur; in effect a co-existence of European and indigenous practice. This research has shown that the persistence of indigenous technology has been driven by a number of factors, such as socioeconomic, political, and environmental conditions. The continuing presence of the *huayrachina* despite changing political and social contexts draws a parallel to metal technology in other parts of the Andes. Batán Grande used the same design of furnace for several hundred years despite major political and social changes.

The analytical work carried out has confirmed the selection of local ores. All styles of archaeological furnaces (European and *huayrachinas*) were used for smelting argentiferous

galena that varied according to zinc, iron, and tin quantities. The scale of production appears to have varied between metallurgical techniques analysed here. Large scale silver production must have been occurring in the European dome style furnaces. However, the demand for fuel would have made this technology costly to run over extended periods. There is still work to be done addressing the organisation of labour with regard to metal production in colonial Porco. It is hoped that this thesis will be used to further understand the region's status within world silver production.

Recent metal production has shown the persistence of indigenous practices within the region. Links between the archaeological and ethnographic observations have been noted. This thesis presents two models (*chaîne opératoires*) to illustrate metal production processes. The use of a web of archaeometallurgical research in this thesis acts as a reflection of my own work process, and hopefully a contribution to the theory of technology, acting as a case study for those who wish to consider the study of technological change and choices. The analytical work done in this research has allowed for a comparison between recent and archaeological methods of smelting. The current day situation reviews the last known working *huayrachina* and has shown that adaptation to an environmental, social, and economic situation is critical for a technology's survival.

This thesis has documented for the first time archaeometallurgical activity spanning the colonial period. It is hoped that the results will contribute to a better understanding of the Porco-Potosí region's history and to Andean metallurgy.

12.5. Future work

The overall material available for archaeometallurgical study from the Porco-Potosí region far exceeds the amount of material that can be studied in a single PhD thesis. In this thesis a small number of sites have been selected for analytical work in order to demonstrate and answer several specific research questions.
However, future work would like to address:

- **A strategy to allow for more accurate dating of archaeological sites.**

  Current dating methods include using ceramic chronology, soil stratigraphy, and the observation of surrounding architecture. I believe that radiocarbon dating should be employed when suitable charcoal samples are available. The use of luminescence dating could also be applied for burnt ceramic or sediments. A more precise dating of archaeological sites will help to further contextualise and monitor technological changes over time.

- **Further investigation into 18th and 19th century *huayrachina* use.**

I would like to conduct a much wider review of smelting activity in the Porco region using material dated to the 18th – 19th century. This period was one of economic and political instability and seems to have been overlooked in historical documentation. There is a need to identify the then current smelting technology and review the technological persistence of *huayrachinas,* and compare that to the current day situation.

I want to consider:

* Who was smelting in the 18th century?
* What ore was selected, silver rich ore or pure galena?
* Where and how was it being refined?
* When did *huayrachina* smelting change from an elite to a peasant technology?
* What stimulated those changes?
* How has the use of illicit ore and how has sociocultural awareness affected the technology?

- **Further ethnographic work**

Ethnographic data has been an important component of this research project and it has raised many more questions related to the continued use of the *huayrachina.* I think there is scope for investigating the recent and current use of *huayrachinas* and other smelting furnaces in other silver producing regions.

- **The different methods used in colonial Porco-Potosí to refine silver.**

The results of analytical work carried out on smelting furnaces (presented in this thesis) support the hypothesis that cupellation was occurring within the early colonial period, and most likely even before. Samples of partially intact hearths, CHM, scorifers and cupels have been documented from surface survey and excavated contexts. These require detailed analyses to understand the technological function and relevance of cupellation within the region.

- **A consideration of *tocochimbos;* the indigenous furnaces claimed to be used for silver refining.**
  * What did *tocochimbos* look like?
  * How did they function?
  * How were they used in relationship to *huayrachinas* and the European metallurgical techniques? Who operated them?
  * Did they require bellows or blow pipes?

To address early-middle colonial silver refining in Porco, archaeological site 35 would be of interest. It contains three large structures within which five metallurgical hearths have been found. In the centre of the site there is a large flattened platform with a number of large *quimbaletes* used for ore beneficiation. The hearths have different shapes and do not correlate to the smelting furnaces studied in this thesis. The site requires a detailed archaeometallurgical review. Its role within the other metallurgical techniques already identified needs to be understood.

13. REFERENCES

Abbott, M. B,. and Wolfe, A.P. 2003. Intensive Pre-Incan metallurgy recorded by lake sediments from the Bolivian Andes. *Science* 301, 1893-1895.

Abercrombie, T.A., 1998. Pa*thways of memory and power. Ethnography and history among an Andean people*. Wisconsin, US: The University of Wisconsin Press.

Alfassi, Z.B., 2001. *Non-destructive Elemental Analysis*. Oxford: Blackwell Science Ltd.

Anguilano, L., Timberlake, S. and Rehren, Th. in press. Excavation, slag analysis and experimental reconstruction of an Early Medieval lead smelting bole from Banc Tynddol, Cwmystwyth, Ceredigion (Wales UK), *Historical Metallurgy special volume*.

Aldenderfer, M., Craig, N.M., Speakman, R.J., and Popelka-Filcoff, R., 2008. Four-thousand-year-old gold artifacts from the Lake Titicaca basin, southern Peru. *PNAS* 105 (13), 5002-5005.

Bachmann, H. G., 1982. *The identification of slags from archaeological sites.* London: The Institute of Archaeology.

Bakewell, P., 1984. *Miners of the red mountain Indian labour in Potosi, 1445-1650.* Albuquerque: University of New Mexico.

Bakewell, P., 1997. Technological Change in Potosi: The Silver Boom of the 1570's. *Mines of Silver and Gold in the Americas* (Variorum), 75-95.

Bargallo, M., 1967. La guaira, horno del fundición del Antiguo Peru. Estudio de las referencias de Cronistas. *Mineria* 79, 43-47.

Bayley, J., 1992. Anglo-Scandinavian non-ferrous metalworking from 16-22 Coppergate (The Archaeology of York 17/7). London: Council for British Archaeology.

Bayley, J., and Eckstein, K., 1995. Silver refining - production, recycling, assaying. In: A. Sinclair, E. Slater and J. Gowlett (eds) Archaeological sciences 1995 : proceedings of a conference on the application of scientific techniques to the study of archaeology, Liverpool, July 1995. Oxford, UK: Oxbow Monograph, 107-111.

Berthelot, J., 1986. The extraction of precious metals at the time of the Inka. In: J. Murra, N. Wachtel, & J. Revel (eds) *Anthropological History of Andean Polities*. Cambridge, UK: Cambridge University Press, 69-88.

Bertonio, L., 1984 (1612). *Vocabulario de la lengua Aymara*. Cochabamba, Bolivia: Centro de Estudios de la Realidad Económica y Social.

Bingham, H., 1911. Potosí. *Bulletin of the Americas Geographical Society* 43 (1), 1-13.

Bolton, R., and Mayer, E., 1977. *Andean kinship and marriage*. US: Special publication of the American Anthropological Association 7.

Boman, E., 1908. *Antiquités de la région Andine de la république Argentine et du désert d'atacama* ., Paris, France: Tome Premier.

Bray, W., 1978. *The gold of El Dorado.* London, UK: Times Newspaper.

Browman, D., 1974. Pastoral nomadism in the Andes. *Current Anthropology* 15 (2), 188-196.

Brandon, D. and Kaplan, W., 1999. *Microstructural Characterization of Materials.* UK: John Wiley & Sons Ltd.

Brundle, R., Evans, C., and Wilson, S., 1992. *Encyclopaedia of materials characterization: surfaces, interfaces, thin films.* Butterworth – Boston, London: Heinemann.

Burgess, C,. 2000. *Valid analytical methods and procedures.* Cambridge, UK: Royal Society of Chemistry.

Capoche, L., 1585. *Relacion General de la Villa Imperial de Potosí.* Ediciones Atlas Madrid.

Cohen, C.R., Rehren, Th., Van Buren, M., Mills, B.H., in press: Current silver smelting in the Bolivian Andes: a review of the technology employed, *Historical Metallurgy special volume.*

Cohen, C.R., Rehren, Th., Van Buren, M., forthcoming a: The *huayrachina* inside and out: an archaeo-metallurgical study of lead smelting technology in Porco-Potosí, Bolivia, *Coloquio Minas y Metalurgias en los Andes del Sur* (in Spanish).

Cohen, C.R., Rehren, Th., Van Buren, M., forthcoming b: When the wind blows: environmental adaptability in current day silver production within the Bolivian Andes, *The 37th ISA Conference Proceedings.*

Cohen, C.R., Rehren, Th., Van Buren, M., forthcoming c: An archaeo-metallurgical study of the use of European furnaces in colonial Bolivia, *Proceedings The 2nd Archaeometallurgy in Europe Conference* held June 2007 Grado, Italy.

Cohen, J.M., trans., 1998. *The discovery and conquest of Peru: a translation of Books I to IV of Agustín de Zárate's History of these events ...* Harmondsworth: Penguin.

Costin, C., Earle, T., Owen, B., and Russell, G., 1989: The impact of Inca conquest on localtechnology in the Upper Mantaro Valley, Peru, Chapter 6. In: S.Van der Leeuw and R.Torrence (eds) *What's New? A closer look at the Process of Innovation.* One World Archaeology 14.

Cranstone, D., and Willies, L., 1992. *Boles and smeltmills.* London: Historical Metallurgy Society.

Craddock, P. T., 1995. *Early Metal Mining and Production.* Edinburgh, UK: Edinburgh University Press.

Craig, A., 1994. Spanish colonial silver beneficiation at Potosi. In: A. Craig & R. West (eds.) *In quest of mineral wealth.* Geoscience and Man (33). Louisiana State University, Baton Rouge: Geoscience Publications, 271-286.

Cresswell, R., 1976. Avant-propos. *Techniques et Culture* (1), 5-6.

Cunningham, C. G., Zartman, R. E., McKee, E. H., Rye, R. O., Naeser, C. W., Sanjines, V., Erickersen, G. E., and Tavera, F., 1996. The age and thermal history of Cerro Rico de Potosi, Bolivia. *Mineralium Deposita* 31(5), 374-385.

Deere, C.D., 1990. *Household and class relations: peasants and landlords in Northern Peru.* US: University of California Press.

Dobres, M-A., 1999. Technology's links and *chaînes:* the processual unfolding of technique and technician. In: MA. Dobres and C.R. Hoffmann (eds) *The social dynamics of technology: practice, politics and world views.* Washington: Smithsonian Institute Press, 124-146.

Douglass, R. E., and Mathewson, E. P., trans., 1923 (1640). *Alvaro Alonso Barba's Arte de los metales en que se enseña el verdadero beneficio de los de oro, y plata por azogue, el modo de fundirlos todos y cómo se han de refinar, y apartar unos de otros.* New York.

Dransart, P., 1991. Lamas, herders and the exploration of raw materials in the Atacama desert. World Archaeology 22 (3), 304-319.

D'Altroy, T. N., 2003. *The Incas.* Oxford: Blackwell Publishing.

D'Altroy, T. N., Lorandi, A. M., Williams, V. I., Calderari, M., Hastorf, C. A., DeMarrais, E., and Hagstrum, M. 2000. Inca rule in the Northern Calchaqui Valley, Argentina. *Journal of Field Archaeology* 27 (1), 1-26.

Edwards, R., and Atkinson, K., 1986. *Ore Deposit Geology and its influence on mineral exploration.* London: Chapman and Hall.

Ellis Jones, J., 1986. The Athenian silver mines of Laurion and the British School at Athens excavations at Agrileza. In: *Aspects of Ancient Mining and Metallurgy: ACTA of a British School at Athens centenary conference at Bangor, 1986.* Wales, Classical Association, 11-22.

Epstein, S. M., 1993. *Cultural choice and technological consequences: constraint of innovation in the Late Prehistoric copper industry of Cerro Huaringa, Peru.* PhD dissertation, University of Pennsylvania, Philadelphia.

Fifield, F.W., and Kealey, D., 2000. *Principles and practice of analytical chemistry.* Oxford: Blackwell Science Ltd.

Fisher, J.R., 1975. Silver production in the Viceroyalty of Peru, 1776-1824. *The Hispanic American Historical Review* 55 (1), 25-43.

Fisher, J. R., 1977. *Silver mines and silver miners in colonial Peru, 1776-1824.* Centre for Latin-American Studies. The University of Liverpool Monograph Series 7.

Foster, G. M., 1965. Peasant society and the image of limited good. American Anthropologist 67 (2), 293-315.

Gosden, C., and Marshall, Y., 1999. The cultural biography of objects. *World Archaeology* 31 (2), 169-178.

Hammond, P. B., 1975. *Cultural and social anthropology: introductory readings in ethnology* (2nd edition). New York, US: Macmillan Publishing Co Inc.

Hamilton, R., and Buchanan, D., 1996. *Narrative of the Incas by Juan de Betanzos from the Palma de Mallorca Manuscript*. Austin, Texas: University of Texas Press.

Hanke, L., 1956. The imperial city of Potosí: an unwritten chapter in the history of Spanish America. The Hague: Nijhoff.

Hanson, E., 1926. Out-of-the-World Villages of Atacama. *Geographical Review* 16 (3), 365-377.

Harris, O., 1995. Ethnic identity and market relations. In B. Larson, O. Harris, and E. Tandeter (eds) *Ethnicity, markets, and migration in the Andes. At the crossroads of history and anthropology.* US: Duke University Press.

Hayden, B., 1998. Practical and prestige technologies: The evolution of material systems. *Journal of Archaeological Method and Theory* 5 (1), 1-55.

Healy, J. F., 1978. *Mining and metallurgy in the Greek and Roman world.* UK: Thames and Hudson.

Hoover, L. and Hoover, H., 1950. *Georgius Agricola's De Re Metallica.* New York: Dover Publications.

Howe, E., and Petersen, U., 1994. Silver and lead in the Late Prehistory of the Mantaro Valley, Peru. In: D.A. Scott and P. Meyers (eds) *Archaeometry of Pre-Columbian sites and artifacts: proceedings of a symposium organised by the UCLA Institute of Archaeology and the Getty Conservation Institute.* Malibu: Getty Conservation Institute, 183-198.

Jackson, C. M., and Smedley, J. W., 2004. Medieval and post-medieval glass technology: melting characteristics of some glasses melted from vegetable ash and sand mixtures. *Glass Technology* 45 (1), 36-42.

Johnson, M., 2003. *Archaeological theory: an introduction.* UK: Blackwell Publishing.

Jones, A., 2004. Archaeometry and materiality: materials-based analysis in theory and practice. *Archaeometry* 46(3), 327-338.

Killick, D., 2004. Social constructionist approaches to the study of technology. *World Archaeology* 36 (4), 571-578.

King, H., 2000. *Rain of the Moon; Silver in Ancient Peru* . New York, US: The Metropolitan Museum of Art, Yale University Press.

Kleier, C., and Rundel, P., 2004. Microsite requirements, population structure and growth of the cushion plant *Azorella compacta* in the tropical Chilean Andes. *Austral Ecology* 29, 461-470.

Kulhanek, B., 2007. The technology of silver processing. A comparison of two sites at Porco, Bolivia. Unpublished thesis in partial fulfilment for the requirements of the degree of MSc in Technology and Analysis of Archaeological Material, IoA, UCL.

La Niece, S., and Meeks, N., 2000. Diversity of goldsmithing traditions in the Americas and the Old World. In: C. McEwan (ed.) *Precolumbian Gold: Technology, Style and Iconography,* 220-239. London, UK: British Museum Press.

Lanning, E. P., 1967. *Peru before the Incas.* New Jersey, US: Prentice-Hall Inc,

Lechtman, H., 1976. A metallurgical site survey in the Peruvian Andes. *Journal of Field Archaeology* 3(1), 1-42.

Lechtman, H., 1977. Style in technology - some early thoughts. In H. Lechtman and R. Merrill (eds) *Material culture; style, organization, and dynamics of technology,* 3-20. US: West Publishing Co.

Lechtman, H., 1984. Andean value systems and the development of prehistory metallurgy. *Technology and culture* 25, 1-36.

Lecoq, P., and Cespedes, R., 1996. Nuevas investigaciones arqueologicas en los andes meridionales de Bolivia. Una vision prehispanica de Potosí. Revista de Investigaciones Historicas, 183-267.

Lehmann, D., 1982. *Ecology and exchange in the Andes.* UK: Cambridge University Press.

Lemmonier, P., 1986. The study of material culture today: towards an anthropology of technical systems. *Journal of Anthropological Archaeology* 5, 147-186.

Lemmonier, P., 2002. Technological choices; transformations in material cultures since the Neolithic. London: Routledge.

Lleras Pérez, R., 2005. *Precious metals. Gold and silver from our ancestors.* Chile: Museo Chileno de Arte Precolombino.

Loney, H.L., 2000. Society and technological control: a critical review of models of technological change in ceramic studies. *American Antiquity* 65(4):646-668.

Lucas, G., 2005. Chapter 4. Case Study: the Life and Times of a Roman Jar. In *The Archaeology of Time.* London: Routledge, 95-113.

Mayer, E., 1982. *A tribute to the household. Domestic economy and the encomienda in Colonial Peru.* Austin Texas, US: Institute of Latin American Studies, University of Texas.

Mayer, E., 2002. *The articulated peasant; Household economies in the Andes.* Oxford, UK: Westview Press.

Martinón-Torres, M. and Rehren, Th., 2005. Alchemy, chemistry and metallurgy in Renaissance Europe: a wider context for fire-assay remains. *Historical Metallurgy* 39[1], 14-28.

Martinon-Torres, M., Rehren, Th., and von Osten, S. A., 2003. The 16th century lab in a 21st century lab: archaeometric study of the laboratory equipment from Oberstockstall (Kirchberg am Wagram, Austria). *Antiquity Project Gallery* 77 (298).

Martinón-Torres, M., Valcárcel Rojas, R., Cooper, J. and Rehren, Th. 2007. Metals, microanalysis and meaning: a study of metal objects excavated from the indigenous cemetery of El Chorro de Maíta, Cuba. *Journal of Archaeological Science* 34(2), 194-204.

McEwan, C. 2000. *Precolumbian Gold: Technology, Style and Iconography* . London, UK: British Museum Press.

Mei, J., and Rehren, Th., 2005. Copper smelting from Xinjiang, NW China. Part I: Kangcun village, Kuche county, c 18th century AD. *Historical Metallurgy* 39, 14-28.

Mills, B. H., 2003. *Flame and Fortune.* Unpublished thesis in partial fulfilment for the requirements of the degree of BSc in Archaeology, IoA, UCL.

Moseley, M., 2001. *The Incas and their ancestors. The Archaeology of Peru.* London, UK: Thames & Hudson Ltd.

Nash, J., 1979. *We eat the mines and the mines eat us: dependency and exploitation in Bolivian tin mines.* New York, US: Columbia University Press.

Oehm, V.P., 1984: *Investigaciones sobre minería y metalurgia en el Perú prehispánico*, Bonner Amerikanistische Studien 12, Seminar für Völkerkunde, Universität Bonn, Bonn.

Parma Cook, A., and Cook, N. D., trans., 1998. *Cieza de León, Pedro de, 1518-1554: The discovery and conquest of Peru : chronicles of the New World encounter.* London: Duke University Press, London.

Patterson, C., 1971. Native copper, silver and gold accessible to early metallurgists. *American Antiquity* 36(3), 286-321.

Peele, R., 1893. A Primitive Smelting Furnace, *School of Mines Quarterly* 15, 8-10.

Pernicka, E., 1990. *Gewinnung und Verbreitung der Metalle in prähistorischer Zeit.* Germany: Romisch-Germanisches Zentralmuseum.

Petersen, G., 1970. *Mineria y Metalurgia en el Antiguo Peru.* Lima, Peru: Museo Nacional de Antropología y Arqueología. Arqueológicas.

Pfaffernberger, B., 1992. Social anthropology of technology. *Annual Review of Anthropology* 21, 491-516.

Pfordte, O.F., 1893. Ancient method of silver and lead smelting in Peru. *Transactions of the American Institute of Mining Engineers* 21, 25-30.

Pike, R., 1972. *Aristocrats and traders: Sevillian society in the sixteenth century.* London: Cornell University Press.

Platt, T., Bouysse-Cassagne, T., and Harris, O., 2006. *Qaraqara-Charka — Mallku, Inka y Rey en la provincia de Charcas (siglos XV-XVII): Historia antropológica de una confederación aymara. Qaraqara-Charka.* La Paz, Bolivia: Institut Français d'Études Andines / Plural Editores / University of St Andrews / University of London / Inter-American Foundation / Cultural Foundation of the Bolivian Central Bank.

Presta, A-M., in press. The first jewel in the crown of the Southern Altiplano: the discovery and initial exploration of Porco, 1538-1576. A paper presented at Crossroads of Globalization: 'Hot Spots' in the early modern World. US: The Ohio State University.

Pryce, T. O., Bassiakos, Y., Catapotis, M., and Doonan, R. C., 2007. *'De Caerimoniae'* Technological choices in copper-smelting furnace design at early bronze age Chrysokamino, Crete. *Archaeometry* 49 (3), 543-557.

Rabey, M.A., 1989. Technological continuity and change among the Andean peasants: opposition between local and global strategies. In *What's New? A closer look at the Process of Innovation* edited by S.Van der Leeuw and R Torrence. One World Archaeology 14, 167-181.

Raffino, R., Iturriza, R., Iácona, A., Capparelli, A., Gobbo, D., Montes, V.G., and Vázquez, R., 1996. Quillay: Centro metalurgico Inka en el noroeste Argentino. *Tawantinsuyu* 2, 59-69.

Ramsay, P. M., and Oxley, E., 1997. The growth form composition of plant communities in the Ecuadorian Páramos. *Plant Ecology* 131, 173-192.

Rasnake, R., 1988. *Domination and Cultural Resistance: Authority and Power among an Andean People.* Durham and London: Duke University Press.

Rishel, J.J., and Stratton, S.L., 2006. *The Arts in Latin America, 1492-1820.* US: Yale University Press.

Roux, V., 1990. Psychological analysis of technical activities: a contribution to the study of craft specialisation. *Archaeological Review from Cambridge* 9(1):142-153.

Reed, S. J. B., 1996. *Electron microprobe analysis and scanning electron microscopy in geology.* Cambridge: Cambridge University Press.

Rehren, Th., 1997. Metal analysis in the Middle Ages. In: G de Boe & F Verhaeghe (eds) *Material Culture in Medieval Europe.* Zellink, 9-15.

Rehren, Th., 2001. Ores, crucibles and cupels past and present possibilities of scientific analysis. *Cahiers d'archéologie du CELAT* 10 (Série archéométrie 1), 65-71.

Rehren, Th., and Klappauf, L., 1995. ...ut oleum aquis Vom Schwimmen des Silbers auf Bleiglätte. *Metalla* (2), 19-28.

Renfrew, C., and Bahn, P., 2000. *Archaeology: theories methods and practise* (3rd Ed). London, UK: Thames and Hudson.

Rice, P.M., 1987. *Pottery Analysis; A sourcebook.* Chicago, US: University of Chicago Press.

Rowlands, M., 1993. The role of memory in the transmission of culture. *World Archaeology* 25 (2), 141-151.

Sallnow, M. J., 1989. Precious metals in the Andean moral economy. In: J. Parry and M. Block (eds) *Money and the morality of exchange.* C.U.P., 209-231.

Saignes, T., 1995. Indian migration and social change in seventeenth-century Charcas. In: B. Larson, O. Harris, and E. Tandeter (eds) *Ethnicity, markets, and migration in the Andes. At the crossroads of history and anthropology.* US: Duke University Press.

Scattolin, M.C., and Williams, V., 1992. Actividades minero metalúrgicas prehispanicas en el noroeste argentino nuevas evidencias y su significación. *Bulletin de Instituto Francés de Estudios Andinos (IFEA)* 21(1), 59-87.

Schlanger, N., 2005. The *chaîne opératoire.*In: C. Renfrew and P. Bahn (eds) *Archaeology the key concepts.* London: Routledge, 25-31.

Schorsch, D., 1998. Silver-and-gold Moche artifacts from Loma Negra, Peru. *Metropolitan Museum Journal* 33, 109-136.

Shackleton, W.G., 1986. Chapter 1. Mineral deposits. In: W.G. Shackleton (ed.) *Economic and applied geology; an introduction.* London: Croom Helm, 1-17.

Shimada, I., 1994. Pre-hispanic metallurgy and mining in the Andes: Recent advances and furture tasks. In: by A. Craig and R. West (eds) *In quest of mineral wealth. Aboriginal and colonial mining and metallurgy in Spanish America.* Geoscience and Man 33. Baton Rouge, US: Gseoscience Publications 37-73.

Shimada, I., Epstein, S., and Craig, K., 1982. Batán Grande: A prehistoric metallurgical center in Peru. *Science* 216, 952-959.

Shimada, I., Griffin, J.A., and Gordus, A., 2000. The technology, iconography and social significance of metals. A multi-dimensional analysis of Middle Sican objects. In: C. McEwan (ed.) *Precolumbian Gold: Technology, Style and Iconography*, 28-61. London, UK: British Museum Press.

Shimada, I., and Merkel, J., 1991. Copper-alloy metallurgy in ancient Peru. Scientific American 265(1), 62-75.

Sillar, W., unpublished. An exploration of the concept of 'Embedded Technologies' and suggestions for its application in archaeology. *Embedded technologies reworking technological studies in archaeology* held at the UCL IoA 8-9th May 2006 coordinated by B. Sillar and B. Boyd.

Sillar, W., 2000a. *Shaping culture – making pots and constructing households; An ethnoarchaeological study of pottery production, trade and use in the Andes.* BAR International Series 883.

Sillar. W., 2000b. Dung by Preference:The choice of fuel as an example of how Andean pottery production is embedded within wider technical, social and economic practices. *Archaeometry* 42 (1), 43-60.

Sillar, W., and Tite, M., 2000. The Challenge of 'Technological Choices' for Materials Science Approaches in Archaeology. *Archaeometry* 42 (1), 2-20.

Silverblatt, I., 1987. *Moon, Sun, and Witches; Gender Ideologies and Class in Inca and Colonial Peru* . Princeton, New Jersey: Princeton University Press,

Sisco, A.G., and Smith, C. S., trans., 1951. *Lazarus Ercker's Treatise on Ores and Assaying translated from the German Edition 1580.* US: Chigaco, Illinois.

Smith, C. S., and Gnundi, M. T., trans., 1959. *Vannoccio Biringuccio's De La Pirotecnia.* US: New York.

Steward JH 1946. *Handbook of South American Indians 2.* New York,US: Cooper Square Publishers Inc.

Tarrago M.N., and Gonzalez, L.R., 1998. La producción metalúrgica prehispánica en el asentamiento de Tilcara (Prov. De Jujuy). In: M.B Cremonte (ed.) *Estudios preliminares sobre nueves evidencias. Los desarrollos locales y sus territorios: arqueología del NOA y sur de Bolivia.* San Salvador de Jujuy, Argentina: Universidad Nacional de Jujuy, 179-198.

Timberlake, S., 2000. 'Treasure of the world, king of the mountains, envy of the kings': the imperial Spanish silver mines of Potosí, Bolivia. *Mining History: The Bulletin of the Peak District Mines Historical Society 14* (4), 31-39.

Torrence, R., and Van der Leeuw, S.E., 1989. Introduction: what's new about innovation? What's new? A closer look at the process of innovation. In: S.Van der Leeuw and R.Torrence

(eds) *What's New? A closer look at the Process of Innovation.* One World Archaeology 14, 1-15.

Urton, G., 1999 *Inca myths.* US: University of Texas Press.

Van Buren, M., 2001. Lead and silver smelting; Carlos Cuiza, Pucapuja Porco, Bolivia. Unpublished report.

Van Buren, M., 2003a. Smelts conducted by Carlos Cuiza in 2003 Pucapujra Porco, Bolivia. Unpublished report.

Van Buren, M., 2003b. Un estudio etnoarqueológico de la tecnología de fundicíon en el sur de Potosí, Bolivia, *Textos Antropológicos* 14(2), 133-148. La Paz, Bolivia: UMSA.

Van Buren, M., 2005. *Inka, Spanish and indigenous silver production in Porco, Bolivia.* Collorado State University, US: National Endowment for the Humanities final performance report (Grant # RZ-20934-02).

Van Buren, M., and Presta, A-M., in press. The organisation of Inca silver production in Porco, Bolivia. In: M. Malpass and S. Alconini (eds) *Provincial Inca.* US: University of Iowa Press.

Van Buren, M., and Mills, B.H., 2005. *Huayrachinas* and Tocochimbos: Traditional smelting technology of the southern Andes. *Latin American Antiquity* 16(1), 3-25.

Velasco, P., 2001 The mineral industry of Bolivia. U.S. Geological survey minerals yearbook.

Veldhuijzen, A.H., and Rehren, Th., 2007. Slags and the city: early iron production at Tell Hammeh, Jordan, and Tel Beth-Shemesh, Israel. In: S. LaNiece, D. Hook and P. Craddock (eds) *Metals and Mines – Studies in Archaeometallurgy.* London, UK: Archetype, 189-201.

West, R.C., 1997. Aboriginal metallurgy and metalworking in Spanish America. A brief overview. In: P. Bakewell (ed.) *Mines of Silver and Gold in the Americas* (Variorum), 41-73.

Winterhalder, B., Larsen, R., and Thomas, R.B., 1974. Dung as an essential resource in a highland Peruvian community. *Human Ecology* 2(2), 89-104.

THE WINDS OF CHANGE: AN ARCHAEOMETALLURGICAL STUDY OF SILVER PRODUCTION IN THE PORCO-POTOSÍ REGION, SOUTHERN BOLIVIA AD 1500-2000

VOLUME II
APPENDICES

CLAIRE REBEKAH COHEN
UCL, INSTITUTE OF ARCHAEOLOGY
JUNE 2008

Volume II is a catalogue of raw data including: photographs, drawings, maps, site details, the ethnographic review of silver production and results of analytical work carried out on selected samples (ethnographic and archaeological). It is designed to compliment Volume I.

"I, *Claire Rebekah Cohen* confirm that the work presented in this thesis is my own. Where information has been derived from other sources, I confirm that this has been indicated in the thesis."

TABLE OF CONTENTS

APPENDIX I - ETHNOGRAPHIC SILVER PRODUCTION

The smelting process – pictorial review (Photos by PAPP and B Mills 2001/2002)

Charcoal making

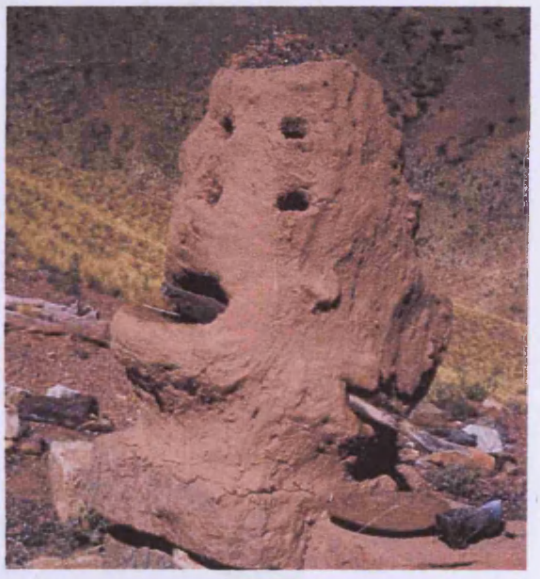

The loaded furnace prior to starting the smelt

Beneficiation of lead ore

Smelting in the *huayrachina*

Cuiza site map (Van Buren and Mills 2005, 16)

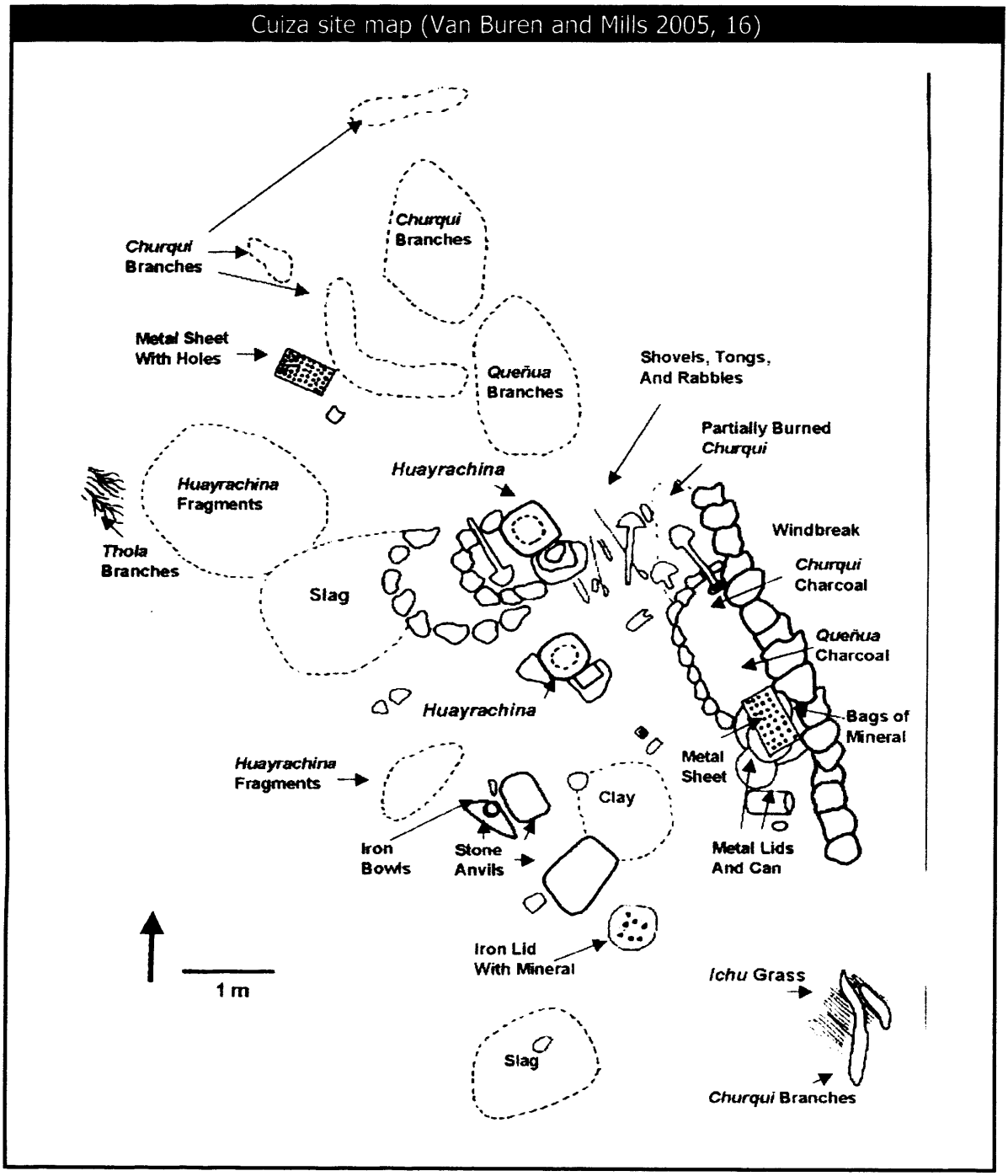

Cuiza's *huayrachinas* visited in during fieldwork in 2005

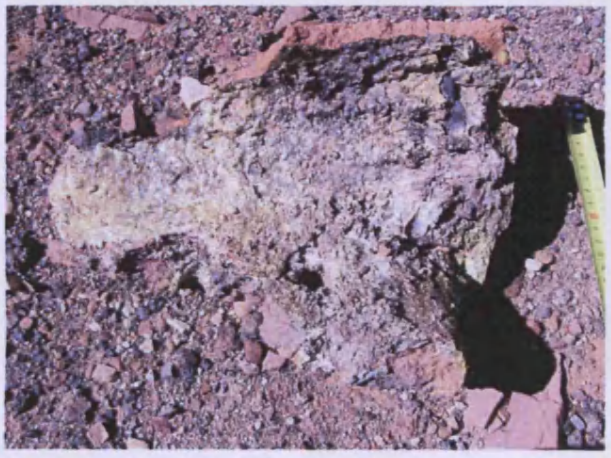

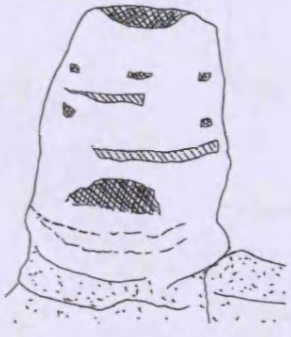

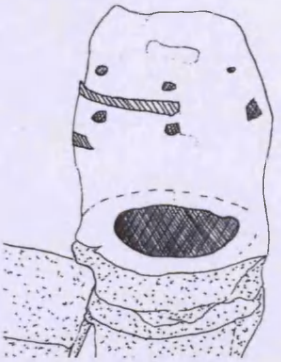

Cuiza's cupellation hut and hearth

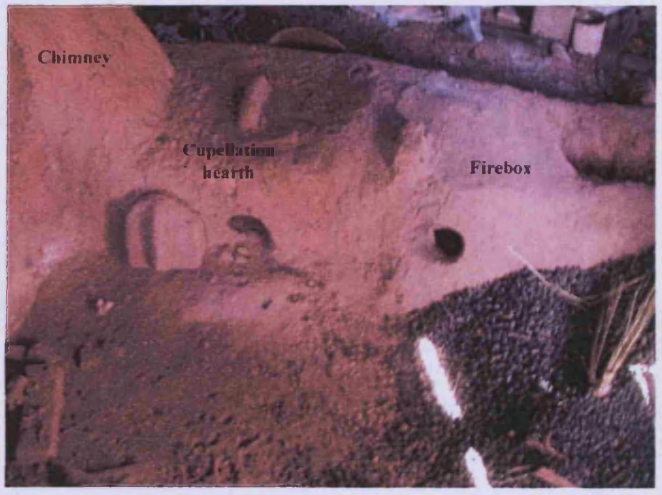

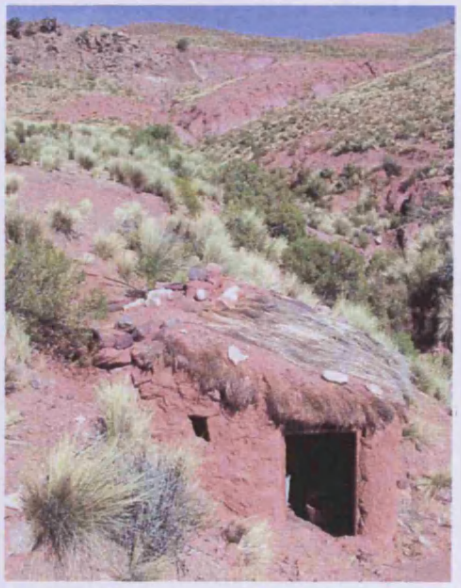

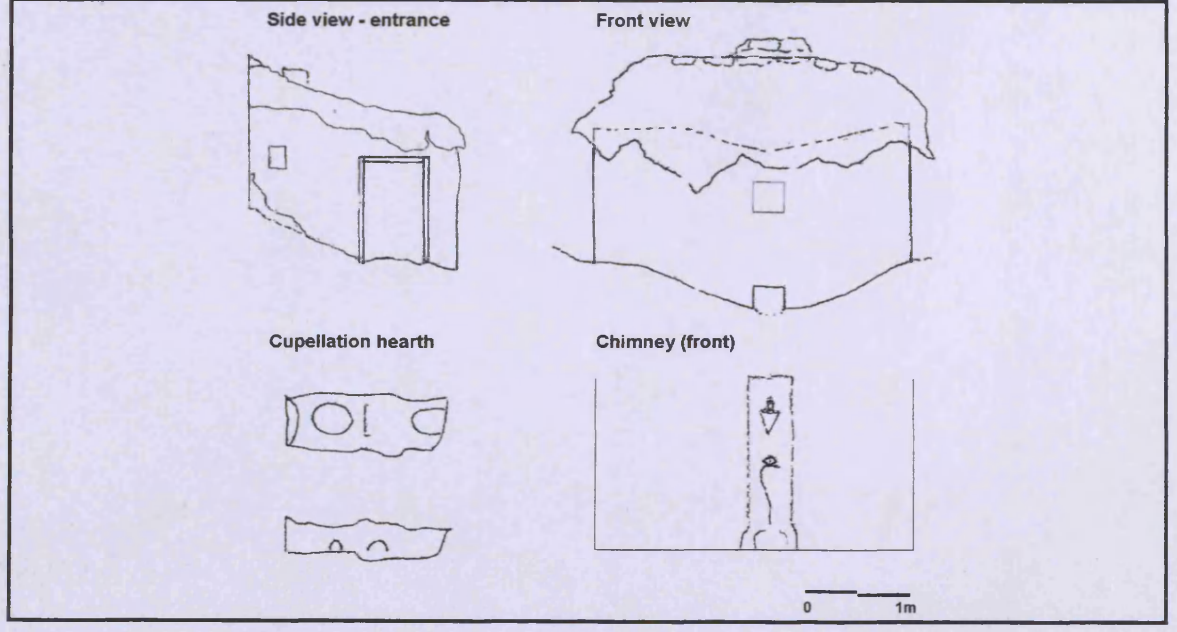

The ethnographic silver production process - details

2001

First day 1st smelt

Time	Action	Details	Notes
11.30	Smelt begins	The fire was lit using dried grass (*ichu*) and burro dung at the base of the *huayra*. The mouths were plugged with firewood and the *huayra* filled from the top with charcoal and dung.	Normal smelting to place in the late afternoon when wind starts to increase.
11.45	Charge was added	Scoop fulls of ore mixture (crushed galena, litharge wetted with urine) were loaded on to *huayra,* alternating layers of charcoal and ore.	~
13.15	The first lead metal was collected	The first lead metal begins to dribble onto the iron dish seated on the side of the *huayrachina*.	Abram (Cuiza's son) said the slag still contained lead. Samples collected from this smelt: labelled: 1-17 2001.
20.00	Smelt terminated	Slag dumped on the side of site. Samples 9 and 9a selected.	

First day 2nd smelt

Time	Action	Details	Notes
12.00	Smelt begins	Same procedure as above (1st smelt).	~
16.00	Smelt terminated	The fire never became hot enough to melt the lead and the smelt abandoned.	No samples taken from this smelt.

Second day 2nd smelt

Time	Action	Details	Notes
11.30	Smelt begins	Partially reacted material from the failed smelt on the first day was re-smelted and then unreacted ore was added.	~
19.00	Smelt terminated	Lead metal produced.	No samples taken from this smelt.

2002

First day 1st smelt

Time	Action	Details	Notes
?	~	Lead ore, litharge and urine (fresh) mixed on a hubcap after beneficiation, the top of the cap was folded over and weighed down. To prevent the mixture drying out.	Carlos said that urine works better than water.
?	*Huayrachina* repaired	Clay from the *quebrada* used to fill in cracks on the *huayrachina*.	~
?	*Ch'allas* offered	*Ch'allas* offered to the furnace, coca leaves, alcohol and he spoke gently to the furnace.	Continued offerings made throughout the smelt.

Time	Action	Details	Notes
9.45	Smelt begins	The *huayra* filled from the top with charcoal and donkey dung. *Ichu* grass used to start the fire, a lot of smoke.	Normal smelting to place in the late afternoon when wind starts to increase.
10.05	Ore mixture added	Scoop fulls of ore mixture (crushed galena, litharge wetted with urine) were loaded on to *huayra*, alternating layers of charcoal and ore.	~
10.35	Slag re-fed	The *huayra* mouth was scraped out and the slag was re-fed back into the top.	The eye holes were poked with an iron rod to move the charge inside the furnace and the mouth was stoked and fresh *quenua* added.
12.45	Lead collect	2 kg of lead collected	~
14.30	Smelt terminated	Last slag is inspected and charge finished, Cuiza decided to finish the smelt, the *huayra* was scraped clean.	~

First day 2nd smelt done in the same *huayrachina*

Time	Action	Details	Notes
13.20	Ore beneficiated	Ore beneficiated by Don Dionisio and Don Juan	~
?	Smelt terminated	Don Carlos smelted the material himself and so there is no data on the second smelt.	~

2001 Cupellation reviewed

Time	Action	Details	Notes
9.30	Cupellation started	The hearth was loaded with 1.8 kg lead and some litharge, the openings were sealed. The fire was started with thola wood from the North end of the fire box.	Cuiza would have normally started earlier but he had to wait for the team to arrive from Potosi.
10.30	Fuel changed	After an hour using *thola* wood, the north opening was sealed with ash and clay and the fire was fed through a side opening with llama and burro dung.	~
12.00	Lead semi-liquid	The lead was semi-liquid gangue skimmed from the surface using an iron hook.	This process of adding small amounts of silver ore, skimming off impurities from the molten lead and stirring the fuel continued constantly until the silver ore was exhausted.
14.00	Silver ore added	The lead was totally molten and the silver ore was added using an iron spoon.	

Time	Action	Details	Notes
6.00 the next morning	Cupellation finished	Silver bullion is removed form the furnace and solidifies immediately	• the opening into the firebox broke was repaired with wet clay • the chimney got plugged • there was too much lead oxide and it absorbed some of the silver. • Cuiza said that some of the lead was absorbed into the hearth lining but he would recycle it in his next *huayrachina* smelt. • Dr Van Buren noted that normally Cuiza would use greater quantities of ore but he made this process smaller so that the team could see the whole process.

2002 Cupellation reviewed

Time	Action	Details	Notes
Unknown	Silver ore beneficiated	Don Cuiza, Don Dionisio and Don Juan beneficiated the ore crushing it to a fine grain powder on a flat rock with mallets.	Cuiza was unhappy with the ore the team had bought, he said it was '*plata blanca*' and had a poor quality. He recommended that they buy '*rosicler*' (ruby silver) this would have been refined more easily and produce purer silver.
Unknown	Llareta ash prepared	The *llareta* ash was screened through a 2 mm sieve. Fresh urine was mixed with the screened ash, to make a semi moist powder. The hearth was lined with this mixture.	~
Unknown	Cupellation started	The fire was started with llama dung, every few minutes handfuls of dried dung was thrown into the furnace. Cuiza said he prefers llama to donkey dung because it creates more heat and less ash.	~
Unknown	*Ch'allas* offered	*Ch'allas* were offered to the furnace, 2-3 plates of different powders were added to the fire box, pure alcohol and *coca* leaves were also given. Mills (2003, 24) noted that Cuiza made later offerings in the name of the 'child Manuel'.	~

Time	Action	Details	Notes
16.15	Cuiza requests more silver ore	Too much lead was present in the system so more silver ore was needed.	~
17.50	Donkey dung added	*Burro* dung was added to the fire box at the end of the process.	~
unknown	Cupellation finished	Silver bullion is removed form the furnace and solidifies immediately	A few problems: the poor silver ore produced very little silver.

2003 Cupellation reviewed

Cuiza was happy with quliaty of the silver ore but a rapture hearth meant that most of the silver metal was lost. Silver metal was trapped in the litharge.

The high quality silver ore required more lead metal which was unavaiblable due to the low lead yield in the *huayrachinas*.

	2001				2002				2003					
Materials	**Input Smelt 1**	**Output Smelt 1**	**Input Smelt 2**	**Output Smelt 2**	**Input Smelt 1**	**Output Smelt 1**	**Input Smelt 2**	**Output Smelt 2**	**Input Smelt 1**	**Output Smelt 1**	**Input Smelt 2**	**Output Smelt 2**	**Input Smelt 3**	**Output Smelt 3**
Lead Ore	12 kg		14 kg		12 kg		11 kg		10 kg		14 kg		16 kg	
Litharge	7 kg		8 kg		6 kg		6 kg		6 kg		11 kg		13 kg	
Urine	0.5 litres		0.5 litres		0.5 litres		0.5 litres		unspecified		0.8 litres		1.5 litres	
Charcoal	12 kg		?		8 kg		8 kg		15 kg		16 kg		10 kg	
Lead Metal		**4 kg**		**6 kg**		**4 kg**		**5 kg**		**2 kg**		**2.5 kg**		**2 kg**
Slag		**?**		**?**		**9 kg**		**7 kg**		**9 kg**		**16 kg**		**10 kg**

Input and output quantities for the documented huayrachina smelts

Materials	2001		2002		2003	
	Input	**Output**	**Input**	**Output**	**Input**	**Output**
Silver ore	0.3kg		1.5 kg		0.5 kg	
Lead metal	1.8 kg		3 kg		6 kg	
Llareta ash	~		~		~	
Dung	12 costales		61.5 kg		66 kg *llama* dung, 1 kg *burro* dung	
Other fuel					1 kg firewood, 0.5 kg dry grass	
Silver metal		**0.145 kg**		**0.013 kg**		**0.227 kg**
CHM	**?**	**?**		**5 kg**		**6 kg**
Slag		**?**		**7.1 kg**		**0.5 kg**

Input and output quantities for the documented silver refining episodes.

Total sample list from the ethnographic samples inherited from Mills 2003

2001

Sample no	Mounted blocks	Description
1		Clay used to repair *huayrachina*
2	2	Lead ore *huayrachina* 1
3	3	Lead ore *huayrachina* 2
4	4	Rejected ore *huayrachina* 2
5	~	CHM added to *huayrachina. Huayrachina* 1
6	6	CHM added to *huayrachina* poss different?
7	7	Lead 1st smelt *huayrachina* 1
8	~	Lead 2nd smelt
9	9	Slag 1st smelt
	9a	
13	13	Silver mineral (gangue)
14	14	Silver metal
15	15 MVB	CHM
	15cc	CHM
16	16 MVB	CHM
	16cc	CHM
	16a	CHM
17	17	*Huayrachina* fragments (OLDER ONES)

2002

Sample no	Mounted blocks	Description
1	~	Ag retrieved from CHM
2	8	CHM/4
3	5	CHM/1
4	19,20	Rejected ore 2nd smelt
5	15,16	Lead 2nd smelt after beneficiation
6	22	CHM 2nd smelt
7	7	CHM/3
8	3	Slag 2nd smelt/1
9	4	Slag 2nd smelt/2
10	9	Furnace fragment/1
11	~	Lead 1st smelt after beneficiation
12	13	AgM {13}
13	10	Slag 1st smelt/3
14	12	Lead metal 2nd smelt/1
15	11	Lead metal 1st smelt/1
16	1	Slag 1st smelt/1
17	2	Slag 1st smelt/2
18	17,18	Rejected ore 1st smelt from beneficiation
19	21	CHM 1st smelt
20	6	CHM/2
21	~	Slag from cupellation furnace
22	~	Llama dung after being scraped out of firebox
23	24	Beneficiated silver mineral used in cupellation
24	~	Clay from *quebrada* for repairing *Huayrachina* 1st smelt
25	25	llareta ash
26	~	*Thola* firewood
27	~	Charcoal *churque* 1st smelt
28	~	Charcoa ; *quenua* 1st smelt

APPENDIX II - ETHNOGRAPHIC SAMPLES

Furnace fragment

Galena - lead ore

Gangue mineral

CHM

Slag

Lead metal

LEAD SMELTING: THE ORE

Don Cuiza and his compadres prepare the galena for smelting. Crushing and sorting the galena from the gangue.

Mounted block	Year of smelt	Description
2	2001	Lead ore 1st smelt
3	2001	Lead ore 2nd smelt
15	2002	Lead ore 2nd smelt
16	2002	Lead ore 2nd smelt
4	2001	Rejected ore 2nd smelt
17	2002	Rejected ore 1st smelt
18	2002	Rejected ore 1st smelt
19	2002	Rejected ore 2nd smelt
20	2002	Rejected ore 2nd smelt

List of ore samples available for analyses

The following catalogue shows selected samples to illustrate the type of samples within the collection.

Ore sample 2 (2001)

a.

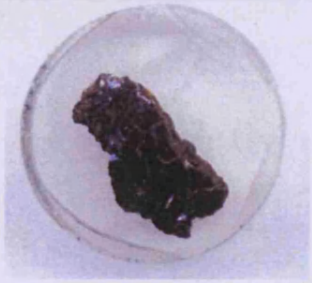

b.

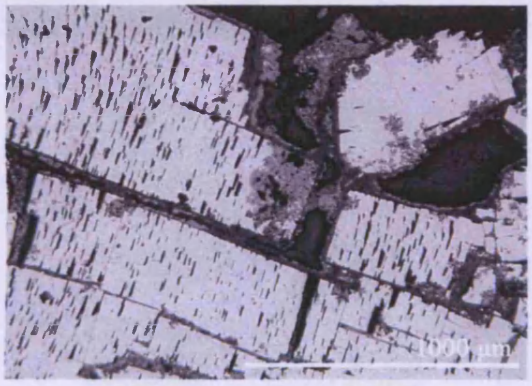

c.

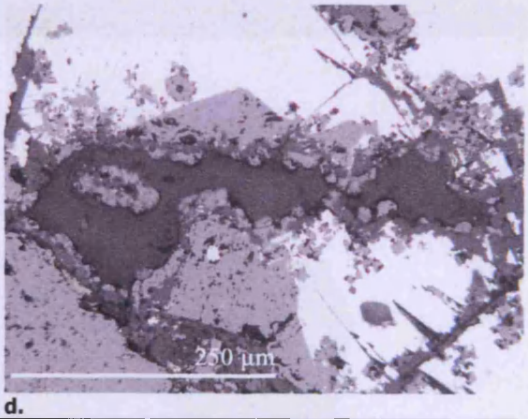

d.

The pure galena used in the *huayrachina* smelt 2001 has a shiny grey hand specimen (a). Prior to analyses it was cut and mounted in epoxy resin (b).

OM images (c and d) show the distinctive triangular pattern of lead sulphide. Inclusions of zinc sulphide (seen as light grey areas in image d) were common.

Ore sample 3 (2001)

a.

Ore sample 3 was beneficiated prior to smelting, crushed to pieces of 1 cm (a). The cut and mounted sample is shown in image b. The OM images showed this sample was not pure lead sulphide, it also contained sphalerite (ZnS) [light grey areas] and pyrite (FeS2), [cream coloured areas in image c and d].

b.

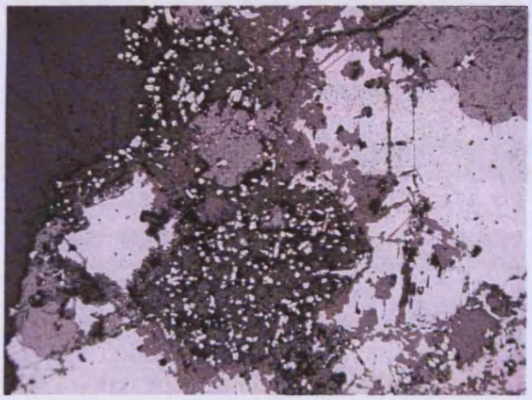

c.

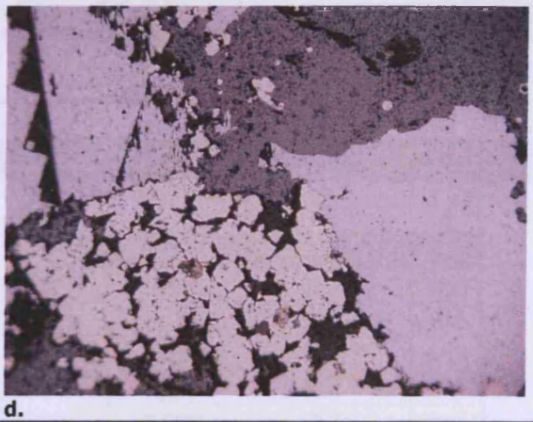

d.

Rejected ore sample 18 (2002) and sample 4 (2001)

Sample 18

2001

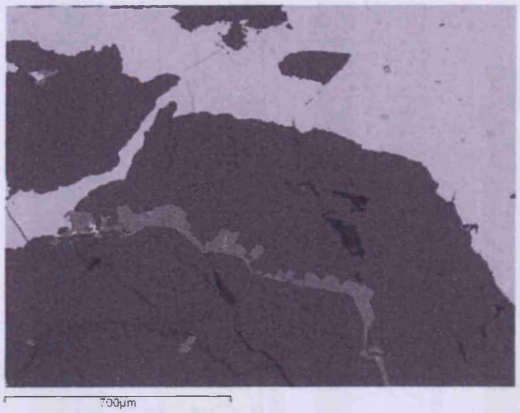

Sample 4 2001 rejected ore

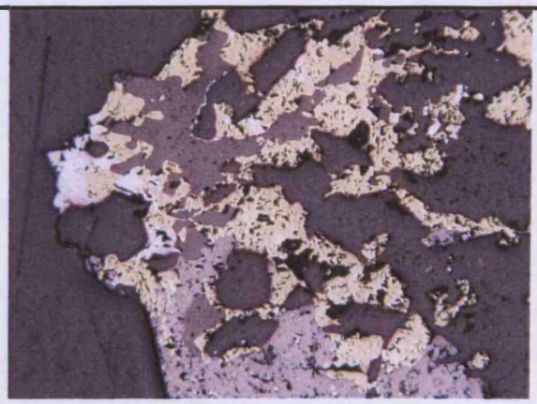

SEM-EDS analyses of the ethnographic ore samples

Samples analysed	S	Fe	Cu	Pb
15 2002	48.6	25.8	25.5	~
15 2002	48.7	26.0	25.3	~
15 2002	48.2	25.8	26.0	~
18 2002	48.6	25.7	25.8	~
18 2002	48.5	25.8	25.7	~
18 2002	48.2	25.0	26.8	~
18 2002	49.1	23.6	23.3	4.1

Scanned area analyses of chalcopyrite presented as normalised to 100 at%.

Samples analysed	S	Fe	Pb
15 2002	51.4	~	48.6
15 2002	50.4	~	49.6
15 2002	52.3	~	47.7
15 2002	48.6	2.3	49.1
4 2001	50.7	~	49.3
4 2001	51.5	~	48.6
18 2002	50.0	~	50.0
18 2002	50.2	~	49.8
18 2002	49.9	2.9	47.2

Scanned area data of galena presented as normalised to 100 at%.

Samples analysed	S	Fe	Cu	Zn
18 2002	48.9	1.2	~	50.0
18 2002	48.5	2.1	1.3	48.2
4 2001	47.8	0.4	~	51.8

SEM-EDS scanned area data of sphalerite normalised to 100 at%.

Samples analysed	MgO	SiO2	CaO	MnO	FeO	ZnO
15 2002	10.6	~	~	4.6	84.8	~
15 2002	16.1	2.6	~	2.9	78.0	~
4 2001	1.8	~	0.5	15.6	80.3	1.7
18 2002	11.5	1.7	~	3.9	82.9	~
18 2002	12.0	1.9	~	4.8	81.4	~
18 2002	13.8	~	~	4.0	82.2	~
18 2002	7.6	~	0.6	3.6	88.2	~
18 2002	16.1	~	~	4.3	79.5	~
18 2002	6.8	3.5	0.6	4.1	85.0	~
18 2002	20.2	~	~	3.0	76.8	~
18 2002	14.2	~	~	3.0	82.8	~
18 2002	7.7	~	0.6	4.2	87.6	~
18 2002	8.6	~	0.5	4.7	86.1	~
18 2002	17.8	~	~	2.9	79.3	~

SEM-EDS scanned area data of gangue – possibly siderite. The data is normalised to 100 wt%.

Element	Na	Mg	Al	Si	S	Cl	K	Ca	Mn	Fe	Pb	As	Zn	Cu	Co	Ni	Ga	Cd	Sb	Hf	Ta	Bi
	%	%	%	%	%	%	%	%	%	%	%	%	%	%	µg/g	µg/g	µg/g	µg/g	µg/g	µg/g	µg/g	µg/g
Selected lead ore 16 2002	1.7	0.3	0.1	0.1	23.9	5.3	0.1	~	~	0.1	68.2	0.1	~	~	159	226	159	17	321	405	174	318
Rej ore 17 2002	1.8	2.1	~	4.7	8.5	2.7	~	0.2	2.3	48.9	28.5	~	0.2	~	420	66	100	39	38	312	128	172
Rej ore 18 2002	0.3	0.9	0.3	57.5	9.2	1.5	~	0.1	0.7	16.7	2.2	~	9.6	0.9	161	129	23	153	5	117	134	29
Rej ore 19 2002	0.9	5.8	0.1	~	1.2	~	~	0.4	4.3	75.2	12.0	~	~	~	352	31	72	4	9	84	30	108

XRF analyses of mounted block ore samples, analysed using Turbo quant and displayed as elements in wt% and normalised to 100%.

Element	Mg	Al	Si	S	Ti	V	Cr	Mn	Fe	Pb	Ni	Cu	Zn	As	Ag	Cd	Sb
Selected lead ore 3 2001	0.04	0.20	1.42	6.73	0.02	trace	0.04	4.19	29.69	45.94	0.01	trace	11.41	0.03	0.21	0.02	0.09
Selected lead ore 5 (MB 15, 16) 2002	0.04	0.02	0.02	10.68	0.01	0.02	0.01	0.02	0.78	75.76	0.01	0.10	12.50	trace	0.07	0.02	0.03

XRF data of lead ore pressed pellets used in *huayrachina* smelts. Analysed via Alloys setting. The data has been normalised to 100 wt%.

Element	MgO	Al2O3	SiO2	SO3	CaO	TiO2	V2O5	Cr2O3	MnO	Fe2O3	PbO	ZnO	As2O5	SrO	Ag	Sb	Tl
	%	%	%	%	%	%	%	%	%	%	%	µg/g	µg/g	µg/g	µg/g	µg/g	µg/g
Rej ore 4 (MB 19, 20) 2002	5.28	0.86	1.23	8.80	0.24	trace	trace	0.01	2.68	58.16	22.58	239	115	143	38	36	533

XRF data of rejected lead ore pressed pellet analysed using Turbo quant. Data has been normalised to 100 %.

LEAD SMELTING: THE CHM ADDED

Mounted blocks	Description
2001	
Unmounted (labelled 5)	CHM added to 1st smelt
6	CHM added to 2nd smelt
2002	
21	CHM added to 1st smelt
22	CHM added to 2nd smelt

CHM added to the *huayrachina*

CHM Sample bag 5

CHM sample bag 6

OM images (CHM sample 6)

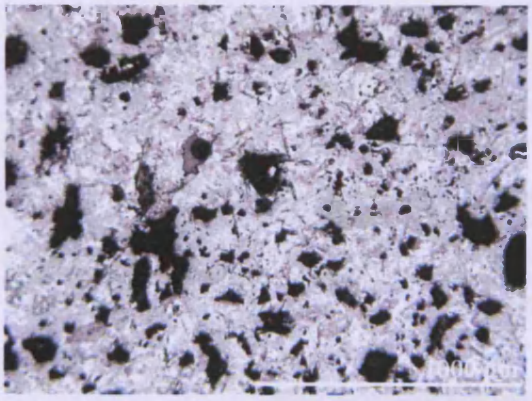

a.

These samples would have been added to the *huayrachina* smelt in 2001. The hand specimens shown above illustrate the variability in colour and texture. OM work indicated that the CHM sample 6 had a number of different layers: the upper (a), middle (b) and lower (c). The lower half of the specimen contains less lead oxide and increased mineral phases. The upper part of the sample is almost pure lead oxide.

SEM-EDS analyses showed that the sample is composed of lead oxide whch has interacted with the hearth lining to form different mineral phases (illustrated in images d and e).

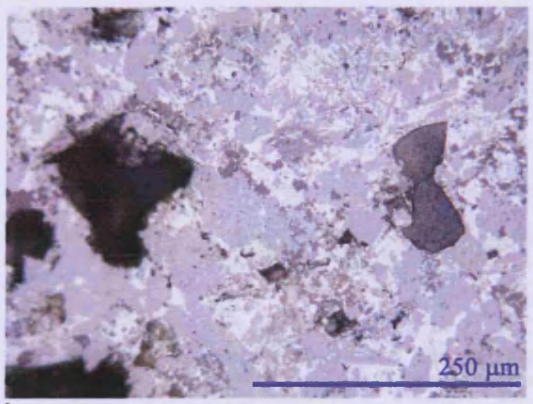

b.

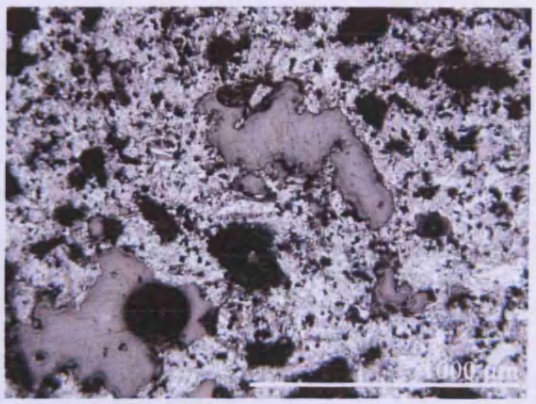

c.

SEM-EDS images and data

d.

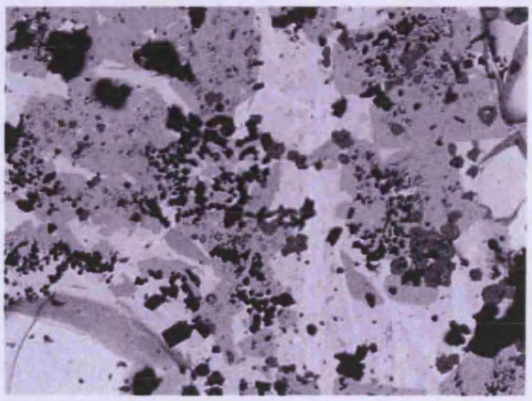

e.

Sampled area	Na2O	MgO	Al2O3	SiO2	K2O	CaO	FeO	ZnO	PbO
1	~	0.8	1.0	8.7	~	7.1	1.6	3.9	77.0
2	~	~	3.4	16	3.2	5.8	0.9	1.4	69.3
3	~	0.9	3.2	17.4	2.3	6.2	0.9	2.0	67.2
4	~	1.1	3.4	16.5	2.5	6.4	0.8	0.8	68.5
5	0.8	1.2	4.3	16.1	2.8	6.0	0.9	1.3	66.6
Average	**0.2**	**0.8**	**3.0**	**14.9**	**2.2**	**6.3**	**1.0**	**1.9**	**69.7**

CHM sample 6 2001 - bulk scanned areas of the CHM avoiding metallic prills, data normalised to 100 wt%

Scanned area	Al2O3	SiO2	CaO	FeO	CuO	ZnO	SbO	PbO
1 (SI6 4)	1.7	4.9	2.6	1.5	1.9	1.4	9.4	76.7

Lead oxide phase enriched with other metal oxides (SEM-EDS area analyses), data normalised to 100 wt%

Spcanned area	MgO	SiO2	CaO	FeO	PbO
1	~	19.4	11.2	~	69.4
2	1.1	20.7	12.9	0.6	64.8

Lead-calcium silicates present within the CHM matrix (SEM-EDS area analyses), normalised to 100 wt%

Spectrum	Na2O	Al2O3	SiO2	K2O	FeO	As	PbO
1	1.0	17.7	23.3	16.5	1.6	~	40.0
2	0.9	25.7	38.4	26.4	2.3	0.3	6.1
3	1.0	17.7	23.3	16.5	1.6	~	40.0

Black lead silicates (SEM-EDS area analyses). Data has been normalised to 100 wt%.

Spectrum	MgO	Al2O3	SiO2	CaO	FeO	ZnO	SbO	PbO
1	1.2	8.4	7.0	22.3	5.9	8.1	37.5	9.6
2	0.9	7.9	1.0	20.7	6.2	20.4	36.5	6.4

SEM-EDS area analyses of dark black angular inclusions (low lead, high antimony & calcium). The data has been normalised to 100 wt%.

Scanned area	Na2O	MgO	Al2O3	SiO2	K2O	CaO	FeO	ZnO	As2O5	PbO
Llareta ash	1.7	4.2	7.5	44.3	8.0	31.9	2.5	0.0	0.0	0.0
CHM 6 2001	0.6	2.8	10.7	52.5	7.7	22.2	3.6	0.0	0.0	0.0

SEM-EDS scanned areas of llareta ash and CHM sample 6 2001.

CHM sample 21 (2002)

a.

A sample from the residual pieces of CHM material that would have been added to the *huayrachina* smelt. The mounted block (a) revealed a layer of lead silicate (brown/yellow) and the llareta hearth lining (purple/grey).OM revealed that the upper layer is a complex lead silicate with different mineralogical structure (b and C). The lower layer is the hearth lining (d). The lead oxide is interacting with the hearth lining, this is seen in image e. SEM images show a lead oxide matrix with different mineral inclusions (f and g).

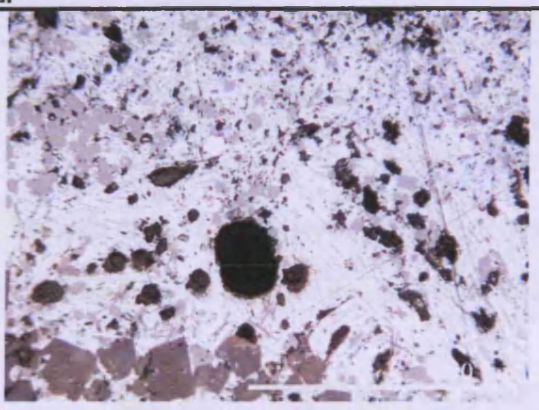

b.

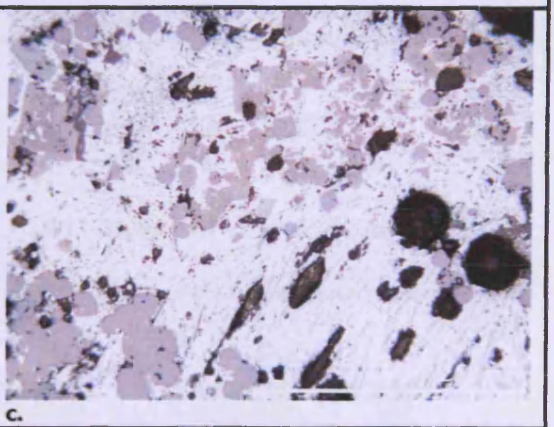

c.

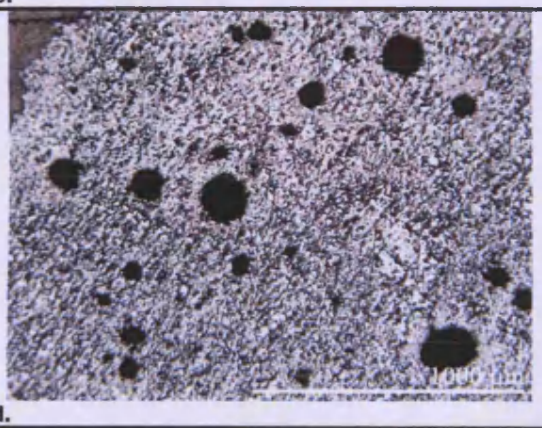

d.

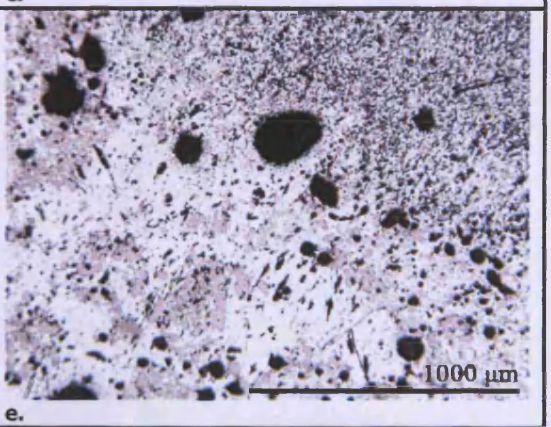

e.

SEM-EDS images and data

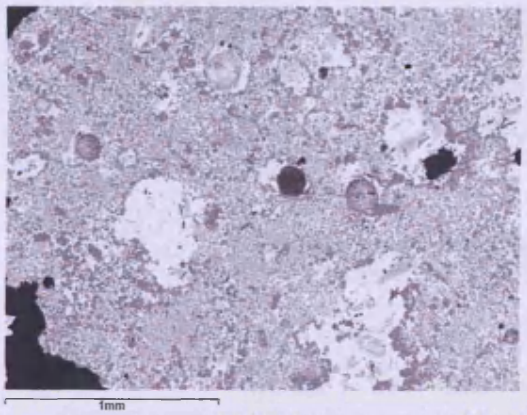

f.

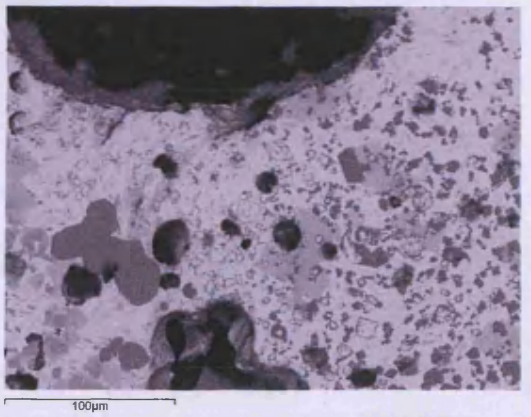

g.

Spectrum	Na2O	MgO	Al2O3	SiO2	CaO	FeO	ZnO	As2Ox3	PbO
1	~	~	1.6	9.5	6.1	2.9	1.4	2.0	76.5
2	0.5	0.8	1.8	9.5	7.6	3.5	2.2	1.1	73.2
3	~	0.9	1.4	9.2	6.2	3.1	1.8	1.0	76.5
Average CHM 21 lower layer	**0.2**	**0.6**	**1.6**	**9.4**	**6.6**	**3.1**	**1.8**	**1.4**	**75.4**

SEM-EDS bulk area analyses of the lower lead oxide layer of sample CHM 21. The data has been normalised to 100 wt%.

Spectrum	Al2O3	SiO2	CaO	FeO	NiO	ZnO	As2Ox3	PbO
1	0.8	3.5	0.7	28.8	1.4	13.9	1.3	49.7
2	~	3.8	0.6	29.6	1.8	12.5	~	51.7
3	0.8	3.1	0.6	28.1	2.0	11.4	1.6	52.5
Average CHM 21 upper layer	**0.5**	**3.5**	**0.6**	**28.9**	**1.7**	**12.6**	**0.9**	**51.3**

SEM-EDS bulk area analyses of the upper layer of sample CHM 21. The data has been normalised to 100 wt%.

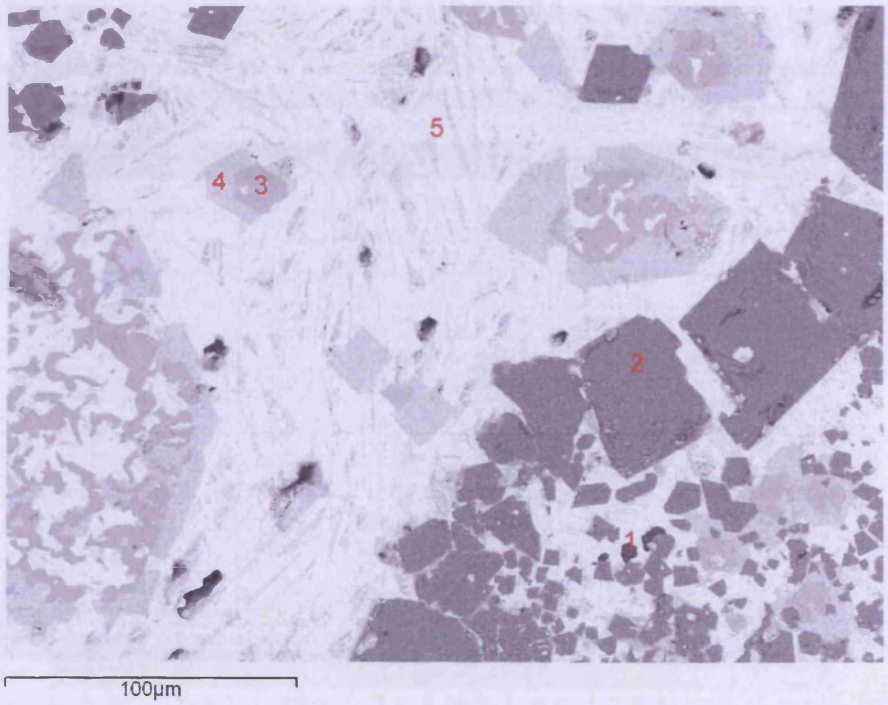

Area 1:

Areas	MgO	Al2O3	SiO2	K2O	FeO	ZnO	PbO
i	~	29.0	39.8	26.5	1.4	0.3	3.2
ii	1.1	29.5	39.8	26.2	0.8	~	2.8
iii	7.1	7.4	30.9	33.6	6.9	5.7	8.5
Average	**4.1**	**21.9**	**36.8**	**28.7**	**3.0**	**5.7**	**4.8**

Darkest small inclusions high in Al and K –leucite The data has been normalised to 100 wt%.

Area 2:

Sampled areas	Al2O3	FeO	CoO	NiO	ZnO	ErO	PbO
1	1.3	66.6	~	8.8	20.8	2.5	~
2	2.9	62.7	~	4.6	23.0	2.9	4.0
3	1.0	66.6	2.1	12.1	18.2	~	~
4	3.1	58.7	2.2	7.7	20.9	~	7.5
5	1.6	67.5	~	4.4	23.6	3.0	~
6	1.2	64.9	2.1	10.9	20.9	~	~
Average	**1.8**	**64.5**	**1.1**	**8.1**	**21.2**	**1.4**	**1.9**

Spinels- Iron and zinc rich phases with nickel rich black euhedral crystals (Labelled 2). Data has been normalised to 100 wt%.

Area 3:

	SiO2	P2O5	CaO	As2Ox	PbO
1	6.7	4.1	22.6	19.4	47.2
2	6.8	4.0	23.0	19.7	46.6
Average	**6.7**	**4.1**	**22.8**	**19.6**	**46.9**

Darker mid grey crystals in PbO matrix (labelled 3). The data has been normalised to 100 wt%.

Area 4:

	Al2O3	SiO2	CaO	FeO	As2Ox	PbO
1	~	20.1	11.7	~	~	68.2
2	~	20.1	12.0	~	0.9	67.0
3	0.6	20.1	11.2	~	1.0	67.1
4	0.8	20.3	11.2	~	~	67.6
5	0.9	15.2	9.9	1.7	5.5	66.8
6	0.7	15.6	11.4	0.6	4.9	66.9
Average	**0.5**	**18.6**	**11.2**	**0.4**	**2.1**	**67.3**

Light grey angular crystals found in association w. mid grey crystals both submerged in PbO matrix (labelled 4). Data has been normalised to 100 wt%.

Area analyses	Al2O3	SiO2	FeO	ZnO	As2Ox	Sb2O3	PbO
1	~	2.9	1.6	~	4.8	1.2	89.6
2	~	3.6	1.6	~	2.1	~	92.7
3	~	3.8	2.7	~	1.4	~	92.1
4	0.7	4.1	2.4	~	1.2	~	91.6
5	0.7	4.1	2.5	0.5	1.5	~	90.8
6	1.2	7.0	2.5	1.1	1.8	~	86.5
7	~	6.9	2.9	0.3	2.0	~	87.9
8	~	2.8	2.1	~	1.0	1.4	92.6
9	~	5.8	3.2	1.7	1.5	~	87.9
10	~	4.3	3.3	~	~	~	92.4
11	~	6.6	3.2	1.0	1.2	~	87.9
12	0.7	4.0	2.6	1.3	~	~	91.4
13	~	5.4	2.1	~	2.1	~	90.4
Average	**0.2**	**4.7**	**2.5**	**0.4**	**1.6**	**0.3**	**90.2**

SEM-EDS scanned area analyses lead oxide/matrix. Data has been normalised to 100 wt%.

Area scan	MgO	Al2O3	SiO2	CaO	FeO	ZnO	Sb2O3	PbO
1	1.2	10.9	2.2	26.0	9.5	7.3	40.5	2.4
2	0.8	10.2	1.5	26.5	11.3	6.8	40.9	1.9
Average	**1.0**	**10.6**	**1.8**	**26.2**	**10.4**	**7.1**	**40.7**	**2.2**

Hexagonal inclusions with high antimony. Data has been normalised to 100 wt%

CHM sample 22 (2002)
SEM-EDS images and data

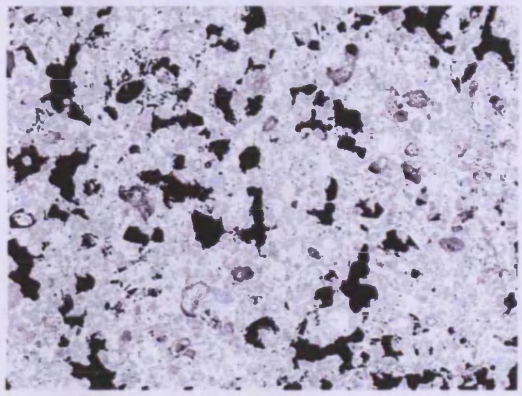

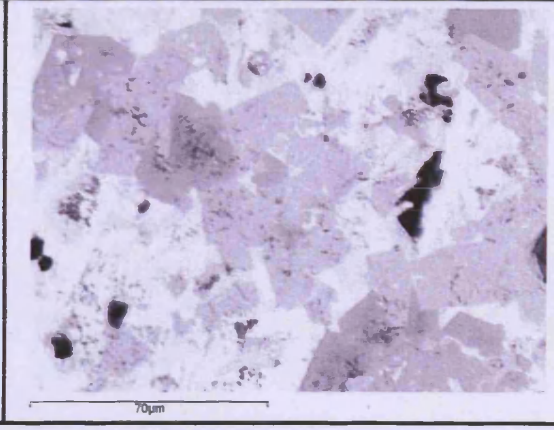

Scanned area	MgO	Al2O3	SiO2	K2O	CaO	PbO
1	0.9	2.5	12.2	~	7.1	77.3
2	1.1	2.2	11.9	~	6.8	78.1
3	1.0	3.4	12.4	~	7.0	76.2
4	1.0	4.1	14.7	1.5	7.4	71.4
5	0.8	2.5	12.2	~	7.0	77.5
Average	**1.0**	**2.9**	**12.7**	**0.3**	**7.1**	**76.1**

SEM-EDS data of the bulk area scans of CHM sample 22 2002. Data has been normalised to 100 wt%.

Spectrum	SiO2	CaO	PbO
1	20.7	12.5	66.7
2	18.9	12.9	68.2
3	20.4	12.7	67.0
3	20.1	11.8	68.1

Lead calcium silicates found in CHM sample 22 (SEM-EDS analyses). Data has been normalised to 100 wt%.

Spectrum	Na2O	MgO	Al2O3	SiO2	SO3	K2O	CaO	PbO
1	1.2	~	18.4	12.4	~	1.5	9.3	57.3
2	0.6	~	18.4	11.7	~	1.4	8.2	59.7
3	1.6		19.0	13.0	2.7	1.8	9.1	52.8
4	1.6	0.6	18.8	12.4	2.4	2.0	8.7	53.5

Lead calcium aluminium silicate (SEM-EDS analyses). Data has been normalised to 100 wt%.

Scanned area	SO3	SiO2	FeO	PbO
1	3.5	~	~	96.6
2	~	~	~	100.0
3	~	4.5	~	95.5
4	~	4.9	1.1	94.0

Lead oxide matrix (SEM-EDS area analyses). Data has been normalised to 100 wt%.

Element Dimension	Na2O %	MgO %	Al2O3 %	SiO2 %	SO3 %	K2O %	CaO %	TiO2 %	Fe2O3 %	PbO %
CHM 21 2002	0.00	1.04	0.77	7.01	10.02	0.55	3.40	0.06	0.94	70.00
CHM 5 2001	2.08	0.20	0.51	2.68	0.00	0.24	3.14	0.04	0.19	90.00

XRF data (major elements) of pressed pellet analyses of CHM added to *huayrachinas*.

Element Dimension	ZnO µg/g	As2Ox µg/g	Sb µg/g	Co3O4 µg/g	NiO µg/g	CuO µg/g	Ga µg/g	SrO µg/g	Ag µg/g	SnO2 µg/g	Ba µg/g	Hf µg/g	Bi µg/g
CHM 21 2002	29169	13163	9498	31	264	1203	317	942	525	221	197	247	1047
CHM 5 2001	304	602	129	58	189	48	169	958	72	0	137	74	23

LEAD SMELTING: THE FURNACE WALL

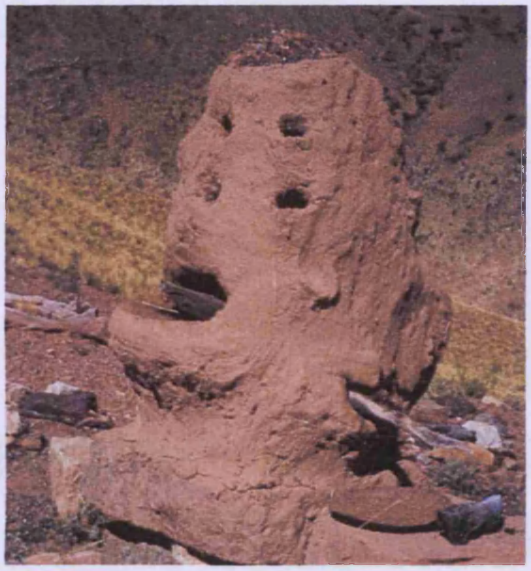

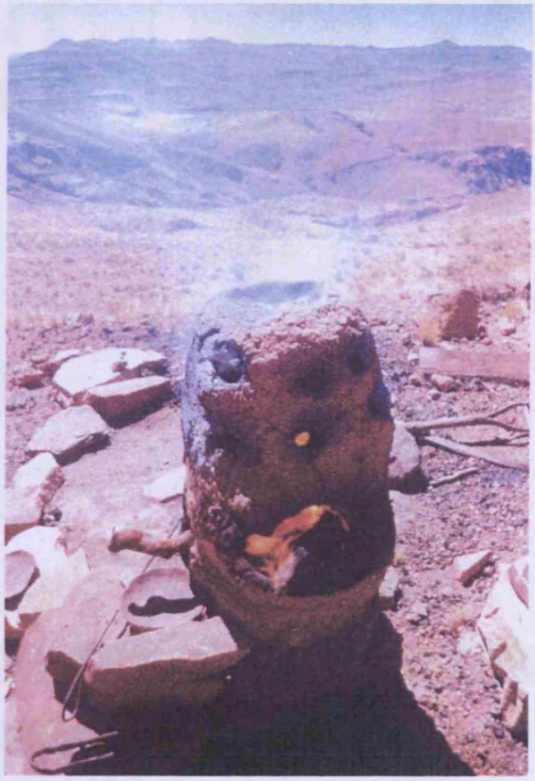

Sample number	Associated Year	Description
17	2001	Old *huayrachina* fragments found at Cuiza's smelting site
9	2002	Furnace fragment
24	2002	Clay from a quebrada/ravine close to Cuiza's smelting site used to repair the *huayrachina* from 1st smelt

Huayrachina ceramic fragments and clay samples available for analysis.

Sample 9 2002

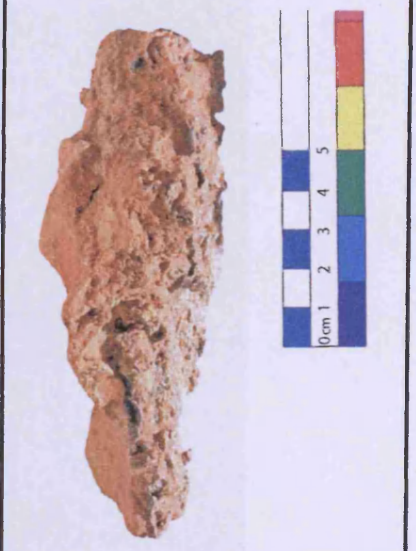

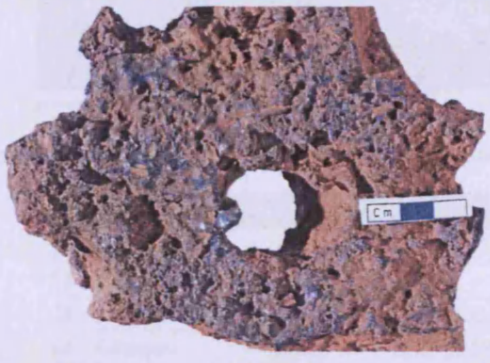

SEM-EDS Data and XRF of the ceramic wall

Samples	Na2O	MgO	Al2O3	SiO2	P2O5	SO3	K2O	CaO	TiO2	Fe2O3	BaO	PbO
24 (2002)	0.4	1.8	20.0	59.3	0.2	1.8	3.5	5.3	0.6	6.4	0.2	0.5
9 (2002)	2.7	0.7	17.9	67.7	0.2	trace	4.1	2	0.5	3.3	0.1	0.7

XRF analysis of pressed pellets of sample 24 clay used to patch *huayrachinas* before use in 2002 and sample 9 a *huayrachina* fragment. The pellets were analysed using Turbo-quant and the data has been normalised to 100 wt%.

Spectrum	Na2O	MgO	Al2O3	SiO2	K2O	CaO	TiO2	FeO
1	0.6	1.1	12.4	74.2	2.9	3.6	0.9	4.5
2	0.9	1.2	14.1	70.7	3.8	4.3	0.7	4.3
3	~	1.3	13.4	71.4	3.2	5.4	0.9	4.4
4	0.4	1.3	13.2	72.4	3.3	4.1	0.6	4.6
5	0.7	0.7	8.1	82.7	1.8	3.1	0.5	2.4
6	~	1.0	11.7	76.6	3.1	4.4	~	3.2
7	~	1.0	11.8	75.9	2.7	4.4	0.5	3.7
8	0.6	1.3	12.6	71.6	3.1	5.2	0.7	5.0
9	0.7	1.2	12.5	74.5	2.8	4.2	~	4.1
10	~	1.1	11.5	76.7	2.7	3.7	0.5	3.9
11	~	1.2	12.8	74.0	2.9	4.5	0.7	4.0
Average	**0.4**	**1.1**	**12.2**	**74.6**	**2.9**	**4.2**	**0.6**	**4.0**
Min	0.4	0.7	8.1	70.7	1.8	3.1	0.5	2.4
Max	0.9	1.3	14.1	82.7	3.8	5.4	0.9	5.0

SEM-EDS bulk area scans of the ceramic body. The data has been normalised to 100 wt%.

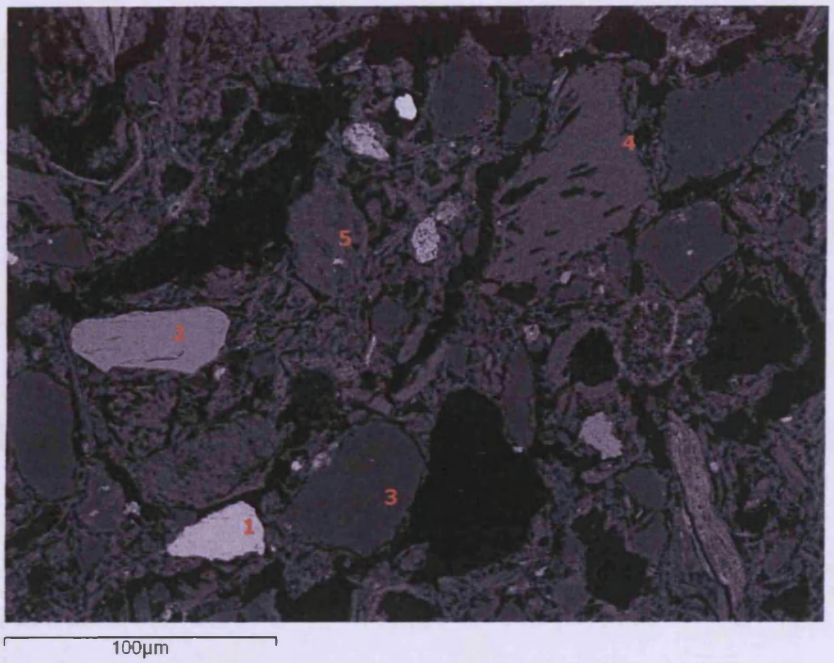

SEM backscattered image of the different composite oxides found in the *huayrachina* sample 9.

Spot area scan	Na2O	MgO	Al2O3	SiO2	K2O	CaO	TiO2	V2O3	MnO	FeO
1 – iron oxide	~	~	~	2.2	~	~	3.7	~	0.5	93.5
2 - titanium oxide	~	~	~	~	~	~	95.9	4.1	~	~
3 - quartz	~	~	~	100.0	~	~	~	~	~	~
4 - feldspar	1.0	~	12.8	76.4	7.9	1.0	~	~	~	0.9
5 - feldspar	0.4	1.6	24.0	59.3	5.6	3.3	1.0	~	~	4.9

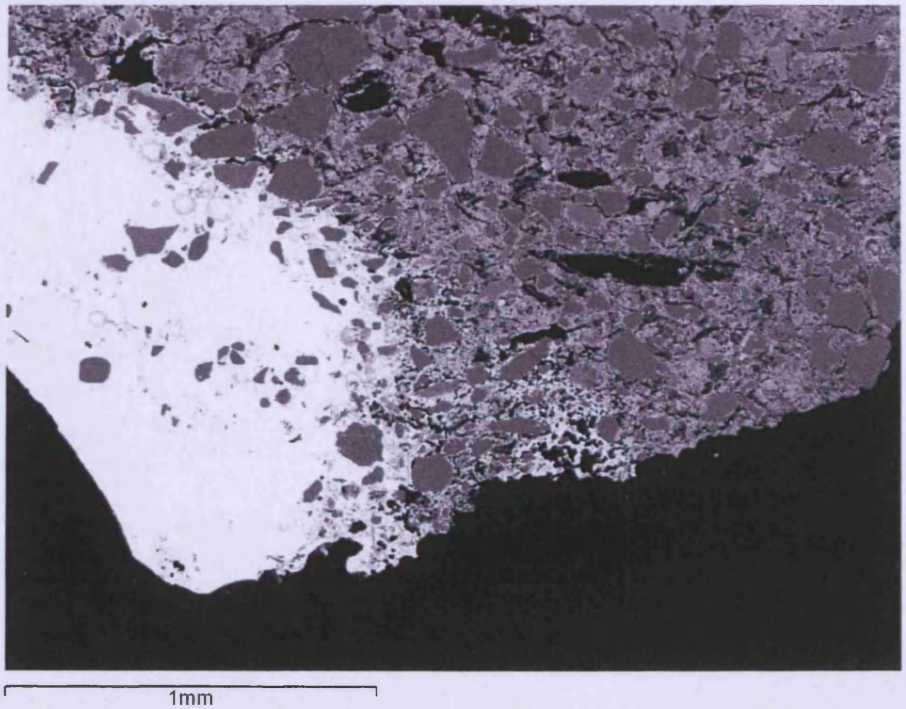

SEM image showing the interaction between the ceramic (grey) and lead silicate layer (white).

Scanned areas	MgO	Al2O3	SiO2	K2O	CaO	FeO	ZnO	PbO
1	~	5.4	27.7	1.3	1.8	2.0	3.8	58.0
2	0.9	6.0	32.4	0.7	3.0	3.6	3.6	49.8
3	0.7	6.1	31.8	1.6	2.7	2.9	3.4	51.0
Average	**0.5**	**5.9**	**30.6**	**1.2**	**2.5**	**2.8**	**3.6**	**52.9**

The vitrified lead silicate layer (illustrated in the figure above) found on the internal side of the huayrachina fragment. SEM-EDS area analyses, the data has been normalised to 100 wt%.

Samples	Na2O	MgO	Al2O3	SiO2	P2O5	SO3	K2O	CaO	TiO2	Fe2O3	BaO	PbO
24 (2002)	0.4	1.8	20.0	59.3	0.2	1.8	3.5	5.3	0.6	6.4	0.2	0.5
9	2.7	0.7	17.9	67.7	0.2	trace	4.1	2.0	0.5	3.3	0.1	0.7

XRF analysis of pressed pellets of sample 24 clay used to patch huayrachinas before use in 2002 and sample 9 a huayrachina fragment. The pellets were analysed using Turbo-quant and the data has been normalised to 100 wt%.

Sample 17 (age unknown)

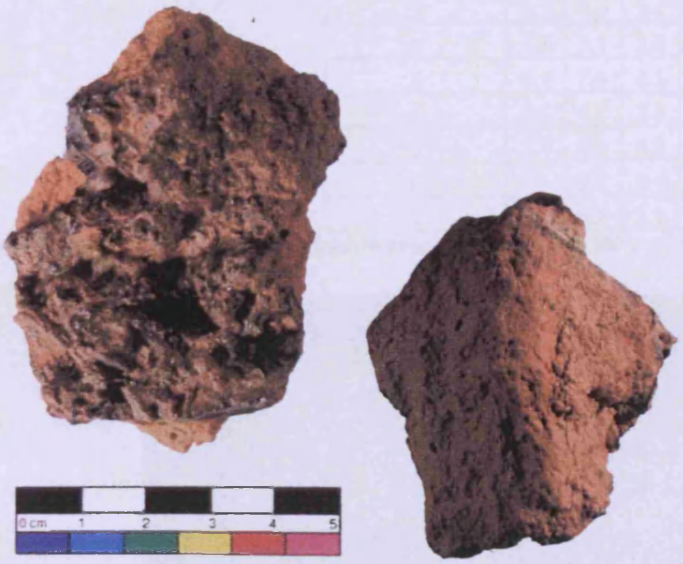

a.

b.

Sample 17 is a furnace fragment found on Cuiza's smelting site. It is a baked red ceramic with a coating of lead silicate slag (a). The mounted block illustrates the 1-1.5 cm slag layer adhered to the furnace wall (b).

SEM imaging shows the ceramic body (c and f) and metallic inclusions of lead metal and rich silver prills (d and e).

SEM-EDS data and XRF of the ceramic wall

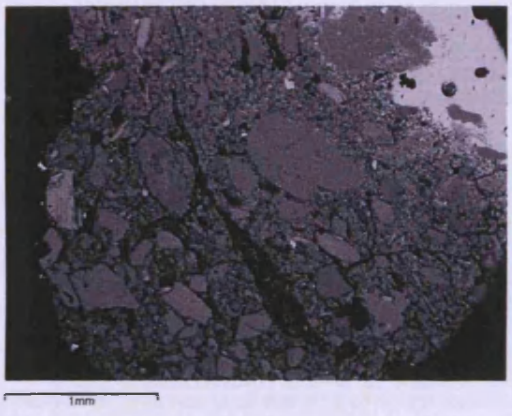

c.

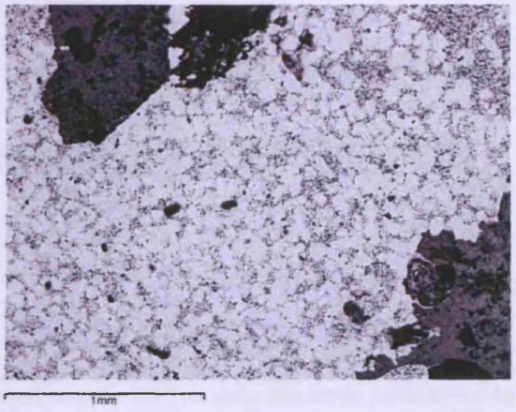

d.

Scanned area	Na2O	MgO	Al2O3	SiO2	K2O	CaO	TiO2	FeO	PbO
1	2.5	1.0	22.1	64.3	2.5	3.5	0.4	3.8	~
2	1.2	1.6	18.1	66.1	2.5	2.9	0.9	5.1	1.7

SEM-EDS bulk area scans of huayrachina fragment sample 17. Data has been normalised to 100 wt%.

Scanned areas	S	Ag	Sb	Pb
1	9.1	4.0	1.1	85.8
2	4.7	7.1	2.8	85.4
3	6.1	7.4	2.1	84.3
4	7.5	6.1	2.2	84.3
5	7.4	6.0	1.9	84.7
6	~	9.7	3.4	86.8
7	~	8.7	3.1	88.3

SEM-EDS area scans of lead sulphide areas (oxygen and silica removed). The data has bene normalised to 100 wt%.

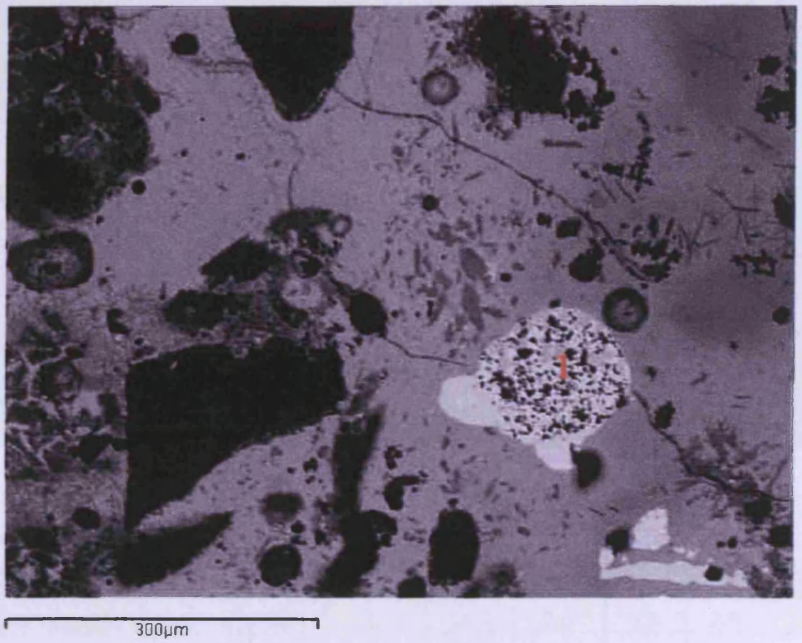

e.

Scanned area	Ag	Sb	Pb
SI2	82.4	11.8	5.8
Area 1 above	24.7	~	75.3

Silver rich prills within lead sulphide (oxygen and silica removed); SEM-EDS. The data has been normalised to 100 wt%

Spectrum	MgO	Al2O3	SiO2	P2O5	K2O	CaO	TiO2	FeO	ZnO	PbO
1	1.4	7.5	37.0	1.1	3.0	5.7	~	4.1	6.4	33.8
2	1.3	6.8	36.1	1.0	2.7	5.2	~	4.4	7.5	35.1
3	1.0	6.4	23.1	~	1.3	3.7	~	2.5	4.5	57.5
4	1.1	6.1	37.4	~	2.1	3.6	~	2.6	4.9	42.2
5	1.4	5.3	32.0	1.7	1.0	8.2	0.5	6.1	12.3	31.6
Average (n=5)	**1.2**	**6.4**	**33.1**	**0.8**	**2.0**	**5.3**	**0.1**	**3.9**	**7.1**	**40.0**

SEM-EDS area scans of the slag of huayrachina fragment sample 17. The data has been normalised to 100 wt%.

Spot	Na2O	Al2O3	SiO2	K2O	TiO2	FeO	ZnO	As	PbO
1	0.4	17.4	58.3	10.9	0.5	0.7	0.8	0.2	10.8

Feldspars recorded in sample 17 , SEM-EDS. The data has been normalised to 100 wt%.

Spectrum	Al2O3	SiO2	K2O	FeO	ZnO	PbO
1	20.7	55.7	20.3	0.9	1.2	1.2

Leucite in the slag (sample 17); SEM-EDS. Data has been normalised to 100 wt%.

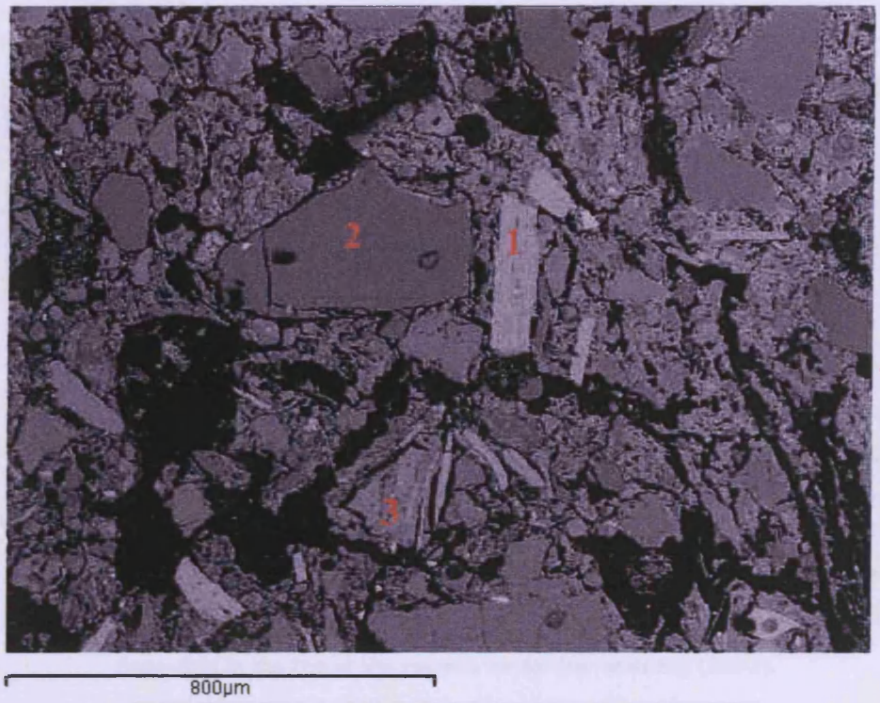

f.

Sampled area	Na2O	MgO	Al2O3	SiO2	P2O5	K2O	CaO	TiO2	FeO
Area 1 - angular long grain	~	8.4	16.1	38.4	2.0	8.9	2.0	4.7	19.5
Area 2 - quartz	~	~	~	100.0	~	~	~	~	~
Area 3 - angular grain	5.8	~	23.7	63.4	~	0.8	6.3	~	~

Minerals identified in the ceramic matrix analysed using the SEM-EDS.
Data has been normalised to 100 wt%.

LEAD SMELTING: THE SLAG

Don Carlos checking the slag collected from the mouth of the huayrachina and re-deposited in the top of the column for further smelting (2002).

The remains of a smelt with broken huayrachina fragments and black discarded slag.

Mounted Block	Associated year	Description	XRF
9	2001	Slag 1st smelt	Pellet
9a	2001	Slag 1st smelt	~
1	2002	Slag 1st smelt	Pellet
2	2002	Slag 1st smelt	~
10	2002	Slag 1st smelt	Pellet & Block
3	2002	Slag 2nd smelt	~
4	2002	Slag 2nd smelt	~
~	2002	Slag 1st smelt	Pellet
~	2002	Slag 2nd smelt	Pellet

Slag samples available for analyses

Slag sample 9 and 9a (2001)

a.

Only one sample of slag from the 2001 smelt was available for analyses (a). It was sampled by taking two different areas of the slag. The OM images of this slag sample showed that the slag was composed of a glassy matrix with mineral and metallic inclusions (b and c). Lead sulphide halos often surround the metallic lead prills. From the hand sample inclusions of charcoal were visible. This was also seen in the OM.

Metallic prills of lead metal were common (d and e).

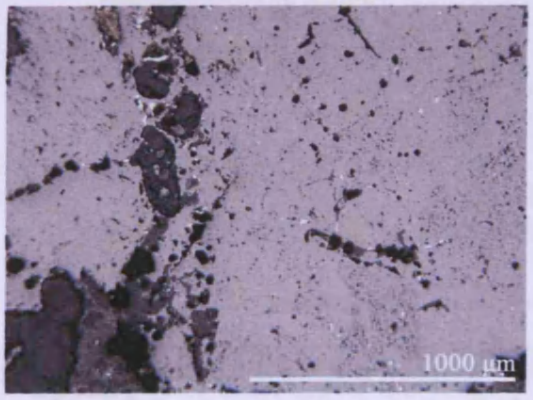

b.

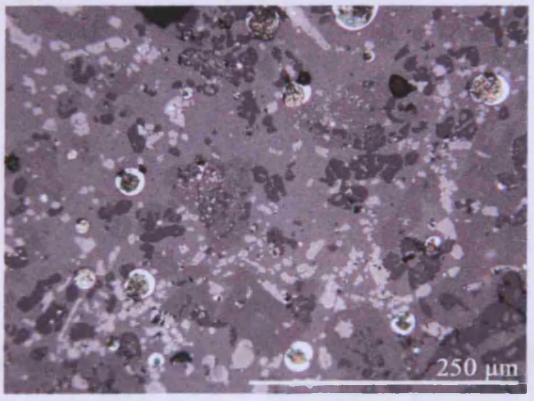

c.

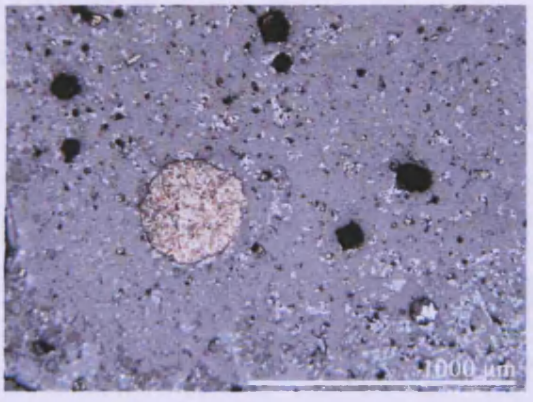

d.

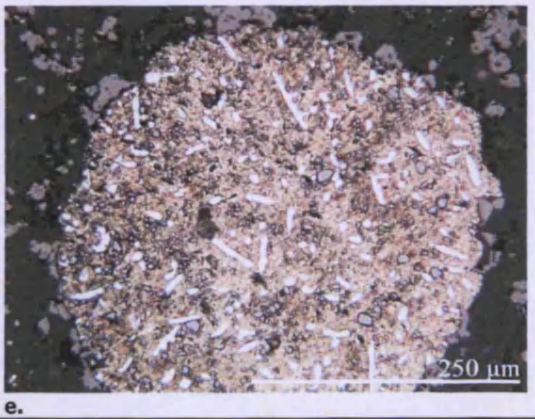

e.

SEM-EDS images and data

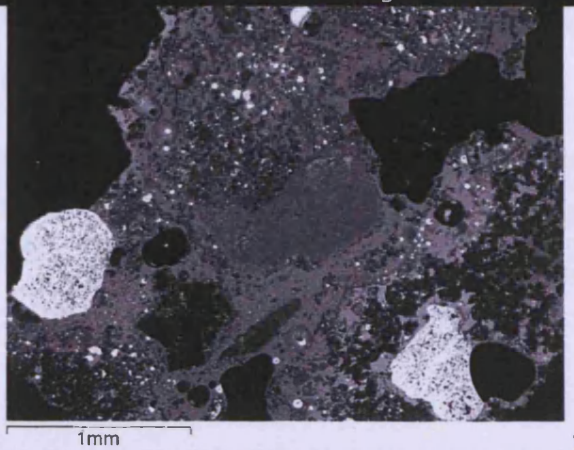

The slag matrix.

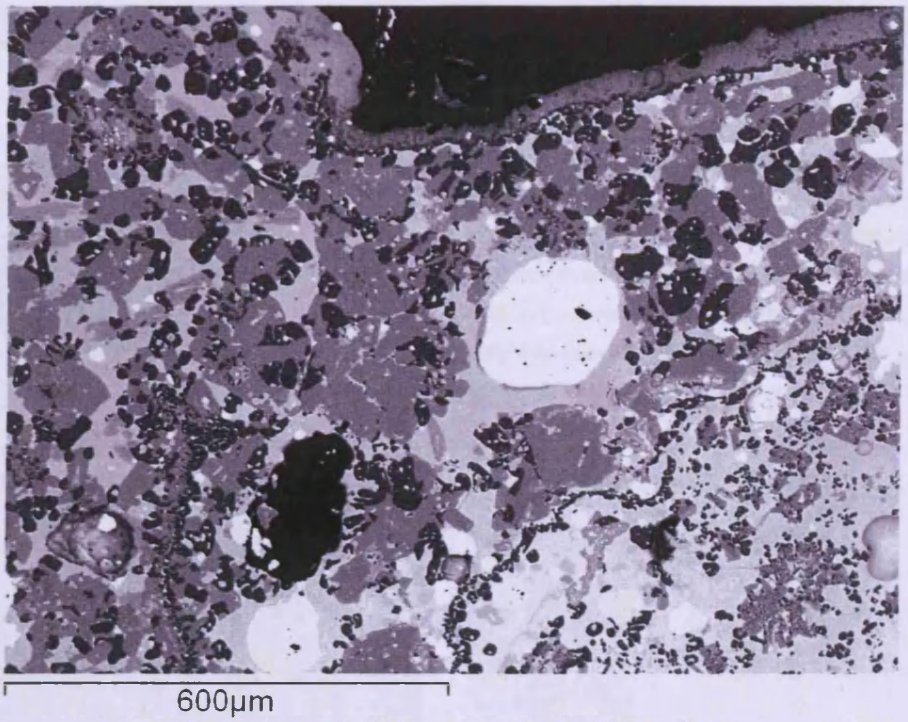

SEM image. The complex slag matrix of slag sample 9a.

Sample analysed	Na2O	MgO	Al2O3	SiO2	P2O5	SO3	K2O	CaO	MnO	FeO	ZnO	PbO
Average 9	1.1	0.5	4.4	30.9	1.6	0.6	1.1	7.0	0.9	12.2	8.9	30.8
Average 9A	~	1.4	3.8	29.2	1.1	0.6	1.6	7.8	0.4	12.8	11.1	30.3
Average 9 + 9A	0.6	1.0	4.1	30.1	1.3	0.6	1.4	7.4	0.6	12.5	10.0	30.5

Area scans of the glassy slag matrix for samples 9a and 9. The date has been normalised to 100 wt%.

Area analyses	S	Ca	Fe	Zn
9 2001	32.7	0.2	6.2	60.9
9a 2001	50.0	~	3.9	46.1

Zinc sulphide. The data has been normalised to 100 at%.

Scanned area	S	Fe	Zn	Pb
9 2001	43.3	~	2.6	54.1

Lead sulphide. The data has been normalised to 100 at%.

Samples	MgO	Al2O3	SiO2	PO2	K2O	CaO	TiO2	MnO	FeO	ZnO	PbO
9 2001	2.1	3.0	40.6	0.2	1.4	30.6	~	~	4.3	15.4	2.3
9A 2001	2.8	3.1	40.9	~	0.4	34.1	~	~	5.1	13.2	0.5

Pyroxenes. The data has been normalised to 100 wt%.

Spectrum	Na2O	Al2O3	SiO2	K2O	CaO	FeO	ZnO	BaO	PbO
9 2001	0.5	20.8	56.6	20.2	~	0.8	0.8	~	~
9A 2001	~	21.4	56.4	21.0	~	0.9	0.3	~	~

Leucite. The date has been normalised to 100 wt%.

Slag sample 1 (2002)

a.

Slag sample 1 is very similar to sample 9 2001. The hand specimen is not particularly glassy and contains large chunks of charcoal (a). The OM analyses showed a glassy matrix with metallic lead (b), inclusions of charcoal (c), different silicate phases such as leucite and pyroxenes(d) and large amounts of partially reacted lead sulphide (usually surrounding lead prills), white minerals (e).

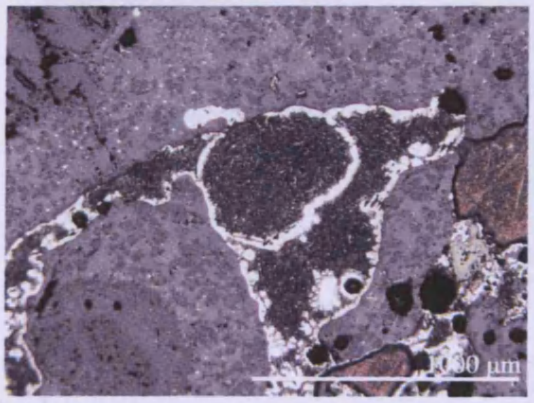

b.

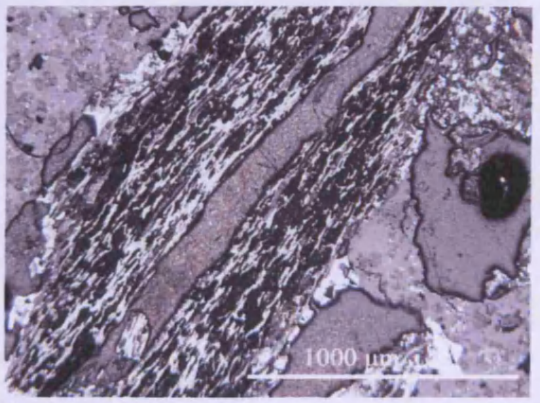

c.

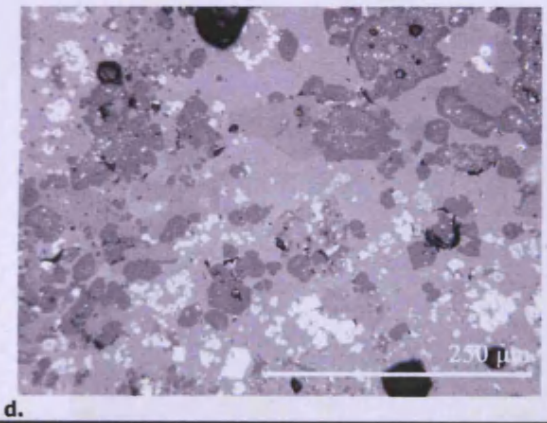

d.

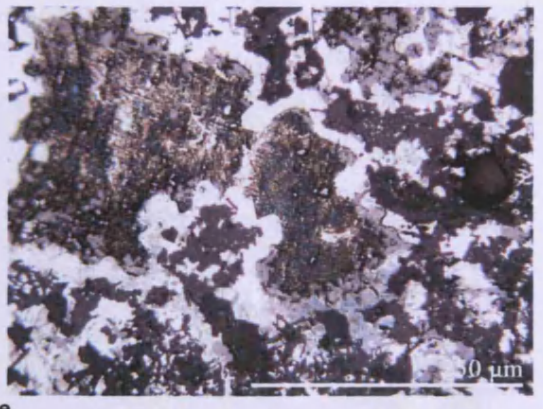

e.

SEM-EDS images and data

Spectrum	MgO	Al2O3	SiO2	P2O5	SO3	K2O	CaO	MnO	FeO	ZnO	PbO
1	1.9	8.7	37.9	0.9	2.7	6.1	13.1	0.8	8.6	6.2	13.3
2	2.4	7.7	39.0	~	3.0	4.6	14.6	0.9	8.4	5.0	14.6
3	2.2	8.0	37.2	~	2.2	4.6	14.1	0.9	8.8	6.4	15.6
4	2.0	8.7	40.0	~	1.6	5.8	14.8	1.0	12.7	7.8	5.7
5	2.3	8.9	41.4	~	1.5	5.4	15.0	1.0	11.7	6.9	6.0
Average	**2.2**	**8.4**	**39.1**	**0.2**	**2.2**	**5.3**	**14.3**	**0.9**	**10.0**	**6.5**	**11.0**
Min	1.9	7.7	37.2	0.9	1.5	4.6	13.1	0.8	8.4	5.0	5.7
Max	2.4	8.9	41.4	0.9	3.0	6.1	15.0	1.0	12.7	7.8	15.6

Bulk area scan of slag sample 1 (2002). The data has been normalised to 100 wt%.

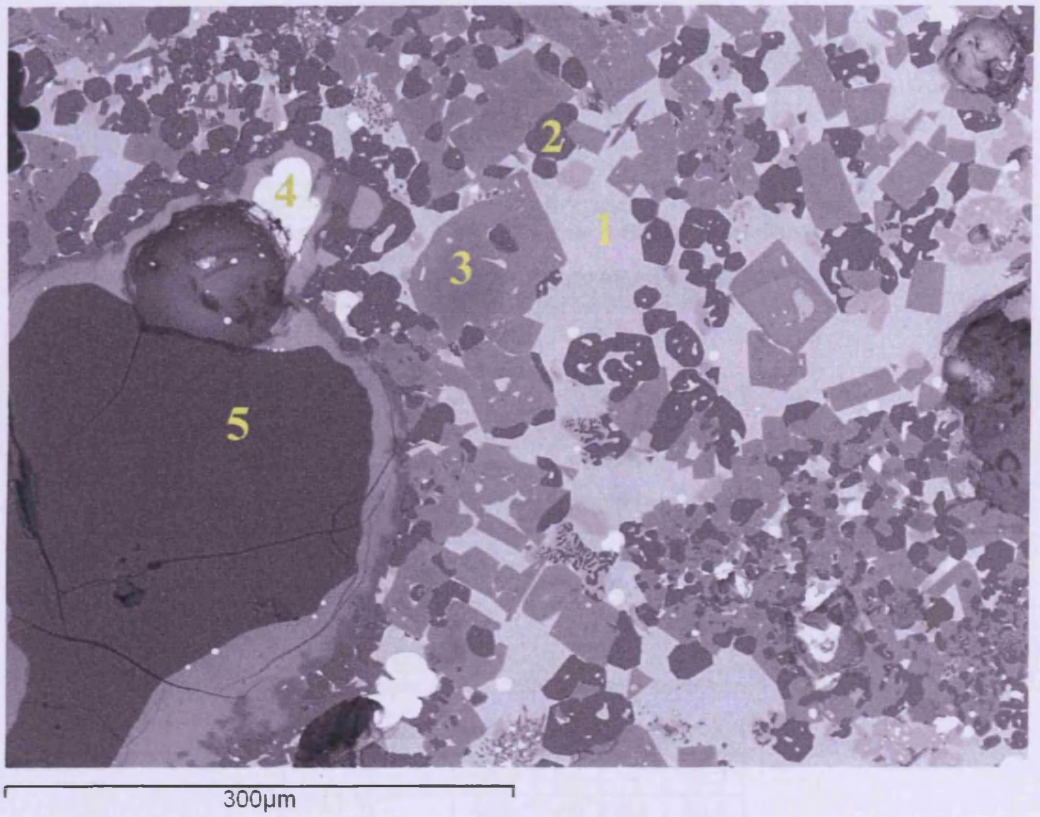

Typical slag seen in the SEM.
1 = glassy slag matrix
2 = Leucite
3 = Pyroxenes
4 = Lead sulphide
5 = Quartz

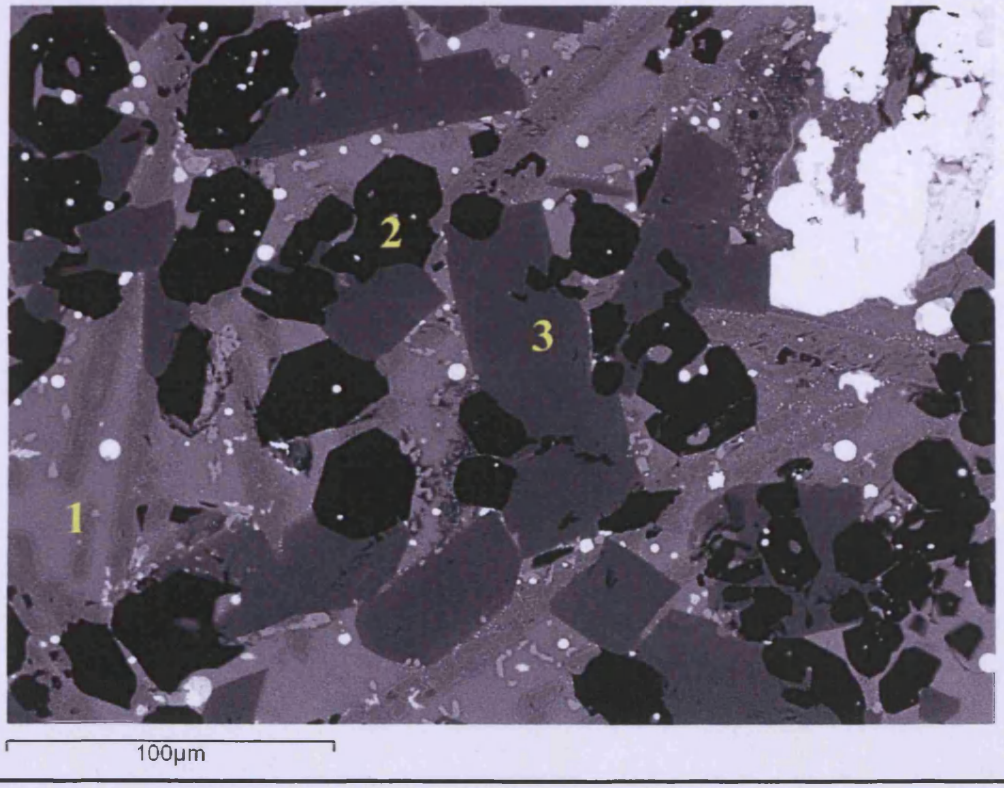

Scanned area	MgO	Al2O3	SiO2	CaO	MnO	FeO	ZnO
1	3.1	3.1	40.9	32.2	0.9	5.9	14.0
2	4.0	2.7	41.6	34.7	~	5.3	11.8
3	3.9	2.1	41.7	34.8	~	4.7	12.8
Average	**3.7**	**2.6**	**41.4**	**33.9**	**0.3**	**5.3**	**12.8**

Pyroxenes recorded in sample 1 (2002). The data has been normalised to 100 wt%.

Scanned area	Na2O	Al2O3	SiO2	K2O	CaO	FeO
1	~	22.0	56.5	20.3	~	1.2
2	~	21.5	57.1	20.4	~	1.1
3	1.4	18.6	55.3	16.2	2.5	4.2
Average	**0.5**	**20.7**	**56.3**	**19.0**	**0.8**	**2.1**

Leucite. The data has been normalised to 100 wt%.

Scanned area	MgO	Al2O3	SiO2	CaO	TiO2	MnO	FeO	ZnO
1	1.4	8.5	5.4	1.5	8.7	1.0	62.8	10.8
2	1.3	7.6	7.5	1.8	8.2	1.2	61.3	11.1
3	1.2	8.7	3.5	1.2	9.6	1.1	63.4	11.3
Average	1.3	8.3	5.5	1.5	8.8	1.1	62.5	11.1

Spinels found in slag sample 1. The data has been normalised to 100 wt%.

Scanned area	S	Fe	Zn	Pb
1	50.3	3.4	~	46.3
2	48.0	4.9	6.3	40.9
3	51.6	~	~	48.4
4	52.7	~	~	47.3
Average	**50.7**	**2.1**	**1.6**	**45.7**

Lead sulphide in slag sample 1. The data has been normalised to 100 wt%.

Slag sample 2 (2002)

a.

The hand specimen of sample 2 is extremely light to the touch and would indicate low lead levels. The centre of the sample has a porous texture (a). The OM analyses showed that the samples is composed of rounded silicates (c), some areas are glassy and contain the usual silicates seen in other huayrachina slags.

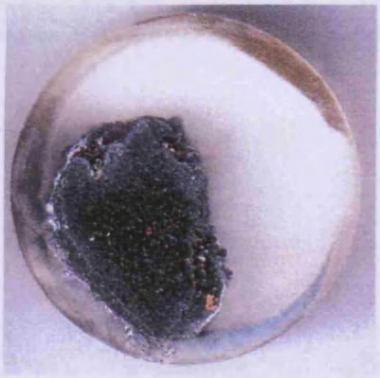

b.

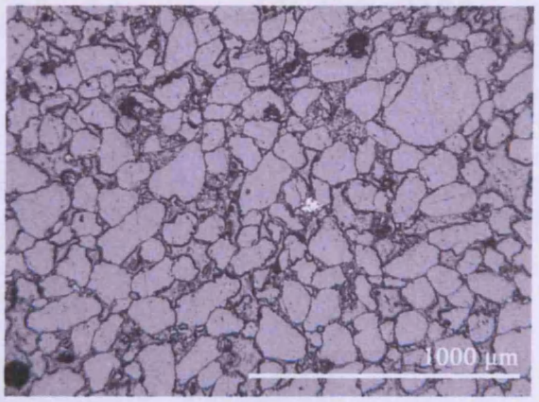

c.

SEM-EDS images and data

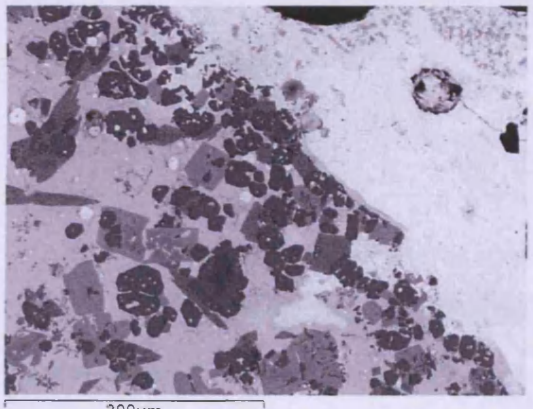

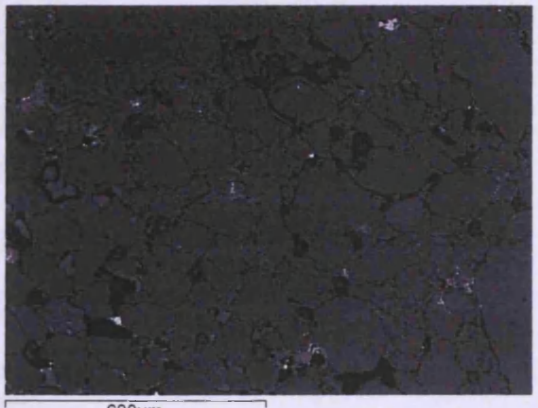

NO BULK AREA SCANS taken as the silicate areas were extremely small and a bulk area scan would have no immediate benefit.

Scanned area	MgO	Al2O3	SiO2	P2O5	CaO	TiO	MnO	FeO	ZnO	PbO
1	5.6	4.5	43.6	1.2	21.6	1.0	0.9	16.4	3.8	1.5
2	1.9	2.4	39.5	~	33.5	~	~	3.6	15.6	3.4
Average	**3.7**	**3.5**	**41.5**	**0.6**	**27.6**	**0.5**	**0.4**	**10.0**	**9.7**	**2.4**

Pyroxenes found in sample 2. The data has normalised to 100 wt%.

Scanned area	Na2O	Al2O3	SiO2	K2O	FeO	ZnO
1	0.7	19.6	57.7	20.9	1.0	~
2	0.7	20.7	57.2	20.7	0.7	~
3	0.7	20.3	56.7	20.6	1.1	0.7
Average	**0.7**	**20.2**	**57.2**	**20.7**	**0.9**	**0.2**

Leucite in sample 2. The data has been normalised to 100 wt%.

Scanned area	MgO	Al2O3	SiO2	P2O5	K2O	CaO	TiO2	MnO	FeO	ZnO	PbO
1	1.0	5.3	34.0	0.8	1.9	6.8	0.6	0.8	12.7	10.3	25.8
2	1.2	5.2	33.4	1.3	1.7	6.4	0.5	1.2	12.9	11.4	24.9
3	1.0	4.7	33.9	0.9	1.8	7.2	~	1.3	15.4	12.8	21.1
Average	**1.1**	**5.1**	**33.8**	**1.0**	**1.8**	**6.8**	**0.3**	**1.1**	**13.7**	**11.5**	**23.9**

Glassy matrix. The data has been normalised to 100 wt%.

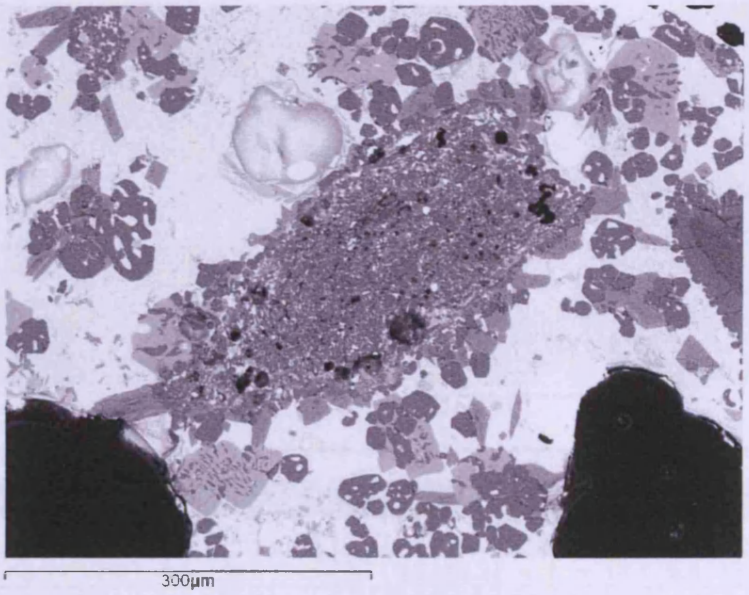

A relict gangue fragment in the middle of the slag matrix in sample 2 (2002).

Area analysed	Na2O	Al2O3	SiO2	SO3	K2O	CaO	FeO	PbO
1	1.0	11.3	68.7	2.3	9.2	1.1	0.8	5.5

An SEM-EDS area analyses of gangue with slag sample 2 (2002); above. Data has been normalised to 100 wt%.

Slag sample 3 (2002)

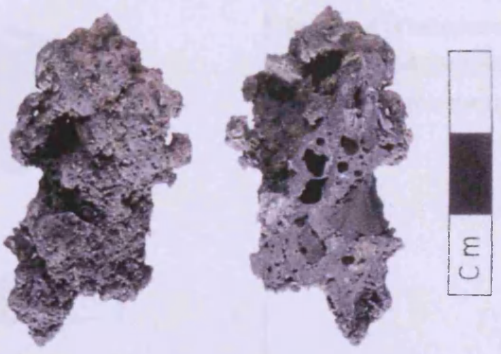

SEM-EDS images and data

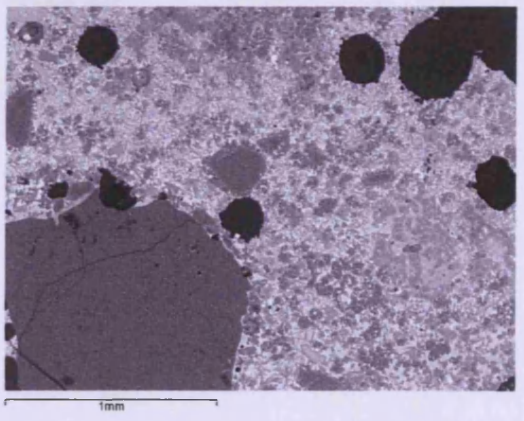

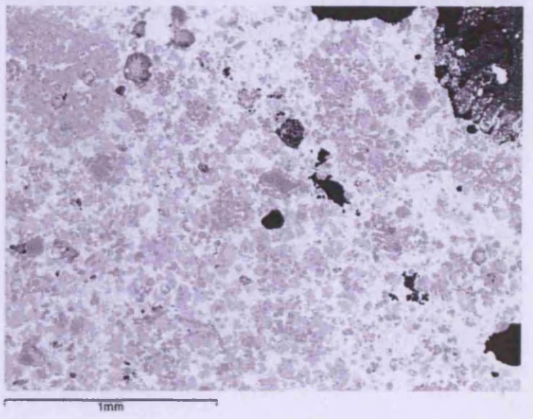

Spectrum	MgO	Al2O3	SiO2	P2O5	SO3	K2O	CaO	TiO2	MnO	FeO	ZnO	PbO
1	2.1	9.1	41.1	1.0	~	4.9	12.5	~	0.6	9.5	8.8	10.4
2	2.0	8.5	38.0	~	2.2	5.0	10.3	~	~	8.4	6.6	19.0
3	1.6	7.3	48.6	~	~	3.8	9.5	0.5	0.8	9.9	8.4	9.6
4	1.4	10.1	54.8	~	~	4.4	5.9	~	~	6.0	4.7	12.7
5	2.2	9.3	43.6	0.9	~	5.4	12.6	~	0.5	8.9	7.0	9.5
Average	**1.9**	**8.9**	**45.2**	**0.4**	**0.4**	**4.7**	**10.2**	**0.1**	**0.4**	**8.5**	**7.1**	**12.2**
Min	1.4	7.3	38.0	0.9	2.2	3.8	5.9	0.5	0.5	6.0	4.7	9.5
Max	2.2	10.1	54.8	1.0	2.2	5.4	12.6	0.5	0.8	9.9	8.8	19.0

Bulk area scans of slag sample 3 (2.1) 2002. The data has been normalised to 100 wt%.

Spectrum	Na2O	Al2O3	SiO2	K2O	CaO	FeO	ZnO	BaO	PbO
Average	0.7	21.2	56.5	20.1	0.1	0.9	0.2	0.1	0.2

Luecite analyses from slag samples. Data has been normalised to 100 wt%.

Samples	MgO	Al2O3	SiO2	K2O	CaO	TiO	FeO	ZnO	PbO
Average pyroxenes	3.7	2.9	41.1	0.1	31.9	0.2	5.3	12.6	2.3

Average pyroxene analyses from all slag samples. Data has been normalised to 100 wt%.

Area analyses	S	Ca	Fe	Zn
Average zinc sulphide	49.5	~	5.9	44.7

Zinc sulphide areas analysed taken using the SEM-EDS. Data has been normalised to 100 at% .

Slag sample 4 (2002)

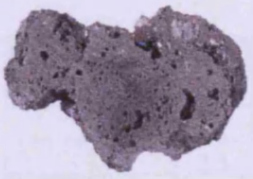

a.

Sample 4 is composed of high quantities of lead sulphide and the hand specimen reflects the low quantity of silicate (a).

SEM-EDS images and data

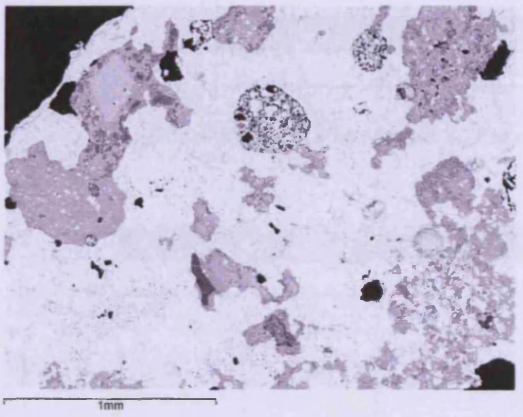

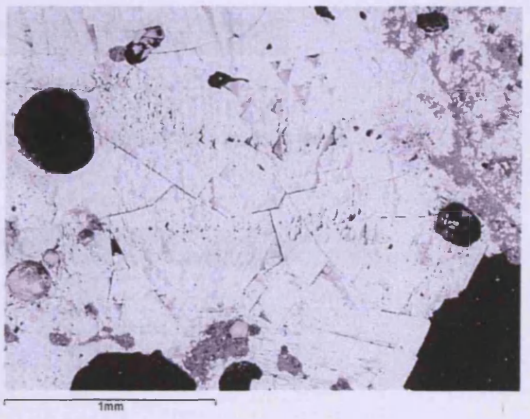

Spectrum	MgO	Al2O3	SiO2	SO3	K2O	CaO	FeO	CuO	ZnO	PbO
1	~	2.1	10.2	19.6	1.6	3.5	3.0	~	4.4	55.6
2	0.8	1.2	10.0	21.9	0.6	7.0	3.3	~	4.7	50.5
3	~	~	2.8	26.8	~	1.5	~	~	~	68.9
4	~	0.9	5.5	21.6	~	3.6	3.3	1.2	1.9	62.0
Average	**0.2**	**1.0**	**7.1**	**22.5**	**0.6**	**3.9**	**2.4**	**0.3**	**2.7**	**59.3**

SEM-EDS bulk area analyses of slag sample 4 (2002). The data has been normalised to 100 wt%.

Scanned area	MgO	Al2O3	SiO2	P2O5	K2O	CaO	MnO	FeO	ZnO	PbO
1	1.4	4.4	31.5	1.4	1.2	5.2	0.7	10.4	11.8	32.2
2	0.9	4.9	34.2	1.4	1.2	7.7	0.5	15.8	14.1	19.5
3	0.7	5.1	32.7	1.4	2.7	8.0	~	9.3	7.9	32.4
Average	**1.0**	**4.8**	**32.8**	**1.4**	**1.7**	**6.9**	**0.4**	**11.8**	**11.3**	**28.0**

The glassy matrix in slag sample 4. The data has been normalised to 100 wt%.

Scanned area	Na2O	Al2O3	SiO2	K2O	CaO	FeO	ZnO	PbO
1	0.4	19.6	55.2	21.2	0.4	1.5	0.8	1.1
2	0.4	20.5	55.2	22.0	~	1.0	~	1.0
Average	**0.4**	**20.0**	**55.2**	**21.6**	**0.2**	**1.2**	**0.4**	**1.0**

Leucite in sample 4. The data has been normalised to 100 wt%.

Scanned area	MgO	Al2O3	SiO2	K2O	CaO	FeO	ZnO	PbO
1	1.9	2.0	37.4	~	32.3	3.2	17.1	6.3
2	3.1	2.4	39.7	0.5	36.4	6.3	11.6	
3	2.1	2.6	38.0	~	33.7	3.8	15.6	4.1
Average	**2.4**	**2.3**	**38.4**	**0.2**	**34.1**	**4.4**	**14.7**	**3.5**

Olivines in slag sample 4. The data has been normalised to 100 wt%.

Scanned area	MgO	Al2O3	SiO2	CaO	TiO2	MnO	FeO	ZnO	SnO2
1	1.3	9.6	1.3	1.0	2.8	~	61.4	21.2	1.4
2	1.2	5.4	~	~	1.6	0.5	69.7	19.7	2.0
Average	**1.3**	**7.5**	**0.7**	**0.5**	**2.2**	**0.2**	**65.5**	**20.5**	**1.7**

Spinels in slag sample 4. The data has been normalised to 100 wt%.

Scanned area	MgO	Al2O3	SiO2	MnO	FeO	ZnO
1	4.7	~	28.0	0.7	13.0	53.7
2	4.0	2.4	26.3	~	16.1	51.2

Zinc silicates in slag sample 4. The data has been normalised to 100 wt%.

Sampled areas	S	Ca	Fe	Zn	Sb	Pb
1	~	~	~	4.1	3.8	92.1
2	~	~	2.2	~	8.1	89.7
3	~	~	4.1	4.6	4.1	87.2
4	~	3.0	5.4	5.7	4.3	81.6
5	~	~	~	~	2.2	97.8
6	~	~	~	5.9	~	90.0
7	7.7	~	~	~	~	92.3
8	~	3.2	4.0	4.7	~	88.1
Average lead prill	**1.0**	**0.8**	**2.0**	**3.1**	**2.8**	**89.9**

SEM-EDS area analyses of lead metallic prills in slag sample 4 (2002). The data has been normalised to 100 wt %.

Slag sample 10 (2002)

a.

Sample 10 is composed of almost pure lead sulphide. The OM images show the distinctive triangular patternation and the presence of zinc sulphide within the partially reacted lead sulphide (b and c).

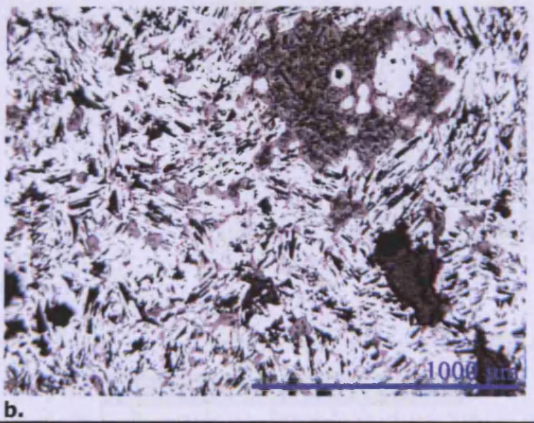

b.

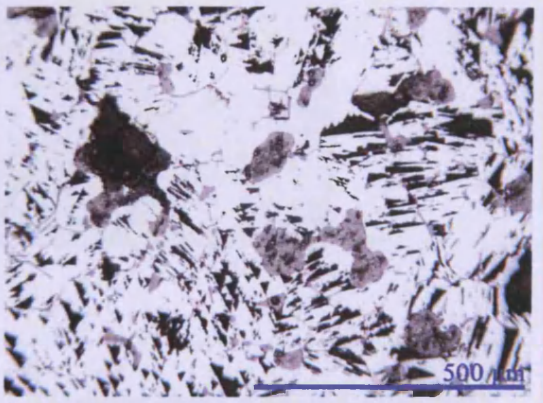

c.

SEM-EDS images and data

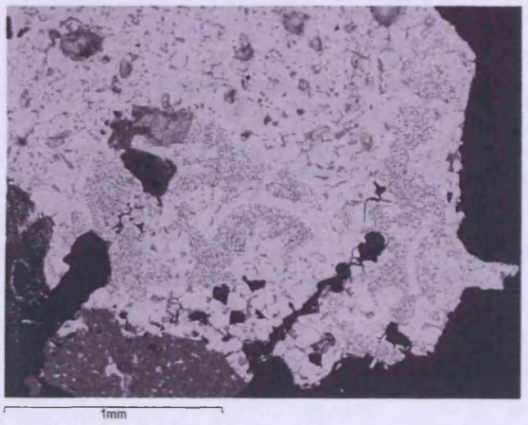

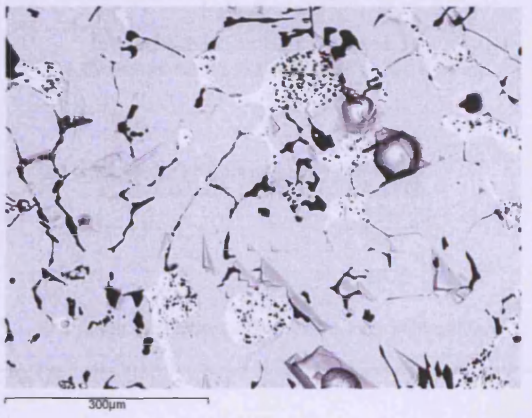

Spectrum	Si	S	Fe	Zn	Pb
1	~	13.9	1.5	3.0	81.7
2	~	14.3	2.5	2.4	80.9
3	~	15.3	2.5	2.2	80.0
4	4.0	10.9	1.5	2.9	84.8
5	3.8	14.9	1.6	2.5	81.0
Average	**1.6**	**13.8**	**1.9**	**2.6**	**81.7**
Min	3.8	10.9	1.5	2.2	80.0
Max	4.0	15.3	2.5	3.0	84.8

Bulk area analyses of sample 10. The data is normalised to 100 wt%.

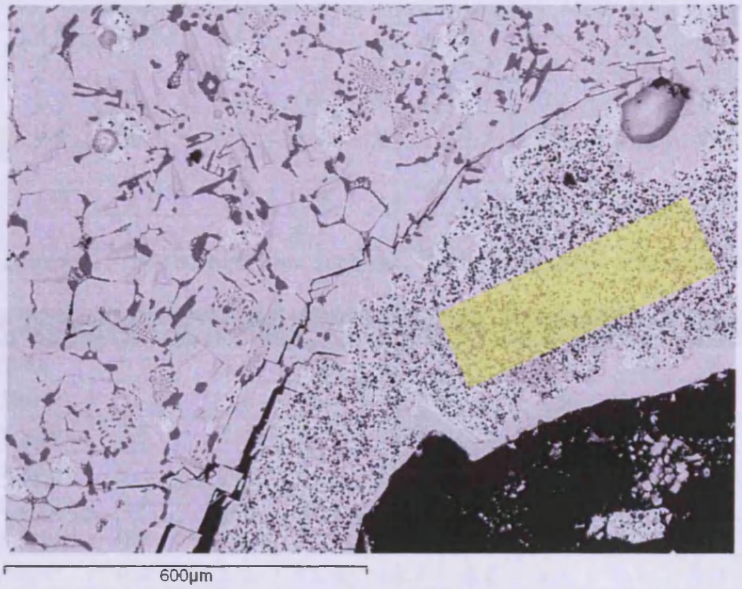

Scanned area	As	Sb	Pb
1	3.3	~	96.7
2	4.2	1.5	94.3
3	3.6	~	96.4
4	3.8	1.8	94.4
5	3.8	~	96.2

Lead metal analysed in slag sample 10.
The data has been normalised to 100 at%.

Scanned area	As	Ag	Pb
SI5 2	~	3.1	96.9
SI7	5.4	3.2	91.4

Scanned area of lead metal which contains 3% silver.
The data has been normalised to 100 at%.

Scanned area	S	Mn	Fe	Zn
1	51.5	0.3	8.9	39.3
2	49.6	~	8.2	42.2
3	49.6	0.5	10.8	39.0

Zinc sulphide in slag sample 10.
The data has been normalised to 100 at%.

Scanned area	S	Pb
1	50.9	49.1
2	50.9	49.1
3	51.8	48.3

Lead sulphide.
The data has been normalised to 100 at%.

Comparison data for all Cuiza's slag samples

Spectrum	MgO	Al2O3	SiO2	P2O5	SO3	K2O	CaO	TiO2	MnO	FeO	CuO	ZnO	PbO
9A	1.9	8.0	37.8	0.7	0.4	4.1	19.7	~	0.3	11.8	~	9.7	5.6
01 1.1 2002	2.1	8.4	39.1	0.2	2.2	5.3	14.3	~	0.9	10.0	~	6.5	11.0
03 2.1 2002	1.9	8.9	45.2	0.4	0.4	4.7	10.2	0.1	0.4	8.5	~	7.1	12.2
Average	**2.0**	**8.4**	**40.7**	**0.4**	**1.0**	**4.7**	**14.7**	**0.0**	**0.5**	**10.1**	**~**	**7.8**	**9.6**
04 2.2 2002	0.2	1.0	7.1	~	22.5	0.6	3.9	~	~	2.4	0.3	2.7	59.3
10 1.3 2002	~	~	1.3	~	26.5	~	~	~	~	1.9	~	2.6	67.7

Comparison of the average SEM-EDS bulk area analyses. The data has been normalised to 100 wt%.

Spectrum	Na2O	Al2O3	SiO2	K2O	CaO	FeO	ZnO	BaO	PbO
9 2001	0.5	20.8	56.6	20.2	~	0.8	0.8	~	~
9A 2001	~	21.4	56.4	21.0	~	0.9	0.3	~	~
01 1.1 2002	0.5	22.7	53.3	20.3	0.8	1.6	0.3	~	~
02 1.2 2002	0.7	20.2	57.2	20.7	~	0.9	0.2	~	~
03 2.1 2002	0.7	21.2	56.5	20.1	0.1	0.9	0.2	0.1	0.2
04 2.2 2002	0.4	20.0	55.2	21.6	0.2	1.2	0.4	~	1.0
Average	**0.5**	**21.1**	**55.9**	**20.7**	**0.2**	**1.1**	**0.4**	**0.0**	**0.2**
Min	0.4	20.0	53.3	20.1	0.1	0.8	0.2	0.1	0.2
Max	0.7	22.7	57.2	21.6	0.8	1.6	0.8	0.1	1.0

Luecite SEM-EDS area analyses from slag samples. Data has been normalised to 100 wt%.

Samples	MgO	Al2O3	SiO2	P2O5	K2O	CaO	TiO2	MnO	FeO	ZnO	PbO
9 2001	2.1	3.0	40.6	0.2	1.4	30.6	~	~	4.3	15.4	2.3
9A 2001	2.8	3.1	40.9	~	0.4	34.1	~	~	5.1	13.2	0.5
01 1.1 2002	3.9	2.6	41.6	~	0.2	34.1	~	0.1	4.9	12.0	0.6
02 1.2 2002	3.7	3.5	41.5	0.6	~	27.6	0.5	0.4	10.0	9.7	2.4
03 2.1 2002	3.7	2.9	41.1	~	0.1	31.9	0.2	~	5.3	12.6	2.3
04 2.2 2002	2.1	2.2	38.0	~	0.2	33.9	~	~	4.0	15.3	4.2
Average	**3.1**	**2.9**	**40.6**	**0.1**	**0.4**	**32.0**	**0.1**	**0.1**	**5.6**	**13.0**	**2.1**
Min	2.1	2.2	38.0	0.2	0.1	27.6	0.2	0.1	4.0	9.7	0.5
Max	3.9	3.5	41.6	0.6	1.4	34.1	0.5	0.4	10.0	15.4	4.2

Pyroxene SEM-EDS area analyses from all slag samples. Data has been normalised to 100 wt%.

Area analyses	S	Mn	Ca	Fe	Zn
9 2001	32.7	~	0.2	6.2	60.9
9a 2001	50.0	~	~	3.9	46.1
01 1.1 2002	48.9	~	4.1	47.0	~
10 1.3 2002	50.1	0.3	~	8.2	41.4
03 2.1 2002	49.5	~	~	5.9	44.7
Average	**46.2**	**0.1**	**0.9**	**14.2**	**38.6**
Min	32.7	0.3	0.2	3.9	41.4
Max	50.1	0.3	4.1	47.0	60.9

Zinc sulphide areas analysed using the SEM-EDS. Data has been normalised to 100 at% .

Scanned area	S	Fe	Zn	Pb
09 2001	43.3	~	2.6	54.1
01 1.1 2002	50.7	2.1	1.6	45.7
02 1.2 2002	47.1	~	~	52.9
04 2.2 2002	48.6	~	~	51.4
04 2.2 2002	46.9	4.2	2.3	46.6
10 1.3 2002	51.1	0.1	~	48.8
Average	**39.4**	**1.1**	**1.1**	**41.8**
Min	43.3	2.1	1.6	45.7
Max	50.7	4.2	2.6	54.1

SEM-EDS scanned area analyses of PbS displayed here in at %.

Samples	Na2O	MgO	Al2O3	SiO2	P2O5	SO3	K2O	CaO	TiO2	MnO	FeO	ZnO	As2O3	PbO
4 2002 extreme area analysed	~	0.1	2.9	17.1		~	0.7	2.1	~	~	5.2	7.6	~	64.4
1 2002	~	6.2	2.4	33.0	1.5	0.2	0.7	6.7	0.1	3.1	36.5	7.3	~	2.7
9 2001	1.1	0.5	4.4	30.9	1.6	0.6	1.1	7.0	~	0.9	12.2	8.9	~	30.8
9A 2001		1.4	3.8	29.2	1.1	0.6	1.6	7.8	~	0.4	12.8	11.1	~	30.3
2 2002	~	1.1	5.3	33.9	1.0	~	1.8	6.8	0.3	1.0	13.5	11.4	~	24.0
3 2002	~	0.3	6.4	36.5	0.7	~	1.4	5.5	0.1	0.7	9.3	11.0	0.6	27.7
4 2002	~	0.9	4.6	32.9	1.3	~	1.4	6.5	~	0.6	12.5	9.6		29.7
Average (9 2001-4 2002)	**0.2**	**0.8**	**4.9**	**32.7**	**1.1**	**0.2**	**1.5**	**6.7**	**0.1**	**0.7**	**12.1**	**10.4**	**0.1**	**28.5**
Min	1.1	0.3	3.8	29.2	0.7	0.6	1.1	5.5	0.1	0.4	9.3	8.9	0.6	24.0
Max	1.1	1.4	6.4	36.5	1.6	0.6	1.8	7.8	0.3	1.0	13.5	11.4	0.6	30.8

SEM-EDS glassy silicate matrix. The data has been normalised to 100 wt%. Samples 4 (extreme area) and 1 have not been included in the average slag matrix because they contain high quantities of lead oxide (sample 4) and high iron oxide (sample 1).

XRF data

Compounds	MgO	Al2O3	SiO2	SO3	K2O	CaO	TiO2	MnO	Fe2O3	PbO	ZnO	As2O3
	%	%	%	%	%	%	%	%	%	%	%	%
1st smelt slag 2002	1.8	5.5	28.4	6.5	2.5	9.1	0.2	0.6	10.5	28.3	5.4	0.6
2nd smelt slag 2002	0.9	2.9	20.3	12.4	1.5	5.7	0.2	0.2	5.4	44.4	5.1	0.3
Slag sample 1 2002	0.3	3.3	37.8	12.6	0.8	2.2	0.1	0.1	2.6	38.1	1.5	0.2

XRF pellet analyses (major elements) of three slag samples analysed using Turbo-quant. Data has been normalised to 100 wt%.

Compounds	Co3O4	NiO	CuO	Ga	SrO	Ag	SnO2	Sb	Ba	Hf	Bi
	µg/g	µg/g	µg/g	µg/g	µg/g	µg/g	µg/g	µg/g	µg/g	µg/g	µg/g
1st smelt slag 2002	431	358	1264	20	1328	249	234	1556	522	208	0
2nd smelt slag 2002	255	487	2195	273	1096	487	95	1466	411	242	160
Slag sample 1 2002	76	252	734	0	655	213	72	692	146	68	0

XRF pellet analyses (minor elements) of three slag samples analysed using Turbo-quant. Data has been normalised to 100 wt%.

LEAD SMELTING: THE LEAD METAL

Lead metal

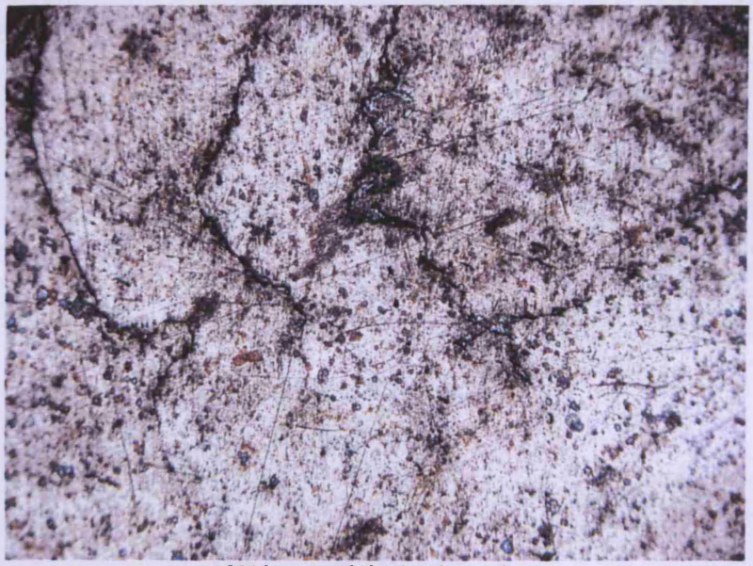

OM image of the lead matrix.

Sample analysed	S	Co	Ni	Cu	Zn	As	Ag	Sb	Pb
Lead metal block 7 (2001)	0.02	0.01	0.02	0.03	0.06	0.09	1.07	0.41	98.28

XRF data of the lead metal produced in the *huayrachina* smelts. The Alloys method was used in the XRF analyses.

SILVER REFINING: THE *LLARETA* ASH

Mounted block	Description	Year
25	Llareta ash	2002

Samples taken for analyses from the silver refining process.

Llareta ash
SEM-EDS images and data

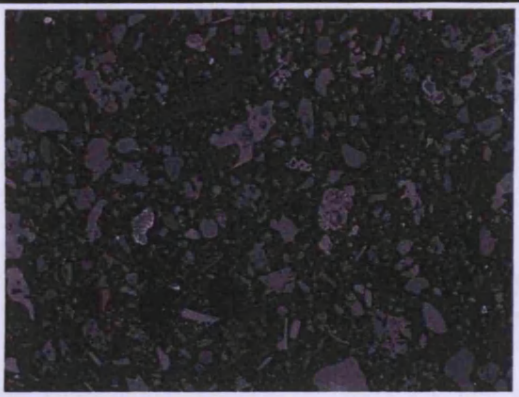

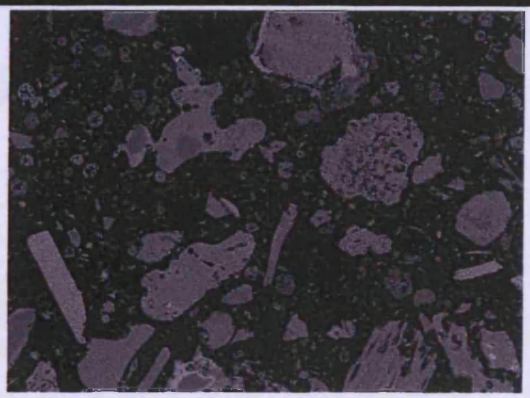

Sample	Na2O	MgO	Al2O3	SiO2	P2O5	SO3	K2O	CaO	Fe2O3
Llareta ash pressed pellet	2.2	4.7	8.7	**36.2**	1.2	2.5	10.6	31.0	3.0

XRF analysis of pressed pellet llareta ash.
The data has been normalised to 100% and oxygen calculated via stoichiometry.

Sampled area	Na2O	MgO	Al2O3	SiO2	K2O	CaO	FeO
1	1.9	5.7	~	46.7	8.8	35.0	1.9
2	1.5	4.0	10.2	44.2	7.0	30.4	2.7
3	1.6	3.8	8.6	43.6	8.2	31.1	3.1
4	1.4	3.8	9.4	43.3	7.9	32.0	2.2
5	1.8	3.8	9.2	43.8	8.0	31.2	2.3
Average	**1.7**	**4.2**	**7.5**	**44.3**	**8.0**	**31.9**	**2.5**

SEM-EDS bulk scanned area analyses of the llareta ash.
Data has been normalized to 100 wt%.

Sample area	Na2O	MgO	Al2O3	SiO2	K2O	CaO	FeO
1	2.7	~	12.8	76.8	6.4	0.8	0.5
2	0.6	~	8.9	82.7	6.2	0.4	1.3
3	0.8	~	11.9	75.5	10.5	0.5	0.8
4	4.2	~	23.9	61.3	1.7	8.9	~
5	~	~	11.5	76.8	10.4	0.7	0.6
6	0.7	~	12.8	71.2	13.1	1.7	0.5
7	6.1	~	23.7	62.4	0.7	7.1	~
8	3.4	0.8	19.3	64.4	8.7	1.5	2.0
9	~	~	11.8	75.5	11.2	0.9	0.6
10	~	~	11.7	76.1	10.9	0.6	0.7
11	2.8	~	11.0	68.4	15.9	0.8	1.1
12	0.8	~	12.1	77.0	8.5	0.8	0.8
Average	**1.8**	**0.1**	**14.3**	**72.3**	**8.7**	**2.1**	**0.7**
Min	0.6	0.8	8.9	61.3	0.7	0.4	0.5
Max	6.1	0.8	23.9	82.7	15.9	8.9	2.0

Round grains within the matrix. Data has been normalised to 100 wt%.

Sample area	MgO	Al2O3	SiO2	P2O5	K2O	CaO	TiO2	FeO
1	11.8	15.4	38.4	~	10.3	~	4.4	19.8
2	10.1	14.4	39.3	2.5	9.0	2.9	4.6	17.2
3	11.7	15.1	38.7	~	10.1	~	4.9	19.5
4	11.4	15.2	38.9	~	10.6	~	5.1	18.8
5	11.1	15.5	38.9	~	11.0	~	4.7	18.8
Average	**11.2**	**15.1**	**38.8**	**0.5**	**10.2**	**0.6**	**4.8**	**18.8**

SEM-EDS area angular inclusions within llareta ash.
Data has been normalized to 100 wt%.

Sample	Na2O	MgO	Al2O3	SiO2	P2O5	SO3	K2O	CaO	Fe2O3	TiO2	MnO
Cuiza *llareta* ash	2.2	4.7	8.7	**36.2**	1.2	2.5	10.6	31.0	3.0	~	~
Beech ash*	0.6	7.0	0.9	**18.0**	15.3	~	20.0	31.0	0.9	0.1	6.2
Oak ash*	0.5	4.3	1.9	**7.1**	3.1	0.7	14.9	64.5	2.5	0.1	0.4

ED-XRF analyses comparing tree ash to the *llareta* ash used by Cuiza. The data has been normalised to 100 wt% and oxygen calculated via stoichiometry.

***Beech and oak ash data taken from Jackson & Smedley 2004, 39.**

SILVER REFINING: THE SILVER ORE

Description	Year	Mounted block
Silver mineral	2001	13
Beneficiated silver mineral used in cupellation	2002	24

Silver ore

a.

a. Rejected silver ore from the 2001 cupellation (sample 13).
b. An OM image of sampel 13 – rejected ore from 2001 smelt. The ore contains large quantities of galena (white), spahlerite (grey).
c. An OM image of sample 24 (selected silver ore 2002). The ore was beneficiated and set in resin prior to analysis.

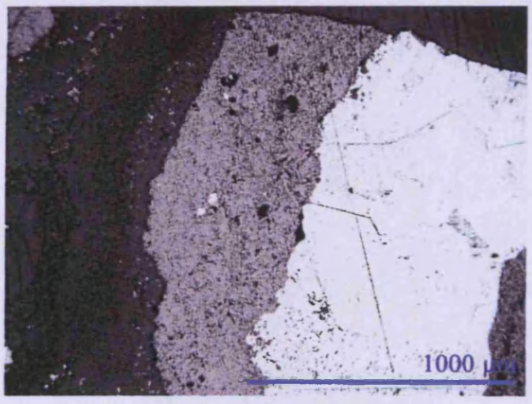

b.

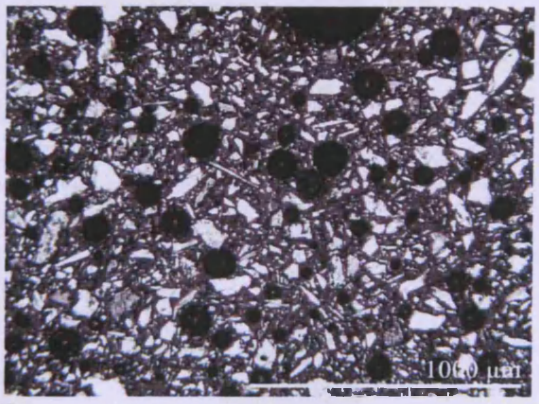

c.

ED-XRF data

Sample analysed	Na	Mg	Al	Si	S	Fe	Pb	Sn	Sb	As	Zn	Cu	Ag
Silver ore 13 MVB 2001	0.8	0.7	0.5	10.9	27.8	4.6	1.5	0.2	0.3	2.1	50.1	0.1	0.1

XRF analyses of mounted block silver ore. The data was collected using the alloy setting, presented in elements and normalised to 100%.

Sample analysed	Si	S	Fe	Cu	Zn	As	Ag	Sb	Pb
Silver ore sample 24 2002	1.0	12.3	1.1	trace	9.0	0.1	**1.6**	15.8	59.0

XRF pressed pellet analyses of silver ore taken from the 2002 refining. The data was collected using the alloy setting, presented in elements and normalised to 100%.

SILVER REFINING: THE CHM

Mounted block	Year	Description
15 MVB	2001	CHM
15 cc	2001	CHM
16 MVB	2001	CHM
16 cc	2001	CHM
16a	2001	CHM
6	2002	CHM/2
7	2002	CHM/3
8	2002	CHM/4

CHM 2001: 15 MVB and 15cc

a.

Sample 15MVB and 15 cc come from sample bag 15, image a shows some unmounted specimens. Sample bag 15 comes from cupellation done in 2001. Two pieces from sample bag 15 were selected for mounting 15 MVB (b left) and 15cc (b right). OM showed that both the samples were porous and exbited a matrix of free lead oxide with some metallic inclusions (c, d [15MVB] and e [15cc]).

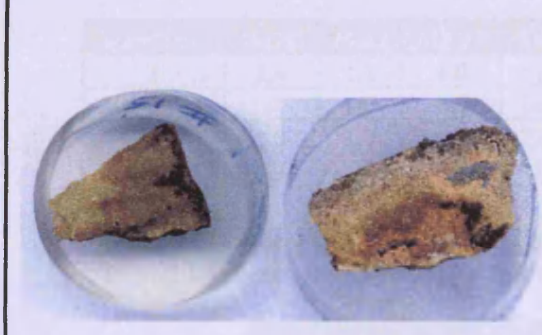

b.

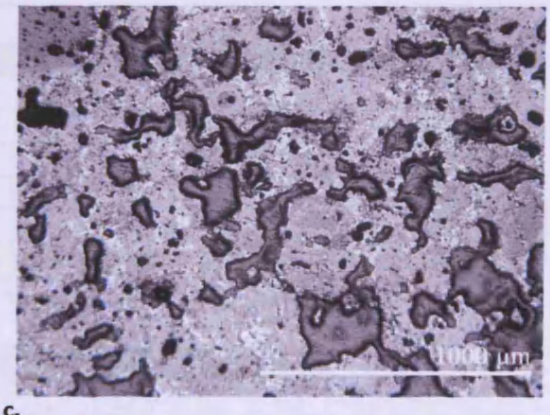

c.

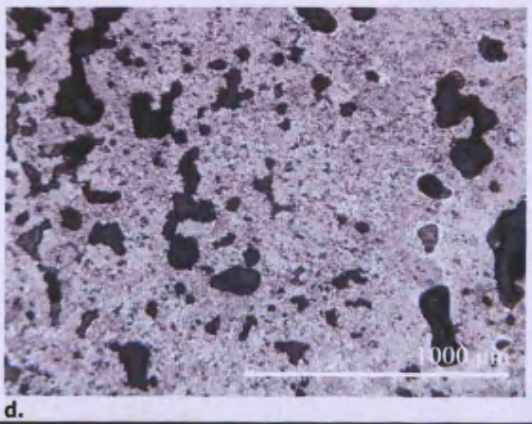

d.

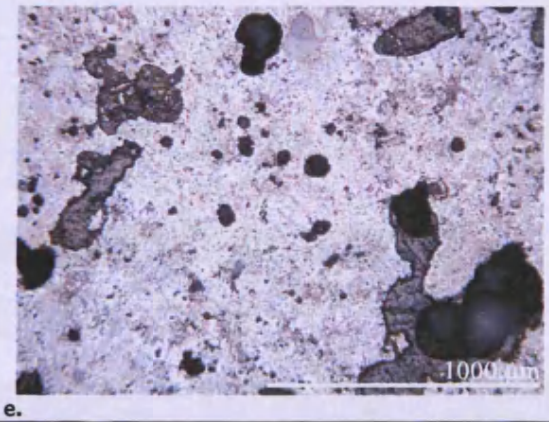

e.

SEM-EDS images and data

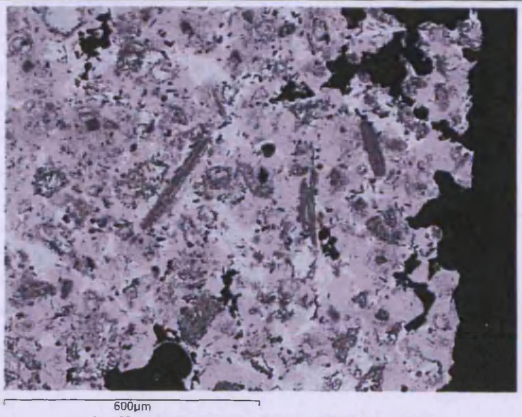

A bulk area scan of the CHM matrix.

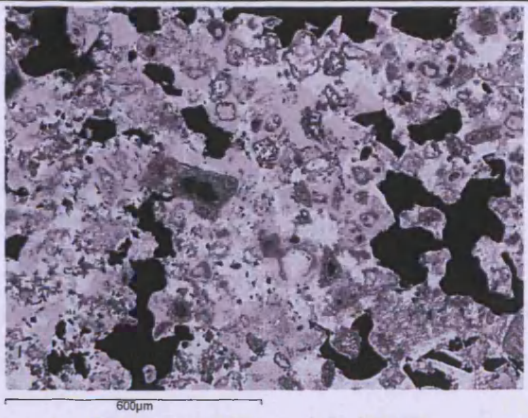

The porous CHM sample 15MVB.

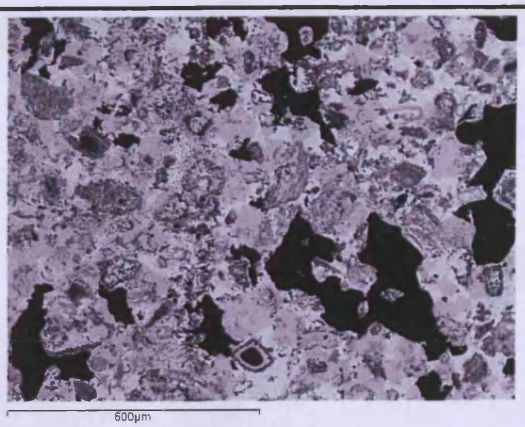

Inclusions of feldspar interacting with the lead oxide are common.

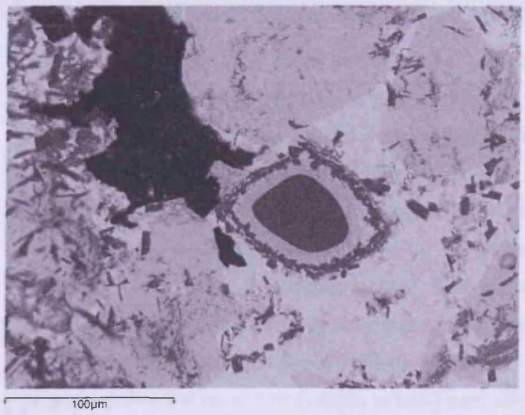

A close-up of the feldspar.

Spectrum	Na2O	MgO	Al2O3	SiO2	K2O	CaO	TiO2	FeO	ZnO	PbO
1	1.4	1.2	4.0	19.9	2.5	11.3	~	2.0	~	57.8
2	~	1.7	4.0	16.6	1.8	8.6	~	2.3	1.2	63.9
3	1.3	1.3	6.0	22.6	5.6	12.2	4.6	2.8	~	43.7
4	4.1	~	4.3	22.0	4.0	13.0	~	1.8	~	50.8
5	2.3	1.1	4.0	17.8	2.9	9.2	~	1.0	1.5	60.2
Average	**1.8**	**1.1**	**4.5**	**19.8**	**3.4**	**10.9**	**0.9**	**2.0**	**0.5**	**55.3**

SEM-EDS area scans of CHM sample 15MVB. The data has been normalised to 100 wt%.

Spectrum	Na2O	Al2O3	SiO2	K2O	CaO	FeO
1	1.1	12.3	71.8	12.9	0.6	1.3
2	5.7	25.1	59.6	1.0	8.5	~
3	2.3	17.7	67.1	12.9	~	~
4	2.3	18.0	66.8	12.5	0.4	~
5	4.8	24.5	58.7	3.7	8.3	~
Average	**3.3**	**19.5**	**64.8**	**8.6**	**3.6**	**0.3**

SEM-EDS data from CHM sample 15 MVB 2001- Feldspar interacting with lead oxide matrix. Data has been normalised to 100 wt%. SEE images above.

Scanned area	Na2O	MgO	Al2O3	SiO2	K2O	CaO	TiO2	FeO	PbO
1	1.9	6.6	8.6	31.1	0.5	28.7	2.1	2.3	18.2

SEM-EDS data from CHM sample 15 MVB 2001- lead/calcium silicates. Data has been normalised to 100 wt%.

Scanned area	Na2O	MgO	Al2O3	SiO2	K2O	CaO	TiO2	FeO	ZnO	As2O5	PbO
Llareta ash	1.7	4.2	7.5	44.3	8.0	31.9	~	2.5	0.0	0.0	0.0
Bulk scans with heavy metals removed (CHM 15 MVB)	4.1	2.4	10.1	44.7	7.6	24.5	2.1	4.5	0.0	0.0	0.0

SEM-EDS scanned area analyses showing the composition of the llareta ash and sample 15 MVB. The data has been normalised to 100 wt%.

CHM 2001: 16 MVB

a.

Selected pieces of CHM from sample bag 16 (a). The CHM sample 16 MVB (c) has a complex structure which has open pores, lead oxide, and metallic prills.d and e. Metallic prills observed using the OM (d). The prills are found within the a lead oxide matrix. The yellow lustre of the prills indicates the presence of silver metal. The smaller of the two prills composed predominately of lead metal. Magnification on the CHM indicates the presence of lead sulphide (white areas) and silver metal (yellow dendritic areas within the brown lead metal (left)), image e.

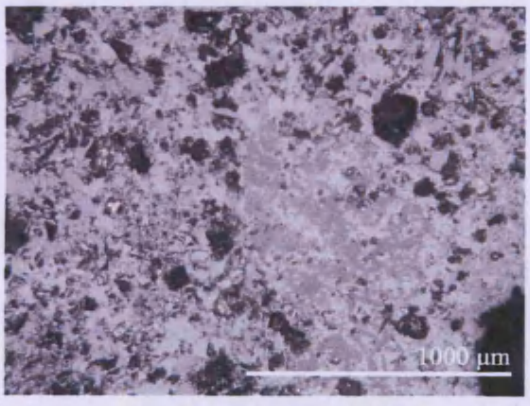

b.

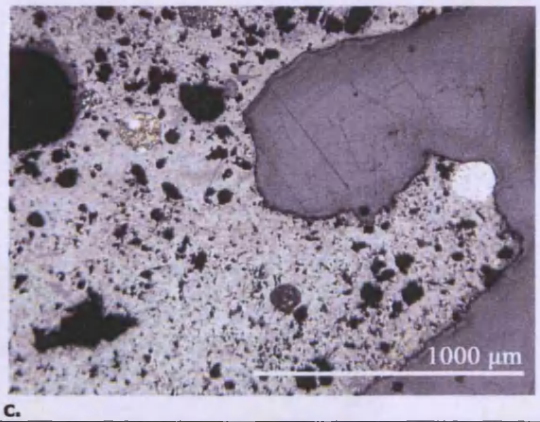

c.

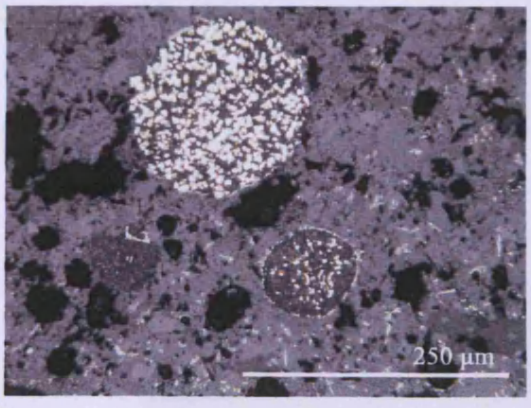

d.

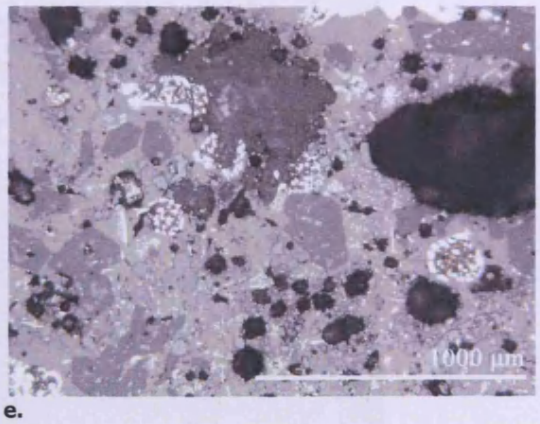

e.

SEM-EDS images and data

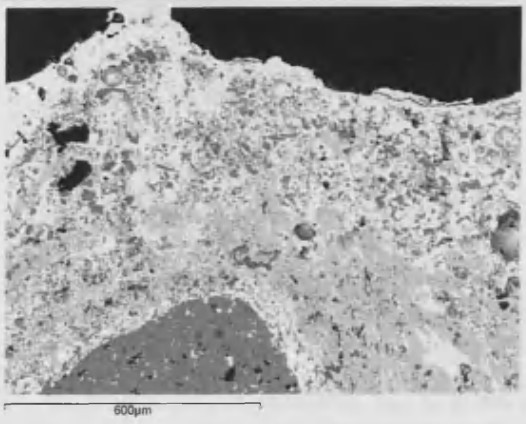

A bulk area image of sample CHM 16 MVB. At the bottom left is a large inclusion of zinc sulphide (grey), surrounded by a lead sulphide halo (white crystals).

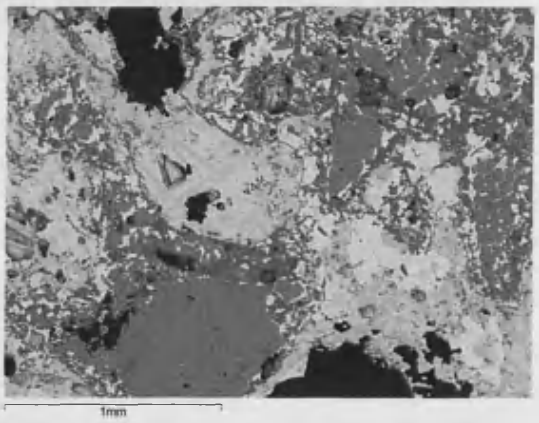

Sample CHM 16 MVB contains large quantities of partially reacted ore: zinc sulphide mid grey), inclusions of quartz (dark grey), in a matrix of free lead oxide (white, light grey).

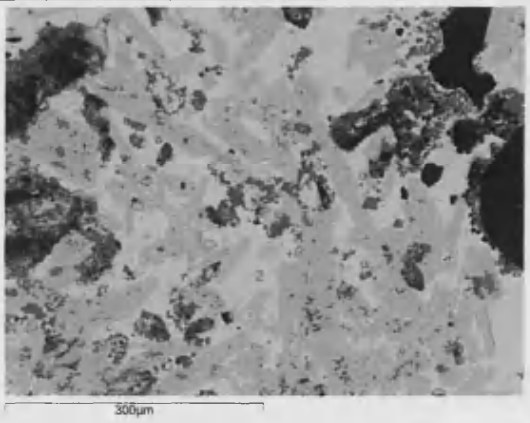

1 = lead, zinc silicate
2 = Lead oxide
3 = Iron, zinc oxide (spinel)

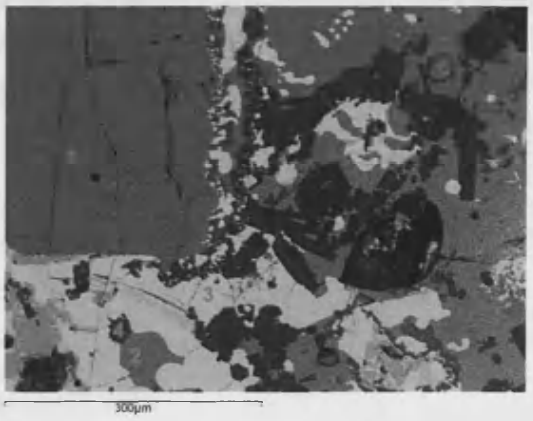

Areas of gangue in CHM 16MVB.
1 = Barite ($BaSO_4$)
2 = Lead, antimony, zinc oxide (spinel)
3 = Lead sulphide
4 = Zinc silicate

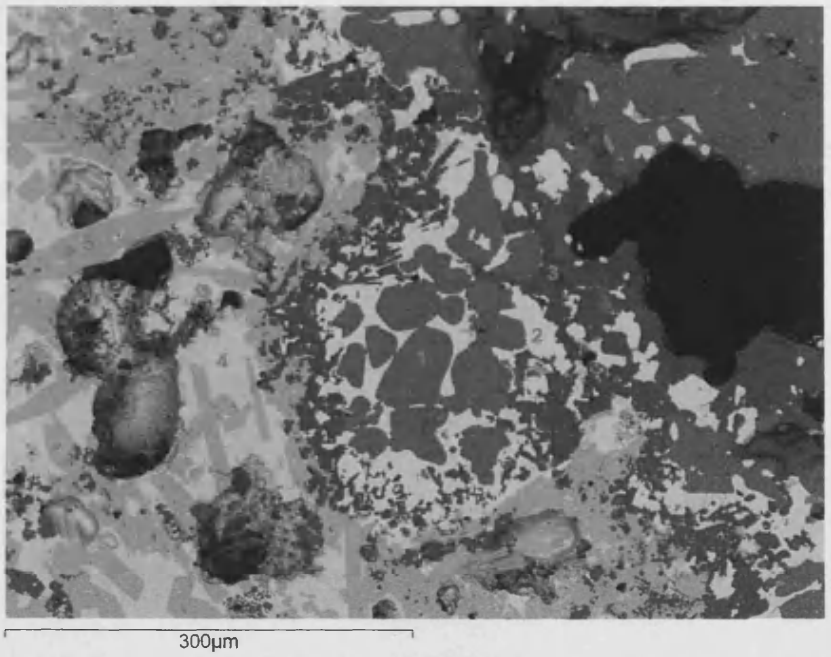

1 = Zinc sulphide, 2 = Lead sulphide, 3 = Zinc, iron silicate, 4 = Lead oxide, 5 = Lead, zinc silicate

Spectrum	Al2O3	SiO2	CaO	SO3	FeO	ZnO	As2Ox	SbO	PbO
1	~	~	~	3.0	1.1	1.0	2.5	2.9	89.7
2	1.8	7.3	~	~	5.1	25.5	1.2	~	59.2
3	~	16.8	~	~	~	25.2	~	~	56.5
4	~	16.2	~	~	~	25.3	~	~	56.2
5	~	17.8	0.8	~	~	24.9	~	~	56.5

SEM-EDS area analyses of the lead oxide matrix.
The data has been normalised to 100 wt%.

Scanned area	Si	Ag	Pb
1	3.7	49.5	46.8
2	~	~	100.0

SEM-EDS area analyses of lead prills in CHM 16MVB.
The data has been normalised to 100 wt%.

Spectrum	SO3	BaO
1	34.1	65.9

Bariam sulphate BaSO4, gangue from galena (CHM 16MVB).
The data has been normalised to 100 wt%.

Spectrum	S	Cu	Zn	Pb
1	13.7	~	~	86.4
2	14.2	~	~	85.8
3	13.4	1.0	3.5	82.0
4	14.4	~	3.0	82.6
5	14.0	~	1.6	84.4
6	33.4	~	1.3	65.4
7	13.7	0.7	1.6	84.0

SEM-EDS bulk area analyses of lead sulphide around lead prills in sample CHM 16 MVB.
The data is normalised to 100 wt%.

Spectrum	S	Fe	Zn
1	33.5	0.4	66.1
2	33.2	1.1	65.7
3	34.2	9.3	56.5

Zinc sulphide measured in three different regions of the sample.
The data is normalised to 100 wt%.

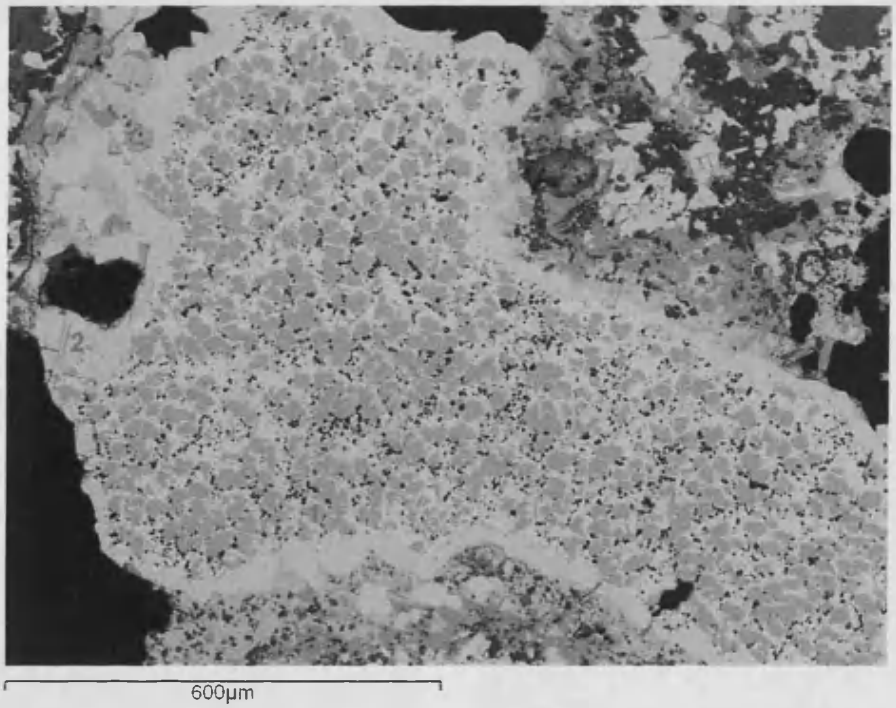

Sample CHM 16MVB contains large metallic areas. In this image the majority of the prill is lead metal, the grey inclusions (1) are silver phases. The area is surrounded by lead sulphide (2).

Spectrum	Ag	Pb
1	95.19	4.81

Silver prills in lead metal islands (in CHM 16MVB).
The data has been normalised to 100 wt%.

CHM 2001: 16cc

a.

Samples 16a and 16cc are chemically and physically similar.
The OM images showed a lead oxide matrix with inclusions of partially reacted ore (lead and zinc sulphide) and metallic prills of lead and silver (see CHM 16a for examples).
a. The mounted and polished sample CHM 16 cc.

SEM-EDS images and data

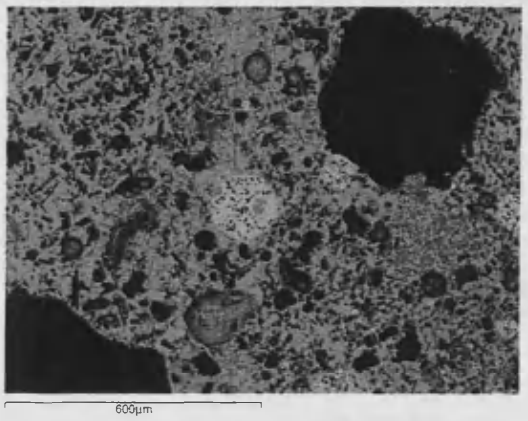

CHM sample with a large metallic lead prill with inclusions of silver (white)and a large hole (black).

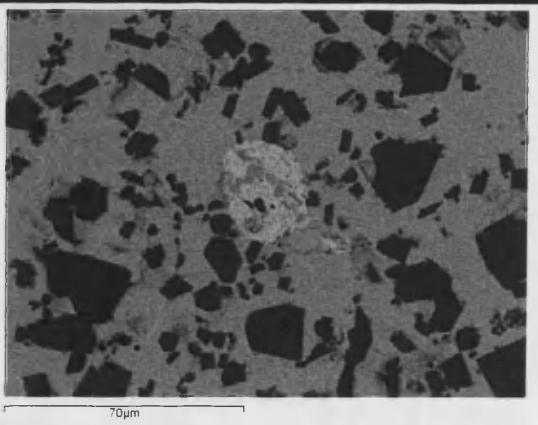

Prill A in a lead oxide matrix and zinc oxide phases.

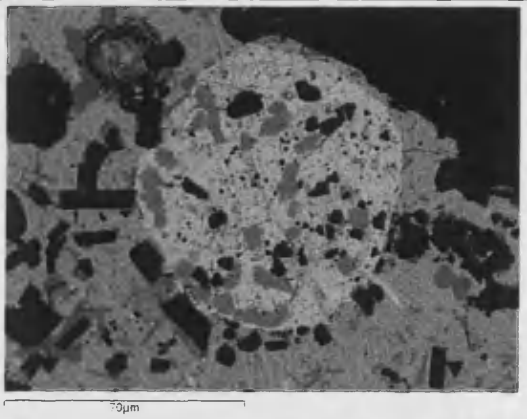

Prill B – a lead-silver metallic prill. The surrounding matrix is lead oxide and zinc, lead silicates.

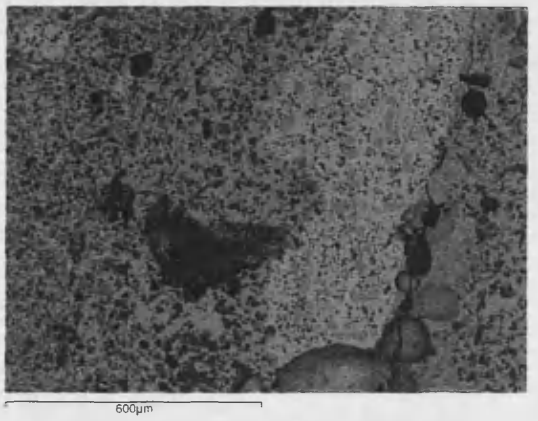

Areas of lead/silver metal within CHM.

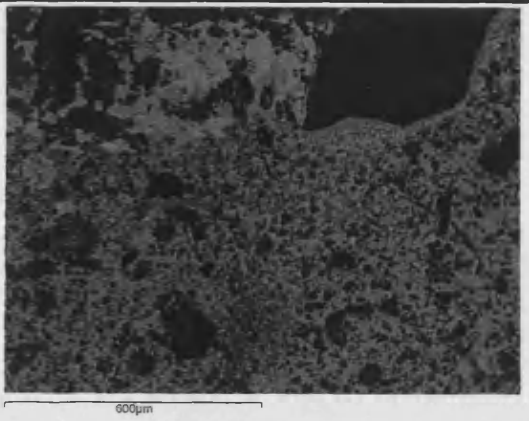

Large areas of zinc sulphide was recorded in the CHM sample 16cc (dark grey area top right).

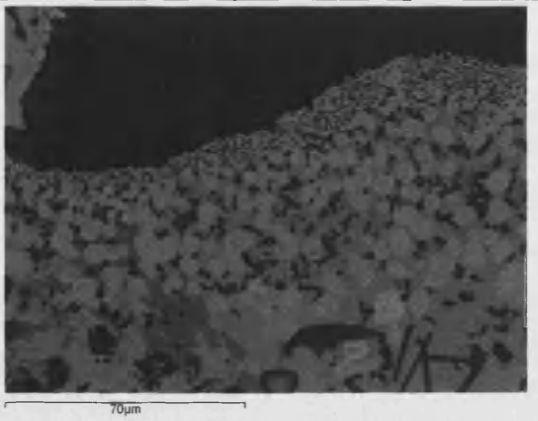

The zinc sulphide reacting with the lead oxide matrix to form lead, zinc silicates.

Prills analysed in CHM 16 cc	Ag	Pb
Prill A (very small prill)	26.5	73.5
Prill B – selected points	4.8	95.2
Prill B – selected points	7.1	92.9
Prill B (large area scan)	14.5	85.5
Prill C	20.4	79.6
Prill D	28.1	71.9
Prill E	28.0	72.0

SEM-EDS area analyses of lead prills within CHM sample 16cc.
The data has been normalised to 100 wt%.

Sampled area	S	Fe	Zn	Pb
1	13.3	~	~	86.7
2	14.6	~	~	85.4
3	33.7	4.6	61.7	~
4	33.9	2.0	64.0	~

SEM-EDS area analyses of partially reacted ore found in sample CHM 16 cc.
The data has been normalised to 100 wt%.

Sampled areas	ZnO
1	100.0
2	100.0

SEM-EDS area analyses of zinc oxide found in sample CHM 16 cc.
The data has been normalised to 100 wt%.

CHM 2001:16a

a.

a. Selected pieces of CHM from sample bag 16.
b. Sample CHM 16a mounted in epoxy resin and polished ready for analytical work.
c and d. Illustrate the typical structure of sample CHM 16a: porous, with lead oxide matrix and inclusions of lead sulphide (bright white), and metallic prills.
e. Metallic prills are common are composed of lead and silver metals and some residual lead sulphide

b.

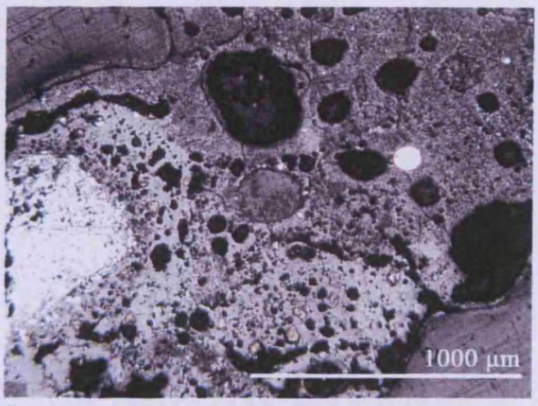

c.

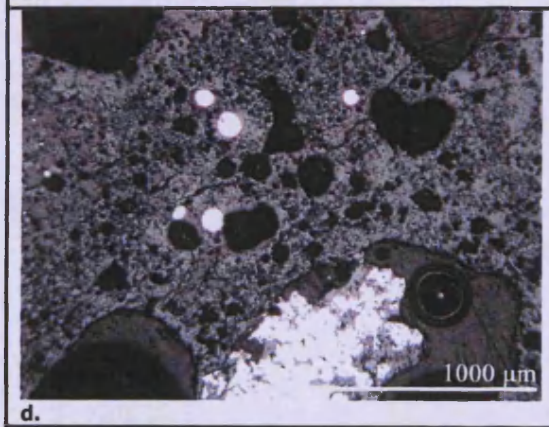

d.

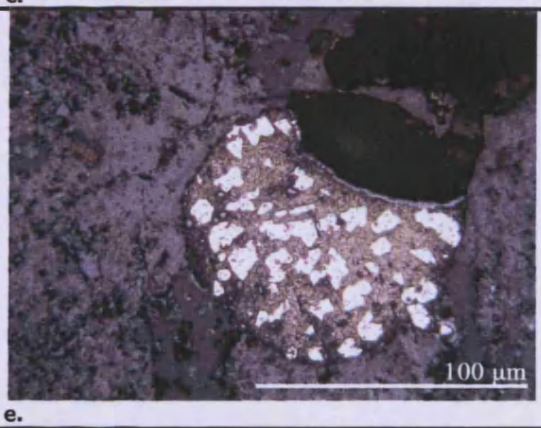

e.

SEM-EDS images and data

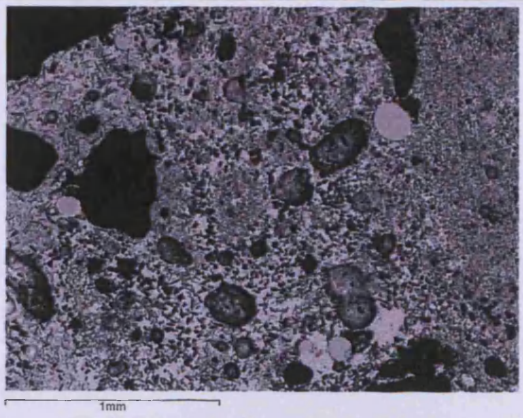

The typical structure of sample 16a.

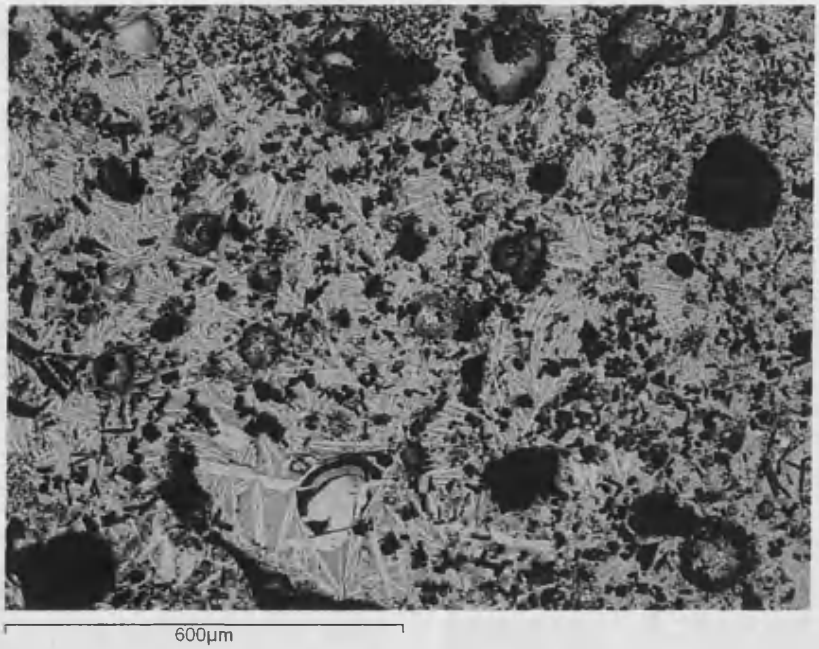

An (backscattered) SEM image of free lead oxide matrix and zinc silicates.

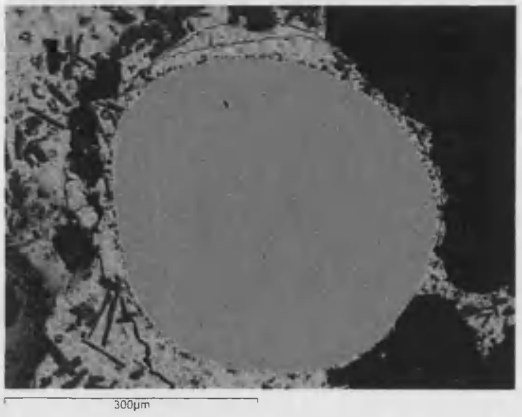

A pure silver prill within the lead oxide matrix.

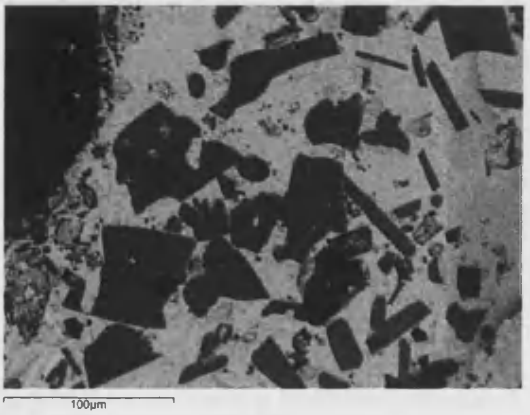

Zinc oxide phases within the lead oxide matrix.

Spectrum	MgO	Al2O3	SiO2	CaO	FeO	ZnO	As2O3	AgO	BaO	PbO
2	0.9	~	5.4	~	3.3	29.5	~	~	~	60.9
3	0.6	1.7	~	~	1.5	25.9	~	2.9	1.0	66.3
4	~	1.3	1.8	~	1.4	23.7	~	1.3	~	70.4
5	~	1.8	1.6	~	1.5	33.0	~	2.1	~	59.9
6	~	0.9	2.0	~	1.0	40.3	~	1.7	~	54.2
7	~	5.2	~	~	3.0	21.9	~	2.0	~	67.9
8	~	1.6	3.5	0.5	2.0	23.8	~	~	~	68.7
9	~	~	6.5	0.7	3.8	25.4	~	~	~	63.7

SEM-EDS area scans of the sample CHM 16a (with metal inclusions). The data has been normalised to 100 wt%.

Spectrum	Mg	Ag
1	0.2	99.8
2	0.3	99.7
3	~	100.0
4	0.3	99.7
5	~	100.0

SEM-EDS area scans of silver prills within sample CHM 16a. The data has been normalised to 100 wt%.

CHM 2002: 6

a.

CHM 6 2002 (image a - one piece shown from all angles). The grey layer is the packed llareta ash, which was wetted into place with urine prior to cupellation. The orange coating is a layer of almost pure lead oxide that has been slowly interacting and sinking into the packed ash.

SEM-EDS images and data

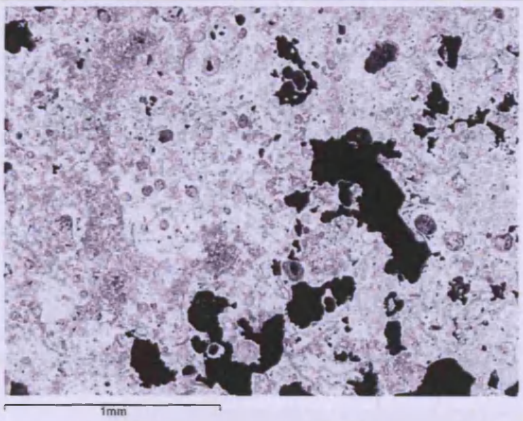

A typical microstructure of CHM 6 2002.

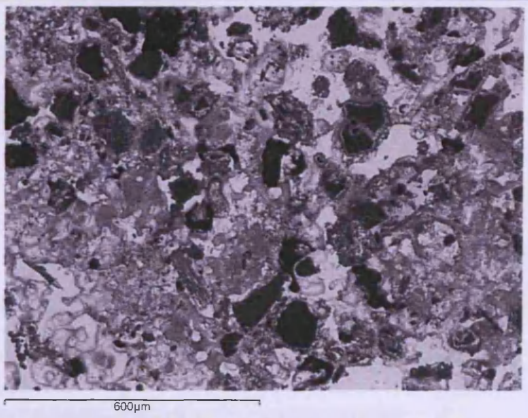

Increasing the magnification revealed the sample was a lead oxide matrix (white) with quartz crystals dissolving in the lead oxide (dark grey).

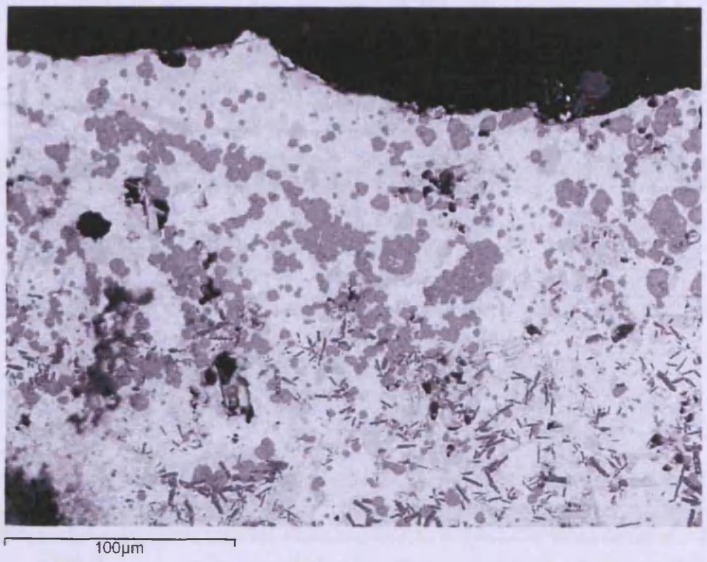

The lead oxide layer includes inclusions of antimony calcium oxides (rounded mid grey crystals).

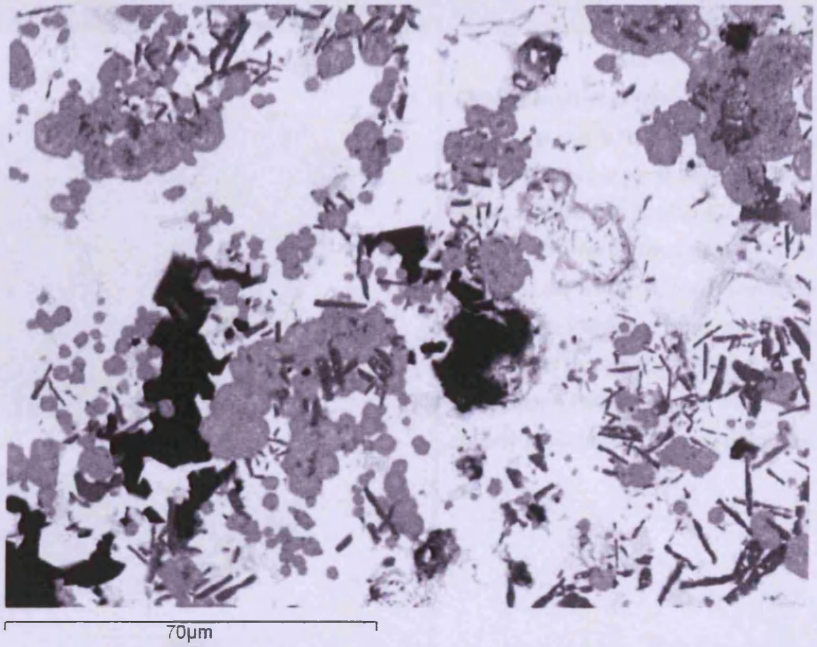

Sample CHM 6 2002 contains large quantities of antimony in different crystalline phases.

Sampled area	MgO	Al2O3	SiO2	K2O	CaO	FeO	ZnO	As2O3	Sb2O3	PbO
1	~	1.5	10.0	~	~	~	2.4	2.9	14.2	69.0
2	~	3.3	20.6	0.9	2.6	0.7	2.3	5.6	~	64.1
3	~	3.2	21.7	1.1	1.3	1.4	2.8	4.0	~	64.4
4	0.6	1.9	14.4	~	~	~	0.9	~	9.8	72.5
5	~	~	3.1	~	~	~	~	1.4	15.0	80.5
6	~	~	~	~	~	~	~	~	14.0	86.0

SEM-EDS area analyses of the lead oxide matrix of CHM from sample 6 2002. Data has been normalised to 100 wt%.

Spectrum	MgO	Al2O3	SiO2	CaO	FeO	ZnO	As2O3	Sb2O3	PbO
1	1.3	13.6	1.8	23.7	3.0	7.9	0.4	43.6	4.8
2	2.4	11.3	2.8	23.0	2.7	9.1	0.1	42.2	6.5
3	2.0	9.7	3.0	23.8	3.7	7.9	~	41.8	8.1
4	1.9	10.5	3.1	23.7	3.2	8.8	~	40.7	8.2
5	1.9	11.2	2.5	23.8	3.1	8.8	~	42.5	6.2

SEM-EDS area analyses of calcium/aluminium/ antimony oxide crystals in sample 6 2002. The data has been normalised to 100 wt%.

Spectrum	Na2O	MgO	Al2O3	SiO2	K2O	CaO	FeO	ZnO	PbO
1	1.4		12.5	76.5	9.6				
2	1.5	0.5	7.0	48.4	4.1	0.8		0.9	36.8
3	0.6	10.7	9.2	55.0	5.9	13.7	1.4		3.7

SEM-EDS area analyses of feldspar grains dissolving in lead oxide sample 6 2002.The data has been normalised to 100 wt%.

Spectrum	Al2O3	SiO2	SO3	CaO	PbO
SI11 3	0.5	3.6	53.9	34.9	7.1
SI10 2	~	2.0	52.8	34.5	10.7

Strange dark crystals, possibly anhydrite ($CaSO_4$) with high sulphur and lime sample 6.

Spectrum	MgO	Al2O3	SiO2	CaO	ZnO	PbO
SI14 2	6.5	2.8	34.5	25.3	6.0	24.8

Lead-calcium silicates in sample CHM 6 2002. The data has been normalised to 100 wt%.

CHM 2002: 7

a.

CHM sample 7 is from Cuiza's cupellation hearth (image a and b (the mounted block)). It has three distinct layers: the upper layer consists of purer lead oxide (c and d), the middle comprises of metallic lead/silver phase (e and f), and the lower is partially reacted hearth lining (this layer has a heavy silicate base and could be the hearth wall/clay) image g. The structure of sample 7 is similar to CHM sample 8. From the OM PbS is clearly present in the upper layers (f).

b.

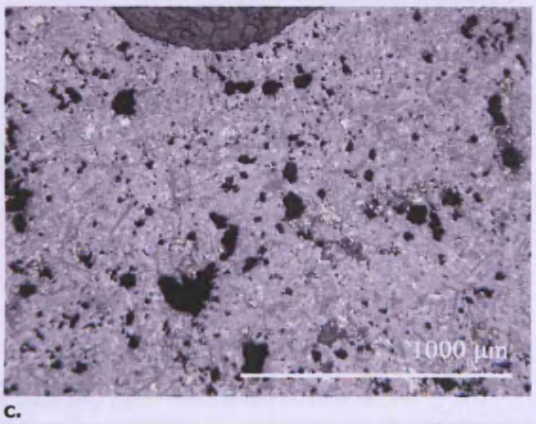

c.

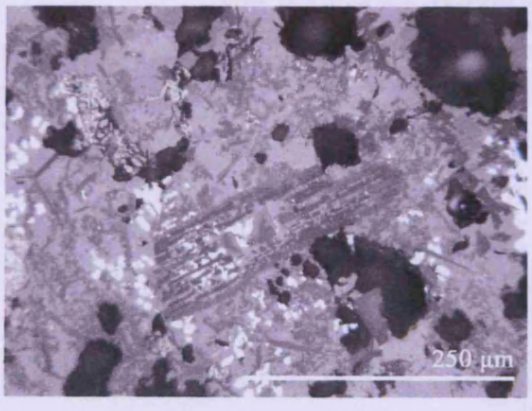

d.

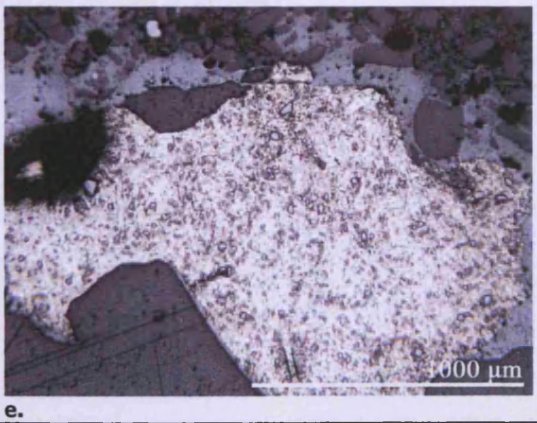

e.

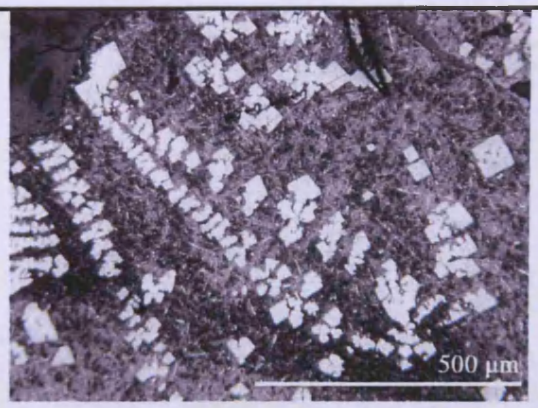

f.

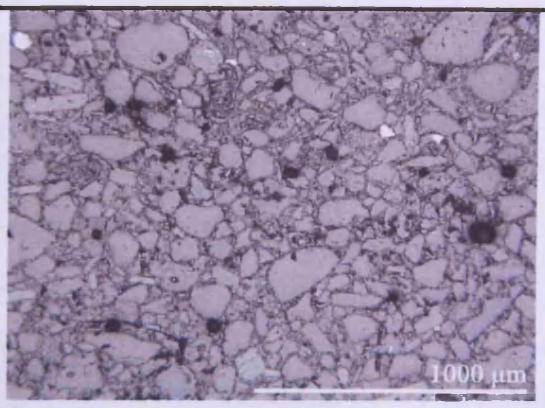

g.

SEM-EDS images and data

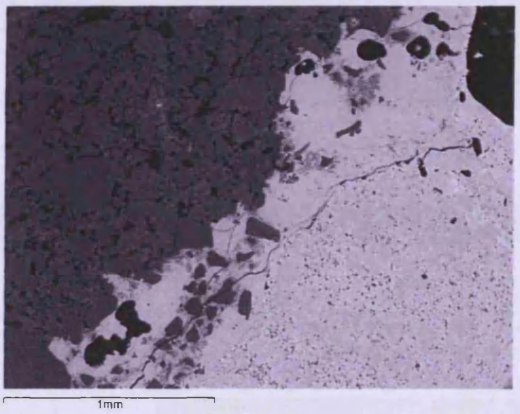

Interaction between lead prill (white) and hearth bottom (dark grey area)

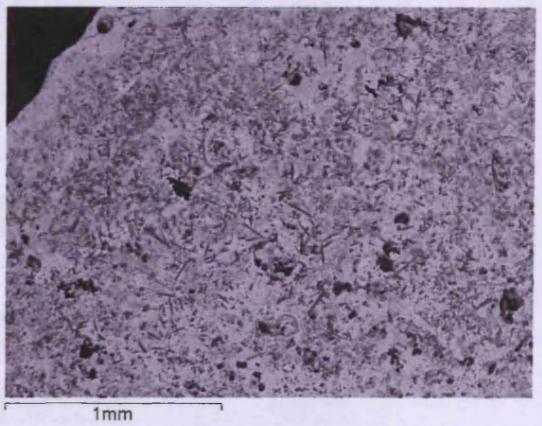

Lead oxide layer

Spectrum	Na2O	MgO	Al2O3	SiO2	K2O	CaO	FeO	ZnO	SbO	PbO
1	~	1.0	2.6	13.6	0.8	6.6	0.7	0.7	13.6	60.4
2	0.6	0.8	2.8	12.7	1.1	5.9	0.9	1.4	12.0	61.8
3	~	1.0	3.2	12.6	1.4	4.4	0.7	2.2	~	74.7
4	~	0.7	2.9	11.6	0.8	6.3	~	2.4	11.0	64.3
5	~	0.9	3.0	14.2	1.3	5.5	0.7	~	13.7	60.8
Average	0.1	0.9	2.9	12.9	1.1	5.7	0.6	1.3	10.1	64.4

SEM-EDS bulk area scans of the CHM sample 7 2002. The data has been normlised to 100 wt%.

Spectrum	Na2O	MgO	Al2O3	SiO2	K2O	CaO	FeO	PbO
Area 1	1.2	0.7	12.2	76.9	3.2	1.6	2.5	1.8

SEM-EDS area scan analysis of the lower section of sample 7.
Indicating the hearth was constructed from a ceramic material.
The data has been normalised to 100 wt%.

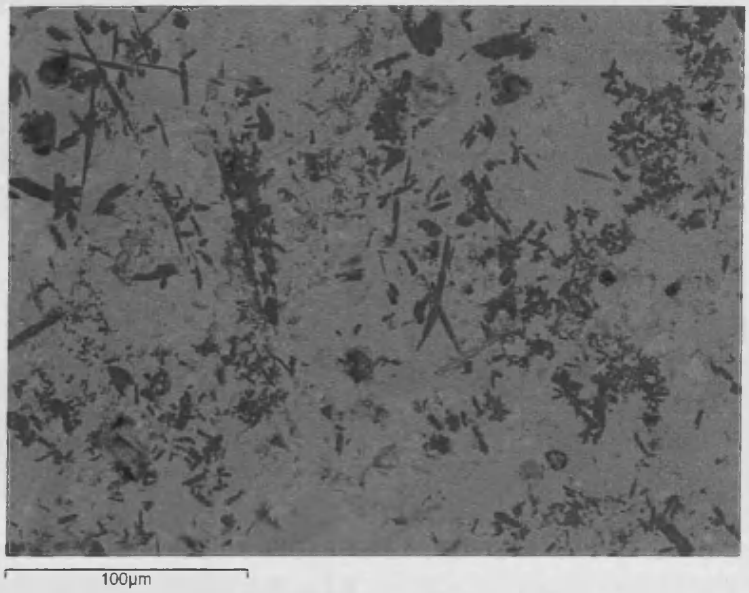

Areas analysed	Na2O	MgO	Al2O3	SiO2	P2O5	SO3	K2O	CaO	ZnO	FeO	PbO
1	1.0	0.9	13.8	28.6	2.8	9.1	6.4	23.5	~	0.8	13.2
2	1.0	0.9	14.2	27.7	2.7	8.5	6.8	24.4	1.5	~	12.4

Black needle-like crystals found in the lead oxide rich areas of CHM sample 7.
Data has been normalised to 100 wt%.

Areas analysed	Na2O	Al2O3	SiO2	K2O	As2O5	SbO	PbO
1	~	19.2	52.4	19.8	0.2	1.4	7.1
2	0.8	26.8	37.4	27.2	0.1	~	7.7

Feldspars (1) and leucite (2) analysed from CHM sample 7.
Data has been normalised to 100 %.

CHM 2002: 8

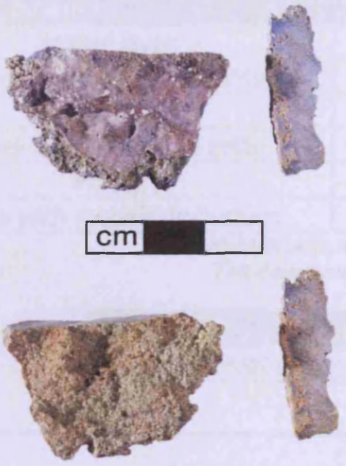

a.

This sample has an upper layer of pure lead oxide, followed by a lower layer that contains recrystallised phases that would have constituted the hearth lining (a).
b. OM images show a free lead oxide upper layer.
c. The sample has metallic prills of silver and lead metal.

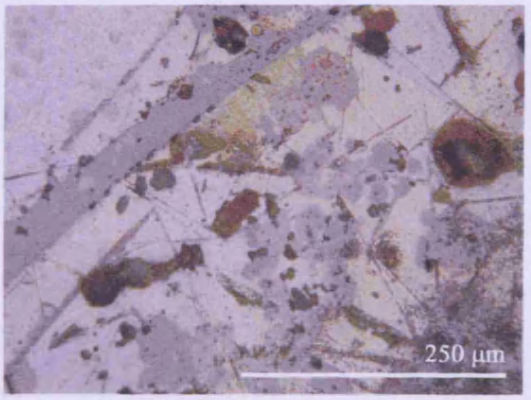

b.

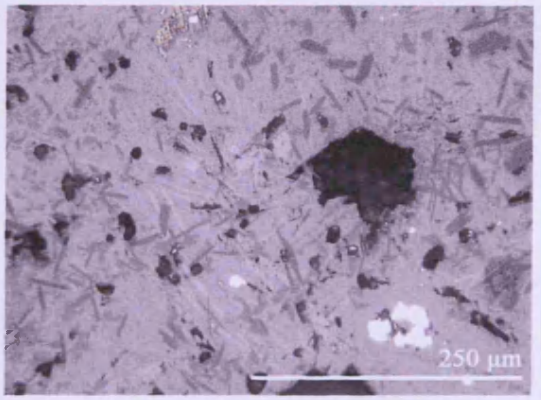

c.

SEM-EDS images and data

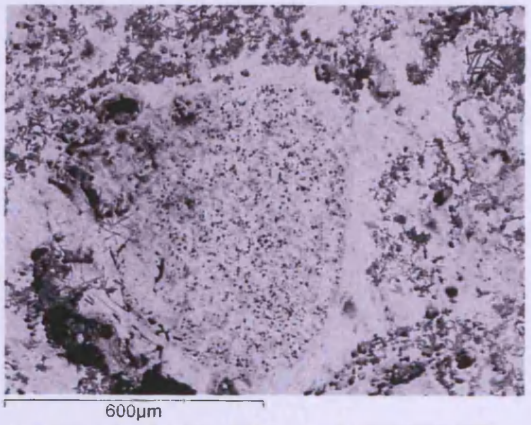

A large lead prill within sample CHM 8 2002.

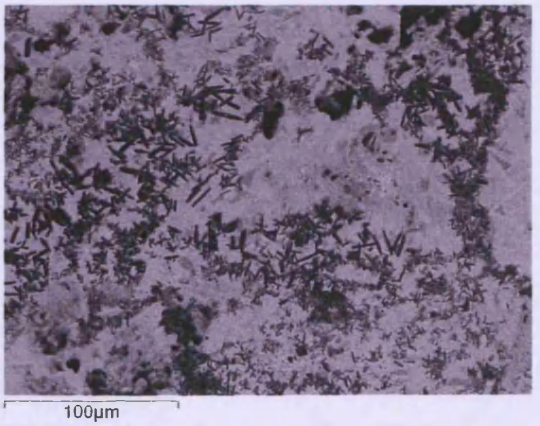

The lead oxide matrix interacting with the hearth lining.

Scanned areas	MgO	Al2O3	SiO2	CaO	ZnO	Sb2O3	PbO
Upper layer	0.6	0.6	4.9	3.8	1.1	~	89.2
Lower layer with lead prills	0.7	1.7	9.6	6.0	1.9	~	80.3
Middle	0.5	1.3	6.6	3.3	2.0	~	86.3
Lower layer with lead prills	0.8	1.7	9.0	7.8	1.9	~	78.7
Middle	1.0	~	8.8	8.0	~	~	82.3
Middle with metallic inclusions	0.8	1.7	6.8	7.5	1.7	11.5	70.0

SEM-EDS bulk area scans of CHM sample 8 2002.
The data has been normalised to 100 wt%.

Scanned area	P2O5	CaO	SnO2
SI5 POSSIBLE RESIDUAL ASH	45.7	53.4	0.9

Combined CHM data

CHM	Na2O	MgO	Al2O3	SiO2	K2O	CaO	SO3	TiO2	FeO	ZnO	As2O3	SbO	AgO	PbO
15 MVB	0.9	2.3	5.4	17.9	4.0	8.4	~	0.3	1.7	0.9	~	~	~	58.3
16 MVB	~	~	1.1	6.4	~	~	1.7	~	5.6	23.9	0.5	0.6	0.3	59.9
16 A	~	0.2	0.7	4.9	~	0.3	~	~	2.5	21.7	0.2	~	0.6	68.8
6 2002	~	1.0	2.3	11.4	0.4	5.4	~	~	0.9	1.9	~	11.9	~	64.8
7 2002	0.1	0.9	2.9	12.9	1.1	5.7	~	~	0.6	1.3	~	10.1	~	64.4
8 2002	~	0.7	1.4	7.4	~	5.7	~	~	~	1.7	~	2.3	~	80.9
Average	**0.2**	**0.9**	**2.3**	**10.2**	**0.9**	**4.3**	**0.3**	**0.1**	**1.9**	**8.6**	**0.1**	**4.2**	**0.2**	**66.2**
Min	0.1	0.2	0.7	4.9	0.4	0.3	1.7	0.3	0.6	0.9	0.2	0.6	0.3	58.3
Max	0.9	2.3	5.4	17.9	4.0	8.4	1.7	0.3	5.6	23.9	0.5	11.9	0.6	80.9

SEM-EDS bulk area analyses of CHM samples. The data has been normalised to 100 %.

Sample	Na2O	MgO	Al2O3	SiO2	K2O	CaO	SO3	TiO2	FeO
CHM 6 to be added to *huayrachina* 2001	0.6	2.8	10.7	52.5	7.7	22.2	~	trace	3.6
CHM 21 to be added to *huayrachina* 2002	0.9	2.8	7.4	43.7	~	30.7	~	~	14.4
CHM 15 2001	3.2	3.5	11.8	44.8	8.8	23.4	~	1.1	3.4
CHM 16 MVB 2001	~	~	7.4	43.2	~	~	11.5	~	37.8
CHM 16A 2001	~	2.3	8.1	57.0	~	3.5	~	~	29.1
CHM 6 2002	0.6	2.8	10.7	52.5	7.7	22.2	~	~	3.6
CHM 7 2002	0.5	3.6	11.9	53.4	4.5	23.7	~	~	2.4
CHM 8 2002	~	4.8	7.4	48.9	~	38.9	~	~	~
Llareta ash	1.7	4.2	7.5	44.3	8.0	31.9	~	~	2.5

Llareta ash vs CHM. A comparison between SEM-EDS analyses of cupellation hearth material (CHM) with the heavy metals removed and the llareta ash (The data has been normalised to 100%). Sample 21 has 14% FeO, this much high quantity is most probably due to a different ore source used for the cupellation.

Element	Na2O %	MgO %	Al2O3 %	SiO2 %	SO3 %	K2O %	CaO %	TiO2 %	V2O5 %	Cr2O3 %	MnO %	Fe2O3 %	PbO %
CHM 5 2001 (to be added to the *huayrachina*ra)	2.08	0.20	0.51	2.68	~	0.24	3.14	0.04	0.00	0.01	0.02	0.19	90.42
CHM 6 2002	0.00	1.98	0.60	6.21	10.74	0.67	2.80	0.05	0.01	0.00	0.00	2.37	67.18
Element	**Co3O4 µg/g**	**NiO µg/g**	**CuO µg/g**	**ZnO µg/g**	**Ga µg/g**	**As2O3 µg/g**	**SrO µg/g**	**Ag µg/g**	**SnO2 µg/g**	**Sb µg/g**	**Ba µg/g**	**Hf µg/g**	**Bi µg/g**
CHM 5 2001 (to be added to the huayra)	58	189	48	304	169	602	958	72	~	129	137	74	23
CHM 6 2002	724	1599	999	14199	496	46291	852	404	137	5046	153	160	1578

ED-XRF analyses of samples CHM 6 and CHM 5 (to be added to the *huayrachina* smelt). The data has been normalized to 100 wt%.

SILVER REFINING: THE SILVER METAL

Mounted block	Year	Description
14	2001	Silver metal
13	2002	AgM {13}
Not mounted	2002	Silver retrieved from CHM

Silver metal

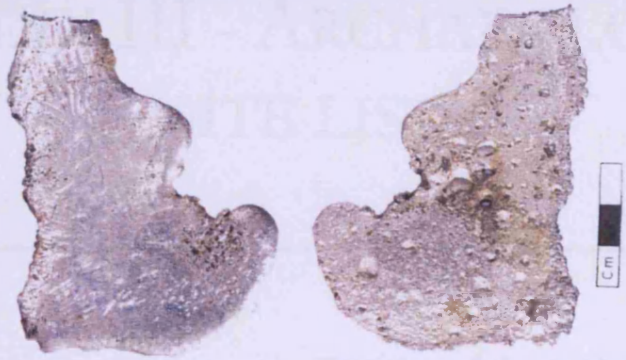

a.

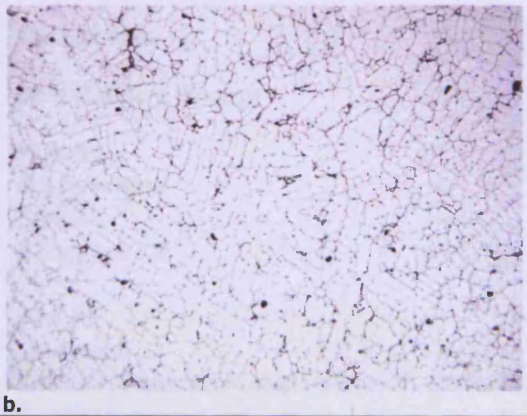

b.

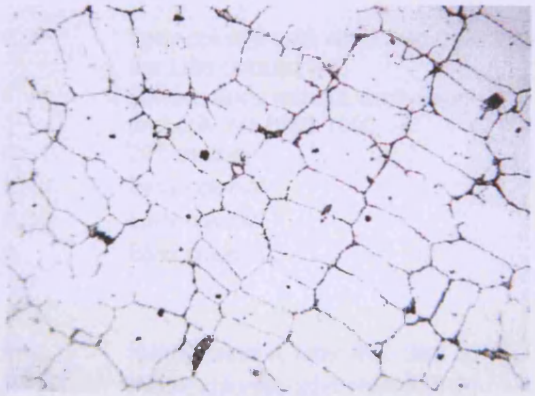

c.

SEM-EDS images and data

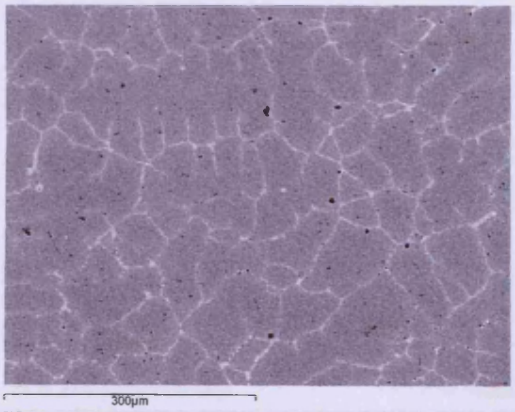

Elements	Ag	Pb	Bi
Average bulk scan areas	97.2	2.8	~
Grain boundaries			
SI4	24.4	14.4	61.3
SI9	17.0	18.0	65.0
SI9	6.6	~	93.4

The data has been normalized to 100 at%.

APPENDIX III - ARCHAEOLOGICAL SITE LIST

Site Name	Site Code	Type of site	Date established for site (See Chapter 3 for the specific dating)
Cruz Pampa	CP	R, F	Early colonial with continued used into the Late colonial era.
Don Martin's Dragon	DMD	F	Surface finds without excavation probably AD 1850-1900
Hornos	H	F	20th century
Huayrachina	Hu	R	Early colonial
Site 24	Hu24	R, H	Early colonial
Structure 23	#23	R	Early colonial
Site 35			
Structure 1	~	F	Middle colonial, later than Site 24
Structure 3 associated with feature E, feature G	~	F	Middle colonial, later than Site 24
Structure 7 associated with feature H	~	F	Middle colonial, later than Site 24
Site 80	#80	R	Early colonial or Inca
Site 123	#123	R, H	?
Uruquilla			
Uruquilla 10 Est and Trinchera	UR10 Est	R, F	Early - middle colonial
Uruquilla 10	UR10	F	Early colonial
Uruquilla 11	UR11	F	Late colonial
Uruquilla 12	UR12	F	Late colonial

H = *Huayrachina* site
R = Residential site
F = Metallurgical sites that do not contain *huayrachinas*

APPENDIX IV - ARCHAEOLOGICAL *HUAYRACHINA* SURVEY

Huayrachina sites	Uruquilla domed furnaces	Dragon furnaces
Cruz Pampa Surface	UR 10	UR EST 10
Huayrachina Alta	UR 11	Don Martin's Dragon
Site 24	UR 12	
Uruquilla West Saddle Surface		
Uruquilla East Saddle Surface		

List of archaeological sites selected for analyses. The column left shows the available *huayrachina* sites.

An archaeological *huayrachina* site (left) and base stone (right)

A map of the Porco area

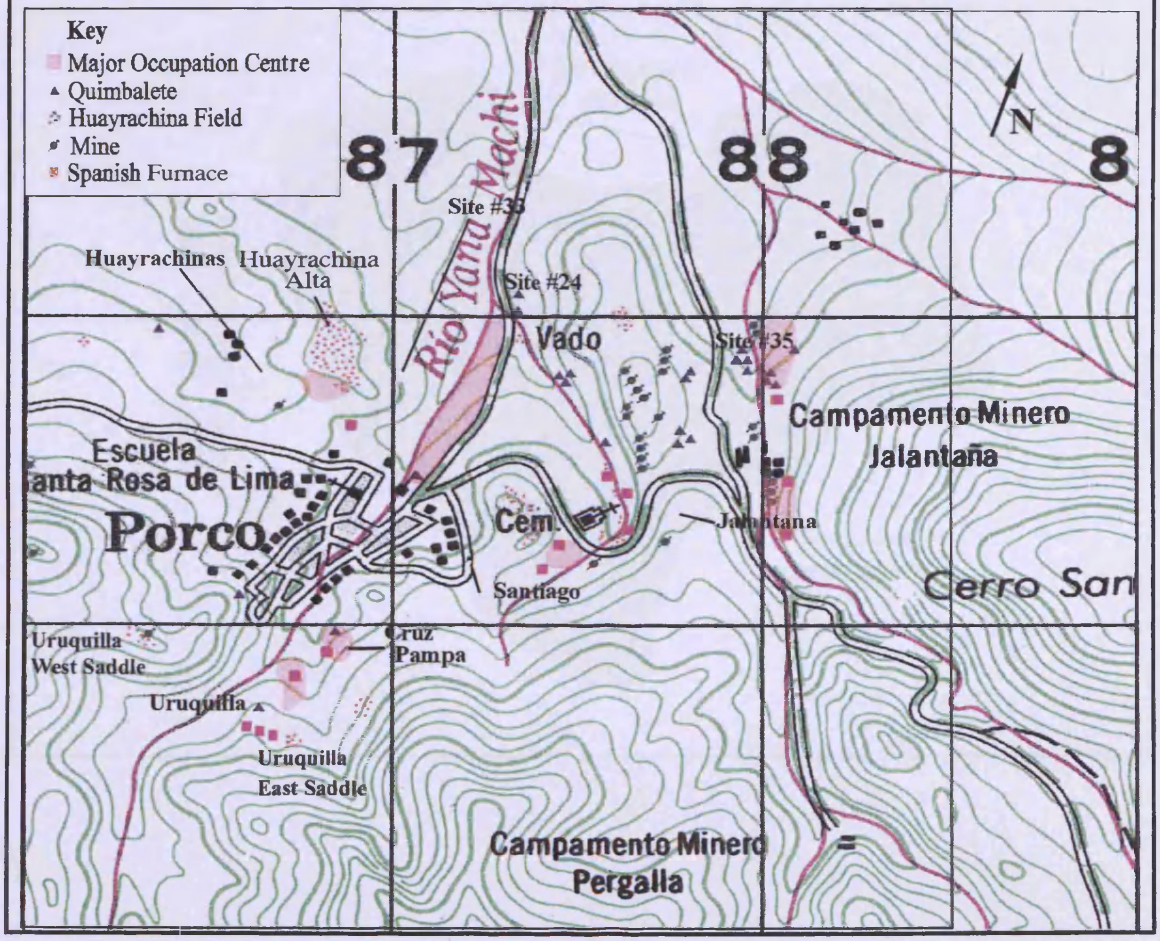

Measuring *huayrachina* fragments

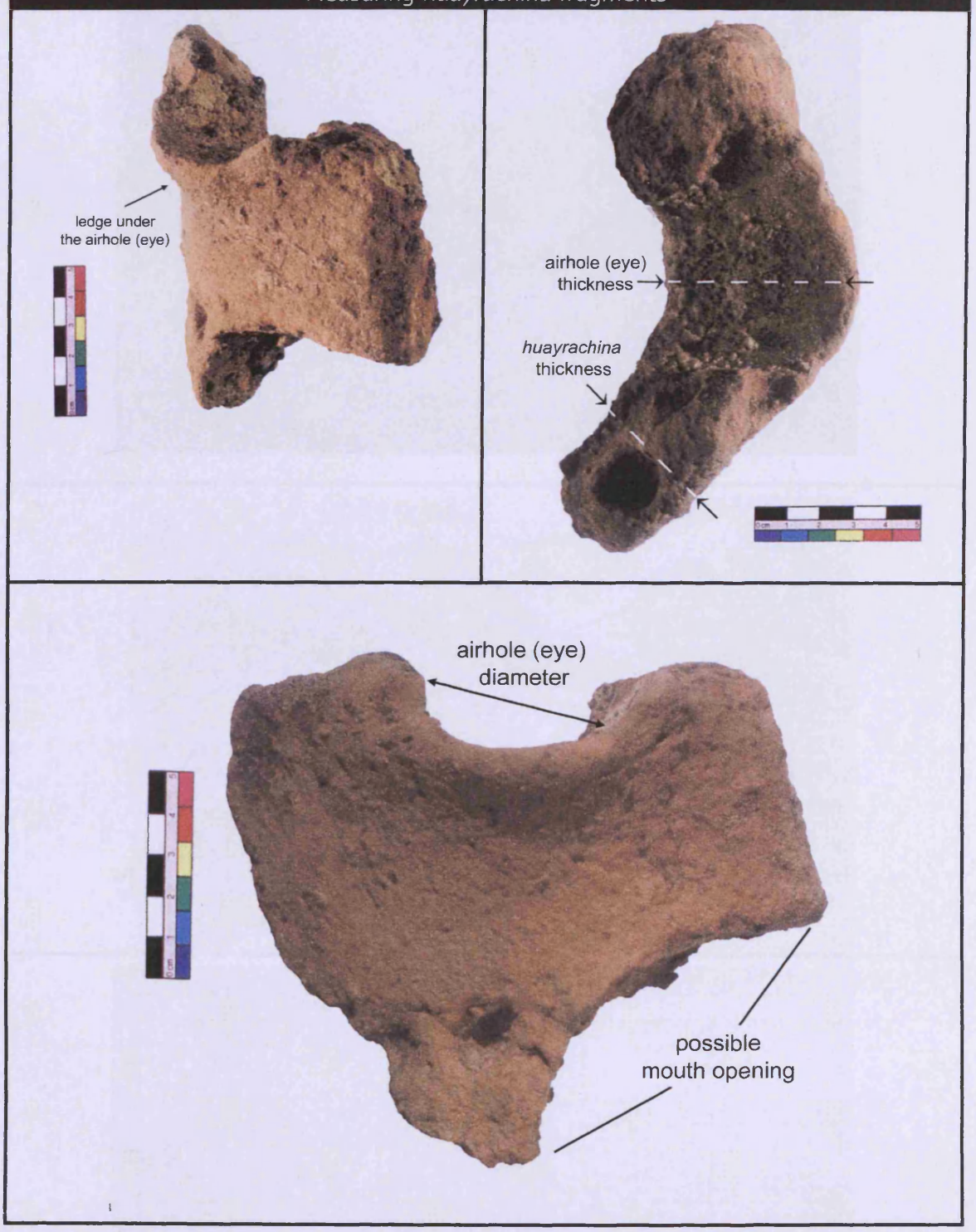

Huayrachina Alta (HuA1) Survey Block A

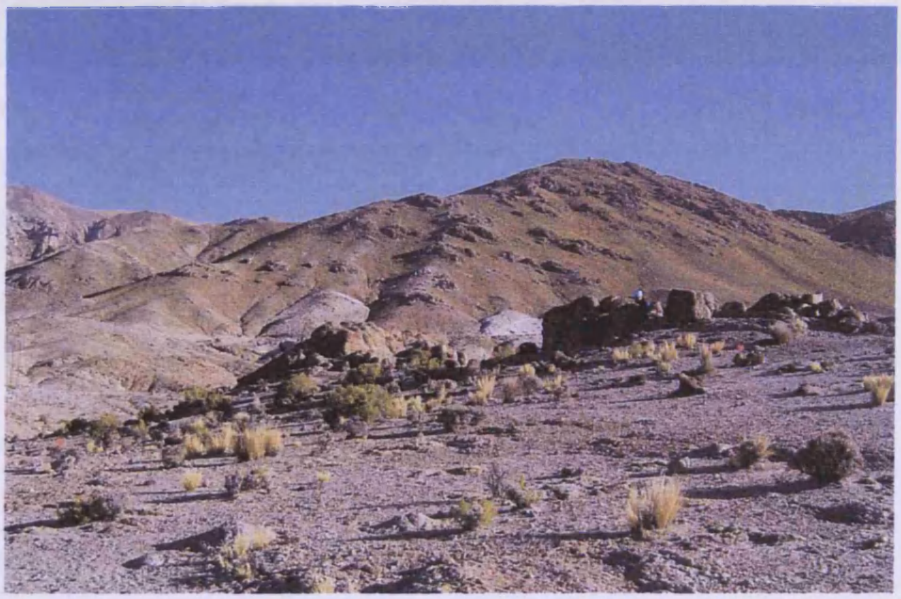

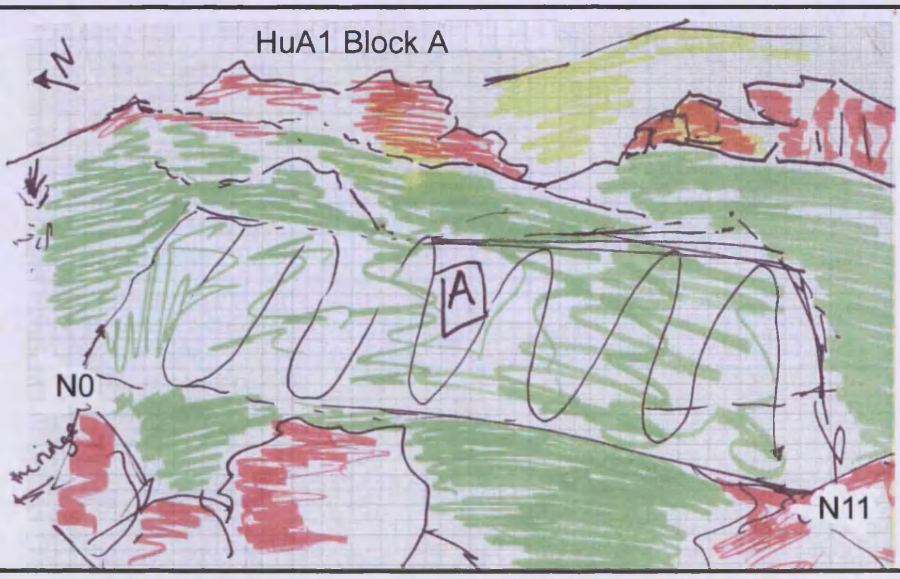

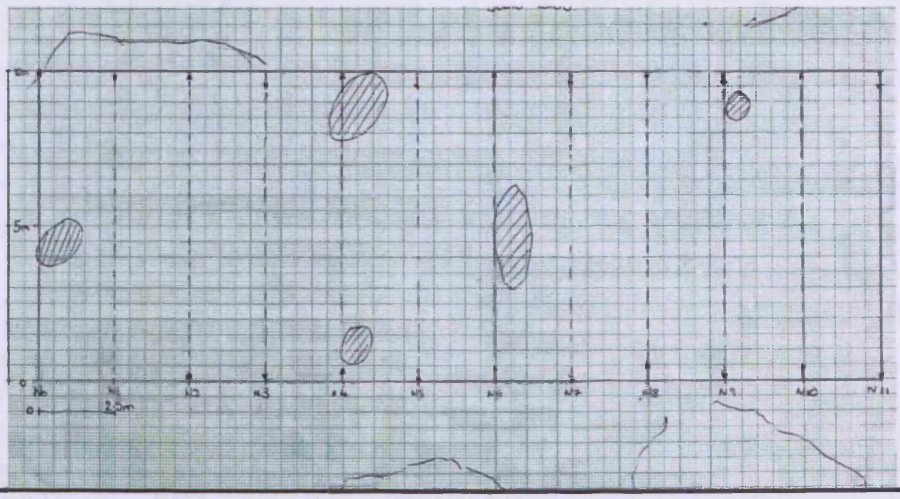

HuA1 Block A - results of the survey

NE	Location	Description	*Huayrachina* thickness(cm)	Eye thickness (cm)	Eye diameter (cm)	Number of layers	Notes
1	N0	*Huayrachina* fragement	1.8	~	~	poss. 2	Thick slag - 1.6cm
2	N0	Quartz Fragment	~	~	~	~	~
3	N0	Glazed pottery - colonial	~	~	~	~	~
4	N1	Possible top fragement of a *huayrachina*, thick white slag	3.0	~	~	1.0	~
5	N1	Large *huayrachina* fragment	3.5	c. 5	5.0	1.0	Slag layer is thin and creamy green in colour
6	N1	*Huayrachina* fragment	3.2-4	~	~	1.0	Slag layer 0.85 cm
7	N1	*Huayrachina* fragment	1.8	~	~	1.0	Thin slag layer 0.3 cm
8	N1	Ceramic with lead silicate	~	~	~	~	~
9	N2	Lots of fine black coated ceramics	~	~	~	~	~
10	N2	*Huayrachina* fragment with eye hole	1.4	1.5	3.7	1.0	Slag layer is light grey 6 cm thick
11	N3	*Huayrachina* fragment with eye hole	3.1	3.2	4.0	1.0	Thin slag layer
12	N3	This transect has lots of ceramic sherds and glassware	~	~	~	~	~
13	N3	Fine grain ceramic black on the inside , possible lead oxide and lumps of slag	~	~	~	~	~
14	N3	*Huayrachina* fragment	2.8	~	~	1.0	Slag layer 3.3 cm
15	N4	*Huayrachina* fragment with two eyes	3.9	3.7	3.7	1.0	Slag layer 1.7 cm
16	N5	Large *huayrachina* fragment possible top	2.5	~	~	1.0	Slag layer 0.8 cm
17	N5	Small *huayrachina* fragment with eye	2.8	2.8	?	1.0	heavily eroded ceramic, slag layer 0.4-0.5cm
18	N5	Very large slag piece	2.0	~	~	~	height = 2.8 cm

NE	Location	Description	*Huayrachina* thickness(cm)	Eye thickness (cm)	Eye diameter (cm)	Number of layers	Notes
19	N5	Small *huayrachina* fragment with eye	2.0	2.0	?	~	~
20	N6	*Huayrachina* fragment with eye	3.5	3.5	4.0	1.0	extremely thin slag
21	N6	*Huayrachina* fragment with two layers	2.5	~	~	2.0	Slay layer 1 cm
22	N6	Ceramic poss. crucible with a layer of slag adherred	~	~	~	~	~
23	N6	Lead silicate coated ceramic crucible	~	~	~	~	Sample taken for analysis
24	N6	*Huayrachina* fragment with two layers	3.4	~	~	2.0	Slay layer 0.5 cm
25	N6	Possible top fragment of a *huayrachina*	2.5	c.3	~	1.0	~
26	N7	very dispersed areas of *huayrachina* fragments, hard to indentify	~	~	~	~	~
27	N7	Chunky *huayrachina* fragment with two eyes	3.3	4-4.5	?	1.0	Thin yellow-gray slag
28	N7	fine grained ceramic with black blobs and yellow lead silicate adherred	~	~	~	~	Sample taken for analysis
29	N7	*Huayrachina* fragment	2.2	~	~	1.0	Ceramic heavily eroded
30	N7	*Huayrachina* fragment with eyes	3.5	4.0	?	1.0	Slag layer 0.7 cm, thick, black slag
31	N7	Potential mouth	~	~	~	1.0	Depth 3 cm
32	N7	*Huayrachina* fragment	~	~	~	~	~
33	N7	Ceramic with lead oxide	~	~	~	~	~
34	N7	*Huayrachina* fragment with two eyes	3.0	3.9 and 4.5	c. 4	1.0	~
35	N7	*Huayrachina* fragment with eyes	4.5	3.0	~	1.0	Thin gray slag
36	N8	*Huayrachina* fragment with eye	2.5	3.0	c.4	1.0	Heavy black slag
37	N8	Large *huayrachina* fragment	4.0	~	~	1.0	Slag 1 cm
38	N8	Mouth fragment	4.0	~	~	1.0	Slay layer 0.8 cm

NE	Location	Description	*Huayrachina* thickness(cm)	Eye thickness (cm)	Eye diameter (cm)	Number of layers	Notes
39	N9	*Huayrachina* fragment with eyes	1.7	3.0	?	1.0	White slag
40	N9	*Huayrachina* fragment	2.4	~	~	1.0	~
41	N9	Ceramic with slag adherred	~	~	~	~	Sample taken for analysis
42	N10	*Huayrachina* fragment with two eyes	~	3 and 4	4.5	1.0	Slag grainy and not very vitreous
43	N11	Poss. mouth	4.0	~	~	1.0	~

	Huayrachina width (cm)	Eye width (cm)	Eye diameter (cm)	Number of layers
Total number finds measured	28	15	8	28
Average	2.9	3.3	4.1	1
Min	1.4	1.5	3.7	1
Max	4.5	5.0	5.0	2

HuA1 Survey Block B

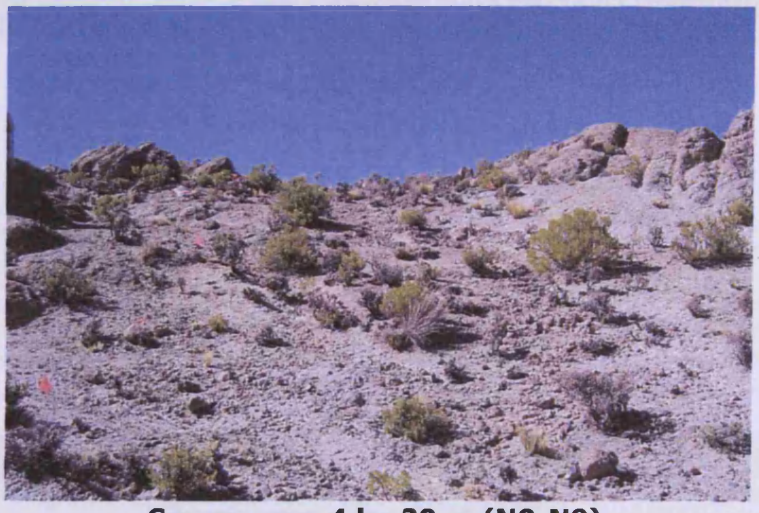

Survey area 4 by 20 m (N0-N9)

HuA1 Block B - results of the survey

NE	Location	Description	*Huayrachina* thickness(cm)	Eye thickness (cm)	Eye diameter (cm)	Number of layers	Notes
1	N0	*Huayrachina* fragement with eyes, thin layer of black slag	~	2.3	~	1.0	Slag layer very thin, but the eye have on the outer side shelves, ledges
2	N0	Ceramic material in association	~	~	~	~	Red eathenware with handles
3	N1	*Huayrachina* fragement with eyes, thin layer of purple/green slag	2.5	4.0	4.0	1.0	Eyes holes have ledges
4	N1	Fine grained crucible fragment with slag adherred, poss. Lead oxide on the outer side	~	~	~	~	~
5	N1	*Huayrachina* fragment with two layers	4.0	~	~	2.0	Slag layer c. 2 cm
6	N2	Thick crucible fragment with lead metal inside	~	~	~	~	Samples taken for analysis
7	N3	Thick crucible fragment with lead silicate inside	~	~	~	~	~
8	N4	*Huayrachina* fragment	~	~	~	~	No distinguishing features

NE	Location	Description	*Huayrachina* thickness(cm)	Eye thickness (cm)	Eye diameter (cm)	Number of layers	Notes
9	N4	*Huayrachina* fragment with 1 eye maybe 2	~	4.0	4.0	1.0	External side very flat
10	N5	*Huayrachina* fragment witheye or opening	4.0	4.0	7?	1.0	One flat side
11	N5	Crucible fragment 2cm thick with lead oxide coating	~	~	~	~	Sample taken for analysis

	Huayrachina thickness(cm)	Eye thickness (cm)	Eye diameter (cm)	Number of layers
Total number finds measured	**4**	**3**	**3**	**5**
Average	3.3	3.4	4.0	1
Min	2.5	2.3	4.0	1
Max	4.0	4.0	4.0	1
2 layers (excluded from averages and min/max)	4.0	~	~	2

UR WS Survey

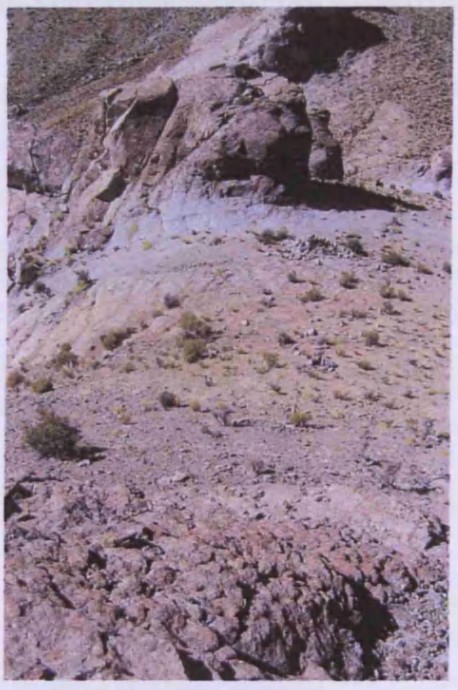

UR WS - results of the survey

NE	Images	Description	*Huayrachina* thcikness (cm)	Eye thickness (cm)	Eye diameter (cm)	Number of layers	Notes
1		*Huayrachina* fragement with two eyes, dense black slag	2.6	4	4 -5cm	1	~
2		*Huayrachina* fragment with two eyes holes, main body not intacted	~	2.6	4 -5cm	1	~
3	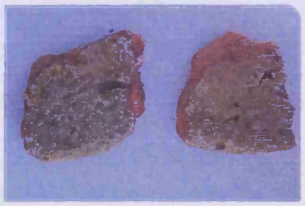	Poss. top fragment	2.7	~	~	1	Vitrified with green lead oxide glaze, drawings taken
4	~	*Huayrachina* fragement with eye, ceramic eroded	2.6	2	5	1	Heavy black slag
5		*Huayrachina* fragment with three layers	4-5.5			3	~
6	~	*Huayrachina* fragment with eye, ceramic eroded	2.3	3.3	?	1	Slag layer 0.8 cm
7	~	*Huayrachina* fragment with eyes badly eroded		2			Severe erosion

	Huayrachina thcikness (cm)	Eye thickness (cm)	Eye diameter (cm)	Number of layers
Total number finds measured	5	5	3	6
Average	2.5	2.8	5.0	1
Min	2.3	2.0	5.0	1
Max	2.7	4.0	5.0	1
2 layer	5	~	~	3

Analysis of the average thickness of *huayrachina* fragments

Huayrachina thickness (cm)	Frequency		
	Block A	Block B	URWS
1.0-1.9	4	~	~
2.0-2.9	10	1	4
3.0-3.9	12	3	~
4.0-4.9	2	~	1
Sum	**28**	**4**	**5**

Comparative work between the dimensions of the ethnographic and archaeological *huayrachinas*

Sample measured	Eye diameter (cm)	Eye thickness (cm)	Notes
1	2.5	3.0	Samples showed evidence for erosion
2	3.0	3.0	
3	3.0	2.5	~
4	3.0	2.5	~
5	3.0	3.0	~
6	3.0	2.0	~
Average surveyed *huayrachinas*	**2.9**	**2.7**	~
Cuiza's intact *huayrachina*	**2.0**	**7.0**	**Upper row of eyes**
	2.0	**10.0**	**Lower row of eyes**

Dimensions of survey ethnographic *huayrachina* eyes (samples 1-6) and the measurements of Cuiza's intact *huayrachina*.

Sample measured	Eye diameter (cm)	Eye thickness (cm)	Notes
Surveyed ethnographic *huayrachinas* average	2.9	2.7	~
Cuiza's intact *huayrachina*	2.0	7.0	Upper row of eyes
	2.0	10.0	Lower row of eyes
HuA1 Block A average	4.2	3.6	~
HuA1 Block B average	3.6	2.7	~
UR WS average	5.0	2.8	~

A comparison of the diameter and width of *huayrachina* eyes from archaeological and ethnographic context. The eyes measured on the intact (ethnographic) *huayrachina* appear to have been partially sealed during the smelt.

Analysis of the average thickness of *huayrachina* fragments

Huayrachina thickness (cm)	Frequency		
	Block A	Block B	URWS
1.0-1.9	4	~	~
2.0-2.9	10	1	4
3.0-3.9	12	3	~
4.0-4.9	2	~	1
Sum	**28**	**4**	**5**

Comparative work between the dimensions of the ethnographic and archaeological *huayrachinas*

Sample measured	Eye diameter (cm)	Eye thickness (cm)	Notes
1	2.5	3.0	Samples showed evidence for erosion
2	3.0	3.0	
3	3.0	2.5	~
4	3.0	2.5	~
5	3.0	3.0	~
6	3.0	2.0	~
Average surveyed *huayrachinas*	**2.9**	**2.7**	~
Cuiza's intact *huayrachina*	**2.0**	**7.0**	**Upper row of eyes**
	2.0	**10.0**	**Lower row of eyes**

Dimensions of survey ethnographic *huayrachina* eyes (samples 1-6) and the measurements of Cuiza's intact *huayrachina*.

Sample measured	Eye diameter (cm)	Eye thickness (cm)	Notes
Surveyed ethnographic *huayrachinas* average	2.9	2.7	~
Cuiza's intact *huayrachina*	2.0	7.0	Upper row of eyes
	2.0	10.0	Lower row of eyes
HuA1 Block A average	4.2	3.6	~
HuA1 Block B average	3.6	2.7	~
UR WS average	5.0	2.8	~

A comparison of the diameter and width of *huayrachina* eyes from archaeological and ethnographic context. The eyes measured on the intact (ethnographic) *huayrachina* appear to have been partially sealed during the smelt.

APPENDIX V – ARCHAEOLOGICAL *HUAYRACHINAS* SITES AND SAMPLES

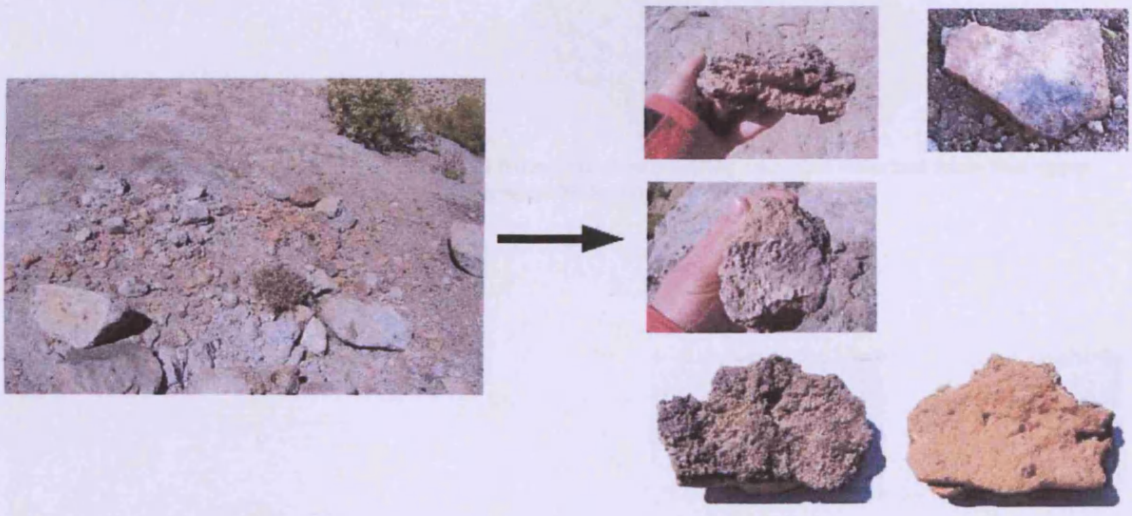

Typical archaeological *huayrachina* sit debris.

CRUZ PAMPA SURFACE (CP)

The two surface hand specimens collection from Cruz Pampa. Slag samples selected from the upper furnace fragment.

CP sample 344A

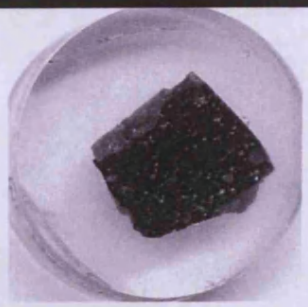

a.

A black slag adhered to a *huayrachina* furnace wall.

a. The mounted and polished sample 344A.

b, c, d and e. The sample contained visible metallic prills trapped inside the slag matrix. Different mineral phases were such as leucite, pyroxenes were identified.

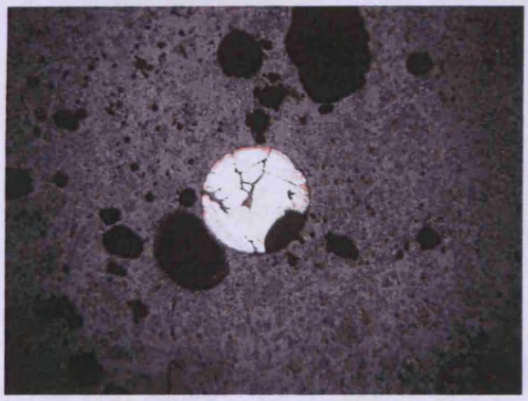

a.

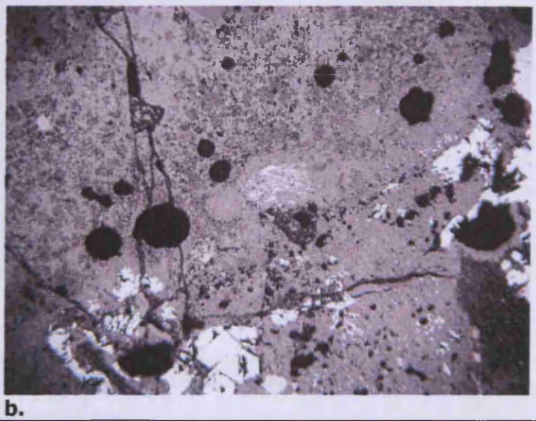

b.

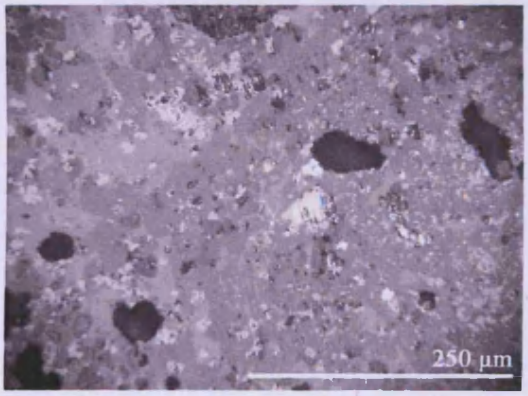

c.

d.

SEM-EDS images and data

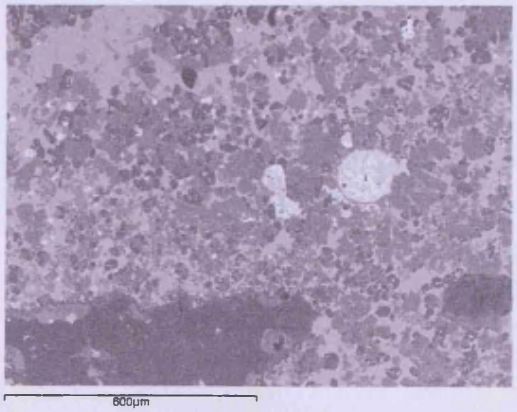

The slag is extremely heterogeneous with different metallic and oxidic inclusions.

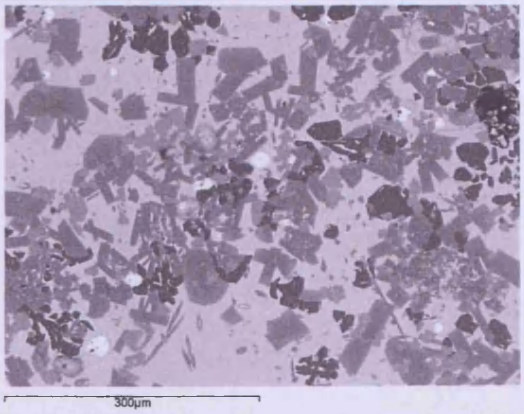

Leucite (dark grey), pyroxene (mid grey) and the glassy matrix (light grey) make up the majority of the slag composition.

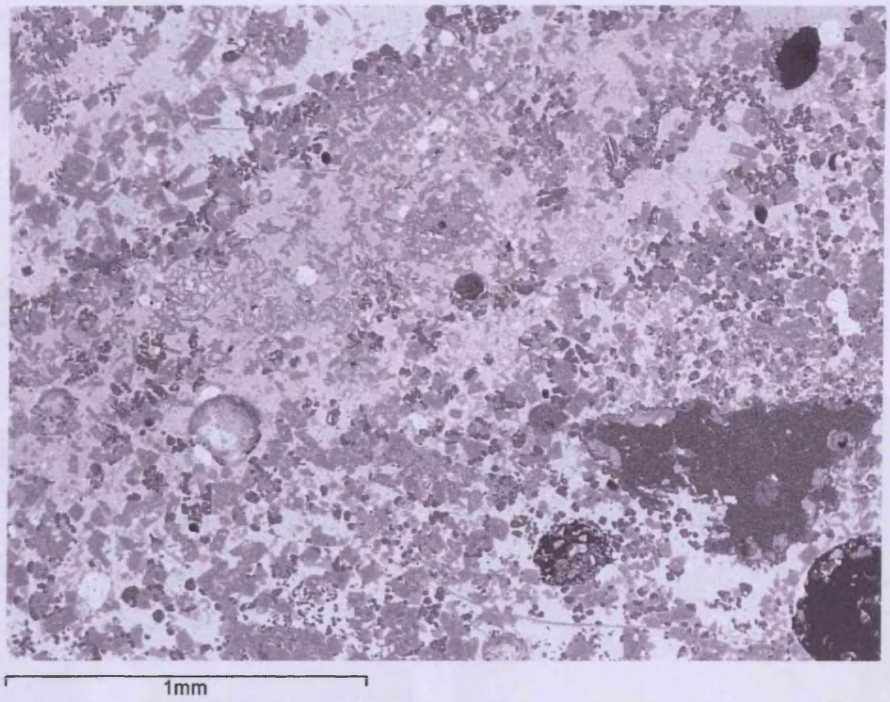

Sample	MgO	Al2O3	SiO2	P2O5	K2O	CaO	TiO2	FeO	ZnO	PbO
CP 344A (n=1)	1.9	5.4	32.3	2.0	3.3	12.4	0.9	10.8	9.3	21.7

SEM-EDS bulk area scan of sample 344A. The data has been normalised to 100 wt%.

CP sample 344B

Another section of slag from a *huayrachina* wall fragment.

a. The mounted and polished sample 344B.

b. A typical OM image from sample 344B.

c. A high magnification of a pure silver prill in sample 344B.

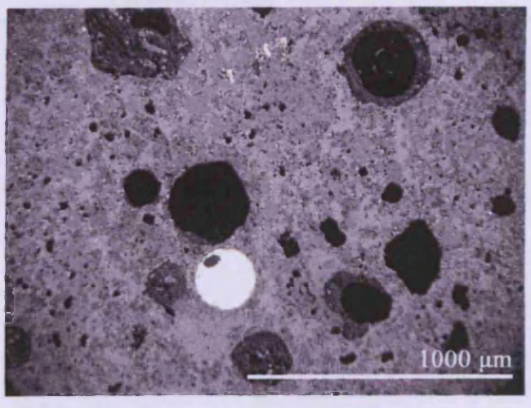

b.

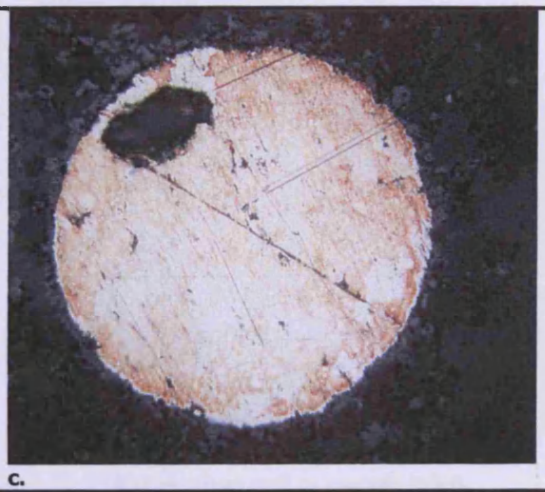

c.

SEM-EDS images and data

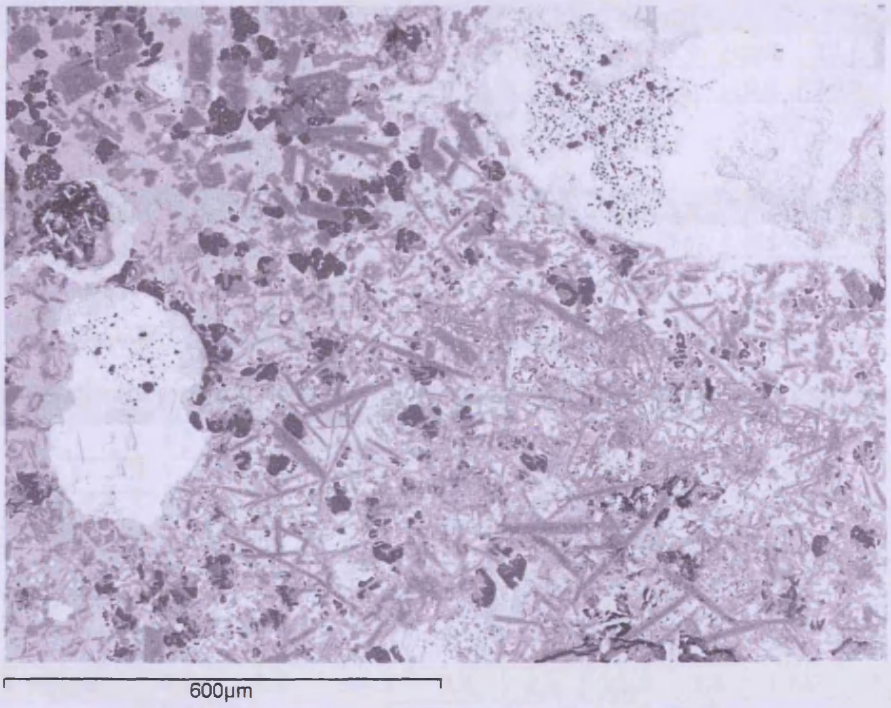

SEM-EDS image of the general slag matrix, metallic prills, leucite (dark black phase), pyroxenes (long angular grey phases) and the slag glassy matrix.

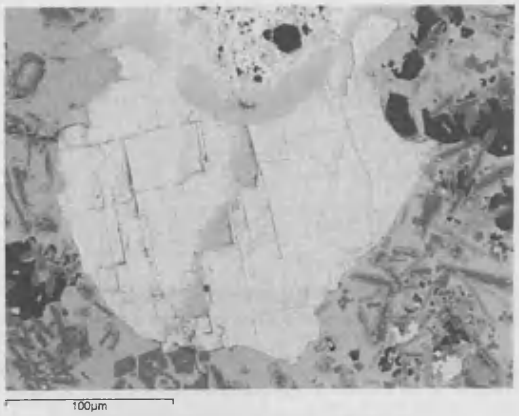

Partially reacted lead sulphide.

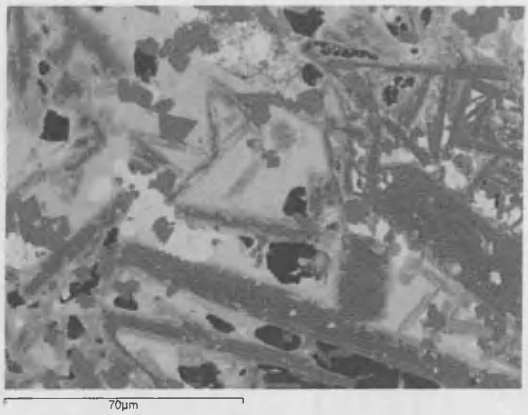

Pyroxenes, leucite and the glassy slag matrix.

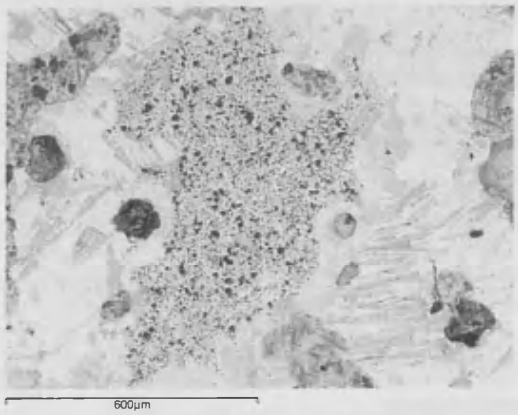

Lead metal in lead sulphide.

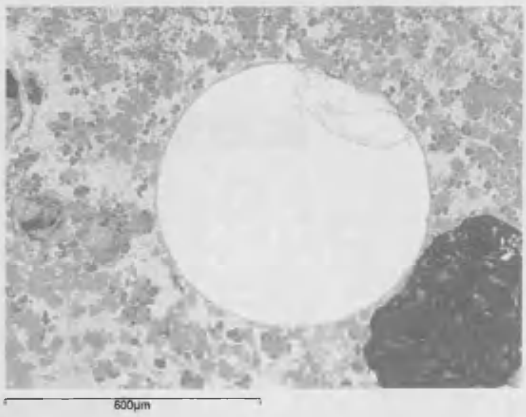

A pure silver prill in sample 344B.

Scanned area	MgO	Al2O3	SiO2	P2O5	K2O	CaO	TiO2	FeO	ZnO	PbO
1	3.2	~	33.9	2.5	3.9	14.0	0.9	10.6	12.1	18.9
2	1.7	3.1	25.2	2.1	1.8	11.7	1.2	9.4	10.6	33.2

SEM-EDS bulk area scans of sample 344B.
The data has been normalised to 100 wt%.

Scanned area	MgO	Al2O3	SiO2	P2O5	K2O	CaO	TiO2	FeO	ZnO	PbO
1	1.3	1.9	28.9	~	1.6	1.7	~	6.4	11.0	47.3
2	1.4	1.9	28.9	1.1	1.5	2.3	1.0	9.3	8.8	43.9
3	~	1.8	18.7	~	~	~	1.1	4.4	2.4	64.3

SEM-EDS area analyses of the glassy slag matrix of CP sample 344B.

Spectrum	MgO	Al2O3	SiO2	P2O5	K2O	CaO	FeO	ZnO	PbO
1	4.2	3.0	39.0	~	0.5	34.0	4.5	10.5	4.4
2	3.3	1.9	38.5	~	0.5	32.0	2.8	15.5	5.6
3	3.1	1.3	39.0	~	0.4	32.7	3.0	15.6	4.9
4	4.5	1.9	40.7	~	0.4	34.9	3.8	12.1	1.9
5	2.8	2.0	38.1	0.7	0.6	30.8	2.7	15.6	6.7
6	6.5	2.1	36.2	~	~	29.4	~	9.3	16.5
7	5.7	1.3	36.8	~	~	29.6	0.9	12.1	13.7
Average	**4.3**	**1.9**	**38.3**	**0.1**	**0.3**	**31.9**	**2.5**	**13.0**	**7.7**

SEM-EDS area analyses of pyroxenes in sample 344B.
The data has been normalised to 100 wt%.

Spectrum	Al2O3	SiO2	K2O	FeO	PbO
1	20.7	57.0	21.1	1.2	~
2	19.9	56.3	21.3	1.6	0.9
3	20.5	56.0	21.1	1.1	1.3

SEM-EDS analyses of leucite in sample 344B.
The data has been normalised to 100 wt%.

Scanned area	MgO	Al2O3	SiO2	CaO	TiO2	FeO	ZnO	SnO	PbO
1	3.6	5.8	~	~	3.6	44.4	24.3	18.3	~
2	2.5	~	0.8	0.5	2.0	59.2	23.3	11.7	~
3	2.7	3.0	1.2		5.6	56.6	21.3	8.1	1.4
4	3.6	4.1	11.5	5.6	4.3	42.5	19.4	6.8	2.1
5	2.6	3.1	~	~	4.8	56.7	22.8	10.0	~

SEM-EDS area analyses of spinels in sample 344B.
The data has been normalised to 100 wt%.

Scanned area	Si	S	Fe	Cu	Ag	Sb	Pb
1	9.8	36.7	1.9	~	3.9	1.9	45.8
2	~	12.2	~	~	~	~	87.8
3	~	41.2	~	~	1.8	~	57.1
4	3.4	45.8	~	~	~	~	50.8
5	~	50.8	~	2.7	~	~	46.5

Areas of lead sulphide in sample 344B.
The data has been normalised to 100wt%.

Scanned area	Ag	Pb
Prill 1	95.9	4.1

SEM-EDS analysis of a silver prill in sample 344B.

Combined data for samples 344A and 344B

Sample	MgO	Al2O3	SiO2	P2O5	K2O	CaO	TiO2	FeO	ZnO	PbO
CP 344A (n=1)	1.9	5.4	32.3	2.0	3.3	12.4	0.9	10.8	9.3	21.7
CP 344B (n=2)	2.5	1.6	29.6	2.3	2.9	12.9	1.1	10.0	11.4	26.1

SEM-EDS bulk area analyses of CP samples. The data has been normalised to 100 wt%.

Sample	Na2O	Al2O3	SiO2	K2O	FeO	PbO
344 A	0.1	21.1	56.1	21.4	1.3	~
344 B	~	20.3	56.4	21.2	1.3	0.7

Leucite recorded in the slag samples CP surface. e data has been normalised to 100%.

Sample	MgO	Al2O3	SiO2	P2O5	K2O	CaO	FeO	ZnO	PbO
344A	3.3	1.3	38.8	~	0.5	31.7	2.6	15.9	6.0
344B	4.3	1.9	38.3	0.1	0.3	31.9	2.5	13.0	7.7

Pyroxenes analysed within the CP slag samples. Data has been normalised to 100%

Sample	MgO	Al2O3	SiO2	CaO	TiO2	FeO	ZnO	SnO2	PbO
344A	3.0	4.3	0.8	0.1	3.6	56.2	20.8	11.0	0.3
344B (n=5)	3.0	3.2	2.7	1.2	4.1	51.9	22.2	11.0	0.7

Spinels analysed in CP slag samples. Data has been normalised to 100%.

HUAYRACHINA ALTA (HUA1)

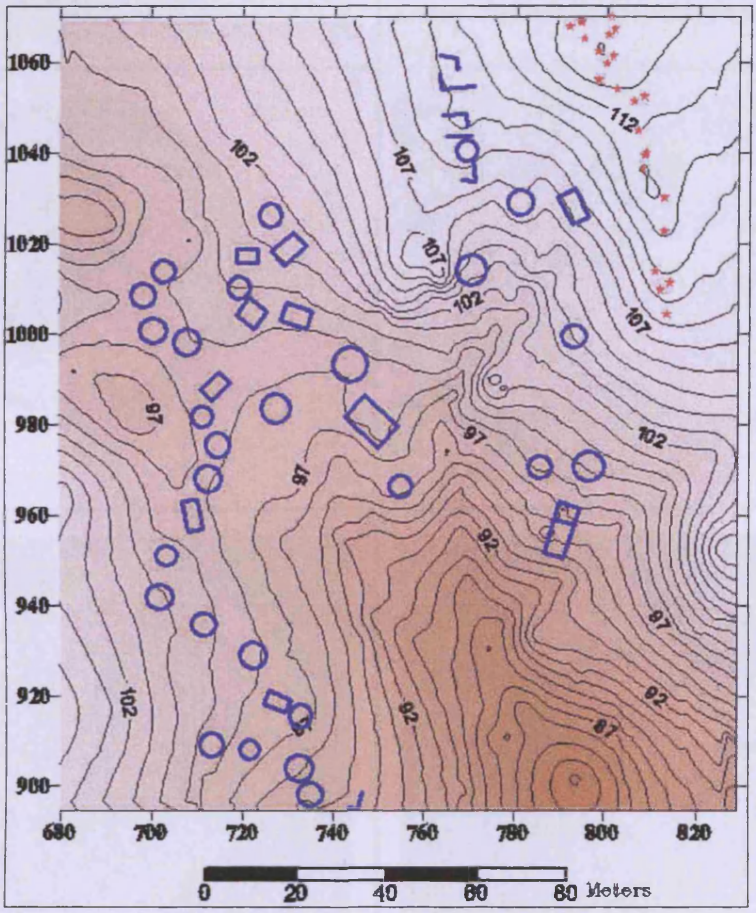

Inca circular and rectangular storage buildings (*qollqas*) are found on the archaeological site of Huayrachina. Huayrachina Alta (HuA1) is located on a ridge above Huayarchina. HuA1 has a large quantity of *huayarchina* remains.

HuA1 sample 26A

a.

Sample 26A is a huayrachina fragment that has a thick layer of black slag. The slag sample has large inclusions of quartz and metallic prills, clearly visable macroscopically (a and b). OM analysis showed a complex slag with different mineral inclusions and metallic prills (c, d and e).
SEM-EDS showed the slag consists of a lead silicate glassy matrix with mineral inclusions such asleucite, pyroxene, and different zinc and lead oxides . Metallic lead prills dominate the sample.

b.

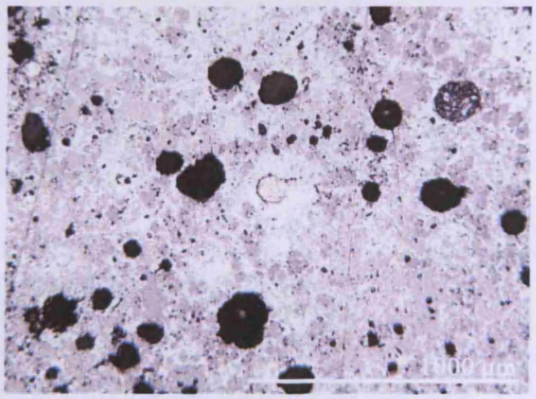

c.

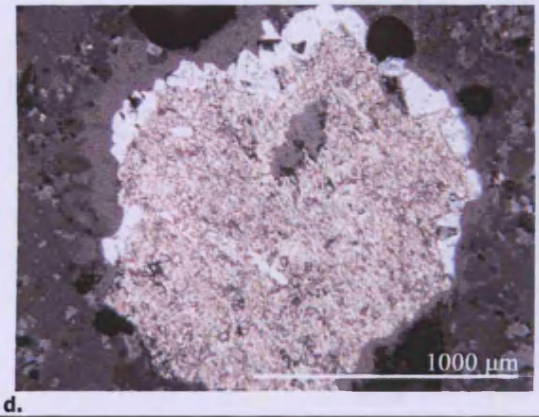

d.

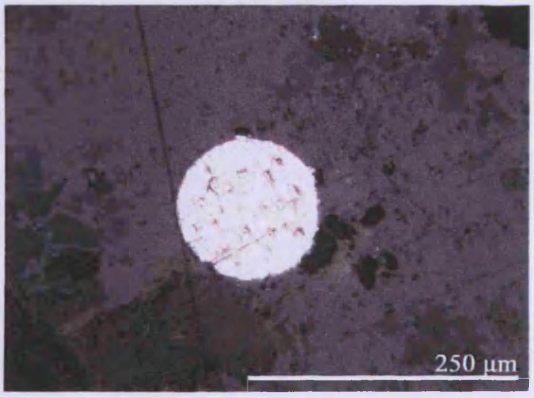

e.

SEM-EDS data and images

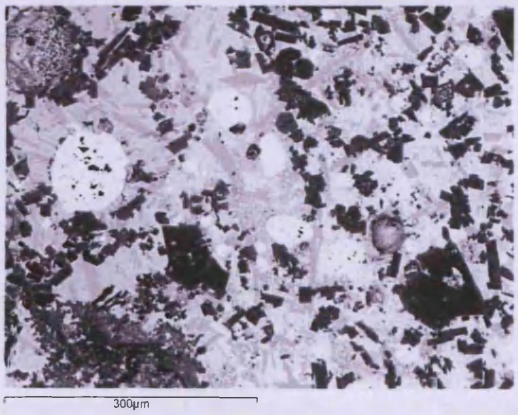

The complex slag structure

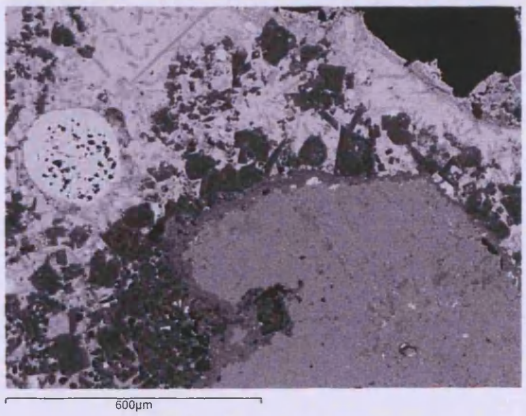

A large inclusions of tin oxide (grey)

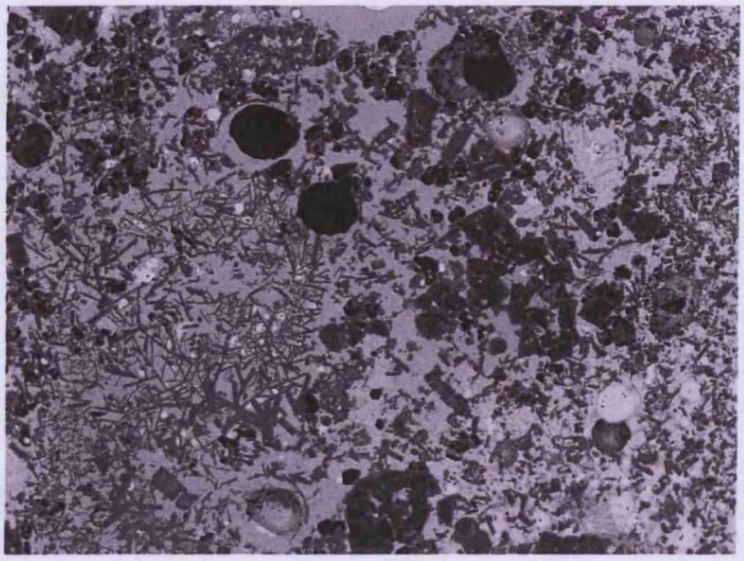

A typical image of sample 26.

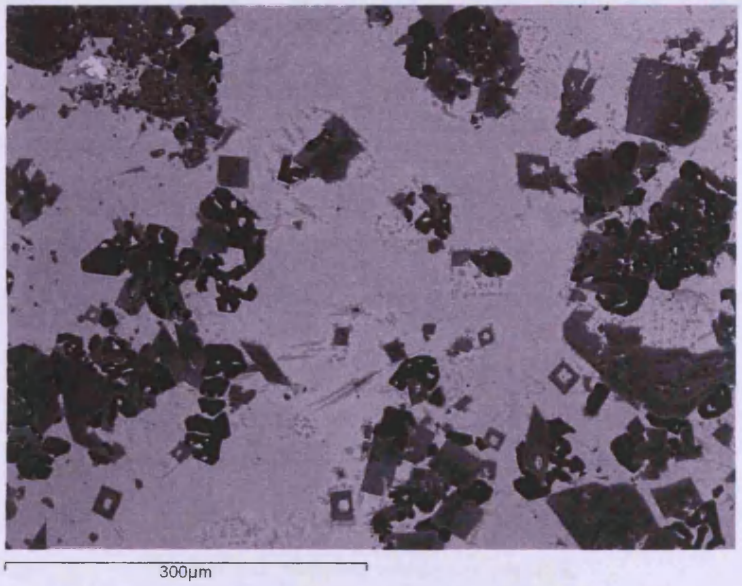

Leucites and pyroxenes in the glassy slag matrix.

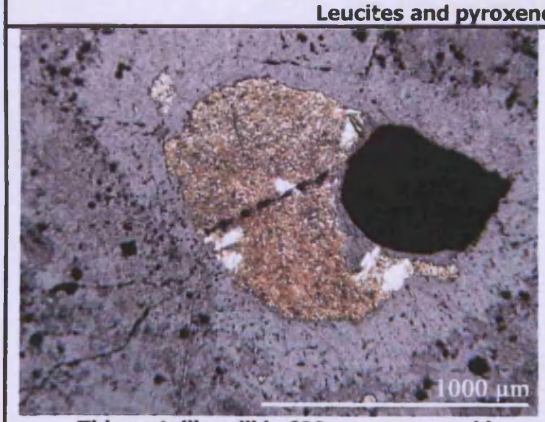

This metallic prill is 600um across and is predominetly lead metal studied with SiC crystals from the polishing process. However, there is a ring of residual ore around the prill.

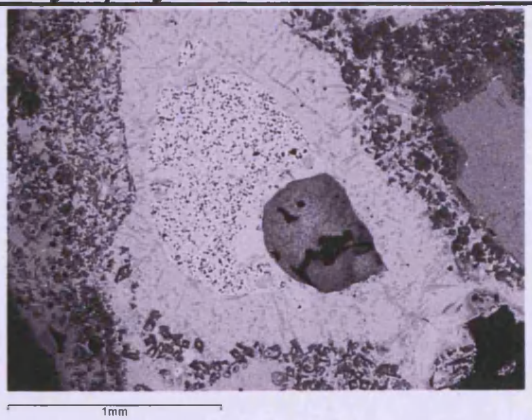

No bulk area scans were done

Scanned area	MgO	Al2O3	SiO2	P2O5	K2O	CaO	FeO	ZnO	As2O3	PbO
1	~	3.9	18.8	~	1.1	2.2	3.1	4.6	1.4	65.0
2	1.1	3.5	22.0	~	0.9	1.9	4.0	5.3	~	61.5
3	~	2.5	13.4	1.3	~	2.2	2.2	1.6	~	77.0
Average	**0.4**	**3.3**	**18.1**	**0.4**	**0.7**	**2.1**	**3.1**	**3.8**	**0.5**	**67.8**

Glassy matrix scanned area within sample 26A. The data has been normalised to 100 wt%.

Spectrum	Al2O3	SiO2	K2O	FeO
1	21.9	56.2	21.2	0.7
2	21.4	56.8	21.2	0.6
Average	**21.7**	**56.5**	**21.2**	**0.6**

Leucite in sample 26A. The data has been normalised to 100 wt%.

Scanned area	MgO	Al2O3	SiO2	P2O5	K2O	CaO	FeO	ZnO	PbO
1	3.2	2.2	38.1	~	~	30.3	1.0	16.1	9.3
2	2.6	2.1	35.3	2.7	~	30.5	1.5	13.6	11.7
3	2.6	2.3	37.9	~	0.4	29.9	3.1	17.5	6.3
Average	**2.8**	**2.2**	**37.1**	**0.9**	**0.1**	**30.2**	**1.9**	**15.7**	**9.1**

Pyroxenes in sample 26A. The data has been normalised to 100 wt%.

Spectrum	SiO2	FeO	ZnO	SnO	PbO
1	1.8	1.2	0.7	92.7	3.6

Tin oxide in sample 26A. The data has been normalised to 100 wt%. SI17

Spectrum	MgO	Al2O3	SiO2	CaO	FeO	ZnO	PbO
1	2.8	~	19.1	1.1	0.9	18.8	57.3
2	2.7	0.7	18.8	1.5	1.0	19.0	56.3

High zinc and lead oxides in sample 26A. The data has been normalised to 100 wt%.

Spectrum	Al	Si	Ag	Pb
1	0.8	8.0	4.9	86.4
2	~	~	3.8	96.2
3	~	4.8	4.0	91.2
4	~	14.7	1.5	83.8

Lead metal analysed within sample 26A.
The data has been normalised to 100 wt%.

HuA1 sample 26B

a.

A thick layer of black very vitereous slag attached to ceramic body. Macroscopically it is clear that this sample contains metallic phase, the optical mircsocopy confirms this. Large metallic lead islands sit surrounded by a multi-phase matrix. PbS prevelant in the sample.
The hand specimen had a large layer of slag adhered to the furnace wall (a). The cut surface of the sample showed large inclusions of lead sulphide and metallic prills (b).

The mounted block contained a section of the furnace wall seen in image c. The slag had a large quantity of partially reacted lead sulphide (d and e). Lead metal was also recorded during the OM analysis (brown area), image f.

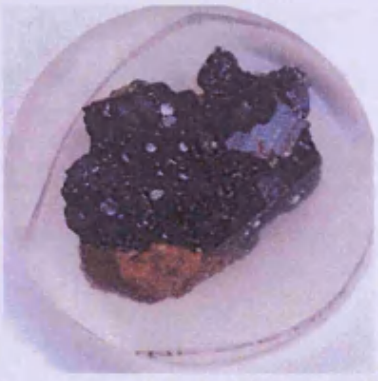

b.

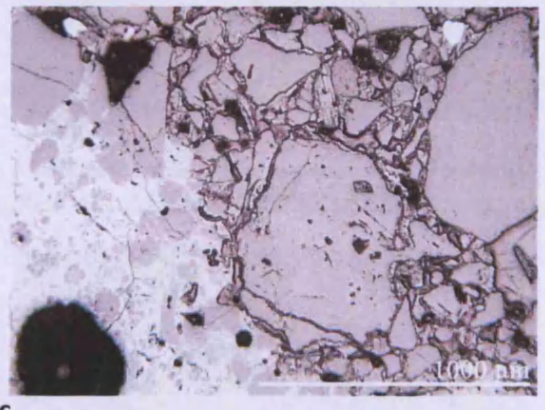

c.

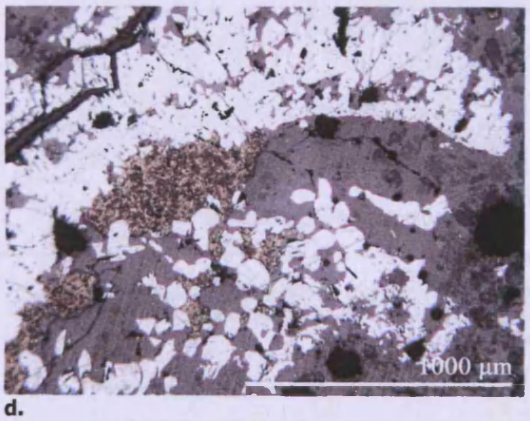

d.

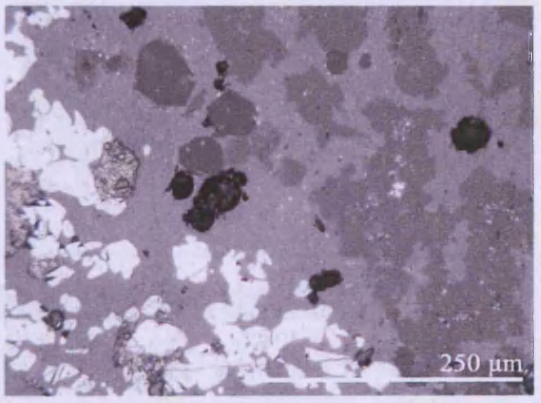

e.

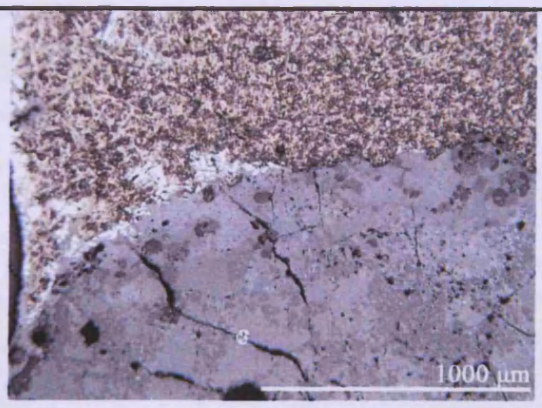

f.

SEM-EDS images and data

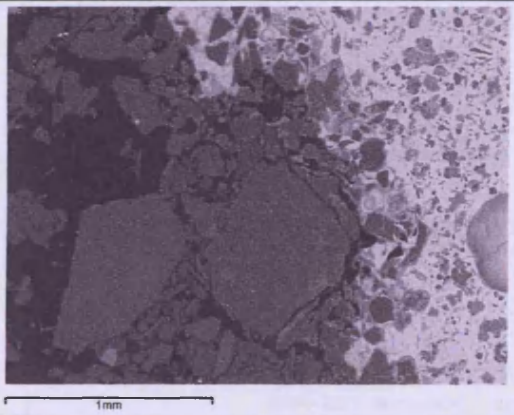

SEM image of the ceramic matrix, being dissolved by the lead oxide creating a lead silicate slag.

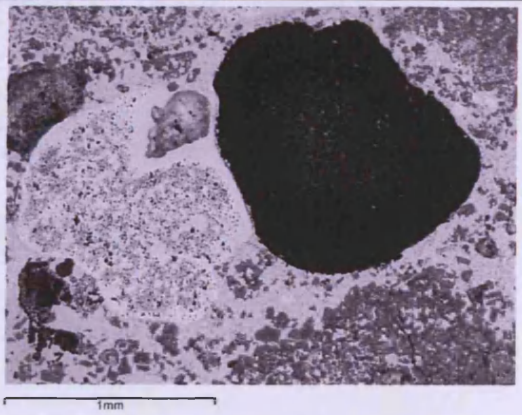

A lead prill surrounded by a halo of lead sulphide (white) in sample 26B.

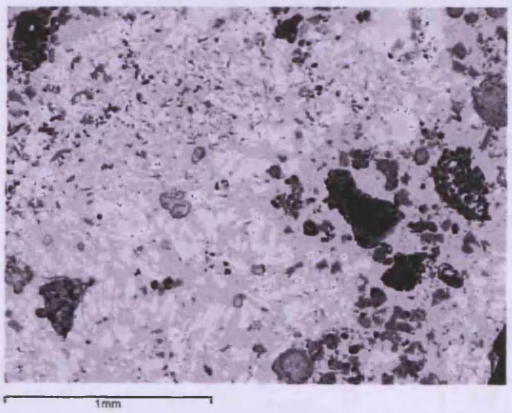

The lead slag with different phases: leucite and pyroxene.

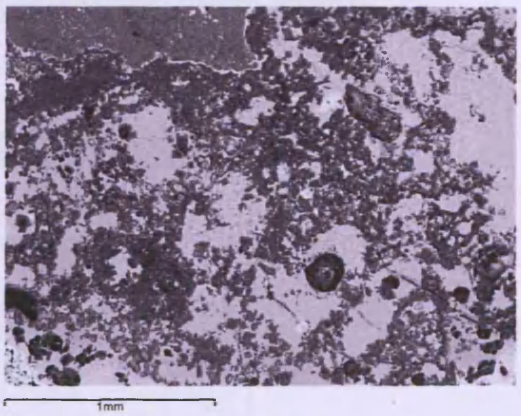

The lead slag.

Scanned area	MgO	Al2O3	SiO2	K2O	CaO	TiO2	FeO	ZnO	PbO
1	1.3	3.2	20.8	0.4	9.2	~	3.9	12.4	48.9
2	0.9	5.0	26.2	3.0	6.3	0.5	2.9	9.7	45.5
3	1.0	4.3	20.2	0.6	8.3	0.5	7.9	23.2	34.1
4	0.9	4.4	22.1	0.8	5.9	~	6.0	20.3	39.6
5	1.0	5.3	25.5	2.6	10.3	~	3.8	10.6	41.0
6	1.0	6.4	26.8	2.5	8.8	0.8	5.1	4.3	44.3
Average	**1.0**	**4.8**	**23.6**	**1.6**	**8.2**	**0.3**	**4.9**	**13.4**	**42.2**

SEM-EDS bulk area analyses of sample 26B.
The data has been normalised to 100 wt%.

Scanned area	MgO	Al2O3	SiO2	K2O	CaO	TiO2	FeO	ZnO	As2O3	PbO
1	~	2.8	19.0	1.6	1.9	~	3.5	10.7	~	60.6
2	~	4.0	19.9	1.4	2.4	0.6	4.0	5.6	0.8	61.5
3	0.7	3.3	19.6	1.4	2.1	~	3.6	7.5	~	61.9
4	~	2.9	15.5	0.7	1.5	~	2.9	7.0	0.6	69.0
5	0.7	3.6	19.5	1.1	1.9	~	3.6	6.3	0.8	62.6
6	~	3.5	20.9	1.1	1.8	~	3.1	7.6	1.8	60.2
Average	**0.2**	**3.3**	**19.0**	**1.2**	**1.9**	**0.1**	**3.4**	**7.4**	**0.7**	**62.6**

SEM-EDS area analyses of the glassy phase in sample 26B.
The data has been normalised to 100 wt%.

Scanned area	Na2O	Al2O3	SiO2	K2O	TiO2	FeO	ZnO	BaO	PbO
1	1.1	16.7	62.8	16.0	~	~	~	1.8	1.6
2	~	20.1	53.9	22.6	0.5	0.6	0.7	~	1.7
3	~	19.8	54.0	22.6	~	1.0	0.9	~	1.5
Average	**0.4**	**18.9**	**56.9**	**20.4**	**0.2**	**0.5**	**0.6**	**0.6**	**1.6**

SEM-EDS area analyses of leucite in sample 26B.
The data has been normalised to 100 wt%.

Scanned area	MgO	Al2O3	SiO2	K2O	CaO	FeO	ZnO	PbO
1	1.9	3.5	34.2	0.2	29.6	2.0	19.5	9.2
2	1.6	6.5	30.9	~	26.2	4.3	24.4	6.1
3	1.4	2.7	34.3	~	27.8	1.3	17.9	14.6
Average	**1.6**	**4.2**	**33.1**	**0.1**	**27.9**	**2.5**	**20.6**	**10.0**

SEM-EDS area analyses of pyroxenes in sample 26B.
The data has been normalised to 100 wt%.

Scanned area	Na2O	MgO	Al2O3	SiO2	K2O	CaO	FeO
1	2.0	0.6	14.9	72.3	6.5	1.3	2.4

SEM-EDS bulk area scans of ceramic body in sample 26B.
The data has been normalised to 100 wt%.

Spectrum	S	Fe	Zn	Pb
1	28.9	7.0	57.4	6.7

SEM-EDS analysis of zinc sulphide in sample 26B.
The data has been normalised to 100 wt%.

Area	Al	Si	Ca	Ag	Pb
1	1.2	7.2	0.7		90.9
2	2.8	11.9	0.4	1.0	84.0
3 LARGE AREA > 1MM	3.0	11.4	0.4	0.9	84.4
4	2.4	4.1			93.5
5	1.8	8.3	0.6	3.2	86.0
6		3.4		1.0	95.6

SEM-EDS analysis of lead metal in sample 26B.
The data has been normalised to 100 wt%.

HuA1 sample 26C

a.

A slag sample from multilayered *huayrachina* ceramic (a and b). Microscopically PbS phases are present in the sample, usually within metallic lead rich phases. The slag also contains a large piece of carbon, giving an indication of the possible fuel used in the furnace (c). The sample has some ceramic body atached (d) which shows interaction with lead oxide. Partially reacted ore (zinc and lead sulphide) and lead metal were also recorded (e, f and g).

b.

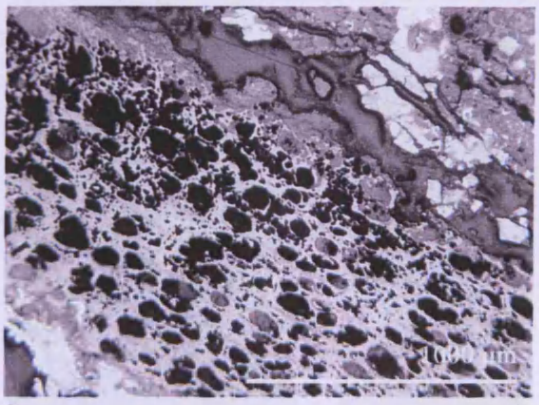

c

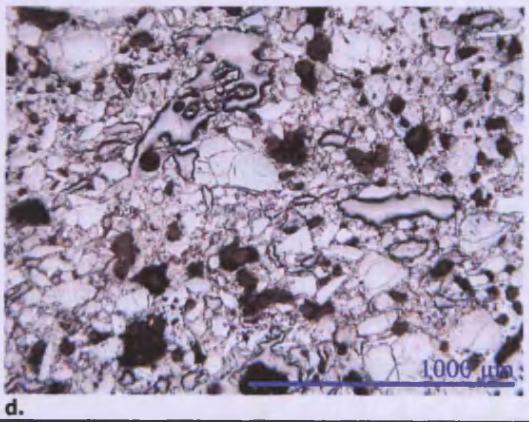

d.

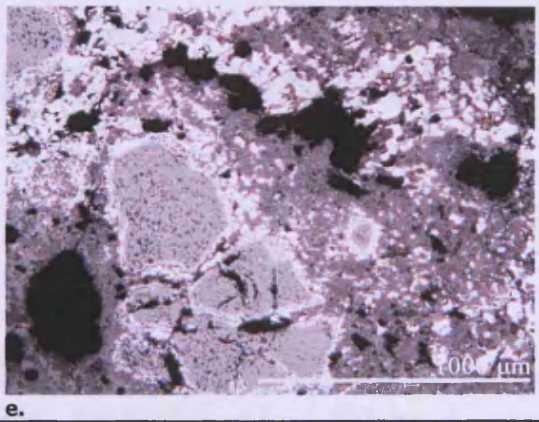

e.

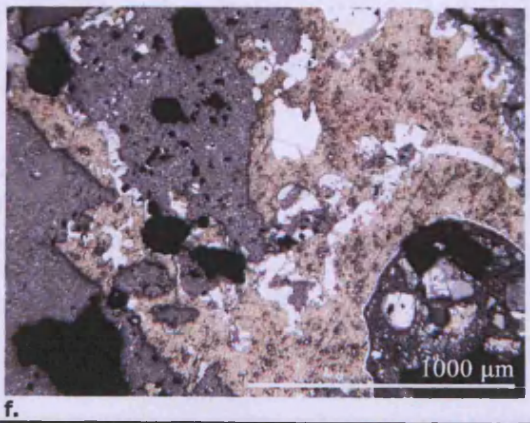

f.

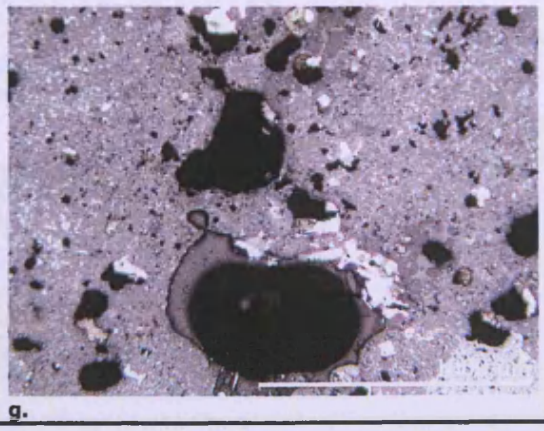

g.

SEM-EDS images and data

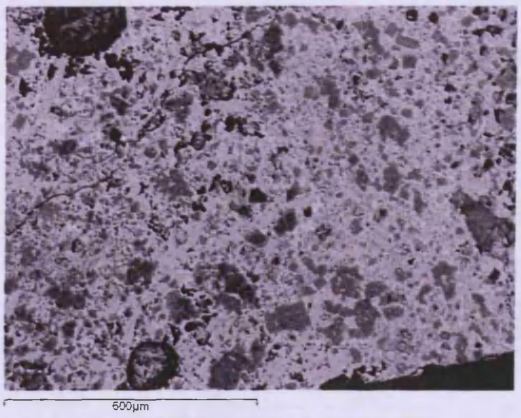

A typical SEM image of sample 26C.

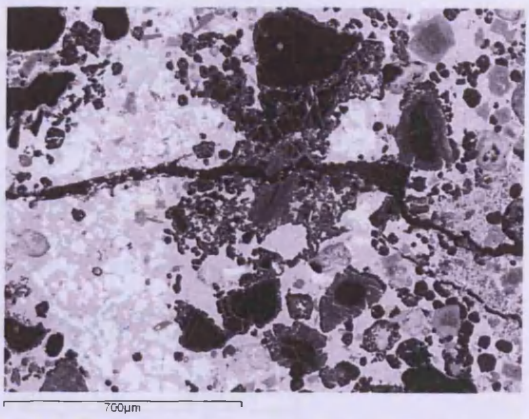

Interaction between pyroxenes and the lead oxide to form lead slag.

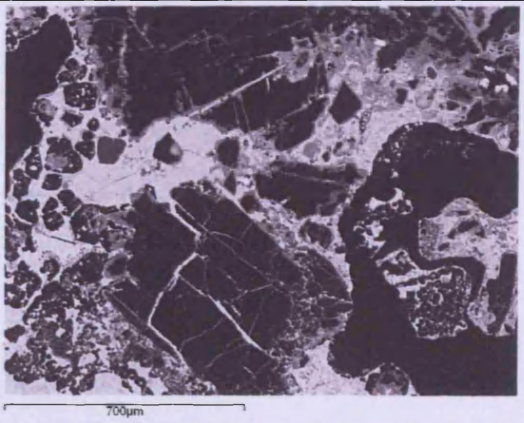

Ceramic dissolving into the lead silicate/lead oxide.

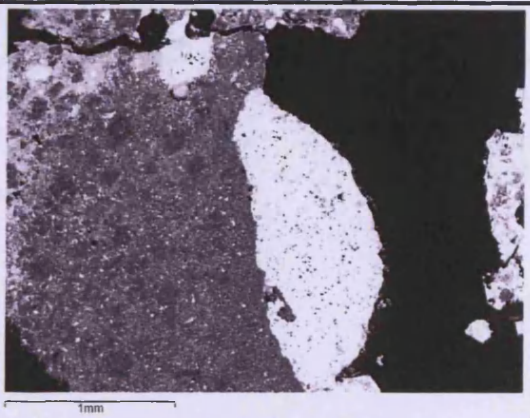

A large metallic prill inside the slag.

Scanned area	MgO	Al2O3	SiO2	SO3	K2O	CaO	FeO	ZnO	As2O3	PbO
1	2.1	5.0	27.3	~	1.9	15.8	10.1	25.1	2.2	10.6
2	0.9	10.3	29.6	4.4	7.0	1.6	2.0	6.4	~	37.9
3	~	3.6	19.6	~	1.2	8.4	3.4	12.9	5.0	46.0
4	~	6.2	17.4	~	1.2	7.2	4.0	17.8	3.9	42.2
Average (n=4)	**0.7**	**6.2**	**23.5**	**1.1**	**2.8**	**8.3**	**4.9**	**15.5**	**2.8**	**34.2**

SEM-EDS bulk area scans of sample 26C.
The data has been normalised to 100 wt%.

Scanned area	Al2O3	SiO2	CaO	FeO	ZnO	As2O3	PbO
1	4.2	19.7	1.5	2.0	6.6	2.9	63.1
2	3.3	21.8	1.2	2.6	5.1	4.5	61.6
Average (n=2)	**3.8**	**20.7**	**1.4**	**2.3**	**5.9**	**3.7**	**62.3**

SEM-EDS area analyses of the glassy matrix in sample 26C.
The data has been normalised to 100 wt%.

Scanned area	Na2O	Al2O3	SiO2	K2O	FeO
1	0.4	22.2	55.9	21.1	0.5
2	~	21.7	56.6	21.2	0.5
3	2.3	18.2	67.2	12.4	~
Average	**0.9**	**20.7**	**59.9**	**18.2**	**0.3**

SEM-EDS area analyses of leucite phases in sample 26C.
The data has been normalised to 100 wt%.

Spectrum	MgO	Al2O3	SiO2	K2O	CaO	FeO	ZnO	PbO
1	2.1	4.9	36.0	0.2	29.7	2.8	22.9	1.4
2	2.2	1.6	36.5	~	29.6	0.7	18.9	10.4
3	1.8	2.5	33.0	~	23.8	1.1	18.6	19.3
Average	**2.0**	**3.0**	**35.2**	**0.1**	**27.7**	**1.5**	**20.1**	**10.4**

SEM-EDS area analyses of pyroxenes in sample 26C.
The data has been normalised to 100 wt%.

Spectrum	S	Pb
SI2	14.5	85.5
SI3	13.6	86.4
SI4	14.4	85.6

Partially reacted lead sulphide.
The data has been normalised to 100 wt%.

HuA1 sample 27 and 27A

a. Sample 27

Two different samples taken from the same sample bag – same area collected. The slags are dark black with metallic and gangue inclusions.

Microscopically the sample contains metallic prills of lead metal. These prills are dispersed in a multi-phase siliceous matrix (a, b c and d). The optical microscopy shows27A has a similar texture to 27 but contains larger metallic inclusions.

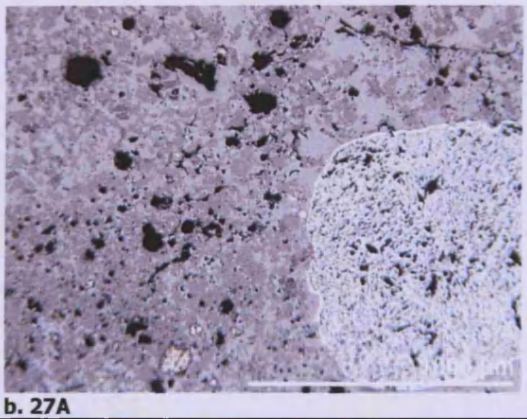

b. 27A

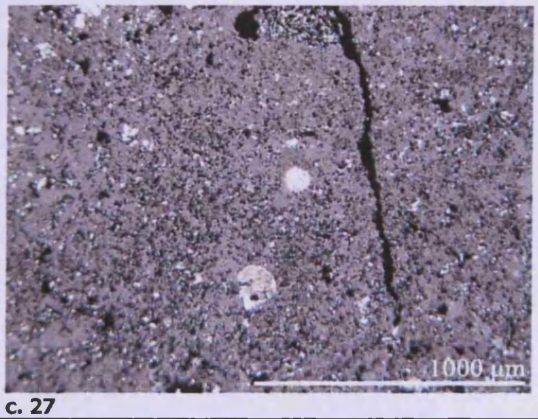

c. 27

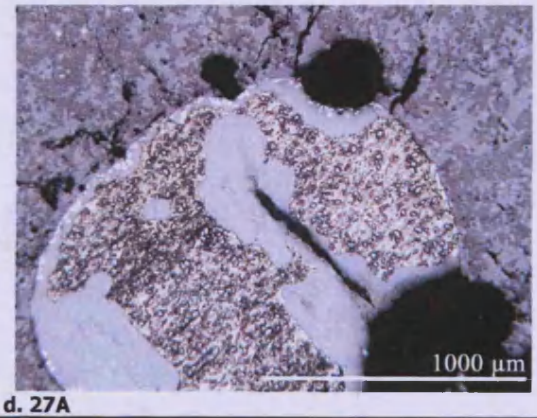

d. 27A

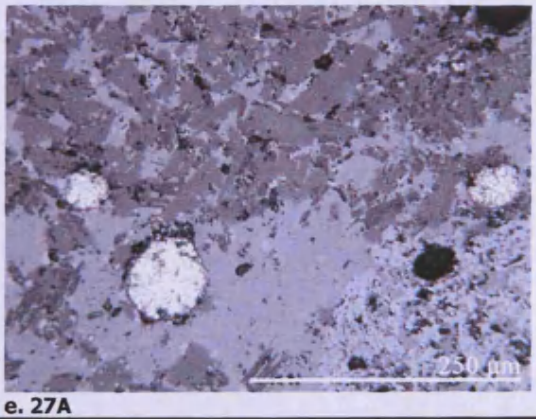

e. 27A

SEM-EDS images and data

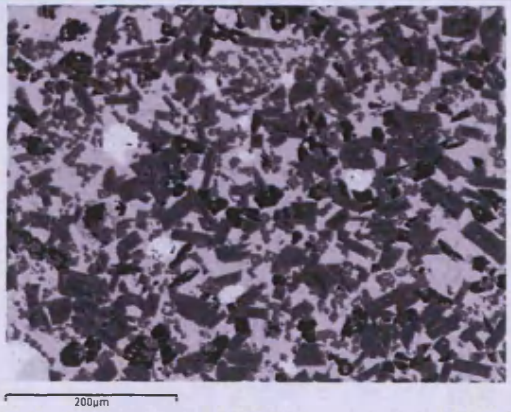

Sample 27A contains different phases: leucite (black), pyroxenes (mid grey angular crystals), glassy matrix (light grey), and metallic prills (white).

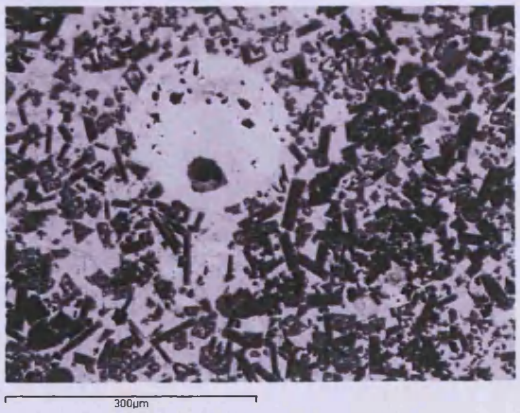

A pure lead prill analysed using SEM-EDS (sample 27A).

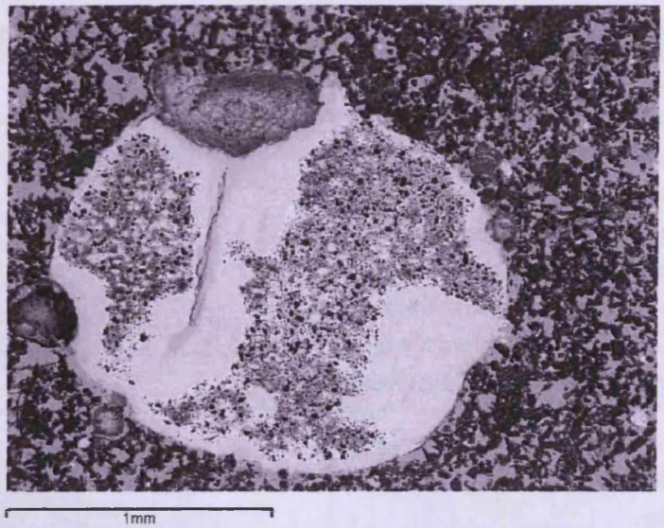

A large lead prill in sample 27A. No silver was recorded. White areas are lead sulphide.

Scanned area	MgO	Al2O3	SiO2	K2O	CaO	MnO	FeO	ZnO	PbO
1	1.7	5.0	25.2	3.4	15.1	0.5	10.6	12.3	26.2
2	1.6	4.4	18.9	2.0	8.5	0.5	17.8	11.0	35.3
3	1.3	5.8	25.6	4.6	13.2	~	6.5	8.7	34.3
4	1.8	6.0	19.2	2.4	8.8	0.6	18.5	12.6	30.1
Average (n=4)	**1.6**	**5.3**	**22.2**	**3.1**	**11.4**	**0.4**	**13.4**	**11.1**	**31.5**

SEM-EDS bulk area scans of sample 27A. The data has been normalised to 100 wt%.

Spectrum	Na2O	MgO	Al2O3	SiO2	K2O	CaO	FeO	ZnO	PbO
1	1.0	0.6	2.4	20.3	2.1	1.1	3.5	4.3	64.9
2	~	0.6	1.8	16.8	1.2	1.6	4.3	4.1	69.6
3	~	~	2.6	12.7	~	1.5	2.6	2.2	78.4
4	~	0.6	2.0	17.1	1.6	1.5	4.1	4.0	69.1
Average (n=4)	**0.2**	**0.4**	**2.2**	**16.7**	**1.2**	**1.4**	**3.6**	**3.6**	**70.5**

SEM-EDS area analyses of the glassy matrix.The data has been normalised to 100 wt%.

Scanned area	Na2O	Al2O3	SiO2	K2O	FeO	PbO
1	0.7	26.4	38.7	31.1	2.5	0.7

SEM-EDS analysis of leucite. The data has been normalised to 100 wt%.

Spectrum	S	Pb
1	13.8	86.2

SEM-EDS analysis of lead sulphide. The data has been normalised to 100 wt%.

Spectrum	S	Fe	Zn
1	31.7	4.2	64.1

SEM-EDS spot analysis of zinc sulphide in sample 27A. . The data has been normalised to 100 wt%.

Spectrum	Si	Ca	Fe	Pb
1	~	~	0.8	99.2
2	1.1	~	1.0	97.9
3	9.7	0.9	~	89.5
4	~	~	~	100.0
5	7.4	~	~	92.6
6	10.6	0.9	~	88.5
7	12.6	0.9	~	86.5
8	~	~	~	100.0

SEM-EDS area analysis of lead metal. The data has been normalised to 100 wt%.

HuA1 sample 29

a.

A multilayed huayrachina fragment, three distinct areas of the sample. The slaggy top layer (inside of the furnace), interaction layer between the ceramic and slag creating a lead oxide phase, and the remaining ceramic body (a and b). Optical microscopy reveals the large number of metallic lead prills trapped within the slag (c, d and e). These show some interesting red phase inclusions that maybe copper/lead alloys.

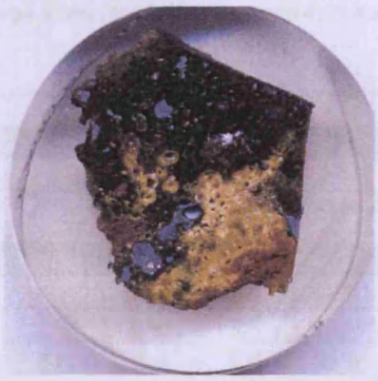

b.

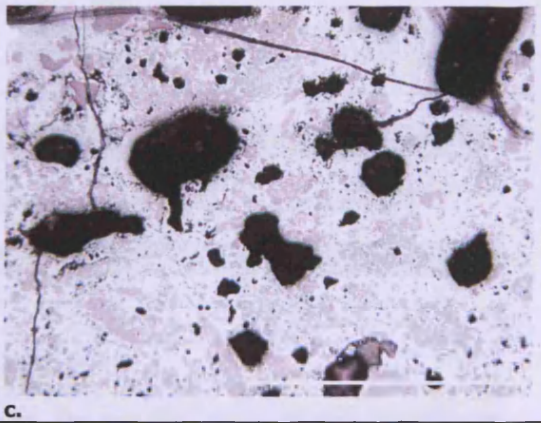

c.

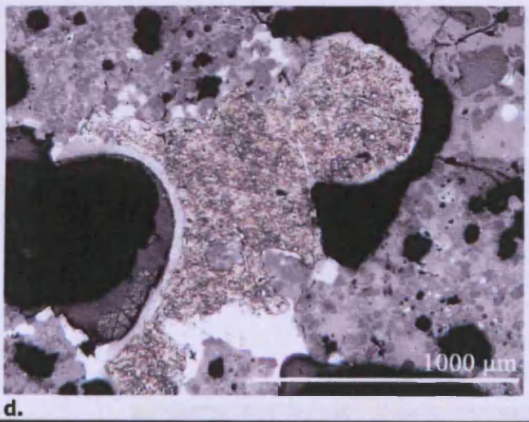

d.

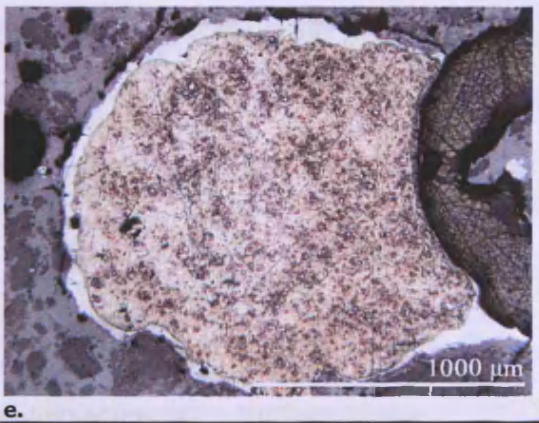

e.

SEM-EDS images and data

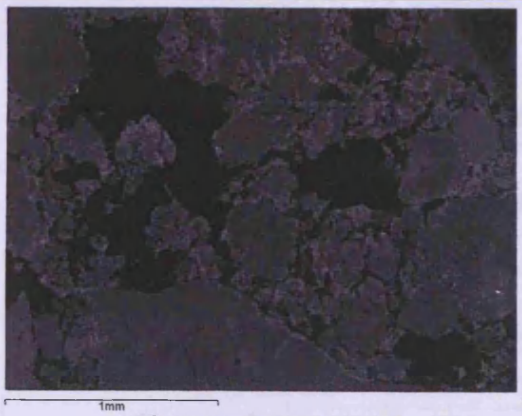

The ceramic furnace wall.

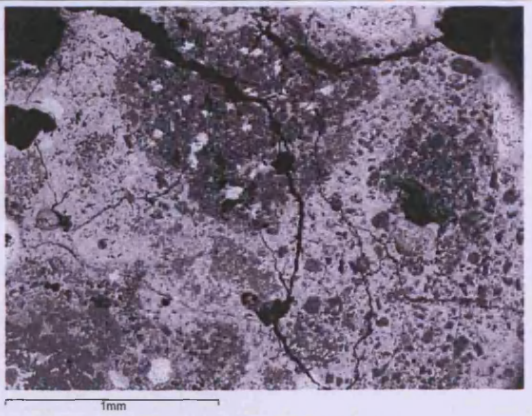

The slag from sample 29.

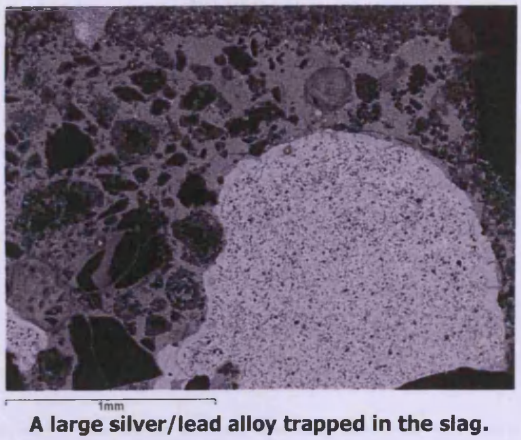

A large silver/lead alloy trapped in the slag.

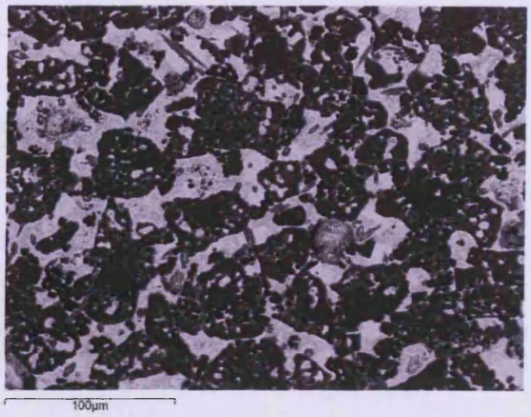

The different phases in sample 29: pyroxenes (dark grey), leucite (black) and lead glassy matrix (light grey).

Scanned area	Na2O	Al2O3	SiO2	K2O	CaO	FeO	As2O3	Sb2O5	PbO
1	0.8	8.2	30.5	2.4	1.0	1.6	1.0	1.8	52.7

Bulk area scans of sample 29. The data has been normalised to 100 wt%.

Spectrum	MgO	Al2O3	SiO2	K2O	CaO	FeO	ZnO	As2O3	Sb2O5	PbO
1	1.4	2.4	15.4	~	1.9	2.9	6.8	1.5	5.5	62.4
2	~	3.6	16.9	~	~	1.5	1.3	~	~	76.7
3	1.1	5.4	21.8	1.5	2.6	4.8	~	~	4.7	58.2
Average	**0.8**	**3.8**	**18.0**	**0.5**	**1.5**	**3.1**	**2.7**	**0.5**	**3.4**	**65.7**

SEM-EDS area analysis of the glassy matrix sample 29. The data has been normalised to 100 wt%.

Spectrum	Na2O	MgO	Al2O3	SiO2	P2O5	K2O	CaO	FeO	As2O5	PbO
1	3.0	0.7	16.6	61.7	1.4	4.5	3.4	2.5	0.2	6.2

SEM-EDS area analysis of the ceramic body in sample 29.
The data has been normalised to 100 wt%.

Spectrum	Al2O3	SiO2	K2O	FeO
1	22.0	56.4	21.0	0.7
2	21.7	55.4	20.8	2.0
3	21.3	57.2	21.0	0.6
Average (n=3)	**21.7**	**56.3**	**20.9**	**1.1**

SEM-EDS area analysis of leucite in sample 29.
The data has been normalised to 100 wt%.

Scanned area	MgO	Al2O3	SiO2	K2O	CaO	FeO	ZnO	PbO
1	3.1	3.1	38.9		33.2	1.8	15.5	4.4
2	6.6	4.3	43.5	0.7	33.2	2.5	4.7	4.3
3	7.3	6.7	41.0	0.6	35.5	2.3	3.4	3.3
Average (n=3)	**5.7**	**4.7**	**41.1**	**0.4**	**34.0**	**2.2**	**7.9**	**4.0**

SEM-EDS area analysis of pyroxenes in sample 29.
The data has been normalised to 100 wt%.

Area	Si	Ag	Pb
1 (small edge of prill 200um)	~	1.7	98.3
2 (overall prill 200um)	4.8	8.8	86.4
4	~	3.5	96.5
SI12	8.5	11.1	80.4

SEM-EDS area analysis of lead metal in sample 29. The data has been normalised to 100 wt%.

Spot analysis	Cu	Si	Ag	Sb	Pb
1	1.1	~	87.7	10.1	1.2
2	~	~	93.2	~	6.8
3	~	0.7	91.5	~	7.9
4	~	~	97.8	~	2.2
5	~	~	96.4	~	3.6

SEM-EDS spot analysis of silver rich areas in sample 29. The data has been normalised to 100 wt%.

HuA1 sample 31

a.

Sample 31 was seleceted from a bag of samples. It is a furnace fragment with a number of different layers of slag.

OM images showed that partially reacted lead sulphide was common in the slag (b). Metallic prills were scarce in sample 31(c).

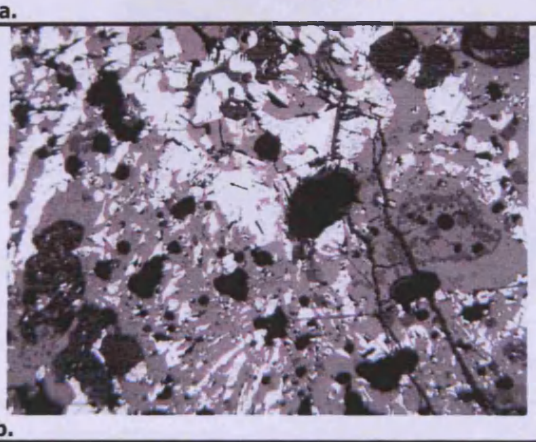

b.

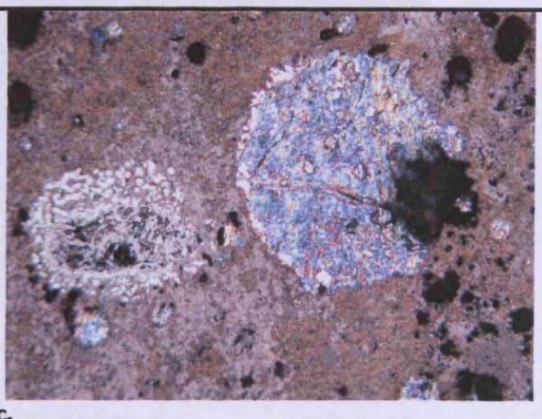

c.

SEM-EDS images and data

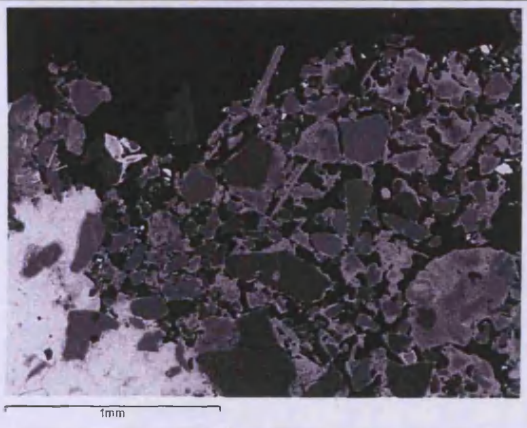

The ceramic wall being dissolved by the slag.

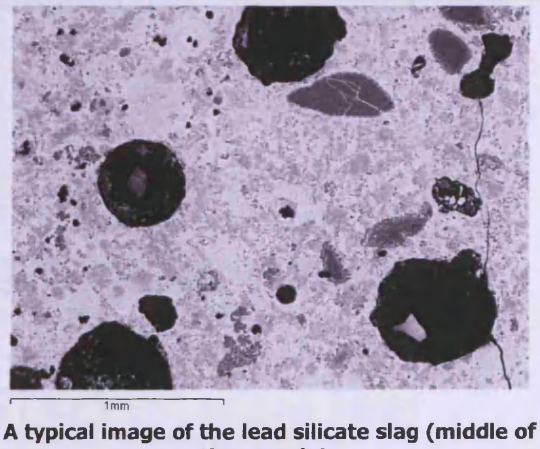

A typical image of the lead silicate slag (middle of the sample).

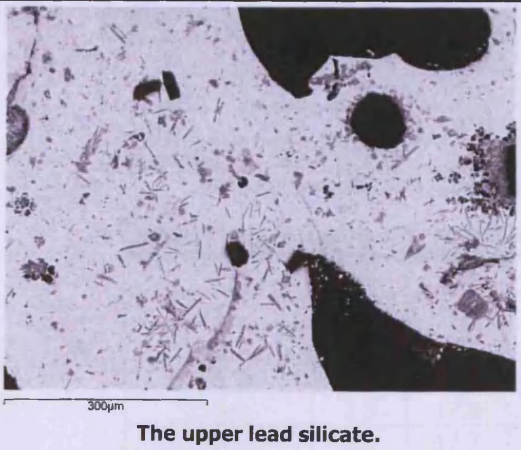

The upper lead silicate.

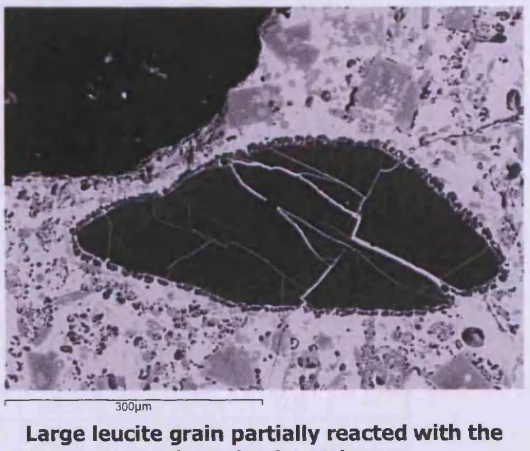

Large leucite grain partially reacted with the glassy lead matrix.

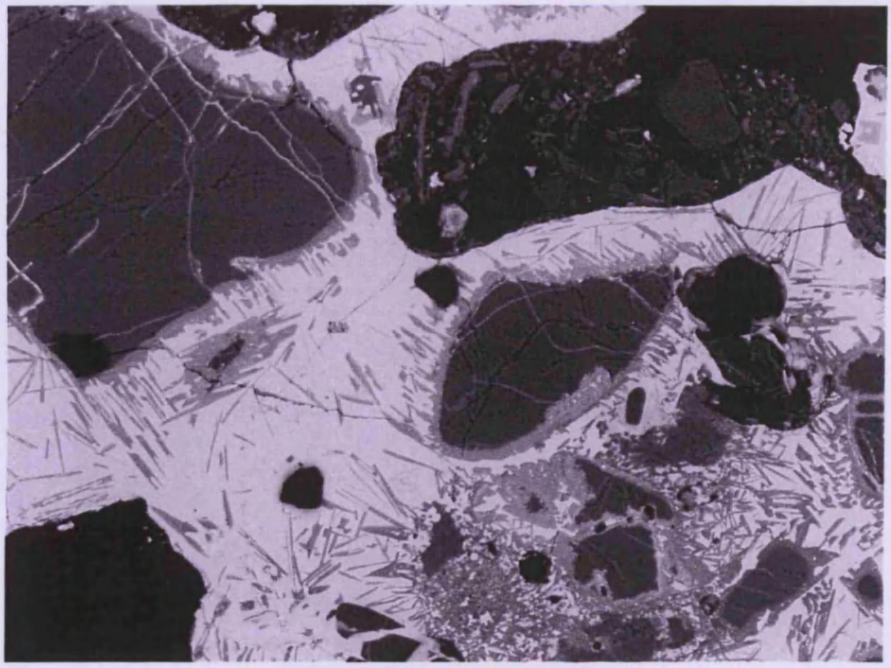

Leucite grains dissolving into the lead slag layer.

Scanned area	Na2O	MgO	Al2O3	SiO2	K2O	CaO	TiO2	FeO	ZnO	PbO
1	~	0.7	6.1	29.3	3.0	7.8	0.6	7.5	15.7	29.4
2	~	1.3	5.5	29.2	2.5	8.1	~	8.7	15.4	29.3
3	~	1.0	5.9	29.1	2.4	8.8	1.3	11.1	15.3	25.2
4	~	0.9	6.0	30.0	1.5	3.7	~	5.6	8.8	43.6
5	1.9	~	11.4	53.1	4.3	0.9	3.6	3.9	~	21.0
Average (n=5)	**0.4**	**0.8**	**7.0**	**34.1**	**2.7**	**5.8**	**1.1**	**7.3**	**11.1**	**29.7**

SEM-EDS bulk area scans of sample 31. The data has been normalised to 100 wt%.

Scanned area	MgO	Al2O3	SiO2	K2O	CaO	FeO	ZnO	PbO
1	0.8	6.5	32.9	1.5	3.6	4.8	6.5	43.5
2	1.0	5.1	30.4	1.1	3.1	4.1	7.4	47.7
3	0.7	6.3	34.7	0.8	~	2.9	2.0	52.8
Average (n=3)	**0.8**	**6.0**	**32.6**	**1.1**	**2.2**	**3.9**	**5.3**	**48.0**

SEM-EDS of the glassy matrix. The data has been normalised to 100 wt%.

Spectrum	Na2O	MgO	Al2O3	SiO2	K2O	CaO	FeO	ZnO	PbO
SI6	~	1.8	3.3	34.0	~	26.6	5.3	21.5	7.5
SI8	~	1.8	2.3	36.6	~	29.7	4.3	18.9	6.4
SI10	1.4	1.0	17.4	52.8	6.3	4.5	1.7	0.9	14.1
Average	**0.5**	**1.5**	**7.7**	**41.1**	**2.1**	**20.3**	**3.8**	**13.8**	**9.3**

Zinc calcium silicates. The data has been normalised to 100 wt%.

Scanned area	Na2O	Al2O3	SiO2	K2O	CaO	FeO	BaO	PbO
1	2.4	18.2	65.6	12.8	~	~	1.1	~
2	~	20.5	56.3	20.5	~	0.8	~	1.9
3	6.0	23.7	62.3	0.7	7.3	~	~	~
4	1.9	17.5	67.0	13.7	~	~	~	~
5	2.5	17.8	66.6	12.1	~	~	0.9	~
6	2.4	17.7	67.3	12.6	~	~	~	~

SEM-EDS area analyses of partially reacted luecite/feldspar? The data has been normalised to 100 wt%.

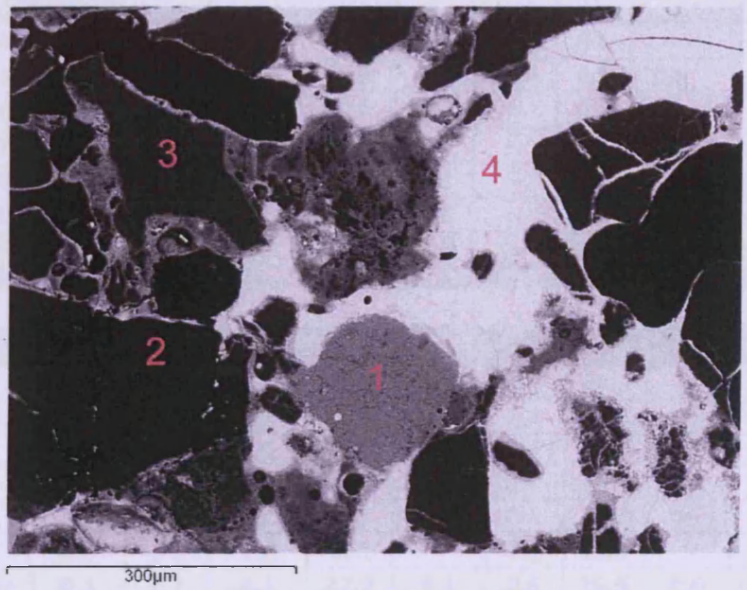

Different phases in sample 31.

Scanned areas	Na2O	MgO	Al2O3	SiO2	K2O	CaO	TiO2	MnO	FeO	ZnO	PbO
Area 1	~	1.0	~	0.6	~	~	53.3	0.7	44.5	~	~
Area 2 - quartz	~	~	~	100.0	~	~	~	~	~	~	~
Area 3 - feldspar	2.5	~	17.8	66.6	12.1	~	~	~	~	~	~
Area 4 – glassy lead silicate	~	0.7	6.3	34.7	0.8	~	~	~	2.9	2.0	52.8

The different phases analysed in sample 31. The data has been normalised to 100 wt%.

Samples	Na2O	Al2O3	SiO2	K2O	TiO2	FeO	ZnO	BaO	PbO
26A	~	21.7	56.5	21.2	~	0.6	~	~	~
26B	0.4	18.9	56.9	20.4	0.2	0.5	0.6	0.6	1.6
26C	0.2	21.9	56.2	21.2	~	0.5	~	~	0.0
27A	0.7	26.4	38.7	31.1	~	2.5	~	~	0.7
29	~	21.7	56.3	20.9	~	1.1	~	~	~
31	~	20.8	56.6	20.8	~	0.9	~	~	0.9
Average Leucite	**0.2**	**21.9**	**53.5**	**22.6**	**~**	**1.0**	**0.1**	**0.1**	**0.5**

Leucite analysed in slag samples from HuA1. Data has been normalised to 100%.

Samples	Na2O	MgO	Al2O3	SiO2	P2O5	K2O	CaO	MnO	FeO	ZnO	PbO
26A	~	2.9	2.7	36.7	0.5	0.3	29.3	~	2.6	16.2	8.9
26B	~	1.6	4.2	33.1	~	0.1	27.9	~	2.5	20.6	10.0
26C	~	2.0	3.0	35.2	~	0.1	27.7	~	1.5	20.1	10.4
27A	~	3.0	2.8	36.4	~	0.9	32.7	0.2	3.3	14.8	6.0
29	~	4.9	4.2	40.6	~	0.3	33.7	~	1.9	9.8	4.5
31	0.5	1.5	7.7	41.1	~	2.1	20.3	~	3.8	13.8	9.3
Average pyroxene	**0.1**	**2.7**	**4.1**	**37.2**	**0.1**	**0.6**	**28.6**	**0.0**	**2.6**	**15.9**	**8.2**

Pyroxenes measured in slag samples from HuA1. Data has been normalised to 100 %.

Sample	MgO	Al2O3	SiO2	CaO	FeO	ZnO	PbO
26B	1.1	1.0	23.9	5.4	4.4	58.5	5.7
26C	7.9	2.4	27.6	~	0.9	57.3	3.8

Willemite (Zn2 SiO4) recorded using SEM-EDS analyses of slag samples from HuA1. Data has been normalised to 100 %.

Samples	Na2O	MgO	Al2O3	SiO2	SO3	K2O	CaO	TiO2	MnO	FeO	ZnO	As2O5	SbO	Pb
26B	~	1.0	4.8	23.6	~	1.6	8.2	0.3	~	4.9	13.4	~	~	42.2
26C	~	0.7	6.2	23.5	1.1	2.8	8.3	~	~	4.9	15.5	2.8	~	34.2
27A	~	1.6	5.3	22.2	~	3.1	11.4	~	0.4	13.4	11.1	~	~	31.5
29	0.8	~	8.2	30.5	~	2.4	1.0	~	~	1.6	~	1.0	1.8	52.7
31	0.4	0.8	7.0	34.1	~	2.7	5.8	1.1	~	7.3	11.1	~	~	29.7
Average	**0.2**	**2.5**	**4.7**	**26.8**	**0.2**	**2.5**	**6.9**	**0.3**	**0.1**	**6.4**	**10.2**	**0.8**	**0.4**	**38.1**
Min	0.4	0.7	4.8	22.2	1.1	1.6	1.0	0.3	0.4	1.6	11.1	1.0	1.8	29.7
Max	0.8	8.2	7.0	34.1	1.1	3.1	11.4	1.1	0.4	13.4	15.5	2.8	1.8	52.7

SEM-EDS bulk area analyses of samples from HuA1. The data has been normalised to 100 wt%.

Samples	Na2O	MgO	Al2O3	SiO2	P2O5	K2O	CaO	TiO2	FeO	ZnO	As2O5	SbO	PbO
26A	~	0.6	3.4	18.7	0.3	0.8	2.0	~	3.2	4.4	0.4	~	66.2
26B	~	0.2	3.3	19.0	~	1.2	1.9	0.1	3.4	7.4	0.7	~	62.6
26C	~	~	3.8	20.7	~	~	1.4	~	2.3	5.9	3.7	~	62.3
27A	0.2	0.4	2.2	16.7	~	1.2	1.4	~	3.6	3.6	~	~	70.5
29	0.3	0.6	4.2	18.6	~	0.7	3.1	~	3.4	1.8	0.8	2.4	64.1
31	~	0.8	4.9	30.3	~	1.0	2.4	~	4.2	6.5	~	~	49.9
Average	0.1	0.5	3.6	20.7	0.1	0.8	2.0	0.0	3.3	4.9	0.9	0.4	62.6
Min	**0.2**	**0.2**	**2.2**	**16.7**	**0.3**	**0.7**	**1.4**	**0.1**	**2.3**	**1.8**	**0.4**	**2.4**	**49.9**
Max	0.3	0.8	4.9	30.3	0.3	1.2	3.1	0.1	4.2	7.4	3.7	2.4	70.5

SEM-EDS area analyses of the glassy slag matrix from samples HuA1. The data has been normalised to 100 wt%.

HUAYRACHINA SITE 24 (HU24)

The layout of site 24.
Stars show concentrations of *huayrachina* remains and squares indicate bolder of the volcanic tuff.

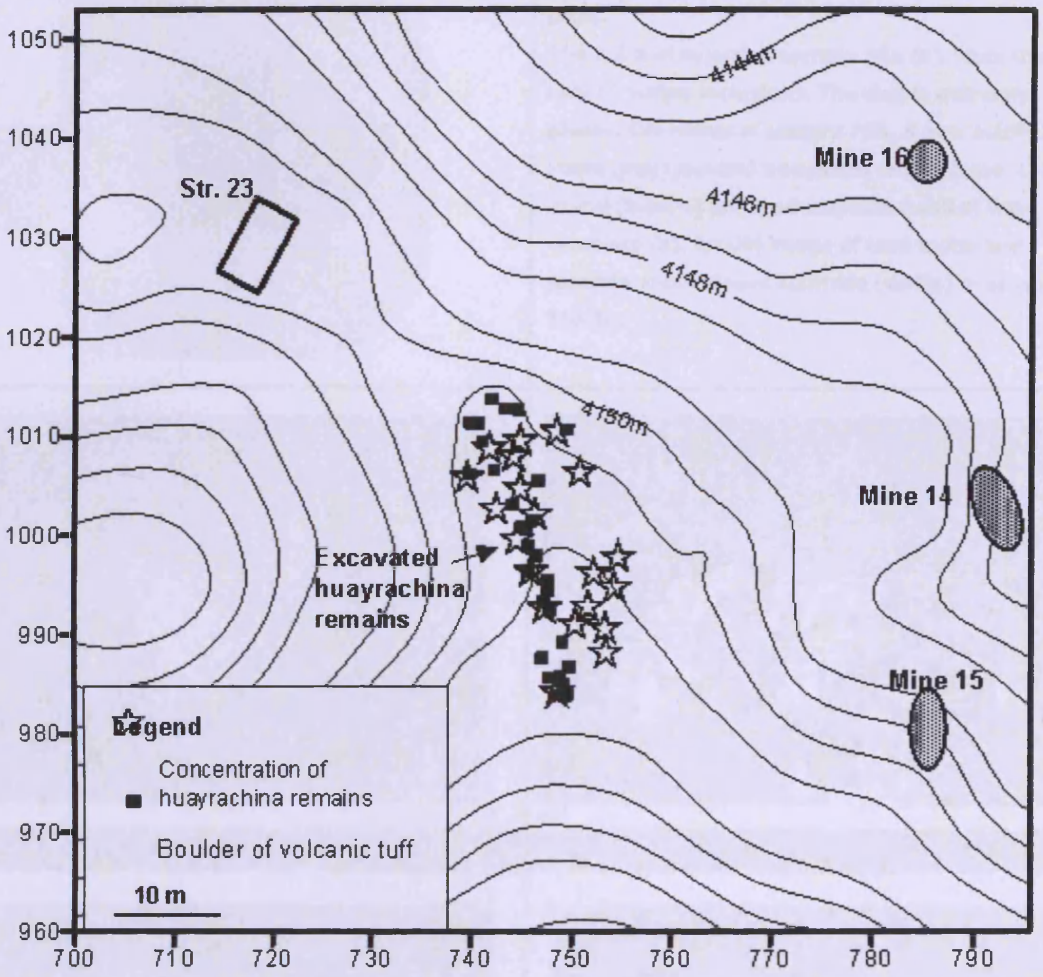

Typical archaeological *huayrachina* debris at Site 24

Hu24 sample 76A

a.

A low phase black slag that contains metallic lead prills.

The cut and mounted sample 76A (a). Note the lack of visible inclusions. The slag is extremly glassy. OM image of sample 76A. A zinc sulphide (light grey) mineral trapped in lead silicate. Lead metal (brown) and lead sulphide (white) were also recorded (b). An OM image of lead metal and partially reacted lead sulphide (white) in sample 76A (c).

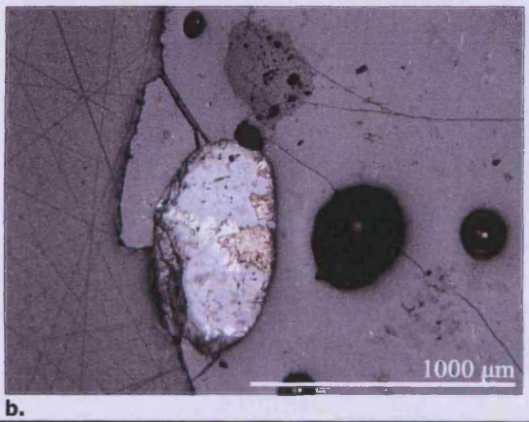

b.

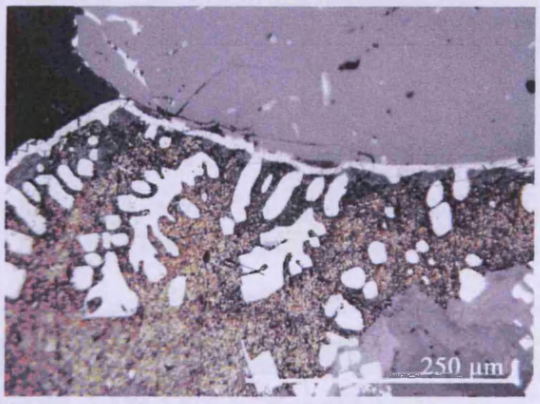

c.

SEM-EDS images and data

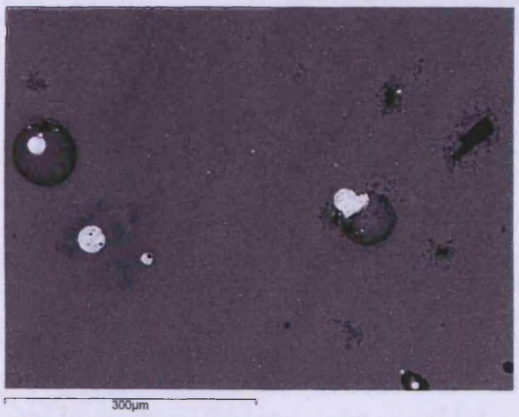

The glassy slag matrix with small metallic prills (white circular areas).

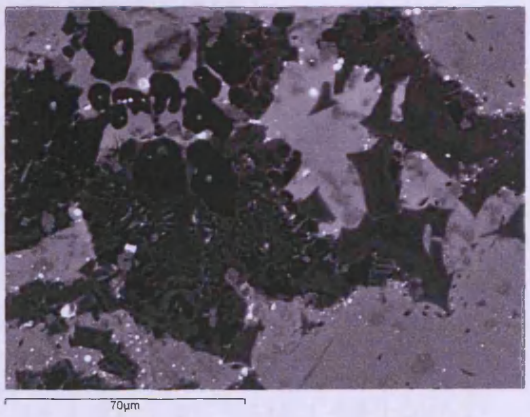

Mineral inclusions within the slag such as pyroxenes and leucite.

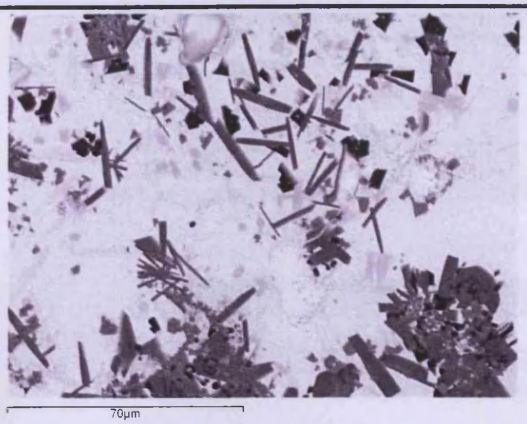

Different mineral inclusions.

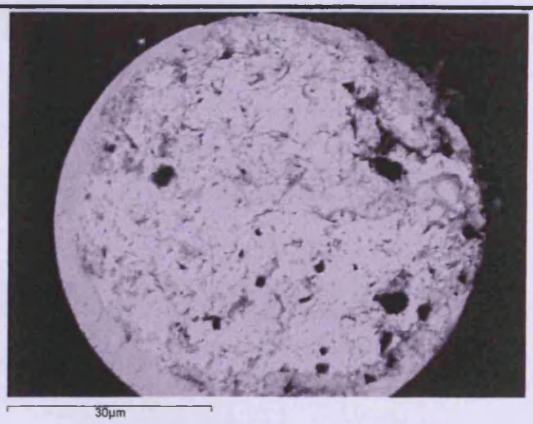

A metallic prill within sample 76A.

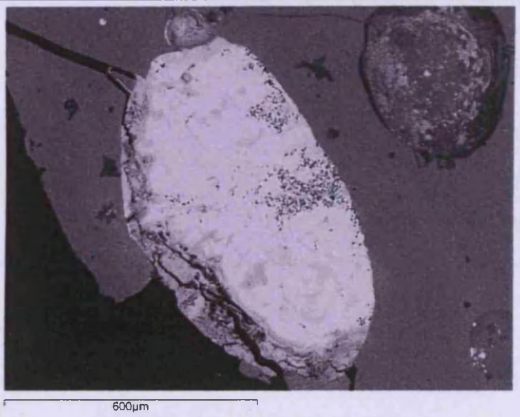

Partially reacted ore inclusions.

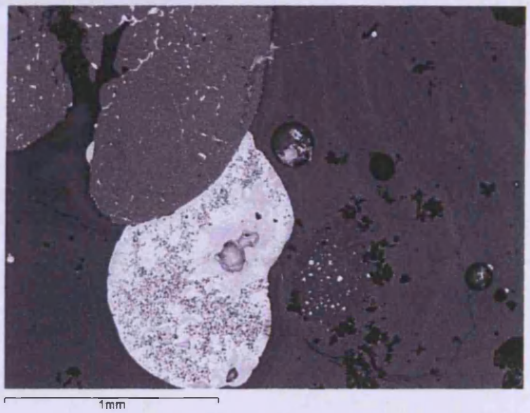

Partially reacted ore.

Scanned area	MgO	Al2O3	SiO2	K2O	CaO	FeO	ZnO	PbO
1 (n=1)	2.2	8.0	33.5	3.7	14.1	14.4	4.9	19.2

SEM-EDS bulk area analyses of sample 76A.
The data has been normalised to 100 wt%.

Scanned area	S	Fe	Cu	Ag	Pb
1	13.8	0.8	0.7	~	84.7
2	11.7	0.7	0.6	~	87.1
3	12.6	0.9	1.9	2.8	81.8
Average	**12.7**	**0.8**	**1.1**	**0.9**	**84.5**

Area of partially reacted ore.
The data has been normalised to 100 wt%.

Scanned area	MgO	Al2O3	SiO2	P2O5	K2O	CaO	TiO2	FeO	ZnO	PbO
1	2.3	8.0	32.6	1.0	3.6	14.0	0.4	14.3	4.5	19.3
2	2.2	7.7	32.7	0.9	3.8	13.8	~	14.6	4.7	19.6
3	2.5	8.1	34.3	1.1	2.9	13.7	~	15.2	4.3	17.9
4	~	7.6	30.7	~	1.4	9.2	0.6	12.5	4.4	31.7
5	2.5	8.1	33.3	~	3.8	14.2	~	14.3	4.6	19.3
6	2.4	7.9	33.3	0.9	3.7	14.4	~	14.5	4.8	18.2
Average	**2.0**	**7.9**	**32.8**	**0.7**	**3.2**	**13.2**	**0.2**	**14.2**	**4.6**	**21.0**

SEM-EDS area analyses of the glassy slag matrix analysed (sample 76A).
The data has been normalised to 100wt%.

Scanned area	MgO	Al2O3	SiO2	K2O	CaO	TiO2	FeO	ZnO	PbO
1	2.9	9.2	38.7	5.3	20.5	0.4	13.5	6.0	3.5
2	~	4.6	40.0	0.4	35.7	~	4.7	7.3	2.3
3	3.3	11.2	35.0	6.9	21.7	~	4.7	5.2	12.2
Average	**2.1**	**8.3**	**37.9**	**4.2**	**26.0**	**0.1**	**7.6**	**6.1**	**6.0**

Pyroxenes measured in sample 76A (SEM-EDS). The data has been normalised to 100 wt%.

Scanned area	Na2O	Al2O3	SiO2	K2O	CaO	FeO	PbO
1	0.53	20.85	54.95	20.49	0.8	1.23	1.14

SEM-EDS area analysis of leucite.
The data has been normalised to 100 wt%.

Scanned area	Si	S	Ag	Sb	Pb
1	3.3	3.9	~	1.5	91.2
2	0.8	~	~	2.8	96.4
3	~	~	~	1.3	98.7
4	0.9	~	1.3	2.4	95.4
5	11.1	~	~	2.6	86.3

SEM-EDS area analyses of lead metal in sample 76A.
The data has been normalised to 100 wt%.

Hu 24 sample 76B

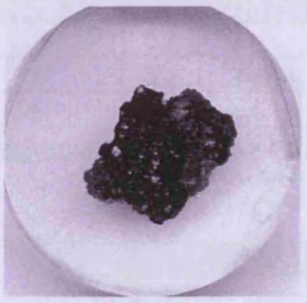

a.

Sample 76B was selected from the same bag as sample 76A. Chemically and physically they appear similar. Macroscopically inclusions of gangue are visible (a).

SEM-EDS images and data

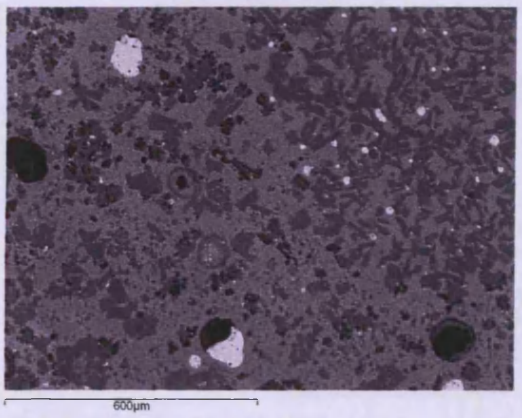

A typical image of sample 76B. A bulk area scan showed that high quantities of zinc was present (equal to lead c. 17%).

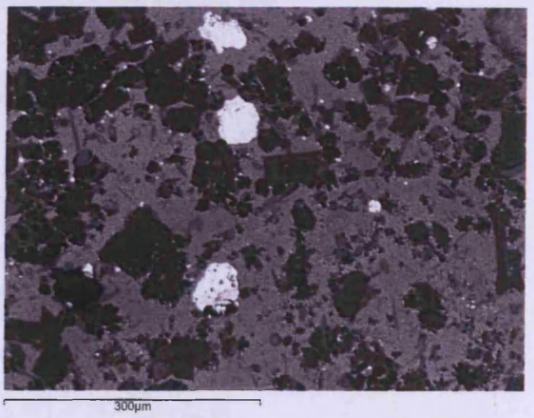

Different phases were recorded in the sample 76B. Pyroxenes, leucite, the lead silicate matrix and lead sulphide prills.

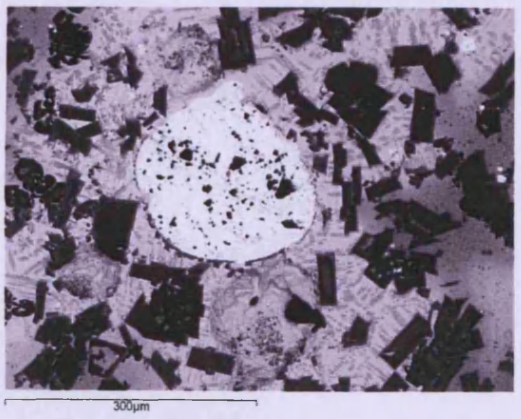

A typical lead prill analysed in sample 76B. Some contain partially reacted lead sulphide.

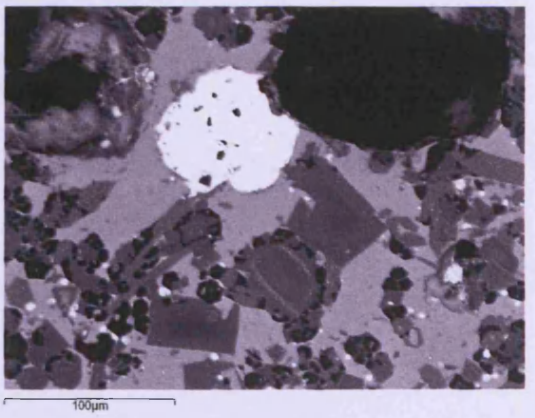

Scanned area	MgO	Al2O3	SiO2	K2O	CaO	TiO2	FeO	ZnO	PbO
1	2.2	6.8	34.0	3.0	13.9	~	7.1	17.9	15.2
2	2.0	7.9	35.5	4.3	11.9	0.5	7.2	17.1	13.7
3	2.1	7.3	34.2	3.7	12.4	~	7.3	16.7	16.4
Average (n=3)	**2.1**	**7.3**	**34.5**	**3.7**	**12.7**	**0.2**	**7.2**	**17.2**	**15.1**

SEM-EDS bulk area scans of sample 76B. The data has been normalised to 100 wt%.

Scanned area	MgO	Al2O3	SiO2	P2O3	K2O	CaO	FeO	ZnO	As2O3	PbO
1	2.2	6.0	31.5	0.8	2.6	8.6	8.5	15.4	~	24.4
2	2.2	5.9	32.9	~	2.8	8.8	9.0	15.9	~	22.5
3	1.6	4.5	29.2	1.0	2.0	6.6	10.2	13.2	1.5	30.3
Average	**2.0**	**5.5**	**31.2**	**0.6**	**2.5**	**8.0**	**9.2**	**14.8**	**0.5**	**25.7**

SEM-EDS bulk area analyses of the glassy slag matrix.
The data has been normalised to 100 wt%.

Spectrum	Na2O	Al2O3	SiO2	K2O	FeO	ZnO	PbO
1	0.3	21.3	55.8	20.9	0.8	0.9	~
2	0.4	21.6	55.7	20.7	0.6	1.0	~
3	~	21.3	53.8	21.1	0.9	1.4	1.5

SEM-EDS bulk area analysis of leucite within sample 76B.
The data has been normalised to 100 wt%.

Scanned area	MgO	Al2O3	SiO2	K2O	CaO	FeO	ZnO	PbO
1	2.3	2.0	38.8	0.3	32.3	2.0	18.3	4.1
2	2.5	1.9	38.7	~	31.7	1.5	18.5	5.2
3	2.5	2.2	39.1	~	32.1	2.6	18.2	3.3

SEM-EDS bulk area analysis of pyroxenes.
The data has been normalised to 100 wt%.

Scanned area	Si	S	Fe	Zn	As	Ag	Sb	Pb
1	12.9	~	~	~	~	~	~	87.1
2	2.0	2.0	~	~	~	~	~	96.0
3	2.9	2.2	~	~	~	1.4	1.5	92.0
4	~	2.5	0.6	1.2	1.4	~	1.3	93.0
5	4.0	~	~	0.8	~	5.3	~	89.9

SEM-EDS area analyses of lead prills analysed in sample 76B.
The data has been normalised to 100 wt%

Hu 24 sample 77A

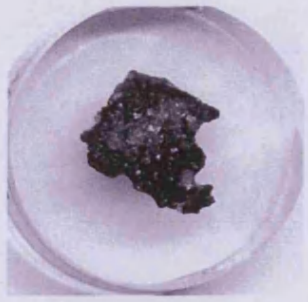

a.

Multiphase siliceous black slag, that contains gangue and metallic phases.

a. Sample 77A, mounted in resin and polished ready for analyses.
b. OM image of sample 77A, the slag is composed of a glassy silicate matrix with different silicate inclusions. Prills of metallic lead were common (top right).
c. OM image of the siilcate matrix.
d. Quartz was also recorded within the slag matrix (OM image).
e. A large metallic prill in sample 77A (OM image).

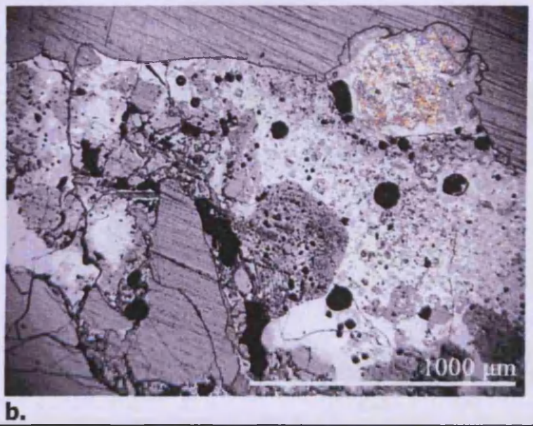

b.

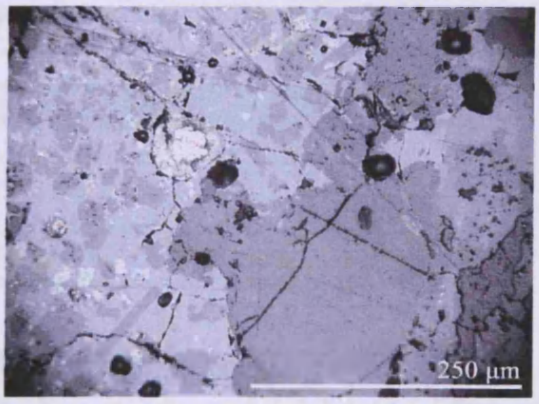

c.

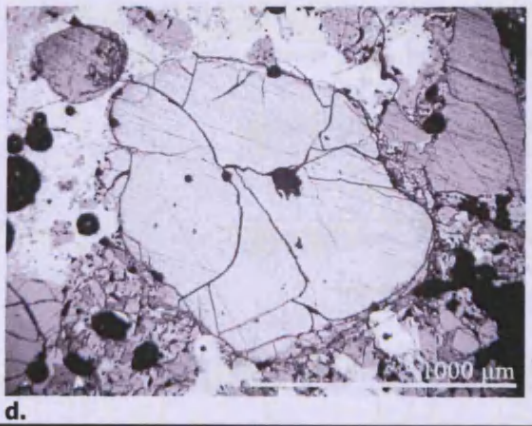

d.

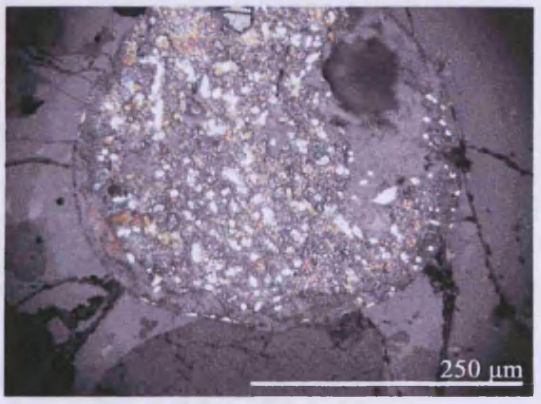

e.

SEM-EDS images and data

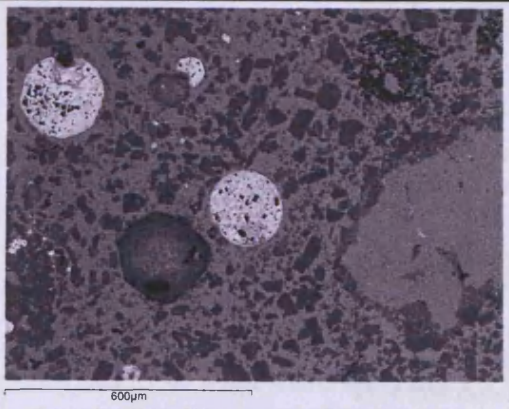

Sample 77A with rounded metallic prills.

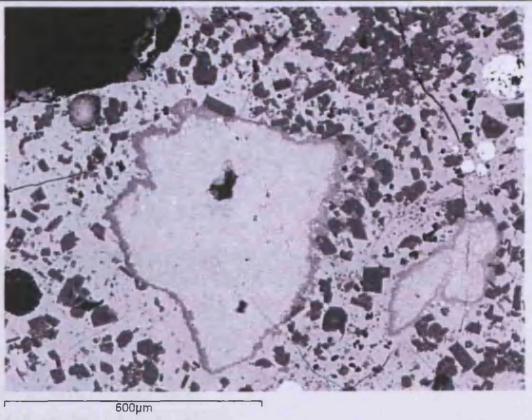

Areas of tin oxide were common in sample 77A.

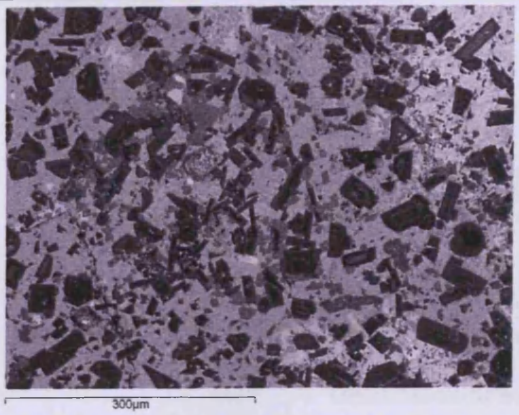

Mixed silicates predominate sample 77A.

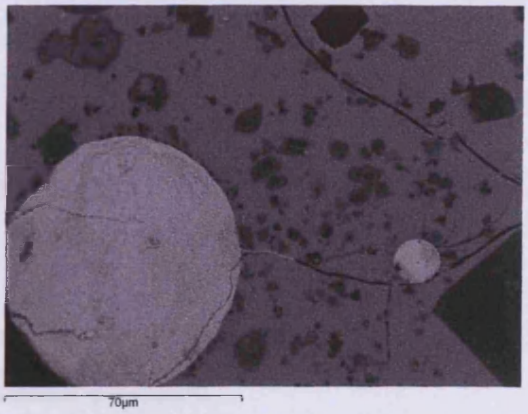

Smaller lead metal prills were found within the main slag body.

Spectrum	MgO	Al2O3	SiO2	K2O	CaO	TiO2	FeO	ZnO	PbO
1	1.3	5.9	22.2	1.1	5.2	1.1	10.4	20.1	32.7
2	1.5	3.3	26.9	1.3	14.7	~	5.9	17.6	28.9
3	1.9	3.4	23.7	~	13.5	~	7.6	17.8	32.1
Average	**1.6**	**4.2**	**24.3**	**0.8**	**11.1**	**0.4**	**8.0**	**18.5**	**31.2**

SEM-EDS bulk area scans of sample 77A. The data has been normalised to 100 wt%.

Scanned area	MgO	Al2O3	SiO2	P2O5	K2O	CaO	FeO	ZnO	PbO
1	1.3	3.6	23.4		2.9	3.7	4.5	15.3	45.3
2	1.7	3.2	22.8	1.3	2.9	2.5	5.8	16.8	43.0
Average glassy matrix	**1.0**	**2.3**	**15.4**	**0.4**	**1.9**	**2.1**	**3.4**	**10.7**	**29.4**

SEM-EDS bulk area scans of glassy matrix scanned area. The data has been normalised to 100 wt%.

Scanned area	AL2O3	SiO2	K2O	FeO	PbO
1	21.0	54.0	20.9	1.2	2.9
2	20.6	57.4	22.0	~	~
Average Luecite	**20.8**	**55.7**	**21.5**	**0.6**	**1.5**

SEM-EDS bulk area scans of leucite.
The data has been normalised to 100 wt%.

Spectrum	MgO	Al2O3	SiO2	CaO	FeO	ZnO	PbO
1	2.2	1.2	36.5	30.9	0.7	20.0	8.5
2	2.1	1.4	36.8	31.0	1.0	19.8	7.9
3	2.9	3.7	36.7	33.0	3.3	13.8	6.6
4	2.3	1.4	37.2	31.3	1.5	19.3	7.0
5	1.8	1.9	36.5	30.4	1.0	21.6	6.7
6	1.9	2.3	37.1	32.1	1.8	20.9	3.9
7	2.2	~	36.2	32.6	1.6	20.1	7.4
Average Olivine	**2.2**	**1.7**	**36.7**	**31.6**	**1.6**	**19.4**	**6.9**

SEM-EDS bulk area scans of pyroxenes.
The data has been normalised to 100 wt%.

Spectrum	MgO	Al2O3	SiO2	TiO2	FeO	ZnO	SnO
1	1.8	19.2	~	1.1	35.0	35.6	7.4
2	2.6	1.3	26.4	~	4.8	64.9	~
3	4.2	4.9	~	~	28.4	35.3	27.2

SEM-EDS bulk area scans of spinels.
The data has been normalised to 100 wt%.

Spectrum	SiO2	FeO	ZnO	SnO	PbO
1	1.4	2.0	~	94.7	1.9
2	~	1.8	~	98.2	~
3	2.1	2.8	~	91.5	3.6
4	2.8	2.2	5.6	85.8	3.7
Average tin oxide	**1.6**	**2.2**	**1.4**	**92.5**	**2.3**

SEM-EDS bulk area scans of tin oxide found in sample 77A.
The data has been normalised to 100 wt%.

Spectrum	Si	S	Cu	Pb
Prill 1 (overall prill)		9.0	2.2	88.8
Prill 2 - A very small prill circa.100 µm	12.3			87.7

SEM-EDS area analyses of metallic lead prills in sample 77A.
The date has been normalised to 100 wt%.

Spectrum	Si	S	Cu	Pb
1	~	9.0	2.2	88.8
2	~	8.6	~	91.4
3	~	9.1	~	90.9
4	3.5	2.1	~	94.4

SEM-EDS area analyses of partially reacted ore with sample 77A.
The date has been normalised to 100 wt%.

Spectrum	S	Fe	Zn
Spectrum 1	31.5	1.0	67.5

SEM-EDS analysis of zinc sulphide found in sample 77A.
The data has been normalised to 100 wt%.

Hu 24 sample 77B

a.

Sample 77B (a) contains two distinct areas: a gangue rich area (c) and a silicate rich area (b). Lead metal prills were recorded in the lead silicate matrix. No silver was recorded. The majority of the sample is lead silicate.

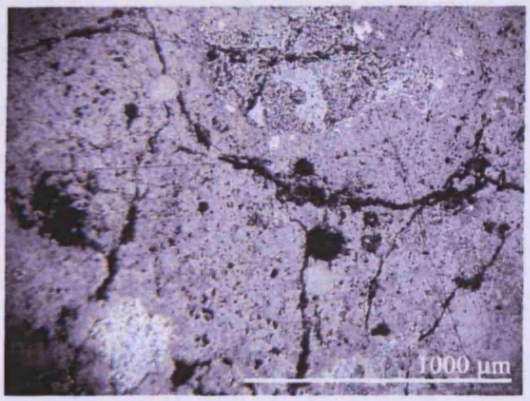

b.

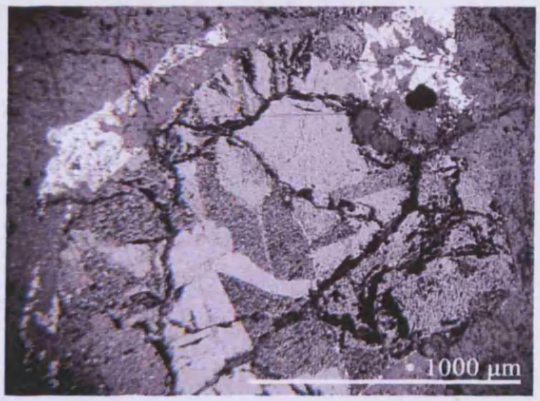

c.

SEM-EDS images and data

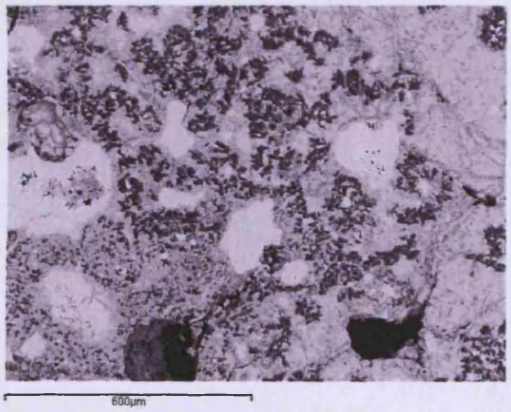

A typical image from sample 77B with inclusions of lead sulphide (white).

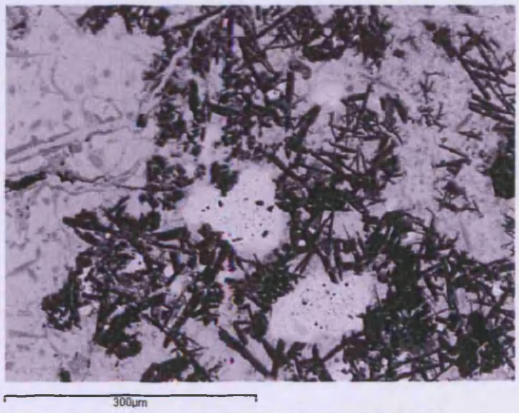

Pyroxenes (angular grey crystals) in a lead silicate matrix.

Scanned area	MgO	Al2O3	SiO2	K2O	CaO	TiO2	FeO	ZnO	PbO
1 (n=1)	1.7	3.3	19.1	0.7	11.7	0.7	5.2	5.4	52.3

Bulk area scans of sample 77B.
The data has been normalised to 100 wt%.

Scanned area	Al2O3	SiO2	CaO	FeO	ZnO	As2O3	SnO2	PbO
1	2.8	21.6		9.9	3.1	1.2	1.9	59.7
2	1.6	11.7	2.8	4.1	1.0	~	~	78.9
3	1.3	18.5	9.0	0.6	~	~	~	70.7
Average	**1.9**	**17.2**	**3.9**	**4.8**	**1.4**	**0.4**	**0.6**	**69.7**

SEM-EDS area analyses of glassy slag matrix scanned area slag sample 77B.
The data has been normalised to 100 wt%.

Spectrum	MgO	Al2O3	SiO2	P2O5	CaO	FeO	ZnO	PbO
1	6.9	2.6	39.4	~	35.6	1.1	6.2	8.2
2	3.5	4.4	38.0	0.3	31.0	2.3	9.9	10.6
3	7.7	1.6	35.5	1.0	40.3	0.9	3.0	10.0
Average	**6.0**	**2.9**	**37.7**	**0.4**	**35.6**	**1.4**	**6.3**	**9.6**

SEM-EDS area analyses of pyroxenes in sample 77B.
The data has been normalised to 100 wt%.

No silver recorded all prills were lead metal.

Hu 24 sample 77C

a.

A low phase siliceous matrix with lead prills dotted throughout the matrix. Microscopically lead metal inclusions were recorded.
a. Sample 77C mounted in epoxy resin.
b. An OM image of zinc sulphide trapped in silicate matrix of sample 77C.
c. OM image of the slag matrix (mid grey) with different silicate minerals. Prills of lead metal (shiny brown, bottom left) and lead sulphide (bright white prills) scatter the slag.
d. OM image of a metallic lead prill in sample 77C.
e. A close up OM image of the metallic prill seen in e. It has a lead sulphide halo.

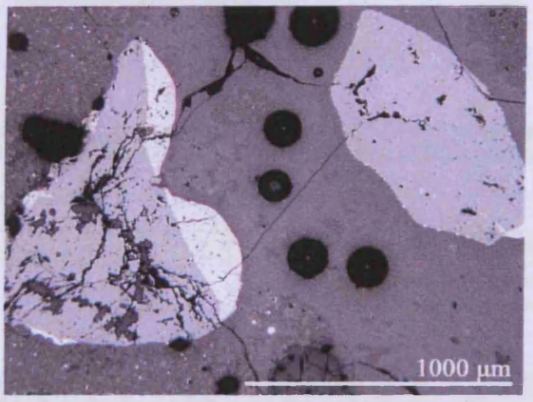

b.

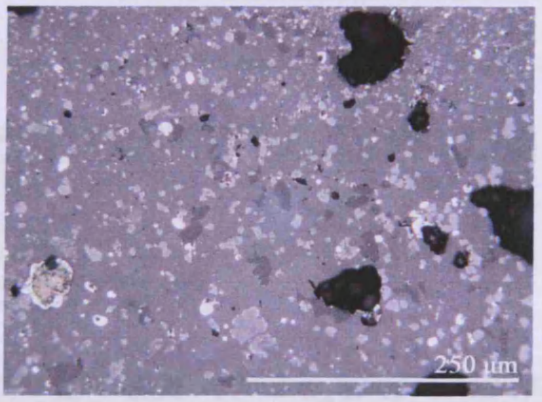

c.

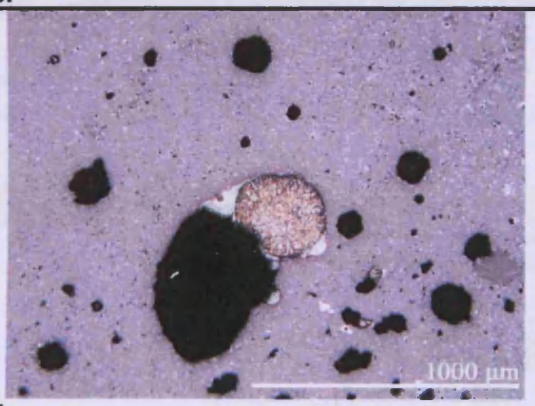

d.

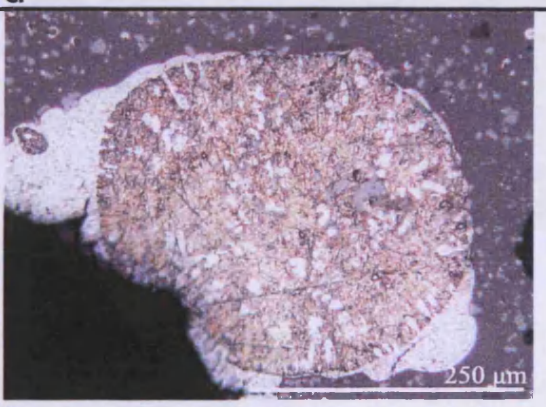

e.

SEM-EDS images and data

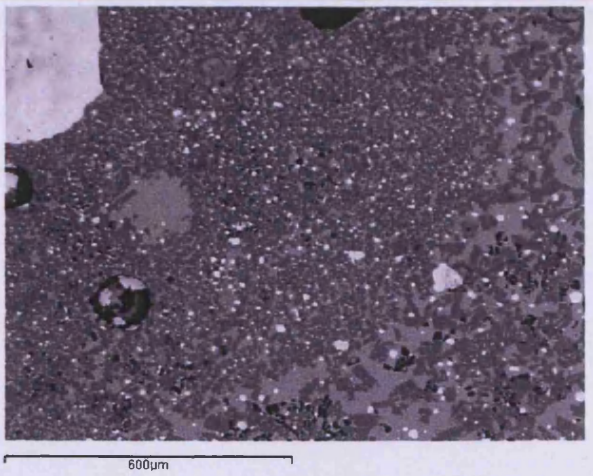

A typical SEM image sample 77C.

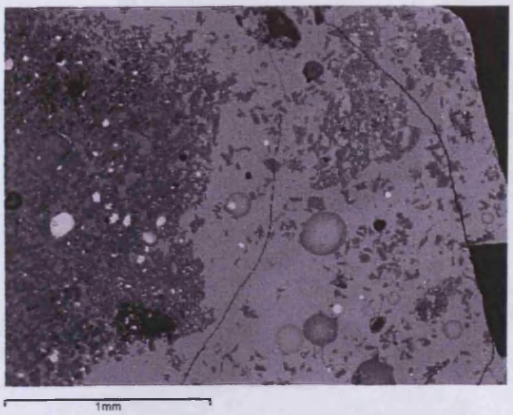

An area of glassy lead slag with pyroxenes

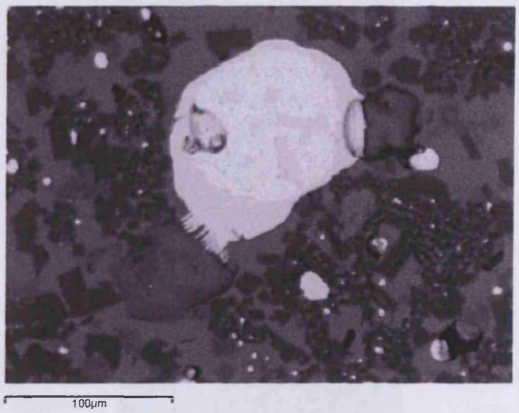

A lead prill in sample 77C.

Scanned area	MgO	Al2O3	SiO2	P2O5	SO3	K2O	CaO	Ti2O	FeO	ZnO	PbO
1	3.8	6.5	33.1	1.2	0.7	2.2	24.1	~	10.1	11.1	7.2
2	3.2	5.4	32.5	1.1	1.1	2.6	22.9	0.4	10.6	12.1	8.2
Average	**3.5**	**5.9**	**32.8**	**1.2**	**0.9**	**2.4**	**23.5**	**0.2**	**10.3**	**11.6**	**7.7**

SEM-EDS bulk area scans of sample 77C.
The data has been normalised to 100 wt%.

Scanned area	MgO	Al2O3	SiO2	P2O5	SO3	K2O	CaO	TiO2	MnO	FeO	ZnO	PbO
1	2.6	5.5	31.7	2.9	1.0	5.8	11.1	0.4	0.4	16.2	11.9	10.6
2	2.6	6.4	31.7	2.8	1.4	6.2	10.1	0.6	0.5	16.4	11.9	9.3
3	3.0	4.1	32.4	3.6	1.8	4.8	11.8	0.5	~	15.1	13.5	9.6
4	2.1	6.0	31.4	3.3	~	5.9	9.7	0.5	~	11.5	11.4	18.2
5	2.2	5.9	32.6	2.9	1.1	6.4	9.0	0.5	~	12.2	12.6	14.6
Average	**2.5**	**5.6**	**31.9**	**3.1**	**1.1**	**5.8**	**10.3**	**0.5**	**0.2**	**14.3**	**12.3**	**12.5**

SEM-EDS area analysis of the glassy matrix in sample 77C.
The data has been normalised to 100 wt%.

Scanned area	Al2O3	SiO2	K2O	FeO	ZnO
1	21.0	55.8	21.6	1.0	0.6

SEM-EDS area analyses of leucite in sample 77C.
The data has been normalised to 100 wt%.

Scanned area	MgO	Al2O3	SiO2	K2O	CaO	FeO	ZnO	PbO
1	3.1	2.6	39.8	0.3	35.9	2.6	14.3	1.4
2	3.5	2.8	40.6	0.4	35.6	2.7	12.9	1.6
3	3.7	4.9	37.7	0.6	33.2	5.4	13.3	1.3
Average	**3.5**	**3.5**	**39.4**	**0.4**	**34.9**	**3.6**	**13.5**	**1.5**

SEM-EDS area analyses of pyroxenes in sample 77C.
The data has been normalised to 100 wt%.

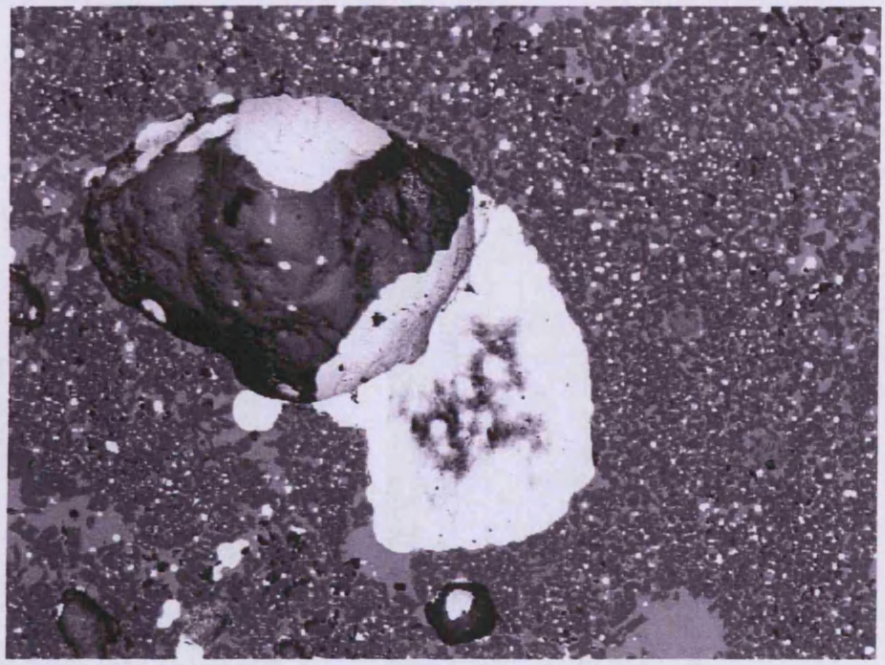

Prill A in sample 77C.

Scanned area	Ag	Sb	Pb
Silver area in prill A	69.8	24.5	5.8

Areas of silver within the above prill 77C.
The data has been normalised to 100 wt%.

Sample	Ca	Ag	Sb	Pb
Prill A	1.5	1.6	2.9	93.7

SEM-EDS area analysis of prill A.
The data has been normalised to 100 wt%.

Scanned areas	Ca	As	Ag	Sb	Pb
1	1.0	18.0		48.8	32.1
2		29.3		52.4	18.4
3		19.5	1.4	49.9	29.3

SEM-EDS area analyses of arsenic antimony prills within lead metal in sample 77C.
The data has been normalised to 100 wt%

Huayrachina site 24 (Hu24)

SAMPLE	MgO	Al2O3	SiO2	P2O5	SO3	K2O	CaO	TiO2	FeO	ZnO	PbO
76A	2.2	8.0	33.5	~	~	3.7	14.1	~	14.4	4.9	19.2
76 B	2.1	7.3	34.5	~	~	3.7	12.7	0.2	7.2	17.2	15.1
77A	1.6	4.2	24.3	~	~	0.8	11.1	0.4	8.0	18.5	31.2
77B	1.7	3.3	19.1	~	~	0.7	11.7	0.7	5.2	5.4	52.3
77C	3.5	5.9	32.8	1.2	0.9	2.4	23.5	0.2	10.3	11.6	7.7
Average slag matrix	2.2	5.7	28.8	0.2	0.2	2.3	14.6	0.3	9.0	11.5	25.1
Min	**1.6**	**3.3**	**19.1**	**1.2**	**0.9**	**0.7**	**11.1**	**0.2**	**5.2**	**4.9**	**7.7**
Max	3.5	8.0	34.5	1.2	0.9	3.7	23.5	0.7	14.4	18.5	52.3

The SEM-EDS bulk area scans of site 24 slag samples.
The data has been normalised to 100 wt%.

SAMPLE	Na2O	MgO	Al2O3	SiO2	P2O5	SO3	K2O	CaO	TiO2	MnO	FeO	ZnO	As2O3	SnO	PbO
76A	0.2	2.0	7.9	32.9	0.7	~	3.2	13.3	0.2	~	14.2	4.5	~	~	20.6
76B	~	2.0	5.5	31.2	0.6	~	2.5	8.0	~	~	9.2	14.8	0.5	~	25.7
77A	~	1.0	3.6	23.6	0.4	~	2.7	3.2	~	~	5.0	15.7	~	~	44.8
77B	~	~	1.7	14.9	~	~	~	2.9	~	~	4.6	1.0	0.5	0.5	73.9
77C	~	2.5	5.6	31.9	3.1	1.1	5.8	10.3	0.5	0.2	14.3	12.3	~	~	12.5
Average glassy slag	0.0	1.5	4.8	26.9	1.0	0.2	2.8	7.6	0.1	0.0	9.4	9.7	0.2	0.1	35.5
Min	**0.2**	**1.0**	**1.7**	**14.9**	**0.4**	**1.1**	**2.5**	**2.9**	**0.2**	**0.2**	**4.6**	**1.0**	**0.5**	**0.5**	**12.5**
Max	0.2	2.5	7.9	32.9	3.1	1.1	5.8	13.3	0.5	0.2	14.3	15.7	0.5	0.5	73.9

Combined SEM-EDS area scans of the glassy slag matrix.
The data has been normalised to 100 wt%.

Spectrum	MgO	Al2O3	SiO2	K2O	P2O5	CaO	TiO2	FeO	ZnO	As2O3	PbO
76A	2.6	7.6	38.4	3.3	~	28.0	0.1	7.0	6.4	~	5.4
76B	2.4	2.3	38.6	0.1	~	31.7	~	2.1	18.5	~	4.3
77A	2.2	1.7	36.7	~	~	31.6	~	1.6	19.4	~	6.9
77B	6.0	2.9	37.7	~	0.4	35.6	~	1.4	6.3	~	9.6
77C	3.5	3.5	39.4	0.4	~	34.9	~	3.6	13.5	0.1	1.3
Average pyroxenes	**3.3**	**3.6**	**38.2**	**0.8**	**0.1**	**32.4**	**~**	**3.1**	**12.8**	**~**	**5.5**
Min	2.2	1.7	36.7	0.1	0.4	28.0	0.1	1.4	6.3	0.1	1.3
Max	6.0	7.6	39.4	3.3	0.4	35.6	0.1	7.0	19.4	0.1	9.6

Pyroxenes analysed using SEM-EDS area analyses in slag samples from site 24.
Data has been normalised to 100 wt%.

Spectrum	Na2O	AL2O3	SiO2	K2O	CaO	FeO	ZnO	PbO
77A	~	20.8	55.7	21.5	~	0.6	~	1.5
77C	~	21.0	55.8	21.6	~	1.0	0.6	~
76A	0.5	20.9	55.0	20.5	0.8	1.2	~	1.1
76B	0.3	21.4	55.1	20.9	~	0.7	1.1	0.5
Average	**0.2**	**21.0**	**55.4**	**21.1**	**0.2**	**0.9**	**0.4**	**0.8**
Min	0.3	20.8	55.0	20.5	0.8	0.6	0.6	0.5
Max	0.5	21.4	55.8	21.6	0.8	1.2	1.1	1.5

SEM-EDS leucite analysed in the slag sample from site 24. Data has been normalised to 100 wt%.

URUQUILLA EAST SADDLE (UR ES)

The UR ES site and typical hand specimens found on site

UR ES 343A

a.

A slag sample without ceramic.
a. Mounted in epoxy resin sample ES 343A.
b and c. Two different metallic prills that were found in sample ES 343A.
d. An OM image of the slag with large pieces of gangue minerals of zinc sulphide.
e. A close up OM image of the zinc sulphide region seen in image d.

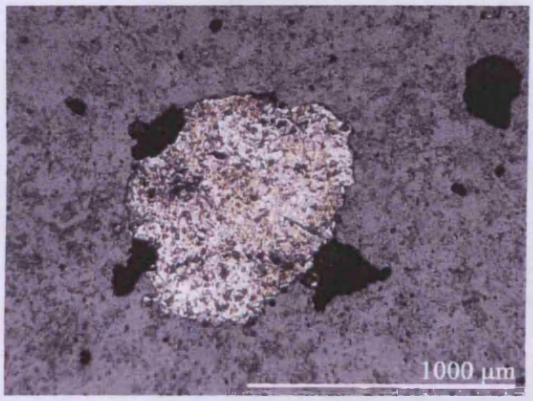

b.

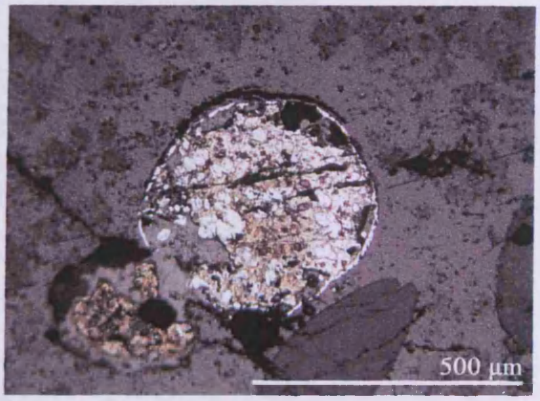

c.

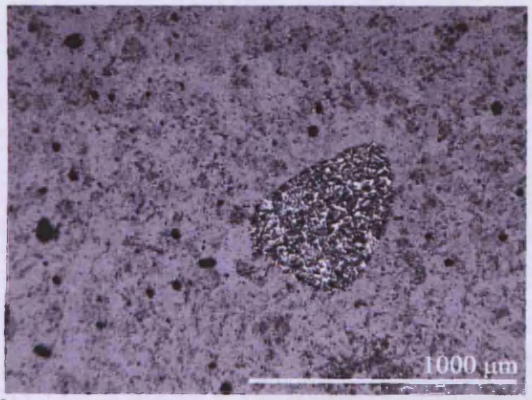

d.

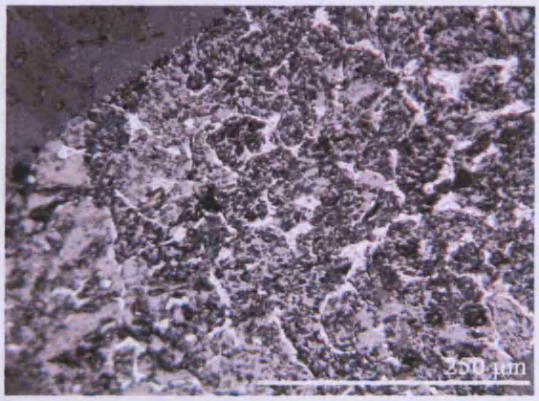

e.

SEM-EDS images and data

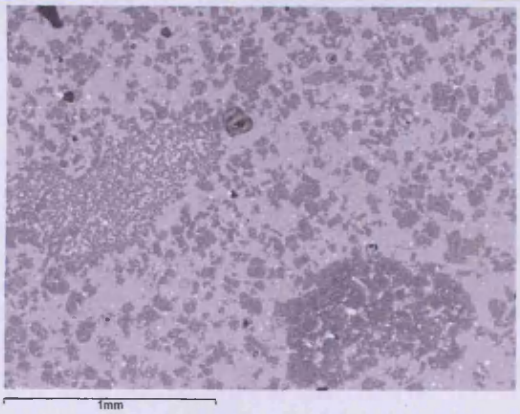

A typical image of sample 343A.

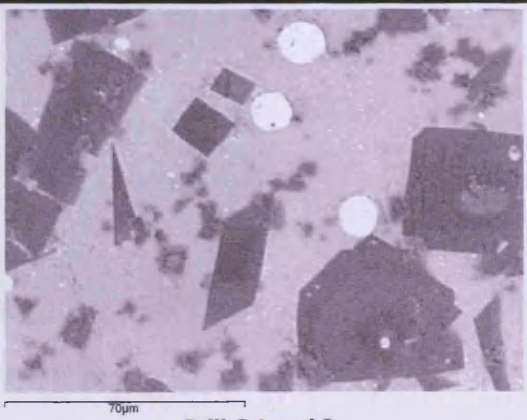

Prill C 1 and 2.

Scanned area	MgO	Al2O3	SiO2	K2O	CaO	FeO	ZnO	PbO
1	2.6	5.4	29.2	2.6	15.7	6.1	23.8	14.6
2	2.4	5.4	28.4	3.2	14.0	6.4	25.1	15.2
3	2.3	5.7	30.8	3.6	13.3	6.0	23.7	14.8
4	2.5	5.2	27.6	2.9	14.1	5.8	25.0	16.8
5	2.2	5.2	29.0	2.9	14.6	6.0	24.7	15.4
Average	**2.4**	**5.4**	**29.0**	**3.0**	**14.4**	**6.0**	**24.4**	**15.4**

SEM-EDS bulk area scans slag sample 343A.
The data has been normalised to 100 wt%

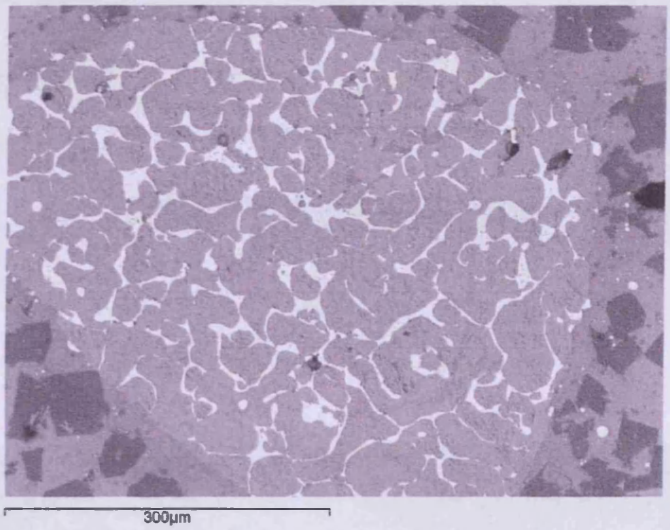

i.

Scanned area	S	Fe	Cu	Zn	Pb
Mid grey phase	46.4	1.4	~	52.2	~
White phase	40.2	6.9	4.0	14.1	34.9
Bulk area of the particle	44.8	1.6	0.5	49.8	3.3

Partially reacted ore found in the slag.
The data has been normalised to 100 at%.

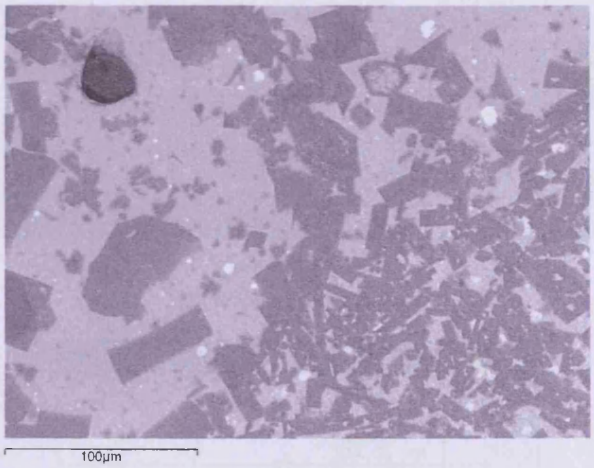

Pyroxenes in sample 343A.

Spectrum	MgO	Al2O3	SiO2	K2O	CaO	FeO	ZnO	As2O3	PbO
1	2.4	2.5	37.3	0.3	33.1	1.4	19.8	~	3.2
2	2.9	2.7	36.2	0.4	32.0	1.5	19.5	0.2	4.5
3	2.6	2.4	37.7	0.2	33.5	1.2	20.4	~	2.0
Average	**2.7**	**2.5**	**37.1**	**0.3**	**32.9**	**1.4**	**19.9**	**0.1**	**3.2**

SEM-EDS area analyses of pyroxenes in sample 343A.
The data has been normalised to 100 wt%.

Area	MgO	Al2O3	SiO2	P2O5	K2O	CaO	FeO	ZnO	As2O3	PbO
1	2.3	4.2	25.7	0.9	4.9	5.2	6.3	22.4	1.0	27.3
2	2.3	3.7	26.8	1.1	5.5	4.8	4.7	25.3	~	25.8
3	2.2	4.8	30.3	0.8	6.0	5.7	5.7	20.8	~	23.8
Average	**2.3**	**4.2**	**27.6**	**0.9**	**5.4**	**5.2**	**5.5**	**22.8**	**0.3**	**25.6**

SEM-EDS area analyses of the glassy slag matrix.
The data has been normalised to 100 wt%.

Scanned area	S	Fe	Cu	Zn	Pb
1	46.4	1.4	~	52.2	~
2	40.2	6.9	4.0	14.1	34.9
3	44.8	1.6	0.5	49.8	3.3

SEM-EDS analyses of partially reacted ore in sample 343A.
The data has been normalised to 100 at%

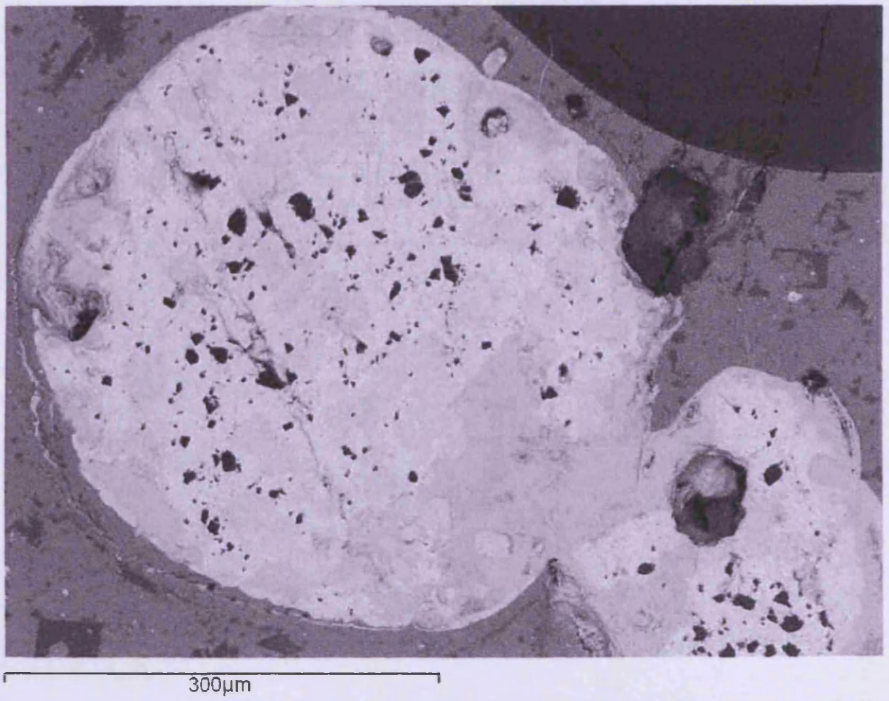

Prill A (sample 343A)

Spot analyses of prill A	S	Cu	Sb	Pb
1	18.5	~	1.6	80.0
2	~	16.0		84.0
3	51.5	~		48.5
4	~	~	1.9	98.1

The data has been normalised to 100 at%.

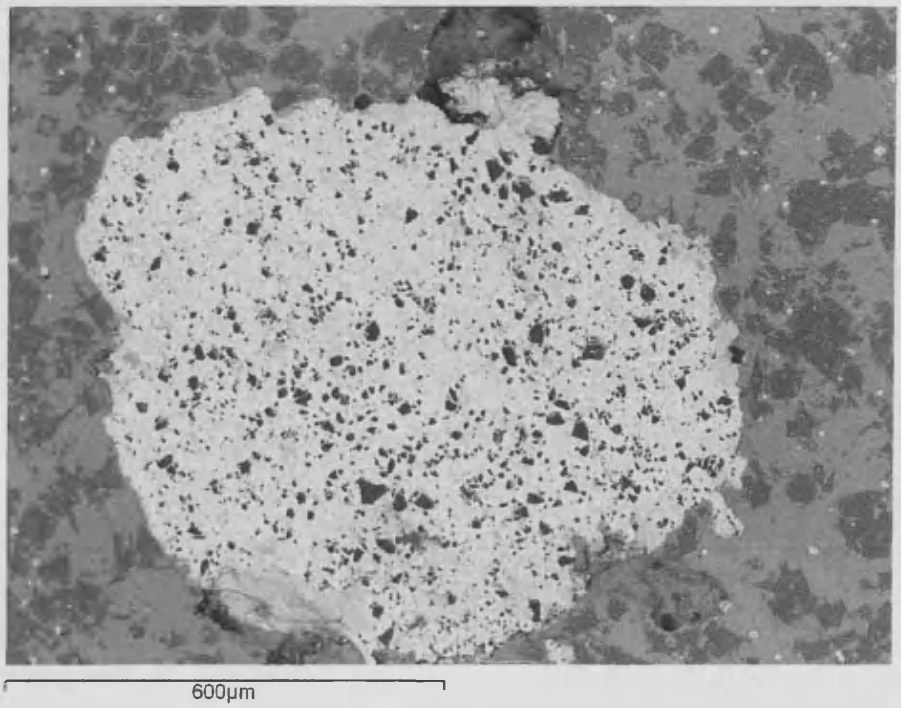

Prill B.

Spectrum	Al	Ag	Sb	Pb
Prill B	13.2	2.8	3.1	80.8

Scanned area	Mg	Al	K	Fe	Cu	Zn	Sb	Pb
Prill C 1	~	2.9	2.2	~	~	13.4	2.0	79.5
Prill C 2	4.6	~	4.5	3.6	3.7	16.8	1.6	65.2

Two prills in sample 343A.
The data has been normalised to 100 at%.

UR ES 343B

a.

The hand specimen for sample 343B was similar to 343A, a grey slag sample not adhered to ceramic. The OM images showed metallic prills of lead metal interspersed between a lead silicate matrix (a and b).

Large lead and silver metallic prills were common within the sample (c and d).

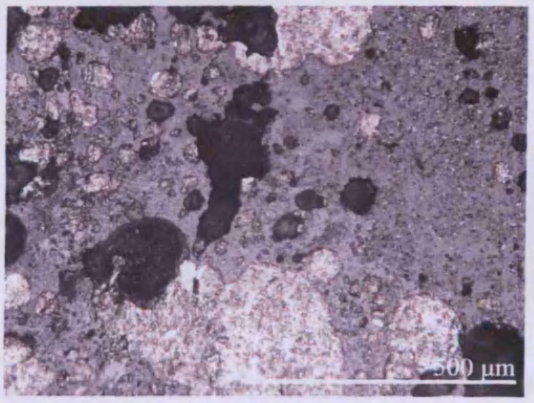

b.

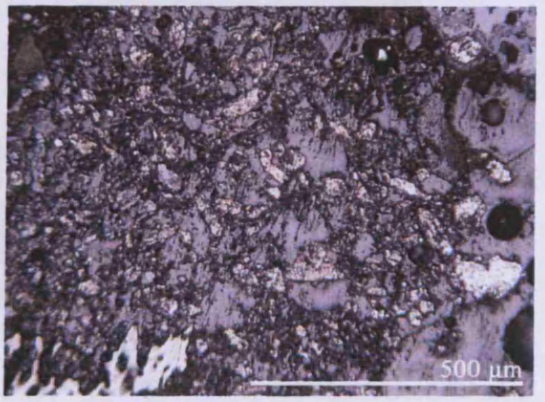

c.

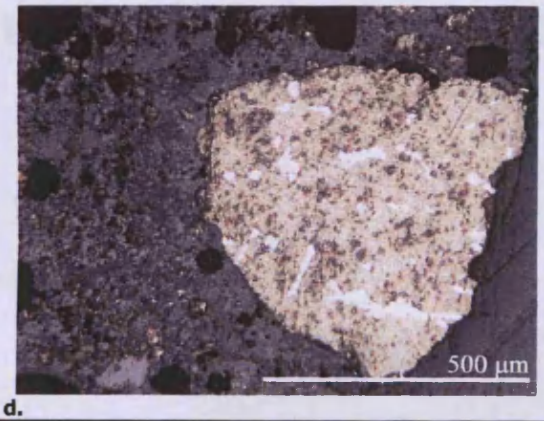

d.

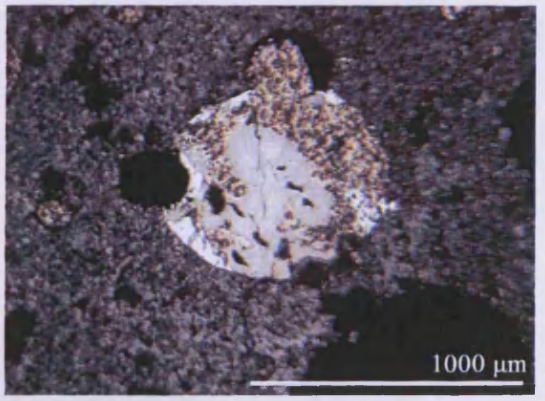

e.

SEM-EDS images and data

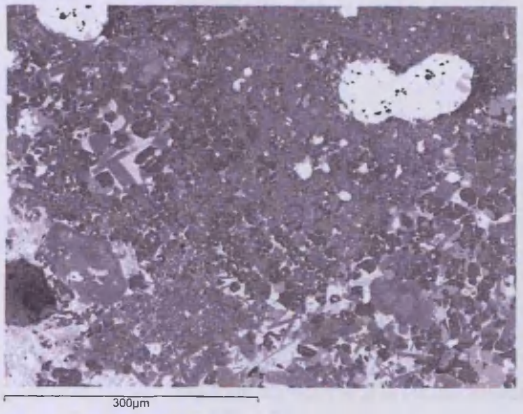

A typical SEM image of slag sample 343B. note the metallic prills (white) trapped within the lead silicate.

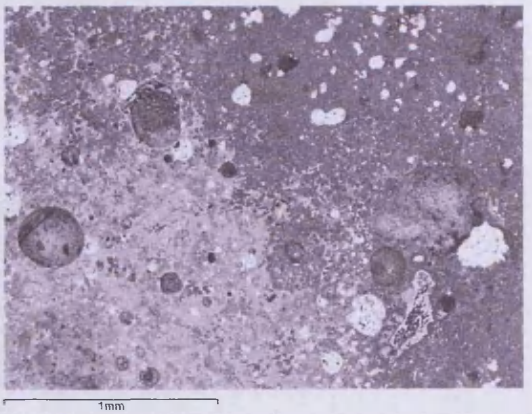

This sample has large areas of tin rich oxides (lighter grey area).

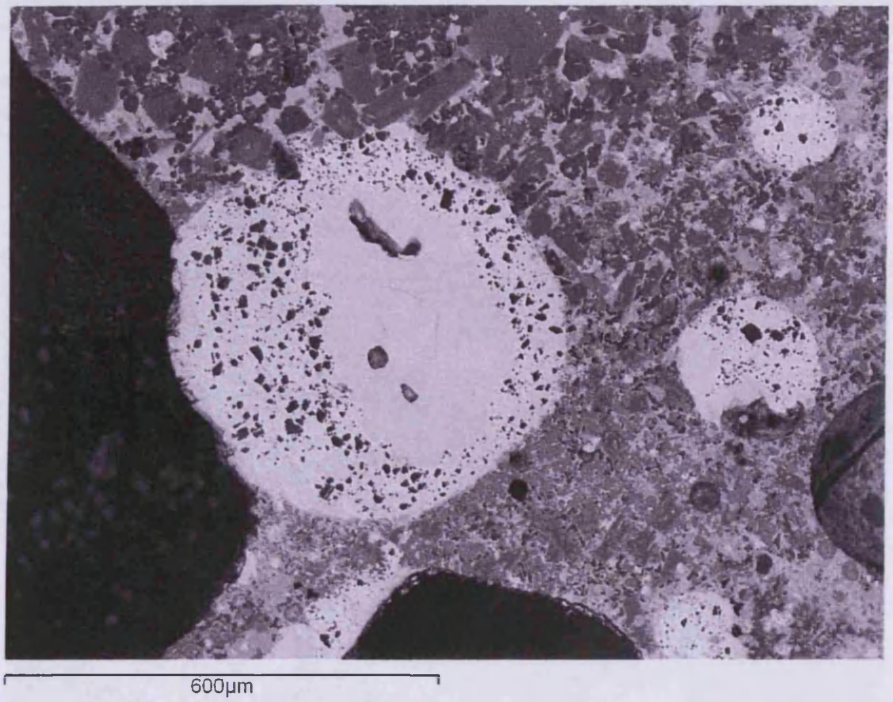

Sample 343B has metallic lead prills that also contain tin and silver.

Spectrum	MgO	Al2O3	SiO2	P2O5	K2O	CaO	FeO	ZnO	SnO2	PbO
SI1	2.0	6.2	30.7	1.5	4.5	15.2	6.5	6.4	13.6	13.5
SI3	2.4	7.9	37.3	2.0	4.2	23.8	9.9	3.8	~	8.9
SI7	1.5	6.9	25.9	1.1	5.4	12.1	5.9	4.1	16.2	21.1
SI14	1.9	8.7	37.8	1.3	5.3	16.9	7.2	8.9	~	12.2
SI15	0.8	3.6	15.0	~	~	8.4	4.6	2.9	33.0	31.7
Average	**1.7**	**6.6**	**29.3**	**1.2**	**3.9**	**15.3**	**6.8**	**5.2**	**12.6**	**17.5**

Bulk area scans of sample 343B. Data has been normalised to 100 wt%.

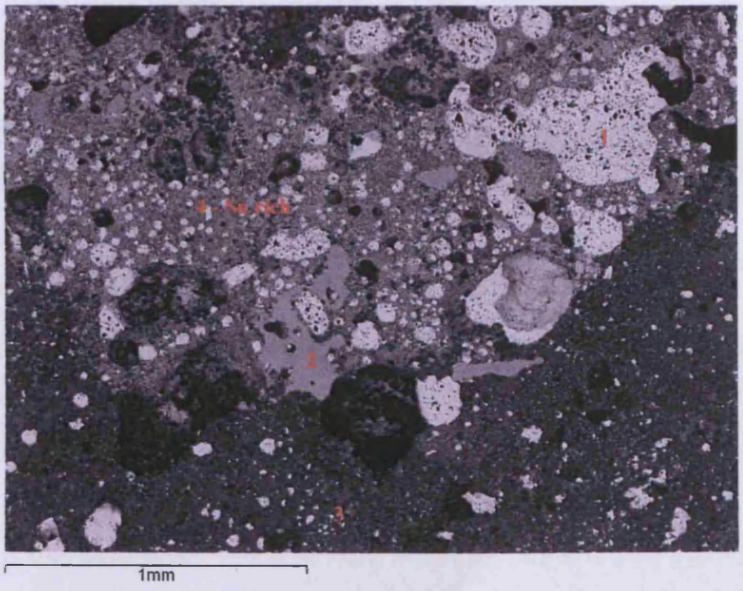

1 = Lead metal with Sn (11 at%)

Spectrum	Mg2O	Al2O3	SiO2	P2O5	K2O	CaO	FeO	ZnO	SnO2	PbO
2-tin oxide	~	0.6	0.7	~	~	~	1.5	0.2	96.1	0.9
3-darker region	2.4	7.7	36.8	3.0	5.5	21.1	9.3	5.1	~	9.0
4-lighter upper region	~	2.6	14.4	~	~	4.5	6.1	1.7	51.4	19.3

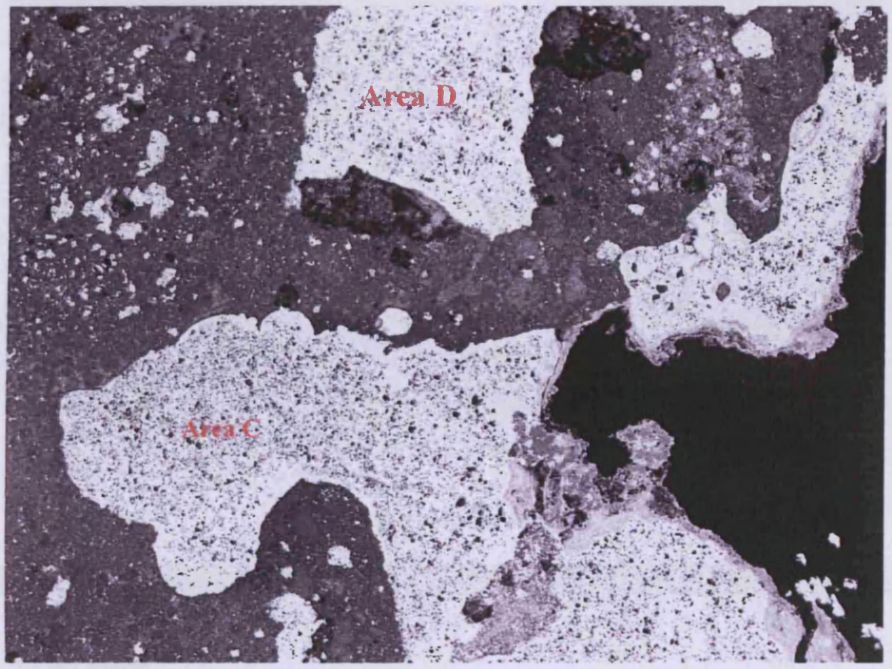

Large areas of lead metal was found inside the slag from sample 343B.

Scanned areas	Ag	Sn	Sb	Pb
Prill A	4.7	10.5	2.4	82.4
Prill B	6.6	6.7	3.8	82.9
Prill C	~	11.1	~	88.9
Area C	3.3	9.7	4.2	82.8
Area D	4.0	11.8	3.8	80.5
Area E	~	16.9	9.4	73.7

SEM-EDS analyses of metallic prills analysed within sample 343B. The data has been normalised to 100 at%.

Spectrum	MgO	Al2O3	SiO2	P2O5	K2O	CaO	FeO	SnO2	BaO	ZnO	PbO
Pyroxene (n=1)	5.5	5.5	38.3	~	0.4	33.4	2.3	~	~	9.2	5.3
Average leucite (n=3)	~	19.9	51.5	1.4	18.5	2.9	2.2	2.0	0.7	~	0.9

Pyroxenes and leucitic phases analysed in sample 343B. The data has been normalised to 100 wt%.

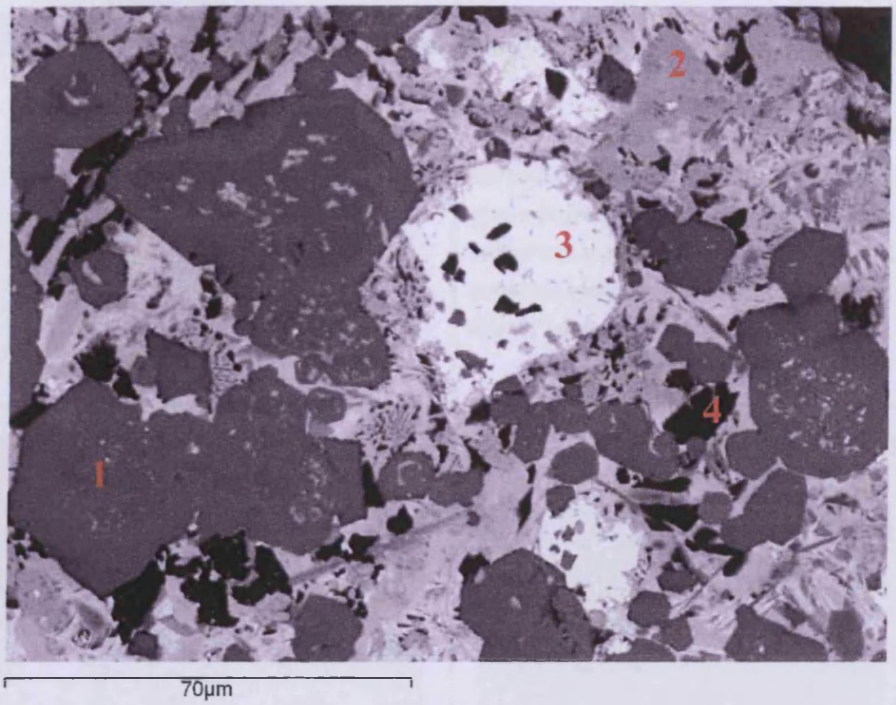

Area 3 – metallic lead

Spectrum	MgO	Al2O3	SiO2	K2O	CaO	FeO	SnO2	BaO	PbO
Area 1 - calcium tine silicate	0.7	7.4	12.4		24.9	8.8	44.0		1.8
Area 2 - tin oxide			1.0			1.1	95.8		2.1
Area 4 - leucite		21.0	54.6	19.6	0.8	2.0		1.0	1.1

UR ES 343C

a.

Sample 343C had a thick ceramic layer with a grey slag adhered (a). OM showed large quartz inclusions within the ceramic matrix (b). The slag contains inclusions of lead sulphide and lead metal, however it has very few prills (c).

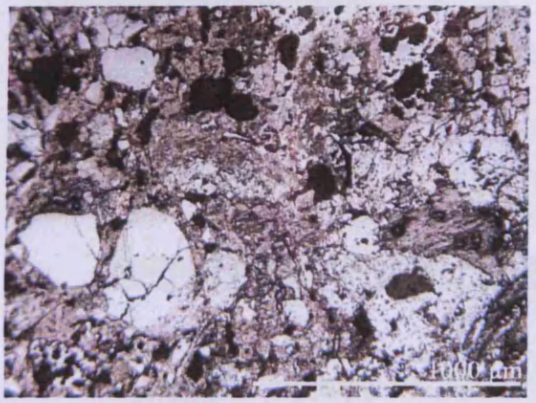

b.

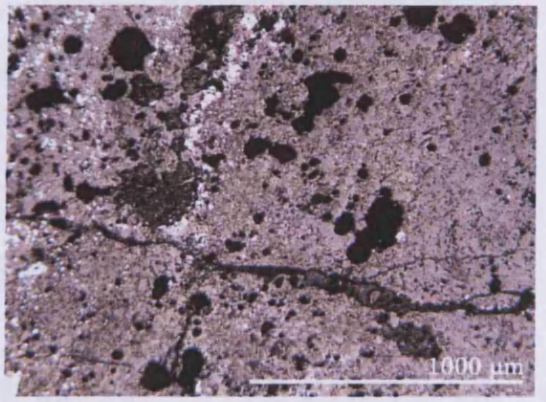

c.

SEM-EDS images and data

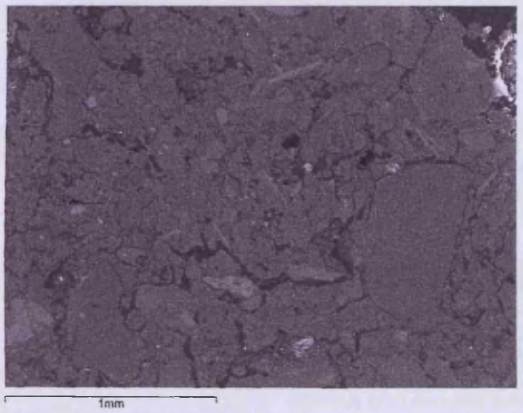

An SEM backscattered image of the ceramic in sample 343C.

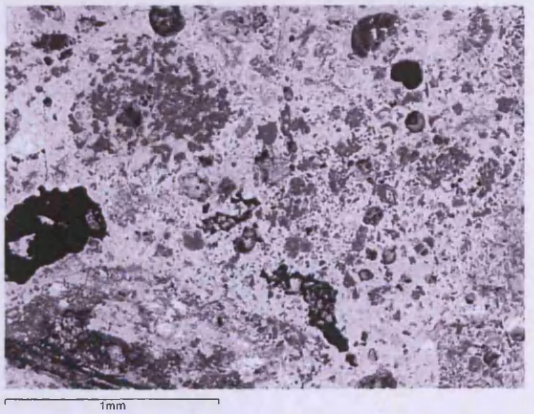

The slag layer on sample 343C. Different mineral phases analysed.

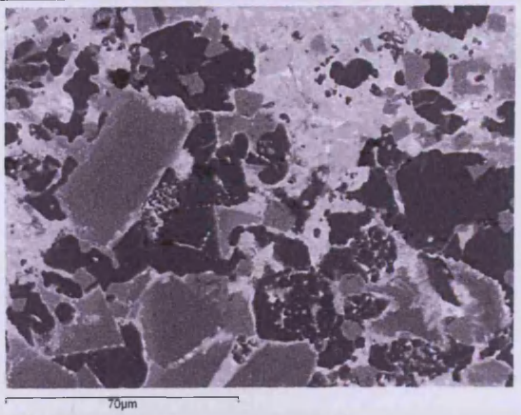

Leuctite and olivine were common in the slag.

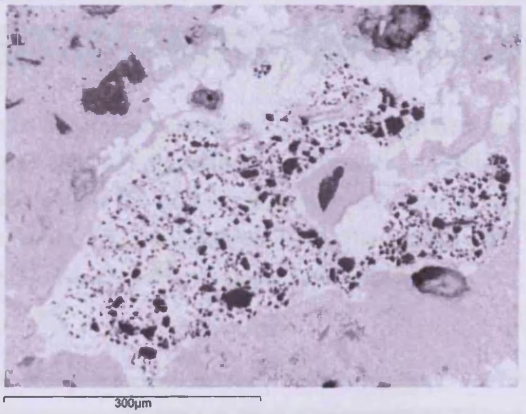

Small prills of Pb metal (3 at% Ag) and PbS.

Scanned area	MgO	Al2O3	SiO2	K2O	CaO	FeO	ZnO	PbO
1	1.3	6.2	22.1	3.2	8.5	3.3	4.9	50.5
2	1.4	5.4	22.0	2.6	9.9	3.7	5.8	49.2
3	0.9	2.9	14.0	~	5.1	2.4	1.4	73.3
Average (n=3)	**1.2**	**4.8**	**19.4**	**1.9**	**7.8**	**3.1**	**4.0**	**57.7**

Bulk area scan analyses of ES 343C. The data has been normalised to 100 wt%.

Scanned area	MgO	Al2O3	SiO2	K2O	CaO	FeO	ZnO	PbO
1	1.8	4.1	24.2	2.4	4.5	1.4	8.2	53.5
2	0.8	2.7	14.1	~	3.8	2.9	2.2	73.5
3	0.9	2.7	15.5	~	5.7	4.1	1.1	70.2
Average	**1.2**	**3.2**	**17.9**	**0.8**	**4.7**	**2.8**	**3.8**	**65.7**

Bulk area scans of the lead silicate matrix. The data has been normalised to 100 wt%.

Scanned area	Na2O	MgO	Al2O3	SiO2	K2O	CaO	TiO2	FeO	PbO
1	1.3	0.8	19.7	65.6	6.1	1.1	0.5	3.7	1.3
2	1.5	0.4	14.1	74.2	7.4	~	0.5	1.9	~
3	0.9	0.8	14.6	73.1	3.6	1.0	0.8	3.5	1.6
Average	**1.2**	**0.7**	**16.1**	**71.0**	**5.7**	**0.7**	**0.6**	**3.0**	**1.0**

SEM-EDS bulk area analyses of the ceramic in sample 343C.
The data has been normalised to 100 wt%.

Spectrum	Na2O	MgO	Al2O3	SiO2	K2O	CaO	FeO	ZnO	PbO
Olivines	~	3.6	2.7	39.1	0.3	32.4	1.6	14.6	5.7
Olivines	~	3.4	3.5	39.3	0.5	33.2	2.1	14.7	3.4
Leucite	0.3	~	21.8	55.1	21.5	~	0.5	~	0.8

Olivine and leucite were recorded in the sample.
The data has been normalised to 100 wt%.

Spectrum	Al	S	Ag	Pb
Area 1	14.1	~	3.0	82.9
Area 2	~	51.8	~	48.2

Metallic lead and lead sulphide were occasionally recorded in sample 343C.
The data has been normalised to 100 at%.

UR ES 343D

a.

The hand specimen of 343D appeared to be purely lead silicate adhered to a red ceramic (a). OM analysis of the ceramic layer grains of quartz and revealed a porous structure (b). The sample did however contain one large lead prill (c).

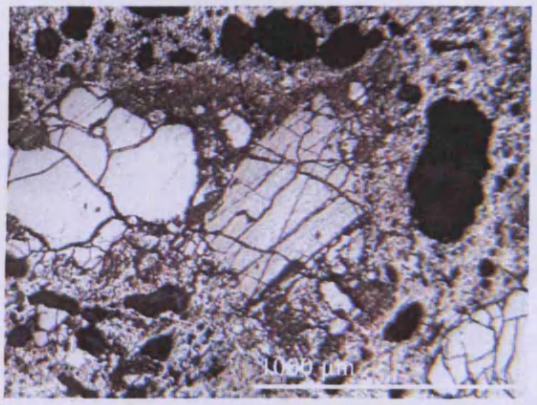

b.

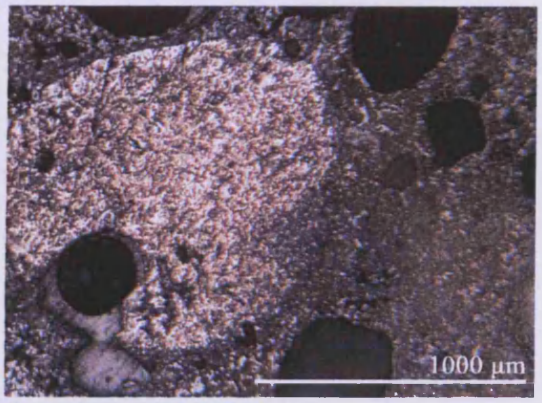

c.

SEM-EDS images and data

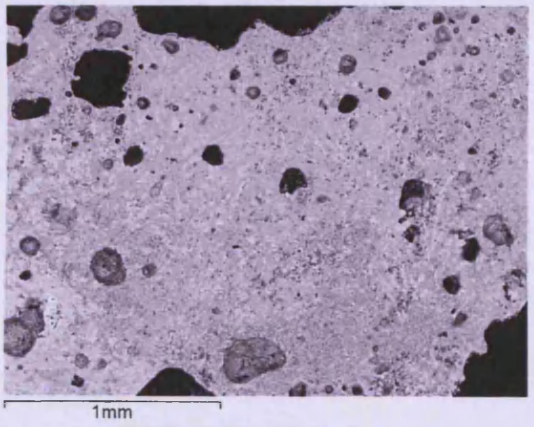

The lead silicate slag layer.

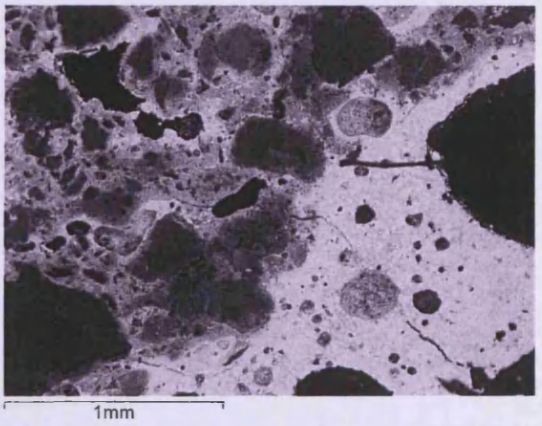

Ceramic grains being dissolved by the lead silicate.

Scanned area	MgO	Al2O3	SiO2	SO3	CaO	FeO	ZnO	As2O3	PbO
1	~	4.6	9.2	~	0.7	0.9	16.1	1.3	67.3
2	1.2	5.8	12.5	~	2.1	1.2	11.8	~	65.6
Average lead silicate (n=2)	**0.6**	**5.2**	**10.8**	**0.0**	**1.4**	**1.0**	**13.9**	**0.7**	**66.4**
Lead oxide	~	~	3.8	4.6	~	~	6.2	~	85.4
Lead oxide	~	~	3.2	5.2	0.6	~	3.9	1.8	85.4

Bulk area scans and lead oxide data from the SEM-EDS. The data has been normalised to 100 wt%.

Scanned area	Na2O	Al2O3	SiO2	K2O	FeO
Bulk area scan of the ceramic	0.9	13.2	79.0	6.0	0.9

A bulk area scan of the ceramic area in sample 343D.
The data has been normalized to 100 wt%.

Scanned area	MgO	Al2O3	SiO2	K2O	FeO	PbO
1	0.6	22.9	63.8	12.0	0.8	~
2	0.6	24.6	59.8	12.5	0.8	1.9

SEM-EDS area analyses of ceramic grains dissolving in the lead silicate (see image above), sample 343D. The data has been normalized to 100 wt%.

Combined data for UR ES

Glassy silicate matrix	Na2O	MgO	Al2O3	SiO2	P2O5	K2O	CaO	FeO	ZnO	As2O3	PbO
Average 343A (n=3)	~	2.3	4.2	27.6	0.9	5.4	5.2	5.5	22.8	0.3	25.6
343B (n=1)	0.9	~	1.7	18.2	~	~	2.4	3.2	~	0.9	72.8
Average 343C (n=3)	~	1.2	3.2	17.9	~	0.8	4.7	2.8	3.8	~	65.7

SEM-EDS area analyses of the glassy matrix of sample UR ES.
The data has been normalised to 100 wt%.

Area analyses	Na2O	MgO	Al2O3	SiO2	K2O	CaO	TiO2	FeO	PbO
Average 343C (n=3)	1.2	0.7	16.1	71.0	5.7	0.7	0.6	3.0	1.0
343D (n=1)	0.9	~	13.2	79.0	6.0	~	~	0.9	~

Ceramic bulk SEM-EDS area analyses of furnace wall sample 343C/D.
The data has been normalised to 100 wt%.

Area analysis	MgO	Al2O3	SiO2	K2O	CaO	FeO	ZnO	PbO
Average 343A (n=3)	2.7	2.5	37.1	0.3	32.9	1.4	19.9	3.2
343B (n=1)	5.5	5.5	38.3	0.4	33.4	2.3	9.2	5.3
Average 343C (n=2)	3.5	3.1	39.2	0.4	32.8	1.8	14.7	4.5

Olivines found and are analysed via SEM-EDS in the UR ES samples.
The data has been normalised to 100 wt%.

Area analysis	Na2O	Al2O3	SiO2	P2O5	K2O	CaO	FeO	SnO2	BaO	PbO
Average 343B (n=3)	~	19.9	51.5	1.4	18.5	2.9	2.2	2.0	0.7	0.9
343C (n=1)	0.3	21.8	55.1	~	21.5	~	0.5	~	~	0.8

Leucite in UR ES samples, area analysed via SEM-EDS.
The data has been normalised to 100 wt%.

URUQUILLA WEST SADDLE (UR WS)

UR WS 342A

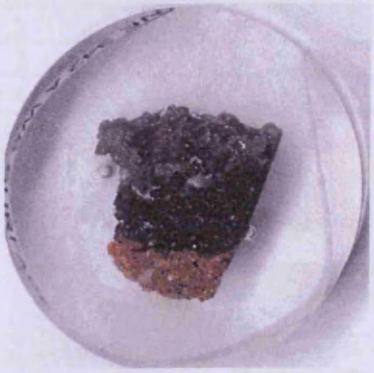

a.

a. Sample WS 342A mounted in epoxy resin. A huayrachina wall ceramic with a layer of black slag adherred.
b. The WS 342A slag matrix which is composed of metallic lead prills (yellow) and numerous silicate phases.
c. OM image of ceramic wall. The silicate slag has partially dissolved the ceramic.
d. This OM image shows the large quantities of zinc sulphide (light grey) which was recorded in WS342A. The areas of zinc sulphide generally have lead sulphide halos.
e. OM image of partially molten lead sulphide in a zinc sulphide matrix. (SI10 SEM image).

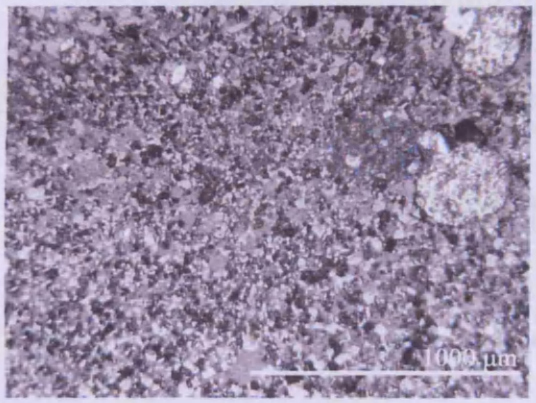

b.

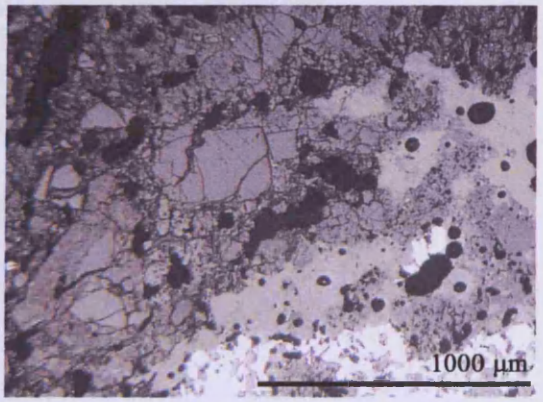

c.

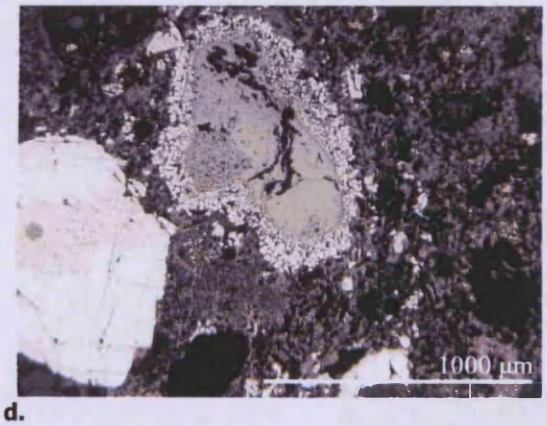

d.

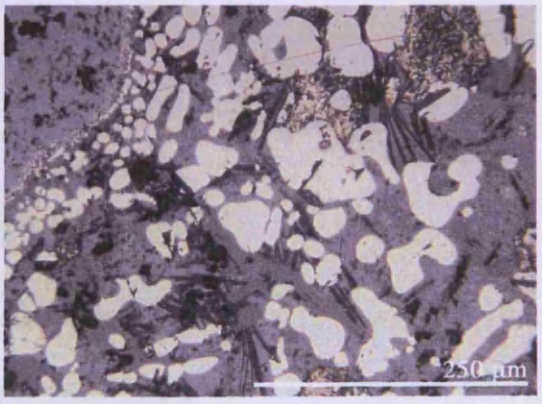

e.

Spectrum	S	Fe	Zn	Pb
Zinc sulphide	47.9	1.7	50.3	~
Lead sulphide	50.1	~	~	49.9
Lead metal	~	~	~	100.0

Spectrum	Al2O3	SiO2	FeO	ZnO	PbO
Area below zinc sulphide	2.4	5.4	21.2	11.4	59.8

Area scanned	Na2O	Al2O3	SiO2	SO3	K2O	CaO	FeO	ZnO	PbO
1	1.2	~	9.6	5.6	~	2.6	11.2	3.8	66.0
2	~	~	4.9	14.3	~	1.1	5.8	6.2	67.7
3	~	1.5	7.4	10.8	~	1.6	8.0	2.8	68.0
4	~	2.5	12.0	18.5	1.0	3.6	10.5	~	51.9
5	~		10.1	13.1	~	~	2.0	~	74.8
Average (n=5)	**0.2**	**0.8**	**8.8**	**12.4**	**0.2**	**1.8**	**7.5**	**2.6**	**65.7**

The bulk area compositions of sample WS 342A.
The data has been normalised to 100 wt %.

Area	Na2O	Al2O3	SiO2	K2O	PbO
1	0.6	12.8	74.8	9.7	2.0

Leucite minerals analysed in sample WS 324A using SEM-EDS area analysis.
The data has been normalised to 100 wt %.

Area	MgO	Al2O3	CaO	FeO	ZnO	AS2O3	PbO
1	~	1.4	0.7	93.7	2.6	~	1.6
2	0.7	1.3	0.5	94.5	2.4	0.6	~

Iron oxide phases found in sample WS 342A (area analysis).
The data has been normalised to 100 wt %.

Area	MgO	Al2O3	SiO2	CaO	FeO	ZnO	PbO
1	3.8	3.1	33.3	24.0	3.0	13.2	19.6
2	3.4	3.4	32.1	23.8	4.5	15.8	17.1

Lead zinc calcium silicates found in sample WS 342A (area analysis).
The data has been normalised to 100 wt %.

Area	MgO	Al2O3	SiO2	CaO	FeO	ZnO	PbO
1	3.2	~	17.9	0.7	1.3	18.5	58.4
2	3.1	~	19.2	0.9	0.9	19.3	56.7
3	2.7	0.9	18.2	1.2	2.0	17.7	57.4

Lead zinc silicates (mid grey) found in sample WS 342A (area analysis).
The data has been normalised to 100 wt %.

Area	Al2O3	SiO2	CaO	FeO	PbO
1	0.8	17.6	8.6	2.0	71.1

Lead calcium silicate found in sample WS 342A (area analysis).
The data has been normalised to 100 wt %.

Area	SiO2	FeO	Sb2O3	PbO
1	13.4	3.5	1.6	81.4
2	4.7	2.3	1.8	91.3

Lead silicate matrix analysed in sample WS 342A (area analysis).
The data has been normalised to 100 wt %.

Area	Ag	Pb
Area 1	7.7	92.4
Area 2	7.4	92.7
SI16 2	13.7	86.3
SI17 1	10.0	90.0

Lead prills analysed in WS 342A (area analysis).
The data has been normalised to 100 at%

Area	S	Pb
1	50.4	49.6
2	52.4	47.6
3	16.6	83.4

Lead sulphide analysed in sample WS 342A. The data has been normalised to 100 at%.

UR WS 342B

a.

a. Sample WS 342B cut and mounted in epoxy resin.
b. OM images lead metal prill with a lead sulphide halo.
c. OM image silicates forming in the slag. Lead sulphide in the right hand corner (white).
d and e. SEM images of the bulk area scans of sample WS 342B.
f. In this SEM image the different phases recorded in the slag matrix can be seen: luecite (black silicates), pyroxenes (mid grey), lead sulphide (brightest white phase).
g. Metallic lead prill with a lead sulphide halo (see OM image b).

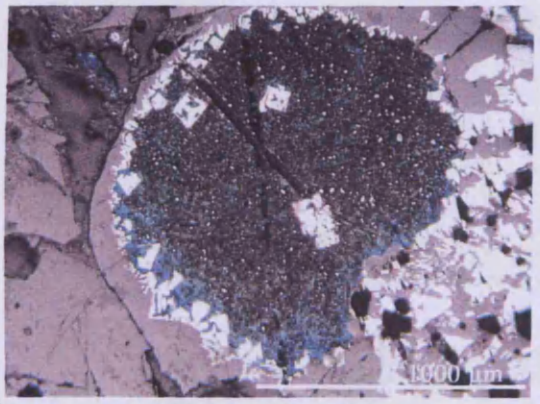

b.

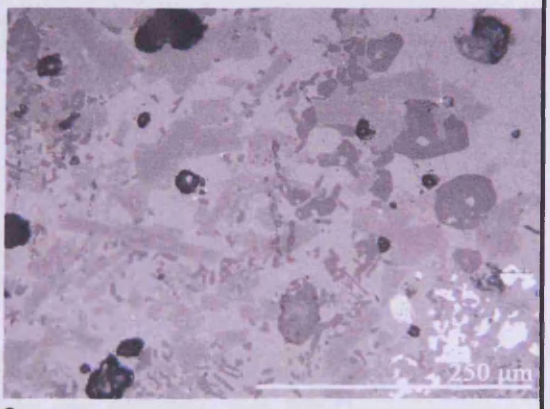

c.

SEM-EDS images

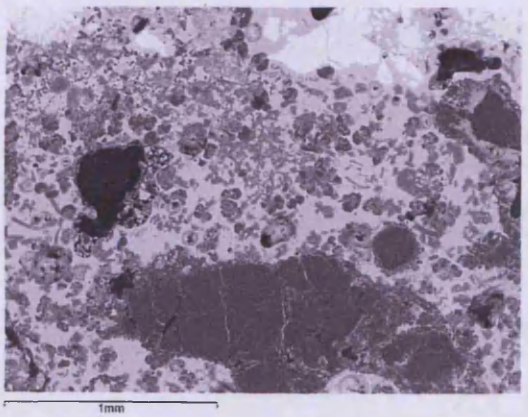

d.

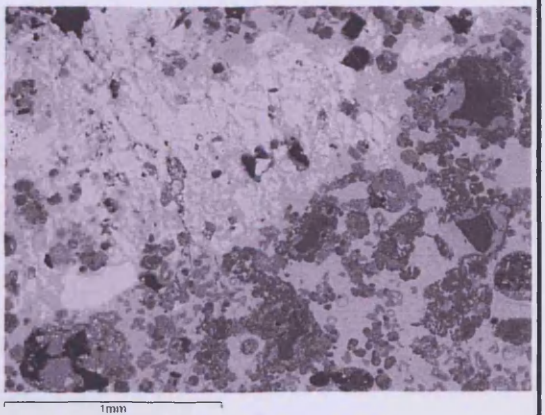

e.

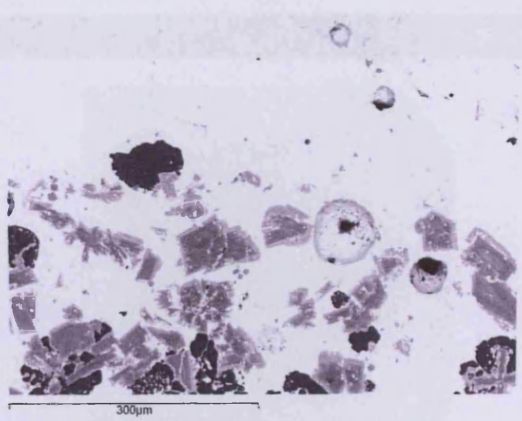

f.

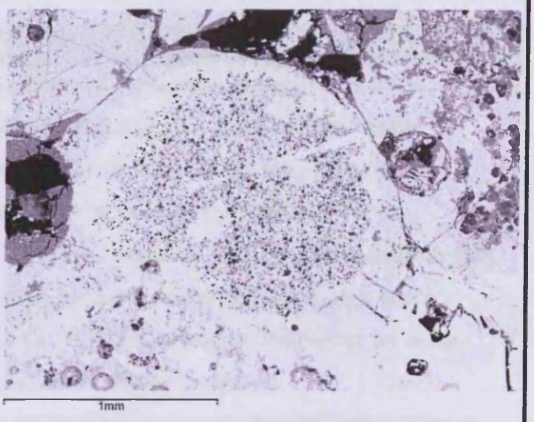

g.

SEM-EDS data

Spectrum	Na2O	MgO	Al2O3	SiO2	SO3	K2O	CaO	FeO	ZnO	PbO
1	1.2	0.9	10.9	39.1	~	4.8	2.7	2.9	2.9	34.7
2	1.3	~	9.9	36.8	~	4.8	2.6	2.5	2.0	40.1
3	~	~	5.6	23.5	7.2	3.9	3.8	2.1	3.8	50.2
4	~	~	4.0	15.1	7.3	1.5	3.0	2.8	7.9	58.5
5	~	1.2	9.3	34.3	~	5.7	6.9	1.6	5.6	35.3
Average (n=5)	**0.5**	**0.4**	**7.9**	**29.8**	**2.9**	**4.1**	**3.8**	**2.4**	**4.4**	**43.7**

Bulk area compositions. The data has been normalised to 100 wt%.

Spectrum	Na2O	MgO	Al2O3	SiO2	K2O	CaO	FeO	ZnO	PbO
Si6 1	1.0	~	4.9	22.1	0.6	1.9	2.1	2.0	65.5
SI10 4	~	1.0	4.6	20.3	0.9	1.3	2.0	3.9	66.0
Average (n=2)	**0.5**	**0.5**	**4.8**	**21.2**	**0.8**	**1.6**	**2.0**	**3.0**	**65.8**

Lead silicate matrix, data has been normalised to 100 wt%.

Spectrum	Na2O	Al2O3	SiO2	K2O	FeO	PbO
SI6 2	0.9	17.4	66.1	15.6	~	~
SI10 2	~	21.9	55.4	20.9	0.7	1.2
Average (n=2)	**0.4**	**19.6**	**60.7**	**18.3**	**0.3**	**0.6**

Pyroxenes (mid grey)

Spectrum	MgO	Al2O3	SiO2	K2O	CaO	FeO	ZnO	PbO
SI10 3	4.2	3.2	38.4	0.4	31.3	1.0	13.6	7.9

Zinc silicate

Spectrum	Al2O3	SiO2	K2O	FeO	PbO
SI9 3	22.2	56.2	20.9	~	0.8
SI10 2	21.9	55.4	20.9	0.7	1.2

Luecite (black silicates)

Spectrum	S	Pb
SI8 1	44.8	55.2
SI8 2	~	100.0
SI10 1	27.8	72.2

Lead sulphide and lead metal recorded. Data has been normalised to 100 at%.

UR WS 342C

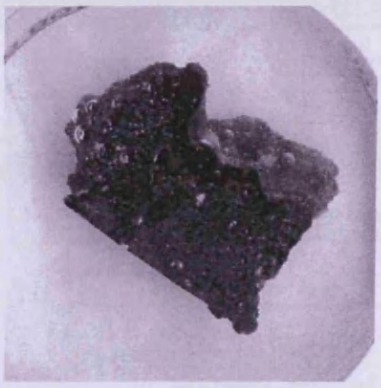

a.

a. *Huayrachina* slag sample WS 342C, shown here in the epoxy resin block.
b. An OM image of the slag body with inclusions of lead sulphide (white).
c. An OM image of lead sulphide which has only partially reacted during the smelt.
d. An SEM-EDS images showing an area used for bulk area scans.
e. SEM-EDS image of the different phases present in WS 342C.

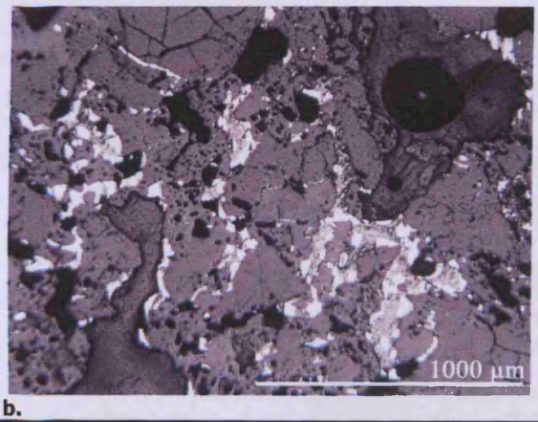

b.

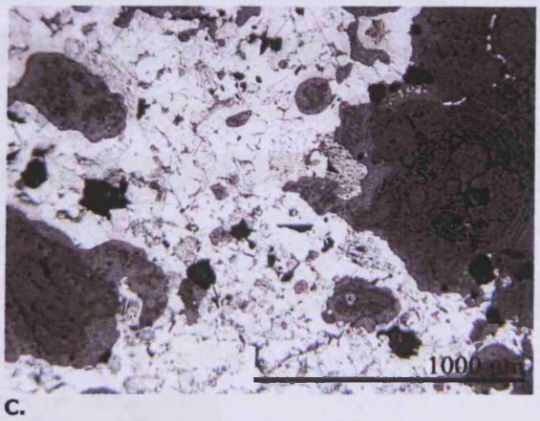

c.

SEM-EDS images

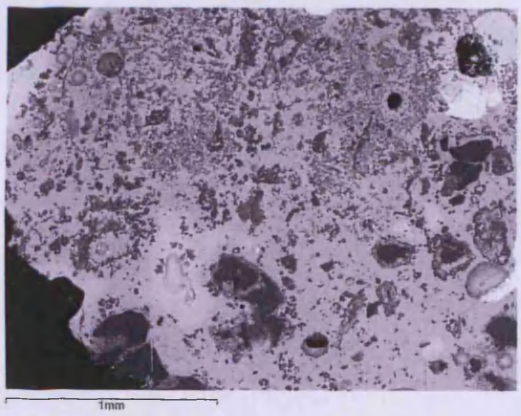

d.

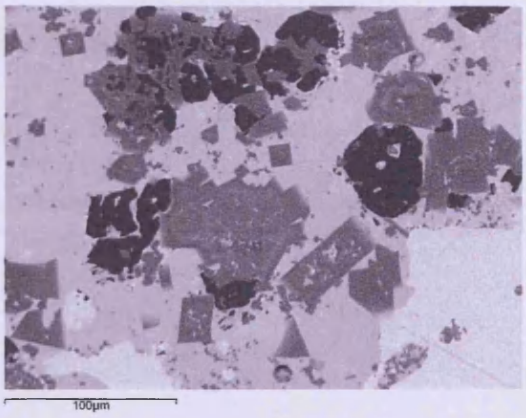

e.

SEM-EDS data

Scanned areas	MgO	Al2O3	SiO2	SO3	K2O	CaO	FeO	ZnO	PbO
1	1.5	9.3	35.7	~	4.8	6.1	6.2	5.5	30.9
2	1.2	7.9	26.4	~	4.5	8.3	4.5	7.8	39.4
3	1.0	5.4	18.6	9.3	1.6	5.8	3.8	24.9	29.7
Average (n=3)	**1.3**	**7.5**	**26.9**	**3.1**	**3.6**	**6.7**	**4.8**	**12.7**	**33.4**

Bulk area scans of slag sample WS 342C. The data has been normalised to 100 wt%.

Scanned areas	Na2O	MgO	Al2O3	SiO2	P2O5	K2O	CaO	FeO	ZnO	PbO
1	1.1	~	3.4	18.8	~	0.8	1.3	3.4	3.1	68.1
2	~	1.7	5.3	28.3	1.4	0.7	4.1	6.4	5.7	46.5
3	~	1.1	3.8	20.8	~	0.8	1.7	4.3	5.6	62.0
Average (n=3)	**0.4**	**0.9**	**4.1**	**22.6**	**0.5**	**0.7**	**2.4**	**4.7**	**4.8**	**58.9**

Lead silicate area scans. The data has been normalised to 100 wt%.

Scanned areas	Na2O	Al2O3	SiO2	K2O	FeO	ZnO	PbO
1	0.4	21.7	55.9	20.3	0.9	~	0.9
2	0.6	20.0	54.2	18.6	2.0	1.5	2.9
3	~	21.9	56.5	20.9	~	0.7	~
Average (n=3)	**0.3**	**21.2**	**55.5**	**19.9**	**1.0**	**0.7**	**1.3**

Scanned areas of leucite present in sample 342C.
The data has been normalised to 100 wt%.

Scanned area	MgO	Al2O3	SiO2	K2O	TiO2	FeO	PbO
SI3	9.2	16.1	36.9	9.4	4.7	21.6	2.1

Iron silicates were found in slag sample 342C. The data has been normalised to 100 wt%.

Scanned areas	MgO	Al2O3	SiO2	K2O	CaO	FeO	ZnO	PbO
1	2.8	1.9	36.5	~	27.3	1.4	15.8	14.3
2	3.2	2.5	38.3	0.2	30.0	3.1	15.0	7.7
3	3.4	3.9	36.6	0.3	28.4	2.2	12.0	13.2
Average (n=3)	**3.2**	**2.8**	**37.2**	**0.2**	**28.6**	**2.2**	**14.2**	**11.7**

Scanned area of pyroxenes present in sample 342C.
The data has been normalised to 100 wt%.

Spectrum	SiO2	FeO	ZnO
SI7 2	28.2	3.3	68.5

Zinc silicates found in 342C. The data has been normalised to 100 wt%.

Spectrum	S	Fe	Zn	Pb
Si7 1	49.6	0.8	49.6	~
Si7 3	47.7	~	10.8	41.5

Lead metal and lead sulphide were found in sample WS 342C. The data has been normalised to 100 wt%.

UR WS 342E

a.

a. The mounted WS 342E sample. Note the three layered structure: ceramic body, lead sulphide (sandwiched in the centre) and lead slag (above).
b. An OM image of the ceramic layer.
c. An OM images of the upper slag layer.

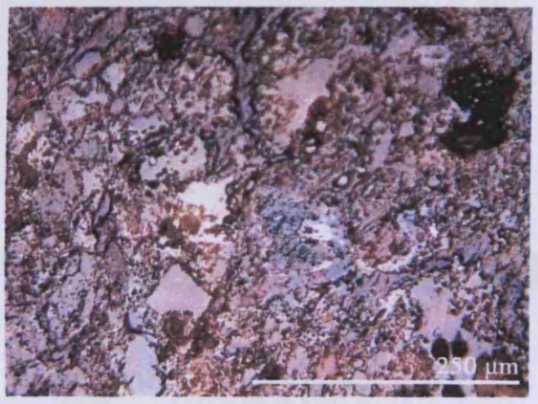

b.

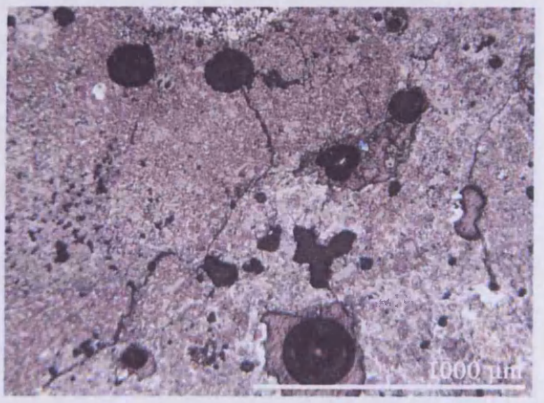

c.

SEM-EDS images

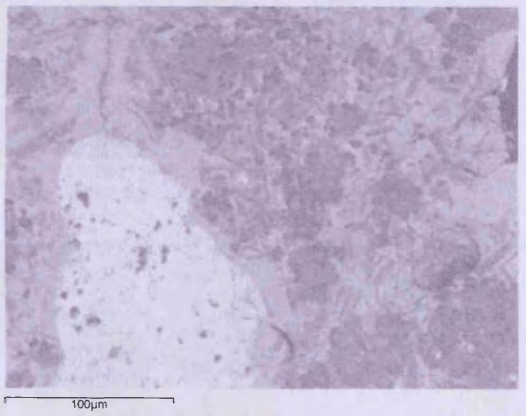

A large metallic prill incide slag 342E.

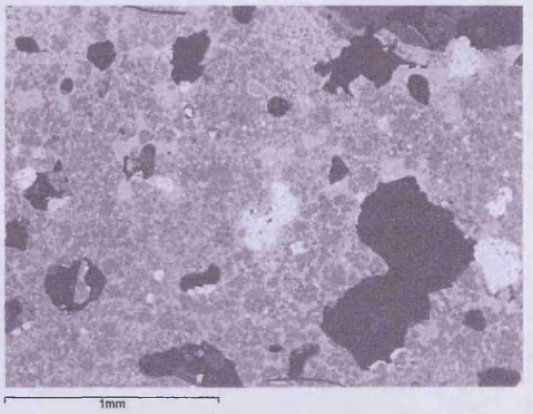

A bulk area scan of the sample 342E.

UR WS 342F

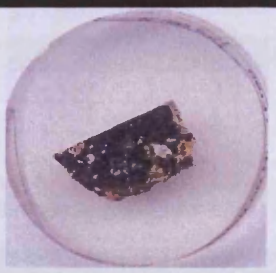

a.

a. A cut and mounted section of sample WS 342F.

b. An OM image of sample WS342F, the siliceous lead slag partially dissolving the ceramic matrix.

c. An OM image of the slag matrix.

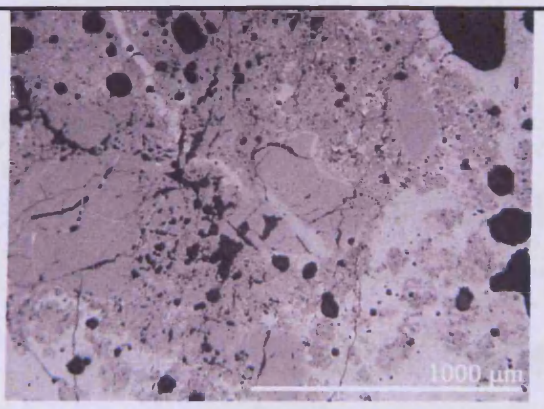

b.

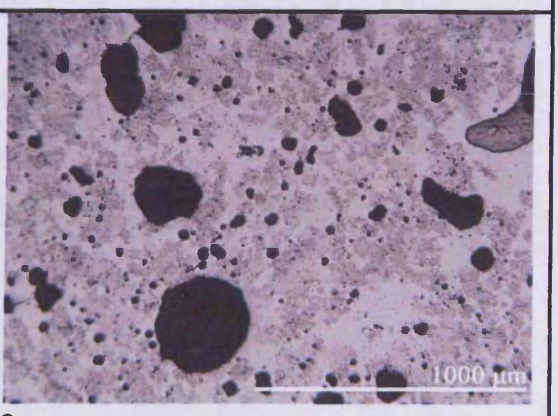

c.

SEM-EDS images:

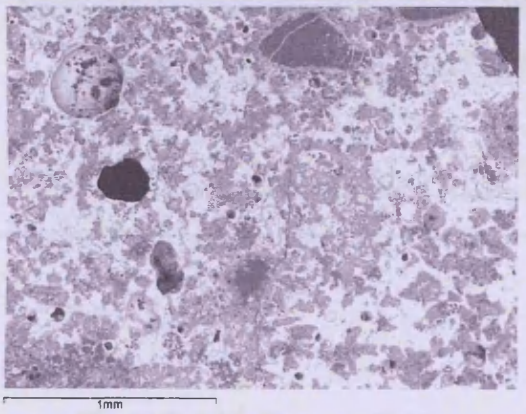

The bulk area of sample 342F.

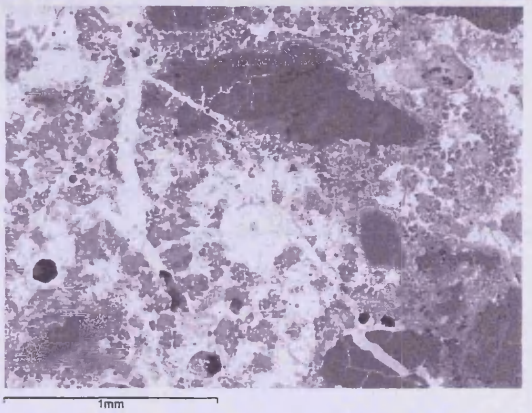

The bulk area of sample 342F with the silicate dissolving leucitic phases.

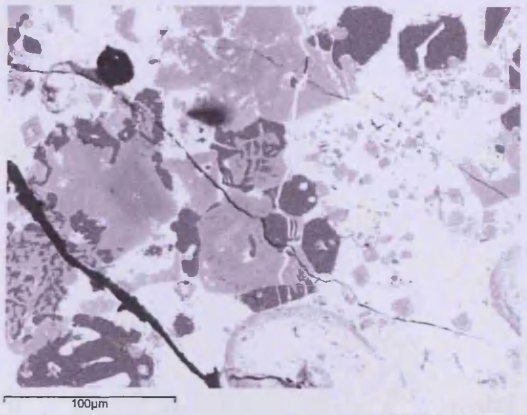

The lead silicate matrix (white)with leucite (black), and pyroxenes (mid grey).

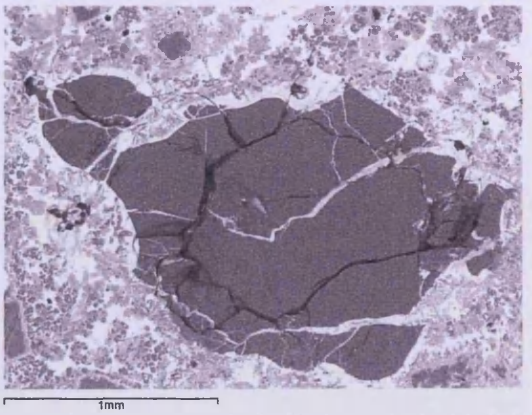

SEM-EDS data

Scanned area	Na2O	MgO	Al2O3	SiO2	P2O5	K2O	CaO	FeO	ZnO	PbO
1	1.3	0.9	10.3	44.8	~	6.4	4.8	2.9	4.2	24.3
2	~	1.4	8.3	33.8	1.3	4.1	9.7	4.1	8.1	29.2
3	1.8	7.7	32.6	1.1	~	4.2	10.7	4.2	8.5	29.4
Average	**1.0**	**3.3**	**17.1**	**26.6**	**0.4**	**4.9**	**8.4**	**3.7**	**6.9**	**27.6**

Bulk area scans of sample WS 342F. The data has been normalised to 100 wt%.

Scanned area	MgO	Al2O3	SiO2	K2O	CaO	FeO	ZnO	Sb2O3	PbO
1	1.2	4.0	23.3	0.6	0.9	2.3	6.0	~	61.3
2	~	4.0	23.4		1.7	2.1	5.9	3.3	59.5
3	1.1	4.5	26.6	1.0	1.4	3.2	5.5	~	56.8
Average	**0.8**	**4.2**	**24.4**	**0.5**	**1.3**	**2.5**	**5.8**	**1.1**	**59.2**

Scanned area analyses of the lead silicate in sample WS 342F. The data has been normalised to 100 wt%.

Scanned area	Na2O	MgO	Al2O3	SiO2	K2O	CaO	FeO	PbO
1	2.1	0.6	15.4	71.2	5.2	1.7	1.7	2.1

Bulk area analysis of the ceramic layer found in sample WS 342F. The data has been normalised to 100 wt%.

Scanned areas	Na2O	Al2O3	SiO2	K2O	FeO
1	0.5	21.9	56.4	20.6	0.6
2	0.7	21.9	56.4	20.6	0.5
3	0.5	21.6	56.5	21.0	0.4

Area analyses of leucite within sample 342F. The data has been normalised to 100 wt%.

Scanned area	MgO	Al2O3	SiO2	K2O	CaO	FeO	ZnO	PbO
1	3.0	5.0	37.9	0.3	30.2	1.9	16.5	5.3
2	2.8	3.3	39.2		30.1	1.2	15.2	8.1
3	2.9	3.4	39.0	0.3	31.7	1.3	15.2	6.1

Pyroxenes in sample 342F. The data has been normalized to 100 wt%.

UR WS 342G

a.

a. Sample WS 342G. Note the small ceramic area to which a thick slag layer is adhered.
b. An OM image of the ceramic layer seen in image a. The ceramic contains large quartz crystals.
c. An OM image of the silicate layer and the different phase.

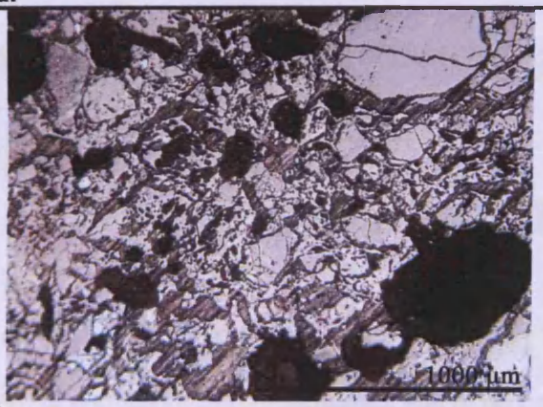

b.

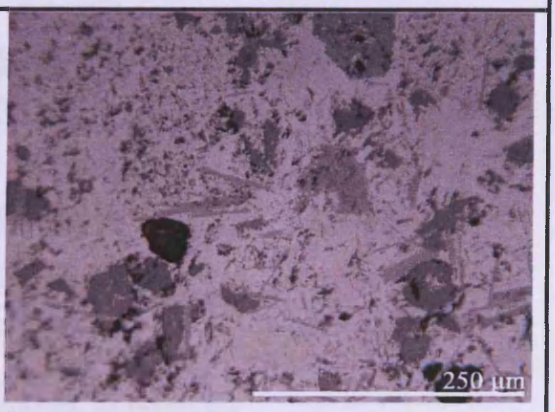

c.

SEM-EDS images and data

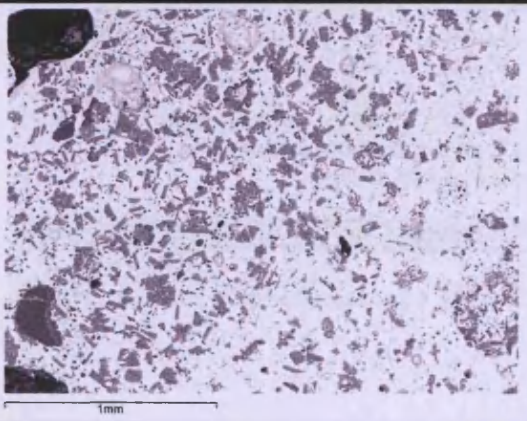

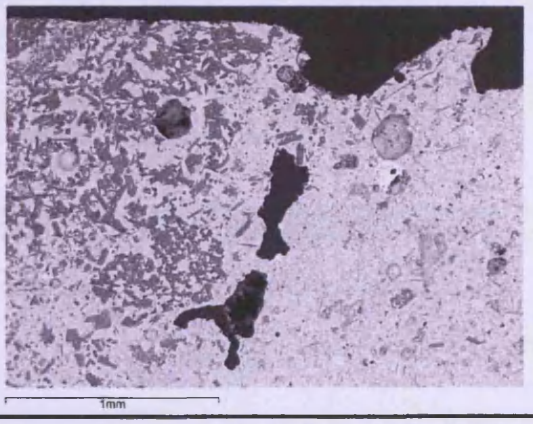

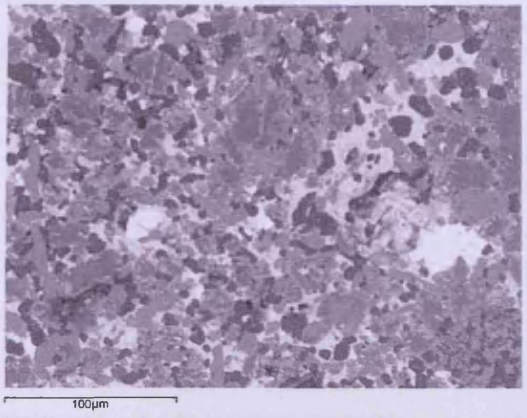

Scanned areas	Mg2O	Al2O3	SiO2	K2O	CaO	FeO	ZnO	PbO
1	1.4	4.8	20.7	2.3	7.6	2.7	4.1	56.4
2	1.6	6.1	25.2	4.0	12.8	3.4	3.8	43.2
3	1.0	3.9	16.6	0.8	5.2	2.4	2.9	67.3
4	1.3	5.1	21.5	2.7	9.3	2.2	3.8	54.2
5	1.1	5.8	21.9	0.7	11.3	4.7	16.3	38.2
Average (n=5)	**1.3**	**5.1**	**21.2**	**2.1**	**9.2**	**3.1**	**6.2**	**51.9**

Bulk area analyses of sample WS 342G. The data has been normalised to 100 wt%.

Scanned area	Al2O3	SiO2	CaO	FeO	ZnO	PbO
1	1.8	16.5	4.2	4.7	~	72.7
2	2.6	16.3	1.9	4.5	0.7	73.9
Average (n=2)	**2.2**	**16.4**	**3.0**	**4.6**	**0.4**	**73.3**

Scanned area analyses of the lead silicate within sample WS 342G. The data has been normalised to 100 wt%.

Spectrum	Na2O	MgO	Al2O3	SiO2	K2O	CaO	TiO2	FeO
Bulk area scan ceramic	1.1	0.7	18.4	68.5	5.3	0.9	1.0	4.2
Phase –feldspar	2.3	~	18.0	67.2	12.5	~	~	~
Silica oxide phases	0.3	~	7.2	90.5	1.5	~	~	0.4

Spectrum	Na2O	Al2O3	SiO2	K2O	CaO	FeO	PbO
1	0.7	26.8	37.7	26.7	2.0	1.5	4.6
2	0.5	30.0	39.5	29.1		0.9	
3	0.4	20.2	52.5	19.0	3.8	2.5	1.7
Average (n=3)	**0.6**	**25.6**	**43.2**	**25.0**	**1.9**	**1.6**	**2.1**

Scanned area analyses of leucite in sample WS 342G. The data has been normalised to 100wt%.

Spectrum	Mg2O	Al2O3	SiO2	K2O	CaO	FeO	ZnO	PbO
1	5.3	4.4	39.7	0.7	33.0	2.4	8.3	6.2
2	5.0	3.0	39.9	0.4	31.2	1.1	10.9	8.5
3	5.3	~	29.4	~	~	4.8	60.6	~
Average (n=3)	**5.2**	**2.5**	**36.3**	**0.4**	**21.4**	**2.7**	**26.6**	**4.9**

Scanned area analyses of pyroxene in sample WS 342G. The data has been normalised to 100wt%.

Spectrum	MgO	Al2O3	SiO2	P2O5	K2O	CaO	FeO	ZnO	PbO
Zinc rich silicates	2.2	7.3	28.8	1.2	2.9	13.0	7.4	26.9	10.5

Zinc silicates in the slag sample 342G. The data has been normalised to 100 wt%.

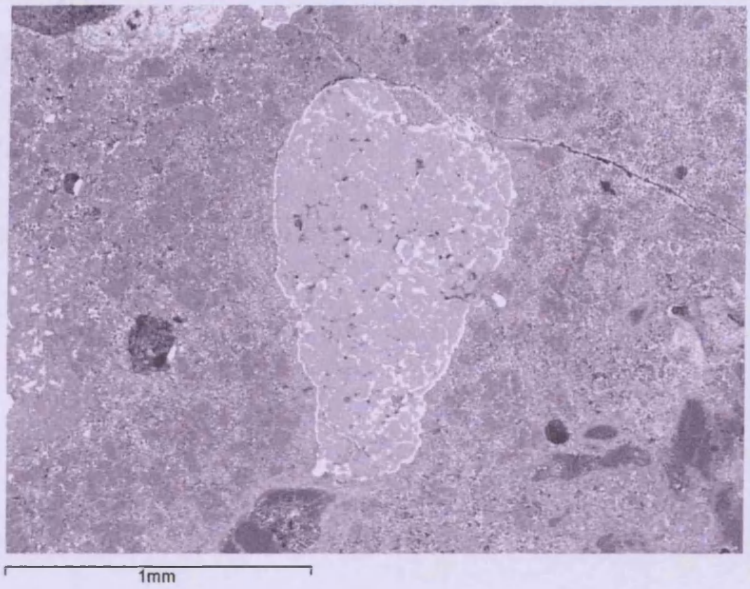

Spectrum	Si	S	Fe	Zn	Pb
Spot scan of ZnS rich area	~	47.8	2.2	49.2	0.9
Bulk area scan	0.9	47.3	2.4	47.6	1.9

Gangue area of zinc sulphide. The data has been normalized to 100 at%.

Area scanned	Na2O	MgO	Al2O3	SiO2	SO3	P2O5	K2O	CaO	FeO	ZnO	PbO
WS 342A (n=5)	0.2	~	0.8	8.8	12.4	~	0.2	1.8	7.5	2.6	65.7
WS 342B (n=5)	0.5	0.4	7.9	29.8	2.9	~	4.1	3.8	2.4	4.4	43.7
WS 342C (n=3)	~	1.3	7.5	26.9	3.1	~	3.6	6.7	4.8	12.7	33.4
WS 342F (n=3)	1.0	3.3	17.1	26.6	~	0.4	4.9	8.4	3.7	6.9	27.6
WS 342G (n=5)	~	1.3	5.1	21.2	~	~	2.1	9.2	3.1	6.2	51.9

Bulk area analyses UR WS slag samples. The data has been normalised to 100 wt%.

APPENDIX VI - ARCHAEOLOGICAL EUROPEAN FURNACES: DRAGON

DON MARTIN'S DRAGON (DMD)

DMD furnace

Side view (note the two holes used to access the the reaction hearth)

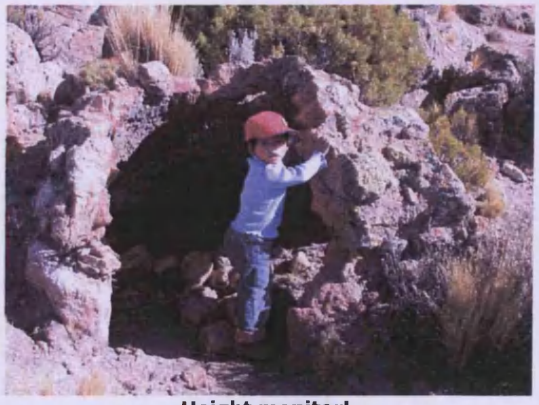

Height monitor!

The chimney.

View of the firebox through the DMD furnace.

The surrounding countryside, view from above the DMD site (Porco is in the horizon).

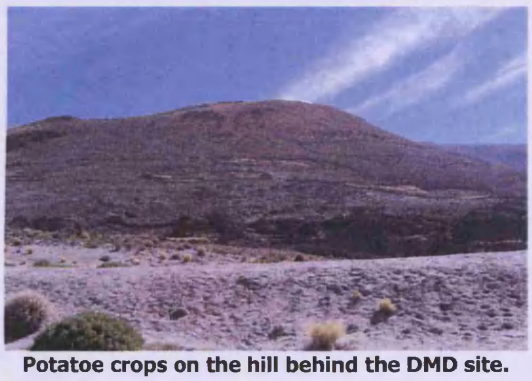

Potatoe crops on the hill behind the DMD site.

Possible domed furnace pieces – scattered around the site.

Sketches of DMD furnace

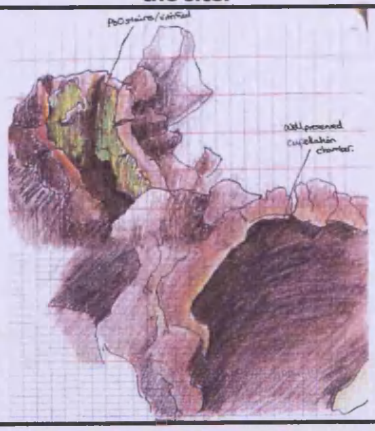

DMD SAMPLES

Date of sample collection	Sample number	Description
06.07.05	**341A**	Dark black heavy slag Vitrieous without inclusions Deep ripples/flow on the top surface
06.07.05	**341B**	Red chunky cermic coated in a lead oxide vitrification.
06.07.05	**341C**	Grey stone layer with a thin coating of lead oxide
06.07.05	**341D**	Most likely a sample of fine soil similar to un-reacted furnace wall or lining

DMD sample 341A slag

a.

The slag from the DMD furnace is extremely glassy (a) indicating that it was created in a furnace that could generate high temperatures sufficient to fully melt the charge. OM analyses showed that the slag has very few mineral inclusions (b and C).

The chemical analyses have shown that the slag contains 60% lead oxide and 22% silica. Very small quantities of lead sulphide in the slag show that conditions must have been highly oxidising. A metallic prill analysed contains silver in a lead matrix, surrounded by a halo of lead sulphide (image b and data below).

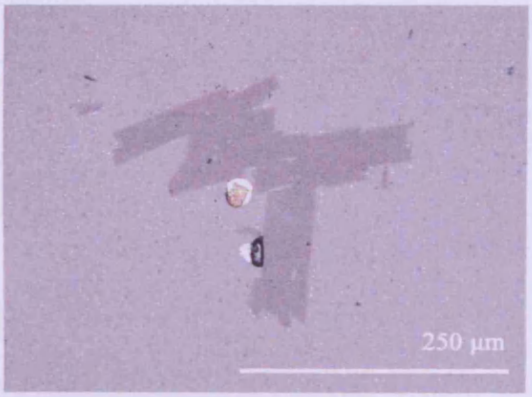

b.

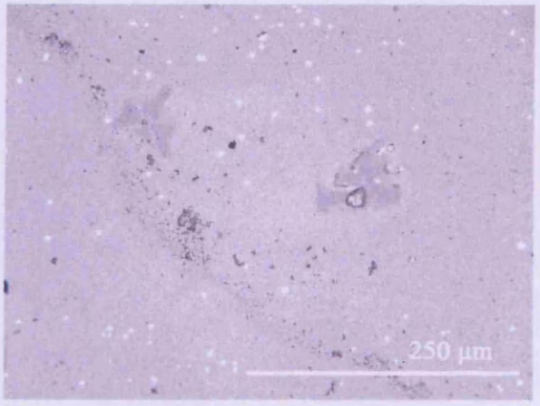

c.

SEM-EDS images and data

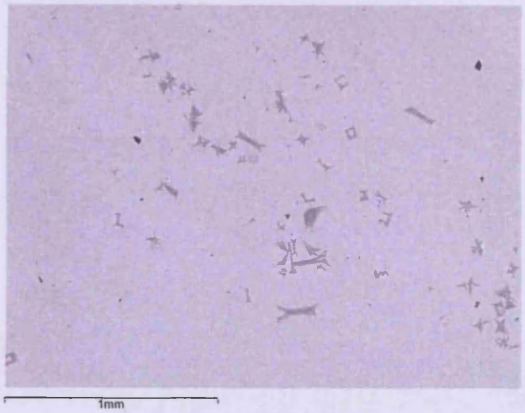

The glassy slag matrix.

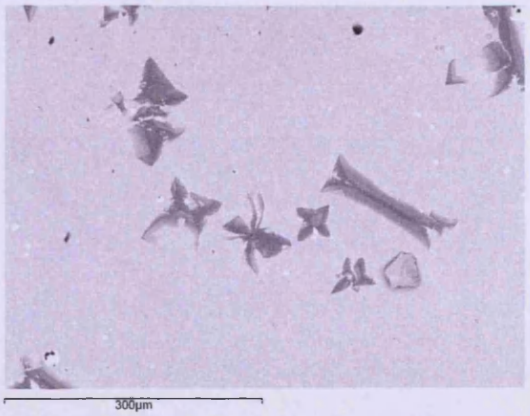

Feldspars in the glassy slag matrix.

Scanned area	MgO	Al2O3	SiO2	K2O	CaO	FeO	ZnO	PbO
Average (n=5)	0.4	2.8	22.2	1.2	4.2	3.2	5.9	60.1

Bulk scanned areas of DMD slag sample 341 (x50 mag, whole area scan).
The data has been normalised to 100 wt%.

Scanned area	S	Zn	Ag	Pb
1	48.1	2.1	~	49.8
2	~	~	7.8	92.2

SEM-EDS area analyses of metallic prills found in the DMD slag sample 341. The has been normalised to 100 at%.

Scanned area	MgO	Al2O3	SiO2	CaO	FeO	ZnO	PbO
1	1.9	1.2	35.8	27.1	1.2	17.2	15.8
2	2.1	1.9	35.2	26.0	1.4	15.6	17.8
3	1.9	2.0	33.6	24.6	1.5	15.6	20.8
4	1.8	1.7	35.6	26.4	0.9	16.5	17.1
5	2.1	2.1	34.4	26.1	1.3	15.7	18.3
Average	**1.9**	**1.8**	**34.9**	**26.1**	**1.2**	**16.1**	**18.0**

SEM-EDS analyses of feldspars within slag matrix. The has been normalised to 100 wt%.

DMD sample 341B

a.

Sample 341B is from the chimney wall/lining. It was taken from area the surrounding the chimney. The fragment selected for analysis are brick coated with red ceramic and lined with a lead silicate (a). OM analysis showed the ceramic body interacting with the lead silicate (b) and the pure lead silicate layer (c).

SEM-EDS analysis confirmed that the silicate layer consisted only of lead oxide and no sulphidc or ore components.

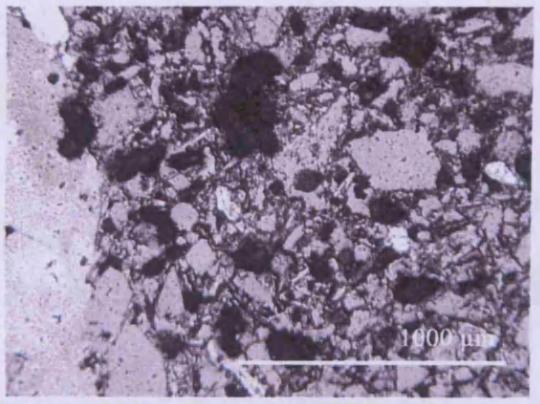

b.

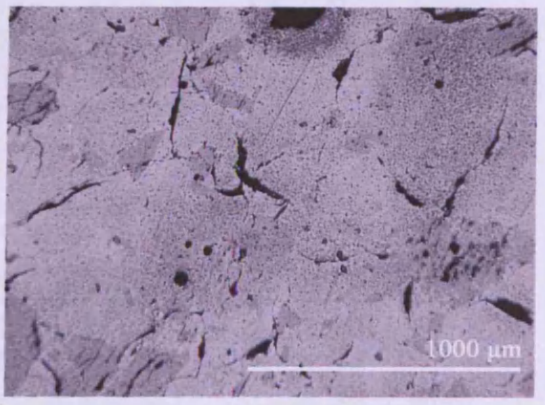

c.

SEM-EDS images and data

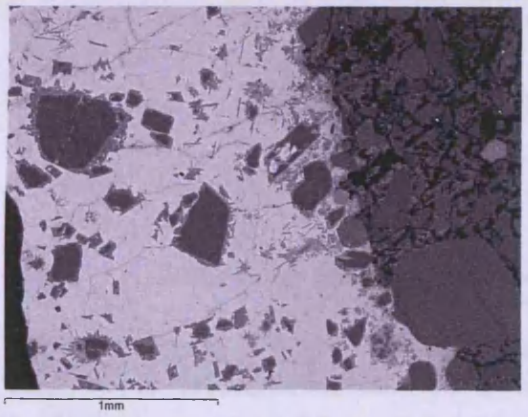

Interaction between the lead silicate layer and ceramic lining.

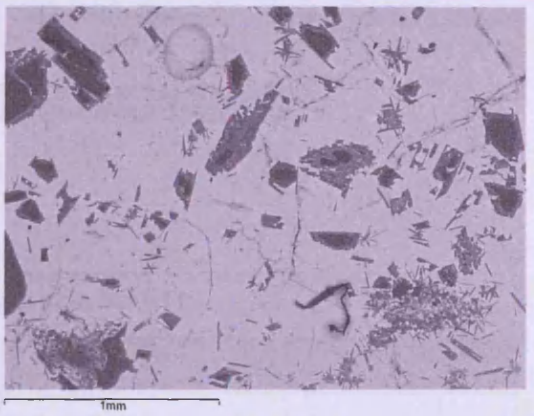

SEM-EDS image of the lead silicate layer.

Scanned area	Na2O	MgO	Al2O3	SiO2	SO3	K2O	CaO	TiO2	FeO	PbO
1	1.5	0.8	16.2	67.9	~	4.0	1.8	1.4	4.7	1.6
2	1.8	0.7	17.3	64.6	~	4.5	2.7	1.7	4.7	2.0
3	1.6	0.7	14.1	70.6	~	5.7	1.4	1.1	3.4	1.5
4	1.9	0.7	16.0	67.8	1.0	4.4	2.5	1.5	4.3	~
5	2.0	0.6	15.9	68.9	~	5.1	1.7	1.0	3.4	1.4
Average	**1.8**	**0.7**	**15.9**	**67.9**	**0.2**	**4.7**	**2.0**	**1.4**	**4.1**	**1.3**

SEM-EDS bulk area scans of sample 341B.
The data has been normalised to 100 wt%.

Scanned area	Na2O	MgO	Al2O3	SiO2	K2O	CaO	TiO2	FeO	ZnO	PbO
1	1.2	0.6	6.5	34.4	1.9	1.5	~	2.1	1.2	50.6
2	0.7	~	6.6	34.3	2.1	1.6	~	1.8	1.1	51.8
3	1.2	~	6.6	33.5	2.0	1.5	~	1.7	~	53.5
4	1.3	~	6.7	33.9	2.2	1.5	~	1.9	~	52.5
5	1.3	~	8.9	36.8	3.6	1.5	~	1.8	~	46.1
6	0.6	0.5	6.4	29.9	1.5	1.2	~	1.6	1.0	57.3
7	1.2	0.7	7.3	35.6	1.7	1.8	1.3	3.1	~	47.3
Average	**1.1**	**0.3**	**7.0**	**34.1**	**2.1**	**1.5**	**0.2**	**2.0**	**0.5**	**51.3**

SEM-EDS area analyses of the lead silicate/green vitrification.
The data has been normalised to 100 wt%.

Scanned area	Na2O	MgO	Al2O3	SiO2	K2O	CaO	TiO2	FeO	BaO
1	0.6	9.0	18.0	39.4	8.5	~	4.3	20.3	~
2	5.3	~	24.3	61.4	0.7	8.2	~	~	~
3	4.7	~	26.1	58.8	0.4	10.0	~	~	~
4	1.6	~	17.4	65.5	13.7	~	~	~	1.8
5	1.5	~	17.0	67.2	14.3	~	~	~	~
6	1.9	~	14.5	70.7	7.7	0.9	0.6	3.8	~

SEM-EDS area analyses of ppartially reacted mineral phases found in the lead silicate glass.
The data has been normalised to 100 wt%.

Scanned area	Na2O	MgO	Al2O3	SiO2	K2O	CaO	TiO2	FeO	PbO
1	1.2	0.7	7.3	35.6	1.7	1.8	1.3	3.1	47.3
2	1.9	~	22.4	47.7	4.7	1.5	~	2.1	19.7
3	1.5	~	17.4	55.9	8.8	~	~	1.0	15.5
4	1.1	~	17.2	59.8	12.8	~	~	0.6	8.6
5	0.7	~	15.4	64.9	10.4	~	0.8	1.3	6.5

SEM-EDS of bulk area of the recrystallised phases that surround the mineral phases in the lead silicate.
The data has been normalised to 100 wt%.

Scanned area	MgO	SiO2	TiO2	MnO	FeO
1	0.7	~	36.3	0.6	62.4
2	0.5	0.7	35.7	~	63.1
3	0.5	0.7	35.7	~	63.1
4	~	2.5	55.5	0.6	40.5

SEM-EDS area analyses of iron titanium oxides within the ceramic matrix.
The data has been normalised to 100 wt%.

Scanned area	Na2O	MgO	Al2O3	SiO2	SO3	K2O	CaO	TiO2	FeO	ZnO	PbO
Chimney wall bulk	1.8	0.7	15.9	67.9	0.2	4.7	2.0	1.4	4.1	~	1.3
Silicate glass	1.1	0.3	7.0	34.1	~	2.1	1.5	0.2	2.0	0.5	51.3
Glass/wall (%)	61.8	38.0	44.1	50.1	~	45.1	73.3	13.2	48.9	~	~

SEM-EDS analyses showing the bulk chimney wall versus the vitrified silicate glass.
The data has been normalised to 100 wt%.

DMD sample 341C

a.

Sample 341C is a section of furnace wall. It is made from a dense grey brick coated in a very thin layer of brown vitrified material (a). OM showed that there were two distinct areas within the sample: the ceramic/brick that would have lined the furnace prior to use (b) and a thin layer of slag/vitrified material (c, d and e).

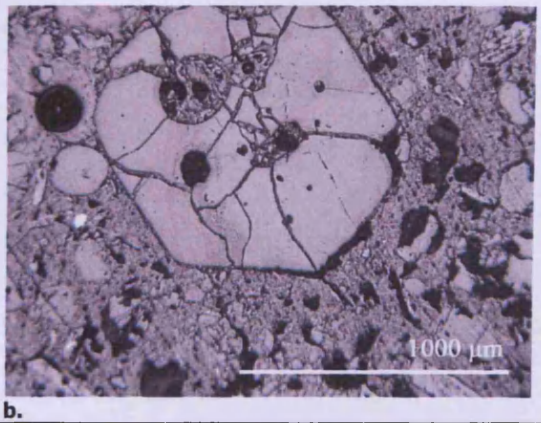

b.

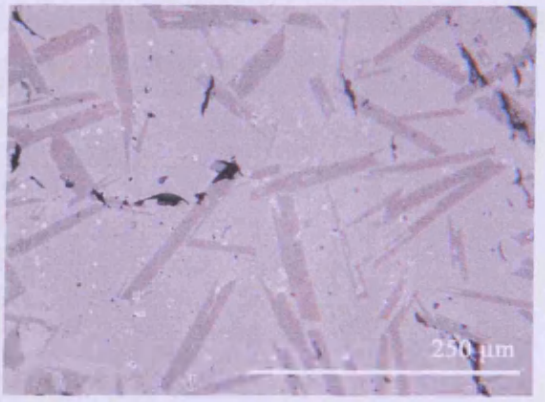

c.

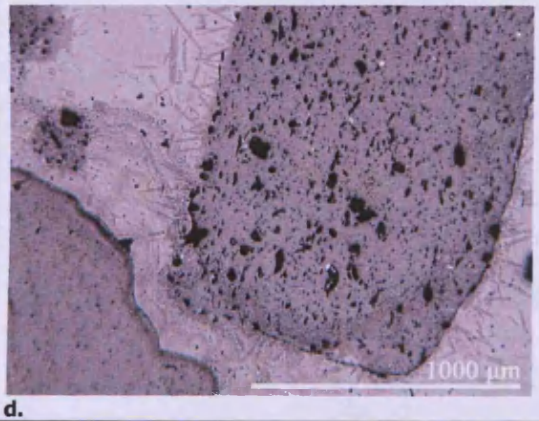

d.

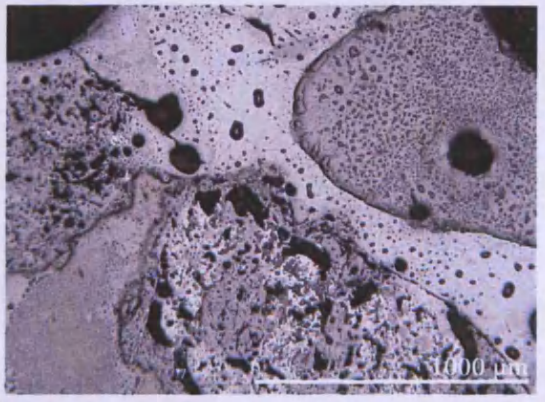

e.

SEM-EDS images and data

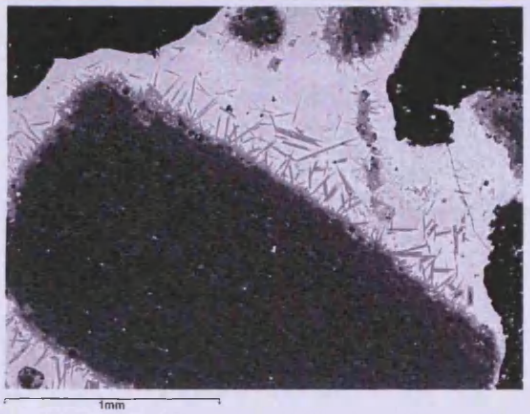

Feldspar inclsuion within ceramic wall being dissolved by lead oxide.

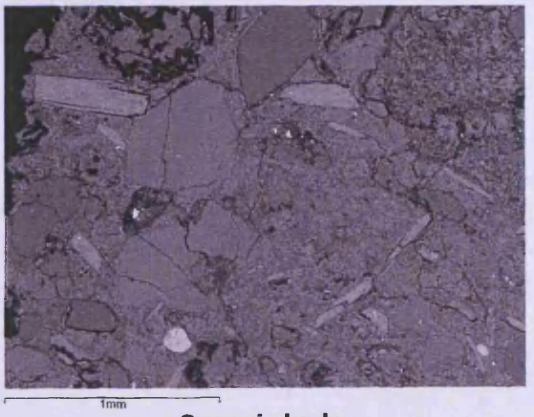

Ceramic body.

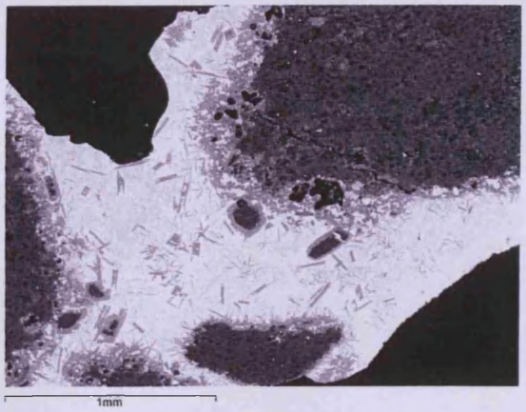

Lead silicate

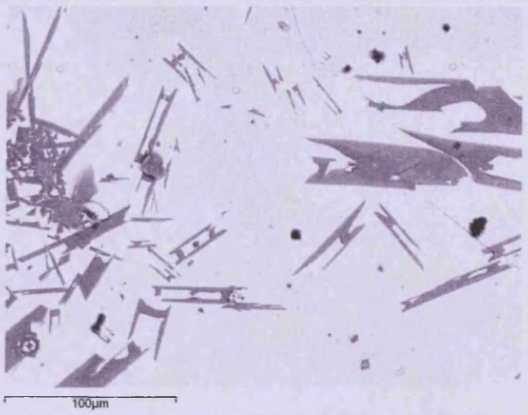

Lead almumium silcates formed within lead silicate.

Scanned area	MgO	Al2O3	SiO2	K2O	CaO	FeO	ZnO	PbO
1	0.6	3.5	21.6	1.1	3.9	3.1	6.1	60.1
2	0.6	3.2	22.3	1.1	4.2	3.1	5.8	59.7
3	0.6	3.4	21.7	1.2	4.2	3.5	5.8	59.6
4	~	~	23.2	1.4	4.2	3.6	5.7	62.0
5	0.8	3.4	22.3	1.2	4.7	2.7	5.8	59.1
6	~	3.3	22.1	1.2	4.0	3.3	6.1	60.1
Average	**0.4**	**2.8**	**22.2**	**1.2**	**4.2**	**3.2**	**5.9**	**60.1**

SEM-EDS bulk area scans of sample 341C.
The data has been normalised to 100 wt%.

Scanned area	MgO	Al2O3	SiO2	CaO	FeO	ZnO	PbO
1	1.9	1.2	35.8	27.1	1.2	17.2	15.8
2	2.1	1.9	35.2	26.0	1.4	15.6	17.8
3	1.9	2.0	33.6	24.6	1.5	15.6	20.8
4	1.8	1.7	35.6	26.4	0.9	16.5	17.1
5	2.1	2.1	34.4	26.1	1.3	15.7	18.3
Average	**1.9**	**1.8**	**34.9**	**26.1**	**1.2**	**16.1**	**18.0**

SEM-EDS area analyses of feldspars within the slag matrix.
The data has been normalised to 100 wt%.

Scanned area	S	Zn	Ag	Pb
1	48.1	2.1	~	49.8
2	~	~	7.8	92.2

SEM-EDS area analyses of metallic prills in sample 341C.
The data has been normalised to 100 wt%.

Scanned area	Na2O	MgO	Al2O3	SiO2	K2O	CaO	TiO2	FeO	ZnO	PbO
Furnace fragment	0.2	0.8	19.2	67.3	4.8	0.4	0.9	5.9	~	0.7
Silicate layer	~	~	8.8	32.5	2.1	1.4	~	3.7	2.0	49.6
Silicate layer/FF (%)	~	~	45.8	48.3	43.2	394.3	~	62.0	~	~

The silicate layer versus main furnace fragment composition.

DMD sample 341D

a.

Sample 341D is most likely a sample of fine soil similar to un-reacted furnace wall or lining (a). From the analytical data and OM work many of the phases present are quartz, feldspars and iron rich silicates (b and c) and these correlate with furnace fragment sample 341C. This indicates that the furnace was built (as expected) from local clay.

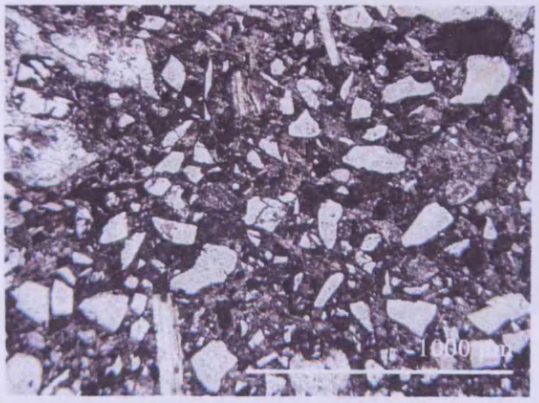

b.

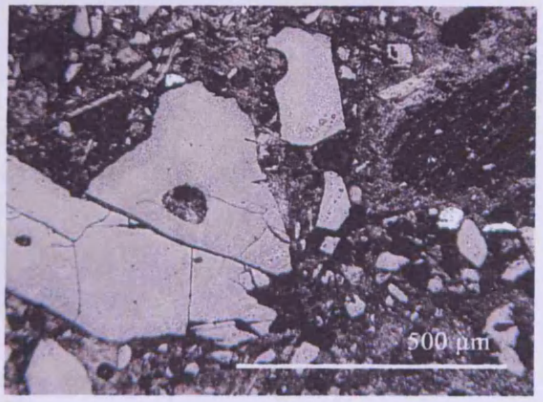

c.

SEM-EDS images and data

Scanned area	Na2O	MgO	Al2O3	SiO2	K2O	CaO	TiO2	FeO	PbO
1	~	0.7	21.3	66.9	5.6	~	1.0	4.5	~
2	0.4	0.9	17.0	67.7	3.9	0.7	0.8	7.3	1.4

SEM-EDS analyses of bulk area of large brick/ceramic inclusions surrounded by the slag (sample 341C-furnace fragment). The data has been normalised to 100 wt%.

Scanned area	Al2O3	SiO2	K2O	CaO	FeO	ZnO	PbO
1	8.8	32.5	2.1	1.4	3.7	2.0	49.6

SEM-EDS analysis a bulk area scan of the vitrified coating on the brick layer (sample 341C- furnace fragment).The data has been normalised to 100 wt%.

Scanned area	Na2O	MgO	Al2O3	SiO2	K2O	CaO	TiO2	FeO	ZnO	PbO
1	~	0.5	7.3	28.3	1.7	1.0	0.7	3.4	1.8	55.4
2	0.8	~	8.0	31.5	1.6	1.2	~	3.7	2.1	51.2
3	~	~	8.1	32.1	2.2	1.2	~	4.2	2.1	50.1
4	0.6	~	7.5	30.5	1.9	1.1	0.6	3.7	1.6	52.5

Bulk area analyses scan of the vitrified matrix, without the phase inclusions (sample 341C-furnace fragment). The data has been normalised to 100 wt%.

Scanned area	Na2O	Al2O3	SiO2	K2O	FeO	PbO
1	0.7	18.8	46.6	7.0	1.6	25.4
2	0.6	18.6	48.4	7.7	1.3	23.4

SEM-EDS area analyses of the silicate phases within the vitrified layer of sample 341C. The data has been normalised to 100 wt%.

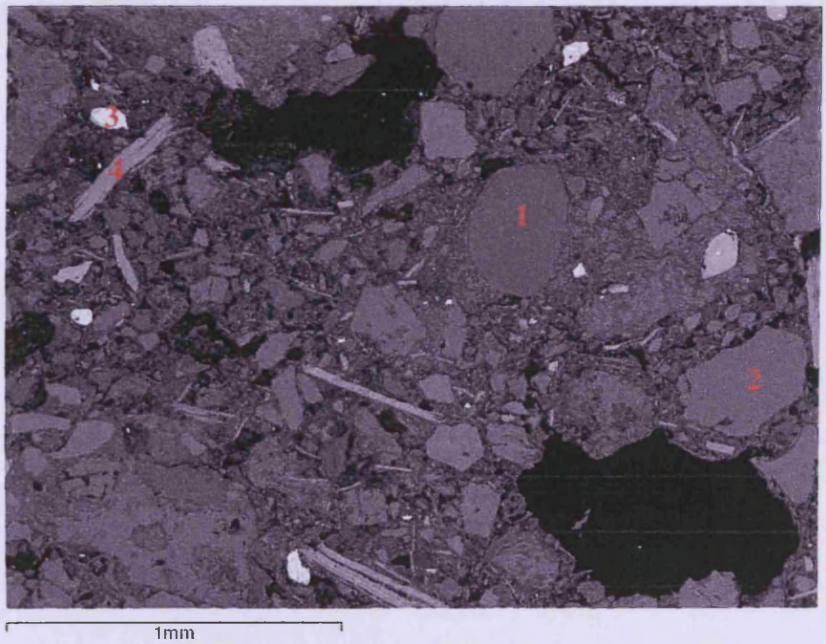

Typical SEM image of DMD sample 341D
1 = quartz
2= Alkaline feldspars
3 = Iron-titanium oxide phases
4 = Iron rich silicates

Scanned area	Na2O	MgO	Al2O3	SiO2	K2O	CaO	TiO2	FeO	BaO
1	1.8	~	13.7	77.0	5.7	~	~	1.7	~
2	2.0	~	15.4	74.4	5.4	~	1.1	1.8	~
3	2.2	~	15.2	73.1	7.7	0.9	0.4	0.6	~
4	1.3	0.5	14.8	73.2	4.7	0.6	1.4	3.5	~
5	1.9	~	17.6	66.5	13.2	~	~	~	0.9

Alkaline feldspars (labelled 2 above) found in sample 341D. Data has been normalised to 100%.

Scanned area	MgO	Al2O3	SiO2	TiO2	MnO	FeO	ZrO
1	~	0.8	1.7	29.1	~	68.4	~
2	0.7	~	2.5	36.2	0.4	56.4	3.9

Iron-titanium oxide (labelled 3 above) phases found in 341D. Data has been normalised to 100%.

Scanned area	Na2O	MgO	Al2O3	SiO2	P2O5	K2O	CaO	TiO2	FeO
1	0.4	8.4	17.3	38.6	~	9.5	~	4.8	21.0
2	~	9.4	16.2	39.2	~	9.9	~	3.9	21.4
3	~	7.4	18.3	41.8	~	8.3	~	4.4	19.9
4	~	9.0	16.4	37.4	2.0	9.8	1.7	4.2	19.5
5	~	9.5	16.3	39.3	~	9.9	~	4.6	20.5

Iron rich silicates (labelled 4 above) area scanned using SEM-EDS of sample 341D. Data has been normalised to 100%.

Scanned area	Na2O	MgO	Al2O3	SiO2	K2O	CaO	FeO	ZnO	PbO
Slag proper 341A	~	0.4	**2.8**	22.2	1.2	4.2	3.2	**5.9**	60.1
Silicate glass 341B	1.1	0.3	7.0	34.1	2.1	1.5	2.0	0.5	51.3
Silicate glass 341C	~	~	8.8	32.5	2.1	1.4	3.7	2.0	49.6
Chimney wall bulk 341B	1.8	0.7	15.9	67.9	4.7	2.0	4.1	~	1.3

SEM-EDS data of the slag proper versus chimney and furnace wall silicates.
The data has been normalised to 100 wt%.

URUQUILLA EST 10 (UR EST 10)

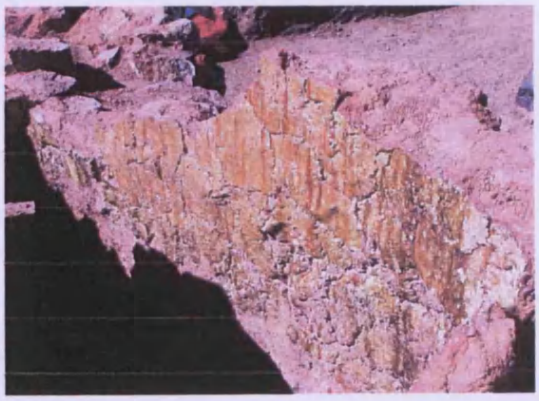

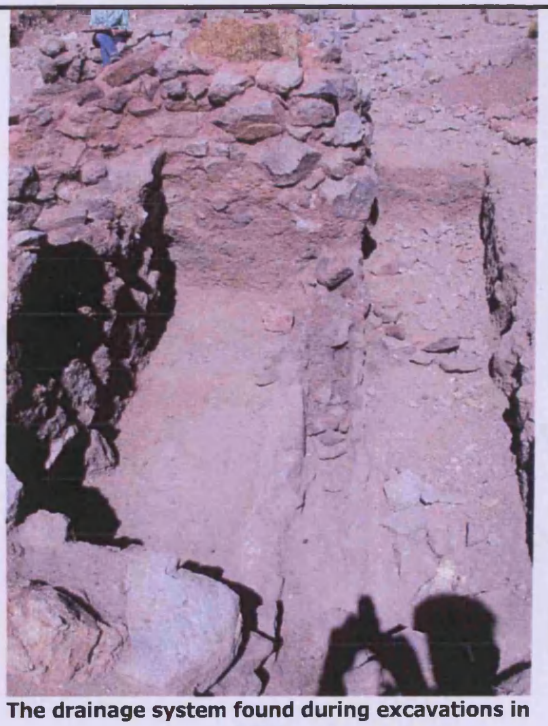

The drainage system found during excavations in 2005.

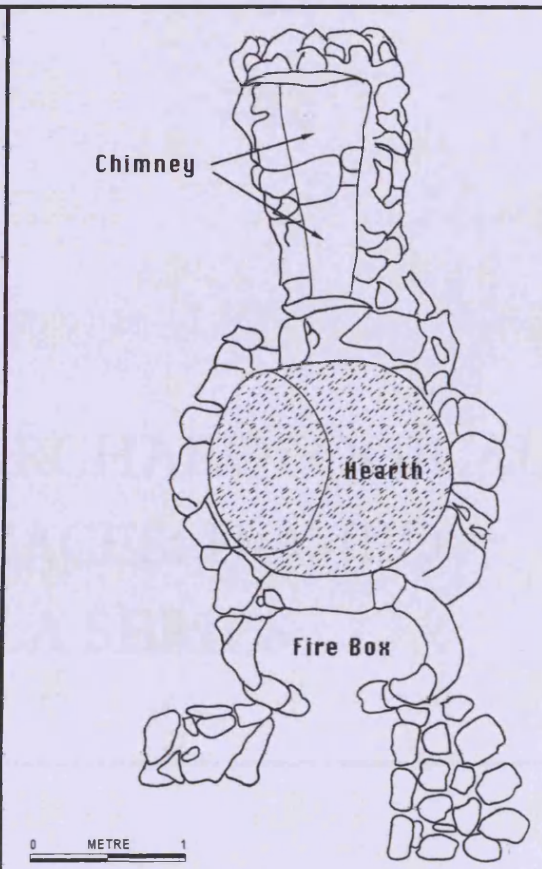

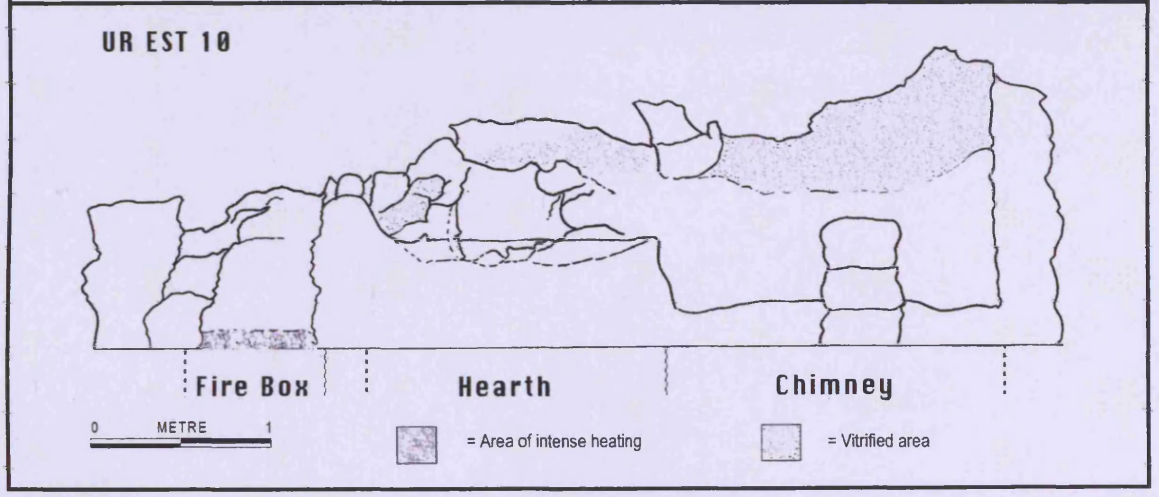

NO SAMPLES ANALYSED from UR Est 10

APPENDIX VII - ARCHAEOLOGICAL EUROPEAN FURNACES: DOMED ~ URUQUILLA SERIES

THE URUQUILLA SERIES

The Uruquilla archaeological area. In the foreground the three furnaces UR10/11/12 (left to right) and in the background in the stone walled settlement (top left) UR Est 10 – The Dragon.

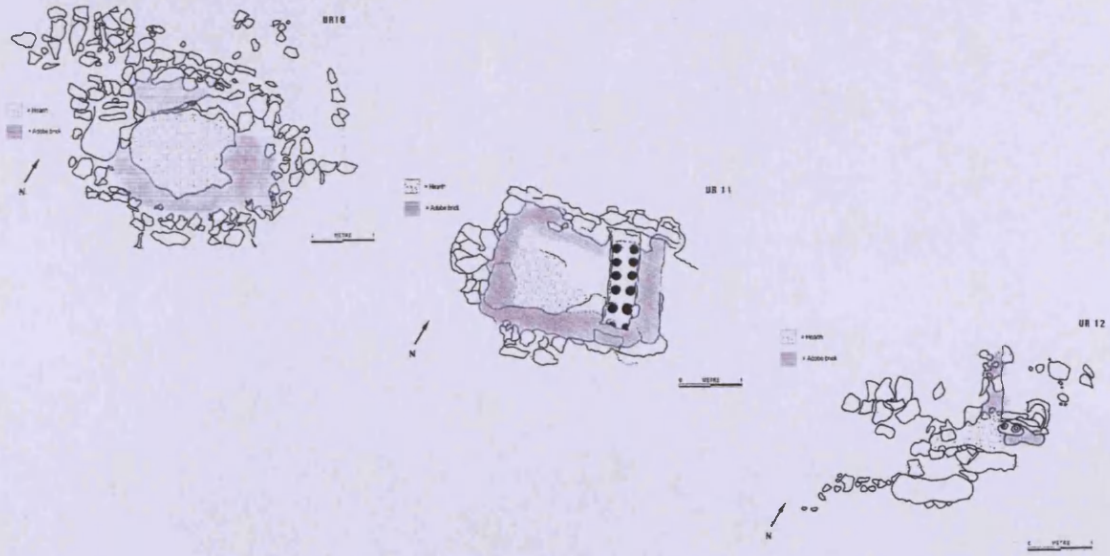

Uruquilla 10 (UR10)

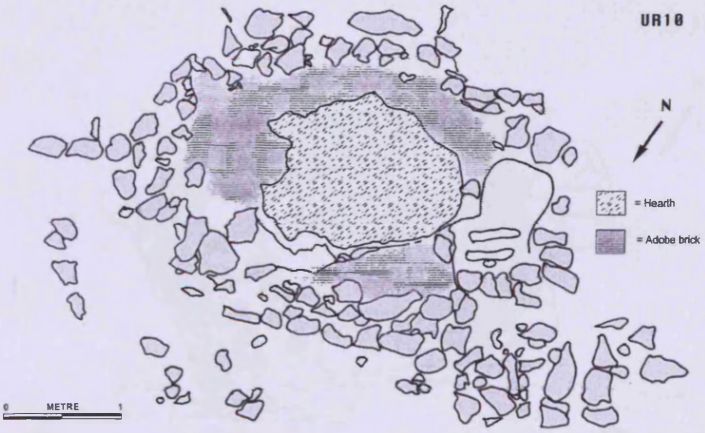

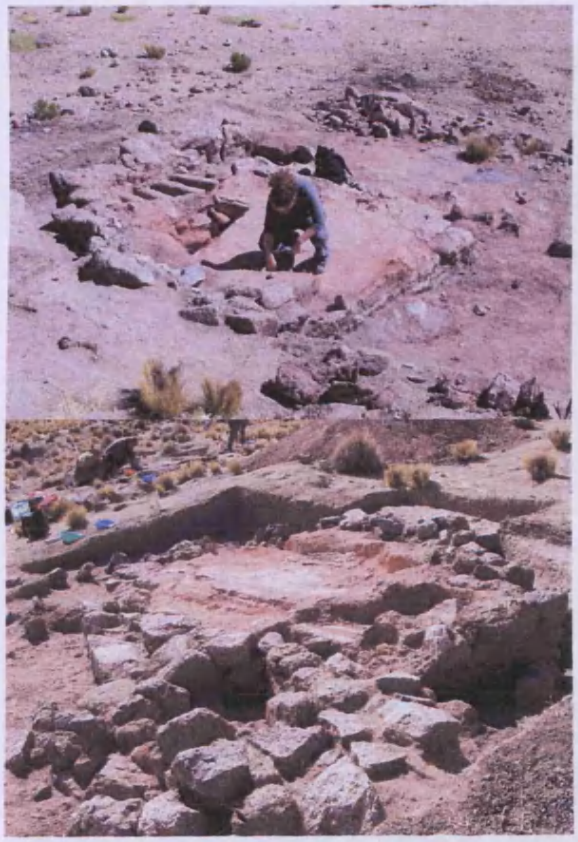

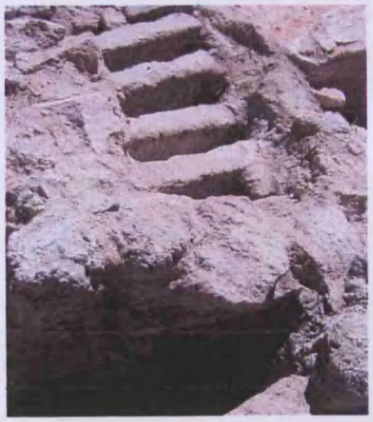

Uruquilla 11 (UR11)

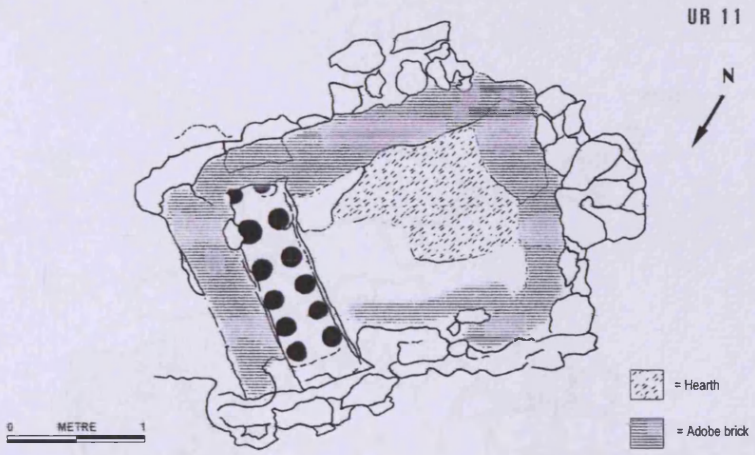

Uruquilla 12 (UR12)

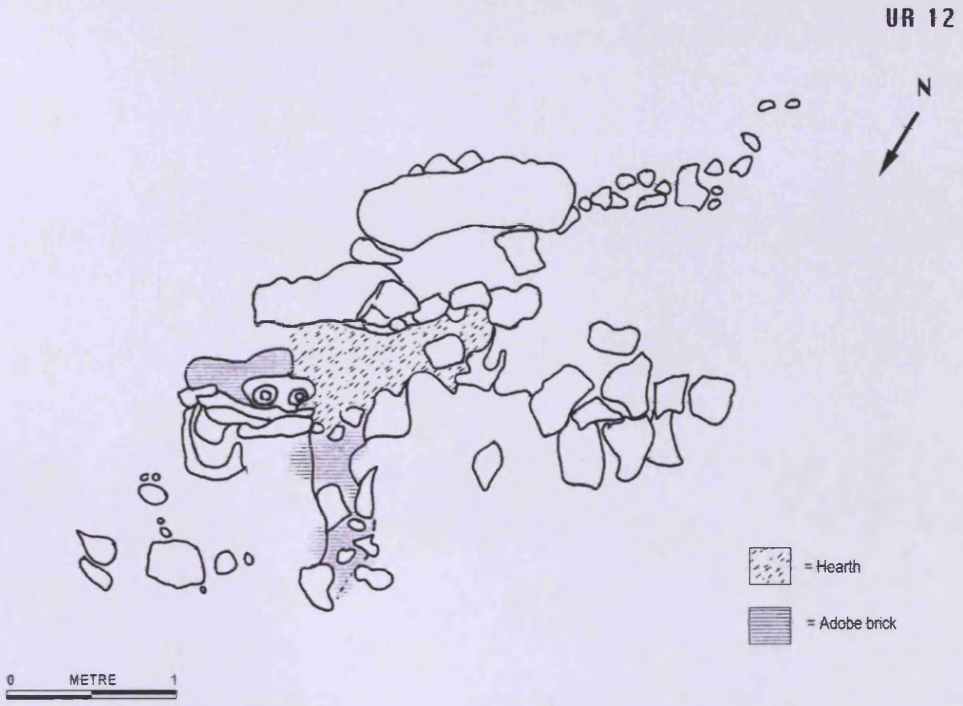

UR SERIES SLAG TYPES – ANALYSES

Type I

Type I - lead rich slags

The hand specimens of the lead rich slags were notably similar. They are extremely black and glassy. Many had a ripple texture on the outer surface (see below). Optical microscopy confirmed the glassy texture seen on the hand specimen was true of the microstructure (image a. UR11 259; image b. UR12 293). Metallic lead prills and prills of lead sulphide were scattered throughout a glassy slag matrix (images c and d. UR10 251, image e. UR10 209, image f. UR10 253B). Other crystalline phases were recorded. SEM-EDS revealed that these are iron and zinc silicates and iron and zinc oxides. The bulk composition of lead rich slags contains relatively high lead oxide (58-72 %). No sulphur was recorded in the overall bulk composition.

The slag also contains silica, iron and zinc oxide, and alumina as the next most important oxides. Very low quantities of lime and potash characterise this slag type. Metallic prills found in the matrix contained silver and lead alloys.

Type I - hand specimens

<table>
<tr><td>  </td><td>  </td><td>  </td></tr>
<tr><td>UR10 209</td><td>UR10 253A</td><td>UR10 253B</td></tr>
<tr><td>  </td><td>  </td><td>  </td></tr>
<tr><td>UR10 254</td><td>UR11 251</td><td>UR11 259</td></tr>
<tr><td>  </td><td>  </td><td></td></tr>
<tr><td>UR11 263</td><td>UR12 293</td><td></td></tr>
</table>

Type I - OM images

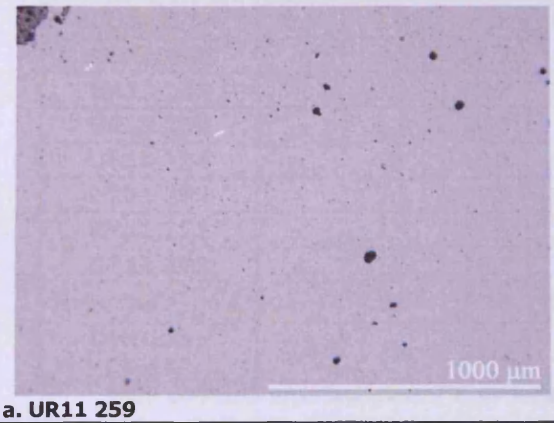

a. UR11 259

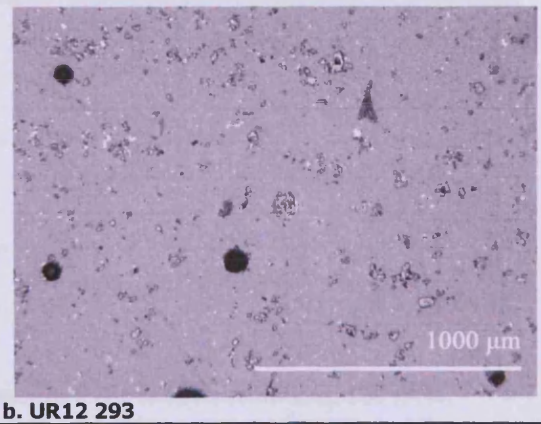

b. UR12 293

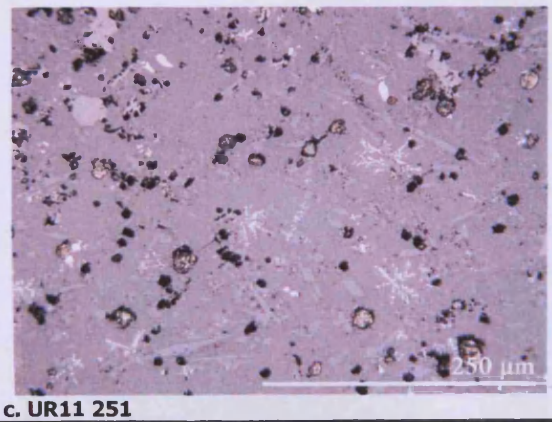

c. UR11 251

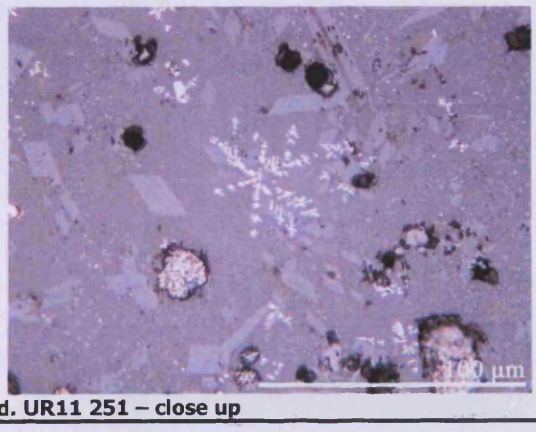

d. UR11 251 – close up

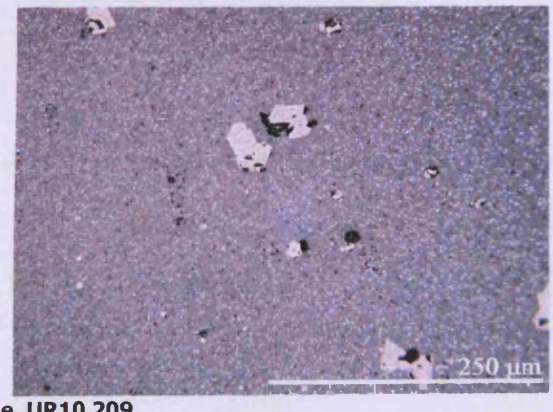

e. UR10 209

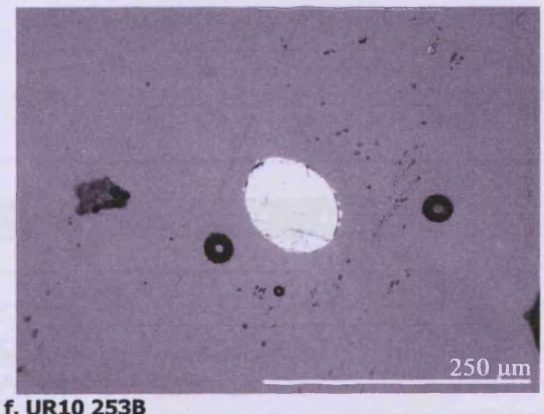

f. UR10 253B

Type I - SEM-EDS images and data

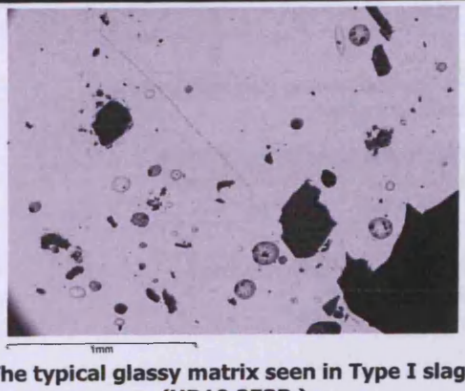

The typical glassy matrix seen in Type I slags (UR10 253B)

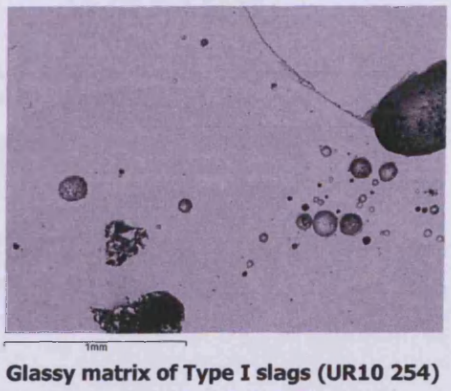

Glassy matrix of Type I slags (UR10 254)

Sample	MgO	Al2O3	SiO2	K2O	CaO	MnO	FeO	ZnO	Sb2O3	PbO
UR10 253A	0.1	3.3	24.8	0.8	0.4	~	5.4	6.6	0.8	57.8
UR10 253B	~	3.5	25.3	0.9	0.8	~	4.7	5.6	0.3	58.8
UR11 263	~	3.5	24.7	0.5	0.5	~	4.5	5.4	0.4	60.4
UR10 209	~	1.9	17.3	~	0.2	1.0	12.4	1.7	~	65.5
UR10 254	~	2.9	18.9	1.5	1.8	~	6.0	2.8	~	66.1
UR11 259	~	2.3	17.9	0.9	1.8	~	5.8	3.0	~	68.3
UR11 251	~	1.4	15.1	~	0.1	~	10.2	1.7	0.3	71.2
UR12 293	~	1.6	16.2	~	0.4	~	5.4	2.3	2.2	71.9
Average Type I	**~**	**2.6**	**20.0**	**0.6**	**0.8**	**0.1**	**6.8**	**3.6**	**0.5**	**65.0**
DMD slag (341A)	**0.4**	**2.8**	**22.2**	**1.2**	**4.2**	**~**	**3.2**	**5.9**	**~**	**60.1**

SEM-EDS bulk area analyses of Type I slag. The data has been normalised to 100 wt%.

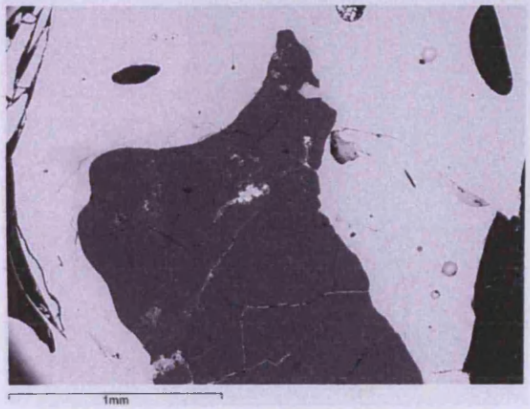

SEM image from slag UR10 253A of partially reacted ore.

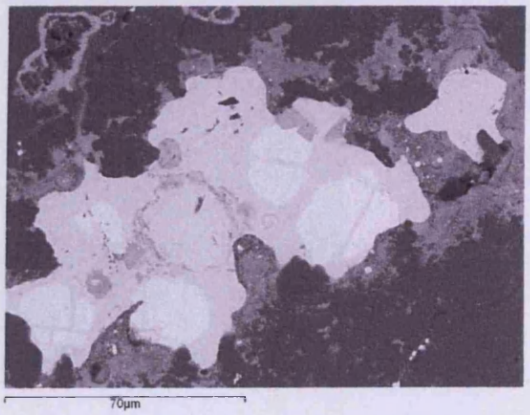

Close up of partially reacted ore in UR10 253A (left). Lead sulphide, silver sulphide and zinc sulphide were recorded trapped in a silica the quartz grain (This is magnified image of the quartz grain where this ore mineral is trapped.).

Scanned area from image above right	S	Fe	Cu	Zn	Ag	Pb
Silver sulphide (mid grey phase)	39.0	~	1.8	~	59.2	~
Zinc sulphide (darkest grey phase)	50.0	8.7	1.3	39.2	0.8	~
Lead sulphide (brightest phase)	50.0	~	~	~	2.3	47.6

SEM-EDS analyses residual ore minerals in slag sample UR10 253A.
Data has been normalised to 100 at%.

Spot analyses	MgO	Al2O3	SiO2	CaO	TiO2	MnO	FeO	ZnO	SnO	PbO
1	0.9	3.1	1.4	0.7	~	1.8	73.5	16.6	2.0	~
2	1.0	8.6	~	~	0.7	1.3	64.3	19.3	3.4	1.5

Iron/zinc rich oxides formed in the lead silicate matrix of slag sample 293.
Data has been normalised to 100 wt%.

Spot analyses	MgO	Al2O3	SiO2	CaO	MnO	FeO	ZnO	SbO	PbO
1	0.8	0.8	19.6	0.5	1.0	4.1	10.0	~	63.0
2	~	2.3	16.2	~	~	4.0	0.4	2.3	75.0

Lead silicates formed in the silicate matrix in sample UR12 293.
Data has been normalised to 100 wt%.

Spot analysed	S	Ag	Pb
1	~	8.4	91.6
2	51.0	~	49.0
3	~	7.1	92.9
4	51.0	~	49.0

Lead metal and lead sulphide spot analyses in sample 251.
Data has been normalised to 100 at%.

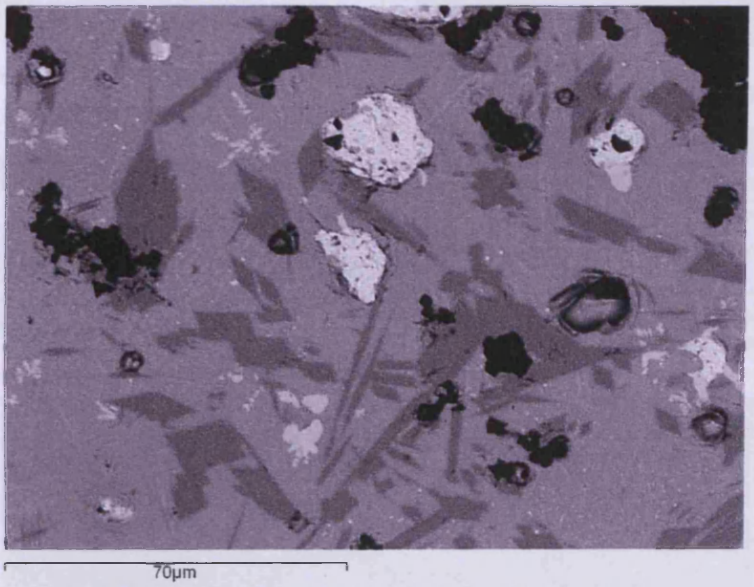

UR11 251 - different oxide phases within the slag.

Scanned area	MgO	Al2O3	SiO2	FeO	ZnO	As2O3	SnO2	PbO
Area 1	~	1.0	1.2	81.7	9.7	0.4	1.8	4.3
Area 2	0.7	1.4	~	86.6	9.4	~	1.9	~

Black crystal phases from sample UR11 251 (see above).
The data has been normalised to 100 wt%.

Scanned area	Al2O3	SiO2	FeO	SnO	PbO
1	1.2	15.4	20.4	5.8	57.3
2	0.5	15.6	19.2	7.1	57.6
3	0.6	15.1	20.2	6.5	57.6
4	0.7	14.7	17.8	10.4	56.5
5	0.7	15.7	19.1	6.4	58.2

Grey silicate phases (image above) from sample UR11 251.
The data has been normalised to 100 wt%.

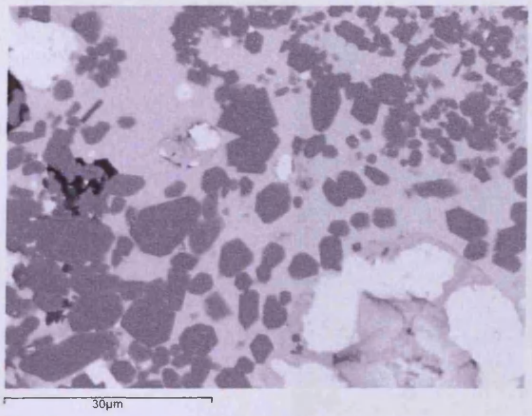

SEM image of zinc silicates within sample UR10 253A.

Scanned area	MgO	SiO2	FeO	ZnO
1	1.1	26.8	4.2	68.0
2	1.1	26.7	4.3	67.9

Zinc silicates in the slag matrix sample UR10 253A seen as mid grey euhedral crystals. Data has been normalised to 100 wt%.

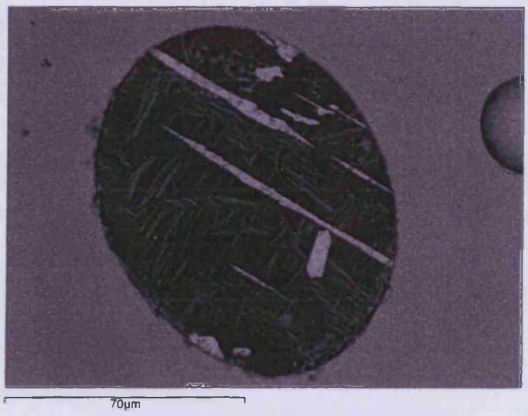

Prill 2 from sample UR10 253B

Scanned area	S	Cu	Ag	Sb	Pb
Prill 1 area 1	3.8	3.8	88.6	1.8	2.0
Prill 1 area 2	7.9	7.9	79.2	1.8	3.1
Prill 2 area 1	33.4	57.0	9.6	~	~
Prill 2 area 2	43.2	22.6	2.3	~	32.0

Prills 1 and 2 analysed using SEM-EDS from sample 253B. The data has been normalised to 100 at%.

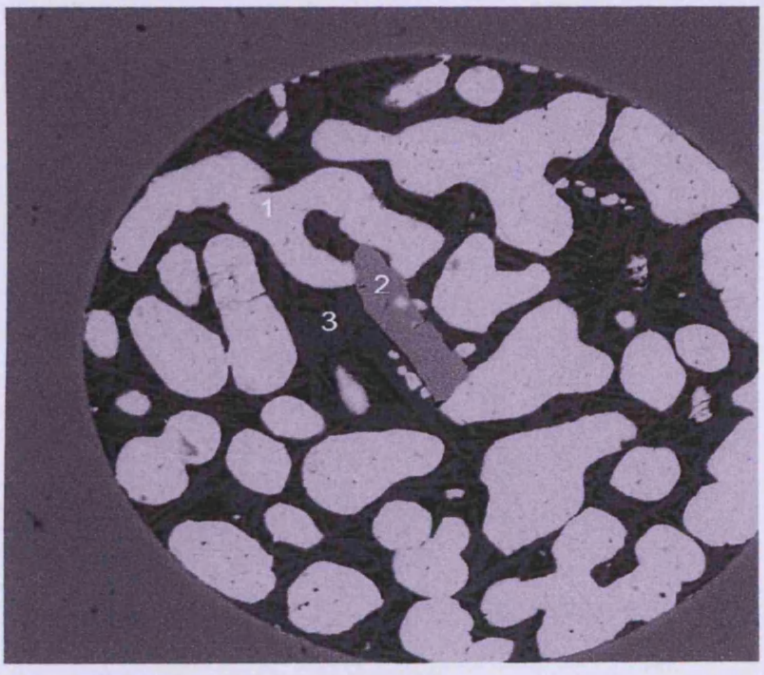

A complex metallic prill found in sample 263. SEM backscattered image of a prill which contains lead sulphide (1) silver (2), and silver/copper sulphide (3).

Spot analyses	S	Cu	Ag	Pb
1 – lead sulphide	50.9	2.7	~	46.4
2 – silver	~	2.5	97.5	~
3 – silver copper sulphide	34.5	33.2	32.4	~

Different metallic phases present in a sample UR11 263 prill (above). The date has been normalised to 100 at%

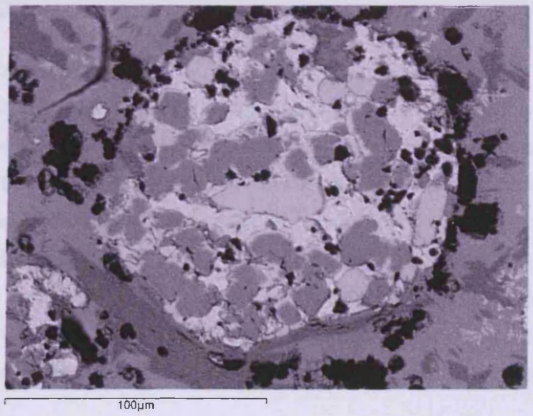

Prill in sample UR11 251.

Spectrum	S	Ag	Pb
Light grey area	~	98.6	1.4
Whitest area	~	~	100.0
Mid grey	51.8	~	48.2

SEM-EDS spot analyses of different metallic phases in SEM image above.
The data has been normalise to 100 at%.

Type II

Type II - zinc sulphide rich slags

The second group of slags is the zinc sulphide rich slags. The SEM-EDS bulk area analyses showed that this group of slags has much lower lead oxide (32 %) compared to Type I slags (65%), but elevated silica, zinc and iron oxides (the majority of the zinc is zinc sulphide). Low quantities of phosphate and lime were present in the slag composition. SEM-EDS analysis confirmed that zinc rich slags all contained ore components such as quartz grains, tin oxide, zinc and lead sulphides. The presence of iron, zinc, arsenic and antimony in the lead silicate matrix can all be attributed to the starting ore. These slags contain crystalline phases that are rich in zinc such as zinc olivines and iron and zinc oxides (spinels). Many of the zinc silicates recorded have different structures and when analysed have variable chemical compositions.

Type II - hand specimens

UR10 250B

UR10 255

UR10 268A
(No pic of the hand specimen so mounted block subsituted)

UR10 268C

UR12 297

OM images

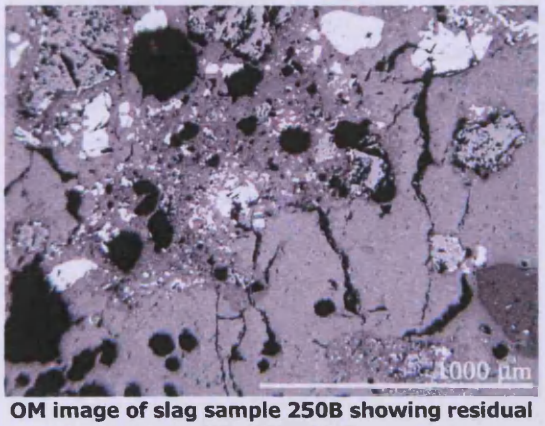

OM image of slag sample 250B showing residual gangue and ore.

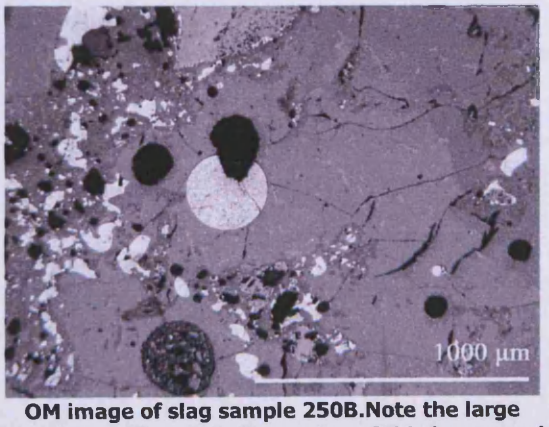

OM image of slag sample 250B.Note the large round metallic prill in the centre of this image and the scattered white lead sulphide prills.

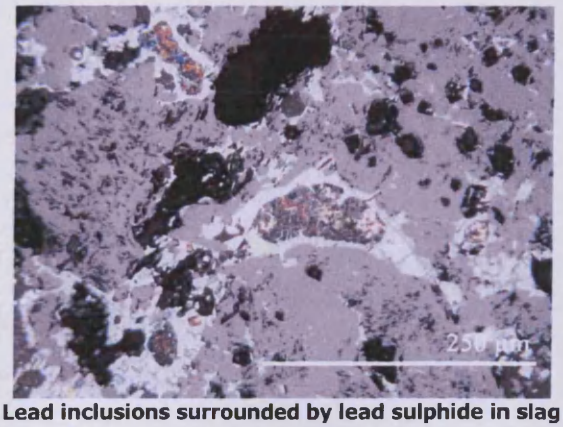

Lead inclusions surrounded by lead sulphide in slag sample 250B

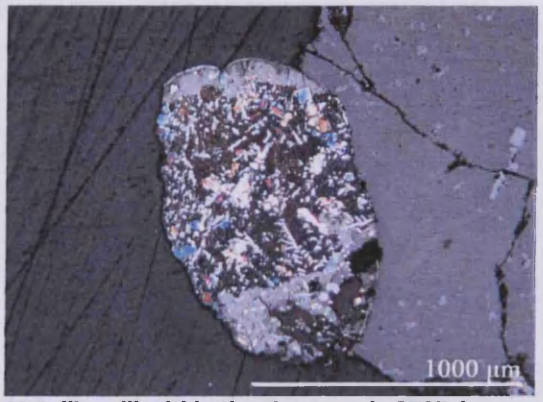

Metallic prill within the slag sample 250B (mag x 200). The matrix is lead metal (brown) with dentritic intergrowths of lead sulphide and prills of silver (creamy yellow).

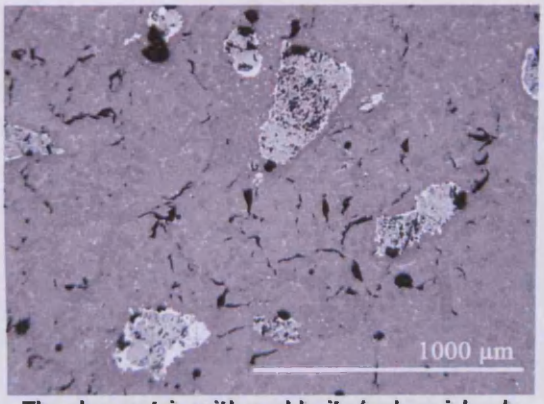

The slag matrix with spahlerite/galena islands

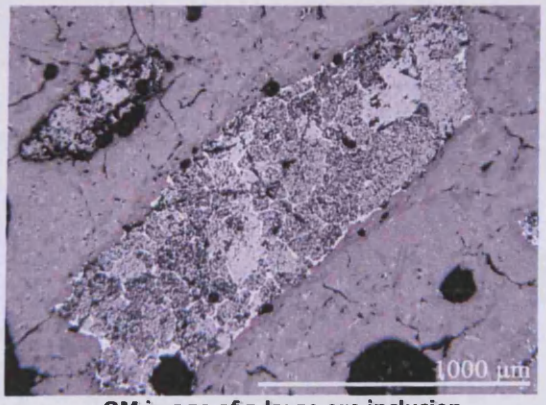

OM image of a large ore inclusion

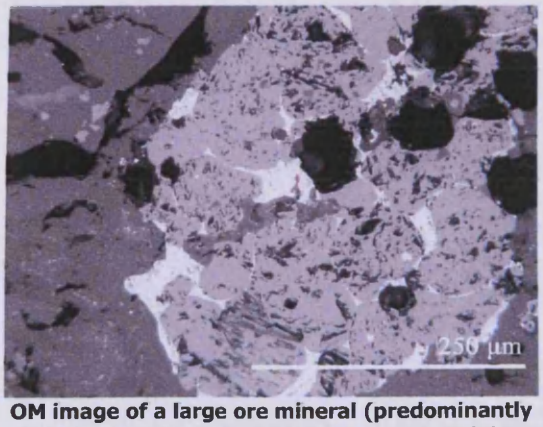

OM image of a large ore mineral (predominantly sphalerite (light grey) and lead sulphide (brightest phase) that has partially reacted with surrounding matrix.

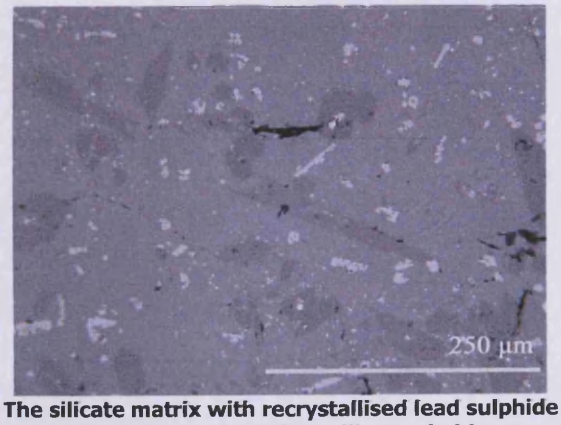

The silicate matrix with recrystallised lead sulphide (white inclusions) and lead silicates (mid grey angular crystals).

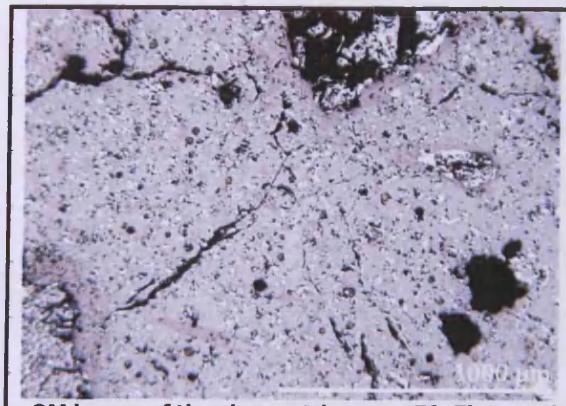

OM image of the slag matrix mag x50. The matrix is dispersed with lead sulphide

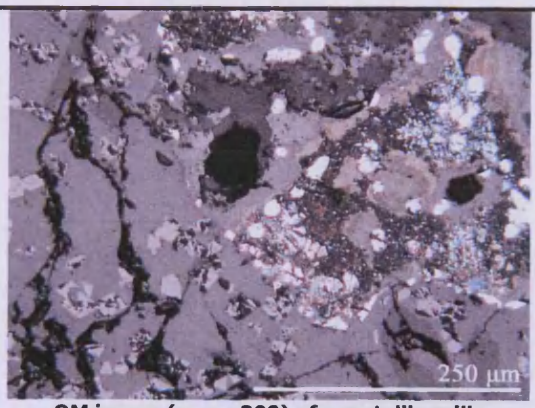

OM image (mag x200) of a metallic prills surrounded by the slag silicate matrix

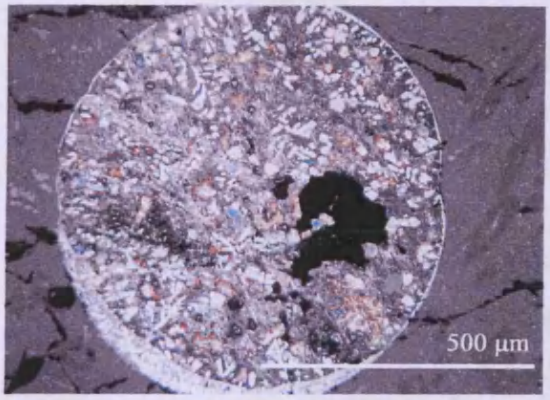

OM image of a metallic prill within the slag. Showing different metallic phases.

Close up of OM image of a metallic prill within the slag. Mid grey inclusions are silver rich dendtrites, dispersed in a lead metal matrix.

SEM images and data

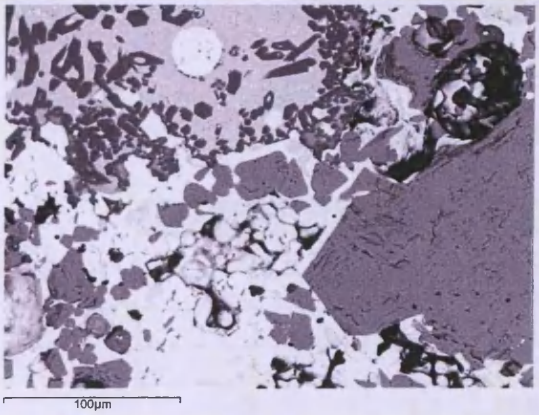

UR10 250B – the different phases in the slag body. Mid grey areas are zinc sulphide.

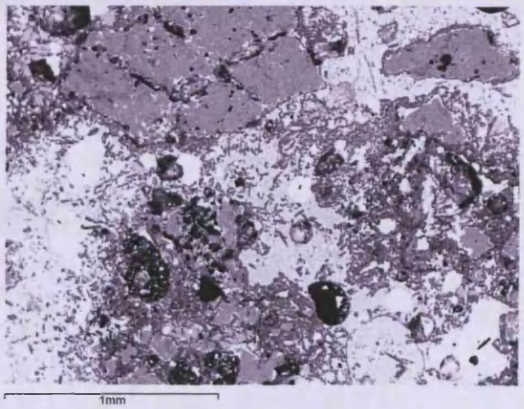

UR10 250B – bulk area scan

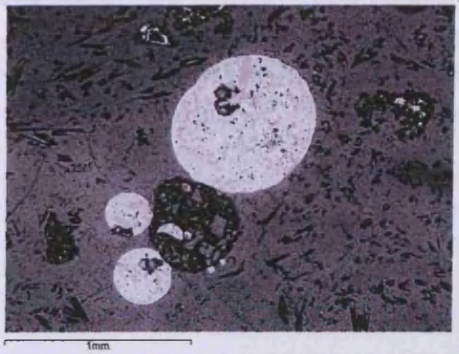

UR10 268A

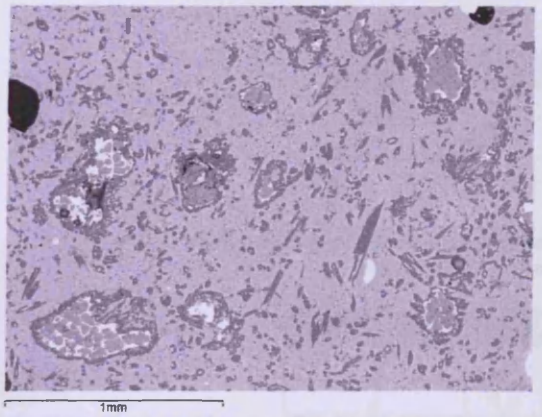

Sample UR10 255 image of the slag matrix with ore inclusions.

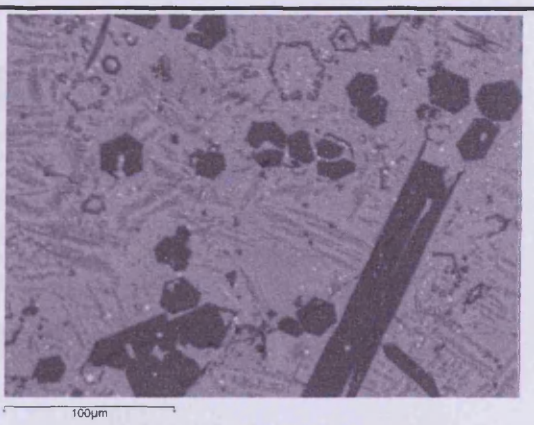

UR10 255 - zinc silicate crystals.

Scanned area	Al2O3	SiO2	P2O5	K2O	FeO	ZnO	As2O3	Sb2O3	PbO
1	2.8	21.3	0.9	0.9	9.2	9.1	2.1	2.5	51.2
2	2.1	16.9	~	0.6	7.5	13.0	1.7	1.4	56.8
3	3.0	22.4	~	1.3	8.1	10.1	2.6	2.3	50.2
4	3.2	22.6	0.8	1.2	8.9	8.1	2.3	2.4	50.6
Average	**2.8**	**20.8**	**0.4**	**1.0**	**8.4**	**10.1**	**2.2**	**2.2**	**52.2**

SEM-EDS area analyses of slag 250B glassy silicate matrix. Data has been normalised to 100 wt%.

Spot analyses	MgO	Al2O3	SiO2	MnO	FeO	ZnO
1	0.7	0.6	25.4	0.4	7.1	66.0
2	~	~	26.1	0.6	10.1	63.3

Zinc silicates found in the UR10 250B slag matrix.
Data has been normalised to 100 wt%.

Scanned area	S	Ag	Sb	Pb
1	51.5	~	~	48.5
2	19.8	72.5	2.9	4.8
3	~	~	~	100.0

Metallic prill analysed in the matrix UR10 250B.
Data has been normalised to 100 at%.

Area analysed	Al2O3	SiO2	K2O	CaO	FeO	ZnO	PbO
1	4.0	29.6	1.3	2.8	12.6	13.5	36.1
2	3.3	29.4	1.6	2.3	10.9	13.6	39.0
3	~	30.1	1.5	2.6	12.1	13.3	40.3
4	3.7	28.6	1.4	2.1	12.9	16.0	35.3
5	3.7	27.9	1.5	2.0	12.2	12.1	40.7
Average	**2.9**	**29.1**	**1.4**	**2.4**	**12.1**	**13.7**	**38.3**

SEM-EDS area analyses of the silicate matrix sample UR10 268A. Data has been normalised to 100 wt%.

Sampled area	MgO	SiO2	P2O5	MnO	FeO	ZnO
1	1.1	28.1	~	~	11.6	59.2
2	~	26.5	~	0.9	13.2	59.4
3	1.6	26.9	~	0.8	10.9	59.9
4	1.4	29.5	~	0.9	9.4	58.8
5	~	26.7	1.2	~	7.2	64.9

Zinc/iron rich silicates found in the UR10 268A slag matrix. Data has been normalized to 100 wt%.

Sampled prill	S	Ag	Sb	Pb
1SEM pics	11.2	33.7	6.5	48.6
2	~	46.0	6.9	47.1
3	26.2	26.8	6.1	40.9
4	7.5	76.3	5.2	11.0

SEM-EDS area analyses of metallic prills within sample UR10 268A.
Data has been normalized to 100 at%.

Sample area	S	As	Ag	Sb	Pb
1	3.1		85.9	9.6	1.3
2	4.6		83.9	10.1	1.3
3	37.8	~	~	~	62.2
4	~	0.7	74.0	22.1	3.2
5	2.7	~	90.2	5.6	1.5
6	~	~	~	~	100.0
7	~	~	~	~	100.0

SEM-EDS area analyses of areas within metallic prills in sample UR10 268A.
Data has been normalised to 100 at%.

Spectrum	Al2O3	SiO2	K2O	CaO	MnO	FeO	ZnO	As2O3	PbO
1	2.3	25.9	0.9	1.1	1.1	8.6	13.5	3.1	43.6
2	2.2	24.9	1.2	1.0	1.1	9.8	12.1	2.8	45.0
3	2.3	25.0	1.2	1.5	~	8.1	8.1	3.6	50.2
4	2.0	23.8	0.9	0.9	~	7.3	13.6	3.2	48.4
5	2.1	26.1	1.4	1.1	0.8	8.6	14.0	2.6	43.3

Analyses of the silicate matrix UR10 268C.
Data has been normalized to 100 wt%.

Spectrum	Al2O3	MnO	FeO	ZnO	SnO
1	4.9	~	75.9	16.6	2.5
2	6.7	0.7	74.3	18.2	~

Iron oxides (probably spinels) formed in the silicate matrix sample UR10 268C.
Data has been normalised to 100 wt%.

Scanned area	MgO	Al2O3	SiO2	MnO	FeO	ZnO	PbO
1	28.9	1.1	12.1	57.9	~	~	~
2	~	~	26.5	1.6	7.1	64.8	~
3	1.3	~	27.9	0.9	9.7	55.7	4.5
4	~	~	28.0	1.0	14.1	57.0	~

Zinc silicates formed in the slag that surround zinc sulphide gangue residues and manganese/magnesium oxide crystals in sample UR10 268C.
Data has been normalised to 100 wt%.

Spot analysed	S	Fe	Zn	As	Pb
1	46.5	3.8	10.2	~	39.5
2	41.5	2.4	8.9	2.4	44.8

Lead sulphide areas analysed in sample UR10 268C, data normalised to 100 at%.

Scanned area	Zn	As	Ag	Sb	Pb
1	~	6.4	~	5.0	88.6
2	~	11.8	8.7	4.0	75.5
3	~	7.1	~	3.3	89.6
4	4.8	6.1	~	4.1	85.0
5	16.6	~	10.9	4.0	68.5
6	14.2	7.3	5.6	3.2	69.8

Metallic prills analysed in the silicate matrix of sample 268C.
Data has been normalised to 100 at%.

Combined SEM-EDS bulk area analyses for Type II slags:

Sample	MgO	Al2O3	SiO2	P2O5	SO3	K2O	CaO	MnO	FeO	ZnO	As2O3	Sb2O3	PbO
UR10 268A	~	3.3	24.6	~	4.6	1	1.5	0.5	11.7	25.2	~	~	27.6
UR10 255	~	3.5	25.9	0.3	8.9	0.9	1.3	0.5	9.5	20.6	~	~	28.6
UR12 297	0.2	5.3	32.8	1.8	1.0	2.2	2.8	~	13.7	10.5	~	~	29.7
UR10 268C	~	2.4	20.4	~	0.5	0.7	0.7	0.4	23.7	16.6	2.6	~	32
UR10 250B	~	1.9	18.4	~	6	0.7	~	~	6.5	22.3	1.3	0.7	42.2
Average zinc sulphide	**~**	**3.3**	**24.4**	**0.4**	**4.2**	**1.1**	**1.3**	**0.3**	**13.0**	**19.0**	**0.8**	**0.1**	**32.0**

SEM-EDS bulk area scans of UR10/11/12 slags - Type II zinc rich slags.
The data has been normalised to 100 wt%.

Type III

Type III - slags with increased lime and phosphate

The third group of slags are the lead silicates with elevated lime and phosphate contents; only two samples can be grouped in this category (UR11 sample 222A and UR12 sample 298).

These two slags have lead oxide levels of 45-50%, they also contain silica, iron and zinc oxides, lime (3%), alumina and phosphate (1%), and potash (1%). Raised quantities of phosphate and lime could have come from the hearth lining or increased fuel ash. Evidence for this still requires further analytical investigation.

UR11 sample 222A

UR12 sample 298

OM images

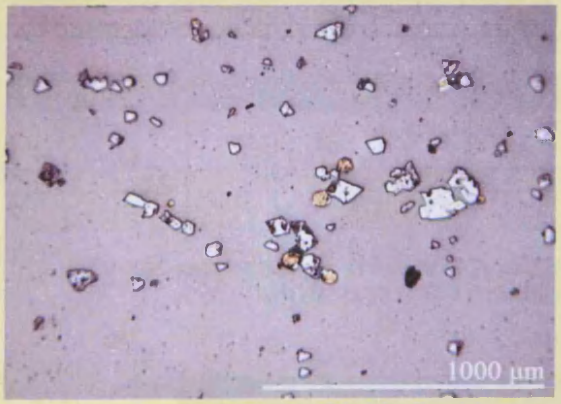

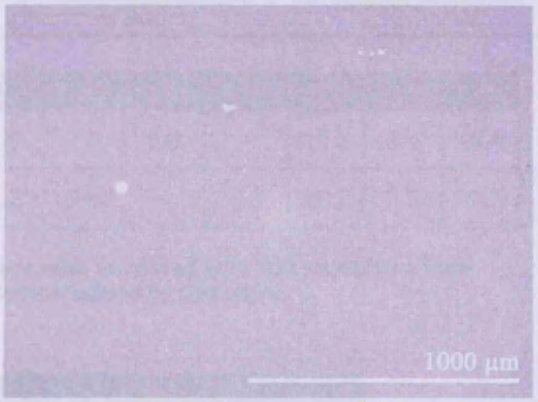

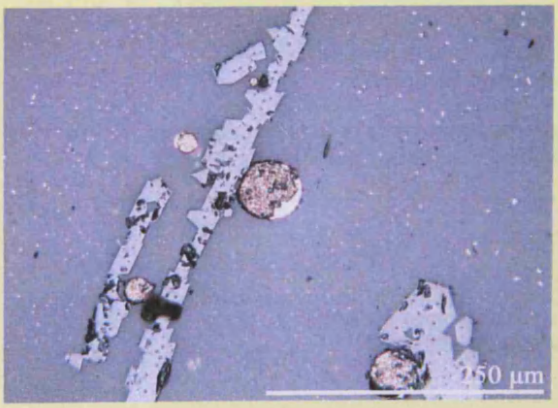

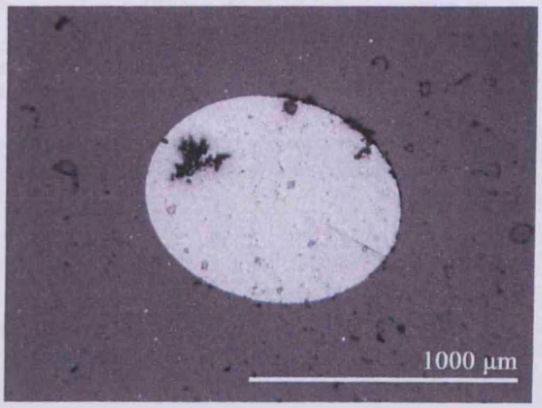

SEM-EDS images and data

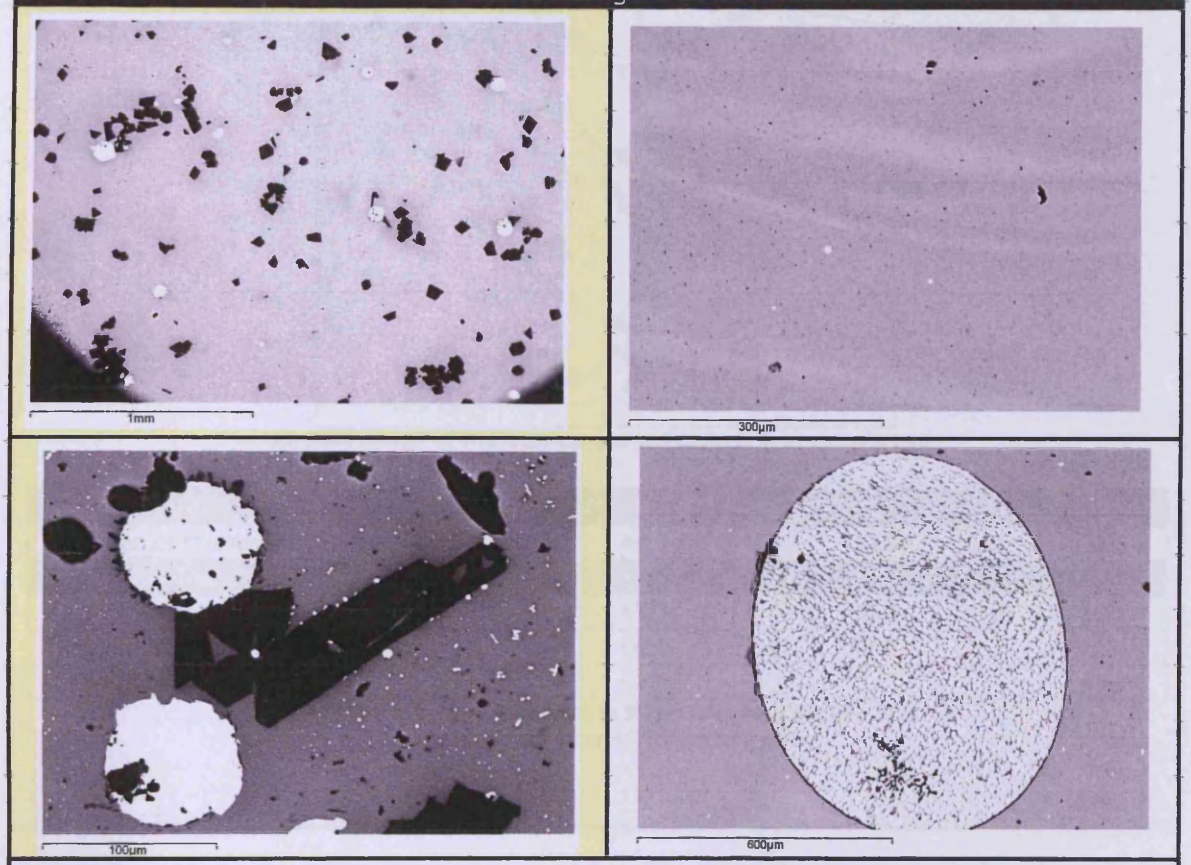

Sample	MgO	Al2O3	SiO2	P2O5	K2O	CaO	MnO	TiO2	FeO	ZnO	PbO
UR12 298 (n=4)	~	3.2	31.4	1.5	1.0	2.0	0.8	~	11.2	3.4	45.4
UR11 222A (n=5)	0.5	3.2	22.6	1.2	1.2	3.0	~	0.3	10.7	8.9	48.5

SEM-EDS data of bulk area scans of Type III - slags with increased lime and phosphate from UR10/11/12. The data has been normalised to 100 wt%.

Area analysis	MgO	Al2O3	TiO2	MnO	FeO	ZnO	SnO2
1	0.9	4.7	1.3	0.4	64.1	22.5	6.1
2	1.1	4.8	4.2	~	63.6	21.5	4.8
3	0.9	3.3	6.1	~	64.7	21.9	3.1
4	1.1	4.7	1.8	0.5	63.8	21.3	6.9

Iron/zinc oxides embedded in the glassy silicate matrix 222A. Data has been normalised to 100 wt%.

Scanned areas	MgO	Al2O3	SiO2	P2O5	K2O	CaO	TiO2	FeO	ZnO	PbO
1	0.5	3.2	23.7	1.4	1.4	3.0	~	7.9	9.0	50.0
2	0.5	3.3	26.8	1.5	1.8	3.7	0.7	5.9	8.2	47.8
3	0.6	3.3	24.4	1.2	1.5	3.2	0.5	7.1	8.4	49.9
4	0.6	3.1	24.1	1.2	1.7	3.4	~	7.6	7.8	50.7

SEM-EDS area analyses of the silicate matrix 222A. Data has been normalised to100 wt%.

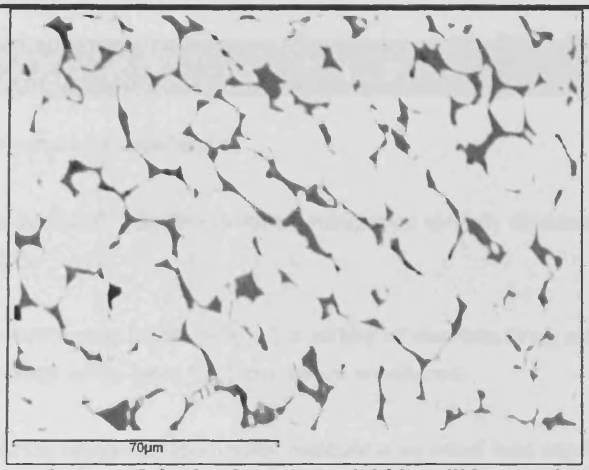

An SEM image of the lead-copper sulphide prill in sample 298.

Analysed area	S	Fe	Cu	Ag	Pb
Area scan of the whole prill	44.9	1.2	22.0	2.3	29.6
Spot analyses					
1 - dark black interphase	45.0	~	38.8	0.8	15.5
2 - White areas	46.1	2.3	47.0	1.7	3.0
3 -mid grey interfill.	49.5	~	1.6	~	48.9

SEM-EDS data of the largest prill found in slag sample 298.
Data has been normalised to 100 at%.

The others

The others - slags that cannot be categorised

Two residual slag samples do not fit into the grouped categories already discussed. Samples 89 and 268B are both from furnace UR10.

Sample 89 is a very high silicate slag (42% SiO_2). Quantities of alumina, lime, potash are elevated when compared to the zinc rich slags while iron, lead and zinc are reduced.

Sample 268B has a very glassy microstructure with residual very small lead sulphide scattered throughout the matrix. It contains 12 wt% antimony which is highly unusual. It also has high quantities of iron and zinc oxides. Silver content in the metallic prills was high with discrete areas of pure silver droplets within metallic lead prills.

UR10 sample 89

a.

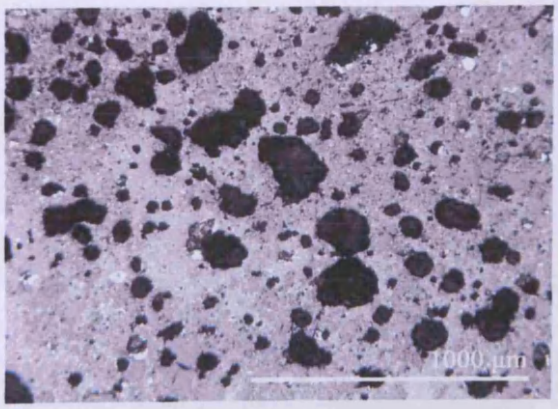

b.

Sample 89 is a complex crystalline slag and has trapped gangue material. It is a lead silicate and contains lead sulphide rich in zinc oxide as remnant ore fragments.
a. Sample 89 hand specimen
b. This OM image shows the area intersecting the partially reacted gangue and the glassy area.
c. OM image of partially reacted gangue area in slag sample 89. This image shows the porosity of this area (dark black holes) and the clusters of partially reacted lead sulphide (galena) the brightest white areas
d. A partially reacted lead/lead sulphide prill embedded in the slag. This prill contains metallic lead in the centre (brown shiny area) and a halo of partially reacted lead sulphide (white)
e. This slag has glassy areas has very little porosity, embedded in glassy matrix are grey crystals and the white minerals which are lead sulphide inclusions.OM image of the crystalline phases in the glassy matrix of sample 89.

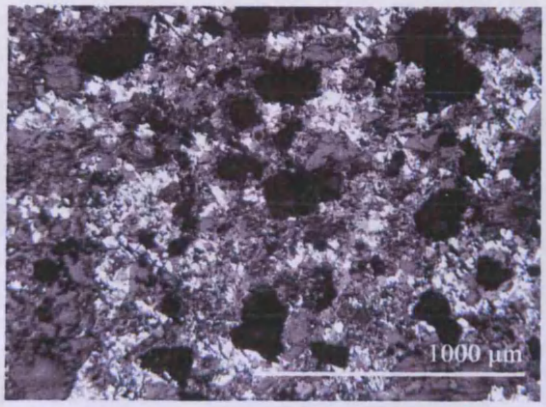

c.

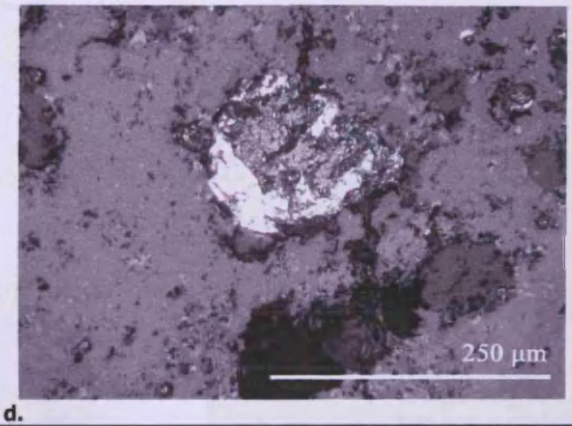

d.

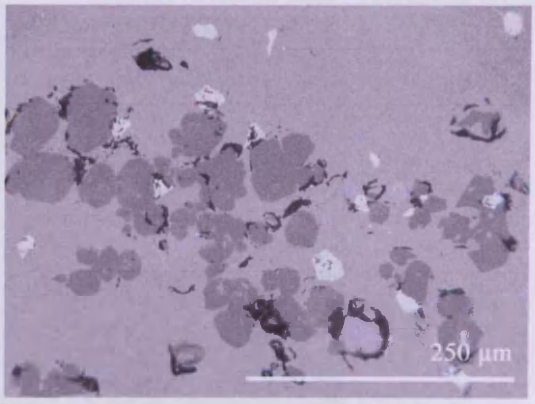

e.

SEM-EDS images and data

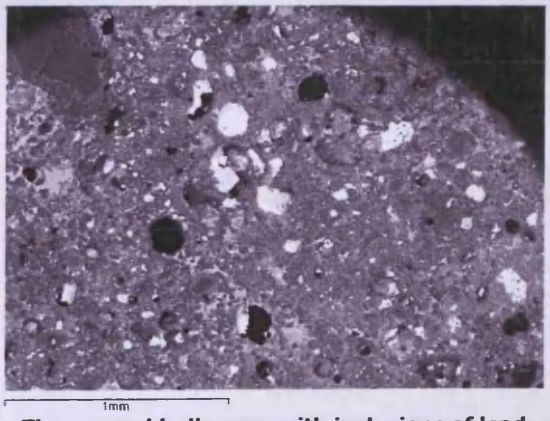

The general bulk area, with inclusions of lead sulphide (whitest phase).

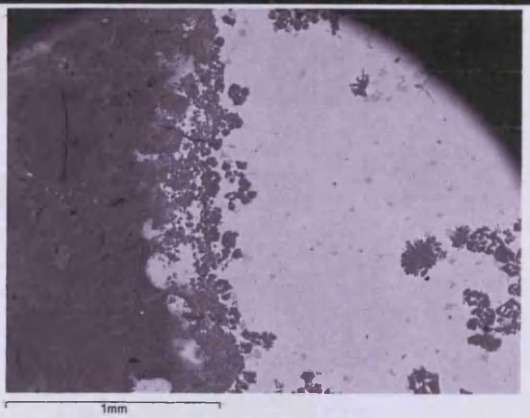

The two different areas of sample 89.

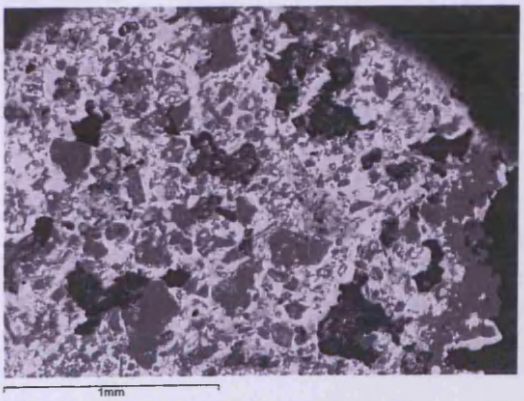

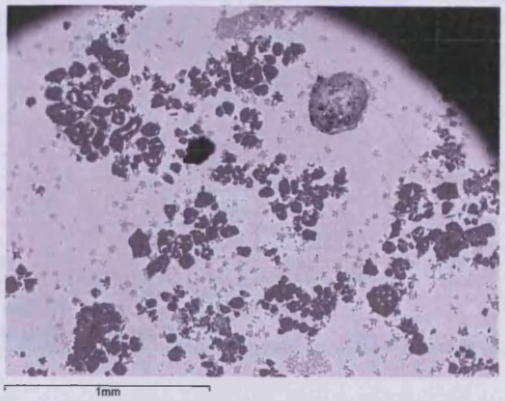

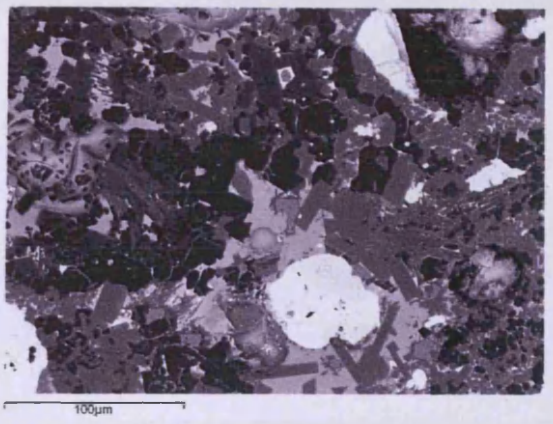

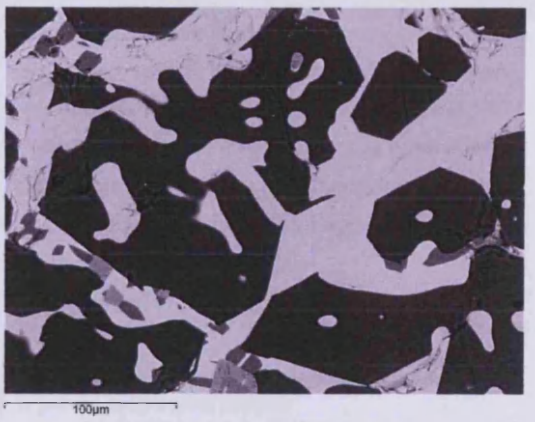

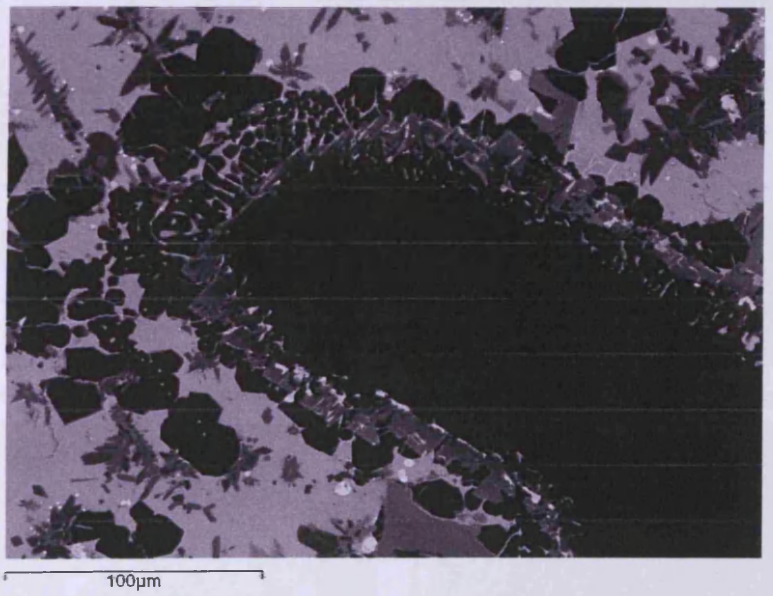

Scanned area	MgO	Al2O3	SiO2	K2O	CaO	FeO	ZnO	PbO
1	0.9	11.1	41.7	5.8	5.3	5.6	5.6	24.0
2	0.9	10.6	41.1	4.7	4.6	5.5	5.2	27.4
3	0.8	10.3	49.0	6.1	3.7	5.3	6.2	18.5
4	1.1	9.0	38.5	4.1	5.5	7.0	8.0	27.0
5	1.1	10.5	40.9	5.7	5.1	6.1	5.8	24.9
Average	**1.0**	**10.3**	**42.2**	**5.3**	**4.8**	**5.9**	**6.1**	**24.3**

Bulk area analyses of slag sample 89. SEM-EDS data has been normalised to 100 wt%.

Scanned area	MgO	Al2O3	SiO2	P2O5	K2O	CaO	TiO2	FeO	ZnO	PbO
1	1.5	7.8	39.2	0.6	2.0	5.8	~	5.4	6.0	31.8
2	1.3	7.7	38.4	~	2.1	5.8	~	6.1	6.9	31.6
3	1.2	5.5	33.7	~	0.8	7.1	~	7.3	9.7	34.7
4	1.3	6.2	35.0	~	0.9	4.9	~	8.6	9.5	33.6
5	2.6	5.4	36.5	2.7	1.0	6.6	0.8	10.9	8.4	25.1
6	0.8	6.3	32.4	~	1.3	6.3	0.5	7.7	12.1	32.7
Average	**1.5**	**6.5**	**35.9**	**0.6**	**1.3**	**6.1**	**0.2**	**7.7**	**8.8**	**31.6**

Area analyses of the glassy silicate matrix from slag sample 89.
The data has been normalised to 100 wt%.

UR10 sample 268B

a.

Slag sample 268B is a black, glassy slag (a). On the upper surface it has a brown/green sheen and the lower base is black with a texture indicating that the liquid slag may have been poured or tapped onto a soft surface. The cut internal surface is black and appears to have no macroscopic inclusions (b).

c. OM image of the slag body.
d. The slag body has different crystalline phases in the slag.
e. OM image of lead prills and grey spinel crystals in the slag matrix

b.

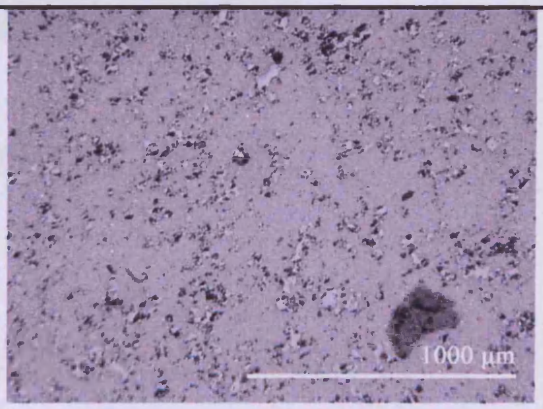

c.

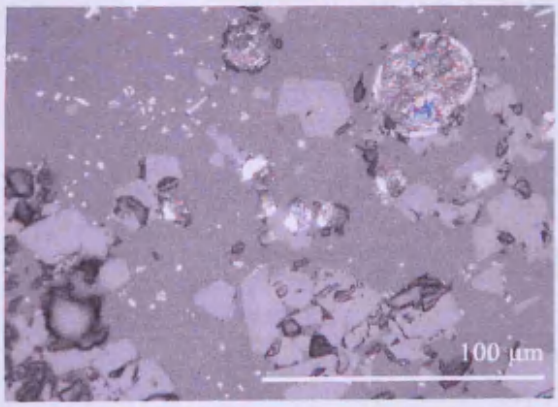

d.

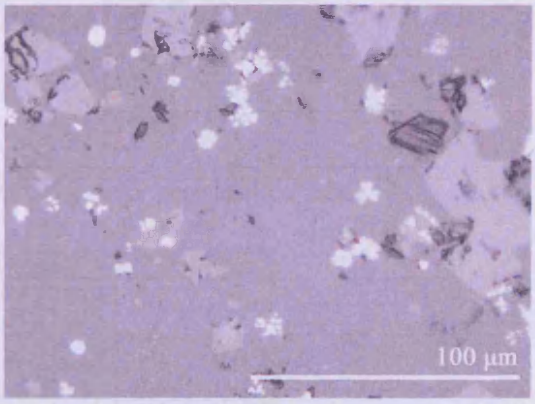

e.

SEM-EDS images and data

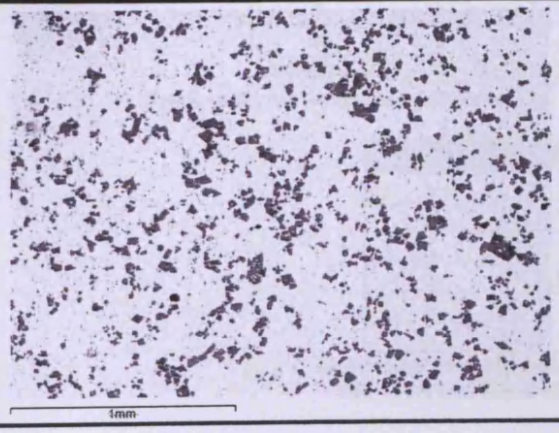

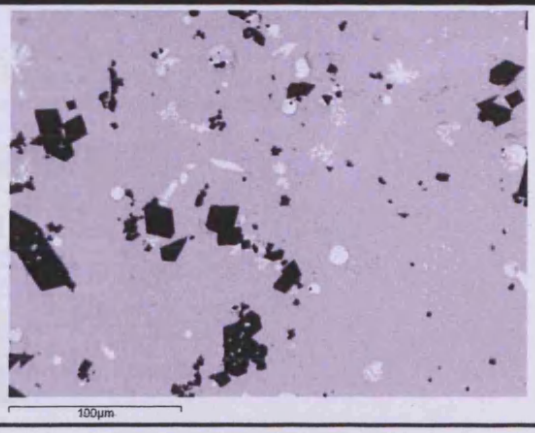

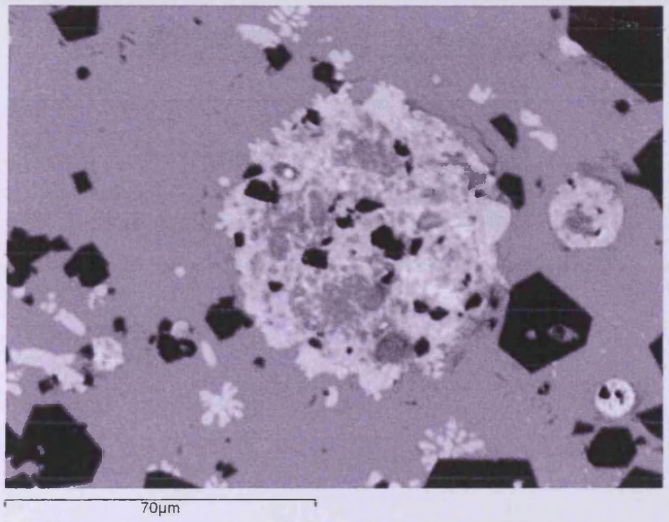

Scanned area	Al2O3	SiO2	K2O	FeO	ZnO	Sb2O3	PbO
1	1.6	12.7	0.6	17.8	7.9	11.6	47.9
2	1.7	12.7	~	17.5	7.3	12.0	48.8
3	1.6	12.7	0.4	15.7	7.3	12.1	50.1
4	1.7	12.5	~	18.0	8.1	11.8	48.0
5	1.7	13.3	~	16.0	7.5	12.1	49.4
Average	**1.6**	**12.8**	**0.2**	**17.0**	**7.6**	**11.9**	**48.8**

Bulk area analyses (SEM-EDS) of slag sample 268B. The data has been normalised to 100 wt%.

Scanned area	Al2O3	SiO2	K2O	FeO	ZnO	As	Sb2O3	PbO
1	1.5	15.7	0.6	4.6	5.5	~	15.3	57.0
2	1.6	15.2	~	4.4	5.6	~	16.1	57.1
3	1.6	15.4	0.6	4.4	4.7	~	15.3	58.0
4	~	16.6	~	4.7	5.3	~	15.8	57.7
5	~	15.9	~	4.2	5.7	~	16.8	57.5
6	1.5	15.5	0.6	4.8	5.7	0.7	15.6	55.7

SEM-EDS analyses of the glassy slag matrix. Data has been normalised to 100 wt%.

Spectrum	Al2O3	SiO2	TiO2	FeO	ZnO	SnO2	Sb2O3
1	3.9	~	~	77.7	16.4	2.0	~
2	3.5	~	~	82.4	14.1	~	~
3	~	1.5	0.4	74.0	20.1	3.1	0.8
4	2.6	~	~	82.0	14.5	0.9	~
5	3.9	~	~	75.5	19.1	1.5	~
6	6.2	~	~	72.3	19.6	1.9	~
7	4.2	~	~	75.3	18.4	2.0	~
8	4.8	~	~	75.5	18.1	1.5	~
Average	**3.6**	**0.2**	**0.1**	**76.8**	**17.6**	**1.6**	**0.1**

Spinels found in the slag matrix. The data has been normalised to 100 wt%.

Spectrum	S	Fe	Zn	Cu	Sb	Pb
1	50.4	~	~	2.0	~	47.6
2	46.2	1.5	1.6		2.8	47.9
3	51.1	~	~	~	~	48.9
4	49.7	1.2	~	~	~	49.1
5	49.8	~	~	~	0.9	49.3
6	50.9	~	~	~	~	49.1

Lead sulphide prills measured using SEM-EDS.
The data has been normalised to 100 at%.

Spectrum	Cu	Fe	Ag	Sb	Pb
1	~	~	4.8	2.0	93.2
2	~	~	39.2	9.1	51.7
3	1.4	~	48.8	9.4	40.4
4	~	2.8	39.1	10.6	47.6

Metallic prills found within slag sample 268B.
The data has been normalised to 100 at%.

APPENDIX VIII - SEM-EDS BULK AREA ANALYSES OF *HUAYRACHINA* AND EUROPEAN FURNACE SLAGS

A comparison of SEM-EDS bulk area analyses of *huayrachina* and European furnace slags.

The data has been normalised to 100 wt% and sorted via lead oxide.

Colour coding = Cuiza's slag (yellow), Archaeological *huayrachina* data (not highlighted), UR furnaces (pink), and DMD furnaces (blue)}.

Average bulk composition	Na2O	MgO	Al2O3	SiO2	P2O5	SO3	K2O	CaO	TiO2	MnO	FeO	ZnO	As2O5	Sb2O3	SnO2	PbO
Cuiza slag sample9a (2001)	~	1.9	8.0	37.8	0.7	0.4	4.1	19.7	~	0.3	11.8	9.7	~	~	~	5.6
Hu24 77C	~	3.5	5.9	32.8	1.2	0.9	2.4	23.5	0.2	~	10.3	11.6	~	~	~	7.7
Cuiza slag sample 1 (2002)	~	2.1	8.4	39.1	0.2	2.2	5.3	14.3	~	0.9	10.0	6.5	~	~	~	11.0
Cuiza slag sample 3 (2002)	~	1.9	8.9	45.2	0.4	0.4	4.7	10.2	0.1	0.4	8.5	7.1	~	~	~	12.2
Hu24 76B	~	2.1	7.3	34.5	~	~	3.7	12.7	0.2	~	7.2	17.2	~	~	~	15.1
ES 343A	~	2.4	5.4	29.0	~	~	3.0	14.4	~	~	6.0	24.4	~	~	~	15.4
ES 343B	~	1.7	6.6	29.3	1.2	~	3.9	15.3	~	~	6.8	5.2	~	~	12.6	17.5
Hu24 76A	~	2.2	8.0	33.5	~	~	3.7	14.1	~	~	14.4	4.9	~	~	~	19.2
WS 342F	1.0	3.3	17.1	26.6	0.4	~	4.9	8.4	~	~	3.7	6.9	~	~	~	27.6
HuA1 31	0.4	0.8	7.0	34.1	~	~	2.7	5.8	1.1	~	7.3	11.1	~	~	~	29.7
CP 344A	~	1.9	5.4	32.3	2.0	~	3.3	12.4	0.9	~	10.8	9.3	~	~	~	21.7
CP 344B	~	2.5	1.6	29.6	2.3	~	2.9	12.9	1.1	~	10.0	11.4	~	~	~	26.1
Hu24 77A	~	1.6	4.2	24.3	~	~	0.8	11.1	0.4	~	8.0	18.5	~	~	~	31.2
HuA1 27A	~	1.6	5.3	22.2	~	~	3.1	11.4	~	0.4	13.4	11.1	~	~	~	31.5
Type II Slags	~	~	3.3	24.4	0.4	4.2	1.1	1.3	~	0.3	13.0	19.0	0.8	0.1	~	32.0
WS 342C	~	1.3	7.5	26.9	~	3.1	3.6	6.7	~	~	4.8	12.7	~	~	~	33.4
HuA1 26C	~	0.7	6.2	23.5	~	1.1	2.8	8.3	~	~	4.9	15.5	2.8	~	~	34.2
HuA1 26B	~	1.0	4.8	23.6	~	~	1.6	8.2	0.3	~	4.9	13.4	~	~	~	42.2
WS 342B	0.5	0.4	7.9	29.8	~	2.9	4.1	3.8	~	~	2.4	4.4	~	~	~	43.7
Type III Slags	~	0.3	3.2	27.0	1.4	~	1.1	2.5	0.2	0.4	11.0	6.2	~	~	~	47.0
WS 342G	~	1.3	5.1	21.2	~	~	2.1	9.2	~	~	3.1	6.2	~	~	~	51.9
Hu24 77B	~	1.7	3.3	19.1	~	~	0.7	11.7	0.7	~	5.2	5.4	~	~	~	52.3
HuA1 29	0.8	~	8.2	30.5	~	~	2.4	1.0	~	~	1.6	~	1.0	1.8	~	52.7
ES 343C	~	1.2	4.8	19.4	~	~	1.9	7.8	~	~	3.1	4.0	~	~	~	57.7
DMD Slag 341A	~	0.4	2.8	22.2	~	~	1.2	4.2	~	~	3.2	5.9	~	~	~	60.1
Type I Slags	~	~	2.6	20.0	~	~	0.6	0.8	~	0.1	6.8	3.6	~	0.5	~	65.0
WS 342A	0.2	~	0.8	8.8	~	12.4	0.2	1.8	~	~	7.5	2.6	~	~	~	65.7
ES 343D	~	0.6	5.2	10.8	~	~	~	1.4	~	~	1.0	13.9	~	~	~	66.4